

"ELECTRICAL AND DIELECTRIC PHENOMENA IN POLYMER FOIL ELECTRETS"

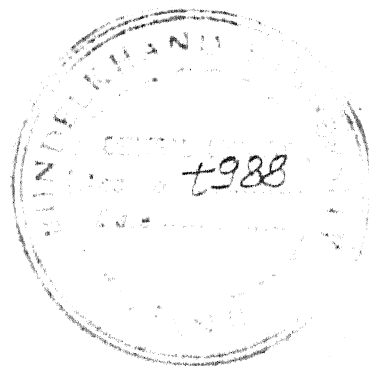
THESIS SUBMITTED TO



BUNDELKHAND UNIVERSITY, JHANSI (U.P.)

For the Award of the Degree of
DOCTOR OF PHILOSOPHY
IN
PHYSICS

By
Ashutosh Verma
M.Sc.

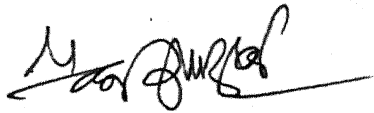


DEPARTMENT OF PHYSICS
BIPIN BEHARI PG COLLEGE, JHANSI (U.P.)

2002

*This Thesis is Devoted
in Memory of
My Loving Mummyji
Late Smt. Krishna Devi*

Forwarded

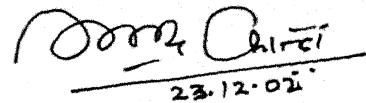


Pawan Kumar Khare

Co-supervisor

Department of P.G. Studies &
Research in Physics

J. B. University, Jabalpur



Dr. Rudra Kant Srivastava

Supervisor

Reader, Department of Physics

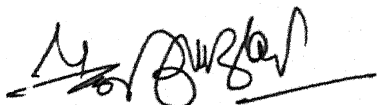
Bipin Behari P.G. College

Jhansi

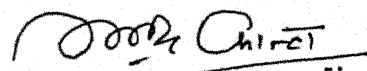
CERTIFICATE

This is to certify that

- (i) *The candidate, **Shri Ashutosh Verma**, has worked for his Ph.D. degree under my guidance and supervision in the Department of Physics, Bipin Bihari P.G. College, Jhansi.*
- (ii) *He has put more than 200 days attendance in the department.*
- (iii) *The thesis entitled "**ELECTRICAL AND DIELECTRIC PHENOMENA IN POLYMER FOILS ELECTRETS**" embodies the original research work done by **Shri Ashutosh Verma** on the approved topic.*
- (iv) *Such work has not been submitted to any other University.*
- (v) *He fulfils all the conditions required under ordinance.*



(Dr. Pawan Kumar Khare)
Co-supervisor




(Dr. Rudra Kant Srivastava)
Supervisor

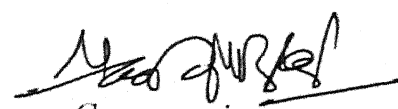
DECLARATION

I hereby declare that with the exception of the guidance and suggestions received from my Supervisor Dr. Rudra Kant Srivastava and co-guidance received from my co-supervisor Dr. Pawan Kumar Khare, the work reported in this thesis is the outcome of my own unaided efforts.

Jhansi

Dated : 23rd December, 2002


ASHUTOSH VERMA


Co-supervisor
(Dr. Pawan Kumar Khare)


Supervisor
(Dr. Rudra Kant Srivastava)

*I am not merely expressing a conventional obligation if I state that the sustained efforts and unistinted direction of my learned Supervisors **Dr. Rudra Kant Srivastava**, Reader, Department of Physics, Bipin Behari Postgraduate College, Jhansi and **Dr. Pawan Kumar Khare**, Reader, Department of Postgraduate Studies and Research in Physics, R. D. University, Jabalpur, the work could not have been brought out in the present form. My most sincere and heartfelt thanks are due to them for their unflinching directions and advise at every stage of work.*

*I also wish to thank **Dr. U. P. Singh**, Principal, Bipin Behari Postgraduate College, Jhansi for giving his kind permission to carry out the present work.*

*Many others have contributed to the realisation of this thesis. Among them, worth to mention here, is the name of **Dr. R. K. Pandey**, Professor, Solid State Research Laboratory, Department of Physics, Dr. H. S. Gaur University, Sagar; **Dr. J. K. Quamara**, Asstt. Professor, Department of Physics, Regional Engineering College, Kurukshetra; **Dr. M. S. Qureshi**, Professor of Physics, Maulana Azad College of Technology, Bhopal; **Er.A.K.Solanki**, Head, Department of Computer Science, B.I.E.T., Jhansi. My very humble obligations are due to them whose valuable, professional knowledge and younger brotherly treat, paid a significant contribution to complete the work.*

*I would also like to acknowledge **Dr. J. P. Srivastava**, Asstt. Librarian, Central Library, Indian Institute of Technology, New Delhi, for providing library facilities as this has enabled me in uplating the literature in the thesis. My sincere thanks are due to him together with **Mr. Devendra Kumar Sahu**, Lecturer SJS in the Department of Physics, School of Sciences,*

Bundelkhand University, Jhansi, who has helped me in various stages of my research work.

The valuable services of Mr. Rajeev Sethi, Zapson Computers for their sincere efforts in getting this thesis into such a flawless computer typing and the help of Mr. Rajendra Singh Thakur and Mr. Hari Shankar Dubey for tracings is gratefully acknowledged.

I am very much thankful to Mr. Sandeep Singh Verma, Bundelkhand University Campus, Jhansi for his constant encouragement.

I am much indebted to my elder brothers, Shri Sanjay Verma and Shri Ajay Verma and two respective Bhabhiji Smt. Suman Verma and Smt. Ritu Verma. My sincere thanks are due to them for constant encouragement and co-operation.

Finally, I offer profound regards to my loving father who have always been a source of constant inspiration, deep love and blessings.

Ashutosh Verma

PREFACE

Electrets create a strong field of about 30 kV/cm which can be utilized for various purposes, like foil electret microphone, in electrophotography, electret gas filters, electrostatic recording, touch transducers, electret motors, generators, etc. Polymers are known to be good electret forming materials. Polymer foil electrets have several applications in modern solid state devices. In all, these devices electrified polymer foils are employed. Recently, it has been shown that with multilayer insulating system, there exist possibility of adjusting polarisation/charge distribution along the film thickness. This adjustable possibility may be very meaningful to applications. The thesis entitled **"Electrical and dielectric phenomena in polymer foils electrets"** is an outcome of a detailed investigations of the polarisation/space charge formation in polymer [polyvinyl pyrrolidone (PVP)] foil electret using thermally stimulated discharge current (TSDC) measurement in short circuit configuration, transient current in charging and discharging modes, steady state electrical conduction and dielectric measurement of polyvinyl pyrrolidone foil electrets. For the sake of convenience, the thesis has been divided into eight chapters.

Chapter I introduces the problem and a review for material used for carrying out the present investigation. It also covers the general introduction to the relevant topics such as different process leading to dielectric absorption, electret state, mechanism of polarization, preparation of thermoelectrets and concept of electrical contacts, etc. This chapter has been concluded with the choice of the material, its properties and applications.

Chapter II deals with various design considerations and fabrication of a suitable sample holders for 'TSDC' studies and preparation of electrets. Various experimental methods for preparation of thin films, measurement of film thickness and electrode deposition on them along with the different equipments used namely, vacuum coating unit, power supply, and electrometers etc. have been discussed.

Chapter III deals with the various theories and mechanism backgrounds of proposed studies of TSDC in short circuit, transient current in charging and discharging modes, electrical conduction and dielectric properties with reviews of work done in relevant studies during last decade.

Chapter IV is devoted to detailed investigations and experimentations of depolarization current studies of PVP foil thermoelectrets under short circuits thermal stimulation of the discharge.

Chapter V emphasises transient behaviour of PVP foil electrets in charging and discharging modes under isothermal conditions. Different models of absorption and desorption transient current have been discussed. Steady state electrical conduction in PVP foil electrets is also reported in this chapter.

Chapter VI reports dielectric properties studies in PVP foil electrets in audio frequency range.

Chapter VII reviews of the results obtained from the above mentioned different studies and discusses the correlation between them.

CONTENTS

Page Nos.

CHAPTER – I

GENERAL INTRODUCTION

1.1	Introduction	1
1.2	The Electret State	3
1.2-1	Hetero and Homo Charges	5
1.2-2	Types of Electerets	6
1.2-3	Charging Polarising Methods	8
1.3	The Polymers–Structure and Properties	10
1.3-1	Classification of Polymers	11
1.4	Choice of Materials	14
1.4-1	Transition in Polymers	15
1.4-2	Factors affecting dielectric behaviour of polymers	17
1.5	Mechanism of Polarization	18
1.5-1	Internal Polarization	18
1.6	Concept of Electrical Contacts	21
1.7	The technique for investigation of electrical properties of insulating material	22
1.8	Material used in the Present Work – Polyvinyl Pyrrolidone (PVP)	27
References	40

CHAPTER – II

EXPERIMENTAL DETAILS

2.1	Introduction	49
2.2	Methods of polymer film formation	49
2.2-1	Thermal evaporation	50
2.2-2	Combination of internal baffles and flash evaporation	50
2.2-3	Laser evaporation	50
2.2-4	Pyrolysis	51

2.2-5	Sputtering	51
2.2-6	Gaseous discharge	52
2.2-7	Hot pressing method	52
2.2-8	Casting method	53
2.2-9	Film blowing	53
2.2-10	Photolytic process	53
2.2-11	Vacuum evaporation	54
2.2-12	Film from polymer solution	54
2.3	Present experimental technique	58
2.4	Measurement of film thickness	60
2.4-1	Mechanical methods	60
2.4-2	Optical methods	61
2.4-3	Electrical methods	62
2.5	Types of Electrodes	63
2.6	Circuit configuration and principal equipments	69
2.6-1	Temperature programming and control	69
2.6-2	Other instruments used and their specifications	70
References	71

CHAPTER – III

THEORETICAL BACKGROUND OF DIFFERENT STUDIES

3.1	Introduction	73
3.2	Transient Currents in Charging and Discharging Modes	74
3.3	Mechanisms of Transient Currents	77
3.3-1	Electrode Polarization Mechanism	77
3.3-2	Dipole Orientation Mechanism	78
3.3-3	Charge injection leading to trapped space charge effects	79
3.3-4	The Hopping Mechanism	80
3.3-5	The Tunnelling Model	81
3.4	Theory of Transient Current in Polar Dielectrics	82

3.5	Last Decade's Work	85
3.6	The Electrical Conduction	86
3.6-1	Generation of Charge Carriers	89
3.7	Mechanisms responsible for conduction	91
3.7-1	Ohmic Conduction Mechanism	91
3.7-2	Schottky-Richardson Emission and Poole-Frenkel Mechanism	91
3.7-3	Space Charge Limited Current (SCLC) Mechanism	93
3.7-4	Ionic Conduction Mechanism	95
3.8	Last Decade's Work on Electrical Conduction	96
3.9	Effect of Various Parameters on Electrical Conduction	108
3.9-1	Electric field	108
3.9-2	Temperature	108
3.9-3	Pressure	109
3.9-4	Moisture	109
3.9-5	Electrode Material	110
3.9-6	Impurity	110
3.10	Thermally stimulated discharge currents (TSDC)	111
3.11	Techniques and Theories of TSDC	118
3.11-1	Current TSDC with shorted electrodes	118
3.11-2	Current TSDC with an air gap	119
3.11-3	Charge TSD by transferring the induced charge to an electrometer	119
3.11-4	Charge TSD by field cancelling method	120
3.11-5	Theory of TSDC due to deorientation of dipoles	120
3.11-6	Theory of TSDC by self motion of charges	124
3.12	Effect of different factors on TSDC thermograms	125
(a)	Polarizing field	125
(b)	Polarizing temperature	125
(c)	Polarizing time	126
(d)	Electrode material	126
(e)	Specimen thickness	127
(f)	Heating rate	127
(g)	Impurity	127
(h)	Humidity	128

3.13	Evaluation of TSDC data	128
3.13-1	Activation Energy	128
(A)	Initial rise method	128
(B)	Bucci <i>et al.</i> method	128
(C)	Half current peak-width method	129
(D)	Heating rate variation method	129
3.13-2	Relaxation Time	130
3.13-3	Charge Released	131
3.14	Last Decade's work on TSDC	131
3.15	Dielectric measurements	141
3.16	Effect of Forming Parameters	143
3.16-1	Temperature	143
3.16-2	Frequency	144
3.16-3	Impurity	146
3.17	Last Decade's Work	147
3.18	Present Investigation	147
References	149

CHAPTER – IV

THERMALLY STIMULATED DISCHARGE CURRENT STUDIES IN PURE POLYVINYL PYRROLIDONE (PVP) FOIL ELECTRETS

4.1	Introduction	164
4.2	Survey of the Mechanisms responsible for TSDC	167
4.3	Method to unravel the various decay processes	169
4.3.1	Choice of polymers for TSDC	169
4.4	Experimental Details	170
4.5	Results and Discussion	172
References	190

CHAPTER – V

TRANSIENT CURRENT STUDIES IN CHARGING AND DISCHARGING MODES AND STEADY STATE ELECTRICAL CONDUCTION IN PURE PVP FOIL ELECTRET

5.1	Introduction	193
5.2	Experimental Details	195
5.3	Results	196
5.3-1	Time Dependence	197
5.3-2	Temperature Dependence	198
5.3-3	Field Dependence	199
5.3-4	Electrode Materials Dependence	199
5.3-5	General Characteristics of Curves	200
5.4	Discussion	202
References	212

CHAPTER – VI

DIELECTRIC PROPERTIES IN PURE PVP FOIL ELECTRETS

6.1	Introduction	214
6.2	Present Investigation	217
6.3	Foil Preparation	217
6.4	Experimental Procedure	217
6.5	Results and Discussion	218
6.5.1	Frequency Dependence of Capacitance	223
6.5.2	Temperature Dependence of Capacitance	224
6.5.3	Electrode Material Dependence on Capacitance	224
6.5.4	Variation in Loss Factor	225
References	227

REVIEW AND CORRELATION OF DIFFERENT RESULTS AND CONCLUDING REMARKS

7.1	Review and Correlation	230
7.2	Concluding Remarks	238
References	241

RESEARCH PAPERS COMMUNICATED TO VARIOUS JOURNALS :

1. Thermally stimulated discharge current study of pure polyvinyl pyrrolidone foil electrets.
2. Transient currents studies in charging and discharging modes in PVP foils.
3. Isothermal electrical conduction in polyvinyl pyrrolidone foils.
4. Dielectric and loss factor studies in polyvinyl pyrrolidone foils.
5. Thermally stimulated discharge current studies of polyvinylidene fluoride foils.

CHAPTER I

GENERAL INTRODUCTION

1.1 INTRODUCTION

The analysis of insulating materials and insulating systems has been advancing on many fronts. Extensive quantitative and qualitative basic research in the subject have been carried out resulting in a huge amount of fruitful information. A major portion of the family of insulators is taken up by polymers.

In the last three decades, scientists have been showing their increasing interest in the basic electrical properties of large energy band gap materials. Most of the literature is available on electrical behaviour, charge storage and transport or most specifically the manifestation of the "Electret state" by some organic solids, waxes, insulating dielectrics, glasses and semicrystalline and amorphous polymers [1]. Studies on polymers have attracted a particular attention due to their useful mechanical properties, unique disordered structure and their potential applications in many technological and engineering areas. The miniaturization of solid state devices has opened up yet another new field for use of polymers, which is very vast, fascinating and promising [2-5]. Extensive research is underway in many laboratories on electrical properties of pure and doped polymers, copolymers, polymeric blends and polymeric compositions.

The existing and anticipated technological potential of charge storage properties of electroactive polymers has

increased tremendously and become almost limitless. Apart from their use as conventional insulators, polymers are now being used in many other fields such as electrets [6], conductive and photoconductive materials in a number of electronic devices [7] such as thin film transistors, thin film memory circuits and cryptron logic.

Polymers have also found valuable applications in bioengineering : for understanding of membranes, neural signals, biological memory in regeneration, electrical mediation in tissue growth and other phenomena. It is expected that they may find many other revolutionary applications in the field of medical science and space technology, etc.

As a result of extensive research carried out in the last decades, a breakthrough has been made in our understanding of designing or synthesizing organic polymer macromolecule to achieve desired properties and processing polymers into preferred morphologies for use in dielectric and electrical engineering applications. The result has been a new generation of polymeric materials providing new strength, stiffness, environmental stability and load bearing capability coupled with elasticity, electrical resistivity, conductivity, and charge and energy absorption and storage capacity. The variety and combination of polymeric materials is limitless and still continues to grow as scientific endeavour and technological application broaden and frequently merge. Infact, the science of polymers today has become one of the

most interdisciplinary field involving efforts of synthetic chemists, material scientists, electronic engineers and theoretical and experimental physicists. The applications involving charge storage and transport properties, particularly, the electret effects are providing the driving force to such an interesting and interdisciplinary research. The structure property relationship and the need to provide new and chemically stable systems have also played an important role. The future will certainly see still more activity in this field and an increasing trend towards tailored and model synthesis in which polymeric materials and their blends are produced with preferred chemical structure, chain conformations, orientations and morphology and these variables are optimized to the utmost for specific applications.

1.2 THE ELECTRET STATE

A dielectric material exhibiting a quasi-permanent electrical charge is defined to be an electret [8]. This implies that a substance will be an electret if the decay time of its stored polarization is long in relation to the characteristic time of experiments performed on the material. The charge of an electret may consist of "real" charges such as surface charge layers, or space charges; it may be a "true" polarization or it may be a combination of these. The true polarization is usually a frozen-in alignment of the real charges comprised of layers of trapped positive and negative

carriers, respectively, often positioned at or near the two surfaces of the dielectric.

The electrostatic attractive properties of waxes, resins and sulphurs which were first described by Gray in 1732, gives us the first studies carried out on electret properties. Subsequently, more work was performed on stored electric fields in dielectrics by Faraday in 1839 [9]. It was very much later that Heaviside coined the word "Electret" in 1892 [10]. He postulated that certain waxes would form permanently polarized dielectrics when allowed to solidify from the molten state in the presence of an electric field. Eguchi [11], in 1919, made the first electret from carnauba wax to verify experimentally this theoretical proposal of Heaviside. The samples prepared by Eguchi were thick plates of carnauba wax turned into electrets by a thermal method. Electret research gradually moved to simpler materials like ionic and organic crystals and polymers where fundamental solid state properties could be correlated with the electret behaviour [12-14]. The electret effect has been studied in biological materials also, the "bioelectret". However, looking at the application prospects, now a days, materials which are mouldable and machinable are being focussed on for the electret studies. Hence, the presently electret research has shifted to thin film polymers like teflon polyfluoroethylene, propylene, polytetra-fluoroethylene, polyvinylidene fluoride, polypropylene and polyethylene [8,15-19], etc.

Initially, electrets were regarded merely as a scientific addity, an object displaying electrostatic phenomenon similar to that of a magnet and its magnetic field. Then the electret was put to its first practical use as a transducer in the form of electret microphones and earphones [20,21]. Subsequently, the electret with its permanent electrification effects was utilized in a wide variety of applications like xerographic reproduction techniques [22], gas filters [23], relay switches [24,25], medicinal appliances like radiation dosimeters [26], optoelectro devices like video/TV cameras [27,28], maritime devices like hydrophones [29-31], electret motors [32] and a host of innovative possible devices like the electret generator [33,34], tachometers [35], vibrational fan [36], measurement of affluents in the space shuttle propulsion system [37], thin film transistors and thin film memory circuits [38], etc.

1.2-1 HETERO- AND HOMO-CHARGES

Eguchi [11] found that non-metallized dielectrics polarized by application of an electric field have on their two surfaces two charges of different nature and of opposite polarity. Gement [39] gave the names "homocharge" and "heterocharge" to these two charges. If the polarity of the charge induced on the surface is the same as that of the adjacent forming electrode, it is called homocharge, while if the polarity is opposite to that of the adjacent forming electrode it is called heterocharge.

To explain the phenomenon, a number of theories were advanced by different workers [40-48] and it turned out that the two charge theory of electret as developed by Gross [41,46-48] was the one which gained widespread acceptance. According to him, the heterocharge is due to dielectric absorption by dipoles in polar substances or ionic charges in other materials, while the homocharge is due to transfer of charges from the electrode to the surface of dielectric across the interface. The formation of the heterocharge which is due to an internal volume effect is not yet clear. Going into details, Gross explained that in polar substances the dipole orientation due to an applied field produces heterocharge but if the field is high enough electrons or ions can be fed into or extracted from the dielectric surface and are transferred to electrodes causing the formation of homocharge on the electret surface. The electret effect in nonpolar dielectrics was explained by Baldus [49] in terms of freezing of induced dipoles during cooling in the presence of an electric field. The two charge theory was later used by Swan [50] to develop a theory for open circuit charge decay which was later expanded for short circuit charge decay by Gubkin [51].

1.2-2 TYPES OF ELECTRETS

Electrets are usually prepared by a number of methods and are given names mostly according to the conditions under which they are formed.

(A) THERMOELECTRETS

These are prepared by simultaneous application of heat and an electric field while polarizing a dielectric [52,53].

(B) ELECTROELECTRET

This is an electret prepared at room temperature under application of a high electric field [48,54,55].

(C) RADIOELECTRET

This is an electret prepared when simultaneously an electric field and high energy radiation such as X-rays, γ -rays, β -rays, monoenergetic electron beam, etc. are used [56-58].

(D) PHOTOELECTRET

These are electrets which are prepared by polarizing a dielectric under the simultaneous action of an electric field and ultraviolet or visible light radiation [59-62].

(E) THERMOPHOTOELECTRET

These are electrets which have been prepared by polarizing at high temperature a photo conducting dielectric by light radiation of high energy under an applied electric field [63,64].

(F) MAGNETOELECTRET

This is an electret obtained by cooling of softened or molten dielectric in a magnetic field [65,66].

(G) TRIBOELECTRET

These are electrets which have been charged due to friction [67].

1.2-3 CHARGING/POLARIZING METHODS

The important charging techniques are given below :

(A) THERMAL METHODS

Here the dielectric is polarized by application of an electric field at an elevated temperature. Subsequent cooling, while the field is still applied, results in a quasi-permanently polarized dielectric [68-71].

(B) CORONA CHARGING TECHNIQUE

This technique produces an inhomogeneous field to generate a discharge in air at atmospheric pressure. The field is generated by application of a voltage between a point-shaped or knife-shaped upper electrode placed at a certain distance from or in contact with one side of the dielectric with a planar back electrode on the other side [71-75].

(C) SPARK DISCHARGE METHODS

In this isothermal technique a sandwich of the film with a much thicker dielectric insert of lower resistivity, acting as a protective series resistance, in the gap between two parallel plate electrodes is used which gives satisfactory charge densities without destroying portions of the film by

arcing [76]. This arrangement will ensure that after application of a voltage there will be a gradual charge transfer by means of a controlled spark breakdown in the minute air gap between the dielectric insert and the film.

(D) LIQUID CONTACT METHOD

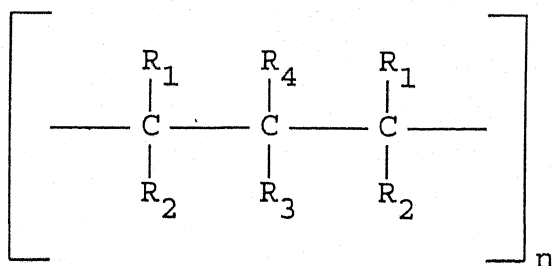
In this charging technique, a polymer film metallized on one surface comes into intimate contact with a wet electrode on the nonmetallized side. This provides a thin liquid layer like water or ethyl alcohol between the dielectric and the electrode. An application of a potential difference between the wet electrode and the metallized surface of the dielectric causes charged double layers to form at both solid-liquid interfaces which brings about a charge transfer to the polymer by the interaction of electrostatic and molecular forces. Large areas of the dielectric can be charged by moving the electrode over the surface [77-79].

(E) ELECTRON BEAM METHOD

Here, monoenergetic electrons are used to irradiate the dielectric samples. Low energy electrons, which get trapped in the dielectric sample after striking it, ensure the charging of the sample. But high energy electrons which pass through the sample bring about charging due to secondary emission and backscattering [80-83].

1.3 THE POLYMERS-STRUCTURE AND PROPERTIES

In a polymer a large number of molecules called monomers are joined together to form a long macromolecular chains, which can assume various conformations in space [84]. These chains may either be separate molecules, or they may form a three dimensional network. A general formula which fits a large number of polymer chain may be written in the form -



where R_1 , R_2 , R_3 and R_4 are different molecular groups and n is the degree of polymerisation which shows how many times the group repeats itself in a polymer chain. The degree of polymerisation may vary from tens to hundreds of thousands of unit and over. A practical polymer consists of a set of molecules differing in molecular weight [85,86].

Polymers in solid state may exist in amorphous or crystalline state. It is usually assumed that in amorphous state the molecules are tangled up in a completely random manner. According to Kargin [87] amorphous polymers are partially ordered systems and are made up of globules or bundles of polymer chains. X-ray pattern of polymers indicate short range order. Generally polymers consist of heterogeneous structure, comprising both the crystalline and amorphous regions [84].

1.3-1 CLASSIFICATION OF POLYMERS

Polymers are substances whose molecules are composed of a great number of repeating units called 'monomeric units'. The number of monomeric units in a molecule is called the 'degree of polymerisation' while the large molecule is called a 'macro-molecule' of polymeric chain. Polymers with high degree of polymerisation are called high polymers while those with a low degree of polymerization are called 'oligomers'. According to composition, polymers may be organic, inorganic or organo-elemental (semi-organic polymers).

(i) ORGANIC POLYMERS

Apart from carbon atoms, these compounds include hydrogen, oxygen, nitrogen, halogen, sulphur and also other elements in their molecules, provided the atoms of these elements are not in the main chain.

As far as the electrical properties are concerned, organic polymers have been the most studied. The name of the polymer is usually derived from the name of the monomer by adding to it the prefix poly. The organic polymers are further sub-divided into the following four groups -

(ii) INORGANIC POLYMERS

These are polymers containing no carbon atoms.

(iii) ORGANO-ELEMENTAL OR SEMI-ORGANIC POLYMERS

These can be divided into the following three groups :

(A) First Group

Compounds whose chains are composed of carbon atoms and hetero-atoms (except nitrogen, sulphur and oxygen atoms).

(B) Second Group

Compounds with inorganic chains, if they contain side groups with carbon atoms connected directly to the chain.

(C) Third Group

Compounds whose main chain consists of carbon atoms and whose side groups contain hetero-atoms (except nitrogen, sulphur, oxygen and halogen atoms) connected directly to the carbon atoms of the chain.

(iv) Linear and Three Dimensional Polymers

Polymers having long chain molecules with a high degree of symmetry are called linear polymers. There are practically no strictly linear polymer molecules; all are branched with three or more side chains. Polymers consisting of long chains connected into a three dimensional network by chemical crosslinks (bonds) are called three dimensional polymers. A two dimensional representation is shown in **Figure 1.1**.

(v) Homo-Polymers and Copolymers

A macromolecule may consist of monomers of identical or different chemical structures. Polymers consisting of identical monomers are called homo-polymers, while polymeric compounds containing several types of monomeric units in their chain are known as copolymers or mixed polymers.



A - IS MONOMERIC UNIT

Fig. 1.1 - Illustration of various type of Polymers.

(vi) Regular and Irregular Polymers

Polymers are also classified in accordance with the regularity with which the side groups are arranged with respect to the main chain. If the polymer chain is conceived to be stretched out in a straight line, the side groups will be arranged either on one side of the chain or they will alternate regularly or alternate at random (isotactic, syndiotactic and atactic polymers, respectively).

(vii) Polar and Nonpolar Polymers

In their different properties, the macromolecules are equivalent to electric dipole with a moment $M = q.l$, where q is the total amount of positive charge (or equivalent amount of negative charge) of a molecule and l is the distance between the centre of gravity of positive and negative charges. If in the absence of electric field, $l=0$, the polymer is said to be nonpolar and if under the same condition $l \neq 0$, the polymer is said to be polar. In the molecule of a nonpolar dielectric, the centres of gravity of positive and negative charges normally coincide in the absence of an external electric field and the dipole moment of the dielectric is zero. The centres of gravity of positive and negative charges, in polar molecules, do not coincide and hence the molecules have permanent dipole moment due to asymmetry in the arrangement of the electron clouds and nuclei of these molecules.

1.4 CHOICE OF MATERIAL

As stated earlier, polymers are composed of a large number of monomer units. They are crystalline or amorphous depending upon the symmetry of the monomer unit. However, even the structure of a crystalline polymer is far from perfect because it is very difficult for all large macromolecules to align themselves in ordered arrays. Crystalline polymers are, therefore, always semicrystalline and contain regions of amorphous phase. Because of their disordered-amorphous structure they contain a high concentration of shallow and deep traps. Consequently, charge trapping on a structural level is quite effective in polymers. They, therefore, yield the best electrets for all practical purposes [88,89].

Most of the interesting properties of polymers are attributable to molecular motions which are very complex. These molecular relaxations exhibit various transitions. A large number of polymers have been investigated in the past.

Among the polymers, there are two obvious choices, viz., polar and nonpolar polymers. A polar polymer is characterized with a distinct dipolar reorientation whereas a nonpolar polymer has a very small dipole moment. The dielectric behaviour of a polymeric system is determined by the charge distribution and also by the polar groups. For polymers in solid or in viscoelastic state, the physical structure is of great importance in determining the dielectric behaviour. With the view to understand clearly the correlation between

structure and dielectric behaviour, current research is largely centred around doped polymers, polymer blends and copolymers.

Some of the most important polar polymers are polyvinyl chloride, polyvinyl alcohol, polyamide, polyvinyl acetate, poly acrylic acid and esters of poly methacrylic acid. While poly vinyl chloride, poly vinyl alcohol and polyamide films have been investigated extensively for their charge storage and transport behaviour. Reports of extensive and thorough investigations on poly methylmethacrylate are very sparse.

1.4-1 TRANSITIONS IN POLYMERS

The characteristic features of polymers are largely due to their extra-rotational degrees of freedom compared with other solid types. The temperature dependence of physical properties changes appreciably due to different kind of molecular motion. This is termed as thermally stimulated transition.

Major chemical and mechanical properties of polymeric materials are affected by changes in temperature. The major transitions occur near the glass transition temperature (T_g) above which a linear polymer exhibits properties characteristic of a rubber and below which it has the properties of a rigid brittle glass.

In the melt, every type of molecular, segmental and submolecular motion is possible. The molecular motion involving main chain segments is not possible in the glassy state, but all molecular motions are not restricted in the glassy state. Transitions in polymers are of relaxation nature. It is customary to denote these transitions starting with the high temperature ones by the Greek letters α , β , γ and δ . The motion of main chain segment produces α relaxation and it occurs at the glass transition temperature. The β relaxation is attributed to the motion of the side groups or elements of chain back bone and it takes place at temperatures below glass transition temperature. Another possibility is rotation of short segments without involving large scale rearrangements of the structure and is usually called Crank-shaft type rotation of groups in the main chain [90]. Such a motion is explained in Figure 1.2. The γ and δ relaxations may have a complicated nature and they have been observed at ultra low temperatures. Activation energy A is characteristic of each relaxation process. Temperature transitions encountered by each polymer depend on its chemical structure. General relation between chemical structure and composition with glass transition is reviewed by Boyer [91]. Mechanisms responsible for relaxation processes and glass transition in polymers and their blends are discussed by many authors [92-94]. Technique employed for the characterization of relaxations in polymers influences the molecules of a

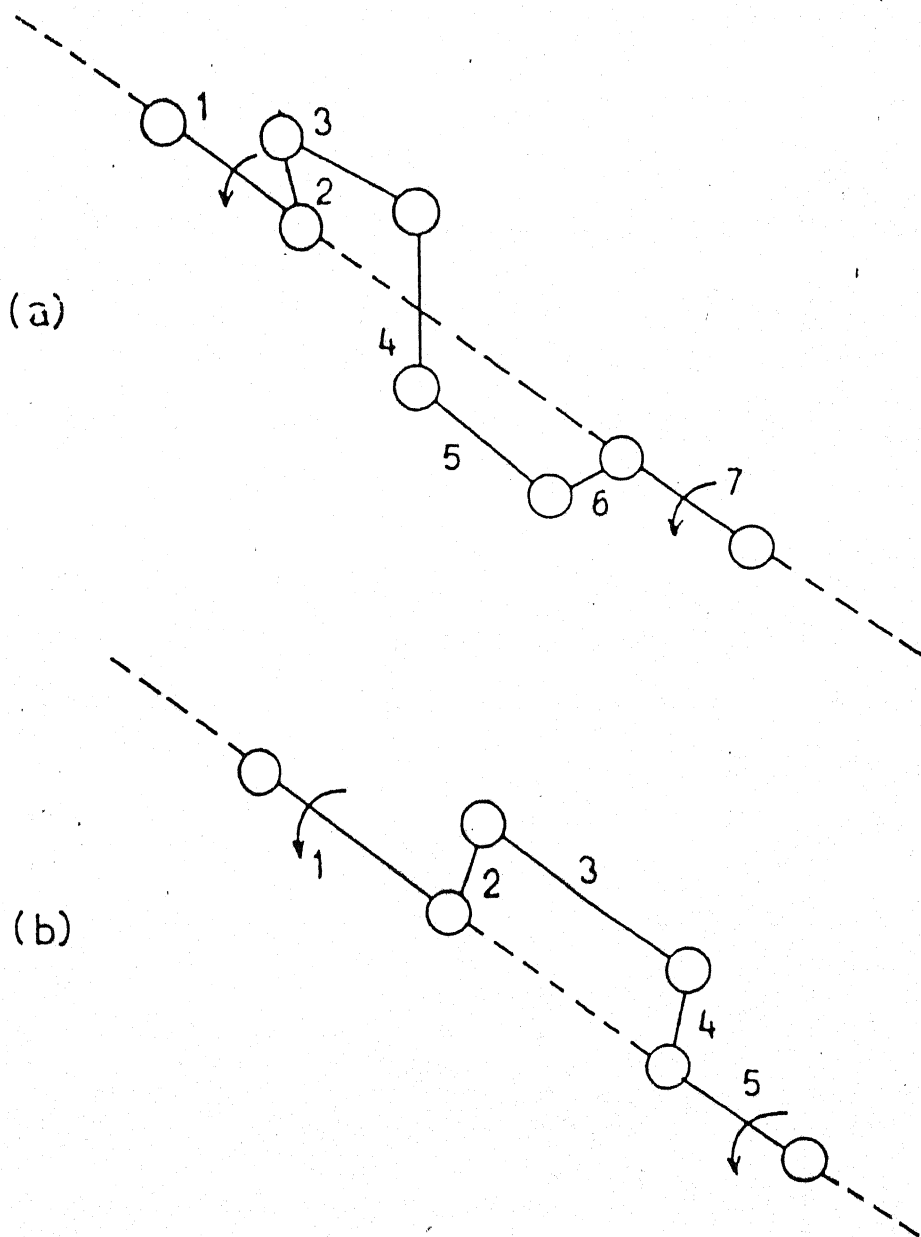


Fig. 1.2 - Illustration of the crank shaft mechanism models proposed by (a) Shatzpi and (b) Boyer.

polymer in a different way and thus the response of a system to different stimuli may be very different.

1.4-2 FACTORS AFFECTING DIELECTRIC BEHAVIOUR OF POLYMERS

(a) Effect of polar groups

The α relaxation is basically dependent on the intra and inter molecular interactions. The greater the inter molecular interaction the less mobile are the molecules and the higher is the relaxation temperature at which maximum loss occurs and larger is the relaxation time. Exchange of non polar substitutes increases dipole-dipole interaction.

(b) Effect of substituents

Introduction of very bulky substituents into the side chains or increasing the side chains decreases the mobility sharply.

(c) Effect of side group isomerism

In case of isomers, magnitude of α and β relaxation are different [95].

(d) Effect of Stereoregularity

The dielectric properties of polymers are substantially dependent on the stereoregular nature of the polymer, because the percentage, the length and quantitative proportion of syndiotactic and isotactic sections have a significant effect on the molecular mobility of polymers.

(e) Effect of Plasticizers

Dielectric relaxation of polymers shift towards lower temperature side on the addition of plasticizers. This is because plasticizers (i) increase molecular mobility, (ii) increase free volume, (iii) decrease T_g of the polymers.

(f) Effect of Cross linking

Cross linking always decreases molecular mobility and increases temperature and relaxation time of α process.

(g) Effect of Copolymerization

Dielectric properties of copolymers vary according to the composition and the ratio of monomeric units [96].

(h) Effect of Pressure

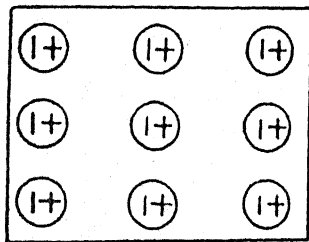
Pressure influences the relaxation times [97] of the process in which the intermolecular interaction plays an important role [98].

1.5 MECHANISM OF POLARIZATION

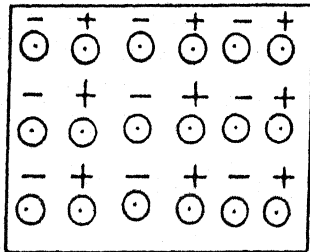
The polarization of a dielectric occurs mainly due to internal and external polarization mechanisms (**Figure 1.3**).

1.5.1 INTERNAL POLARIZATION

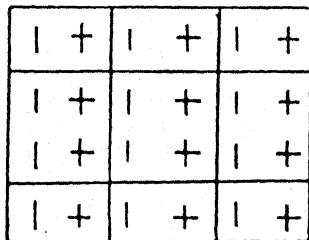
This is brought about by the rotation, migration of charges which have originated and remain within the volume of the dielectric. They lead to the formation of "heterocharge" or "true polarization" as the case may be. Internal polarization is further classified under the following types :



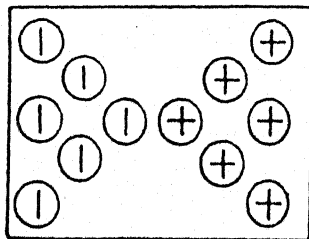
ATOMIC POLARIZATION



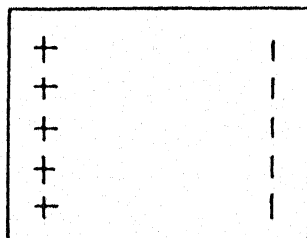
DIPOLAR POLARIZATION



INTERFACIAL POLARIZATION



SPACE POLARIZATION



EXTERNAL POLARIZATION

Fig. 1.3 - Polarization mechanisms in dielectric materials.

(A) Electronic or Microscopic Polarization (P_e)

This happens when the negative electron cloud of the atoms of a system is displaced with respect to the nucleus. This causes a deformation of the electronic shell inducing a dipole moment and the phenomenon is thereby called Electronic Polarization (P_e).

(B) Atomic Polarization (P_a)

Molecules are usually made up of chemically different atoms whose charges may differ from others. An external field acting upon them causes their equilibrium position to change thus inducing the polarization known as "Atomic Polarization".

(C) Dipole or Orientational Polarization (p_o)

If the centres of gravity of the positive and negative charges in a molecule made up of different atoms do not coincide, the molecule will have a permanent dipole moment. This dipole moment may be a deliberate part of the structure or may be accidental or unavoidable impurities. There is no net dipole moment for a sample in normal thermal conditions which has the dipoles randomly arranged. But on application of an external field, the dipoles align themselves in the direction of the field and we are left with a system with a net electric moment and the appearance of "Dipole or Orientational Polarization".

(D) Transitional or Space Charge Polarization (P_s)

In the volume of any sample there may be a small number

of intrinsic free charges, i.e., ions or electrons or both. These are randomly arranged and so when one takes the average overall the charges the net dipole moment is zero. When an electric field is applied to such materials, the positive and negative charges get displaced in opposite directions with cations accumulating near the cathode and anions near the anode producing what is known as "Transitional" or "Space Charge" Polarization.

(E) Interfacial Polarization (P_i)

Inhomogeneous dielectrics often have microscopic domains or grains separated by highly resistive interfaces. In such dielectrics the free charge carriers can move freely only within the grains. On application of an external field the free charges are displaced to the domain boundaries, i.e., amorphous crystalline in semicrystalline and grain boundaries in polycrystalline materials. The resultant polarization is called "Maxwell-Wagner-Sillars (MWS) or Interfacial or Barrier Polarization".

(F) External Polarization (P_x)

A large electric field of 10^5 volts/cm and above will cause charge carriers to be directly injected into the material from the electrode (Schottky emission). Electronic or ionic charge carriers can be deposited or injected on either surface from a dielectric electrode-interface breakdown. This causes a formation of homocharges, originating from real charges and is called external polarization.

The total polarization in a dielectric is thus the total sum of the above kinds of polarizations, i.e.,

$$P = P_e + P_a + P_o + P_s + P_i + P_x$$

The relative contribution of these basic processes and their retentions very according to the chemical nature of the dielectric and the experimental conditions.

1.6 CONCEPT OF ELECTRICAL CONTACT

The temperature voltage dependent current in dielectrics depends to a large extent on the nature of electrodes, the work functions and Fermi level positions. When two materials with different Fermi levels are brought into contact, free carriers will flow from one material into another until equilibrium is established, i.e., until Fermi levels of both materials are aligned. Such a net carrier flow will set up a positive space charge on one side and a negative space charge on the other side forming an electric double layer. This double layer is generally referred to as the potential barrier, and the potential across it is called as the contact potential. The nature of contact is a complex affair.

(A) Neutral Contact :

In case of neutral contact no space charge will exist and no band bending will be present within the dielectric so that both conduction and the valence band edges will be flat right upto the interface (Figure 1.4 a and b).

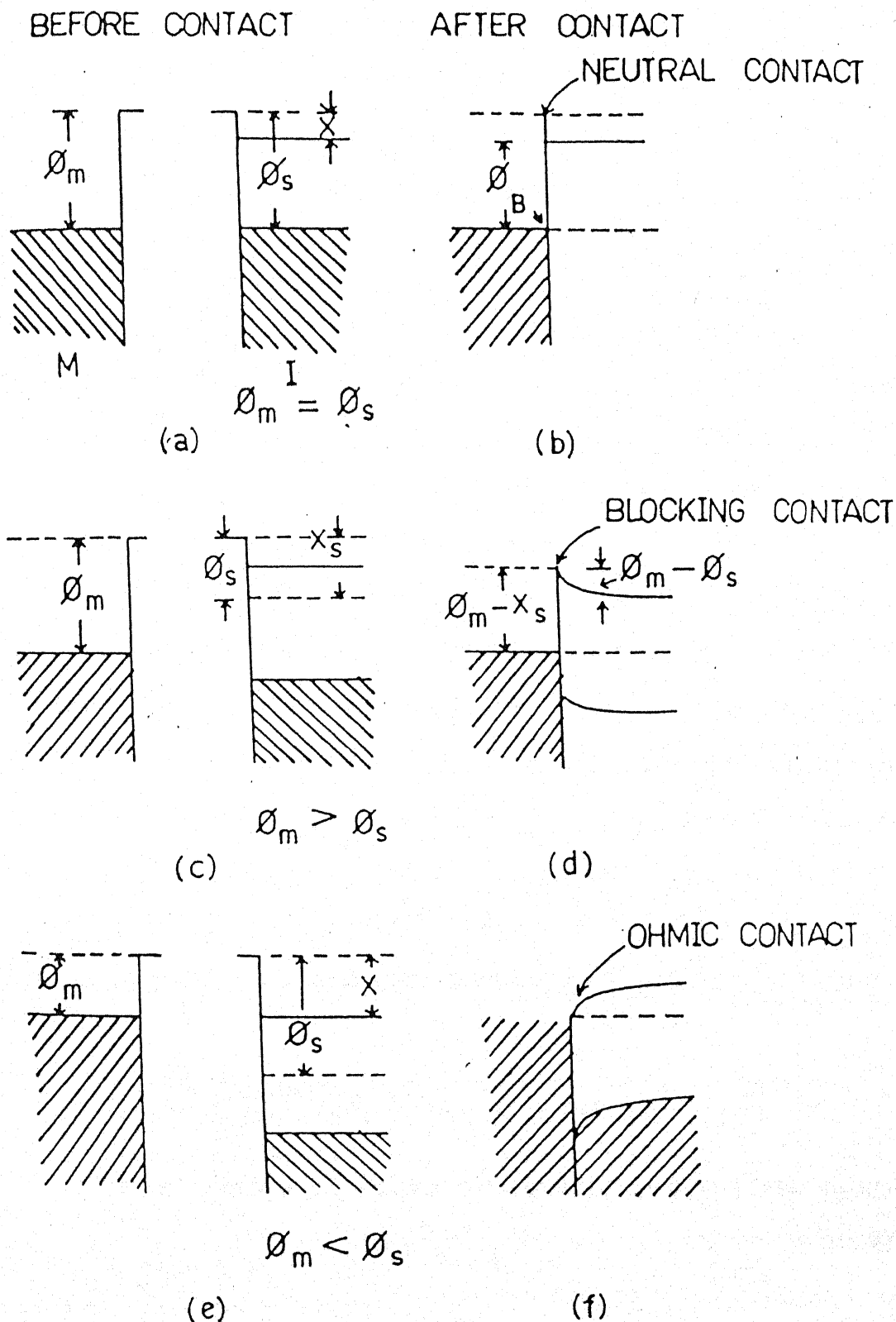


Fig. 1.4 - Energy level diagram for a neutral contact (a, b) blocking contact (c, d) ohmic contact (e, f).

(B) Blocking Contact :

In case of a blocking contact, a depletion layer extending from the interface to the inside of the dielectric is created. With this contact, the thermionic emission tends to be saturated. Electron emission from a metal across the blocking contact may be due to either a thermionic process or a high field tunneling process (Figure 1.4 c and d).

(C) Ohmic Contact :

In this case the free charge carrier density at and in the vicinity of the contact is very much greater than that in the bulk of the insulator or semiconductor so that the contact may act as a reservoir of carriers. The ohmic current creates accumulation of charge carriers extending from the interface to the inside of the insulator. The terminology ohmic is inappropriate in so far as the current voltage relationship is not linear. In general, the conduction is ohmic at low fields, when the metal does not inject excess carriers and becomes non-ohmic if the carrier injection from the electrode or the space charge effect becomes prominent (Figure 1.4 e and f).

1.7 THE TECHNIQUES FOR INVESTIGATION OF ELECTRICAL PROPERTIES OF INSULATING MATERIALS

The knowledge of basic electrical properties such as the type and origin of charge carriers, their storage and transport in the polymeric dielectric are extremely important for making stable and useful electrets. Information about

these can be obtained from the following experimental techniques

- (i) Transient Currents in charging and discharging modes,
- (ii) Dark conduction Currents,
- (iii) Dielectric measurements, and
- (iv) Thermally Stimulated Discharge Current.

1.7-(i) Transient Currents in Charging and Discharging Modes

Transient charging and discharging currents have been investigated extensively to understand time dependent polarization effects in organic polymers [99-104] and to find suitable substitutes to the conventional electrophotographic, photoconductor and semiconductor materials. A number of mechanisms have been proposed to understand the behaviour of these currents, the most important of which are electrode polarization, dipole polarization, charge injection leading to trapped space charge effect tunnelling of charge carrier from the electrodes to empty traps and hopping of charge carriers from one localized state to the another. The above processes have been reviewed by several scientists and it has been established that the observed time dependence alone does not permit any discrimination to be made between various mechanisms. The argument for and against a particular mechanism is to be found by considering the variation of these currents on various other experimental parameters also, such as temperature field and frequency etc.

It is well known that the transient current flowing through a dielectric after the application or removal of a step voltage decays generally following the Curie-Von Schweidler law. The origin of these dielectric absorption and resorption currents is still the subject of much controversy in the literature. The absorption current technique and the TSDC technique are the main tools for investigating the charge storage and relaxation mechanism in polymer films. Though the electrical conductivity of polymers varies exponentially with temperature, it is also a function of time and may vary with electric field.

1.7-(ii) Dark Conduction Currents

In polymeric dielectrics, the internal charge decay processes are governed by electrical conduction and dielectric relaxation. Apart from the study of dc conduction and dielectric behaviour, many other techniques have been developed to measure the electrical parameters and to explore the internal phenomena responsible for the formation and decay of electret charge.

The movement of charge carriers in dielectrics has been receiving a large volume of attention commensurate with the importance of this subject in Science and Technology. Example of this include leakage currents in electrical insulation, charge injection from electrodes which may lead to premature breakdown, all forms of photo-conduction and of transient

pulse drift Including electron bombardment, Induced conductivity and the wide field of xerography. All these problems involve the transport of distributions of charged particles which may therefore, be treated as quasi continuous clouds rather than as individual particles. By contrast there are various approaches which deal with the movement of individual charges, like free electrons or holes by moving in a crystalline lattice under the action of thermal excitation with mean free paths extending over many interatomic spacings or slowly mobile hopping electrons or ions under the action of electric field. Thus, the nature of electrical conduction in solid dielectrics has long been target of extensive research all over the world, because of its vital technical importance for electrical insulating materials in power apparatuses, and also for the electronic application of electrostatic photography, semiconductor device isolation, etc.

The conduction in polymers is complex which is due to intrinsic charge carrier generation and charge carrier injection from contacts at high fields. Various mechanisms are responsible for electrical conduction.

1.7-(iii) Thermally Stimulated Discharge Current

The measurements of Thermally stimulated discharge current (TSDC) have been widely used to determine the trapping parameters, i.e., the density, depth and energy distribution of traps in polymers [157,158]. The analysis of TSDC spectra

of polymeric materials provides useful information on various aspects of charge storage mechanism and relaxation phenomena in polymers [159-163].

For TSDC analysis, the dielectric is polarized to form an electret. The electret is then heated at a constant rate and the depolarization current is recorded as a function of temperature. The TSDC spectrum shows maxima which correspond to various decay processes. In polymeric electrets, these modes correspond to various polymeric relaxations.

Charge decay of an electret takes a longer time at room temperature. Gross [164], Murphy [165] and Gubkin [166] used the technique based on thermal stimulation.

1.7-(iv) Dielectric measurements

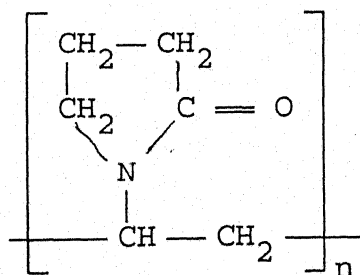
Choice of polymeric dielectric for each concrete case depends on its dielectric and other physical properties over a wide range of temperature and electrical field frequencies. Investigation of dielectric properties is also one of the most convenient and sensitive methods for studying polymer structure. It is, therefore, important that their dielectric behaviour is fully understood. This involves complete knowledge of variation of the complex dielectric constant, i.e., capacitance and losses over a wide range of frequencies and temperature. Whenever a dielectric is subjected to an electric field, dissipation of power depends on the voltage and frequency. These losses of power in a dielectric are

commonly known as dielectric losses. Dielectric properties also depend on the type of material (polar, non-polar), temperature, structural changes, frequency, field, humidity and impurity.

To understand the dielectric properties, the mechanism of polarization of the material is to be understood fully.

1.8 MATERIAL USED IN THE PRESENT WORK - POLYVINYL PYRROLIDONE (PVP)

Polyvinyl pyrrolidone is a water soluble polymer characterised by its unusual complexing and colloidal properties and its physiological inertness. Special pharmaceutical grades of PVP are available under the trademarks Plasdone and Plasdone C (GAF Corporation) and Kollidon 25 and 17 (Badische Anilin- und Soda-Fabrik). Peregall ST levelling and stripping agents (GAF Corporation) and Albigen A (Badische Anilin- und Soda-Fabrik) are aqueous solutions of PVP offered to the textile industry for special applications [167].



PVP is available as a white free-flowing powder and also in the form of aqueous solutions. It is offered in four

viscosity grades. The commercial uses of PVP are related to its outstanding properties. Its film-forming and adhesive qualities are utilized in aerosol hair sprays, adhesives, and lithographic solutions. As a protective colloid, it is used in drug, and detergent formulations, cosmetic preparations, polymerization recipes, and in pigment or dyestuff dispersions. The textile industry makes use of its dye-complexing ability to improve the dyeability of synthetic fibers and as a dye-stripping assistant. Since it complexes with tannin-like compounds, PVP is used as a clarifying agent for vegetable beverages, particularly beer.

Polyvinyl pyrrolidone is manufactured in four viscosity grades, PVP K-15, K-30, K-60 and K-90. The number average molecular weights are about 10,000, 40,000, 160,000 and 360,000, respectively.

In 1932, Fikentscher in an attempt to relate the relative viscosity of any polymer solution to concentration, proposed the following formula :

$$\ln \eta_{\text{rel}} = \left[\frac{k + 75 k^2}{1 + 1.5 kc} \right] c$$

The constant k in this equation, known as Fikentscher's constant, is a function of molecular weight. In the early development of PVP, the polymers were characterised by measuring the relative viscosity and calculating a constant, K , using a slightly modified "Fikentscher's formula".

$$\log \eta_{rel} = \frac{75 K_o^2}{1 + 1.5 K_o c} + K_o$$

where, $K = 1000 K_o$, c = concentration in g/100 ml solution,
 η_{rel} = viscosity of solution compared with solvent.

Since the measurements are made only with $c = 1.00$, the formula reduces to :

$$\log \eta_{rel} = \frac{75 K_o^2}{1 + 1.5 K_o} + K_o$$

The use of K value become well established and is retained today as a means of expressing relative molecular weight.

Increasing the temperature of aqueous solutions of PVP has considerable effect in lowering the viscosity. One of the unusual properties of PVP is its solubility in a wide variety of different solvents. The solubility of PVP in water is limited only by the viscosity of the resulting solution. PVP K-30 containing up to 5% water is soluble in alcohols, aliphatic acids, chlorinated solvents containing hydrogen, nitroparaffins, and amines. Desiccated material containing less than 0.5% water is moderately soluble in cyclic ethers such as dioxanes or tetrahydrofuran but essentially insoluble in aliphatic ethers. Dry PVP is also moderately soluble in aliphatic esters, ketones, fully chlorinated hydrocarbons such as carbon tetrachloride, and in the aromatic hydrocarbons. It is insoluble in aliphatic hydrocarbons, but solutions can be prepared in such solvents as kerosene, heptane, and Stoddard solvent by using butyl alcohol as a cosolvent. Solutions in

the chlorofluoroalkane propellants can be made using 20-30% ethanol.

Films of PVP which are clear, transparent, glossy, and hard can be cast from a number of different solvent systems such as water, methyl alcohol, or chloroform (4). Moisture retained or taken up from the air by PVP acts as a plasticizer for the film. In addition, the hardness of the film may be altered by adding compatible plasticizers without affecting the clarity or luster of the films. PVP films become tacky at 70% rh, and at 50% rh they contain 18% moisture. In the use of PVP films as hair fixatives, the incorporation of plasticizers and humidity control agents is necessary to obtain the best properties.

PVP is compatible with many natural and synthetic resins as well as with many other chemicals and most inorganic salt solutions. For example, PVP can be combined in solution or in a film with ethyl cellulose, polyethylene, poly(vinyl chloride), and poly(vinyl alcohol). It is compatible with glycerides such as olive oil and lanolin and with poly(ethylene oxide). Aqueous PVP solutions have good tolerance for inorganic salts such as ammonium chloride, copper sulphate, ferric chloride and sodium pyrophosphate.

In aqueous solution, PVP forms complexes with many types of compounds. Insoluble complexes are formed with polyacids such as poly(acrylic acid) or tannic acid. A 1:1 addition

compound of PVP with poly(acrylic acid) was isolated in 70% yield. These complexes are insoluble in water, alcohol, and acetone, but are dissolved by dilute alkali which apparently destroys the bond by neutralizing the polyacid. Dyes are strongly held by PVP, and this action accounts for the successful use of PVP as a dye stripping agent. Conversely, the introduction of PVP into other polymers through grafting or merely mixing greatly improves the dyeability of the polymers. PVP forms complexes with many toxins, viruses, drugs, and toxic chemicals, thereby reducing toxicity and irritation. Chemicals such as potassium cyanate, formamide, nicotine, phenols, chlorbutanol are complexed by PVP as are mercuric chloride, silver oxide, cobaltous oxide, ferric chloride, and iodine.

The complex with iodine is being marketed because of its excellent germicidal properties combined with the greatly reduced toxicity and absence of the staining action of the iodine. The iodine is held so tightly in this complex that it is not removed by extraction with chloroform and no appreciable vapour pressure of iodine is apparent above the complex.

PVP is permanently insolubilized by heating with strong alkali at 100°C. Aqueous PVP will gel when treated with ammonium peroxysulfate at 90°C, with hydrazine and hydrogen peroxide, or with gamma rays from a Co⁶⁰ source. These gels are apparently formed from permanently crosslinked PVP, since

they are substantially insoluble in large amounts of water. The alkaline sodium phosphates will do the same thing. When dried under mild conditions, these gels retain their uniform structure and capacity to swell again by absorbing water. Crosslinked PVP containing glycerine is used as a dialysis membrane. The volume of a number of (biological) protein solutions was reduced 5-15 times by dialysis (reverse osmosis) against a concentrated (25-30%) solution of PVP using a cellophane membrane. PVP is preferred because the molecular size is sufficiently large so as not to pass through the membrane, leaving the concentrated protein solution free of PVP. PVP is also rendered insoluble by the action of oxidizing agents such as bichromate and diazo compounds under the influence of light. Resorcinol and pyrogallol also precipitate PVP from aqueous solution, but the complex redissolves in additional water and does not precipitate from alcoholic solutions.

PVP is highly susceptible to grafting and has been used to form graft copolymers of styrene and acrylic esters, employing emulsion polymerization techniques. Improved nylon-6,6 with a high degree of wet-crease recovery has been made by grafting PVP. The PVP is activated with hydrogen peroxide, dried, and then added to molten hexamethylenediammonium adipate at 210°C . The mixture is heated 2-1/2 hr to 285°C in a steam atmosphere to give a melt-spinnable polymer (72).

Table 1.1
Nonpharmaceutical Grades

Viscosity grade	Form	K range	Water, %	Ash(dry basis), %	Residual monomer, ^a %
PVP K-15	powder	12-18	5 max	0.02 max	1.0 max
PVP K-30	powder	26-35	5 max	0.02 max	1.0 max
PVP K-60	aqueous solution	50-62	55 max	0.02 max	1.0 max
PVP K-90	aqueous solution	80-100	80 max	0.02 max	1.0 max
PVP K-90	powder	80-100	5 max	0.02 max	1.0 max
Polyclar AT brand	powder	crosslinked	5 max

^a
Calculated as vinylpyrrolidone, % based on dry solids.

Specifications

The specifications for nonpharmaceutical and pharmaceutical grades of PVP are shown in Tables 4, 5 and 6.

Pharmaceutical grades of PVP (all powders) are marketed under the Plasdone and Plasdone C trademarks. Three viscosity types for nonplasma use are : K-26-28, K-29-32 and K-33-36, having the specifications shown in Table.

Table 1.2

Pharmaceutical Grades for Nonplasma Use

moisture content	less than 5%
unsaturation (calculated as monomer)	less than 1%
ash	less than 0.02%
heavy metals content	less than 20 ppm
arsenic content	less than 2 ppm
nitrogen content	12.6% \pm 0.4%

Plasdone C pharmaceutical grade PVP, specifically for plasma use, has the specifications is shown in the Table below.

Table 1.3

Pharmaceutical Grades for Plasma Use

K-value	30 \pm 2
K-value distribution	not more than 15% greater than K-41 not more than 25% lower than K-16
moisture content	less than 5%
unsaturation (calculated as monomer)	less than 1%
ash	less than 0.02%
heavy metals content	less than 20 ppm
arsenic content	less than 2 ppm
nitrogen content	12.6% \pm 0.4%
acetaldehyde content	less than 0.5%

Shipping Containers

PVP K-15, K-30 and K-90, powder, are shipped in polyethylene bags inside fiber drums (100 lb net). PVP K-60 and K-90, aqueous solutions, are shipped in aluminium tank cars, and 55 gal polyethylene-lined fiber drums.

USES

Cosmetics (qv) and Toiletries

PVP is used in hand creams, pomades, hair lotions, shaving creams, shampoos hair tints (48), pre-electric and after-shave lotions etc, because of its emulsifying, thickening, emollient, and dye-solubilizing properties. Its film-forming ability and excellent adhesion to hair has led to its widespread use in aerosol hair sprays. Dentrifrices containing PVP have enhanced ability to remove dental stains.

Textiles

Incorporation of PVP into hydrophobic fibres, such as polyacrylonitrile, polyesters, nylon, visose, natural rubber (93,94) and polypropylene greatly increases their dyeability with most classes of dyestuff. PVP K-30 is a stripping agent for removing vat, sulfur, and direct colors from dyed fabrics. As a suspending agent, it is used in the scouring of nylon to remove graphite (used in lace manufacture) and in print washes to scavenge loose color. PVP is a suspending agent for titanium dioxide in delustering nylon-6. It is used in fugitive tints and as an auxiliary retarding agent in pastel

dyeing. PVP is used in sizing glass fibers. Graft copolymers of PVP with nylon-6,6 exhibit improved wet-crease recovery and moisture regain.

Detergents

PVP is compatible in clear, liquid, heavy-duty detergent formulations. It prevents soil redeposition, particularly on synthetic fibers and resin treated fabrics. It also acts as a loose color scavenger during laundering because it has dye-binding properties.

Beverages

The ability of PVP to complex with certain tannins has been applied to the clarification and chillproofing of various vegetable beverages. The addition of 0.01-0.02% to the brew kettle results in improved taste and reduced chill haze while allowing a reduction in the hops used. PVP is used similarly in wines, whisky, vinegar, etc. A special high-molecular-weight crosslinked grade of PVP, Polyclar AT clarifier, insoluble in water, organic solvents, and strong mineral acid and alkali, is particularly effective in clarifying beer and other vegetable beverages. It also controls browning in wines.

Pharmaceuticals

A special grade, Plasdone C pharmaceutical grade PVP is marketed for this purpose. Its suspending and drug-retardant

proportions are utilized in injectible preparations of antibiotics, hormones, analgesics, etc. PVP is used as tablet binder and tablet coating. It is used in aqueous or organic solvent systems, including effervescent products prepared in an anhydrous medium. PVP is used in layered tablets and timed-release capsules. PVP is effective in stabilizing vitamins and aspirin tablets. It acts as a protective colloid and reduces drug irritation in ophthalmic and topical preparations. The ability of PVP to form a stable complex with iodine has led to the development of PVP-Iodine. This product retains the germicidal properties of iodine while drastically reducing the iodine's toxicity towards mammals. Aqueous solutions of PVP-Iodine form fibers that protect open wounds but are water-washable and do not permanently stain skin, natural fibres, or hard surfaces. PVP-Iodine has been effective as surgical scrub and in treatment of burns. Gargles, tinctures, and ointments containing PVP-Iodine are being marketed under the trademark Isodine (Purdue Fredericks Co.).

Plasma Extenders

During World War II, more than a million persons of all ages received emergency administration of PVP solutions to combat shock due to blood loss. In the period 1948-50, thousands of units of PVP were evaluated in clinical tests of human volunteers in the USA. Together with cooperative research by the National Research Council on synthetic plasma

expanders, these studies resulted in approval for the emergency stockpiling of PVP by local communities. PVP has been used with outstanding success in the treatment of shock due to severe burns, accidents, or surgical procedures. Moreover, it is nonantigenic, requires no crossmatching and avoids the dangers of infectious hepatitis which are inherent in natural blood. However, plasma or blood of the proper type is still preferred by American medical authorities and PVP solutions are for emergency use when the former are unavailable.

Dyestuff and Pigment Dispersions

In inks based on dyes, PVP improves solubility and gives greater colour value per pound of dye. In pigmented inks, PVP is used in the milling operation to give higher tinctorial strength, dispersion stability, and better gloss. It has found use in the preparation of color dispersions for latex paints, paper coatings, and plastics.

Automotive Products

Copolymers of PVP and alkyl acrylates are used in formulations for high-detergency motor oil, automatic transmission fluids, and grease.

Plastics

In two-phase polymerization systems for styrene, vinyl chloride, vinyl esters, acrylics, and other monomers, PVP acts

as a particle size regulator, suspending agent, and viscosity modifier. PVP is also used as a post polymerization additive to improve dyeability and stability of various latexes. The addition of PVP to polyoxymethylene (see Acetal resins) improves heat stability of the dried polymer.

Miscellaneous

In wax and polish formulations, PVP functions as a protective colloid and film former to give better cleansing action and gloss. In the paper industry, PVP is used in the control of deposition of pitch, in the deinking of waste paper, in decolorizing rag stock, and as a viscosity modifier for paper coatings. Its use in lithographic plates and in the preparation of photographic emulsions has been cited. Uses in water-remoistenable and pressure-sensitive adhesives have been mentioned. PVP functions as a protective colloid in cement mixtures, retarding the separation of water, in preventing caking of fertilizer mixes, and preparation of conductive coatings for television or cathode-ray tubes.

REFERENCES

1. Wintle, H.J. IEEE, Transactions on Electric Insulation 25, 1 (1990).
2. Gerhard Mulhaupt, R., Kunstler, W. and Danz, R. (Eds.) Proc. 7th International Symposium on Electrets, Berlin, 25-27 Sept., 1991 (Available IEEE Service Centre 445, Hes Lane, Piscataway, N.J. 08854 USA).
3. Chen Ying Chang, Jpn. J. Appl. Phys. 30, 90A, 2101 (1991).
4. Wider, H.H. and Kaufman, Z. Electr. Eng. (USA) 72, 511 (1953).
5. Fabel, G.W. and Henish, H.K. Phys. Stat. Soli.(a) 6, 535 (1971).
6. Sessler, G.M., Electrets, Berlin, (1980).
7. Seymour, R.B. Conductive Polymers, Plenum Press, New York (1981).
8. Sessler, G.M. (Ed.) "Electrets", 2 Springer Verlag, Berlin (1980).
9. Farady, M. "Experimental Researches in Electricity", Richard and John Edwar Taylor, London (1839).
10. Heaviside, O. "Electrical Papers", Chelsea, New York, 448 (1892).
11. Eguchi, M. Philos. Mag. 49, 178 (1925).
12. Bucci, C. and Fieschi, R. Phys. Rev. Lett. 12, 16 (1964).
13. Campos, M. et al. Phys. Rev. Lett. 27, 1432 (1971).
14. Van Turnhout, J. "Thermally Stimulated Discharge of Polymer Electrets", Elsevier, Amsterdam (1975).
15. Karanja, P. and Nath, R. IEEE Trans. 1,2, 213 (1994).
16. Ochiai, S. et al. IEEE Trans. 3, 487 (1994).
17. Mizutani, T. IEEE Trans. 1,55, 923 (1995).
18. Sun, K.S. et al. IEEE Trans. 2,1, 1 (1995).
19. Sun, K.S. et al. IEEE Trans. 1,2, 224 (1994).

20. Walker, R.R. and Morgan, A.J. Post. Off. Elect. Eng. J. 72, 15 (1979).
21. Gutman, F. Rev. Mod. Phys. 20, 457 (1948).
22. Schaffert, R.M. "Electro Photraphy" Wiley, New York (1975).
23. Turnhout, J. Van Staub. Reinholt luft 36, 36 (1976).
24. Andrykschemko, V.A. Autom. Remote Control, U.S.S.R. 21, 93 (1961).
25. Dreyfus, G. and Lewiner, J. J. Applied Phys. 46, 4357 (1975).
26. Atlix, F.A. and Roesch, W.C. (Eds.) "Radiation Dosimetry", Academic Press, New York (1968).
27. Lines, M.E. and Glass, A.M. "Principles and Applications of Ferroelectrics and Related Materials", Clarendon Press, Oxford (1977).
28. Garn, L.E. and Sharp, E.J. IEEE Trans. PHP-10, 208 (1970).
29. Miller, G.K. "Electret Tape Transducers", GIE Sylvania, F30602-75-6-0075".
30. Miller, G.K. "High Pressure Transducers", GIE Sylvania, N0014-72C-307.
31. Hennian, C. and Lewiner, J. J. Acoust. Soc. Am. 63, 1229 (1978).
32. Jefimenko, O.D. "Electrostatic Motors", in Electrostatics and its Applications, Ed. by A.D. Moore Wiley, New York (1975).
33. Jefimenko, O.D. and Walker, D.K. IEEE Trans. IA.14, 537 (1978).
34. Nazarov, V.G. Elektrichestro 7, 60 (1954).
35. Van Turnhout, J. J. Electrostat. 1, 147 (1975).
36. Toda, M. and Osaka, S. Proc. IEEE 67, 1171 (1979).
37. Susko, M. J. App. Meteorol 18, 48 (1979).
38. Holland, E.R. et al. J. Appl. Phys. 75, 12 (1994).
39. Gement, A. Philos. Mag. 20, 929 (1935).

40. Thiessen, P.A. et al. Z. Physik. **37**, 511 (1936).
41. Gross, B. Brit. J. Appl. Phys. **1**, 289 (1950).
42. Swan, W.F.G. J. Franklin Istt. **250**, 219 (1950).
43. Gemant, A. Direct Current **1**, 145 (1935).
44. Gubkin, A.N. Sov. Phys. Tech. Phys. **2**, 1813 (1957).
45. Adamas, E.D. J. Franklin Ist. **204**, 469 (1927).
46. Gross, B. J. Chem. Phys. **17**, 866 (1949).
47. Gross, B. An. Aead Bros. **17**, 219 (1945).
48. Gross, B. J. Chem. Phys. **60**, 26 (1944).
49. Baldus, W. Z. Tech. Phys. **6**, 481 (1954).
50. Swan, W.F.G. J. P. Franklin Ist. **255**, 513 (1955).
51. Gubkin, A.N. Sov. Phys. Tech. Phys. **2**, 1813 (1958).
52. Eguchi, M. J. Appl. Phys. (Japan) **1**, 10 (1922).
53. Pillai, P.K.C. et al. Phys. Stat. Sol.(a) **13**, 341 (1972).
54. Sessler, G.M. and West, J.E. J. Appl. Phys. **17**, 507 (1970).
55. Sessler, G.M. and West, J.E. J. Appl. Phys. **43**, 922 (1972).
56. Murphy, T. et al. J. Chem. Phys. **38**, 24 (1963).
57. Gross, B. et al. J. Appl. Phys. **47**, 96 (1976).
58. Gross, B. Phys. Rev. **107**, 368 (1987).
59. Nadzhakov, G. Z. Physik. **39**, 225 (1938).
60. Fridkin, V.M. and Zherudev, I.S. "Photoelectrics and Electrophotographic Processes", Focal Press, New York (1973).
61. Rosenberg, H. Phys. Rev. **97**, 1996 (1955).
62. Kallman, H. Rev. Mod. Phys. **33**, 1533 (1961).
63. Padgett, E.D. Radio Electronics **2**, 61 (1955).

64. Pillai, P.K.C. and Goel, M. Int. Conf. on Electrets, Electro Chem. Soc., Miami Beach, Florida (1972).
65. Bhatnagar, C.S. Indian J. Pure and Appl. Phys. **2**, 331 (1964).
66. Khare, M.L. and Bhatnagar, C.S. Indian J. Pure & Appl. Phys.
67. Ohara, K. Wear **48**, 409 (1978).
68. Van Turnhout, J. and Gasiot, J. "Thermally Stimulated Relaxation in Solids", Springer-Verlag, Berlin (1979).
69. Gubkin, A.N. et al. Vysokomol Sayed **A12**, 602 (1970).
70. Day, G.W. J. Appl. Phys. Rev. Lett. **40**, 413 (1974).
71. Hayakawa, R. and Wada, Y. Adv. Polym. Sci. **11**, 1 (1973).
72. Ieda, M. et al. Electr. Eng. Journ. **88**, 67 (1968).
73. Mortazavi, M.A. et al. J. Opt. Soc. Am. **B6**, 732 (1989).
74. Page, R.H. et al. J. Opt. Soc. Am. **B7**, 1239 (1990).
75. Martinez, D.R. et al. J. Appl. Phys. **75**, 8, 4273 (1994).
76. Seiwatz, H. and Bro, J.J. Phys. Ann. Ref. Conf. Electr. Insul. Dielectr. Phenomenon (NAS) Washington, D.C. (1966).
77. Chudleigh, P.W. Appl. Phys. Lett. **21**, 547 (1972).
78. Chudleigh, P.W. J. Appl. Phys. **47**, 4475 (1976).
79. Engelbrecht, S. J. Appl. Phys. **45**, 3421 (1974).
80. Gross, B. J. Polym. Sci. **27**, 135 (1958).
81. Sessler, G.M. and West, J.E. Appl. Phys. Lett. **17**, 507 (1970).
82. Matsokawa, T. et al. J. Appl. Phys. **45**, 773 (1974).
83. Gross, B. et al. J. Appl. Phys. **45**, 1 2841 (1974).
84. Jenkins, A.D. (Ed.) "Polymer Science" Vol. 1, Ch.2, 3 and 4.
85. Tobolosky, A.V. "Properties and Structure of Polymers", John Wiley and Sons, New York (1968).

86. Tager, A. "Physical Chemistry of Polymers", Mir Publications, Moscow (1978).
87. Kargin, V.A., Kitaigorodskii, A.I. and Sdonomskii, G.L. Kolloid Zh. 19, 131 (1957).
88. Perlman, M.M. (Ed.) Electrets charge storage and transport in dielectrics, Electrochemical Society, Princeton (1973).
89. Braulich, P. (ed.) Thermally Stimulated Relaxations in Solids, Topics in Applied Physics 37, Springer-Verlag, New York (1979).
90. Schatzki, T.F. J. Polym. Sci. 57, 496 (1962).
91. Boyer, R.F. Rubb. Chem. Technol. 36, 1303 (1963).
92. Shogo Saito and Tatseyi Nakajima. J. Appl. Polym. Sci. Vol.2, 93 (1956).
93. Richard, H. Boyd. Polymer , Vol. 26, 1123 (1985).
94. Bryan B. Sauer, Benjamin and Hsiao, S. J. Polym. Sci., Part-B Polym. Phys. Vol.31, 917 (1993).
95. Ishida, Y. Kolloid Z. 174, 124 (1961).
96. Gupta, A.K., Singhai, R.P., Bajaj, P. and Agrawal, A.K. J. Appl. Polym. Sci. 28, 1167 (1983).
97. Shoga, Saito, Hiroyuki, Sasabe, Tatseyi Nakajima. J. Polym. Sci. Part A-2, Vol.6, 1297 (1968).
98. Sasabe, H. and Saito, S. J. Polym. Sci. Pt. A-2, 6, 1401 (1968).
99. Neagu, E.R. and Neagu, R.M. Phys. Stat. Solidi(a) 144, 429 (1994).
100. LakshmiNarayanaa, K., Dasaradhu, Y. and Narasimha Rao, V.V.R., Polymer International 35, 315 (1994).
101. Vanderschueren, J. and Linkens, A. J. Appl. Phys. 49, 4195 (1978).
102. Khare, P.K., Indian J. Pure & Appl. Phys. 34, 249 (1996).
103. Khare, P.K., Pramana J. of Phys. 46, 109 (1996).
104. Khare, P.K., Pandey, P.K., Chourasia, R.R. and Jain, P.L., Polymer International 49, 719 (2000).

105. Emtage, P.R. and Tantraporm, W., Phys. Rev. Lett. **8**, 267 (1962).
106. Rogger, A.V., Phys. Rev. Lett. **9**, 368 (1962).
107. Christy, R.W., J. Appl. Phys. **35**, 2179 (1964).
108. Carter, G.M., Thakur, K.K., Chem, Y.J. and Hryniewicz, J.V., Appl. Phys. Lett. **47**, 157 (1985).
109. Lengyel, G., J. Appl. Phys. **37**, 807 (1966).
110. Lane, J.A., Brighton College of Tech. Project Report 156 (1967).
111. Miyoshi, Y. and Chino, K., Jpn. J. Appl. Phys. **6**, 181 (1967).
112. Gregor, L.V. and Kaplan, L.H., Thin Solid Films **2**, 95 (1968).
113. Gregor, L.V., Thin Solid Films **2**, 95 (1968).
114. Lilly, A.C. and McDowell, J.R., J. Appl. Phys. **39**, 141 (1968).
115. Lilly, A.C. and Lowitz, J. Appl. Phys. **39**, 4360 (1968).
116. Idea, M., Kosaki, M., Ohshima, H. and Shimohara, U., J. Phys. Soc. Jpn. **25**, 1742 (1968).
117. Kosaki, M., Sugiyama, K. and Ieda, M., J. Appl. Phys. **42**, 3388 (1971).
118. Gupta, D.K. and Barbarez, M.K., J. Phys. D. **D6**, 867 (1973).
119. Hanscomb, J.R. and Caldarwod, J.H., J. Phys. D. **6**, 1093 (1973).
120. Lupo, A. and Battog, I., J. Polym. Sci. **12**, 2399 (1974).
121. Kamisako, K., Akiyama, S. and Shinohara, K., Jpn. J. Appl. Phys. **13**, 1780 (1974).
122. Kryszewski, M. and Swiatek, J., Acta Phys. Polon **A-45**, 119 (1974).
123. Suzuki, M., Takahashi, K. and Mintani, S., Jpn. J. Appl. Phys. **14**, 74 (1976).
124. Hogarth, C.A. and Iqbal, T., Phys. Stat. Sol(a) **65**, 11 (1981).

125. Agrawal, V.K. and Mitasuhashi, H., Thin Solid Films **41**, 271 (1977).
126. Mahendru, P.C., Pathak, N.K., Jain, K. and Mahendru, P., Phys. Stat. Sol(a) **42**, 403 (1977).
127. Phadke, S.D., Sathianadan, K. and Karekar, N., Thin Solid Films **51**, 49 (1978).
128. Chutia, J. and Barus, K., Thin Solid Films **55**, 387 (1978).
129. Hogarth, C.A. and Iqbal, T., Thin Solid Films **3**, 201 (1969).
130. Tyczkowski, J., Zielinski, M. and Kryszewski, M., Thin Solid Films **55**, 253 (1978).
131. Staryga, E. and Swiatek, J., Thin Solid Films **56**, 311 (1979).
132. Sachar, E., IEEE Elect. Insul. **EI-14**, 85 (1979).
133. Diaconu, I., Dumitrescu, S. and Siminonescu, C., Eur. Polym. J. **15**, 1155 (1979).
134. Chutia, J. and Barua, K., J. Phys. D. **13**, L9 (1980).
135. Sharma, B.L. and Pillai, P.K.C., Polymers **23**, 19 (1982).
136. Tyczkowski, J., Czeremuskin, G. and Kryszewski, M., Phys. Stat. Sol(a) **72**, 751 (1982).
137. Sodolaki, M., Phys. Stat. Sol(a) **89**, 647 (1985).
138. Sessler, M., Hahn, B. and Yoon, D.Y., J. Appl. Phys. **60**, 318 (1986).
139. Hogarth, C.A. and Zor, M., Phys. Stat. Sol(a) **98**, 611 (1986).
140. Zor, M. and Hogarth, C.A., Phys. Stat. Sol(a) **99**, 513 (1987).
141. Murthy, S.S.N., J. Phys. D. **21**, 1171 (1988).
142. Paul, N. and Radhakrishnan, M.K., Ind. J. of Pure & Appl. Phys. **28**, 279 (1990).
143. Singh, S. and Singh, H.P., Ind. J. of Pure & Appl. Phys. **28**, 490 (1990).
144. Chakraborty, S.C. and Patil, N.B., Ind. J. of Pure & Appl. Phys. **29**, 478 (1991).

145. Das, S.K. and Basu, S., Appl. Phys. **29**, 478 (1991).
146. Narayan, A. and Singh, H.P., Ind. J. Pure & Appl. Phys. **29**, 814 (1991).
147. Mahendru, P.C., Phys. Stat. sol. **42**, 403 (1977).
148. Khare, P.K., Gaur, M.S., Bajpai, Alka, Pandey, R.K. and Srivastava, A.P., Indian J. Pure & Appl. Phys. **31**, 326 (1993).
149. Khare, P.K., Gaur, M.S. and Srivastava, A.P., Indian J. **32**, 14 (1994).
150. Khare, P.K. and Chandok, R.S., J. Polym. Mater. **12**, 23 (1995).
151. Khare, P.K., Jain, S.K. and Paliwal, S.K., Bull. Mater. Sci. **20**, 699 (1997).
152. Upadhyay, J.K., Khare, P.K., Ashish Verma and Paliwal, S.K., J. Polym. Mater. **15**, 281 (1998).
153. Khare, P.K., Pandey, R.K. and Jain, P.L., Bull. Mater. Sci. **22**, 1003 (1999).
154. Khare, P.K., Pandey, R.K. and Jain, P.L., Bull. Mater. Sci. **23**, 325 (2000).
155. Khare, P.K. and Srivastava, A.P., Thin Solid Films **208**, 233 (1992).
156. Khare, P.K., Jain, P.L. and Pandey, R.K., Bull. of Mater. Sci. **23**, 419 (2000).
157. Ieda, M., Sawo, G. and Kato, S. J. Appl. Phys. **42**, 3737 (1971).
158. Jain, V.K., Gupta, C.L., Jain, R.K. and Tyagi, R.C. Thin Solid Films **48**, 175 (1978).
159. Srivastava, R.K., Qureshi, M.S. and Bhatnagar, C.S. Japan J. Appl. Phys. **17**, 1537-1542 (1978).
160. Srivastava, R.K., Qureshi, M.S. and Bhatnagar, C.S. Ind. J. Pure & Appl. Phys. **18**, 923-926 (1980).
161. Srivastava, R.K., Khare, M.L. and Bhatnagar, C.S. Ind. J. Pure & Appl. Phys. **18**, 20-23 (1980).
162. Srivastava, R.K., Qureshi, M.S. and Bhatnagar, C.S. Ind. J. Pure & Appl. Phys. **18**, 957-960 (1980).

163. Srivastava, R.K. and Bhatnagar, C.S. Ind. J. Pure & Appl. Phys. **19**, 19-23 (1981).
164. Gross, B. J. Chem. Phys. **17**, 866 (1949).
165. Murphy, P.V., and Riberio, S.C. J. Appl. Phys. **34**, 2061 (1963).
166. Gubkin, A.N. and Matsonashirli, B.N. Sov. Phys. Solid State **4**, 878 (1962).
167. Encyclopedia of Chemical technology Vol.21, Edited by E.J.Palaski (John Wiley, USA), 1970, 427; Plasma extenders in Krik Othmer, Encyclopedia of Chemical technology, Vol.10 (1st edition), A. Slander and J.Scott (Editors) (Interscience Publishers, New York), 421.

CHAPTER II

EXPERIMENTAL DETAILS

2.1 INTRODUCTION

Virtually, all the polymers are either amorphous or partially crystalline macromolecular compounds. However, the crystalline regions are macroscopic ($\geq 1000 \text{ \AA}$) in size. Since it is not possible to obtain crystals of polymers large enough to allow proper handling, these have to be studied either in the form of compressed pellets or slabs cast from the melt, or thin films. The increasing demand for microminiaturisation of components for electronic applications has further stressed the need for growth and development of thin insulating polymer films. Consequently, thin films of pure polymers, polymer composites and polymer blends are being extensively studied instead of pellets or slabs [1-2]. Also, the results on pellets are viewed with suspicion because of interfacial effects, role of surface conduction and large anisotropy.

This chapter describes the experimental details of the investigations presented in the thesis. We briefly discuss methods of preparation of thin film and measurement of their thickness, types of electrodes and vacuum coating unit.

2.2 METHODS OF POLYMER FILM FORMATION

Thin films of polymers are obtained by a large variety of methods. Some excellent reviews [3-6] have appeared in the literature on the methods of preparation which are discussed briefly in the following sections.

2.2-1 THERMAL EVAPORATION

Thin films are produced from polymers by thermal evaporation of bulk material. Here the material to be deposited is heated to a high temperature at a very low pressure and in extremely clean conditions where it vapourises. The vapour is then allowed to condense on a substrate placed above the source to form a film. Thermal evaporation was reported to lead to a wax like deposit on a substrate, together with gaseous fractions and solid residue. Evaporated polymer films are contaminated due to the vigorous boiling action of the molten polymer, and due to the rapid evolution of breakdown products. However, uncontaminated films can be obtained by choosing a low evaporation temperature and thus a slow rate of deposition and by specially designed thermal evaporation methods pot [7], combination of internal baffles and flash evaporation [8] and laser evaporation.

2.2-2 COMBINATION OF INTERNAL BAFFLES AND FLASH EVAPORATION

In this technique, the polymer to be evaporated is taken in the powder form and is made to drop in the form of fine particles from a mechanically agitated hopper on to a hot crucible fitted inside, with baffles so that numerous discrete evaporations may occur.

2.2-3 LASER EVAPORATION

Here the material is heated by the enormous power of a laser source. The evaporation in this process generally takes

place from the surface of the material only. Very thin films can be obtained as the amount of energy released in each burst is very large.

2.2-4 PYROLYSIS

The thermal decomposition of a compound to yield a deposit of the stable residue is called pyrolysis. Szwarc [9] discovered that the vacuum pyrolysis of xylene, on condensation could lead to poly-p-xylene which were contaminated by low molecular weight by-products. Gorham [10] used di-p-polymer which is pyrolysed in vacuum at 600 C. This process forms two molecules of p-polymer which instantaneously polymerize when incident on a substrate maintained at less than 30 C. The above formed polymer is a high molecular weight leniaca poly-p-polymer. The advantage in this process is that the films seemed to have better electrical, mechanical, optical properties compared to the other types of preparation.

2.2-5 SPUTTERING

The ejection of atoms from the surface of a material by bombardment with energetic particles is called sputtering. The ejected or sputtered atoms can be condensed on a substrate to form a thin film. The chief advantage of this method is that the deposition rate remains constant. Various sputtering systems such as glow discharge and rf-sputtering are based on the effect that the free electrons ejected from the evaporant can be accelerated in an electric field to cause further

ionization of the residual gas and such ionization will result in further bombardment of the surface of the target and a self sustaining reaction. Some other systems are based on increasing the electron path lengths so that the self sustained system can work at relatively low pressures.

2.2-6 GASEOUS DISCHARGE

Thin films of polymers can be obtained when a gas discharge is maintained in the vapour of monomer. Since the pressure maintained is of the order of 1 mm Hg. The discharge is a cold one and no hot cathode emission is necessary. The problems associated with high gas pressures and substrate heating have been minimised by utilizing a longitudinal magnetic field to compress the glow discharge in a tube and rf electrodeless excitation.

2.2.-7 HOT PRESSING METHOD

The first method of film fabrication was hot pressing. In this method the polymer powder is placed in between two ferrotype photographic plates and hot pressed at a temperature 10-15 C above the crystalline melting point under pressure. The film is then removed from the press and immediately quenched in ice water in order to prevent any crystallization, if necessary. Then the film is stretched in order to obtain necessary thickness.

2.2-8 CASTING METHOD

Preparation of thin films of polymers from solvent casting is a very satisfactory method of film formation. In this method, the polymer dissolved in the appropriate solvent is poured on a clean surface of glass plate and is spread to an even thickness with a doctor blade. A dust shield is placed above the solution and the film is allowed to form in air. When the film is dry, the plate is immersed in water and the film floats. In most cases the film is then dried in a vacuum chamber for about 8 hrs followed by exposure to room temperature.

2.2-9 FILM BLOWING

Biaxial stretching by applying a pressure difference across the film or by elevated temperatures gives rise to thin film. This method consists of placing the polymer film under a hold down ring that secures the film over a circular opening in a heavy teflon disk. Pressure is then applied to one side of the polymer film and a "balloon" blows through the opening in the teflon disk. The entire assembly is placed in a vacuum oven which allows heating under an inert atmosphere or vacuum. Some polymer films are successfully blown to thickness of 10 to 30 μm . The blowing process is very difficult to control and have to be done at a high temperature, near the crystalline melting point.

2.2-10 PHOTOLYTIC PROCESS

Photolytic process is used for the formation of thin

dielectric layers for use in thin film circuit insulation. In this process the films are obtained when the surface is irradiated with ultraviolet light in the presence of monomer vapour. Polymer films formed in this method are quite stable and the reliability is excellent down to 50 Å⁰. Dielectric properties of photopolymer films have been studied in many cases and found to possess the properties of the bulk polymer.

2.2-11 VACUUM EVAPORATION

Hogarth and Iqbal [11] have prepared thin films of polypropylene by vacuum evaporation technique. Polypropylene was evaporated at a pressure of 6×10^{-5} torr from a stainless steel blade which was maintained at a temperature of 335 C. The film was deposited on to a previously deposited copper or aluminium base electrode. However, the polymer films prepared by this method are generally not free from pin holes.

2.2-12 FILM FROM POLYMER SOLUTION

All the methods for film preparation discussed above involve immediate polymerization. As such, they are not expected to give useful films for research purposes. Further, the polymer formed by these techniques may have different degree of polymerization and may contain undesired impurities. Polymer films prepared by vacuum deposition technique are also not useful as they are not expected to be free from pin holes. Moreover, polymer blend films cannot be obtained by the above methods as it is difficult to control the quantities of

constituent polymers during evaporation and polymerization. Films with uniform degree of polymerization and high purity can be prepared from polymer solution using highly pure polymer as solute and inert solvents of AR grade. The blending percentage can also be controlled easily by dissolving known amounts of the constituent polymers in solution.

There are two main methods available for preparing thin films from polymer solution :

- (a) Isothermal immersion technique, and
- (b) Casting from solution.

(a) Isothermal Immersion Technique

Solution of suitable concentration is kept at a desirable temperature and substrate is immersed into it vertically for a given period of time depending upon the required film thickness. When the film is deposited, the substrate is slowly taken out and dried by hot air. The deposited film is then gently detached using a sharp knife edge [12-13]. Polyblend films can also be prepared by dissolving desired quantities of constituent polymers in a solution. Rastogi and Chopra [14] have studied this method in detail and found that the thickness of the film depends upon the concentration of the solution, its temperature, nature of the substrate and the time for which substrate is kept immersed in the solution.

This method requires a great care in selecting the temperature and concentration of the solution. Also, sophisticated mechanical instrumentation is required for taking out the substrates from the solution, keeping them exactly vertical to the solution surface. Lack of proper instrumentation and care may result in the films containing air bubbles and of nonuniform thickness.

(b) Casting from Solution

The polymer solution of known concentration and quantity is spread over an optically plane clean glass plate of known area which is placed horizontally over a mercury pool. Solvent is allowed to evaporate at a suitable constant temperature and the resulting film is gently detached from the substrate. Films of different thicknesses may be obtained using solutions of different concentrations. The films obtained by this method are of uniform thickness and perfectly plane surface, if prepared carefully. Also, an elaborate cleaning procedure must be adopted for substrates.

(i) Choice of substrate and its cleaning

An ideal substrate should not react with the polymer or its solvent or the surrounding atmosphere; it should be resistant to chemical corrosion, especially to those which are commonly used for cleaning purposes. Its surfaces must be smooth and easily washable for repeated use. Its softening and melting points should lie much higher than the temperature of

investigation. It should be made of hydrophobic material. Out of various substrates, like metal foils, crystals, glass etc., glass is the best of all. In the present investigations, microglass slides of "Blue Star" were used as substrates for deposition of capacitor structures. The glass substrates dimensions were of the order of $4.0 \times 2.5 \text{ cm}^2$ and in most of the other investigations possess almost all the listed qualities of a good substrate. The glass plates were first kept in a freshly prepared hot chromic acid for one hour. They were washed in tap water using a liquid detergent like "Genteel" and rinsed in double distilled water and in acetone respectively. Then the cleaned substrates were dried by blowing hot air. The glass substrates cleaned in this way were used for the deposition of bottom electrode. They are cheap and ready for repeated use after cleaning. Metal foils have an inherent disadvantage that they usually react with the ambient oxygen to form an oxide layer over their surfaces. Similarly, crystals like NaCl are more or less hygroscopic and their surfaces are easily contaminated.

(ii) Choice of Solvent

To grow the best quality, smooth films, free from pin holes the rate of vaporization of the solvent should be kept sufficiently slow. This can be achieved by using a solvent of high boiling point.

(iii) Solution Concentrations

It is preferable to use the solution of low

concentration for the film deposition. Experiments indicate that the films grown from thick solutions have considerably different thicknesses at different spatial points. They may also trap air bubbles in their structure. The best procedure is to keep the slides immersed in thin solution over a small period of time about (20 minutes).

(iv) Solution Temperature

Temperature of a solution markedly affects the growth of films. Hot solution give rise to thinner depositions due to a lower value of viscosity. It is better to use the solution whose temperature lies in the neighbourhood of room temperature. It is necessary since the substrate acquires the temperature of the solution when dipped into it and if it is much higher than room temperature, the rate of vaporization of solvent would greatly enhance during the process of drying which is undesirable. The temperature of solution is kept a bit higher (about 5 C) than room temperature so as to make the compensation for temperature fluctuations arising due to change in the weather. A magnetic stirrer is used to eliminate the temperature gradients.

2.3 PRESENT EXPERIMENTAL TECHNIQUE

Thin polymer films were deposited by the solution grown technique which involves the isothermal immersion of a substrate into the polymer solution of suitable concentration held at a constant temperature of a certain time. The rate of

growth of the polymer film and thickness of the film depends on the nature of the substrate and the solvent and also on the concentration and solvent temperature, and on the subsequent time for which the substrate is left immersed in the solution.

Polyvinyl pyrrolidone (PVP) films were deposited from the solutions of fixed concentration (1.5 grams of PVP dissolved in 50 cm³ of chloroform. The solution of the particle concentration was prepared in a glass beaker by dissolving the required amount of PVP in the solvent at 40 C temperature. The solution was continuously stirred by means of magnetic stirrer for about 45 mins. The solution was stirred and heated simultaneously until it ensures a homogeneous mixing.

Freshly and neatly cleaned blue star micro-glass slides with vacuum deposited lower electrodes were used for the deposition. The substrates were held inside the constant temperature bath vertically above the solution. Then the solution and substrates acquired the required temperature the substrates were isothermally immersed in the solution for fixed time. After withdrawal of the filmed substrates from the solution, they were washed in the solvent and then dried in hot air oven for more than 24 hours maintained at a temperature of 40°C. (Fig 2.1)

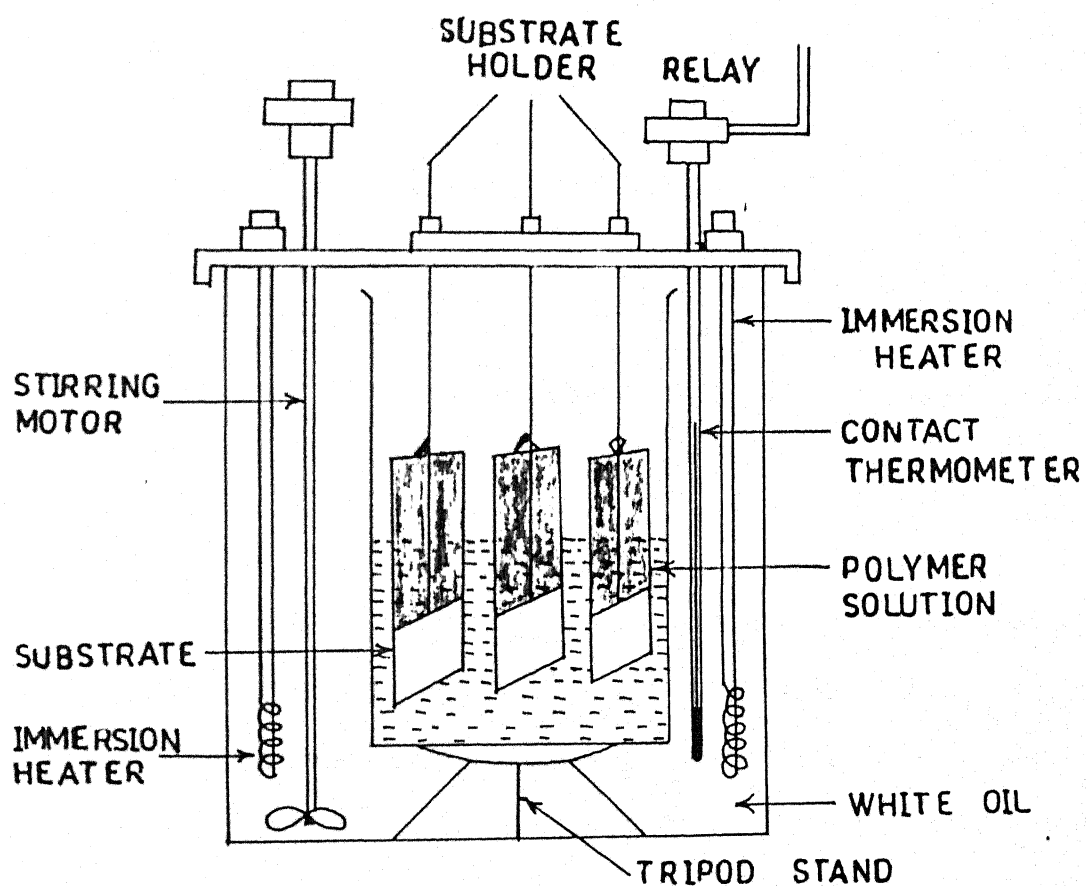


Fig.2.1 A diagram of the Isothermal Immersion Technique for growing the thin Films.

2.4 MEASUREMENT OF FILM THICKNESS

The thickness of polymeric films can be measured by a variety of methods. They may be described under the following three categories :

- (i) Mechanical methods,
- (ii) Optical methods, and
- (iii) Electrical methods.

2.4.1 MECHANICAL METHODS

This includes two important methods, namely Stylus method and Weighing method.

(A) Stylus Method

In this method, a fine pointed stylus is moved over a stepped surface formed by the edge of the film on the substrate. The transverse displacement suffered at the step is fed to an electronic circuit for amplification and recording, and the thickness of the film is computed. The method is very simple but its accuracy is very low [15-17].

(B) Weighing Method

This method is applicable only to films of uniform thickness. Since mass is defined as density multiplied by volume, and the area and the mass of the film can be measured precisely using vernier callipers and physical balance, the thickness of the film can be computed by the formula :

$$d = \frac{M}{\rho \times a}$$

where M , ρ , a and t are the mass, density, area and thickness of the film, respectively. Obviously, the sensitivity of the method depends upon the measuring accuracy of M and a . Though it is not always possible to cut the substrate in a well defined area. Further, the area selected for thickness measurement may not be representative of the area under investigation [17,18].

2.4-2 OPTICAL METHODS

Ellipsometry, interferometry and light sectioning methods are the important methods belonging to this category -

(A) Ellipsometry

This method is used for the measurement of thickness of transparent films. It is based on evaluating the change in the state of polarization of light reflected from the film and the substrate. However, as it is time consuming and involves complicated mathematical calculations [19].

(B) Interferometric Methods

Interferometric methods include those devices which make use of interference of light, e.g., Newton's ring set up, Michelson interferometer, Fabri-Perrot etalon, etc. Film thickness is determined by observing the shift in the interference fringes (due to change in path difference of reflected or transmitted light rays) on moving from film surface to the substrate. The technique is mainly used for measuring thickness of optically smooth films yielding consistent results [20].

(C) Light Sectioning Methods

In case of thin films of more than 1 mm thickness, measurement can be made using travelling microscope movable in vertical direction. Light sectioning microscope can also be used for precise thickness measurements, however, the method becomes quite inaccurate for films of uniform thickness. A brief description of this method is as follows :

Light from a slit is projected on to the sample surface at an angle of 45° . An observing microscope making an angle of 45° to the sample surface and 90° with the illuminating light beam is used for observing the separation of slit images. In case of opaque films slit is projected across a step in the film; however, in the case of transparent films step is not necessary as the two images are obtained because of reflection from the upper and lower surfaces of the film [21-22].

According to Brown [23], the separation of slit images due to reflection across the step can be measured with an eyepiece micrometer to an accuracy of 0.1 mm in 1 to 400 m range. In case of transparent films, the actual film thickness d can be calculated from the apparent film thickness d' and the index of reflection n of the medium using the relation :

$$d = d' (2n^2 - 1)^{1/2}$$

2.4-3 ELECTRICAL METHODS

Thickness of thin films can also be determined

conveniently by measuring the capacitance of a condenser having film as a dielectric. This method gives accurate result for uniform films. Vacuum evaporated electrodes are deposited on both the surfaces of the film to form a parallel plate condenser. Plane metallic electrodes can also be used for very good uniform surfaces. Capacitance of thin condenser thus formed is measured and the thickness is calculated using the observed value of the capacitance, area of the metallic electrodes and dielectric constant of the film. Absence of pin holes and uniformity of film surfaces are the two main advantages of this method. It is, therefore, most suitable for solution grown thin films.

2.5 TYPES OF ELECTRODES

The following four types of electrodes are used for making electrical contacts with polymer films for studying the electrical storage and transport properties :

- (i) Pressed metal-foil electrodes,
- (ii) Painted electrodes,
- (iii) Liquid contact electrodes, and
- (iv) Vacuum deposited electrodes.

2.5-(i) PRESSED METAL-FOIL ELECTRODES

Film is sandwiched between two plane metallic foil electrodes of desired shape, area and good surface finish. Springs are used to ensure uniform pressure throughout the film surface. However, in the case of polymers, when

measurements are carried out at high temperatures, such electrodes are disadvantageous. At high temperatures, the polymer is softened. Due to pressure of the electrodes on the film, its thickness is reduced and this sometimes results in breakdown of the polymer film. Further, under ambient humid atmospheric conditions, practically all metallic electrodes except gold and platinum form oxide and other chemical coating over their surfaces. This affects the experimental results by contaminating the film surface as improper transfer of charges takes place through contaminated surfaces.

2.5-(ii) PAINTED ELECTRODES

Electrodes of desired shape and area can be painted on film surface using conducting graphite or silver paints. However, the use of painted electrodes is not possible on most of the polymers, since the thinner present in the conducting paint may attack the film surface. Hence, the use of painted electrodes is restricted to those polymers only, which are inert to the thinner used with conducting paints.

2.5-(iii) LIQUID CONTACT ELECTRODE

In this method, non-metallized surface of an unilaterally metallized film specimen is kept in contact with a liquid such as water or ethyl alcohol so that a thin uniform layer of liquid rests over the non-metallized surface of the film. A potential is applied between the metallic electrode and rear unmetallized surface of the film. A double charge

layer is formed at the solid-liquid interface and as a result of interaction between electrostatic and molecular forces, charge transfer to polymer film takes place. Electrodes should be withdrawn and liquid evaporated before removal of voltage to ensure charge retention on the specimen surfaces. Recently, non-wetting liquid-insulator contact electrodes have also been employed. Monocharge electrets have also been prepared using liquid contact electrode obtained by filling one side metal polymer gap with liquid and leaving the other filled by air.

2.5-(iv) VACUUM DEPOSITED ELECTRODES

Vacuum deposition method is probably the best and most convenient for depositing metallic electrodes of desired size and shape. The metal can be vacuum evaporated on any metallic or non-metallic substrate or film specimen. No air gap exists between the evaporated electrode and the substrate. The electrodes can be very conveniently used for measurements at low as well as high temperatures, provided the melting point of electrode metal is higher than the temperature of measurements.

In the present investigation, vacuum deposited metal electrodes are used.(Fig. 2.2 & 2.3)

2.5-(v) VACUUM COATING UNIT SYSTEM

The metal electrodes were deposited by vacuum evaporation technique using a Vacuum Coating Unit. The Vacuum Coating system was assembled using necessary accessories. The

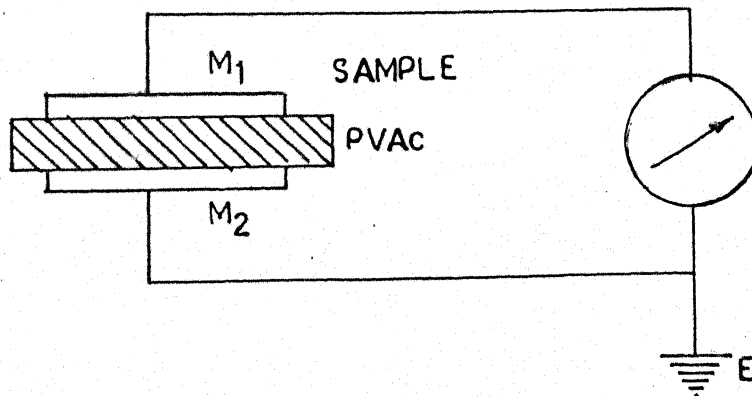
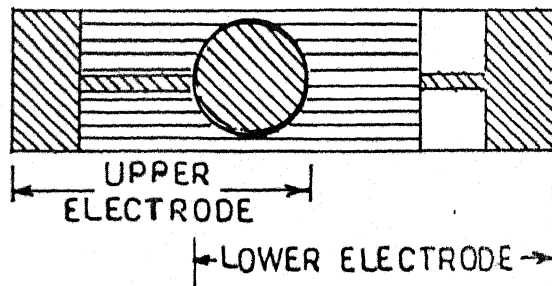
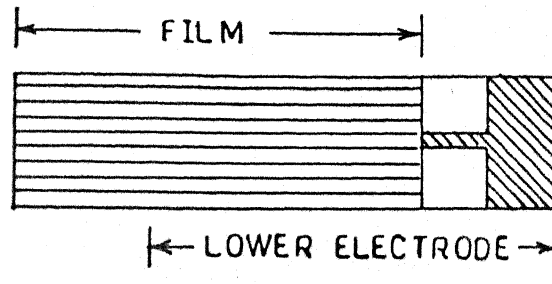


Fig.2.2 Circuit diagram for measurement of current in electrode-Sandwich Configuration.

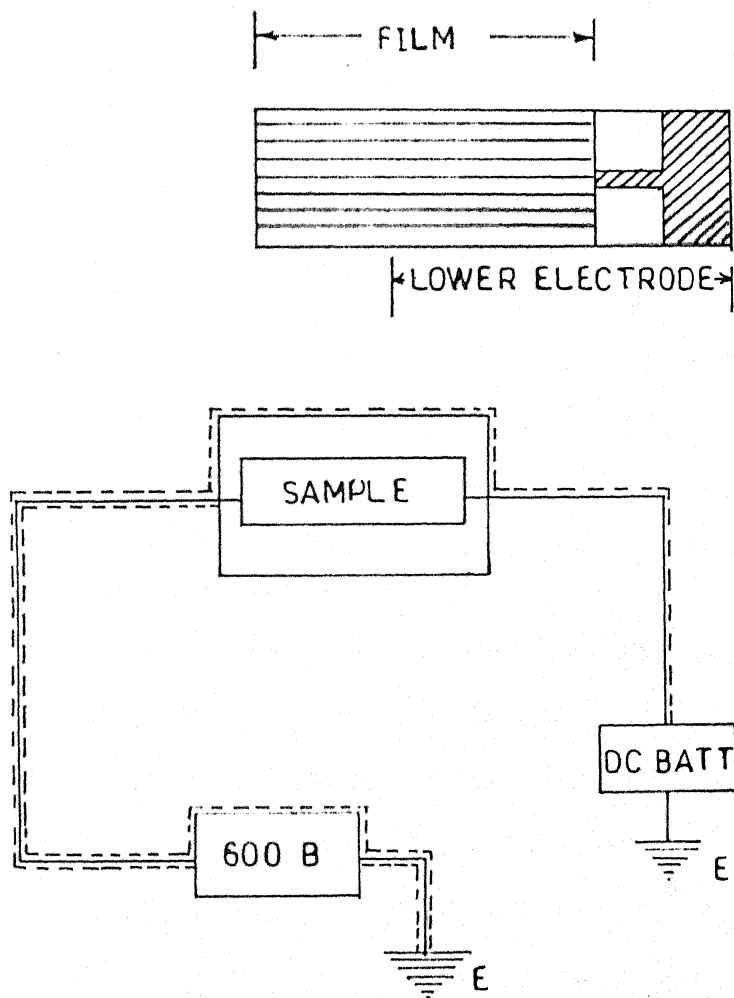


Fig.2.3 Schematic diagram of circuit.

vacuum coating unit has been employed to achieve a vacuum of 2×10^{-6} torr, in the evaporation chamber. A pirani-penning gauge system measures the vacuum in the belljar. A low tension transformer capable of providing 100 amperes at 10 Volts was used for resistive heating of tungsten spiral/boat to which the material to be evaporated was fed. Metals like aluminium, copper and silver of high purity of 99.99% are used for the deposition of electrodes.

Vacuum evaporated metal electrodes were deposited on polyblend thin films using Hind High Vacuum Coating Unit, Model 12-A4.

(a) MAIN PARTS OF THE COATING UNIT

The unit consists of the following parts :

1. Vacuum chamber : This consists of

- A. Hemispherical glass belljar with a L-shaped rubber gasket for air sealing,
- B. Support for substrate or specimen to be coated,
- C. Molybdenum boat or a tungsten filament for heating the material to be evaporated,
- D. Hinged metallic shield for controlling the deposition rate of the material,
- E. High tension discharge unit (electrodes) for ionic bombardment, and
- F. Substrate rotator.

2. Rotary pump

3. Diffusion pump
4. Pirani gauge (for measuring coarse vacuum)
5. Penning gauge (for measuring high vacuum)
6. Electric supplies to the chamber :
 - A. A low tension supply - for filament and boat,
 - B. A high tension supply - for glow discharge cleaning of the substrate, and
 - C. Variac for LT and HT supply.
7. Valves :
 - A. Backing valve (V_1) - this connects the rotary pump with the diffusion pump,
 - B. Roughing valve (V_2) - this connects the rotary pump with the vacuum chamber,
 - C. Baffle valve (V_3) - this connects the diffusion pump with the vacuum chamber,
 - D. Air admittance valve (V_4) - this allows air to enter into the vacuum chamber, and
 - E. Gas inlet valve (V_5) - this allows gas to enter into the chamber at the desired rate.

(b) OPERATION OF THE COATING UNIT

At the start all valves were closed and the rotary pump was turned on. It initially evacuates the tubes connecting the rotary pump and the junction of the backing and roughing

valves. When the pressure shown by the pirani gauge attained a value less than 0.5 torr, the backing valve V_1 was opened for connecting the rotary pump with the oil diffusion pump. Circulation of water in the tubes surrounding the diffusion pump was started and the heater of the diffusion pump was turned on.

Approximately half an hour later with the diffusion pump ready, the backing valve V_1 was closed and the roughing valve V_2 was operated for connecting the vacuum chamber directly with the rotary pump. The pressure inside the vacuum chamber was allowed to fall to 10^{-2} to 10^{-3} torr. After which the high tension supply was switched on. This caused ionization of the rarefied air inside the vacuum chamber with the net result that the substrate was cleaned by ionic bombardment. The HT was switched off after 5 minutes.

The pressure inside the vacuum chamber was allowed to fall up to 0.002 torr so as to establish a rough vacuum. After this valve V_2 was closed and valve V_1 was opened again so that the rotary pump was connected to the diffusion pump for maintaining the backing vacuum. With valve V_1 open, the baffle valve V_3 was opened to connect the diffusion pump with the vacuum chamber. The vacuum was maintained by reading the pressure on the Penning gauge. When the vacuum had reached a pressure value of 10^{-5} torr, the low tension supply was switched on. When the Al pellet kept in the spiral tungsten filament started to evaporate, the hinged metallic shield was

swung out to allow the deposition of the metal vapour on the surface of the specimen. In this way aluminium electrodes of 5.5 cm diameter were prepared.

With the deposition over, the filament and heater currents were switched off. Valve V_3 was closed and the fine vacuum Penning gauge was switched off. After 10 min the air admittance valve V_4 was opened to leak air into the vacuum chamber making the bell jar free to be removed and the electrodes deposited film to be taken out. The coating unit was closed down by first turning off the diffusion pump heater with the rotary pump still running and the backing valve open. After 15 minutes when the boiler of the diffusion pump was cooled, the backing valve was closed and the rotary pump was switched off. Finally the water circulation in the diffusion pump was stopped. (Fig. 2.4)

2.6 CIRCUIT CONFIGURATION AND PRINCIPAL EQUIPMENT

The instruments used were practically common to all the studies undertaken in this thesis. The experimental circuitry was not complicated in all the cases. The current measuring cell with its constructional details and the specifications of the other measuring instruments are described in the following subsections.

2.6-1 TEMPERATURE PROGRAMMING AND CONTROL

During various experiments, a constant temperature was

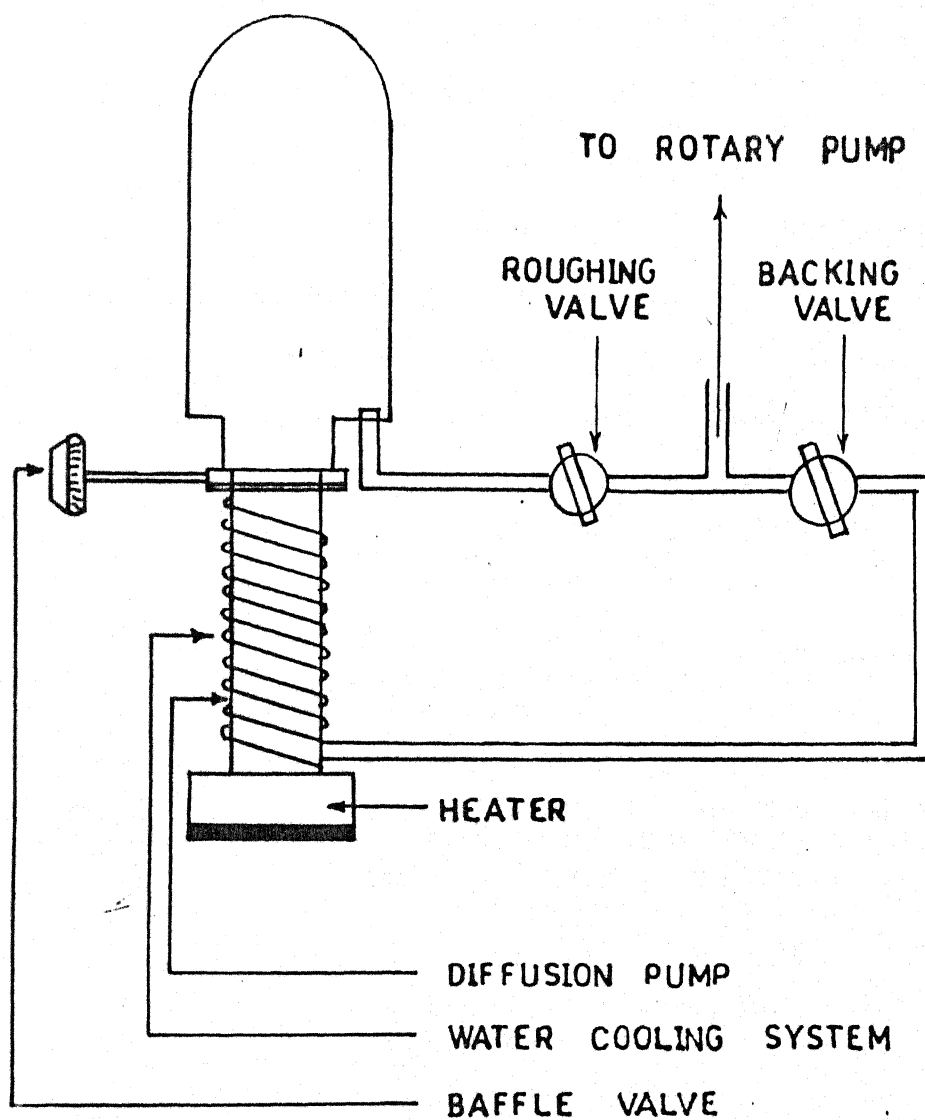


Fig.2.4 Block diagram of Vacuum Coating Unit.

achieved in the oven with an accuracy of ± 1 C. The temperature programming was done in the oven with the help of a Laxson's programmable temperature controller, type 1600-2/B supplied by Laxson's Electric Private Ltd., Bombay. With the help of this instrument, it was also possible to provide a linear heating rate of 3 C/min to the specimen, during thermally stimulated discharge experiments.

2.6-2 OTHER INSTRUMENTS USED AND THEIR SPECIFICATIONS

(i) Electrometer Amplifier - Model 600B KEITHLEY

Current	:	10^{-5} to 10^{-14} amps (full scale for both polarities)
Accuracy	:	3%
Voltage range	:	10 mV to 10 V (full scale for both polarities)
Accuracy	:	$1\% \pm 0.1$ mV
Input impedance	:	Greater than 10^{14} ohms in open position of input impedance switch (voltage measurements)

(ii) High voltage unit - Type 4800 B

Manf.	:	Electronic Corporation of India Ltd., Hyderabad
Output voltage:	:	± 50 to $+3,000$ volts

(iii) Stabilizer - Nelco stabilizer

Regulation	:	$\pm 1\%$ from no load to full load
------------	---	-------------------------------------

REFERENCES

1. Gupta, C.L. Indian Journal of Pure and Appl. Phys. **15**, 684 (1977).
2. Mahendru, P.C., Jain, K. and Mahendru, P. J. Phys. D. Appl. Phys. **9**, 83 (1976).
3. Gregor, L.V. Physics of thin films, Ed. G. Hass and R. E. Thun, Vol. 3, (1966).
4. Mano, E.B. and Durao, L.K. J. Chem. Ed. **50**, 228 (1973).
5. White, M. Thin Solid Films **18**, 157 (1973).
6. Jackson, G.N. Thin Solid Films **5**, 209 (1970).
7. Luff, P.P. and White, M. Vacuum **18**, 437 (1968).
8. Perveer, A.F. and Muranova, G.A. Priboory in Technika Eksperimenta **4**, 200 (1969).
9. Szwarc, M. Disc. Faraday Soc. **2**, 46 (1947).
10. Gorham, W.F. J. Polym. Soc. **4**, 3027 (1966).
11. Hogarth, C.A. and Iqbal, T. Thin Solid Films **51**, L45 (1978).
12. Hogarth, C.A. and Zor, M. Thin Solid Films **27**, L5 (1975).
13. Koutsky, J.A., Walton, A.G. and Bear, E. J. Polym. Sci. **4**, 611 (1966).
14. Rastogi, A.C. and Chopra, K.L. Thin Solid Films **18**, 187 (1973).
15. Jain, K. and Chopra, K.L. Phys. Stat. Sol(a) **20**, 167 (1973).
16. Wagner, M.E. Thermochemica Acta **23**, 93 (1978).
17. Nakagawa, K. and Ishida, Y. J. Polym. Sci., Polym. Phys. **11**, 1503 (1973).
18. Gazro, J. Thin Solid Films **21**, 43 (1974).
19. Galang, R. In the handbook of thin film technology, Eds. L.I. Maissel and R. Glang (McGraw-Hill NY, 1970).
20. McCracklin, F.L. J. Res. NBS **674**, 363 (1963).

21. Kondratenko, M.M. and Malik, A.I. Instrument and Expt. Tech. (USA) 17, 855 (1974).
22. Borbat, A.M. and Goban, I.S. Optical Measurements in Tekhnika Kiev (1967).
23. Brown, R. Am. Cerem. Soc. Bull. 45, 206 (1966).

CHAPTER III

THEORETICAL BACKGROUND OF STUDIES

3.1 INTRODUCTION

Transient currents in dielectrics observed upon the application of a step voltage have been studied extensively to give an insight into the polarization processes in the materials undertaken for the study. It is generally accepted that the transient currents in an insulating material, on the application or removal of a step voltage, may be attributed to one or more of the following mechanisms : (i) electrode polarization, (ii) dipole orientation, (iii) charge storage leading to trapped space-charge effects, (iv) tunneling of charge from the electrodes to empty traps; (v) hopping of charge carriers through localized states. The above processes have been reviewed by several scientists and it has been established that the observed time dependence alone does not permit any discrimination to be made between various mechanisms. The argument for and against a particular mechanism is to be found by considering the variation of transient currents on various experimental parameters also, such as temperature, field and frequency. Polymers contain a large number of structural disorders and, therefore, contain discrete traps levels in their bulk. The role of various polarization processes and their relative contributions to the electret state of the polymer is not yet fully understood. Particularly, the space charge structure including the trap distribution of energy and also over the volume of the polymer, are still to be well understood. Such informations are also being obtained by carrying out the measurements of

absorption and short circuit isothermal desorption (discharging) currents at various temperatures. The d.c. step response technique in which the current response is measured as a function of time after d.c. voltage is applied to, or removed from the sample, is the isothermal analogue of TSDC measurement, as it determines the discharging current at constant temperatures instead of varying temperatures.

Polyvinyl pyrrolidone (PVP) is a polar polymer that exhibits excellent chemical resistance and good mechanical properties. In spite of its activeness for many applications, the conduction mechanism is presently not well understood. In the present thesis, we have attempted to identify the nature of the transient conduction and thermally stimulated discharge currents in pure polyvinyl films by comparing the observed dependence on parameters such as electric field, electrode material, temperature, time and relation between the charge and discharge currents, in the light of characteristic features of various proposed mechanisms.

3.2 TRANSIENT CURRENTS IN CHARGING AND DISCHARGING MODES

The charging or absorption current is obtained immediately after the application of a step voltage on a dielectric specimen, while the discharging or desorption current is obtained on removal of the step voltage provided the temperature is kept constant. Both the charging and

discharging currents decay approximately as t^{-n} , where t is the time elapsed after the application or removal of the step voltage, and the exponent n is a constant depending upon the properties of the material and the experimental conditions [1]. Charging current decays with time until a steady state current, usually known as conduction current, is reached. On the other hand isothermal discharging current decays for a long time depending upon the internal phenomenon taking place irrespective of the steady state current level.

The nature of transient charging and discharging currents differ from material to material depending upon the mechanism involved. The origin of these transient currents is still a subject of much controversy in the literature [2] and a large number of mechanisms have been proposed by various workers [3-10]. The combined effect of one or more may be responsible for the observed decay pattern of the transient currents. The discharging current is usually mirror image of charging current, provided that a steady state current does not occur. Hence, discharging currents can yield information about charging processes even when the corresponding charging current is masked by conduction current at charging. Quantitative as well as qualitative analysis can be made on comparing the experimental values of the decay exponent obtained under various experimental conditions [10]. The results of this technique can also be compared with those of some other electrical studies, like thermally stimulated

discharge current (TSDC) and isothermal surface charge decay, etc. to get clear and justified conclusions.

This technique is time consuming hence it is not very popular, but results of this long time technique are most consistent than any other technique because the electrical disturbances and instantaneous variations in other experimental parameters affect these experiments much less as compared to those involved in the fast discharge processes.

The origin of isothermal charging and discharging currents has not been clearly accounted for in most of the dielectric materials because of lack of experimental data covering an adequate range of experimental parameters, i.e., field, temperature, electrode material etc. However, the results are available for many materials although covering very few experimental conditions, which are insufficient to yield clear and firm conclusions.

In view of this it becomes worthwhile to undertake a detailed study of transient currents and to correlate the results obtained with those of other studies. This is expected to give a proper clarification of the transient response of charging and discharging in polymers, which is of prime importance for the analysis of the electret effect in polymer dielectrics.

3.3 MECHANISMS OF TRANSIENT CURRENTS

We find that there is a little consensus on the way absorption currents originate in polymers. This lack of agreement is evident from the fact that several mechanisms have been proposed to arrive at an explanation. But it has been seen that the applicability of each is limited and specific. The principal mechanisms are -

3.3-1 ELECTRODE POLARIZATION MECHANISM

Free charges are frequently available in the polymer bulk and have thermally activated mobilities. There is movement of these free charges towards electrodes of opposite polarities on application of a polarizing voltage and they start piling up near the electrode. We find that the electrode polarization or blocking mechanism (occurring in ionic materials) is characterised by linear dependence of the isochronal current on the field (though theory predicts a nonlinear region at low field), and a current that is thermally activated. It is also found that no definite confirmation exists on the dependence of the isochronal current at constant field with the specimen thickness. The current fall is initially proportional to $t^{-1/2}$ followed by a severe change, where n is greater than 1. The charging and discharging currents are mirror images of each other [12,13].

3.3-2 DIPOLE ORIENTATION MECHANISM

If we have randomly distributed dipoles inside a polymeric sample, they will not produce a net dipole moment. However, these dipoles possess a definite relaxation time and activation energy with the relaxation time being thermally activated. On application of an external electric field at an elevated temperature, the dipoles start orienting in the field direction. Image charges are induced on the metal electrode surface during the orientation of dipoles, causing a net current to flow in the external circuit. The value of this absorption current depends on the rate of dipole orientation and decreases gradually with time at a fixed temperature and time. After removal of the polarizing electric field, the dipoles start deorienting, producing the desorption current in the external circuit.

Dipole relaxation [12,13] can account for a t^{-n} absorption current, if a wide distribution of relaxation times exist for the dipoles uniformly distributed through the bulk of the material. The distribution has been theoretically analysed by Cole and Cole [14]. These relaxations are thermally activated and the current temperature curves taken at a fixed polarization time (isochronals) give an activation energy $A(1-\alpha)$, where A is the activation energy, and α is the distribution parameter, for times $t/\tau \ll 1$, where τ is the relaxation time. When $t/\tau \gg 1$, the current falls with increasing temperature, with an apparent negative activation

energy $A(\alpha-1)$. In dipole orientation there is no contact effect, i.e., there is no dependence on the electrode material. The current varies as $I \propto t^{-n}$, where $0 \leq n \leq 2$. The isochronal current at constant field is independent of the thickness and is directly proportional to the field. To apply the dipolar relaxation model to nonpolar polymers, we require a sufficient concentration of adventitious polar groups. Since the current being observed is small, we presume that this concentration is usually there.

3.3-3 CHARGE INJECTION LEADING TO TRAPPED SPACE CHARGE EFFECTS

There are usually a high concentration of trapping sites in the forbidden energy gap of polymers. These trapping sites are the outcome of impurities or due to the internal molecular arrangements in macromolecules. The application of an electric field to the polymer sandwiched between two metallic electrodes causes electrons or holes to be injected which get trapped in the trapping sites available, the distribution depending on the energy and trap depths. The charges which get trapped inside the bulk form a space charge which opposes further trapping of charge carriers. The trapping process causes the charging current to flow while removal of the external field produces the discharging current. The space charge model [12,13] needs a sufficiently high concentration of deep trapping levels to be present. Under this model, the isochronal current at constant field is independent of thickness.

3.3-4 THE HOPPING MECHANISM

Insulators have a wide energy band gap and low carrier mobility. The structure of these materials is such that the bonding between molecules is mainly due to Vander Waals or London forces and is rather weak, and also the overlap of the molecular orbitals and the intermolecular electron exchange are small which is not conducive for charge transport. These materials may have a large number of localized states within the bulk, with a wide distribution of activation energy and trap depths. These states may be filled with charge carriers like electrons, or holes. These states are separated from one another by potential barriers which prevent electrons or holes from moving from, say one molecule to a neighbouring molecule. Under application of an electric field, a carrier can move from one molecule to another by jumping over the potential barriers. This kind of charge transport by random jumps is known as the hopping model and will take place when $\tau_v < \tau < \tau_e$, where τ_v is the intramolecular vibration period, τ is the electron relaxation time and τ_e is the intermolecular vibration period [23].

In transient currents, the hopping model [11,13] will exhibit the following characteristic features. The isochronal current will be directly proportional to the field. At constant fields, the isochronal current will be independent of the thickness of the sample. The current will also be independent of the electrode material. The current will be

thermally activated and its time dependence will be of the form t^{-n} with $0 \leq n \leq 2$. The charging and discharging currents will be mirror images of each other.

3.3-5 THE TUNNELLING MODEL

This model [15,12,13] assumes the presence of a trap level or trap levels in the dielectric. It may so happen that charge carriers may lack enough energy to surmount the potential barrier existing between these traps and hence take part in the current process. This model [16] assumes that an electron in a π -molecular orbital on one molecule, when excited to a higher energy level (in our case by application of an external field at elevated temperature) can tunnel through a potential barrier to a non-occupied state of a neighbouring molecule. Traps are an essential part of the tunnelling model. It has been observed that the current-time curve is mainly due to the trap level closest to the Fermi level of the injecting electrode, whereas trap level which are deep and located well inside the band gap have been postulated. Deep traps have been reported [17] in corona charged samples which in fact may be ion traps. The lack of substantial evidence on the presence of deep traps may be due to an inhomogeneous distribution leading to a weaker concentration of deep traps in the bulk as indicated by Davies [11].

The tunnelling model points to a field which is directly proportional to the isochronal current. Here, the isochronal current at constant field is inversely proportional to the thickness. The current is strongly dependent on the electrode material and is independent of the temperature. The current is dependent on time as $I \propto t^{-n}$ with $0 \leq n \leq 2$.

3.4 THEORY OF TRANSIENT CURRENT IN POLAR DIELECTRICS

When an electric field is applied to a dielectric specimen kept between two plane metal electrodes, an absorption current flows in the external circuit. This current is composed of two components namely the polarization current component and the conduction current. Assuming that the polarization is due to dipoles of a single relaxation frequency $\alpha(T)$, the polarization current can be written as

$$\frac{dP_s(t)}{dt} + \alpha(T) P_s(t) = \epsilon_0 (\epsilon_s - \epsilon_\phi) \alpha(T) E \quad \dots (3.1)$$

where T is the absolute temperature, t is the time, ϵ_0 is the permittivity of free space and ϵ_s and ϵ_ϕ are the static and high frequency dielectric constants, respectively. The density of current generated by decay in polarization is given by

$$i_p(t) = \frac{dP(t)}{dt} = -\alpha(T) P_s(t) + \epsilon_0 (\epsilon_s - \epsilon_\phi) (T) E \quad \dots (3.2)$$

the conduction current i_c at a fixed temperature T and field E is defined as

$$i_c = \sigma(T) E \quad \dots (3.3)$$

where $\sigma(T)$ is the conductivity of the material at a fixed temperature T . Thus, the total absorption current will be the sum of both the components, i.e.,

$$i_{ab} = i_c + i_p(t) = \left[\epsilon_0 (\epsilon_s - \epsilon_\phi) \alpha(T) + \sigma(T) \right] E - \alpha_s P_s(T) \quad \dots (3.4)$$

The desorption current is obtained when the sample is short circuited and the field is made zero. Thus, from eq.(3.2) we have

$$\frac{dP_s(t)}{dt} + P(t) \alpha(T) = 0 \quad \dots (3.5)$$

where $\alpha(T)$ is a time dependent parameter. The above equation is a differential equation with constant coefficients. Its isothermal solution can be written as

$$p_s(t) = p_o \exp \left[- \int_0^t \alpha(T) dt \right] \quad \dots (3.6)$$

The current generated during deorientation of dipoles is only due to polarization. There is no conduction current since the external field is zero. The desorption current is thus given by

$$i_d(t) = - \frac{dP_s(t)}{dt} = \epsilon_0 E f(t) = \left[\alpha(T) P_o \exp[-\alpha(t)t_o] \right] \quad \dots (3.7)$$

where E is the steady charging field, $f(t)$ is the dielectric response function, P_o is the initial polarization and $\alpha(T)$ is the dielectric response loss peak in frequency domain.

Alternatively, this can also be expressed in terms of the frequency response of the complex dielectric constant, $\epsilon(\omega)$,

$$\epsilon(w) = \epsilon'(w) - i \epsilon''(w) (1+iw)^{-1} \quad \dots (3.8)$$

where, $\epsilon'(w)$ and $\epsilon''(w)$ are the real and imaginary part of the dielectric constant.

Thus, isothermal depolarization current measurements differ an alternative technique for dielectric constant and dielectric loss measurements as a function of temperature and frequency.

Frequency dependence of dielectric loss factor can also be obtained using Hamon's approximation [18], i.e.,

$$\epsilon''(t) = \frac{i(t)}{2 \pi f C V} \quad \dots (3.9)$$

where $i(t)$ is the magnitude of the transient current at time t , C is the geometrical capacitance of the electrode assembly without the sample, V is the applied step voltage and f is Hamon's frequency ($= 0.1/t$). This approximate method gives good accuracy in calculation of dielectric loss provided there is a broad distribution of relaxation times.

The time dependence of transient currents can be expressed according to the Curie-von-Scheidler [19] law expressed in the following form

$$i(t) = k t^{-n} \quad \dots (3.10)$$

In the optimum time range if the charging phenomena persists for a time t_p , then according to the principle of superposition, time dependence of the transient currents can be expressed by the following equation

$$i_d(t) \propto (T)(t) = i_p(t) - i_p[\alpha(T) + t] \quad \dots (3.11)$$

Using eq.(3.11) we have,

$$-i_d(t) \propto (T)(t) = -k t^{-n} \left[1 - \left\{ \frac{\alpha(T)}{(t+1)} \right\}^{-n} \right] \quad \dots (3.12)$$

which gives for $t \ll 1/\alpha(T)$

$$i_{d,\alpha(T)}(t) = -k t^{-n} \quad \dots (3.13)$$

and

for $t \gg 1/\alpha(T)$

$$i_{d,\alpha(T)}(t) = -n \alpha(T) k t^{-n-1} \quad \dots (3.14)$$

where $0 < n < 1$.

3.5 LAST DECADES'S WORK

Transient charging and discharging currents in dielectrics have been studied extensively. Dasgupta and Joyner [20-22] observed the transient charging and discharging currents in polypropylene and PET films over a wide range of temperatures and electric fields as a function of electrode materials and sample thicknesses. Vanderschuren and Linkens [23] measured the transient charging and discharging currents in several polymers from room temperature to the glass transition temperature and the effect of varying parameters such as field strength, electrode material, sample thickness, method of polymer preparation and addition of impurities was investigated in some of them. The absorption currents in polystyrene (PS) and its donor-acceptor complex with chloranil (PS-CA) and in a blend of polycarbonate and polypropylene have

been observed [24,25]. Transient currents were measured in discharging [26] and charging mode [27] with ethyl cellulose foil samples. Ranjeet Singh and S.C.Datt [28] have also reported transient currents in polypropylene and concluded that the observed currents are governed by charge injection processes leading to space charge effect. Charging transient currents on ethyl cellulose foil samples have been measured by Dubey et al [29]. Transient (charging and discharging) currents in polyvinyl alcohol-polyvinyl pyrrolidone polymer blend films and polyethylene terephthalate were measured as a function of temperature, field strength and electrode materials by LakshmiNarayan et al [30] and Neagu and Neagu [31]. Recently, Khare [32,33] and his co-researchers [34-43] measured charging and discharging transient currents in various polymers as a function of electrode materials, sample thicknesses, poling fields and results have been interpreted on the basis of available theories.

3.6 THE ELECTRICAL CONDUCTION

The electrical conduction in polymeric dielectrics is mainly due to transport of free charge carriers present in the bulk of the polymer and from a number of different conduction processes taking place simultaneously depending upon the experimental conditions. The structure of these materials are sensitive to their electrical, mechanical and thermal history so that the mode of conduction differs from polymer to polymer and the sensitivity of measurement is different for different

materials. When a polymer is subjected to different conditions they often undergo structural transitions making charge carrier generation and transport phenomenon more complicated. No universally accepted theory has been propounded till date which can explain the conduction phenomenon in all the polymeric dielectrics. However, attempts have been made to explain the observed conduction behaviour on the basis of various existing theories.

Many workers have tried to explain the dark conduction in polymers in their own way, such as traps and their energy distribution [44-46], tunnelling of charge carriers [47-50], Schottky emission [51-55], avalanche breakdown [56], etc. Still, despite inconsistencies in understanding the conduction mechanism, one can conclude on the basis of various studies reported in the literature that some of the phenomena occurring during electrical conduction in polymers are similar and have physical origin similar to those observed in solids of poor electrical conductivity.

In general, polymers are amorphous or semicrystalline substances. The transport mechanism in amorphous bodies is more complicated than the crystalline materials, especially for monocrystals where long range order exists. Thus, the charge transport mechanism in dielectric solids can be better understood from modifications applied to the quantum mechanical band theory of solids. Hence, band model of disordered materials has some of the gross features of that of

crystalline structure, but with significant differences concerning details. Electronic conduction may be due to the motion of free electrons in the conduction band or holes in the valence band or alternately due to the motion of quasi localized carriers.

If the concepts of band model are applied directly to organic solids, a very large energy gap between valence and conduction bands is expected, so that thermal activation in the normal temperature range is too small to transfer an electron from the valence band to the conduction band.

In amorphous substances, there are many localized charge carrier levels and carrier mobility is very low. The low lying states may be treated as trapping sites (levels) but in comparison with crystalline substances they are not related to the discrete activation energy values because they are situated in the broadened edges of conduction band and valence band. Hence, it is difficult to consider the transport behaviour of polymers in terms of a generalised theory. It is, therefore, not surprising to see controversies on transport theories in the literature [57-63] or no single mechanism is able to explain the entire conduction in these materials. However, the theories proposed for amorphous and polycrystalline inorganic solids are normally applied to describe the conduction behaviour of these materials with a few limitations.

3.6-1 GENERATION OF CHARGE CARRIERS

Most of the materials reveal in dark an exponential temperature dependence of conductivity (σ) of the form,

$$\sigma = \sigma_0 \exp(-A/kT) \quad \dots (3.15)$$

where A is the activation energy, k is the Boltzmann constant and T is the temperature. This led the earlier workers to assume that carriers are intrinsic in nature and hence they equated the experimental activation energy to half the band gap.

The resistivity of polymers is high because both the mobility and carrier concentration are low. The concentration of carriers produced intrinsically by thermal ionization is also very low since the band gaps are several electron volts. Hence, it seems more likely that ionization of impurities is responsible for any outstanding concentration of carriers. Impurities may also provide carriers by internal field emission in the presence of gross doping.

The charge carrier generation through the injection of electrons and holes from the electrodes has been widely accepted and this is probably the main source of carriers in high polymers. It is important to note here that the carrier density within the material should be much greater than the material being treated, i.e., the contact should act as the reservoir of carriers. Carriers once injected have appreciable mobilities and life times. Several workers have studied the

injection of charge carriers in polymer [64-66]. Hofman [67] has shown that conduction in atactic polystyrene (PS) depends on the injection of excess of electrons from metals. Davies [68] studied injection in polyvinyl fluoride and has shown that injection continues for a long time and for both polarities of applied potentials, although some asymmetry is indicated.

Despite a great deal of work done, there are still plenty of unanswered questions about the origin of free charge carriers, which take part in conduction under electrical stream. It is still not evident whether the measured current is by the motion of charge carriers inherent to the polymers or those injected from the electrodes. Adamec and Calderwood [69] measured current in polymethyl methacrylate (PMMA) under two conditions; first when the specimen was in direct contact of the electrode, and second when an insulating air gap was present between the specimen and electrode. The finding that the conductivity determined by the experiment with contactless electrodes is the same as that obtained with evaporated electrodes supports the contention that the free charge carriers originate in the bulk of the polymeric dielectric.

Doping of polymers with donors and acceptors and blending of two or more polymers increases/decreases the conductivity by several orders of magnitude and also modifies the charge carriers response for conduction.

3.7 MECHANISMS RESPONSIBLE FOR CONDUCTION

Some important conduction mechanism are now discussed briefly :-

3.7-1 OHMIC CONDUCTION

Ohmic conduction is attributed to a linear relationship between the conduction current and applied voltage at a constant temperature. The value of ohmic conductivity in polymer dielectric is given by :

$$\sigma = e (n_+ \mu_+ + n_- \mu_-) \quad \dots (3.16)$$

where μ_+ and μ_- are trap modulated mobilities and n_+ and n_- are the concentrations of positive and negative charge carriers, respectively. Because of large energy band gap in polymers, the charge carriers concentrations, i.e., n_+ and n_- are very small as long as radiation effects are absent. The mobilities μ_+ and μ_- are also very small in electret forming materials. Thus, the ohmic conduction current can be regarded as a universal source of conduction current in polymers. The origin of free charge carriers in PMMA and other polymers also indicate some possibility of intrinsic charge carrier conduction in polymer dielectric [70].

3.7-2 SCHOTTKY-RICHARDSON EMISSION AND POOLE-FRENKEL EFFECT

In the presence of an applied field barrier profiles are altered. If the applied field is high enough and the electrode makes ohmic current with the insulator, the charge carriers

are injected into the insulator by lowering of the barrier at the metal-insulator interface. This effect is referred to as the Schottky-Richardson (SR) emission.

The expression for current due to SR emission is given by [55],

$$I = ZST^2 \exp\left[\frac{-\theta_s}{kT} + \beta_{SR} E^{1/2}\right], \quad \dots (3.17)$$

where Z is the Richardson-Dushman constant ($120^\circ \text{ A cm}^{-2}$ in theory), S is the dielectric sample area, θ_s is the Schottky potential barrier, k is the Boltzman constant, T is the temperature and E is the applied field across the sample. β_{SR} is Schottky field lowering constant, which is given by

$$\beta_{SR} = \frac{1}{kT} \left[\frac{e^3}{4 \epsilon' \epsilon_0} \right]^{1/2}, \quad \dots (3.18)$$

where e is the charge on the electron, ϵ_0 is the permittivity of free space, ϵ' is the high frequency dielectric constant of the material.

The first term of eq.(3.17) shows a linear relationship between $\ln(1/T^2)$ and $(1/T)$ and the slope of the curve represents the Schottky potential barrier. Equation 3.17 also shows a linear relationship between $\ln I$ and $E^{1/2}$ with a slope β_{SR} for a given temperature.

Apart from the Schottky-Richardson emission [71], the linear dependence of $\ln I$ on $E^{1/2}$ is also predicted by the Poole-Frenkel effect. If a charge carrier gets trapped in a Coulombic potential well, then it can be detrapped on lowering

of the trap depth by an applied electric field. The current due to the Poole-Frenkel [72] effect is given by,

$$I = ZST^2 \exp\left[\frac{-\theta_{PF}}{kT} + \beta_{PF} E^{1/2}\right], \quad \dots (3.19)$$

where β_{PF} is the field lowering constant and θ_{PF} is the trap depth, which is given by

$$\beta_{PF} = \frac{1}{kT} \left[\frac{e^3}{\pi \epsilon' \epsilon_0} \right] \quad \dots (3.20)$$

Thus from eqs. (3.20) and (3.19),

$$\beta_{PF} = 2 \beta_{SR} \quad \dots (3.21)$$

The main difference between the Poole-Frenkel and the Schottky-Richardson models is that in the former the conductivity is bulk-limited whereas in the later it is electrode-limited.

3.7-3 SPACE CHARGE LIMITED CURRENT (SCLC)

If the electrode-insulator contact is ohmic and the insulator is trap free, the accumulation of carriers near the electrode results in the space charge build up. Mutual response between individual charge limits the total charge injected into the sample. The resulting current is said to be Space charge limited current (SCLC).

A complete mathematical analysis of time-independent space-charge current is so complex that no explicit explanation has yet been obtained. Mott and Gurney [73] were the first to emphasize the importance of an injecting contact

between a metal and an insulator. The expression relating the current density J to the applied voltage V , for a trap-free insulator is given by,

$$J = \frac{q}{8} \epsilon_0 \mu \epsilon' \frac{V^2}{d^3}, \quad \dots (3.22)$$

where ϵ_0 is the permittivity of free space, ϵ' is the dielectric constant of the sample, μ is the dipole moment, d is the thickness of the sample and q is the elementary charge on the charge carrier.

If traps are present in the insulator, the space-charge-limited current is decreased by several orders. Rose [74] and Lampart [75] modified the theory of SCLC independently. Expression, given by Rose [74], for a trap dependent current density is

$$J = \frac{q}{8} \epsilon_0 \mu \theta \frac{V^2}{d^3} \quad \dots (3.23)$$

where θ is the ratio of trapped charge to free charge, and is called the trap limiting factor.

Assuming that the carriers are trapped at shallow traps of average depth E , that remain in the thermal equilibrium state with the concerned band, θ is given by,

$$\theta = \frac{n_{\text{eff}} \exp(-E_r/kT)}{N + n_{\text{eff}} \exp(-E_r/kT)} \quad \dots (3.24)$$

where n is the density of states in the conduction band and N is the density of traps.

Assuming $N \gg n_{\text{eff}} \exp(-E_r/kT)$, θ becomes,

$$\theta = \frac{1}{N} \left[n_{\text{eff}} \exp\left(-\frac{E_r}{kT}\right) \right] \quad \dots (3.25)$$

and,

$$J = (q/8) n_{\text{eff}} \exp\left[-\frac{E_r}{kT} - \frac{\epsilon_0 \epsilon \mu V^2}{Nd^3}\right] \quad \dots (3.26)$$

Deviation from eq.(3.26) due to the dependence of the current density J on powers of V greater than 2 has been observed. This is explained on the basis of existence of deep traps and continuous distribution of trapping sites in the forbidden gap. Space charge limited currents (SCLC) in solids depend on the carrier transport and trapping and is independent of carrier generation. The fact that only very few organic solids show ohmic conduction has led to the belief that the conduction in organic solids is mainly extrinsic.

3.7-4 IONIC CONDUCTION

Ionic conduction occurs in materials which contain ionic groups or to which ionic materials have been added. In these materials, adsorption of water plays a dominant role because it can act as a source of ions, as a high dielectric impurity or as a local structure modifier. In amorphous polymers, ionic conduction can also occur due to the drift of defects on the application of an electric field. In various polymers, particularly those with halogens in their molecular structure conduction has been proved to be qualitatively ionic. Based on a model of diffusion of lattice defects or ions and a carrier hopping process [76], the expression for steady state current (I_s) at high fields is given by,

$$I_s = I_o (-A/kT) \exp(e^* \cdot L/kT), \quad \dots (3.27)$$

where L is the hopping (jump) distance and A is the activation energy. Eq.(3.27) show a relationship between $\ln(I)$ and A.

Ionic conduction is characterized by a high activation energy, noticeable polarization and a large transit time for ions. For materials with defect centres, the ionic conduction also exhibits different slopes in $\ln(I)$ vs $(1/T)$ or the $\ln(I/T^2)$ vs $(1/T)$ plots [77]. Activation energies are larger at higher temperatures than at lower temperature.

Studies of the structure of the polymer its physical and chemical properties and electrical properties will characterise the polymer and given an insight into the various mechanisms responsible for the different properties exhibited by it. Here an attempt has been made to characterise the polymer, polyvinyl formal, in thin film form.

3.8 LAST DECADE'S WORK ON D.C. ELECTRICAL CONDUCTION

The studies of electrical conductivity of these polymer films would enable us to understand their behaviour with temperature and the nature of conduction mechanism prevalent in them. A number of workers have investigated the nature of conduction mechanisms in a variety of polymers. Excellent reviews dealing both theoretical and experimental results have appeared in the literature [78-81]. A brief review of the work reported in the literature is given below.

Bashara and Doty [82] studied the current voltage characteristics and resistivity measurement in very thin polybutadiene films of thickness range 100 to 500 Å. It was found that the space charge limited conduction mechanism was the dominant mechanism in their films. It was also observed that the tunnelling takes place through the interface partly.

Lengyel [83] studied the voltage-current characteristics and conductivity measurements of polyethylene-terephthalate and polyvinyl formal films prepared by vacuum evaporation method, in the temperature range 40 C to 120 C. The above two material films displayed the familiar Richardson-Schottky characteristics for fields between 20 to 200 kV/cm and temperatures 25 to 100 C.

Lilly et al [84] studied the high field (2-1400 kV/cm) conduction in Mylar and teflon films of thickness ranging from 1 to 10 mils as a function of temperature (70-163 C). In the above films, the Schottky theory was found to be responsible for conduction mechanism by two space charges, ionic and electronic, each dominant at a different field level.

Davies [85] studied the carrier transport in iodine doped polythene films which were sandwiched between two metal electrodes, the film thickness was approximately 1 mm. It was observed that the presence of iodine increases the carrier mobility over the pure film.

Babcock and Christy [86] studied the electrical capacitance, conductance and photo conductance of tetramethyl tetraphenyl trisiloxane thin films of thickness 150 \AA formed by electron bombardment, on glass substrates in the sandwich configuration. They have successfully explained the conduction mechanism by field assisted thermal ionization of donors heavily compensated by acceptors.

Gupta and Barbarez [87] measured the D.C. conductivity of polyethylene films over a thickness range $25\text{-}75 \text{ }\mu\text{m}$ in sandwich configuration. The results were applied to a model proposed by Adachi et al [88] and good agreement was found between experimental results and the model.

Gazso [89] studied the variation of electrical conduction with applied voltage in vacuum deposited polyethylene films of 2000 \AA thick, in the sandwich configuration. He also studied the effect of irradiation by gamma rays on the conduction of polyethylene films.

Boonthanom and White [90] studied D.C. and A.C. electrical conductivities in the polyethylene polymer films with copper dispersed in its matrix. They observed the large increase in electrical conductivity due to doping with copper. The results were explained by the mechanism of hopping traps in localised states close to fermi level.

Kryzewski and Swiatek [91] studied the current voltage characteristics of polyvinyl carbazole and polystyrene films prepared by glow-discharge method. The studies were made over a temperature range 290-373 K. They found that above room temperature, conduction was controlled by surface limited and bulk limited depending on the electrical field strength.

Suzuki et al [92] studied the electrical conductivity and Hall effect on vacuum deposited thin films of polyacronitrile and made them semi-conductive by heat-treatment in nitrogen atmosphere. The results suggested that the conduction should be understood in terms of hopping transport of charge carriers in the localised states.

Rastogi and Chopra [93] studied the current-voltage characteristics of pure and iodine doped polyvinyl chloride thin films prepared by solution growth technique, both in sandwich and surface configuration over a temperature range 120-400 K. In the case of pure films, the conduction was ascribed to hopping mechanism at low temperatures and at high fields and at high temperatures to Schottky emission mechanism. The electrical resistivity of polyvinyl chloride films decreases considerably by the addition of iodine. They also found that the activation energy depends upon the type of configuration in which the studies were made.

Vollmann and Poll [94] studied the current-voltage characteristics at thin polymer fluoro-carbon films with

thickness between 0.02 and 1.5 μm deposited by different methods and with different contact materials. They observed the uniform conduction mechanism over the entire field strength not depending upon the method of preparation and the contact materials. The results were interpreted by means of a modified Poole-Frenkel effect for insulators with high impurity density.

Desbarax et al [95] studied the electrical conductivity of polysiloxane thin films formed by glow-discharge method. They observed that in the steady state, Poole-Frenkel mechanism seems to be mainly responsible for the conduction.

Mahendru et al [96] studied the electrical conduction in polypropylene films and found that the Schottky field assisted by thermionic emission was the dominant conduction mechanism in the temperature range 390-440K.

Electrical conductivity studies in pure and iodine doped polyvinyl acetate films were made by Mahendru et al [97]. They prepared the films by solution growth technique and studies were made in the sandwich configuration. The electrical conductivity of polyvinyl acetate films was found to be increased by large amount due to doping of iodine. The results were interpreted in terms of Poole-Frenkel charge transfer mechanism.

Gupta et al [98] carried the conductivity measurements of pure and doped polyvinyl fluoride thin films, prepared by

solution growth technique, whose thickness was about 50 μm . Conductivity measurements on pure and doped PVF films in the temperature range 300-500K have been reported. Here, vanadyl ions were found to affect the mode of conduction in the PVF matrix by contributing two additional activation energies of conduction. In unannealed films, the conduction was a thermally activated process while in annealed films the conduction was the combination of more than one thermally activated process.

Jain et al [99] studied the temperature dependence of electrical conductivity of solution grown films of pure and doped polyvinyl alcohol. The thickness of these films was of the order of 100 microns and they were doped with different impurities, viz., CuSO_4 , CuCl_2 , FeCl_3 , ZnCl_2 , NaCl and rhodamine. These impurities found to affect the electron traps in the forbidden band of dielectric and modulate the current flow.

Phadke et al [100] studied the electrical conduction mechanism in polyferrocene films prepared by plasma polymerization. They found that space charge limited conduction was the dominant mechanism.

Hanscomb and Kaahwa [101] studied the high temperature electrical conduction in polyethylene terephthalate in the temperature range 10-180 C at field strengths extending to $2.4 \times 10^8 \text{ V m}^{-1}$. The data was found to be well fitted to electronic or hole, Poole-Frenkel conduction or ionic

conduction resulting from field assisted dissociation of protons.

Takai et al [102] studied the high field conduction in poly(p-xylylene) thin films. The dark currents under fields upto 6 MV/cm were investigated for a poly(P-xylylene) film with Au and Al as electrode materials.

Audenaert et al [103] studied the D.C. electrical conductivity of poly(2-vinyl pyridine)-iodine films of thickness 80-100 μm as a function of iodine concentration and temperature in the range 200-300K. The electrical conduction mechanism was governed by electronic hopping between random localised states.

Rao and Chopra [104] investigated the electron transport properties of Cu doped polyvinyl chloride films. D.C. conductivity, A.C. conductivity, dielectric relaxation and thermally stimulated discharge current measurements were made on Cu doped PVC films as function of Cu concentration upto 12%. The results were explained in terms of tunnelling mechanism. The A.C. conductivity of these films favoured the hopping conduction.

The electrical properties of thin films of glow discharge polymerized hexamethylcyclotrisilazane were investigated by Tyezkowski et al [105] in order to determine the mechanism of electrical conduction. The I-V characteristics were studied at room temperature and

measurements of activation energy were made in temperature range 300-370K. The results of field dependence, temperature dependence and film thickness on the conductivity supported by the results of TSC measurements, suggested electrode limited conduction in the material investigated.

Staryga and Swiatek [106] studied the electrical conductivity of polycrystalline p-terphenyl films as a function of electric field, temperature and film thickness. The experimental data was interpreted in terms of hopping process between localised sites through potential barrier lowered by the electric field according to the modified Poole-Frenkel equation.

Bahri and Singh [107] investigated electrical conduction mechanism in the metal-polyvinyl chloride (1500 Å)-metal sandwich structure using Al, Ag and Cu electrodes. Two kinds of switching properties were found. The symmetric sandwich with Al electrodes exhibited voltage controlled negative resistance (VCNR) with memory, while asymmetric structures displayed current controlled negative resistance (CCNR) with memory. The VCNR mechanism was explained on the basis of high field domains and the CCNR phenomenon was explained on the basis of filamentary model.

Sawa et al [108] studied the electrical conduction mechanism in polypyromellitimide films in the temperature range 120-180 °C as function of electric field. An attempt was

made to fit the experimental results to the theoretical values for the ionic hopping conduction.

Miyairi and Ieda [109] observed new type of I-V characteristics in polyethylene terephthalate films of thickness $6\text{ }\mu\text{m}$ as function of different electrode materials. In the case of Au electrodes, two current peaks were observed around 5V and 20V at higher temperatures 160 and 170 C, whereas in Al electrodes single peak was observed at 160 C.

Kulshrestha and Srivastava [110] studied the electrical conduction of solution grown polystyrene films of thickness about $15\text{ }\mu\text{m}$ in the field and temperature ranges of about 6×10^5 to $3 \times 10^7\text{ Vm}^{-1}$ and 300-400 K respectively. The results showed that the Poole-Frenkel (PF) mechanism as modified by Jonscher and Ansari was the dominant conduction mechanism.

Bahri and Singh [111] studied the conduction mechanism and I-V characteristics of pure polyvinyl chloride films of thickness range 500-1500 \AA obtained by the isothermal immersion technique. The conduction process was examined in a broad temperature range 260-507 K, with applied electric fields ranging from 4.6×10^5 to $1.5 \times 10^7\text{ V cm}^{-1}$. At low temperature (below 325K) and at high fields ($> 1.5 \times 10^6\text{ V cm}^{-1}$) the current transport was ascribed to a tunneling mechanism. At high temperatures (above 325K) and at high fields ($> 1.5 \times 10^6\text{ V cm}^{-1}$) it was concluded that although the analytical form of I-V characteristics was similar to that obtained for both

Schottky emission and Poole-Frenkel effect the experimental value of β_{exp} was incompatible with the theoretical values of β_{RS} or β_{PF} . The resistivity of the PVC films was about $10^{13} \Omega \text{ cm}$ at room temperature and at a field of 10^7 V cm^{-1} . The activation energy was 0.60 eV at temperatures above 325K and at a field $1.5 \times 10^6 \text{ V cm}^{-1}$. Finally the annealing of PVC films at temperatures around 500K resulted in increased resistivity.

Cros-Lee Gloan and St-Onge [112] studied the electronic conduction in polyethylene films in a high electric field. A study was made on the effects of applied voltage, temperature, electrode materials and polyethylene density. The results were interpreted in the light of existing physical models of space charge and electron trapping.

The electrical conduction of Nylon was studied by Nakamura et al [113]. The results were interpreted in terms of the migration of a fixed number of ions existing in the polymer towards counter electrode. Lipinski et al [114] studied the electrical conductivity of p-terphenyl TCNE structures. The increase in conductivity by two orders was explained by the existence of charge transfer complex formation. Sharma and Pillai [115] studied the electrical conduction in kapton polyimide films at high electric fields and results were interpreted in terms of ionic conduction. Bahri [116] studied the D.C. electrical conduction in pure and iodine doped polystyrene films and the results were interpreted on the

basis of charge transfer complexes. The effect of iodine on electrical conduction in polyvinyl fluoride films was studied by Chand et al [117] and the results were explained on the basis of charge transfer. Tyezkowski et al [118] studied the Poole-Frenkel centres in dielectrics of plasma polymerized organosilicon films. Jayarama Reddy and Syrajuddin [119] studied the electrical conduction in pure and iodine doped polyvinylfluoride films. The results were explained on the basis of charge transfer between polymer and iodine. The D.C. electrical measurements on evaporated thin films of copper phthalocyanine was studied by Gould [120]. Lee et al [121] studied the conduction phenomenon of the polypropylene films. Four regions of conducting currents were observed and were attributed to ionic conduction a Poole-Frenkel region, a Schottky region and a negative resistance region. Kojima et al [122] studied the electronic conduction in polyethylene terephthalate at high electric fields. The results were explained by the impact ionization. The electrical conduction phenomena in polyimide (Kapton) films was studied by Sessler et al [123] with a particular attention to the separation of interface and bulk phenomena. The current-voltage characteristics were found to be ohmic at low fields while space charge characteristics were found to be ohmic at low fields and space charge limited at high fields.

Tawanski et al [124] investigated the D.C. electrical conduction in polyvinyl alcohol films. The ohmic type of

conduction was found to be operative below 303 K whereas space charge limited above 303 K.

Narasimha Rao et al [125] studied the electrical conduction mechanism in pure and doped polyvinyl formal films. The results were attributed to the Poole-Frenkel conduction mechanism. Das Gupta and Doughty [126] studied the dielectric and conduction processes in polyether ketones. It was suggested that several mechanisms may be relevant and may all be involved in the conduction mechanism in a complicated manner. Narasimha Rao and Kalpalatha [127] studied electrical conduction mechanism in polyvinyl pyrrolidone films. The results were interpreted in terms of Poole-Frenkel type conduction mechanism. Electrical conduction in polyacrylic acid was studied by Narasimha Rao et al [128] and two conduction regions were observed. Basha et al [129] studied the electrical transport in polyvinyl alcohol films containing transition metal halides. The transport of carriers was attributed to hopping mechanism between localized states.

Narasimha Rao and Subba Rao [130] studied the electrical conduction in polyacrylamide polymer films in the temperature range 300-450K and field strengths ranging from 0.48×10^6 - 24.1×10^6 V m⁻¹. The electrical conduction was explained as due to the simultaneous action of Richardson-Schottky and Poole-Frenkel mechanisms. Narasimha Rao et al [131] studied the electrical conduction mechanism in polyvinyl alcohol films in the temperature range 300-450K and was found Richardson

Schottky mechanism operating over the entire range. Sathyanarayana et al [132,133] studied the electrical conduction mechanism in polyacrylamide films.

3.9 EFFECT OF VARIOUS PARAMETERS ON ELECTRICAL CONDUCTION IN INSULATORS

The electrical conductivity has been found to vary with various experimental parameters. However, the extent and the nature of variation differs from material to material. A brief description about the variation of electrical conductivity with various parameters, in general, is as follows -

3.9-1 ELECTRIC FIELD

The dc conductivity has been found to increase with the applied electric field and is generally attributed to the Schottky-Richardson and Poole-Frenkel emissions. Kramer [134] have studied the field dependence of conductivity over a number of plastic films.

3.9-2 TEMPERATURE

The temperature dependence of the conductivity can be emphasized considering insulating and semiconducting behaviour of the materials. At absolute zero, most of the semiconducting properties are brought about by thermal excitation of trapped charges or thermally stimulated charge carrier generation. Therefore, a rise in temperature is always associated with an increase in conduction current.

Current-voltage or current-temperature curves are sometimes not identical during increase and decrease of the field or temperature. This type of hysteresis effect has been observed in case of carnuba wax, sugarcane wax, polyethylene and many other compounds. The temperature dependence of conductivity has been studied by various scientists. Conductivity variation with linear temperature increase has been studied by Adamec [135].

3.9-3 PRESSURE

DC conductivity has also been found to increase with pressure. Akamatu and Inokuchi [136] have found that the resistivity of the isoviolanthrone power decreases with pressure. Increase in conductivity followed by lowering of activation energy [137,138]. At highest pressure it was found to be about 6 times the atmospheric value. The pressure dependence of conductivity has been studied by many workers [139] and the materials studied include pentacene [140,141], ferrocene [142], and many other materials [143-147].

3.9-4 MOISTURE

Conductivity is also affected by the presence of moisture in the insulator. Inokuch and Shirotani [139] have studied in detail the effect of moisture on pellets of organic solids. Barker and Tomar [148] have reported that humidity affects the steady state conduction in two ways : first being

the increase in dielectric constant with the increase of humidity which gives rise to a net increase in ion concentration by reducing the effective dissociation energy and second being the increase in effective conductivity with moisture. At higher fields departure from the other law was observed as a result of activation perturbation. Increase in dc conductivity with humidity has also been studied by Manthia et al [149].

3.9-5 ELECTRODE MATERIAL

The conductivity is also affected by the electrode material as the metal-insulator contact plays a genuine role in deciding the various conduction mechanisms. The injection of holes or electrons from the electrode material to the insulator is governed by the electrode material and insulator work function. Effects of electrode material over electrical conduction in a large number of insulators have been studied by various workers [150-161].

3.9-6 IMPURITY

The presence of impurity content in the insulators has also been found to increase the conductivity of materials. The effect of impurity over electrical conductivity is so pronounced that the conductivity can be indicated as a characteristic of the sample purity. In the opposite way, the addition of limited impurity can be used to alter the dc conductivity in a desired proportion. It has been observed

that the conductivity always increases with dopants even when the dopants are more resistive to the host materials.

3.10 THERMALLY STIMULATED DISCHARGE CURRENTS (TSDC)

The thermally stimulated depolarization current (TSDC) is a general method for investigating the electrical properties of high resistivity solids via the study of thermal relaxation effects and as such offers an alternative scheme to the conventional bridge methods or current-voltage-temperature measurements. The method has special advantages of its own which are (i) conductivity does not interfere in the measurements, (ii) the motion of small chain segments whose processes have very low losses can be detected, (iii) since time and temperature can be and are simultaneously changed in TSDC methods, therefore, the phenomena which vary with time or temperature can be analysed, and (iv) low frequency behaviour of the dielectrics can be elucidated in a simple way.

The TSDC technique involves measuring with a definite heating scheme, the currents generated by the release of a polarized state in a solid dielectric sandwiched between two electrodes. We find that TSDC being used for studying the fundamental mechanisms of charge storage and release in non-metallic solids and hence the present stage of experimental and theoretical development of TSDC is such that we have a vast number of theoretical models formulated to clarify the experimental data obtained on various types of

charge storage mechanisms. But it can be seen that the proposed mathematical expressions rely on much simplified and unrealistic assumptions leading to similar descriptions of the polarization process. We find that the immeasurability of the microscopic parameters lead to glaring discrepancies between the propounded theory and the experimental data. It can be observed that one of the major problems of the measurements is to unequivocally determine the physical origin of the observed current peaks.

The microscopic origin of a given current spectrum is obtained by comparing the predictions of the general theories related to the main polarization process with the available experimental data. Workers in the field ascribe the polarization of a solid dielectric - subjected to an external electric field - to a number of mechanisms involving either microscopic or macroscopic charge displacement. The mechanisms are (i) electronic polarization resulting from the deformation of the electronic shell requiring about 10^{-15} seconds, (ii) atomic polarization occurring from the displacement in molecules with heteropolar bonds requiring 10^{-14} to 10^{-12} seconds, (iii) dipolar or orientational polarization which can occur in pico seconds or months and occurs in materials containing permanent molecules or ionic dipoles, (iv) or space-charge polarization which occurs in materials containing intrinsic free charges (ions or electrons or both) and can take place in millisecond or years, (v) interfacial

polarization also known as Maxwell-Wagner-Sillars (MWS) polarization happens in systems with a heterogeneous structure within the time range of millisecond to years [162]. The present thesis highlights the theories of dipolar, space-charge and MWS polarization with special emphasis on the much discussed dipolar mechanism.

The Thermally Stimulated Depolarization Current (TSDC) is an useful and powerful technique to understand charge storage and charge decay processes in electrets. Now-a-days this technique is being utilized widely to investigate the molecular relaxation mechanism, trapping parameters and charge storage behaviour of insulating materials including polymers. The method consists of mainly two parts : Polarization of a specimen under the specified conditions of electric field, and temperature for a stipulated period. The poled sample (Thermoelectret) is afterward depolarized through a current recording device under stimulation of linear heating.

As an inherent property of regaining charge neutrality, electrets discharge by means of various processes. Depending upon the nature of polymer electret, any one or two or even more than two processes can play a prominent role in the discharging process. In the electrets made from the polar materials, the disorientation of dipoles plays a prominent role. The disorientation of dipoles involves the rotation of a coupled pair of positive and negative charges, and requires a

certain energy which in solids may amount to a few eV per dipoles.

Often the disorientation energy (activation energy) differs for different dipoles (or charges). Therefore, the low activation energy dipoles respond at low temperature, while the high activation energy dipoles at high temperature. Consequently, TSC (thermogram) generally consists of many peaks. If the difference of activation energy is not large, these peaks overlap and merge into a broad peak (β -peak).

Such broad peaks are often seen as a result of disorientation of polar-side groups in polymers at low temperature. Another possible cause for the appearance of broad peak is a difference in the rotational mass of the dipoles. These differences occur in a polymer when it is heated to its softening temperature, where the dipoles are disoriented by the motion of main chain segments. This disorientation is responsible for the α -peak, which responds at glass-rubber transition temperature, T_g .

Polarization of dielectric can also occur due to any shift-of-ion from its equilibrium to a new position; the shift may be in the form of trapping at the position slightly away from their equilibrium position. Heating of dielectric provides activation of any such trapped ions to be detrapped and return to their original positions which results in the

decrease of total polarization in the form of a peak of TSDC thermograms.

In addition to dipoles and trapped ions, polarization appears in an electret (dielectric) in the form of nonuniformly stored immobilized space charges, usually stored densely near electrodes [163-165]. Heating mobilizes them, which results in neutralization of such mobilized ions either at electrodes or in the sample by recombination with charges of opposite sign. In general, at higher temperature field controlled self drift persuades driving (motion) of any such charges. Space-charge peaks (referred as β peaks) appear at high temperatures [163,165-168] because disorientation of dipoles, merely involves a flip from one position to other while neutralization of space charges requires them to move over many atomic distances. In polymers, at very high temperature (near and above T_g), the self motion of space charges usually is accompanied with a second neutralization mechanism; namely, recombination with thermally generated carriers. These carriers are generated uniformly in the entire specimen by dissociation of neutral entities. These carriers may be electronic or ionic in nature and are responsible for conductivity of material. In polymers these seem to be impurity ions which contribute most of the ohmic conduction, because polymers show an appreciable conduction only above glass-transition temperature when enough free volume is available for ions to move. In the TSD of shorted electrets it

passes completely unnoticed, the net conduction current being zero because there is no voltage across the sample.

Self motion of the space charges can be described in two ways. If the charges are ions, they are generally considered to be free to move with a thermally activated mobility. This can also be visualized as hopping from one vacancy to another across a potential barrier equal to the activation energy. If, however, the charges are electrons or holes, it is more appropriate to visualise them as being immobilized in local traps from which heating releases them into a band of energies in which they can freely diffuse to the electrodes.

In heterogeneous systems consisting of amorphous and crystalline phases, another kind of trapping known as interfacial trapping occurs [163,165-168]. The interfacial charges are due to difference in conductivity of phases. During polarization, these carriers will either accumulate or be depleted near a particular interface in the form known as Maxwell-Wagner effect depending on whether the incoming local conduction current is greater or smaller than the outgoing one. The difference in local conduction current are also responsible for the dissipation of the charges in the subsequent TSD, because the current then flow in the opposite direction.

Polarization in a dielectric also arises from charges injected from electrodes [162], when the material is

sandwiched between two electrodes bearing high electric field. Injected charges may either be trapped or form space charge. This injection takes place due to Richardson-Schottky emission of electrons or holes from the metal electrodes. Such charges can be captured in the dielectric at different sites. Perlman [169] based on his observation of TSDC of corona charged electrets containing no aligned dipoles, has classified the charge storage sites into three structural levels. The primary levels are atomic sites of molecular chains, secondary levels are the cages between adjacent molecules where charges can be trapped and the tertiary level trapping involves charge storage in the region where material changes its phase, i.e., interfaces. The charge released from the primary levels depend upon the motion of the group of atoms. The charge released from the tertiary level depends upon the main chain motion on their drift under space charge limited conduction [170-181]. Release of trapped charges takes place in two stages, first is detrapping while second is related with transportation of released ones.

The magnitude of the TSDC current depends on the charge retained by the electret. However, the time interval of current cannot be equal to the charge originally present, because all the decay processes do not contribute fully to the external current, e.g., charge neutralisation by ohmic conduction in shorted electrets does not contribute to the external current at all. Self drift of charges, particularly

when neutralization requires them to move over relatively short distances, is also an inefficient current generating process. Diffusion is likewise an inefficient current generating process. With ohmic electrodes the charges diffuse systematically outwards and no current is generated at all. The only process whose efficiency is 100% is the disorientation of dipoles.

3.11 TECHNIQUES AND THEORIES OF TSDC

Thermally stimulated decay of an electret can be studied by any one of the following four techniques -

- (i) Current TSDC with shorted electrodes,
- (ii) Current TSDC with an air gap,
- (iii) Charge TSDC by transferring the charge induced on the upper electrode to a sensitive electrometer, and
- (iv) Charge TSDC by field cancelling technique.

3.11-1 CURRENT TSDC WITH SHORTED ELECTRODES

The method was developed for bimetallized specimens by Freis [182] and subsequently successively applied by other workers. The particular name is derived from the fact that the voltage drop across the electrodes is zero. Owing to the virtual short circuit, the main electric field E_p and the mean ohmic conduction current within the electret are so small that only a displacement current makes observable influence. Therefore, the resultant external current is due to the image

charges escaping from the evaporated electrodes which are induced by dipoles and space charges.

3.11-2 CURRENT TSDC WITH AN AIR GAP

To study the decay of unilaterally metallized homoelectrets, Turnhout [176] has modified Freis method [182] by introducing an air gap between non metallized side of the specimen and adjacent metal electrode. When such a assembly is heated, a displacement current is generated by image charge released from the noncontacting electrodes as the air gap prevents the electret charges from recombining with the image charges of the upper electrode. Since, the electret itself is not shorted, the electric field within the electret is no longer zero and infact becomes quite large. Consequently, the ohmic conduction current flowing through the electret produces an appreciable displacement current, whereas it remains obscured in current TSD of shorted electrodes.

3.11-3 CHARGE TSD BY TRANSFERRING THE INDUCED CHARGE TO AN ELECTROMETER

Various methods have been developed to investigate charge TSD by employing an air gap between nonmetallized side of the dielectric and adjacent electrode. A common method is to move the nonadhering electrode periodically away in order to transfer the image charges induced on it to an integrating electrometer. However, no continuous record of the decaying charge can be obtained and hence it is difficult to determine accurately the temperature of the fastest decay.

3.11-4 CHARGE TSDC BY FIELD CANCELLING METHOD

Current TSDC measurements have been found to be unfavourable in case of one side metallized homoelectret foils for which the ratio between the air gap and electret thickness cannot be made small. In such a case, the decaying electret induces most of its image charge on the grounded adhering electrode instead of the probing electrode. A novel version of the air gap charge TSD developed by Turnhout [176]. The method which also allows a continuous monitoring of decaying charge is based on the field cancelling technique, according to which the external field of the foil is nullified by driving the noncontacting electrode with an adjustable bias voltage V_g of the same value and polarity as the equivalent voltage of the electret. Since the upper electrode in such a system is virtually floating, the external current is zero and hence the method is referred to as the charge TSD in open circuit.

The discharge of a shorted electret usually takes place either due to dipole relaxation or space charge relaxation. These two processes are described by separate theories which have been discussed in the following sections.

3.11-5 THEORY OF TSDC DUE TO DEORIENTATION OF DIPOLES

Consider a polar material containing N dipoles per cubic metre with a dipole moment P . The dipole will be oriented during the charging by field E , and produce a final polarization, P_o ,

$$P_0 = N P \sqrt{\cos \theta} \quad \dots (3.28)$$

where θ is the angle the dipole makes with the direction of the field. The alignment that is forced on the dipoles by the charging field E is counteracted by their thermal motion. For non interacting dipoles, i.e., when the dipolar concentration is sufficiently low, we have for the average orientation,

$$\cos \theta = \frac{\epsilon_0 P \epsilon}{3 k T} \quad \dots (3.29)$$

where ϵ is the dielectric constant of the medium, ϵ_0 is the dielectric constant of free space and T is the temperature.

During subsequent TSDC, the aligned dipoles will randomly deorient at a rate proportional to the number of dipoles still aligned. The polarization will, therefore, decay according to the Debye rate equation,

$$\frac{dP(t)}{dt} + \alpha(t) P(t) = 0 \quad \dots (3.30)$$

where $P(t)$ is the dipolar polarization at a given time t and $\alpha(t)$ is the reciprocal relaxation time or relaxation frequency which is assumed to be the same for all dipoles. The current density generated by the decay in polarization may then be expressed as

$$I(t) = - \frac{dP(t)}{dt} = -\alpha(t) P(t) \quad \dots (3.31)$$

where $P(t)$ follows from eq.(3.30) after integration

$$P(t) = P_0 \exp \left[- \int_0^t \alpha(T) dT \right] \quad \dots (3.32)$$

Since the temperature is raised linearly with time, the

current density may also be written as a function of temperature,

$$I(T) = -\alpha(T) P_0 \exp\left[-\int_{T_0}^T \alpha(T) dT\right] \quad \dots (3.33)$$

Here, h is the inverse heating rate dt/dT . Because $\alpha(T)$ is small at low temperature, the electret will retain its charge for a long time when stored at room temperature. During heating, $\alpha(t)$ increases strongly following Arrhenius equation,

$$\alpha(T) = \alpha_0 \exp(-A/kT) \quad \dots (3.34)$$

where α_0 is the natural relaxation frequency and A is the activation energy required to disorient a dipole.

The energy A can be considered as a potential barrier, which the dipole has to surmount before it can readjust its direction [174,183,184]. Equation (3.34) broadly applies to relaxations involving the rotation of small molecular groups. However, this equation fails in the case of major relaxations in polymers, which occur when the polymer passes from the glassy to rubbery state. This glass rubber transition involves the configurational rearrangement of various parts of long main chains. Their relaxation in this case obey Wagner-Landale-Ferry (WLF) equations [174,185-191].

$$\alpha(T) = \alpha_g \exp\left[C_1 (T-T_g) (C_2+T-T_g)^{-1} \right] (T>T_g) \quad \dots (3.35)$$

For most amorphous polymers

$$\alpha_g = 7 \times 10^{-3} \text{ s}^{-1}, \quad C_1 = 40 \text{ and } C_2 = 52 \text{ K.}$$

Often the activation energy of dipoles is not the same. Dipoles with low activation energy orient at low temperature

while those with high activation energy respond at high temperatures. Apart from the distribution in activation energy, there may be a distribution in rotational mass of dipoles which will then lead to distribution in the pre-exponential factor α , in eq.(3.34). These distributions are described by the following relations,

$$\alpha_i(T) = \alpha_o \exp(-A_i/kT) \quad \dots (3.36)$$

and

$$\alpha_i(T) = \alpha_o \exp(-A/kT) \quad \dots (3.37)$$

In the case of distribution in natural frequency α_o , the polarization is given by,

$$P(t) = P_o \int_0^\infty F(\alpha_o) \exp\left[-\alpha_o \int_0^t \exp(-A/kT) dT\right] d\alpha \quad \dots (3.38)$$

and in the case of distribution in activation energy, the same is given by,

$$P(t) = P_o \int_0^\infty g(A) \exp\left[-\alpha_o \int_0^t \exp(-A/kT) dT\right] dA \quad \dots (3.39)$$

where $F(\alpha_o)$ and $g(A)$ are the distribution function in natural frequencies and activation energies. These functions represent the contribution between $\alpha_o \rightarrow \alpha_o + d\alpha_o$ and $A \rightarrow A + dA$ to total dipolar relaxation strength $\epsilon_s - \epsilon_\infty$. Actually, they are relative contribution to $\epsilon_s - \epsilon_\infty$ because they are normalised, so that

$$\int_0^\infty F(\alpha_o) d\alpha_o = \int_0^\infty g(A) dA = 1. \quad \dots (3.40)$$

The corresponding expressions for TSDC are obtained by differentiation of Eq.(3.38) and (3.38),

$$i(t) = P_0 \exp(-A/kT) \int_0^\infty \alpha_0 F(\alpha_0) \exp\left[-\alpha_0 \int_0^t \exp(-A/kT) dT\right] d\alpha_0 \quad \dots (3.41)$$

$$i(t) = P_0 \exp \alpha_0 \int_0^\infty g(A) \exp\left[-(A/kT) - \alpha_0 \int_0^t \exp(-A/kT) dT\right] dA \quad \dots (3.42)$$

3.11-6 THEORY OF TSDC BY SELF MOTION OF CHARGES

Apart from the dipolar polarization, the polarization can also arise due to space charge formation in the sample. As we know that a dielectric never insulates perfectly, particularly, not at high temperature when an increasing number of thermal carriers are generated. During polarization these carriers move in the applied field and when the dielectric is cooled, some of them are trapped in various available traps existing in the sample. Owing to this process thermally formed electrets usually contain a space charge polarization. Space charges can also be injected from the electrodes, specially at high field strengths [163,166-168].

At low temperature the space charges remain frozen in, but when the temperature is raised, these charges get thermally activated and remobilized. During heating in short circuit these space charges move under the influence of the internal field of the electret, giving rise to thermally

stimulated discharge current in the external circuit. Some of the mobilized space charges move to the electret [174,166-168] and recombine with their image charges while some of them recombine with their counter parts within the electret.

In the case of space charge TSDC, the current obtained in the external circuit is thus given by,

$$I(t) = C \exp(-A/kT) - (\beta\tau_0)^{-1} \int_{T_0}^T \exp(-A/kT) dT \quad \dots (3.43)$$

where A is the activation energy, C is a constant, β is heating rate, k is the Boltzmann constant and τ_0 is the pre-exponential factor of relaxation time.

3.12 EFFECT OF DIFFERENT FACTORS ON TSDC SPECTRA

(a) Polarizing Field (E_p) :

In order to form electrets, specimen is subjected to electric field, known as polarizing field E_p . In the TSDC spectra, the peak due to dipolar or volume polarization increases linearly with E_p , whereas the space charge polarization varies non linearly with polarizing fields [192].

(b) Polarizing Temperature (T_p) :

The temperature at which sample is polarized, is polarizing temperature. The polarizing temperature T_p affects the position and magnitude of peak current significantly. For a process with single relaxation time, the peak in the TSDC spectra remains unaltered while its magnitude increases with

increasing (T_p). In a distributed relaxation process, both the position and magnitude of peak current depend on T_p .

(c) Polarizing Time (T_p) :

The position and intensity of peak current in the TSDC spectra depend on the polarizing time. According to Turnhout [140], (T_p) should change logarithmically to obtain charges of the same magnitude as with the charge of T_p .

(d) Electrode Material :

Effect of electrode material on TSDC spectra of thermoelectrets has been studied and it has been shown that a good correlation exists between the charge acquired by the thermoelectret and the work function of the metal electrode used during polarization [193,194-196]. Shrivastava et al [193] studied effect of electrode material on TSDC of poly(styrene) (PS) films and concluded that the first stage of charging of PS films, as a result of contact with the metal, is charge injection which decreases with the increase in metal work function. The second stage is entrapment of these charges in the border layer. Mahendru et al [196] observed that thermally stimulated discharge current is negative with electrode metals of lower work function, whereas it is positive when the metals used as electrodes are of higher work function during the depolarization of identically polarised specimen of poly(vinyl acetate).

(e) Specimen Thickness :

The charge on an electret has been found to depend upon its thickness [197].

(f) Heating Rate :

When the heating rate is slow, the polymer responds sooner in giving a current at a lower temperature. Its intensity is lowered by a factor equal to the ratio of the increase in heating rate. The current is decreased because the final charge released is the same. The peak temperature and heating rate are related according to the following equation for dipolar relaxation processes,

$$\tau = \frac{kT_m}{\beta A_a}$$

where k is the Boltzmann's constant, T_m is the peak temperature, β is the rate of heating, A_a is the activation energy and τ is the relaxation time at peak temperature.

Variation in heating rate provides information regarding the nature of traps and type of relaxation mechanisms in an insulator. This method has been recently exploited by a large number of workers [198-201].

(g) Impurity

Whenever, a polymer matrix is impregnated by an impurity, a Charge Transfer Complex (CTC) is formed. CTC formation sometimes changes the structure of polymer. The magnitude and shifting of a current maximum has been observed by many workers in polyethylene [202-204].

(h) Humidity

Humidity also affects the TSDC thermogram. At different pH values the absorption of moisture is different. Some polymers form complexes also with water [205].

3.13 EVALUATION OF TSDC DATA

3.13-1 ACTIVATION ENERGY

Now, we discuss the various methods for evaluation of activation energies from the observed TSDCs thermograms.

(A) INITIAL RISE METHOD

In this method, suggested by Garlick and Gibson [206], the activation energy A is obtained from the straight line portion of $I(t)$ vs $1/T$ curves in the range where the TSDC current rises initially.

If we differentiate the TSD current over initial rising part with respect to $1/T$, we have

$$\frac{d \ln I(t)}{d(1/T)} = - \frac{A}{k} \quad \dots (3.44)$$

(B) BUCCI-FIESSHI AND GUIDI (BFG) METHOD

According to this method [207], the activation energy A can be calculated from the relation

$$\alpha(T) = \frac{I(t)}{P(t)} = \frac{I(t)}{\beta} \int_T^{\infty} I(t) dT \quad \dots (3.45)$$

where $\alpha(T)$ is the reciprocal relaxation time of relaxation

frequency, β is the heating rate and T the absolute temperature.

(C) HALF CURRENT PEAK-WIDTH METHOD

Using this method, the activation energy A can be evaluated from the relation

$$\frac{\Delta T}{T_m} \approx 2.47 \frac{k T_m}{A} \quad \dots (3.46)$$

where ΔT is the half width of the current peak and T_m is the peak temperature.

(D) HEATING RATE VARIATION METHOD

Activation energy can also be estimated by changing the heating rate of the electret. If heating is changed, the activation energy can be deduced by observing the shift of the peak temperature from T_1 to T_2 . On differentiating Eq.(3.42) we find that the current maximum occurs when

$$\frac{d}{dT} \left[\frac{1}{\alpha(T)} \right] = -\beta \quad \dots (3.47)$$

which, for an Arrhenius type d-T relation, transforms into

$$\frac{\alpha(T_m) \beta k T_m^2}{A} = 1 \quad \dots (3.48)$$

For the two heating rates, we then have

$$\beta_1 T'_1 \alpha(T_1) = \beta_2 T'_2 \alpha(T_2) = \text{constant} \quad \dots (3.49)$$

If the heating rate is changed more than twice, it is advantageous to find A from βT_m^2 vs $1/T_m$ plot [208]. Such a plot need not be based solely on the TSDC maxima. The other points of the TSDC peaks may also be involved. This is done in the method suggested by Solunov et al [209,210].

3.13-2 RELAXATION TIME (τ_0)

The low temperature tail of equation 3.43 is given by

$$\log i(T) = \text{Const} \left(- \frac{A}{kT} \right) \quad \dots (3.50)$$

Thus, from equation (3.50) the activation energy A of the discharge process responsible for the peak can be obtained from a plot of $\log I$ versus $1/T$.

On differentiating equation (3.43) with respect to temperature and equating it to zero $\left(\frac{di}{dT} = 0 \right)$, one obtains the temperature (T_m) where maximum current occurs. T_m is given by -

$$\tau_0 = \frac{k T_m^2}{\beta A \exp \left(\frac{A}{kT_m} \right)} \quad \dots (3.51)$$

Finding T_m from current versus temperature plots, one can calculate τ_0 . Knowing τ_0 we can easily calculate the relaxation time at T_m and at any temperature, i.e.

$$\tau(\tau_m) = \tau_0 \exp \left(\frac{A}{kT_m} \right) \quad \dots (3.52)$$

Calculations of $\tau(\tau_m)$ from equation (3.52) requires the value of τ_0 one can, however, calculate $\tau(\tau_m)$ without knowing τ_0 . From equation (3.51), we have

$$kT_m^2 = \beta A \tau_0 \exp \left(A/kT_m \right)$$

$$= \beta A \tau(\tau_m)$$

$$\text{or } \tau(\tau_m) = \frac{k T_m^2}{\beta A} \quad \dots (3.53)$$

Knowing T_m from experimental plots $\tau_{(\tau_m)}$ can be obtained directly from 3.53.

3.13-3 CHARGE RELEASED (Q)

Charge released (Q) during the discharge was calculated by integrating the current versus temperature/time curves using Simson's rule.

3.14 LAST DECADE'S WORK ON TSDC

Polymers are generally good dielectrics which are capable of storing the charge in them permanently when subjected to field temperature treatment. Such dielectric materials bearing persistent charge are called thermoelectrets. When thermoelectrets are subjected to a programmed heat treatment, they give rise to a current in the external circuit and this is called thermally stimulated discharge current (TSDC). Thermally stimulated discharge current technique is a convenient and sensitive method for studying the charging and discharging process in dielectrics. These currents are due to dielectric relaxation behaviour and motion of free charges in the polymer. Hence the TSDC technique can be used to understand the low frequency dielectric relaxation in solids and the relaxation between dielectric behaviour and process on the atomic scale. Because of the high sensitivity of this technique, it is also used to investigate the low concentration of dipolar impurities,

formation and aggregation of impurity vacancy complexes, phase transitions, photographic response of silver halides etc.

Studies on thermoelectrets started as early as 1922 by Eguchi on Carnuba wax. Since then various dielectrics both plastic and ceramics have been studied extensively by different workers. Excellent reviews on this subject both theoretical and experimental have appeared in the literature [211]. Some of the work recently reported in literature on polymer thermoelectrets is briefly reviewed below to get a comprehensive picture of the present state of research on this subject.

Thermally stimulated discharge currents (TSDC) in carnuaba wax electrets were studied by Perlman [212] using a linear heating rate for various polarizing fields, temperatures, times and thicknesses of the sample. Three peaks were observed at 47, 59 and 69 C respectively. Microscopic displacement of ions with trapping was proposed as the possible mechanism for the TSDC.

Caserta and Serra [213] have made simultaneous measurements of current voltage characteristics, isothermal discharge currents and thermally stimulated discharge currents to determine the mechanism of formation of electrets in carnuaba wax. Homocharge from the electrodes and hetero charge with the material are found to be responsible for TSDC.

The electret effect in shellac wax was investigated by TSD current (TSDC) by Pillai et al [214] prepared under different polarizing conditions. They observed only one peak for the TSDC spectra. They have attributed the TSDC spectra to the dipolar orientation and microscopic displacement of charges with trapping.

Jain et al [215] studied TSD currents in solution grown polyvinyl butyral films as a function of the polarization field (750 to 25000 V/cm) and iodine dopant concentration. Polarized PVB films exhibited two glow discharge peaks one at 350K (β) and the other at 430K (α) corresponding to activation energies of 0.19 and 0.53 eV respectively. It was observed that the β -peak disappeared at low polarizing fields (750 V/cm). The α -peak was attributed to the depolarization of the aligned dipoles connected to the main chain whereas the β -peak due to the local motion or twisting of the side groups connected to main chain. On doping with iodine, both un-polarized and polarized films exhibited TSD currents. This is attributed to the formation of charge complexes.

Mahendru et al [216] studied TSD currents in polyvinyl acetate thin films as a function of polarizing field (0-9 kV/cm) and thickness (1000-7000 Å⁰). They reported three peaks at 326, 389 and 468K. The peaks at 326 and 389K were attributed to the motion of the side groups and the orientation of the dipoles of the main polymer chain

respectively, whereas the peak at 368K was related to the relaxation process which was due to the release of the trapped space charges.

Mahendru et al [217] studied electret effects in polyvinyl fluoride thin films. They observed only one peak in the TSDC spectra. The results of these studies were explained in terms of the disorientation of dipoles and/or the migration of charges over microscopic distances with trapping.

Thermally stimulated discharge currents from polyacrylonitrile were studied by Comstock et al [218]. Electrically polarized films of stretched and unstretched polyacrylonitrile were studied with the thermally stimulated discharge technique. Preferential orientation of nitrile side groups in polarized specimens was inferred from birefringence and X-ray diffraction experiments but the contribution of observed persistent electrical polarization appeared to be small. The major contribution was found to be due to trapped space charges, some of which was found to be due to trapped space charges, some part of which was associated with residual solvent molecules. Small ordered regions within polyacrylonitrile were expected to play a role in development of each contribution to the final persistent electrical polarization.

Thermostimulated currents from polychlorotrifluoroethylene electrets were studied by Latour and Murphy [219].

Thermostimulated current profiles were obtained for electrets of chlorotrifluoroethylene poled under various conditions of field strengths, temperature and electrode contact. The principal current peak was located at 145 C for electrets poled at an elevated temperature (100-178 C) and at 125 C for electrets poled at room temperature (20 C). Increase in the poling field from 3 to 300 kV/cm produced continuous variations in the discharge current profile consistent with a transition from hetero-charge to homo-charge. Both hetero-charge and homo-charge appeared to be released simultaneously at the principal current peak. Similar curves were obtained for samples poled with corona.

Studies on electron traps in polyethylene terephthalate by thermally stimulated current and photostimulated detrapping current analysis was made by Takai et al [220]. A broad peak of TSDC was observed around 100 C at which the motion of the COO group was released and a plateau was observed around 0 C. The apparent activation energy of the former peak was estimated to be about 0.23 eV by the partial heating technique. On the other hand, TSDC spectra at 185 C showed an existence of deep traps at 2.3 eV, which could be thermally cleaned by heating only upto 70 C. These facts clearly showed the effect of molecular motions on the carrier detrapping process during heating.

Thermally stimulated depolarization studies of PVC polymer electrets were made by Talwar and Sharma [221].

Thermally stimulated depolarization (TSDC) of polyvinyl chloride thermoelectrets prepared at polarizing temperatures of 80, 100 and 120 C with field strengths of 10, 12.5 and 14 kV/cm was studied. A sharp peak appeared at 97 C and was associated with the activation energy of the trap at a depth of 0.44 ± 0.03 eV.

Miyairi and Yanagisawa [222] studied thermally stimulated current in polyethylene terephthalate in the high temperature region. Electrical conduction in polyethylene terephthalate (PET) at high temperature was dominated by ionic process.

Thermally stimulated depolarization current (TSDC) of polypyromellitimide was measured by Tanaka et al [223] in order to obtain knowledge of the charging and discharging mechanisms of carriers in polypyromellitimide. Two peaks were observed one at 173 C (α) and the other at 50 C (β) in the dried film. The β peak was attributed to dipole orientation polarization. The α -peak showed non-linear dependence on polarization electric field E_p . The peak showed electrode material dependence. The α -peak was considered to be due to space charge polarization due to trapping of electrons injected from the cathode in the vicinity of the polymer film surface.

Kojima and Maeda [224] studied thermally stimulated currents from polyethylene terephthalate due to injected charges. Thermally stimulated currents from polyethylene

terephthalate (PET) electrets was investigated in the temperature range from -190 to +120 C. Both dependence of TSC on electrode metals (Au, Al) and the polarity of an applied field were remarkable in the temperature range above -40 C. The results indicated that electrons injected from the Al cathode greatly contributed to the TSC above -40 C and that the TSCs below -40 C for Al electrode and at all temperatures for Au electrodes were mainly induced by the depolarization of dipoles.

Bhargava and Srivastava [225] investigated thermally stimulated discharge currents in polystyrene thin films grown by the solution growth technique. Films in the thickness range (2000-10000 Å) were polarised at 130 C under the influence of different field strengths (2-10 kV/cm). Two relaxation peaks were observed at 77 C and 112 C. The occurrence of 112 C peak was explained in terms of space charge injection from electrode and ionic effect. The occurrence of 77 C peak was shown to be due to release of trapped charges due to local movements of polystyrene molecular chains.

TSDC study of pyrene picrate charge transfer complex was made by Srivastava and Mathur [226]. They observed two peaks. The first peak was attributed to bulk polarization whereas the second peak due to Maxwell-Wagner charging. Iqbal and Hogarth [227] studied the trap depth in evaporated polypropylene from measurements of thermally stimulated currents. The occurrence of thermally stimulated currents in thin evaporated films of

polypropylene was demonstrated and an analysis of the curve gave an electron trap depth of 0.33 eV to this material.

Jain et al [228] studied the charge storage properties in solution-grown polyvinyl butyral (PVB) thin films as a function of poling field (2.50×10^4 - 2.00×10^6 V/m), temperature (333-398 K), time (5.40×10^3 - 1.44×10^4 sec), thickness of the films (0.8-4.5 μm) and heating rates of depolarization (2.8-10 K/min) by the TSDC technique. Two relaxation processes one at 347K and the other at 423K were observed having activation energies of 0.36 ± 0.02 eV and 0.66 ± 0.02 eV respectively. The peak at 347K was found to be due to the deorientation of the aligned dipoles involving the acetate/hydroxyl groups. The peak at 423K was attributed to the release of trapped electrons/holes. The increase in the activation energy associated with the peak at 423K and the shift in its position towards higher temperatures with increase in the poling time and temperature suggested that the peak was associated with a distribution of relaxation times.

Srivastava et al [229] studied electrical polarization in polystyrene films of thickness 20 μm by measuring the TSDC at different polarizing fields, temperatures and heating rates. One peak was observed at 105 C which was unaltered by a change in the field. The occurrence of peak was due to a mechanism involving dipole orientation process.

Narasimha Rao and Narsingh Das [230] studied the TSDC in polyacrylic acid polymer films. Polyacrylic acid films of thickness $15\text{ }\mu\text{m}$ were grown by the solution growth technique. Thermally stimulated discharge currents (TSDC) were studied on these polymer films as a function of polarizing field strength and polarizing temperature at a constant heating rate of 0.08 KS^{-1} . In all these studies, one TSDC peak was observed and the temperature corresponding to this peak was found to shift to higher temperatures as the polarizing temperature increases. But for given polarizing temperature, the temperature corresponding to the peak was independent of polarizing field strength. The activation energies and relaxation parameters were evaluated. The origin of the TSDC was attributed to the dipolar orientation process.

Narasimha Rao and Kalpalatha [231] studied thermally stimulated discharge currents in polyvinyl pyrrolidone polymer films. Polyvinyl pyrrolidone films of thickness $17.6\text{ }\mu\text{m}$ were grown by the isothermal solution growth technique. Thermally stimulated discharge currents were studied on these films as a function of polarizing field strength and polarizing temperature at a constant heating rate of 0.15 KS^{-1} . In all these studies only one TSDC peak was observed and it was attributed to the space charge process.

Verma and Sinha [232] studied TSDC in bakelite (polyphenol formaldehyde) thermoelectrets. α and β peaks were

obtained for different poling temperatures and fields. Dou-Yol Kang et al [233] studied TSC in polypyromellitimide (polyimide). They observed three peaks A, B and C. The C peak was shown to be due to the polarization of ionic space charge which was measured as a function of forming time, forming temperature, forming voltage. Chand and Kumar [234] studied the effect of doping on TSD relaxation in polyvinylidene fluoride (PVF_2) films. TSD spectra of both pure and methylene blue dye doped PVF_2 films showed two relaxation peaks, however, in the latter case the peak positions, peak currents and charges depend strongly on the concentration of the dopant. TSC peaks in undoped poly(p-phenylene vinylene) were observed by Onoda et al [235]. Akuetey and Hirsch [236] reported TSD and TSC measurements of PVK films over the temperature range 85-530K. The only peak reported was found to lie at 250K and the corresponding activation energy was deduced to be 0.55 ± 0.05 eV. Thermally stimulated depolarization current (TSDC) spectra of polychlorotrifluoroethylene with relatively low crystallinity were studied by Shimizu and Nakayama [237]. These TSDC peaks were observed in the range of 85 to 400K.

Narasimha Rao and Subba Rao [238] studied the thermally stimulated depolarization currents in polyacrylamide polymer films between polarizing field strengths $0.48 \times 10^6 \text{ Vm}^{-1}$ to $24.1 \times 10^6 \text{ Vm}^{-1}$ and temperature range from 305 to 368K for different heating rates and polarizing times. The spectra

showed only one peak at low polarization temperatures whereas two peaks at high polarization temperatures. The origin of first TSDC peak was attributed to the dipolar orientation and peak II was attributed to the space charge polarization with the injection of charge carriers from the electrode and subsequent trapping and detrapping.

3.15 DIELECTRIC MEASUREMENTS

The dielectric behaviour of polymeric films is of direct interest to both the basic studies of electrical conduction through such films and their application in capacitors for micro-electronics. To obtain high values of capacitance, the dielectric constant should be high and the thickness be small. Due to the difficulty of obtaining structurally continuous and stable ultra-thin films, capacitor applications are generally limited to thick films.

The evaluation of dielectric properties of insulator films is carried out by measuring simultaneously the capacitance and the dissipation factor over a wide range of frequencies and temperatures. As all the other electrical parameters of dielectrics, the permittivity depends on the changeable external factors such as the frequency of voltage application, temperature, pressure, humidity, etc. In a number of cases these dependences are of great practical importance.

Less has been reported on dielectric properties of PVP and it seems to carry out further investigations to understand the dielectric behaviour of the polymer. This chapter reports on capacitance and dielectric loss factor of pure PVP films as a function of temperature and frequency. Besides basic types of polarization [239-242] like electronic, ionic, dipolar, migrational polarization plays a dominant role in polymeric materials. Electronic polarization is present in all types of dielectrics. It occurs almost instantaneously. Relaxation time of this polarization is 10^{-15} sec. Ionic polarization is the mutual displacement of ions forming a hetero polar (ionic) molecule. The time required for it is also short but longer than that of electronic polarization (10^{-13} sec). Both electronic and ionic polarizations are fast and do not entail dielectric losses. The third type, i.e., dipolar polarization is exhibited by polar dielectrics. In the absence of an electric field, the dipoles are randomly distributed. Electric field introduces certain orderlines in their positions. Orientational polarization belongs to slow or relaxation type of polarization. The relaxation time may vary from 10^{-12} sec to tends of seconds depending upon the size of the molecules and viscosity of the medium. Dipole polarization dissipates electric energy which is transformed into heat in a dielectric. Migrational polarization arises due to the inhomogeneity in the electrical properties of a dielectric. The formation of space charges in a dielectric under the

action of an external field and other causes which initiate the redistribution of charges with time are some of the factors responsible for introducing inhomogeneities. It is also called interfacial polarization and arises only when $\epsilon_1 \sigma_2 \neq \epsilon_2 \sigma_1$, where ϵ_1 and σ_1 are permittivity and conductivity of the first phase and so on. The accumulation of charges at the interfaces requires flow of current through the dielectric phases which may require seconds, minutes or even hours depending upon the relative values of ϵ and σ of two phases. Because of very high relaxation time, this type of polarization does not appear in dielectric measurements. It also involves dissipation of energy. The dielectric losses in polymers are convolution of two effects, viz., the presence of dipoles which get coupled to the electric field and suitable thermal motion in the polymer to give rise to a dispersion. The polar group includes polymer like polyvinyl chloride, polyacrylonitriles, polyvinyl acetate.

3.16 EFFECT OF FORMING PARAMETERS

The properties markedly depend on the forming parameters, i.e., temperature, frequency of operation and impurity, etc.

3.16-1 TEMPERATURE

Temperature affects the dielectric properties by decreasing the number of polarized ions per unit volume due to thermal expansion. Expansion of lattice results in increase of

the polarizability [243]. At constant volume, macroscopic polarizability depends upon the temperature, Debye's equation [244] for dielectric is :

$$\frac{E-1}{E-2} = \frac{4\pi N}{3} \left(\alpha_o + \frac{\mu^2}{3kT} \right) \quad \dots (3.54)$$

where N - Number of molecules per cc, α_o - Polarizability of the molecule, μ - Permanent electric dipole moment of the molecule.

In case of polar polymers dielectric constant is temperature dependent [245]. Effect of temperature, frequency on organic material have been studied by many workers [246,247].

3.16-2 FREQUENCY

Dielectric losses depend on a wide range of frequencies. In case of polar substances dielectric constant changes at a characteristic frequency when a dielectric substance is subjected to an alternating field. Complex dielectric constant ϵ'' is represented by :

$$\epsilon'' = \epsilon' - i\epsilon'' \quad \dots (3.55)$$

where ϵ'' is a real part (observed dielectric constant) and ϵ' is imaginary part called dielectric loss :

$$\tan \delta = \epsilon''/\epsilon' \quad \dots (3.56)$$

where δ is the phase angle between displacement and field. $\tan \delta$ is termed as loss tangent.

According to Frohlich modification, the following expressions

$$\epsilon' = \epsilon_{\infty} + \frac{\epsilon_0 - \epsilon_{\infty}}{1 + iW\tau} \quad \dots (3.57)$$

and the magnitude of dielectric dispersion

$$\epsilon_{\infty} - \epsilon_0 = 3\epsilon + 2\epsilon_0 \left(\frac{\epsilon_{\infty} + 2}{3} \right)^2 \frac{4\pi n g \mu^2}{3 k T} \quad \dots (3.58)$$

ϵ_0 = static permittivity,

ϵ_{∞} = optical or high frequency permittivity

W = angular frequency of applied field

where,

ϵ_0 = zero frequency permittivity

ϵ_{∞} = optical or high frequency permittivity

τ = relaxation time

ω = angular frequency

η = concentration of dipoles

μ = dipole moment

and q = parameter relating to dipole interaction.

Equation

$$\epsilon'' = \frac{(\epsilon_0 - \epsilon_{\infty})\omega\tau}{1 + \omega^2\tau^2} \quad \dots (3.59)$$

shows that the loss approaches zero for both small and large values of $W\tau$, while it is maximum for $Wm\tau = 1$ or

$$\tau = \frac{1}{W_m}$$

Hence, the maximum loss

$$\epsilon''_{m''} = \frac{\epsilon_0 - \epsilon_{\infty}}{2} \quad \dots (3.60)$$

and maximum permittivity

$$\epsilon'_{m'} = \frac{\epsilon_0 + \epsilon_{\infty}}{2} \quad \dots (3.61)$$

The polymers do not follow the Debye's equation. They show a broader dispersion curve and lower maximum loss than would be expected from eq. (3.59) and (3.61), respectively. Cole-Cole [248] pointed out that this anomaly arises due to the fact that the long chain molecular compounds do not have a single relaxation time. On the contrary their relaxation times are distributed within certain minimum and maximum limits. Physically it can be visualized as follows [249]. Every molecular dipole in a given chain is coupled to neighbouring dipoles of the same chain by primary valence bonds so that the motion of any dipole affects the motion of its neighbours and they in turn influence its response to a torque. Furthermore, in the various configurations which a chain molecule can assume, we can find one or another segment of chain acting effectively as a co-operative electrical unit and these segments will, of course, vary in length between the improbable extremes of a single monomeric unit and the whole extended chain. Such a state of affair leads to distribution of relaxation time. Nevertheless, it is still possible for most purposes to consider that the practical situation is represented by a composite single relaxation time.

3.16-3 IMPURITY

Impregnating of polymer with impurity affects the dielectric constant and losses as well. Previously Tiwari [250] and Kulshreshtha [251] have also reported changes in capacitance and losses values.

3.17 LAST DECADE'S WORK ON DIELECTRIC MEASUREMENTS

Relaxation mechanism of number of polar, non-polar polymers and organic compounds have been reported. Low temperature relaxation behaviour of polyethylene and related hydrocarbon polymers have been reported by Phillips [252] and Thomas [253]. Dielectric relaxation behaviour of polyvinylidene fluoride (PVDF) [254,255], poly methacrylates (PMMA) [256,257] have also been reported. Reported work/papers are also available on poly chlorotrifluoro ethylene [258] and polyacrylonitrile [259]. Co-polymers have also been investigated in past years. Reports are available on acrylonitrile [259], acrylonitrile butadiene [260] and polymethyl trifluoro propyl siloxane [261]. In the literature, the subject has been discussed [262-264].

Reports are available on Xanthene [265], parachloro aniline [266], and Anthraquinone [267]. Field is also one of the important parameters, particularly in case of polar polymers. Chatterji and Bhadra [268], McMohan [269], Elgard [270] and others [271,272] have observed isotropic increase in dielectric constant with field but no satisfactory interpretation has been given for this effect so far.

3.18 PRESENT INVESTIGATION

In the present investigation, attention has been paid to lower frequencies and temperature range (30-210°C). Frequency range selected is from 500 Hz to 30 kHz.

The present investigation is intended to get an insight into various molecular relaxation processes which occur in polyvinyl pyrrolidone under the influence of alternating field. This chapter describes the permittivity and loss variation of PVP as a function of frequency and temperature.

The following procedure was adopted to measure the complex dielectric constant as a function of frequency and temperature. The temperature of the specimen was recorded with the help of a fine copper-constantan thermocouple placed close to the sample. A direct reading potentiometer was used for the determination of thermo e.m.f. Before starting the measurements the sample was allowed to attain the equilibrium temperature for a sufficiently long time. The oscillator was set for the desired frequency and the null detector was tuned to it. The bridge balance was done by repeated adjustment of capacity selector, capacity and dissipation knobs till the null detector indicated the least deflection. The oscillator was then set for the next frequency and the bridge was balanced in a similar manner. After covering the entire frequency range, the temperature was changed and the measurements were repeated over the entire frequency range and so on.

REFERENCES

1. Adamec, V., Perlman, M.M. and Kabayama, M.A. Dielectric Properties of Polymers, Ed. F.F.Karasz, Plenum Press, New York (1972).
2. Wintle, M.J. J. Non Crystalline Sol. **15**, 471 (1974).
3. McDonald, J.R. J. Chem. Phys. **54**, 2026 (1971).
4. Sutton, P.M. J. Am. Ceram. Soc. **47**, 219 (1966).
5. Daniel, V.V. Dielectric Relaxations (London-Acad. Press, 1967), Chapter IV.
6. Walden, R.H. J. Appl. Phys. **43**, 1178 (1972).
7. Wintle, H.J. J. Appl. Phys. **42**, 4724 (1971).
8. Lindmayer, J. J. Appl. Phys. **36**, 196 (1965).
9. Wintle, H.J. J. Appl. Phys. **44**, 2514 (1973).
10. Lewis, T.J. Conf. on Electrical Properties of Organic Solids, Inst. Phys. Chem., Wraclaw Tech. Univ., Poland Ser. No. 7, Conf. No.1, 146.
11. Davies, D.K. J. Phys. **D6**, 1017 (1973).
12. Wintle, H.J. J. Non Cryst. Solids **15**, 471 (1974).
13. Das Gupta, D.K. and Joyner, K. J. Phys. D. Appl. Phys. **9**, 829 (1976).
14. Cole, K.S. and Cole, R.H. J. Chem. Phys. **90**, 341 (1941).
15. Kao, K.C. and Hwang, H.W. "Electr. Transport in Solids", Pergamon Press, Oxford (1981).
16. Adamec, V. Kolloid **249**, 1085 (1971).
17. Aras, L. and Baysal, B.M. J. Poly. Sci. Poly. Phys. **222**, 1453 (1984).
18. Hamon, B.V. Proc. IEEE London **99**, 151 (1952).
19. Von Schweidler, E. Ann. Physik. **LP3, 24**, 711 (1907).
20. Das Gupta, Doughty, K. and Brockley, R.S., J. Phys. D. Appl. Phys. **13** (1980).
21. Das Gupta, D.K. and Joyner, K., J. Phys. D. Appl. Phys. **9**, 829 (1976).

22. Das Gupta, D.K. and Joyner, K., J. Phys. D. Appl. Phys. **9**, 2041 (1976).
23. Vanderschueren, J. and Linkens, A., J. Appl. Phys. **49**(7), (1978).
24. Pillai, P.K.C. and Rashmi, European Polymer Journal **17**, 611 (1981).
25. Pillai, P.K.C., Narula, G.K., Tripathi, A.K. and Mendiratta, R.G., Phys. Stat. Sol(a) **77**, 693 (1983).
26. Keller, J.M., Datt, S.C., Singh Ranjit, Jain Vinita and Verma Girish, JEEE, 177 (1991).
27. Datt, S.C., Keller, J.M., Singh, Ranjit, Dubey, Rajendra and Singh, Reeta, ISE-7, IEEE, 171 (1991).
28. Singh Ranjit and Datt, S.C., Proc. 5th Intern. Symp. Electrets, Heidelberg, 202 (1985).
29. Dubey, R.K., Keller, J.M., Singh, R. and Datt, S.C., Indian Journal of Pure & Appl. Phys. **31**, 433 (1993).
30. Lakshmi Narayana, K., Dasaradhu, Y.S. and Narasimha Rao, V.V.R., Polymer International **35**, 315 (1994).
31. Neagu, E.R. and Neagu, R.M., Phys. Stat. Sol(a) **144**, 429 (1994).
32. Khare, P.K., Pramana **46**, 109 (1996).
33. Khare, P.K., Indian J. Pure & Appl. Phys. **34**, 249 (1996).
34. Khare, P.K. and Singh Ranjit, Polymer International **34**, 407 (1994).
35. Khare, P.K. and Chandok, R.S., Polymer International **36**, 35 (1995).
36. Khare, P.K., Chandok, R.S. and Srivastava, A.P., Pramana **44**, 9 (1995).
37. Gour, M.S., Singh Reeta, Khare, P.K. and Singh Ranjit, Polymer International **37**, 33 (1995).
38. Khare, P.K. and Chandok, R.S., Polymer International **38**, 153 (1995).
39. Khare, P.K., Chandok, R.S. and Srivastava, A.P., Indian J. Phys. **69**, 627 (1995).

40. Khare, P.K. and Jain, S.K., Indian J. Pure & Appl. Phys. **35**, 408 (1997).
41. Khare, P.K., Pandey, R.K., Chourasia, R.R. and Jain, P.L., Polymer International **49**, 719 (2000).
42. Khare, P.K., Jain, P.L. and Pandey, R.K., Bull. Mater. Sci. **23**, 325 (2000).
43. Khare, P.K., Jain, P.L. and Pandey, R.K., Bull. Mater. Sci. **23**, 419 (2000).
44. Antenen, K. Z. Angew. Math. Phys. **6**, 478 (1955).
45. Marry, A., Symphoni, M.M., Weisz, S.A. and Levinson, J. J. Phys. Chem. Solids **22**, 285 (1961).
46. Lampert, M.A. Rep. Progr. Phys. **27**, 329 (1964).
47. Rose, A. R.C.A. Review **12**, 302 (1951).
48. Eley, D.D. and Parfitt, G.D. Trans. Faraday Soc. **51**, 1529 (1955).
49. Gardew, M.H. and Eley, D.D. Discussion Faraday Soc. **17**, 115 (1957).
50. Fischer, J.C. and Glaever, I. J. Appl. Phys. **32**, 172 (1961).
51. Lengyel, G. J. Appl. Phys. **37**, 807 (1966).
52. Wintle, H.J. IEEE Trans. Electrical Insulation **25**, 27 (1990).
53. Eley, D.D. and Spirey, D.I. Trans. Faraday Soc. **56**, 1432 (1960).
54. O'Dwyer, J.C. J. Appl. Phys. **37**, 599 (1956).
55. Simmons, J.G. Phys. Rev. Letts. **15**, 967 (1965).
56. Advani, G.T., Gotting, J.S. and Osman, M.S. Proc. IRR **50**, 5030 (1962).
57. Warfield, R.W. Testing of Polymers, Ed. Schmitz, T.V., Vol.1, Wiley, New York, 287 (1965).
58. Bahri, R. and Singh, H.P. Thin Solid Films **62**, 291 (1979).
59. Kulshreshtha, Y.K. and Srivastava, A.P. Thin Solid Films **69**, 269 (1980).

60. Chutia, J. and Barua, K. Phys. Stat. Sol.(a) 55, K13 (1979).
61. Staryga, E. and Swiatek, J., Thin Solid Films 56, 311 (1979).
62. Narasimha Rao, V.V.R. and Kalpalatha, A. Polymer 28, 648 (1987).
63. Sekhar, R., Tripathy, A.K., Goel, T.C. and Pillai, P.K.C. J. Appl. Phys. 62, 4126 (1987).
64. Sessler, G.M. and Seggern "Charge Storage, Charge Transport and Electrostatics with their Application", Kyoto, Japan 9-12 Oct. (1978).
65. Hughes, R.C. J. Non Cryst. Solids (Netherlands) 35-36, 1005 (1988).
66. Duart, H. and Ramos, Electricidade (Portugal) 143, 151 (1979).
67. Hofman, R. Ber. Bunsenges Phys. Chem. 83, 441 (1979).
68. Davies, R.K. (Ed.) 3rd International Conf. on Dielectric Materials Measurements and Applications, Birmingham, England, 1013 Sept., 342 (1979).
69. Adamec, V. and Calderwood, J.M. J. Phys. D. Appl. Phys. 11, 781 (1978).
70. Gutman, F. and Lyons, L.E., Organic semiconductors (New York, Wiley 1967).
71. Schottky, W. Z. Physik. 15, 872 (1914).
72. Frankel, J. Phys. Rev. 54, 647 (1938).
73. Mott, N.F. and Gurney, R.W. Electronic Processes in ionic crystals, Oxford University Press (1948).
74. Rose, A. Phys. Rev. 97, 1538 (1955).
75. Lampart, M. Rep. Prog. Phys. 27, 329 (1964).
76. Newman, B.A., Yoon, C.H., Pal, K.D. and Scheinhein, J.I. J. Appl. Phys. 50, 6095 (1979).
77. Zheluder, I.S. Physics of Crystalline dielectrics, 2, Plenum Press, New York (1971).
78. Blythe, Electrical Properties of Polymers,

79. Donald A. Seanor, Electrical conduction in polymers, Academic Press, New York (1982).
80. Simmons, J.G. Hand Book of Thin Film Technology (Edited by L.I.Maissel and R.Glang), McGraw Hill, New York (1970).
81. Lamb, D.R. Electrical conduction mechanisms in thin insulating films, Methuen and Co. Ltd., London (1967).
82. Bashara, N.M. and Doty, C.T., J. Appl. Phys. 35, 3498 (1964).
83. Lengyel, G. J. Appl. Phys. 37, 807 (1966).
84. Lilly, A.C. and Mcdowell, J.R. J. Appl. Phys. 39, 141 (1968).
85. Davies, D.K. J. Phys. D. 5, 162 (1972).
86. Babcock, L.E. and Christy, R.W. J. Appl. Phys. 43, 1423 (1972).
87. Gupta, D.K. and Barbarez, M.K. J. Phys. D. Appl. Phys. 6, 867 (1973).
88. Adachi, H., Shibata, Y. and Ono, S. J. Phys. D. Appl. Phys. 4, 988 (1971).
89. Gazso, J. Thin Solid Films 21, 43 (1974).
90. Boonthanom, J. and White, M. Thin Solid Films 24, 295 (1974).
91. Kryzewski, M. and Swiatek, J. Acta. Physica Polonica 45, 119 (1974).
92. Suzuki, M., Takahashi, K. and Nitani, S. Japan J. Appl. Phys. 14, 741 (1975).
93. Rastogi, A.C. and Chopra, K.L. Thin Solid Films 26, 61 (1975).
94. Vollmann, W. and Poll, H.H. Thin Solid Films 26, 201 (1975).
95. Desbarax, N., Segui, Y. and Ai Bui, Phys. Stat. Sol(a) 33, 247 (1976).
96. Mahendru, P.C., Pathak, N.L., Singh Satbir and Mahendru, P. Phys. Stat. Sol(a) 38, 365 (1976).

97. Mahendru, P.C., Pathak, N.L., Jain, K. and Mahendru, P. Phys. Stat. Sol(a) 42, 403 (1977).
98. Gupta, C.L. and Tyagi, R.C. Indian J. Pure and Appl. Phys. 16, 428 (1978).
99. Jain, V.K., Gupta, C.L. and Jain, R.K. Indian J. Pure and Appl. Phys. 16, No.6, 625 (1978).
100. Phadke, S.D., Sathianandam, K. and Karekar, R.N. Thin Solid Films 51, L9 (1978).
101. Hanscomb, J.R. and Kaahwa, Y. J. Phys. D. 121, No.4, 579 (1979).
102. Takai, Y., Kato, H. and Ishii, K. Japan J. Appl. Phys. 18, No.9, 851 (1979).
103. Audenaert, M., Gusman, G., Mehmod, M., Deltour, R., Niorhomme, B. and Vander Donckt, E. Solid State Communications 30, 797 (1979).
104. Rao, T.V. and Chopra, K.L. Phys. Stat. Solid(a) 53, No.1, 43 (1979).
105. Tyezkowski, J. and Zeelinski, M. Thin Solid Films 55, No.2, 253 (1979).
106. Staryga, E. and Swiatek, J. Thin Solid Films 56, No.3, 311 (1979).
107. Bahri, R. and Singh, H.P. Thin Solid Films 62, 291 (1979).
108. Sawa, G., Nokamura, S., Leide, K. and Ieda, M. Japan J. Appl. Phys. 19, No.6, 1067 (1980).
109. Miyairi, K. and Ieda, M. Japan J. Appl. Phys. 19, No.6, 1067 (1980).
110. Kulshrestha, Y.K. and Srivastava, A.P. Thin Solid Films 69, No.3, 269 (1980).
111. Bahri, R. and Singh, H.P. Thin Solid Films 69, 281 (1980).
112. Cros Lee Gloan, A. and Onge, H. St. Rev. Gen. Electr (France) 89, No.2, 121 (1980).
113. Nakamura, S., Sawa, G. and Ieda, M. Jap. J. Appl. Phys. 20, 47 (1981).
114. Lipinski, A., Staryaga, E. and Swiatek, J. Mater. Sci. VII, 231 (1981).

115. Sharma, B.L. and Pillai, P.K.C. Polymer 23, 17 (1982).
116. Bahri, R. J. Phys. D. Appl. Phys. 15, 677 (1982).
117. Chand, S., Radhakrishnan, S. and Mahendru, P.C. J. Phys. D. Appl. Phys. 15, 2499 (1982).
118. Tyezkowski, J., Czeremuskin, G. and Kryszewski, M. Phys. Stat. Sol(a) 72, 751 (1982).
119. Jayarama Reddy, P. and Syrajuddin, M. Presented at International Conference on Metallurgical Coatings, Sandeigo, U.S.A., April 1984.
120. Gould, R.D. Thin Solid Films 125, 63 (1985).
121. Joom-Ung Lee, Young-Joo-Kum and Bang-Henpkin. Trans. Korean. Inst. Electr. Eng. 34, 349 (1985).
122. Kojima, K., Takai, Y. and Ieda, M. J. Appl. Phys. 59, 2655 (1986).
123. Sessler, G.M., Hahn, B. and Yoon, D.Y. J. Appl. Phys. 60, 318 (1986).
124. Tawanski, A., Migahed, M.D. and El.Hamid, M.I.A. J. Polymer Sci. Pt. B. Polym. Phys. 24, 2631 (1986).
125. Narasimha Rao, V.V.R., Subba Rao, T. and Narsingh Das, N. J. Phys. Chem. Solids 47, 33 (1986).
126. Das Gupta, P.K. and Doughty, K. IEEE Trans. Electr. Insul. E1-22, 1 (1987).
127. Narasimha Rao, V.V.R. and Kalpalatha, A. Polymer 28, 648 (1987).
128. Narasimha Rao, V.V.R., Mahender, T. and Subba Rao, B. J. Non Crystl. Solids 104, 224 (1988).
129. Basha, A.F., Amin, M., Abdel Samad, H.A. and Darwish, K.A. J. Polym. Mater. 5, 161 (1988).
130. Narasimha Rao, V.V.R. and Subba Rao, B. Acta Polymerica (accepted for publication and may appear in 9(1991) issue).
131. Narasimha Rao, V.V.R., Jeevana Krishna, K. and Subba Rao, B. Paper presented at 33rd IUPAC International Symposium on Macromolecules held at Montreal Canada, July 8-13, 1990.

132. Satyanarayana, K.V., Subba Rao, U.V. and Narasimha Rao, V.V.R. J. Mater. Sci. Lett. (UK) Vol.9, No.1, 3-4 (1990).
133. Turnhout, J. Van. Thermally stimulated discharge of polymer electrets, Elsevier, Amsterdam, (1975).
134. Kramer, M. and Memner, D. Electro. Tech. Z. (ETZ) A95,9, 435 (1974).
135. Adamec, V. and Maletova, E. Polymer 16, 166 (1975).
136. Akamatu, H. and Inokuchi, I. J. Chem. Phys. 18, 810 (1950).
137. Cooper, J.R. J. Phys. Lett. 36,9, 219 (1975).
138. Chu, C.W., Gebalk, T.H., Harper, J.M.E. and Green, R.L. Phys. Rev. Lett. 31,25, 149 (1973).
139. Inokuch, H., Shirotani, I. and Minomura, S. Bull. Chem. Soc. 37, 3257 (1964).
140. Samara, G.A. and Drickamer, H.G. J. Chem. Phys. 37, 474 (1962).
141. Aust, R.B., Samara, G.A. and Drickamer, H.G. J. Chem. Phys. 41, 2003 (1964).
142. Holzapfel, W.B. J. Chem. Phys. 50, 4424 (1969).
143. Simpson, J.D. and Offen, H.W. J. Chem. Phys. 42, 1573 (1970).
144. Beardske, R.A. and Offen, H.W. J. Chem. Phys. 42, 6016 (1970).
145. Ludwig, J. and Kommandeur, J. J. Chem. Phys. 52, 2302 (1970).
146. Bently, H.W. and Drickamer, H.G. J. Chem. Phys. 42, 1573 (1965).
147. Shimonura, K., Hatono, M. and Nakda, I. Phys. Soc. Jpn. 23, 578 (1967).
148. Barker, R.E. Jr. and Thomar, C.R. J. Appl. Phys. 35,11, 3203 (1964).
149. Manthia, S.B., Kronick, P.L. and Labes, M.M. J. Chem. Phys. 37, 2503 (1962).

150. Bhatnagar, S.N. and Shrivastava, A.P. Madhya Bharti J. University of Sagar (India) **17**, Pt. II, Sec. A. **13**, 69 (1968).
151. Mullikan, R.S. J. Am. Chem. Soc. **74**, 811 (1952).
152. Kallmann, H. and Pope, M. Symposium on Electrical Conductivity in Organic Solids, Ed. Kallmann, M. and Silver, M. Inter Science Pub. (1961).
153. Rose, A. J. Appl. Phys. **35**, 2664 (1964).
154. Weast, R.C., Selby, S.M. and Hodgeman, C.D. (Eds.) Handbook of Chemistry and Physics, Chemical Rubber Co. Pub. (1964) 517.
155. Lyone, L.E. J. Chem. Soc., 5001 (1957).
156. Kallmann, H. and Pope, M. Nature **186**, 31 (1960).
157. Kallmann, H. and Pope, M. J. Chem. Phys. **36**, 2482 (1962).
158. Silver, M. Organic Semiconductors MacMillan Co. New York, Ed., 27 (1962).
159. Mark, P. and Helfrich, W. J. Appl. Phys. **33**, 205 (1962).
160. Eley, D.D. and (Miss) Thomer, P. W. Trans. Faraday Soc. **64**, 1513 (1968).
161. Reucroft, P.J. J. Chem. Phys. **36**, 1114 (1962).
162. Braunlich, S.P. (Ed.) "Thermally Stimulated Relaxation in Solids", Springer Verlag, Berlin (1979).
163. Sessler, G.M. Electrets, Topics in Applied Berlin, (1980).
164. Perlman, M.M. Ed. Electret Storage and Transport in Dielectric, Electrochemical Society, Princeton (1973).
165. Braunlich, P. Ed. "Thermally Stimulated Relaxation in Solids", Topics in Applied Physics, Springer Verlag, New York, 37 (1979).
166. Turnhout, J. Von "Thermally Stimulated Discharge of Polymer Electrets", Elsevier, Amsterdam (1975).
167. Sores de Campose M. Ed., "International Symposium on Electrets and Dielectric", Acad. Brasil. de ciencias, Rio de Janeiro, (1977).

168. Fillard, J.P. and Turnhout, J. Van Eds. "Thermally Stimulated Process in Solids, New Prospects", Elsevier, Amsterdam, (1971).
169. Perlmann, M.M., J. Electro Chem. Soc. 119, 892 (1972).
170. Fabel, G.W. and Henish, H.K. Phys. Stat. Sol(a) 6, 535 (1971).
171. Sessler, M.G. and West, J.E. J. Appl. Phys. 43, 722 (1972).
172. Seggern, H. Von, J. Appl. Phys. 52, 4086 (1981).
173. Seggern, H.Von, J. Appl. Phys. 52, 4081 (1981).
174. Mccrum, N.G., Read, B.E. and Willium, G. "An elastic and dielectric effect in polymeric solids", Wiley, New York, (1967).
175. Perlman, M.M. and Unger, S., J. Appl. Phys. 45, 2389 (1974).
176. Turnhout, J. Van "Thermally Stimulated Discharge in Polymer Electrets".
177. Chueren Vanolers, J. Polym. Sci. Polym. Phys. 15, 873 (1977).
178. Ponevski Ch. and Solunov, S., J. Polym. Sci. Polym. Phys. 15, 1467 (1975).
179. Sessler, G.M., West, J.E. and Seggern, H.Von, J. Appl. Phys. 53(6), 4320 (1982).
180. Khazanovich, T.N., "Hand Book of Physics", Mir Publ., Moscow (1977).
181. Hill, N.E., Vaughan, W.E., Price, A.H. and Davies, M., "Dielectric Properties Molecular Behaviour", Van Nostrand - Reinhold, Lonodn, (1969).
182. Freis, H. and Groetzinger, G., Phys. Sik. 2, 37, 720-724 (1936).
183. Hill, N.E., Vaughan, W.E., Price, A.H. and Davies, "Dielectric Properties and Molecular Behaviour", Von Nostrand-Reinhold, London (1959).
184. Frohlich, H. "Theory of Dielectrics", 2nd Ed., Oxford University Press, Oxford (1958).
185. Ferry, J.W., "Visco Elastic Properties of Polymers", Wiley, New York, (1970).

186. Hedwing, P., "Dielectric Spectroscopy of Polymers", Hilger, A., Bristol (1977).
187. Roberts, G.E. and White, E.F.T. "Relaxation Processes in Amorphous Polymers", Cited in Physics of Glass Polymers, Ed. by Howard, R.N., Appl. Sc. Pub., London (1978).
188. Ward, I.M., "Mechanical Properties of Solid Polymer", Pub. Wiley Inter Sc., London (1971).
189. Mazurin, O.V., J. Non. Crys. Solids 25, 130 (1977).
190. Moynihan, C.T., Easleal, Wilder, J. and Tacker, J., J. Phys. Chem. 78, 2673 (1974).
191. Kovacs, A.J., Hutchinson, J.M. and Aklonis, J.J., Cited in "Structure of Non Crystalline Solids", Proc. Symp., Cambridge, 153 (1977).
192. Turnhout, J. Van, "Thermally Stimulated Discharge of Electrets", Elsevier, Scientific Pub. Co. Amsterdam (1975).
193. Shrivastava, S.K., Ranade, J.D. and Srivastav, A.P. Polymer 22, 1645 (1981).
194. Pillai, P.K.C., Nair, P.K. and Nath, R., Polymer 17, 92 (1976).
195. Pillai, P.K.C., Goel, T.C. and Xavier, S.F., Europ. Polymer J. 15, 1149 (1979).
196. Mehendru, P.C., Jain, K. and Mehendru, Praveen, J. Phys. D. : Appl. Phys. 11, 1431 (1978).
197. Vanderschurren, J. and Linkens, A., J. Appl. Phys. 51, 4697 (1980).
198. Pillai, P.K.C. and Jain, K., Phys. State Solidi(a) 17, 221 (1973).
199. Gupta, V.K. and Bhawalkar, D.R., Indian J. of Pure & Appl. Phys. 10, 878 (1975).
200. Hino, T., Jap. J. Appl. Phys. 12, 611 (1973).
201. Dasgupta and Joyner, J. Appl. Phys. 45, 42 (1975).
202. Jain, V.K., Gupta, C.K., Jain, R.K. and Tyagi, R.C., Thin Solid Films 48, 175 (1978).
203. Fischer, P. and Rohi, P., J. Polym. Sc. West Germany 14, 531 (1976).

204. Stupp, S.I. and Carr, S.H., J. Polym. Sci. 15, 485 (1977).
205. Mahendru, P.C., Jain, K. and Mahendru, P., J. Phys. D. Appl. 10 (1977).
206. Gerlick, G.F.J. and Gibson, A.F., Proc. Phys. Soc. (London) 60, 574 (1948).
207. Bucci, C., Fieschi, R. and Guiddi, G., Phys. Rev. 148, 816 (1966).
208. Tradten, W. Hoogens, Phylips Res. Rep. 13, 575 (1958).
209. Solunov, C. and Ponevski, C., J. Poly. Sci. Polym. Phys. 14, 1801 (1976).
210. Solunov, C. and Ponevski, C., J. Poly. sci. Polym. Phys. 15, 969 (1977).
211. Braunlich, P. Thermally Stimulated Relaxation in Solids, Springer-Verlag, Berlin, (1979).
212. Perlman, M.M. J. Appl. Phys. 42, 2645 (1971).
213. Caserta, G. and Serra, A. J. Appl. Phys. 42, 3778 (1971).
214. Pillai, P.K.C., Jain, K. and Jain, V.K. Phys. Stat. Sol(a) 17, 221 (1973).
215. Jain, K., Rastogi, A.C. and Chopra, K.L. Phys. Status Solid A 21, 2, 685 (1974).
216. Mahendru, P.C., Jain, K., Chopra, V.K. and Mahendru Praveen. J. Appl. D. Appl. Phys. 8, 305 (1975).
217. Mahendru, P.C., Suresh Chand and Pathak, N.L. Thin Solid Films 44, L13 (1977).
218. Comstock, R.J., Stupp, S.D. and Carr, S.H. J. Macromel. Sci. Phys. B13, 101 (1977).
219. Latour, M. and Murphy, P.V. J. Electrostat. 3, 163 (1977).
220. Takai, Y., Mori, K., Mizetani, T. and Ieda, M. Japan J. Appl. Phys. 16, 11, 1937 (1977).
221. Talwar, M. and Sharma, D.L. J. Electrochem. Soc. 125, 434 (1978).

222. Miyairi, K. and Yanagisawa, I. Japan J. Appl. Phys. 17, 595 (1978).
223. Tanaka, T., Hirabayashi, S. and Shibayama, K. J. Appl. Phys. 49, 784 (1978).
224. Kojima, K. and Maeda, A. Japan J. Appl. Phys. 17, 1735 (1978).
225. Bhargava Bharat and Srivastava, A.P. Indian J. Phys. 53A, 47 (1979).
226. Srivastava, S.K. and Mathur, O.N. Indian J. Phys. 53A, 91 (1979).
227. Iqbal, T. and Hogarth, C.A. Thin Solid Films 61, 23 (1979).
228. Jain Kamlesh, Kumar Naresh and Mahendru, P.C. J. Electrochem. Soc. 126, 11 (1979).
229. Srivastava, S.K., Ranade, J.D. and Srivastava, A.P. Thin Solid Films 67, 201 (1980).
230. Narasimha Rao, V.V.R. and Narsing Das, N. J. Vac. Sci. Technol. A4(1), 75 (1986).
231. Narasimha Rao, V.V.R. and Kalpalatha, A. Materials Chemistry and Physics 17, 317 (1987).
232. Verma, J.P. and Sinha, T.H.D. Ind. J. Pure and Appl. Phys. (India), Vol.26, No.7, 462 (1988).
233. Dou-Yol Kang, Won-Jae Lee, Hyung-Du Kim, Trans. Korean Inst. Electr. Eng. (South Korea) 37, No.8, 540 (1988).
234. Chand, S. and Kumar, N. Ind. J. Pure and Appl. Phys. (India) 26, No.9, 579 (1988).
235. Onoda, M. et al. J. Phys. Condens. Matter UK 1, 1, 113 (1989).
236. Akuetey, G. and Hirsch, J. J. Phys. D. Appl. Phys. (UK) 22, 1, 174 (1989).
237. Shimizu, H. and Nakayama, N. Japan J. Appl. Phys. 2 Lett (Japan) 23, 9, L1616 (1989).
238. Narasimha Rao, V.V.R. and Subba Rao, B. Acta Polymerica (accepted for publication and may appear in 8 (1991) issue).
239. Sharma, S.P. and Bhatnagar, C.S., Ind. J. Pure Appl. Phys. 10, 729 (1974).

240. Bhatnagar, S.N. and Srivastava, A.P., Ind. J. Pure Appl. Phys. **10**, 272 (1972).
241. Heijbour, J., British Polymer **1**, 3 (1969).
242. Nozaki, M., Jap. J. Appl. Phys. **10**, 179 (1971).
243. Havinga, E.E., J. Phy. Chem. Sol. **18**, 253 (1961).
244. Debye, P., Polar Molecules Chemical Catalogue Co., NY (1929).
245. Smyth, C.P. and Hitchcock, C.M., J. Am. Chem. Soc. **50**, 1547 (1928).
246. Hara, T. and Okamoto, S., J. Phys. Soc. Japan **20**, 1291 (1965).
247. Hara, T., Nozaki, N. and Okamoto, S., Japan J. Appl. Phys. **6**, 1138 (1967).
248. Cole, K.S. and Cole, R.H., J. Chem. Phys. **18**, 1417 (1951).
249. Rastogi, A.C., Ph.D. Thesis, I.I.T., New Delhi (1975).
250. Tiwari, A.R., Ph.D. Thesis, University of Saugar (1983), Sagar (M.P.), India.
251. Kulshrestha, Y.K., Ph.D. Thesis, University of Saugar (1980), Sagar (M.P.), India.
252. Phillips, W.A., Proc. Roy. Soc. A(GB) **319**, 565 (1970).
253. Thomas, R.A., Appl. Phys. Letts. (USA) **26**, 406 (1974).
254. Uembra, S., J. Polym. Sc. Polym. Phys. **12**, 1177 (1974).
255. Nakagawa, K. and Ishida, Y., J. Polym. Sc. Polym. Phys. **11**, 1503 (1973).
256. Shimzu, K., Yano, Y., Wada, Y. and Kawamura, Y., J. Polym. Sc. Polym. Phys. **11**, 1541 (1973).
257. Nroisewa, T.T. and Chirkov, M.N., Polym. Sc. (USSR) **15**, 2304 (1973).
258. Baird, M.E. and Sen Gupta, C.R., Polym. (GB) **9**, 1099 (1973).
259. Gupta, A.K., Chand, N., Singh, R. and Mansingh, A., Europ. Polym. J. **15**, 129 (1979).

- 260. Ikado, E. and Watanbe, J., J. Polym. Sc. Polym. Chem. 10, 3457 (1972).
- 261. Baird, M.E. and Sen Gupta, C.R., Polym. (GB) '15, 608 (1974).
- 262. Link, G.L., J. Electrochem. Soc. 120, 84C (1973).
- 263. Budenesteyn, P.P., Ed. Digest of Literature on dielectrics, 36 (1972).
- 264. Haward, R.N. (Ed.) Barking Essex, England Appl. Sc. Pub., (1973).
- 265. Agrawal, D.P., Ph.D. Thesis, University of Saugar (1974), Saugar (M.P.), India.
- 266. Pateria, A.P., Ph.D. Thesis, University of Saugar (1975), Saugar (M.P.), India.
- 267. Sharma, A.D., Ph.D. Thesis, I.I.T., New Delhi (1981), India.
- 268. Chatterji, S.D. and Bhadra, T.C., Phys. Rev. 98, 1728 (1955).
- 269. McMohan, W., J. Am. Chem. Soc. 14, 3290 (1956).
- 270. Elgard, A.M., Fiz. Tverd. Tela 4, 1320 (1962).
- 271. Lal, H.B., Ind. J. Pure Appl. Phys. 7, 370 (1969).
- 272. Kittle, C., 'Introduction to Solid State Physics', 2nd edn., John (1956).

CHAPTER IV

THERMALLY STIMULATED DISCHARGE CURRENT STUDIES IN PURE POLYVINYL PYRROLIDONE (PVP) FOIL ELECTRETS

4.1 INTRODUCTION

Non-isothermal dielectric relaxation of a polymer exhibit a spectacular relaxation phenomenon which is due to hindrance of the motions of the permanent dipoles and free charges of the polymer by frictional forces and since internal friction depends exponentially on temperature, the response time τ_0 of permanent dipoles and free charges changes markedly with temperature. This response time gets accelerated by heating the polymer. This brought the idea of thermally stimulating the discharge of the sample and thus performing the decay experiment within a reasonable time. This new method, first proposed by Frei and Groetzinger [1], is commonly known as thermally stimulated discharge current (TSDC) technique and consists in slowly heating the electric between two electrodes, connected to a sensitive electrometer that measures the ensuing current.

This TSDC technique has been extensively practised by many workers of electrets, previously the temperature rise was not programmed since their interest lay chiefly in ultimate charge released. Later on, VonAltheim [2] pointed out that the charge release is controlled by molecular motions which depend strongly on temperature. For this reason, Bucci et al [3] advocated the linear rise of temperature, say 3°C per minute. In this modified form, the technique has made encouraging progress and has heighten the status of electret.

A wide literature [4-15] is available on TSDC in polymers. The technique has been widely used in the study of trapping parameters in luminescent and photo-conducting materials. Lilly et al. [16] investigated TSDC in mylar and teflon. Stupp and Carr [17] suggested an ionic origin for high temperature discharge currents in poly acrylic nitrile. Guillet and Seytre [18] conducted a detailed study of the complex relaxation modes observed in poly-L-proline, Takeda and Naito [19] studied temperature change of dielectric constant of polystyrene using TSDC measurement. TSDC in corono charged polymers have been investigated by Perlman [9] and those in electron beam irradiated, polymers have been investigated by Sessler [20]. Ong and Turnhout have concluded in favour of the existence of a continuous distribution of relaxation times. Recently, similar conclusions have been inferred by Fischer and Rohl [21] and Hino [22] from studies on secondary peak of polyethylene and polyethylene terephthalate respectively. Chaitan et al. [5], however, have found in polyamides that the low temperature peaks could generally be decomposed in several discrete Debye processes.

It has been shown by theoretical argument and by experiment [23] that only in the case of a first order kinetics, polarization do the TSDC peaks occur invariably at a fixed temperature. Otherwise their position is shifting in a characteristic way with changing initial polarization. In the case of a space charge release, for example, the maximum

temperature is increasing with polarization temperature and polarization time. Thus, peak position data for varying polarization conditions allow one to decide in particular whether a peak is due to a first order depolarization process, e.g. complex reorientation or to the release of a space charge.

TSDC of polar materials [24] shows several bands or peaks. This indicates that the depolarization is realized by several different processes. Two such processes are well known, the relaxation of aligned dipoles and the relaxation of a space charge caused by mobile carriers accumulated at the electrodes. But there are still other processes which cause TSDC peaks and have not yet been identified. It is one of the fundamental problems of any TSDC investigation to relate the observed peaks to specific depolarization processes. TSC peak may be characterized by the maximum positions, the magnitude of the peak is eventually a measure of the number of defects causing the polarization. The determination of activation is a delicate task if the peaks overlap too much, possible no meaningful value can be obtained at all. Dependence of peak position on initial polarization provides information on the depolarization processes.

TSDC spectra are unique to the material under study. They are finger prints of them and are sensitive to impurities, additives, discharges, humidity, i.e. to any chemical or morphological change. They provide a sensitive

analytical tool that could be used to guide the production of materials with fixed electrical properties. TSC is an electrical spectroscopy and have practical application to electrical quality control. Recently, several workers [25,26] have used TSC technique to investigate changes produced in polymers due to doping of them with suitable impurities. Gupta and Tyagi [25] doped polyvinyl fluoride with rhodamine, alizarine, dichlorofluorescein and iodine and utilized TSC to find out the changes produced by doping. Srivastava et al. have reported relaxation parameters by doping polystyrene with copper-phthalocyanine, ferrocene, anthracene, pyrene, iodine and chloranil [26].

Mahendru et al. [27] have reported TSDC in PVAc films. They observed three TSC peaks at 53, 116 and 195°C and studied the effect of film thickness on TSDC spectra of PVAc. The 53°C peak was found to grow slightly with thickness. The magnitude of 116°C peak was observed to increase with film thickness and 195°C remained uninfluenced with the thickness. Total charge under all the three peaks grew linearly with the film thickness which led them to conclude uniform volume polarization in PVAc. Effect of iodine doping on TSDC spectra of PVAc has been considered by Mahendru et al. [28].

4.2 SURVEY OF THE MECHANISM RESPONSIBLE FOR TSDC

The processes taking place during TSD are similar to those occurring during sample formation and so all the

processes which occur during electret formation are also expected to take place in TSDC.

The net charge of the sample usually arises from aligned dipoles and space charges of which the latter are called excess charges. However, before electret formation, the neutral polymer already contained free charges; they manifest themselves in a conduction current when forming field is applied. So in addition to excess charges there must be equilibrium charges in the sample which do not contribute to its net charge but are responsible for its ohmic conductivity [29].

The decay of the net charge of an electret and its consequence manifestation as TSD will result from dipole reorientation, excess-charge motion and ohmic conduction. The decay of each of them should give rise to a TSD peak, because of the temperature activated mobilities. Initially, as the temperature increases, the thermal agitation will reorient the dipoles in the side group of the polymers and will manifest to give a current maximum at lower temperature but as the temperature further increases, reorientation of the main chain segments also starts together with that of side chain and causes the appearance of second peak near the glass transition temperature. At the temperature above than the glass transition, conformational motion of macromolecules start which leads to motion of excess charges and cause the third current peak. Therefore, current maximum due to dipole

reorientation occurs at a lower temperature than that of excess charge motion because the first process requires only a rotational motion of molecular groups, whereas the latter process involves a motion of molecular groups over a macroscopic distances [29].

4.3 METHODS TO UNRAVEL THE VARIOUS DECAY PROCESSES

TSDC of a polymer depends on its properties, the forming conditions and effect of different electrode materials.

4.3-1 CHOICE OF POLYMERS FOR TSDC

By the choice of polymer we can change, in particular the dipole contribution and the ohmic conduction. There are two obvious choices, viz. polar and non-polar polymers. When the polymer is polar, we will have a dipole reorientation, whereas in a non polar polymer we will have none. Moreover, non-polar polymers show high ohmic conduction, since this arises partly from the absorbed water, which may amount to few percent in polar materials, the high polarity will also enhance the formation of free carriers by facilitating the dislocation of impurities. Consequently, in polar polymers we might expect storage of dipoles and excess charges. Their high concentration often enables the excess charges. Their high concentration often enables the excess charges to contribute discernibly to the TSDC of shorted electrets, unnoticed by ohmic conduction. In the present study we have taken polar material, polyvinyl pyrrolidone (PVP).

The dependence of TSD on the forming conditions and different electrode materials have already been given in Chapter 3.

4.4 EXPERIMENTAL DETAILS

The isothermal immersion technique was utilized for preparing thin films of polyvinyl pyrrolidone (PVP). The solution was prepared in a glass beaker by first dissolving 2.4 gm PVP in 30 ml of chemically pure chloroform at room temperature and continuously stirred for 60 min by means of a teflon coated magnetic stirrer. Thereafter, it was stirred and heated to 50°C to yield a homogeneous solution. The glass beaker containing the solution was then immersed in a constant temperature oil bath. Films were cast on to a metal coated microscopic glass slides by isothermal immersion technique. Vacuum coated electrodes were used in the present study. For sandwich structure (Al-PVP-Al/Cu/Ag/Sn) in the films, lower electrode was deposited on optically plane glass slide and then it was suspended vertically for 20 min. in the glass beaker, containing polymer solution of desired concentration. Later these films were kept in an oven at 45°C for 24 hrs to remove all the traces of solvent. This was followed by room temperature outgassing at 10^{-5} torr for a further period of 24 hrs. After the film deposition on lower electrode, the glass slide with the polymer film on it, was wrapped in an aluminium mask having a window of 1.33 cm^2 . When exposed to

metal in vacuum, the metal was deposited on the polymer films, thus a sample in the sandwich structure of area 1.33 cm^2 was obtained. The deposition of electrode was done by vacuum coating unit, supplied by M/s Hind High Vacuum Co. Ltd., Bangalore.

The thickness of the samples was determined by measuring its capacitance at 10 kHz using a dielectric constant $\epsilon = 3$. Different steps for the preparation of thermoelectret are as follows :

- (i) The sample is heated to the desired polarizing temperatures (T_p),
- (ii) It is kept at T_p for some time to reach temperature equilibrium,
- (iii) Then an electric field is applied at T_p and kept on for a period of polarizing time t , and
- (iv) It is cooled under the field application to room temperature (or below). The field is then removed.

In the present investigation, the samples are thermally polarized with fields of 5, 10, 25, 50, 75 and 100 kV/cm at temperatures 40, 50, 60, 70 and 80°C respectively. The field was applied with the help of a power supply (EC-4800D) and the current was recorded by a sensitive electrometer (Keithley 600C).

4.5 RESULTS AND DISCUSSION

The TSDC thermograms of pure PVP foil electrets formed by incorporating for similar Al-Al configuration are shown in Figs. 4.1 to 4.5 for various polarizing fields E_p ($= 5, 10, 25, 50, 75$ and 100 kV/cm) at instant polarising temperature T_p . The value of T_p taken are $40, 50, 60, 70$ and 80°C . PVP film of about $20\text{ }\mu\text{m}$ in thickness is employed and the samples are heated at the rate of 3°C per minute. Each thermogram show the effect of various polarising fields at a particular constant temperature. It can be seen that there appear two distinct current peaks which occur at temperatures 90 and $170\pm 5^\circ\text{C}$ and designated as α and ρ peaks, respectively. There is no appreciable shift in the positions of two peaks for various polarizing fields (In reality, there is small shift both ways, right and left, which is due change in the relative magnitudes of the various peaks as the polarizing field increases). For the ρ peak, the current is higher than for α peak. The height of current peaks is found to rise in magnitude with the increase in polarizing field.

The TSDC thermograms of pure PVP foil electrets for other similar Ag-Ag systems are shown in Figs. 4.6 to 4.8 for various polarizing fields as mentioned above at constant temperature T_p . The values of T_p taken are $40^\circ, 60^\circ$ and 80°C . Film thickness and heating rate used here is the same as in Al-Al system. All the curves show three distinct current peaks

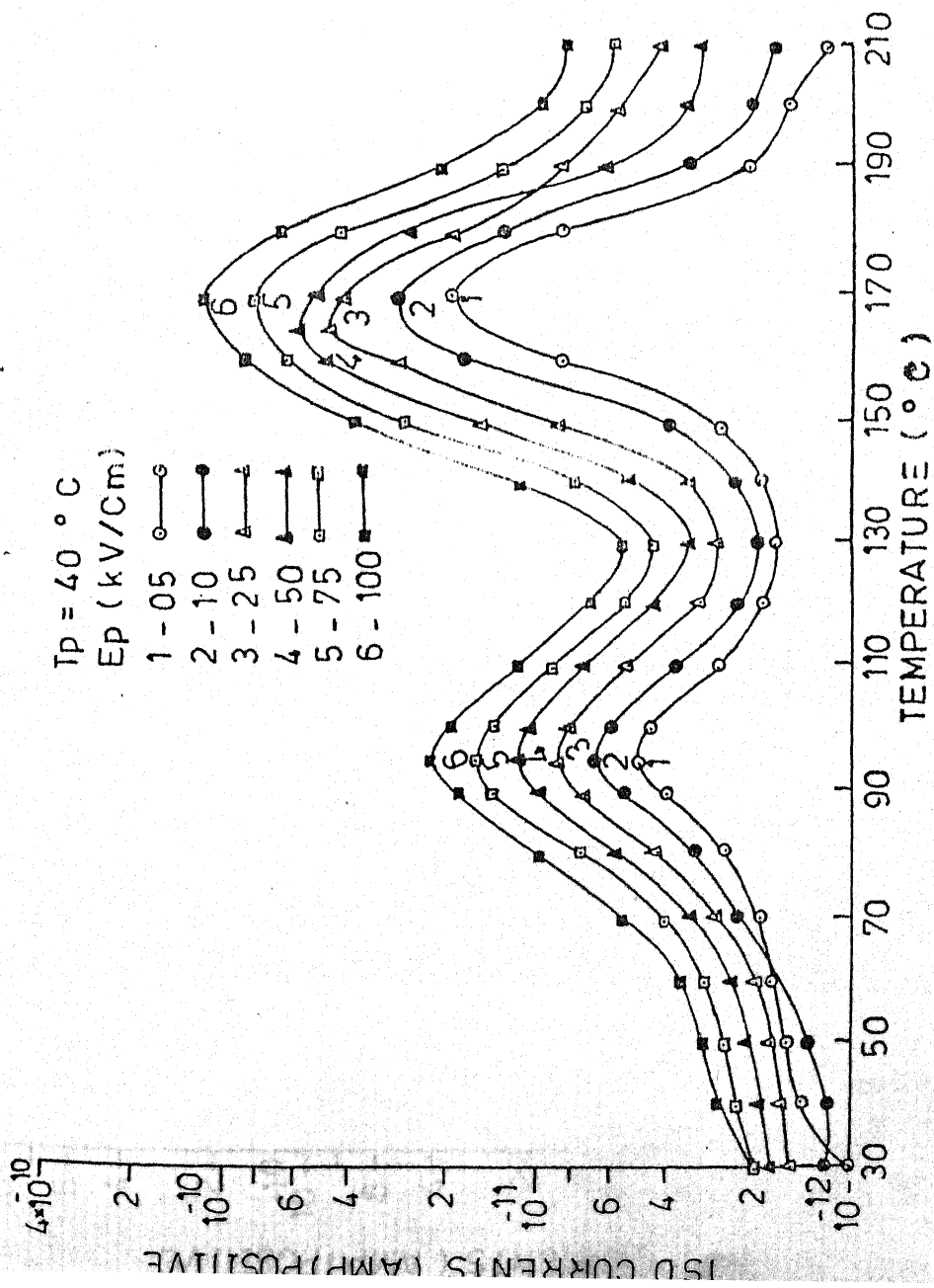


Fig 4.1 Effect of various polarising fields on TSDC.C. thermograms of samples (20 μm thick, poled at given temperature with Al-Al system.

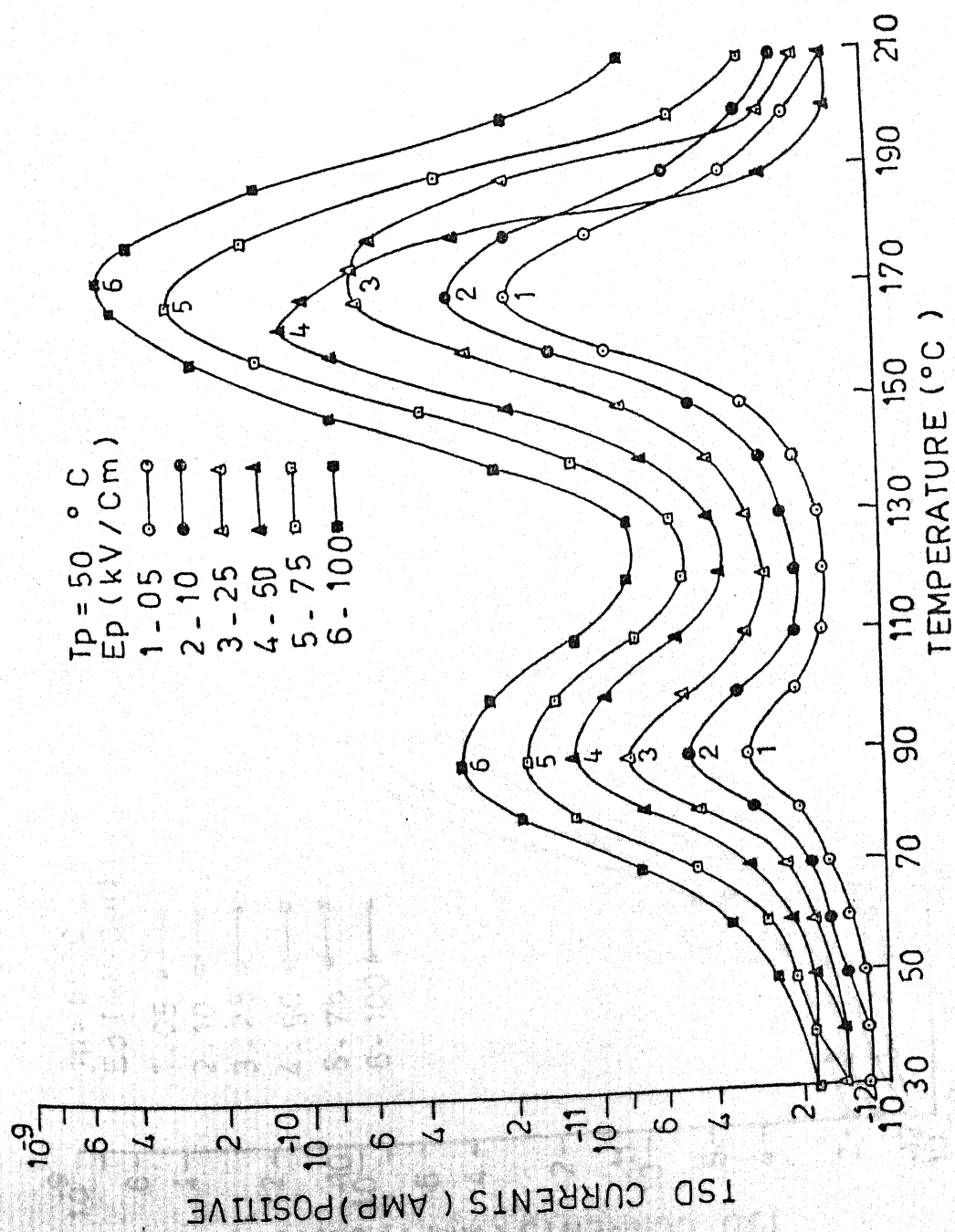


Fig. 4.2 Effect of various polarising fields on TSDC thermograms of samples (20 μm thick) poled at given temperature with Al-Al system.

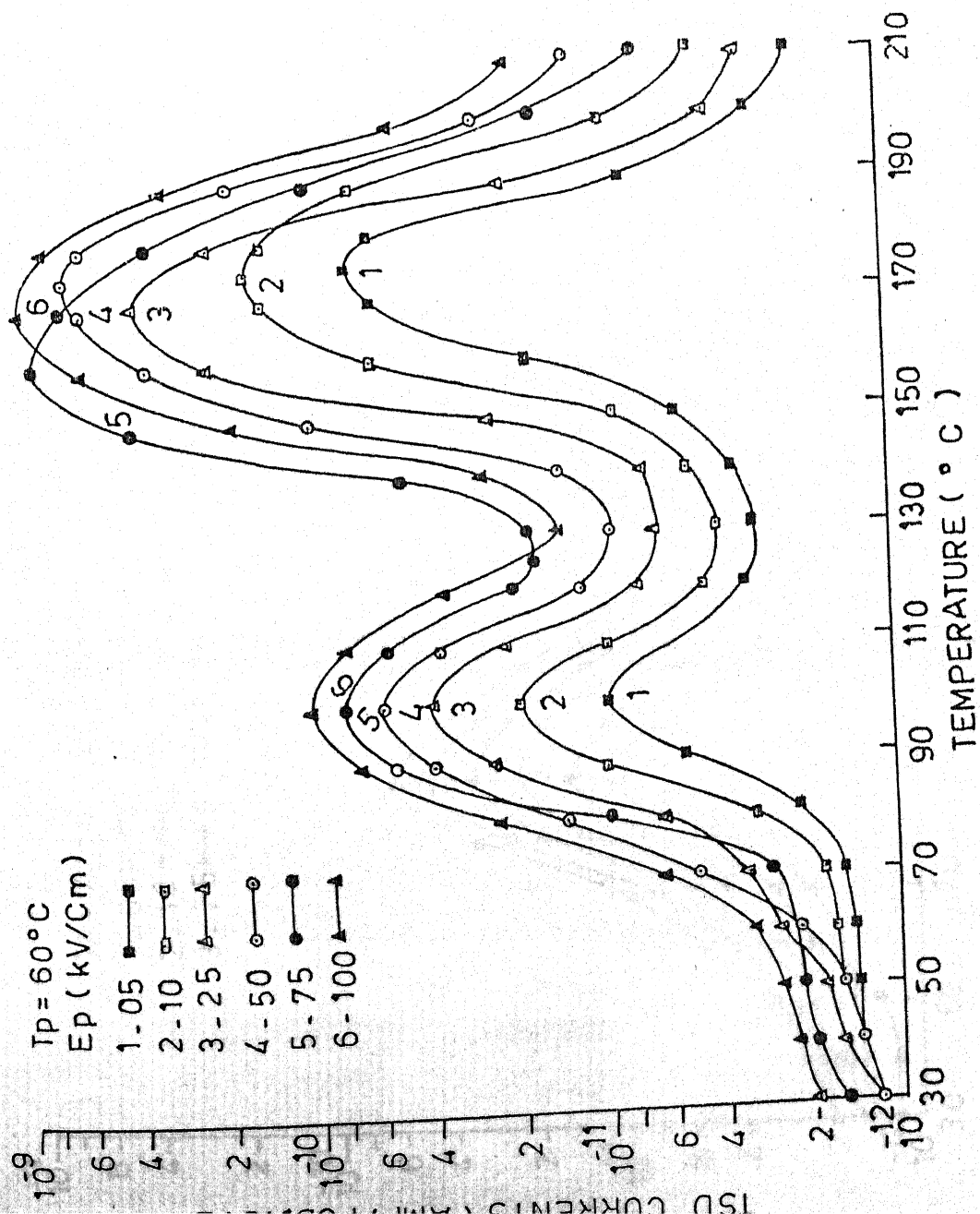


Fig. 4.3 Effect of various polarising fields on TSDC thermograms of samples
 ($20\ \mu\text{m}$ thick) poled at given temperature with Al-Al system.

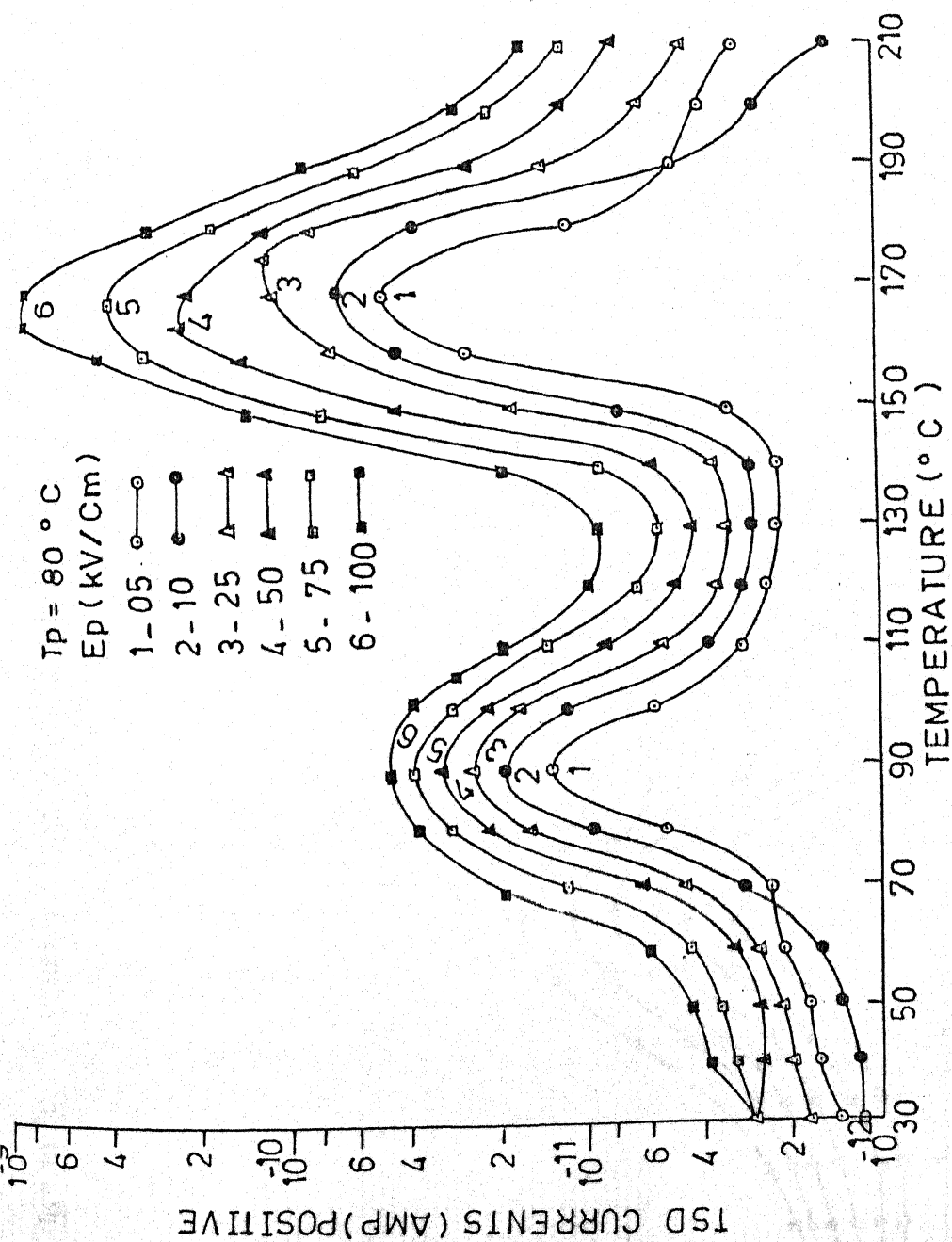


Fig 4.5 Effect of various polarising fields on TSDC thermograms of samples
 (20 μm thick) poled at given temperature with Al-Al system.

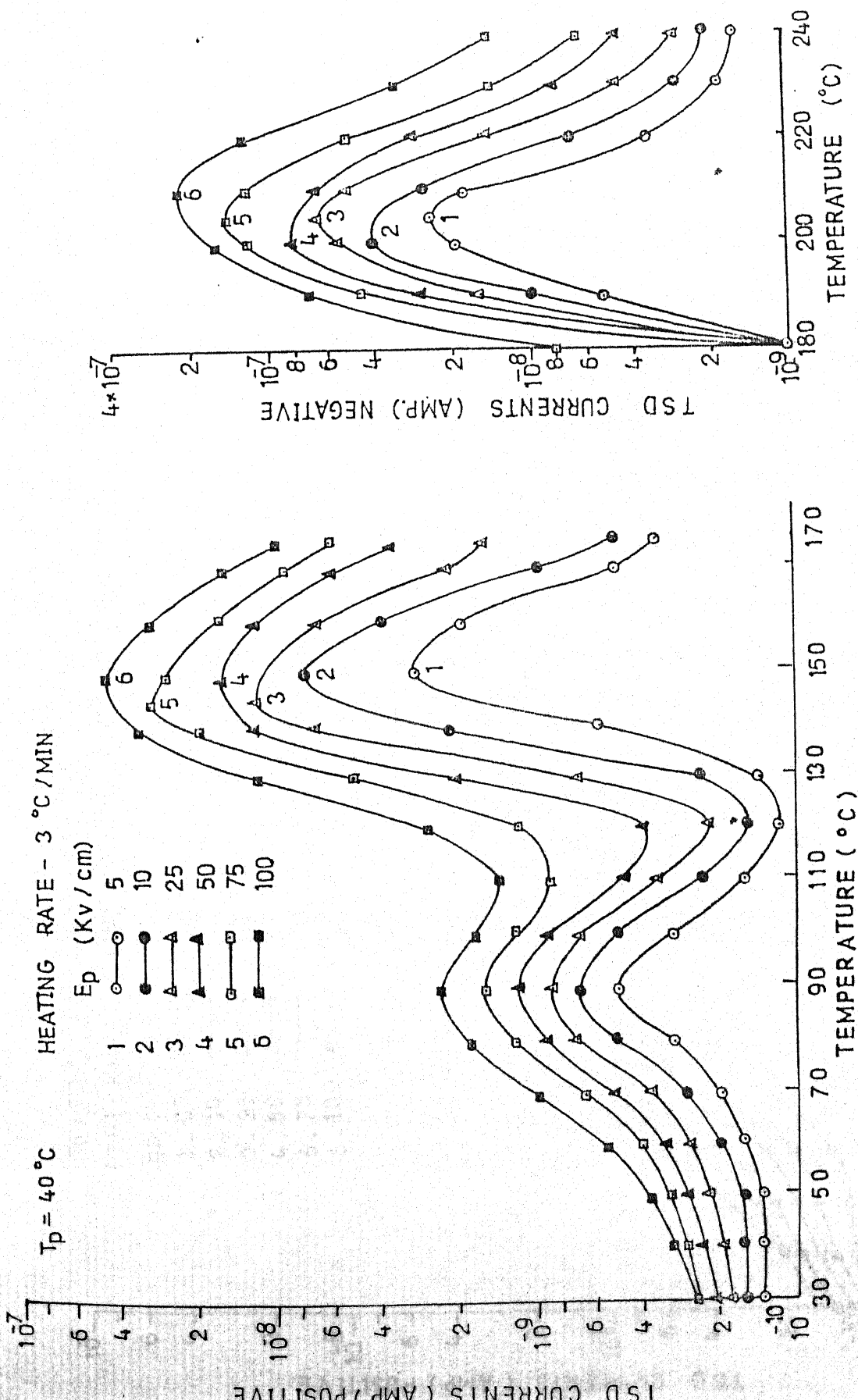


Fig. 4.6 Effect of various polarising fields on TSDC thermograms of samples
 ($20\ \mu\text{m}$ thick) poled at given temperature with Ag-Ag system.

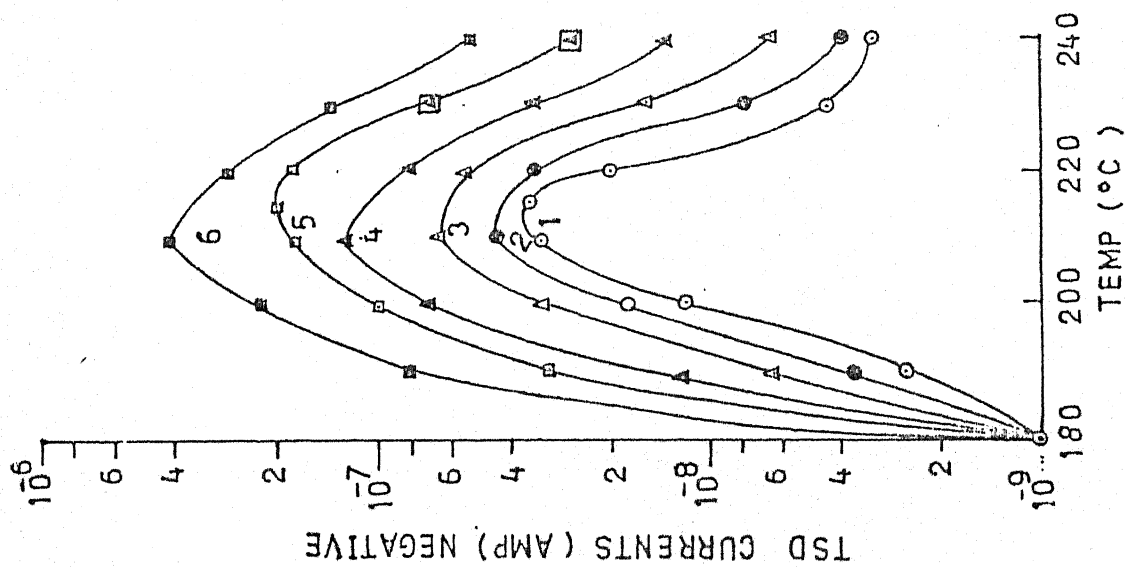
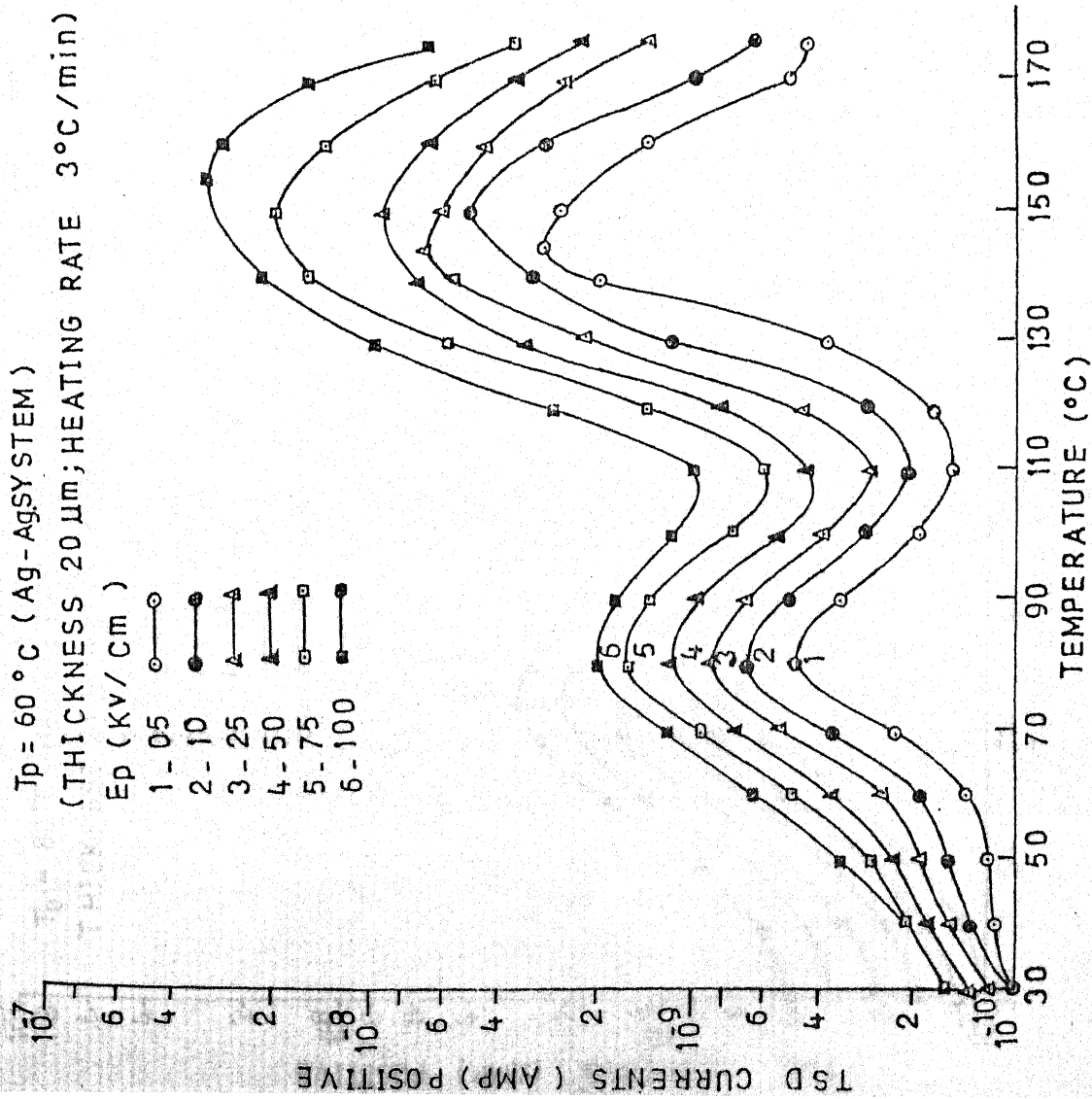


Fig. 4.7 Effect of various polarising fields on TSDC thermograms of samples ($20\mu\text{m}$ thick) poled at given temperature with Ag-Ag system.

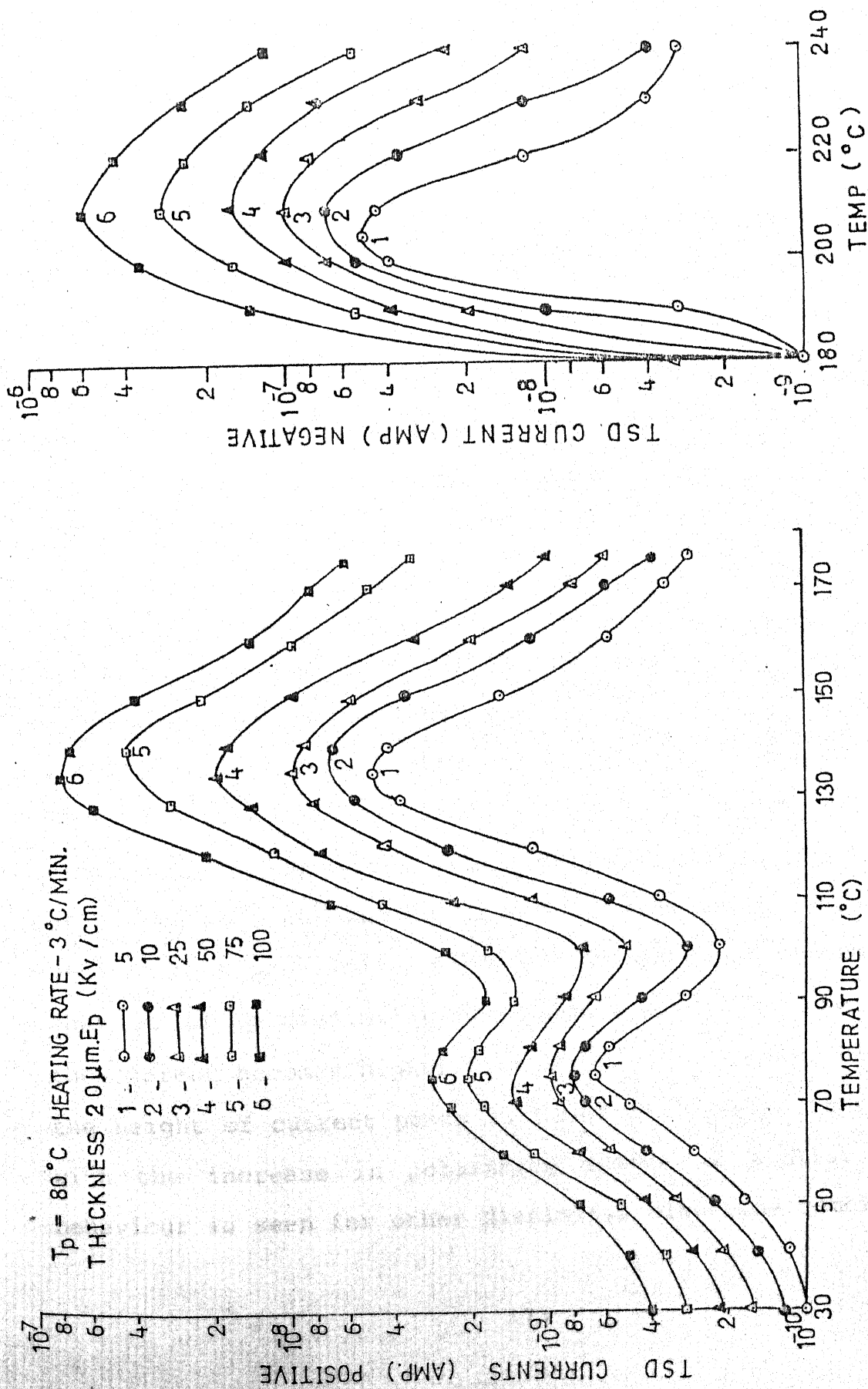


Fig. 4.8 Effect of various polarising fields on TSDC thermograms of samples
 ($20\mu\text{m}$ thick) poled at given temperature with Ag-Ag system.

which occur at temperatures 95 ± 5 ; 170 ± 10 ; $200 \pm 5^\circ\text{C}$ and designated as α , ρ and ρ' peaks, respectively. The α and ρ peaks have been found in a similar manner as observed in Al-Al system whereas, an additional peak ρ' has been found in a direction which is opposite to both the peaks. There is no shift in the position of three peaks for different polarizing fields. For the ρ peak, the current is higher than for α peak, whereas for the ρ' peak, the current is higher than for α peak and lower than ρ peak but in opposite direction. The height of the current peaks is found to increase in magnitude with the increase in polarizing fields. A similar type of behaviour is also observed for Cu-Cu system shown in Figs. 4.9 to 4.11 and for Sn-Sn configuration, shown in Figs. 4.12 to 4.14 for the same polarising fields and temperature under identical conditions.

The TSDC thermograms of pure PVP foil electrets for dissimilar electrode system Al-Ag configuration are shown in Figs. 4.15 to 4.17 for same polarizing fields E_p as used in similar electrode system at constant temperature T_p . The value of T_p are 40° , 60° and 80°C . All the thermograms show similar behaviour as observed in Ag-Ag, Cu-Cu and Sn-Sn systems except that in Al-Ag dissimilar electrode system, for the ρ' -peak, the current becomes higher than for α and ρ peaks. Here also, the height of current peaks is found to increase in magnitude with the increase in polarising fields. A similar type of behaviour is seen for other dissimilar electrode combinations,

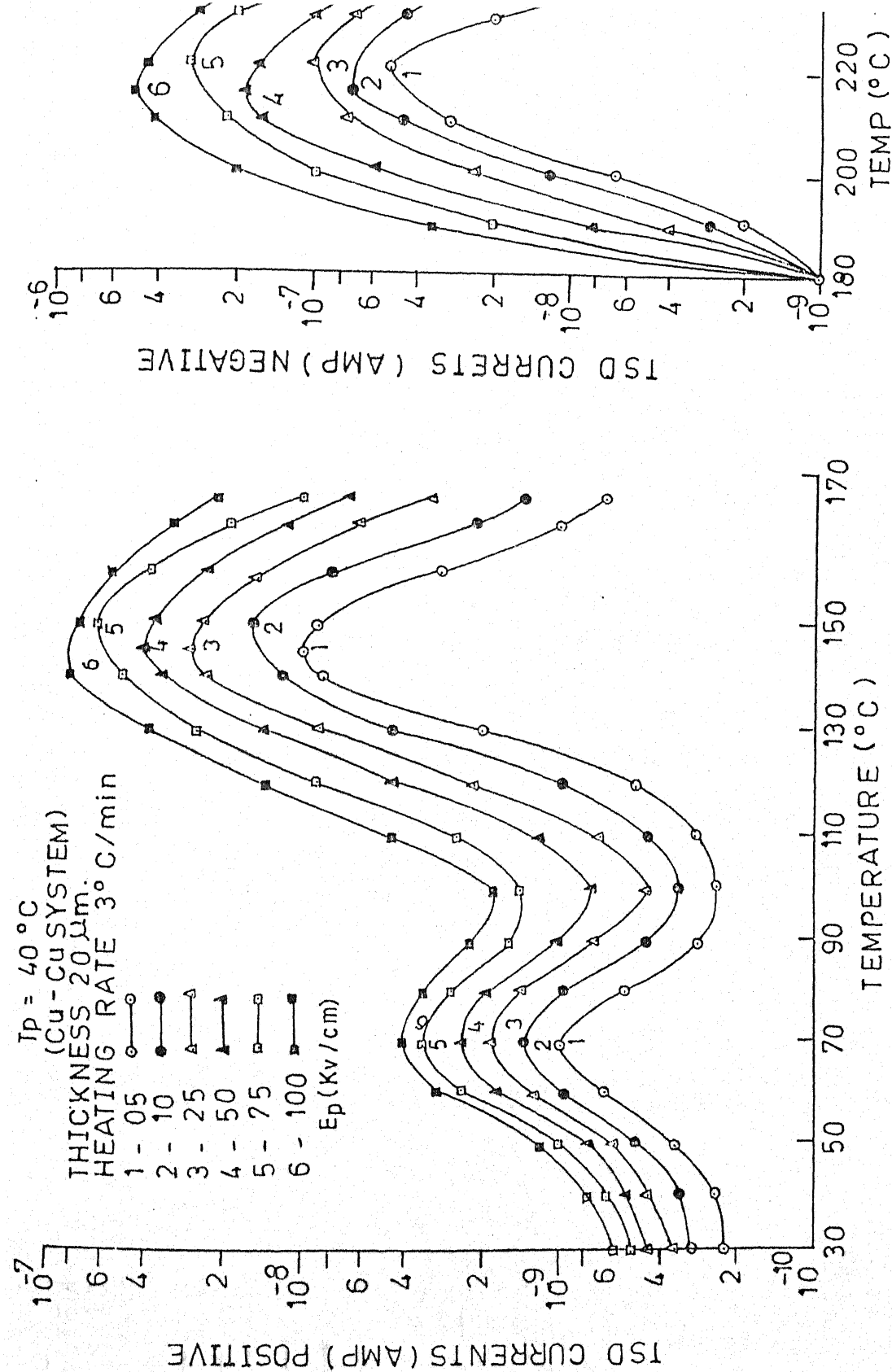


Fig. 4.9 Effect of various polarising fields on TSDC thermograms of samples ($20\mu\text{m}$ thick) poled at given temperature with Cu-Cu system.

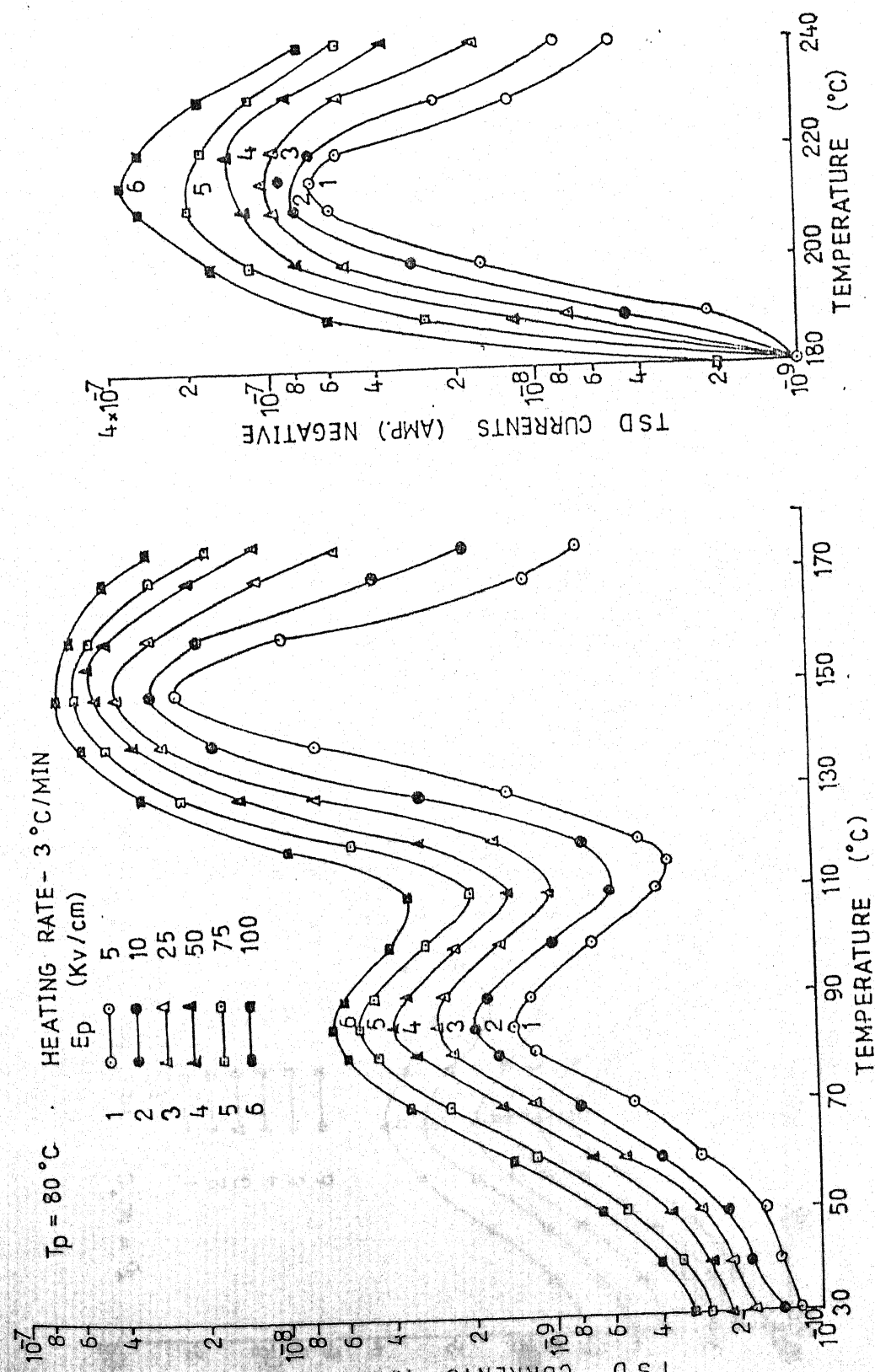


Fig. 4.11 Effect of various polarising fields on TSDC thermograms of samples
 ($20\ \mu\text{m}$ thick) poled at given temperature with Cu-Cu system.

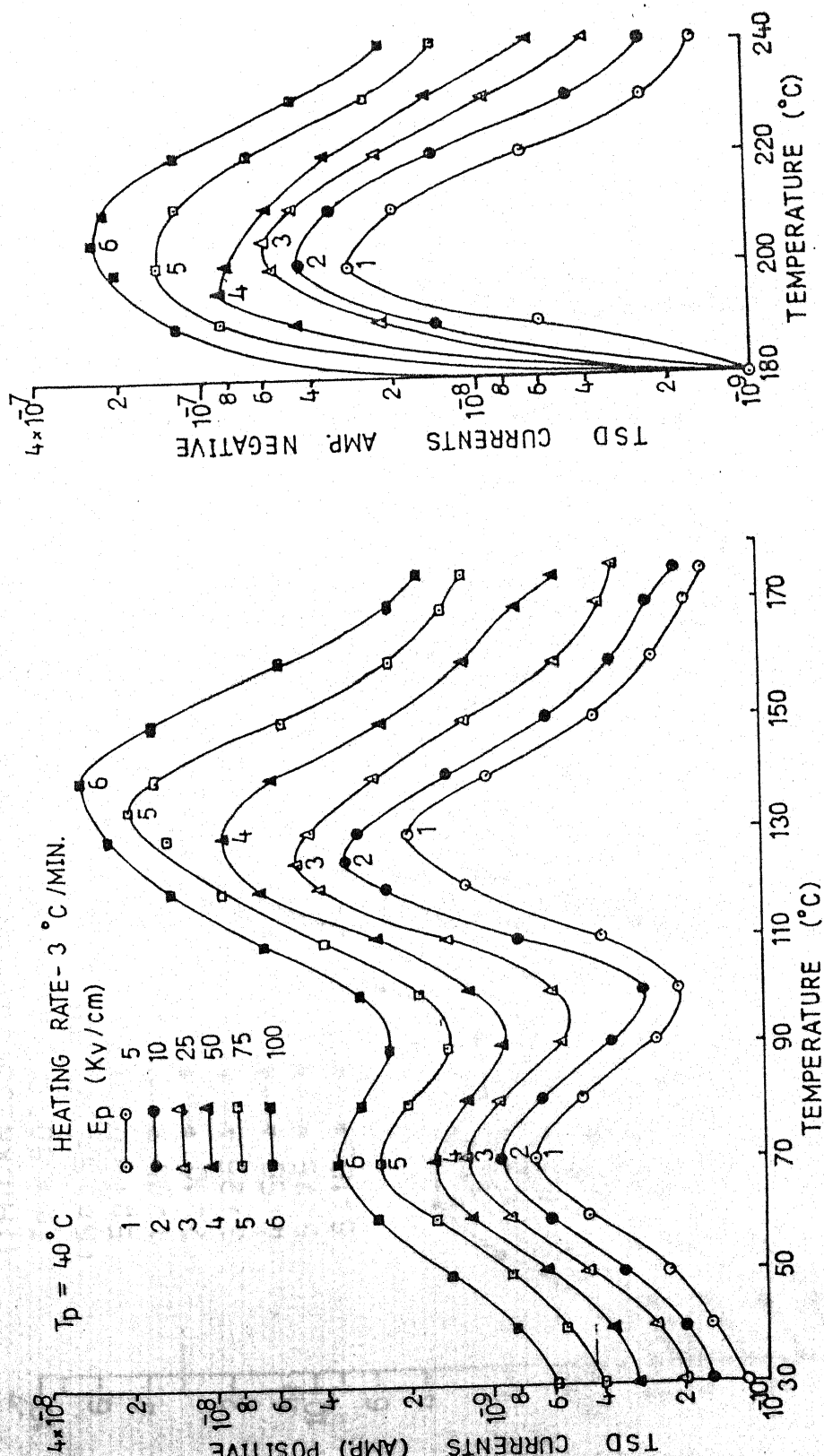


Fig. 4.12 Effect of various polarising fields on TSDC thermograms of $(20\ \mu\text{m})$ thick samples poled at given temperature with Sn-Sn system.

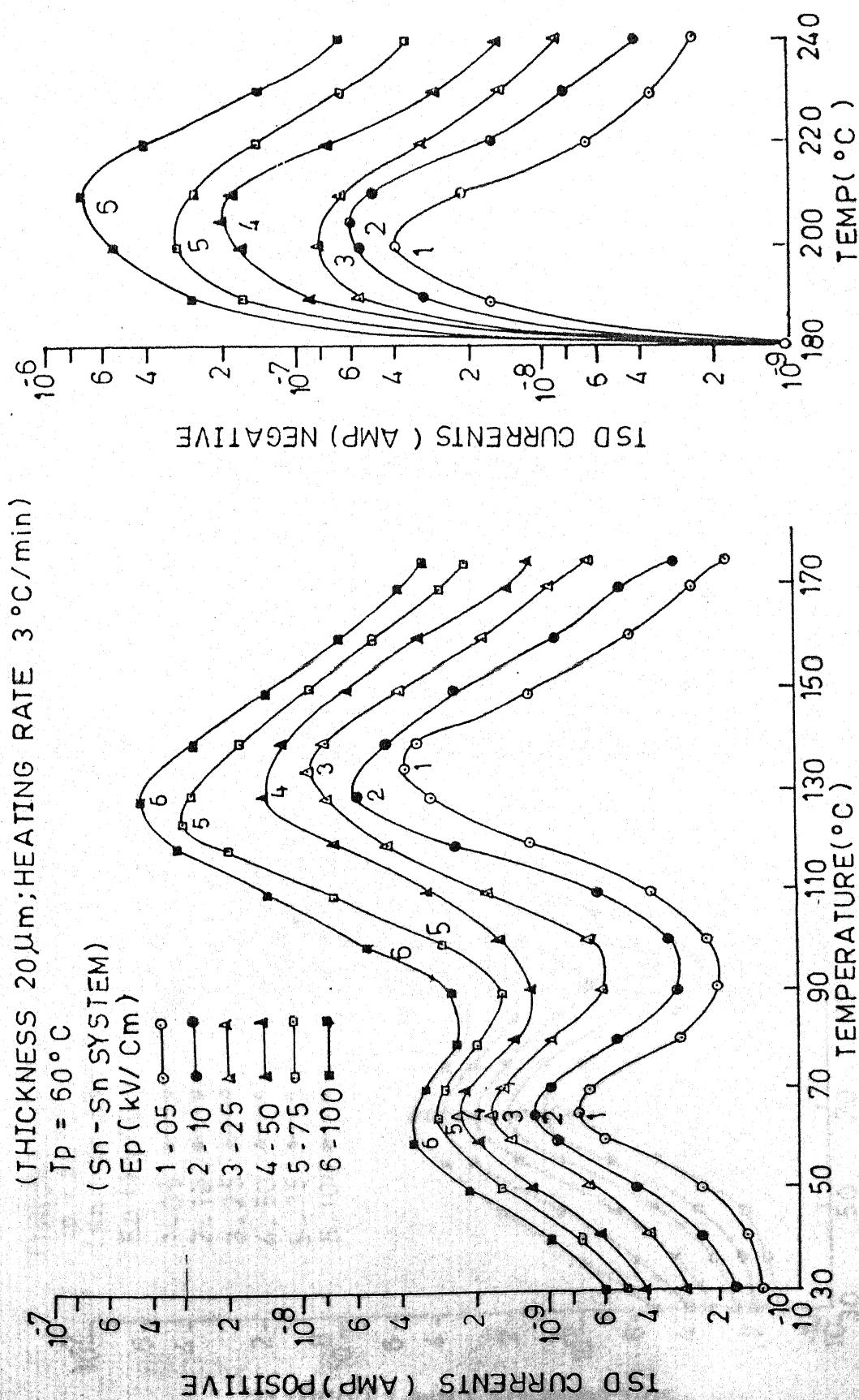


Fig. 4.13 Effect of various polarising fields on TSDC thermograms of (20 μm thick) samples poled at given temperature with Sn-Sn system.

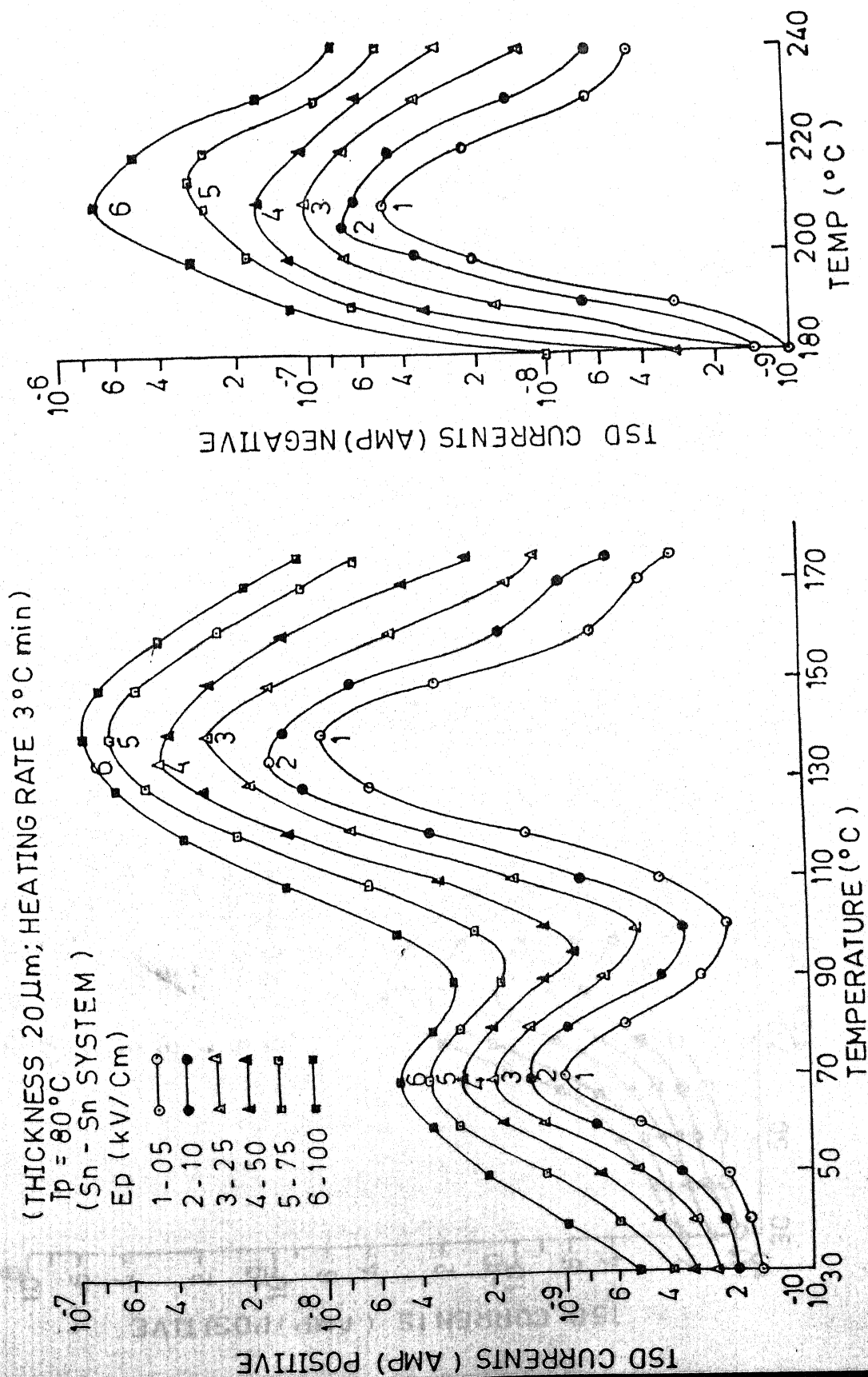


Fig. 4.14 Effect of various polarising fields on TSDC thermograms of (20 μm thick) samples poled at given temperature with Sn-Sn system.

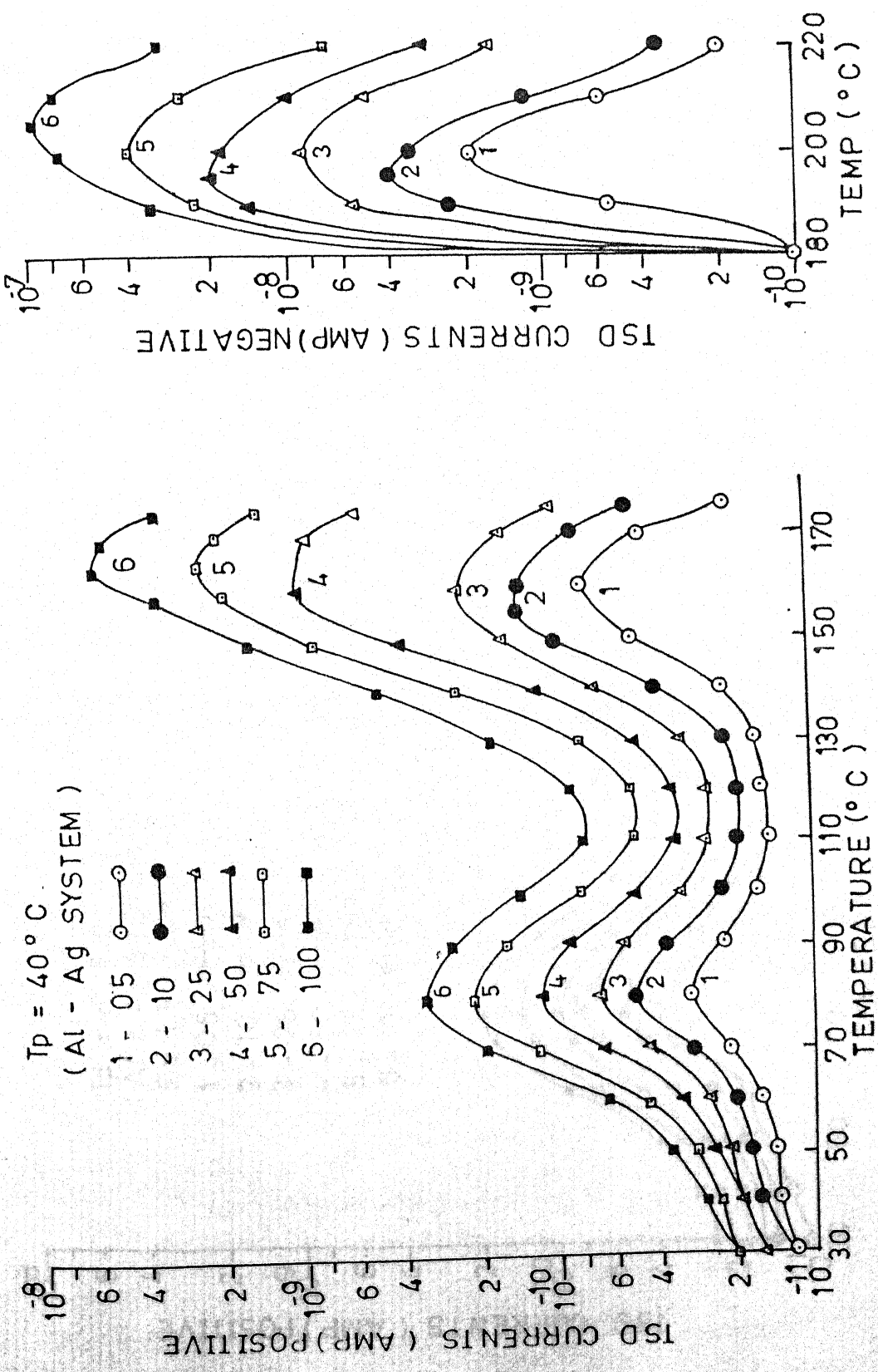


Fig. 4.15 Effect of various polarising fields on TSDC thermograms of (22. μm thick) samples poled at given temperature with Al-Ag system.

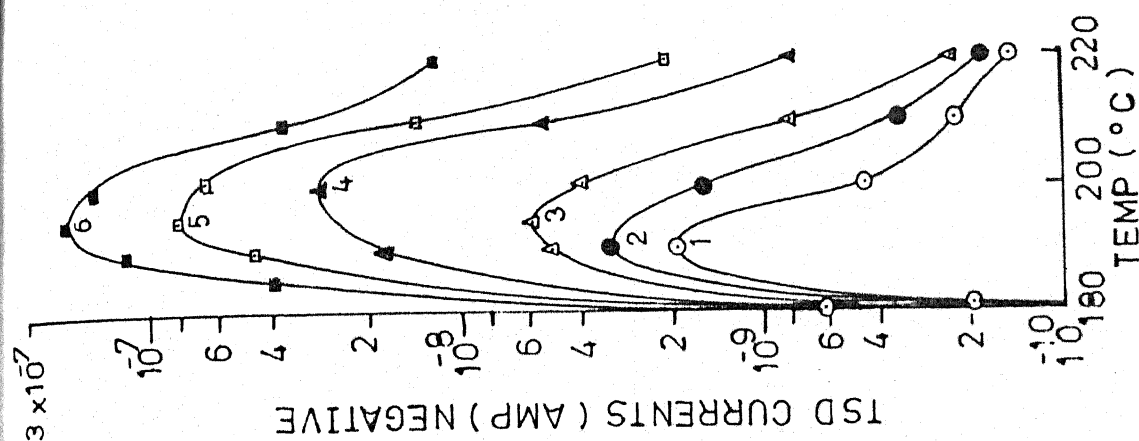
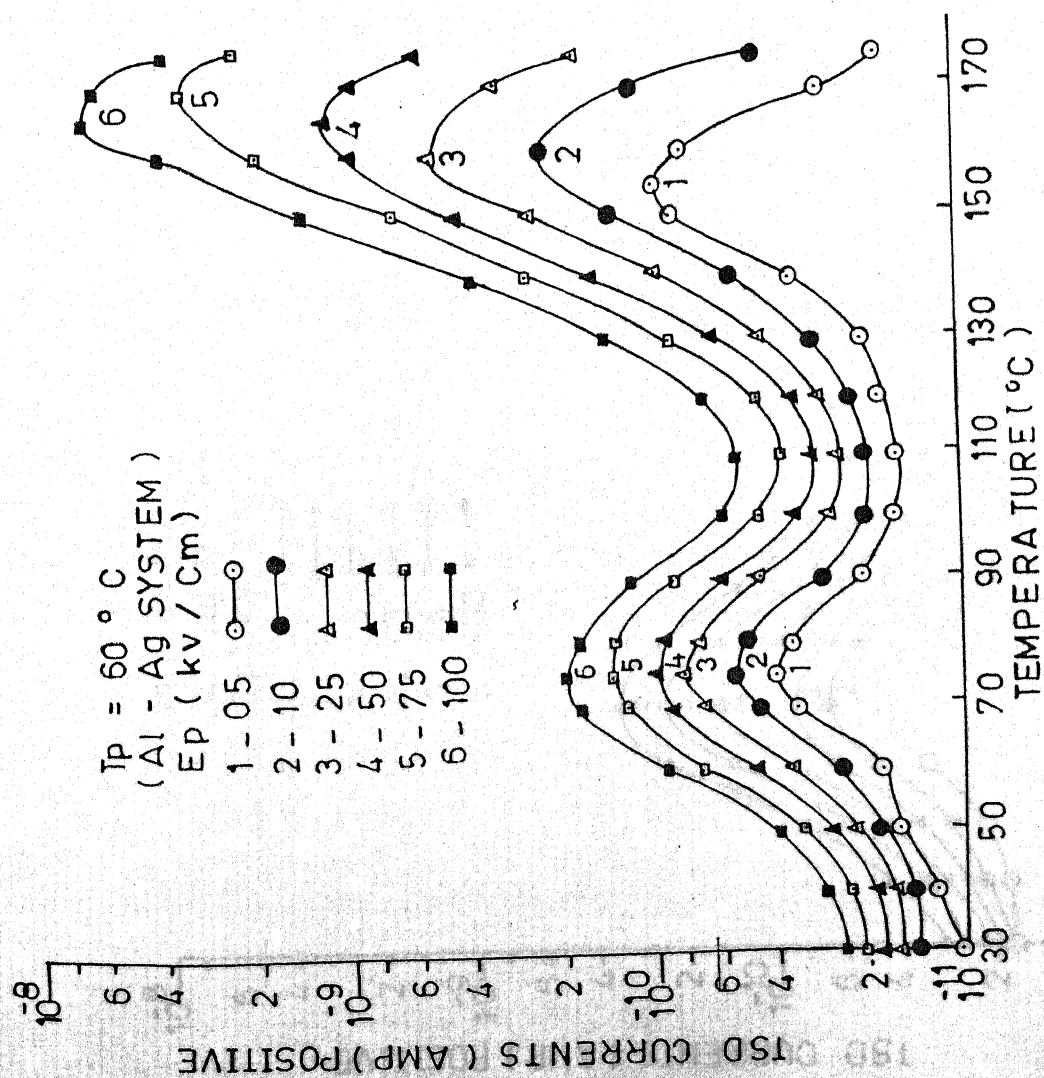


Fig. 4.16 Effect of various polarising fields on TSD thermograms of (20 μm thick) samples poled at given temperature with Al-Ag system.

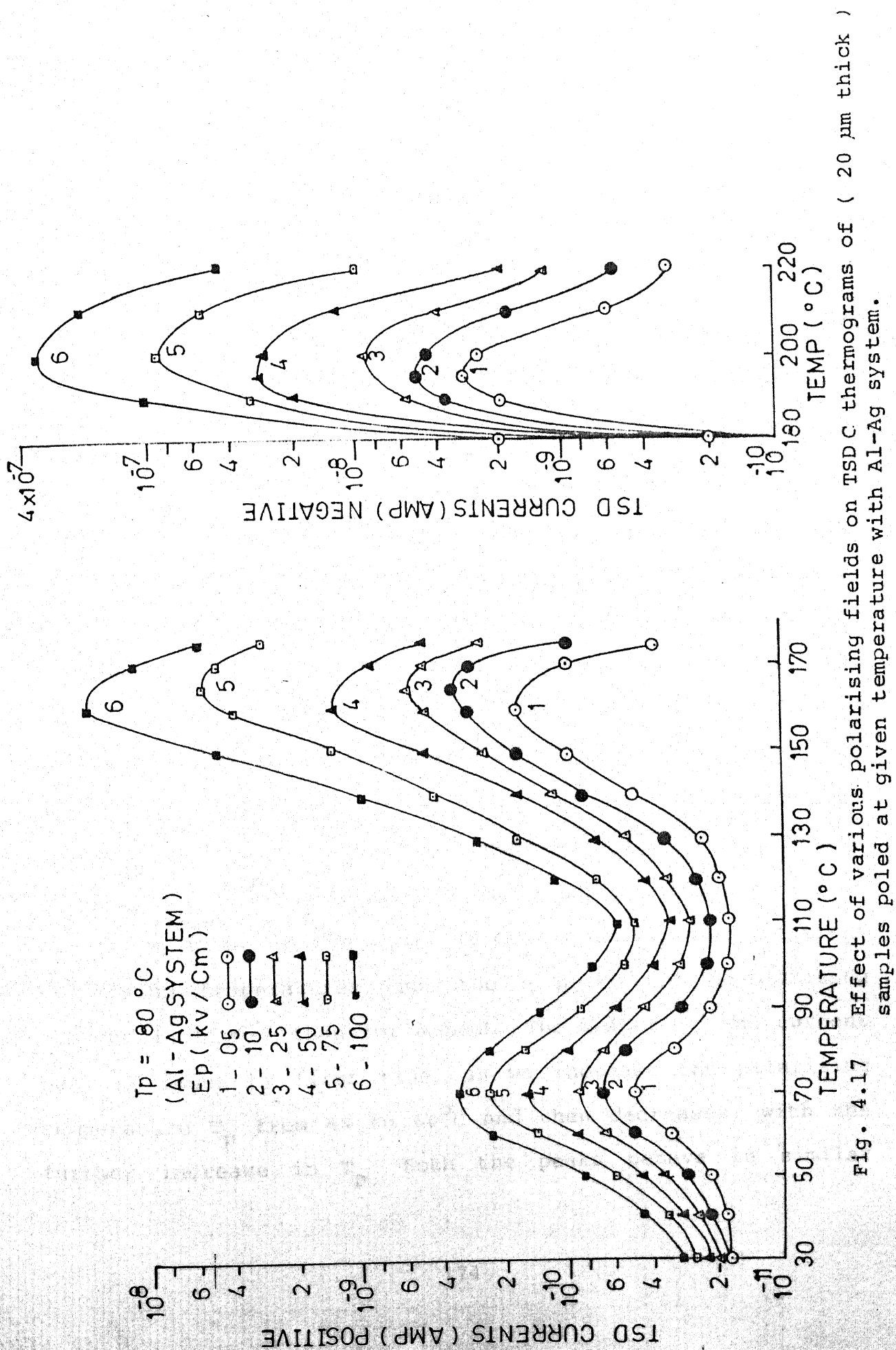


Fig. 4.17 Effect of various polarising fields on TSDC thermograms of (20 μm thick) samples poled at given temperature with Al-Ag system.

Al-Cu and Al-Sn as shown in Figs. 4.18 to 4.20, 4.21 to 4.23, respectively.

The depolarization kinetic data, i.e. activation energy, charge released and relaxation times for the observed peaks have been calculated using initial rise method of Garlick and Gibson and Bucci et al described earlier in theoretical chapter initial rise plots of Garlic and Gibson are shown in Figs.4.23(a), (b) and (c) and their values are listed in Tables 4.1 to 4.23.

Figs. 4.24 to 4.65 show the effect of different polarising temperatures on the TSDC thermograms of PVP foil electrets. Samples are prepared for different polarising temperatures T_p ($= 40, 50, 60, 70$ and 80°C) at constant polarising field E_p . The values of E_p taken are 5, 10, 25, 50, 75 and 100 kV/cm for different electrodes configurations. Film thickness is 20 μm and heating rate of 3°C per minute is used. Figs. 4.24 to 4.29 are for Al-Al system. All the thermograms show two distinct peaks which occur at temperatures 90 and $170 \pm 5^\circ\text{C}$ and 200°C designated as α , ρ and ρ' peaks. There is almost no shift in the position of two peaks with different polarising temperatures. For the ρ peak, the depolarising current is higher than for α peak. The height of the current peak is found to first rise, as we increase the polarising temperature T_p from 40 to 60°C and then decreases, with the further increase in T_p . Both the peaks behave in similar

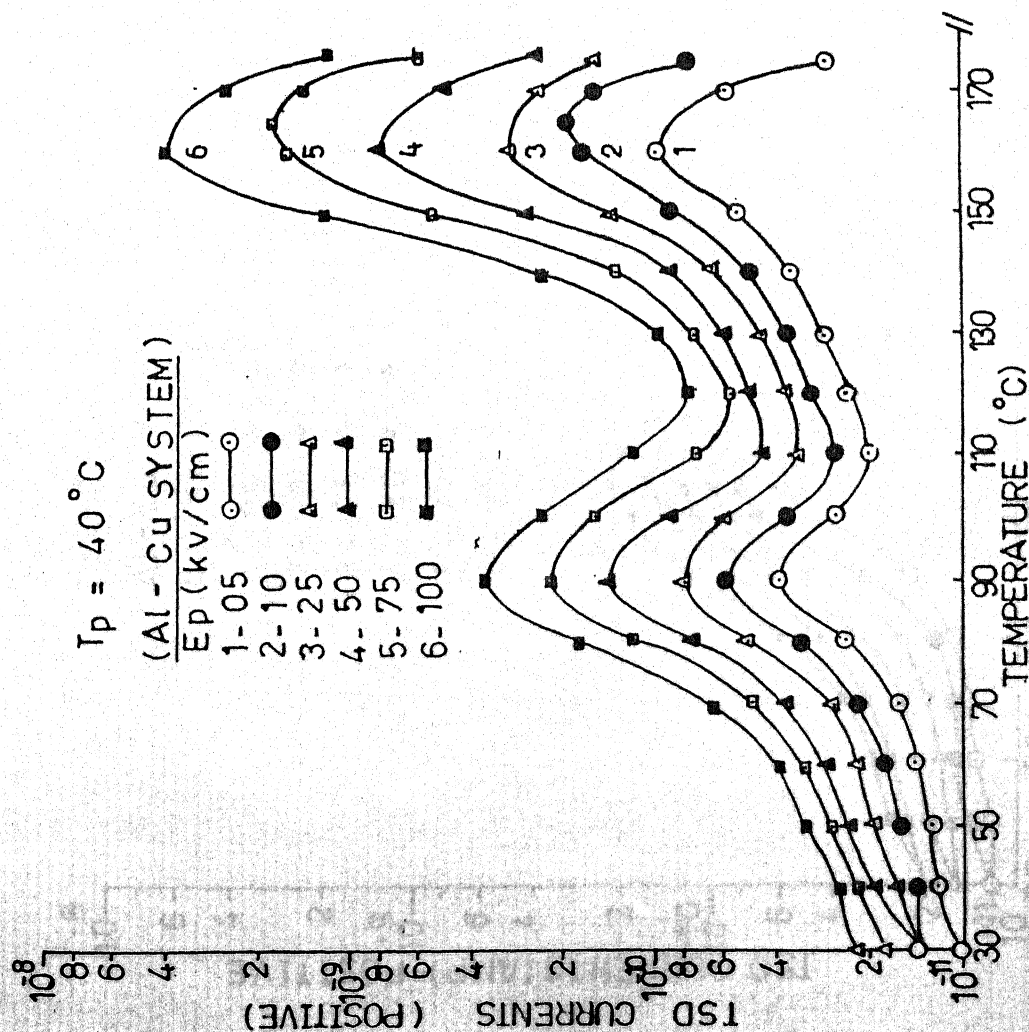
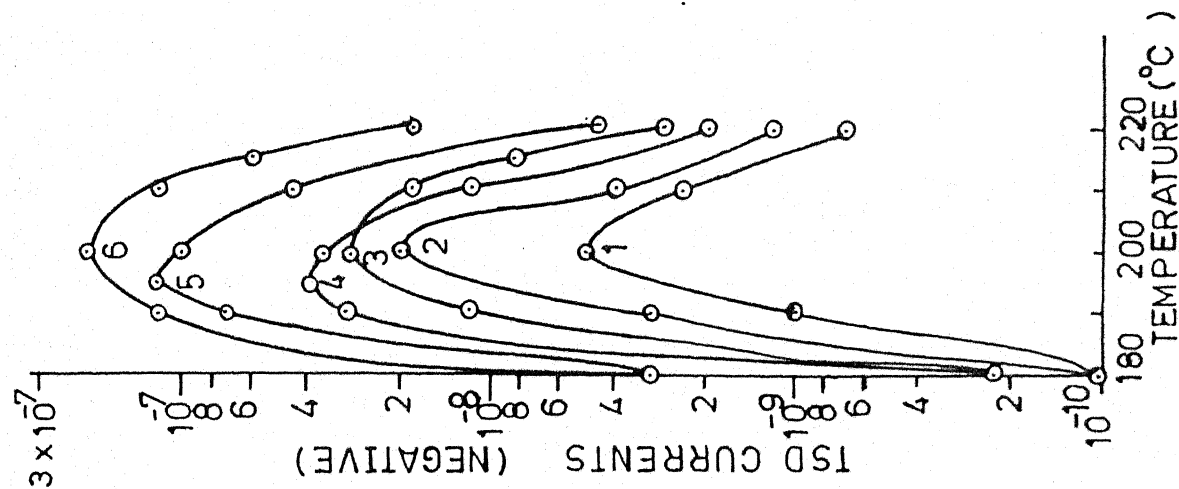


Fig. 4.18 Effect of various polarising fields on TSD thermograms of (20 μm thick) samples poled at given temperature with Al-Cu system.

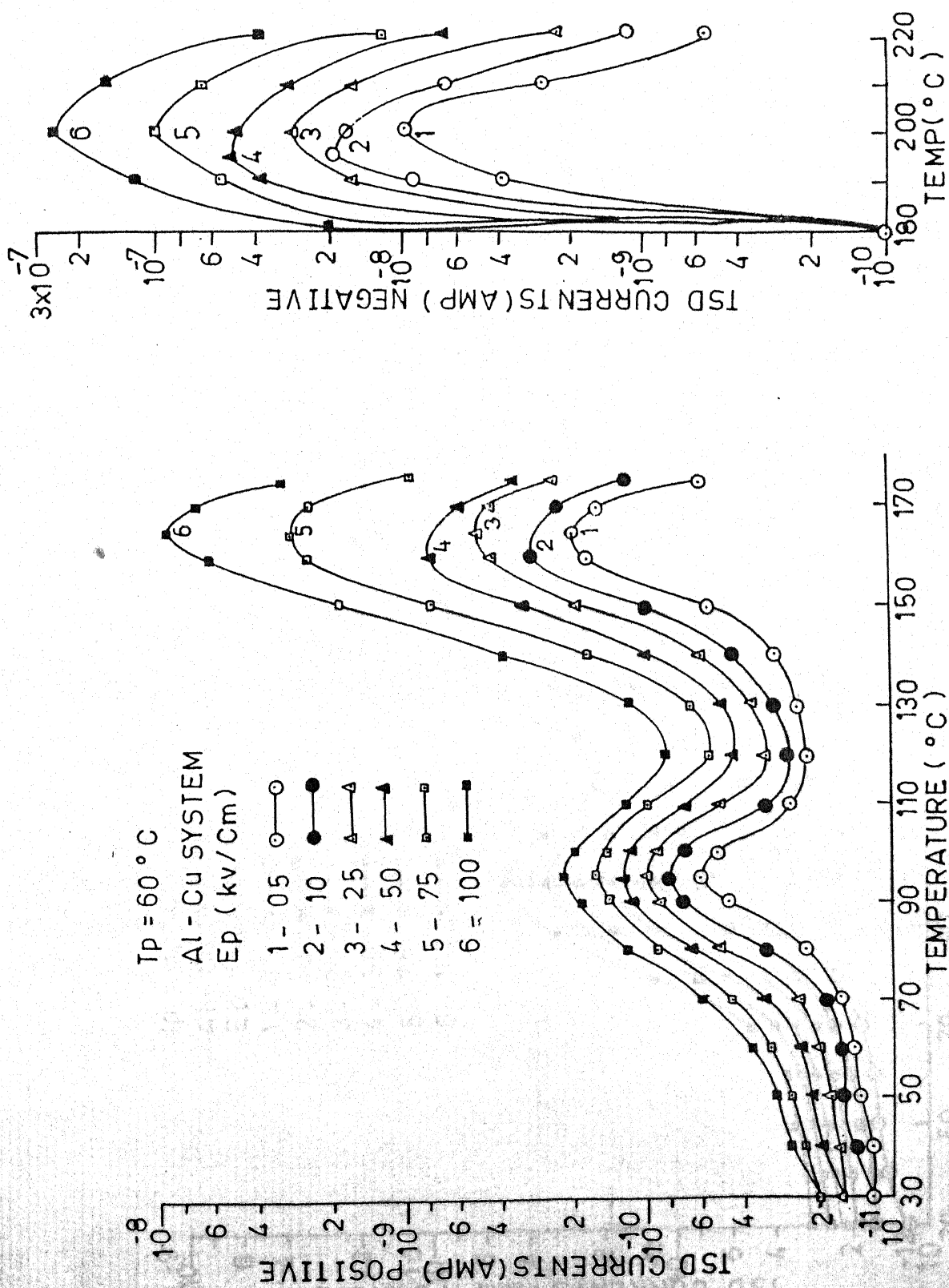


Fig. 4.19 Effect of various polarising fields on TSDC thermograms of (20 μm thick) samples poled at given temperature with Al-Cu system.

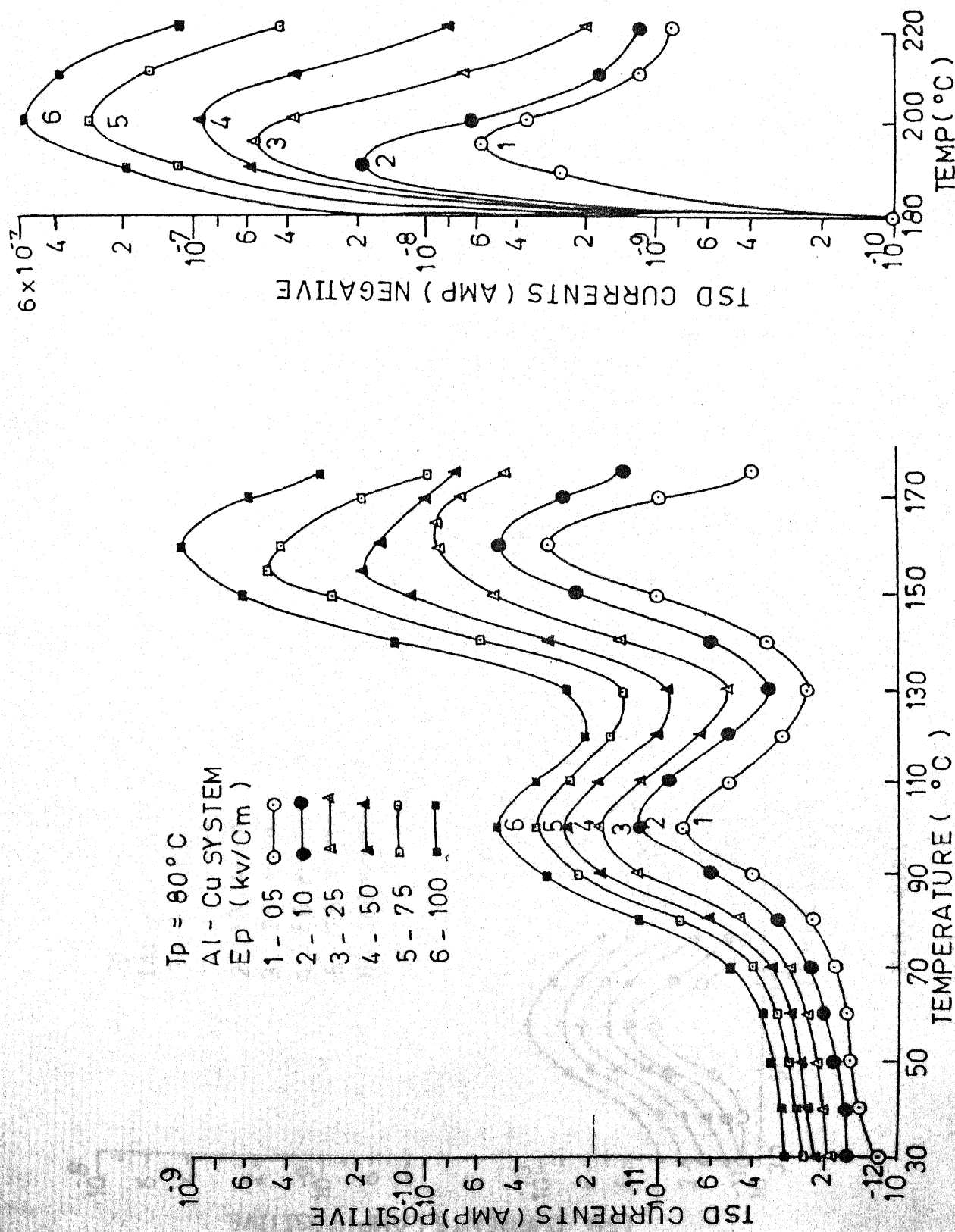


Fig. 4.20 Effect of various polarising fields on TSDC thermograms of (20 μm thick) samples poled at given temperature with Al-Cu system.

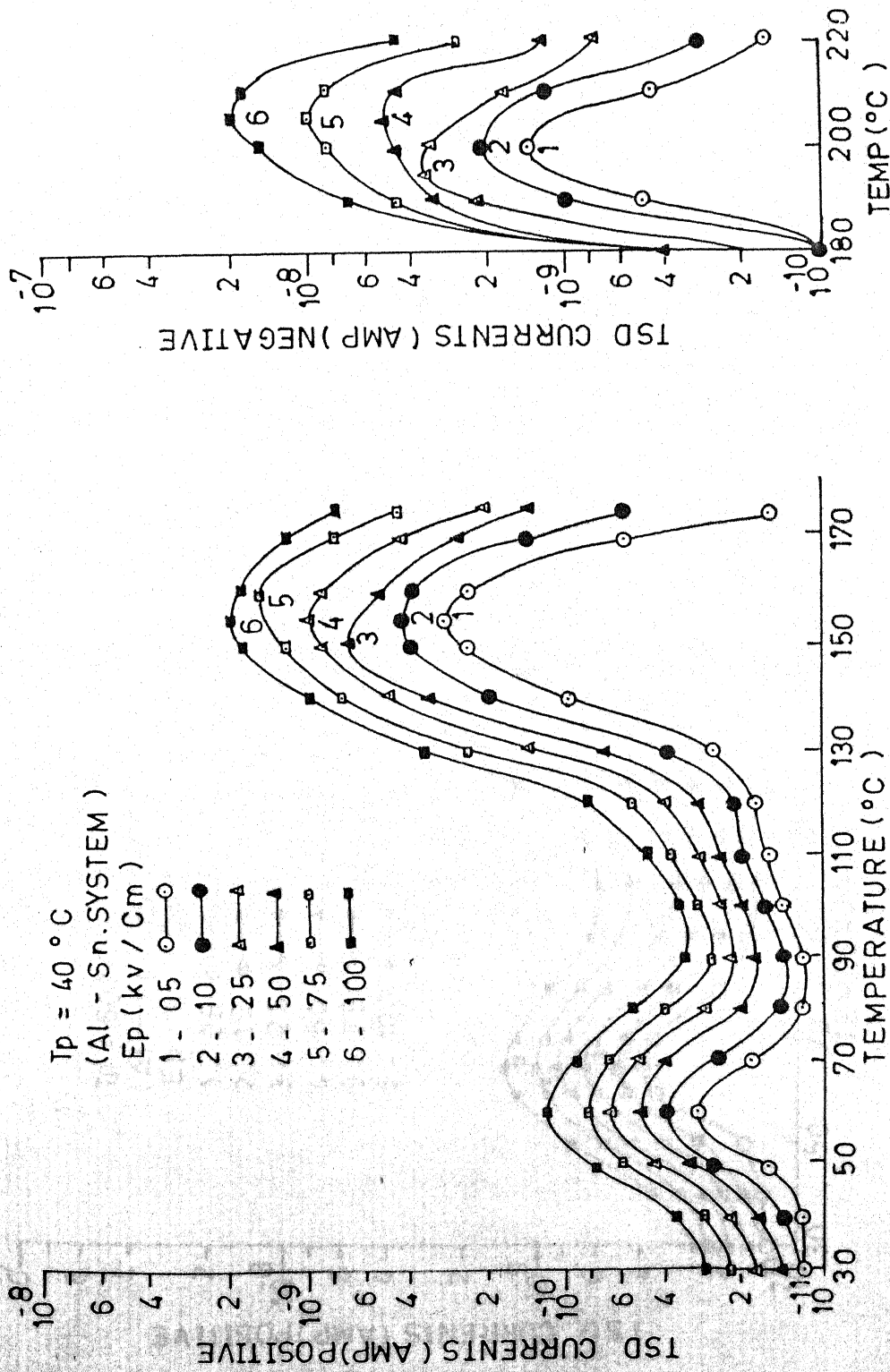


Fig. 4.21 Effect of various polarising fields on TSDC thermograms of (20 μm thick)
 Samples poled at given temperature with Al-Sn system.

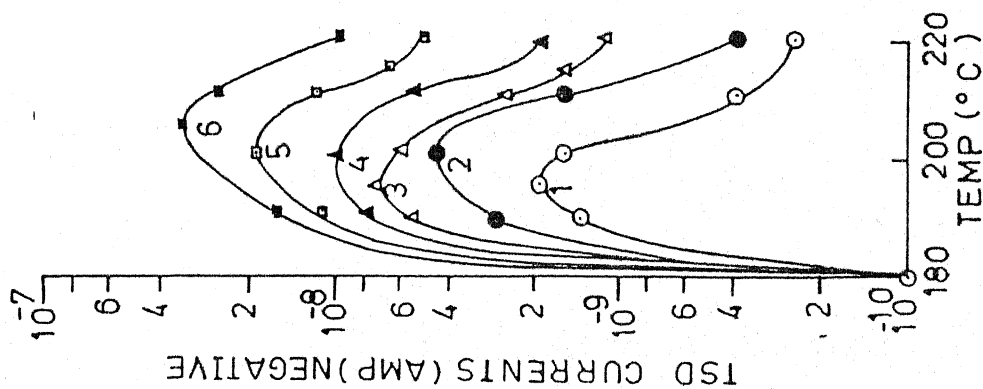
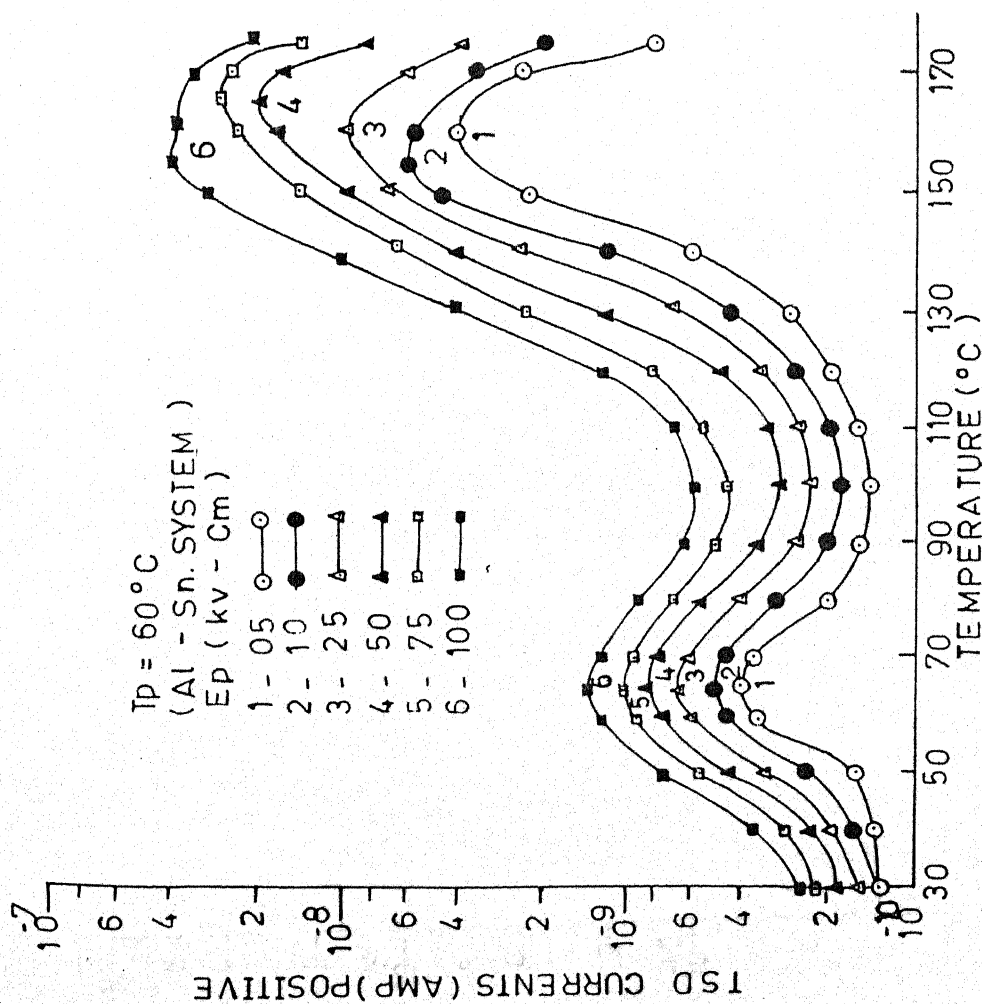


Fig. 4.22 Effect of various polarising fields on TSD thermograms of (20 μm thick) samples poled at given temperature with Al-Sn system.

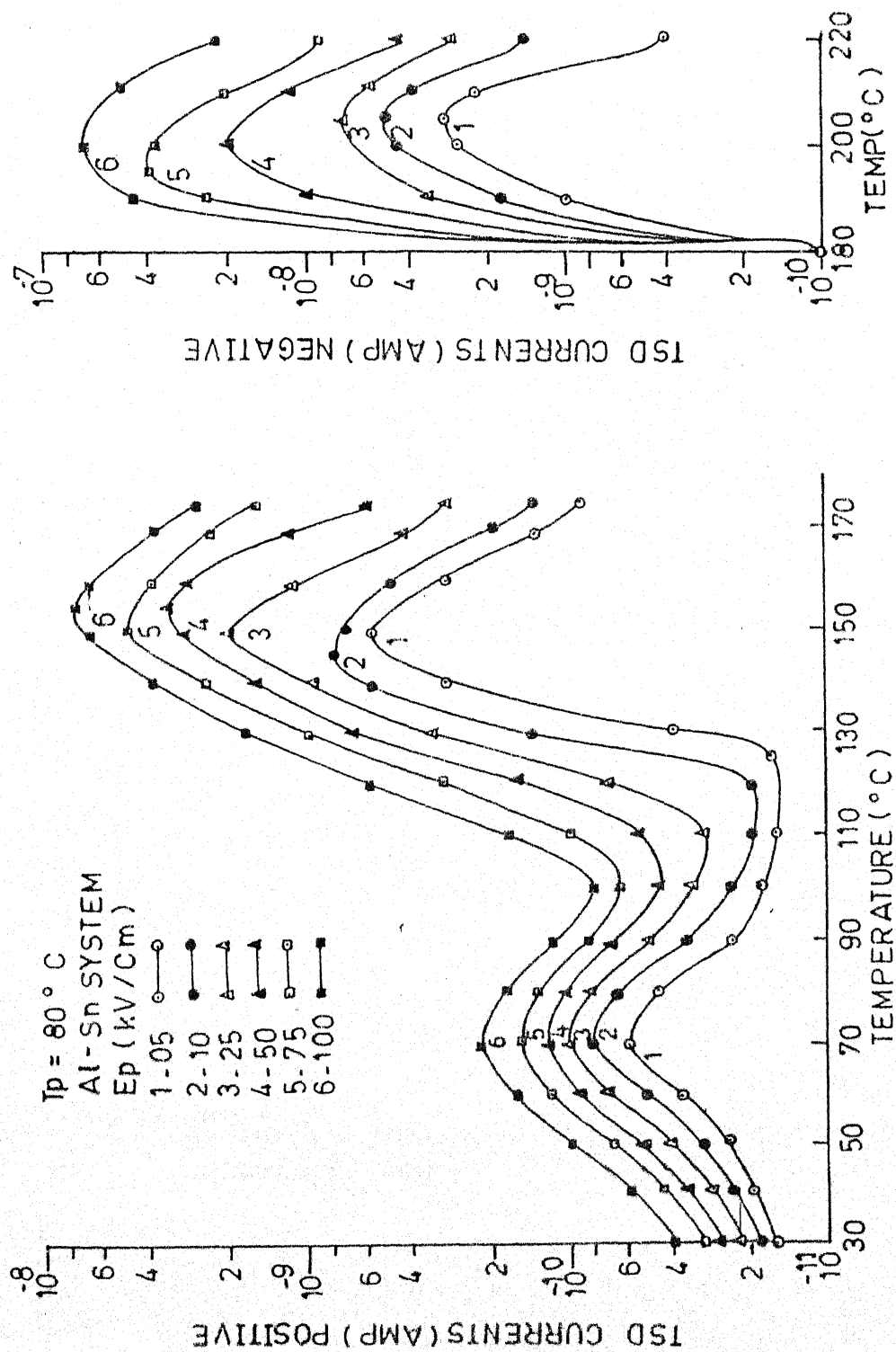


Fig. 4.23 Effect of various polarising fields on TSDC thermograms of (20 μm thick) samples poled at given temperature with Al-Sn system.

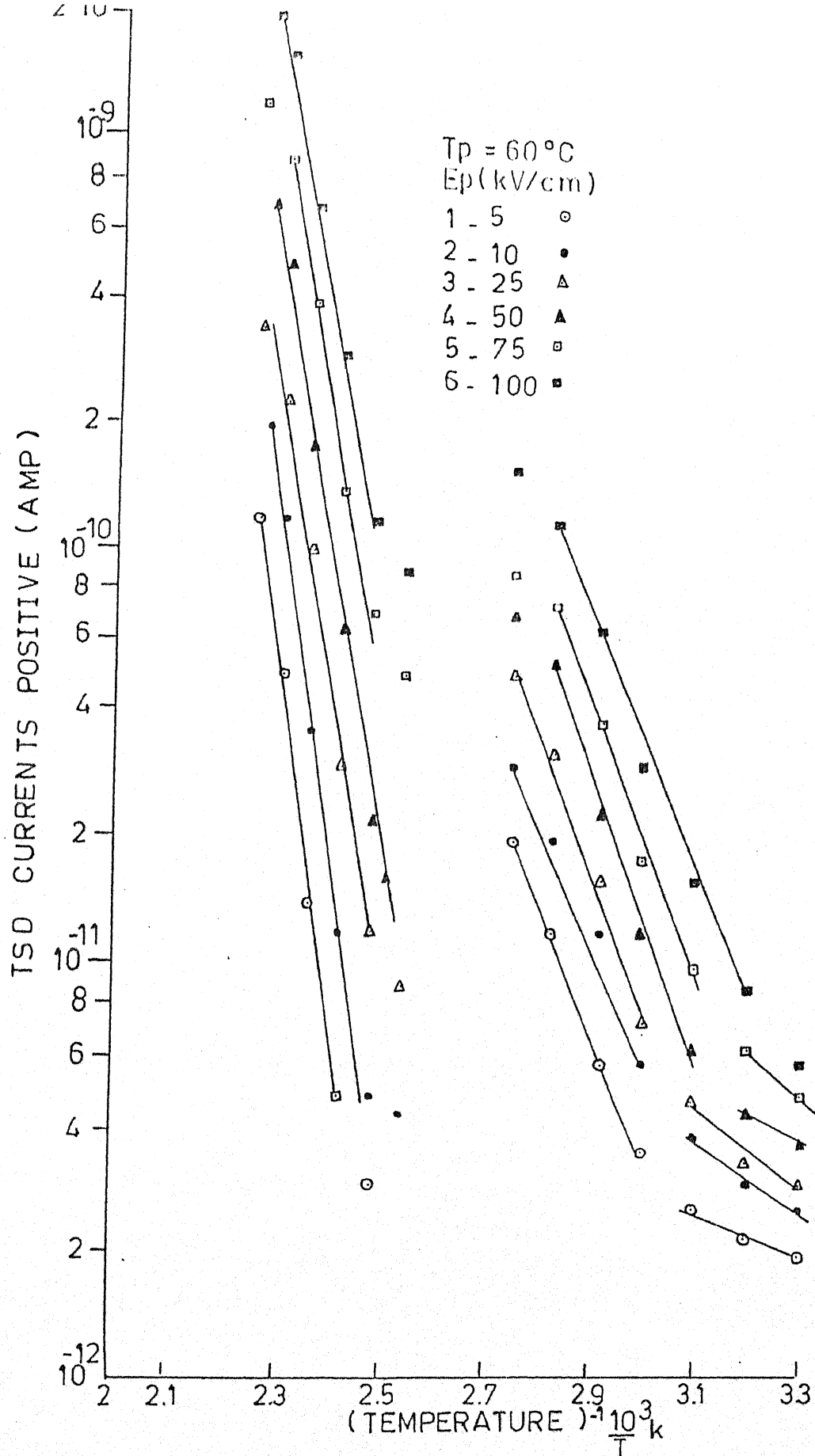


Fig. 4.23 (a) Initial rise plot for (5 μm thick) samples poled at given polarising temperature and different fields for Al-Al system.

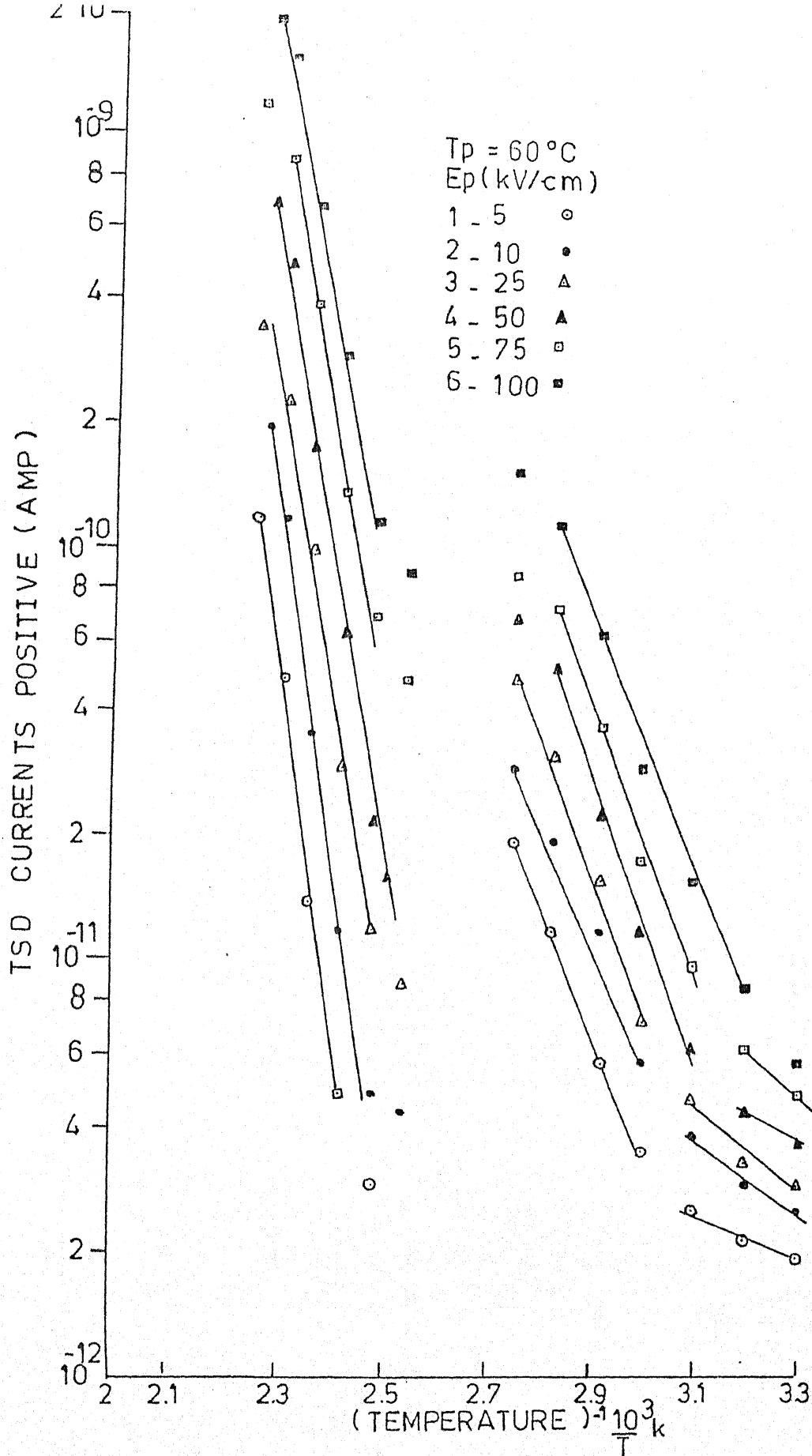


Fig. 4.23 (a) Initial rise plot for (5 μm thick) samples poled at given polarising temperature and different fields for Al-Al system.

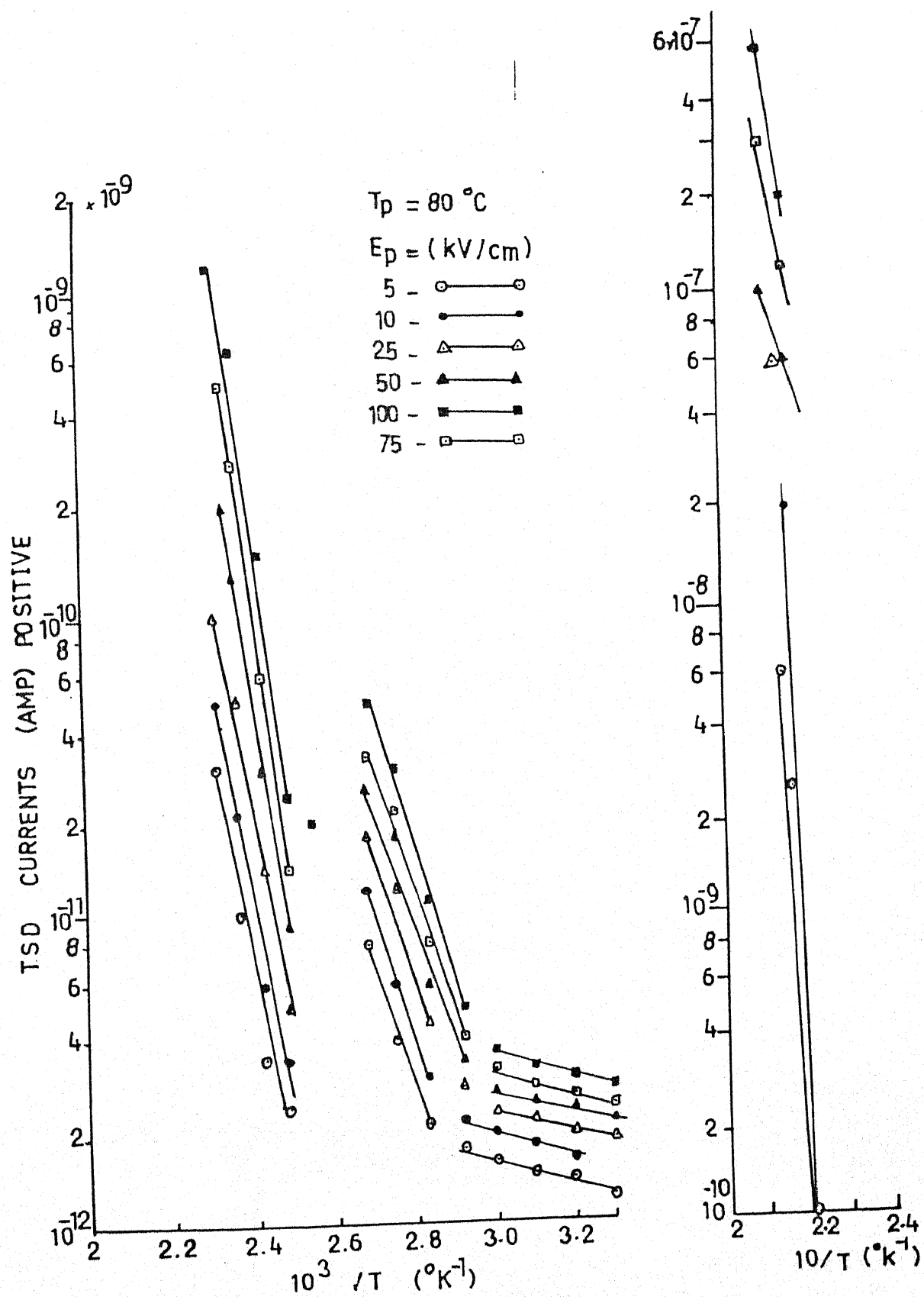


Fig.4.23(b) Initial rise plot for (20 umthick) samples poled at given polarising temperature and different fields for Al-Cu System.

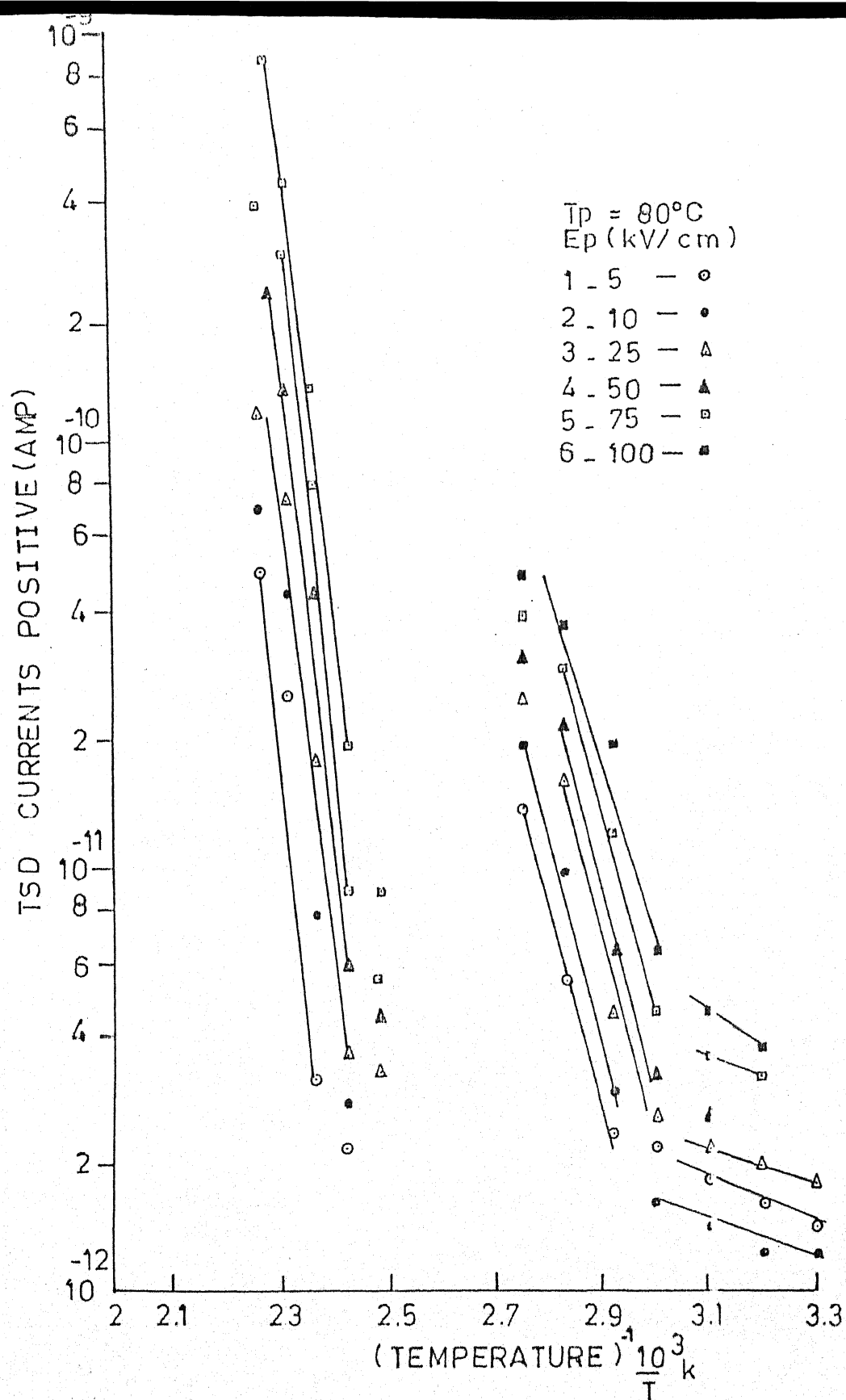


Fig. 4.23 (c) Initial rise plot for (25 μm thick) samples poled at given polarising temperature and different fields for Al-Al system.

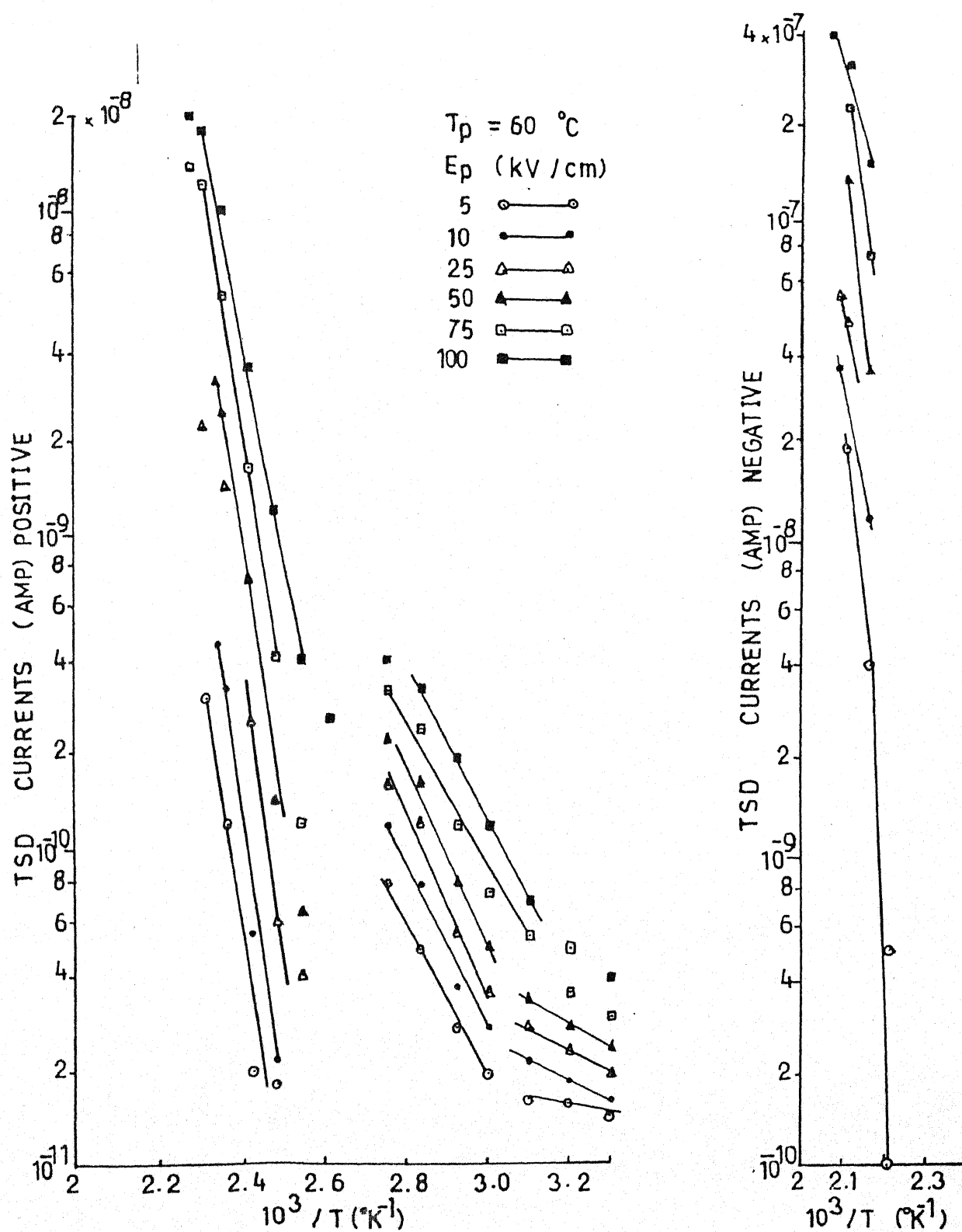


Fig.4.23(a) Initial rise plot for (5 μ m thick) samples poled at given polarising temperature and different fields for Al- Cu System.

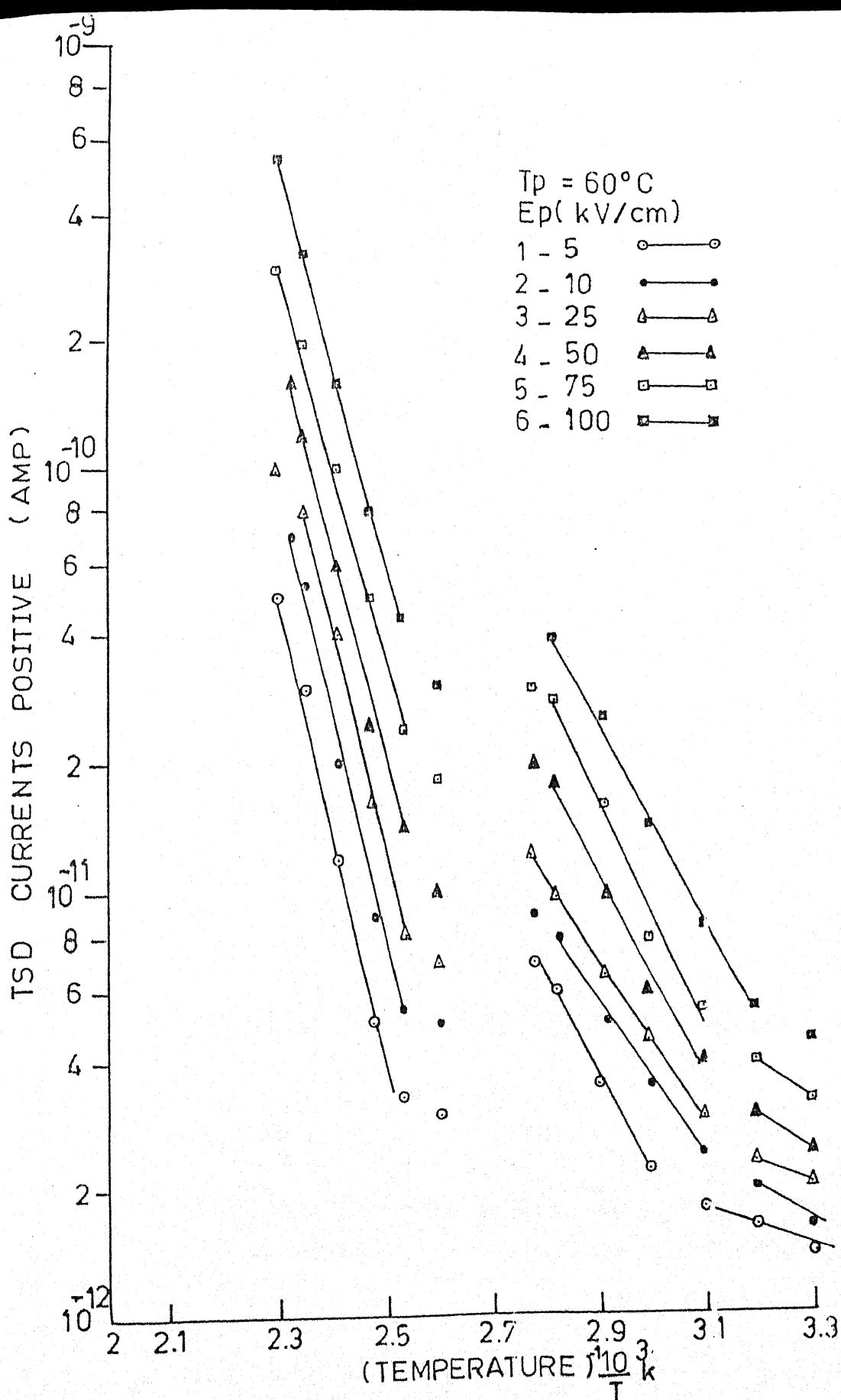
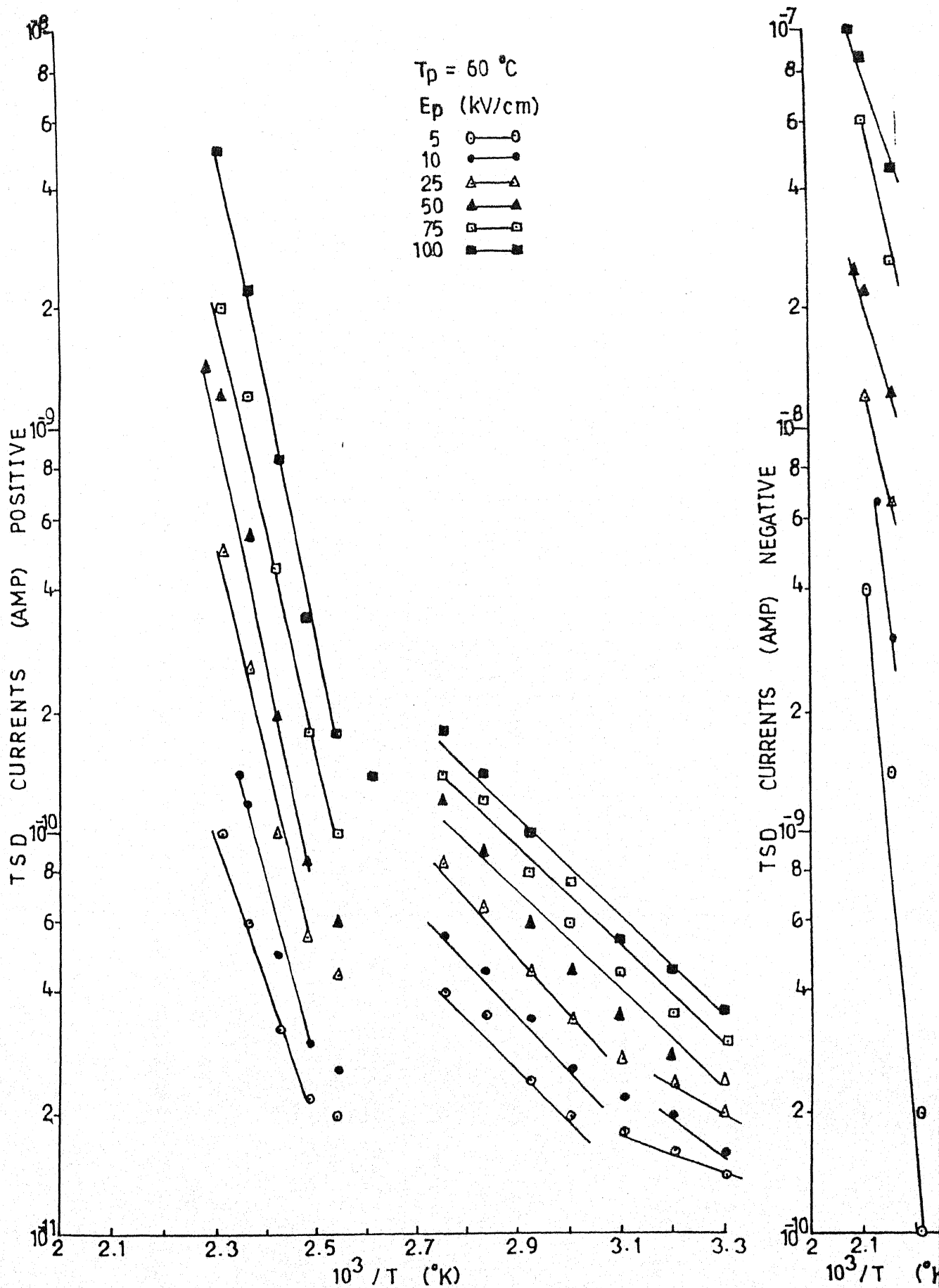


Fig. 4.23 (b) Initial rise plot for (20 μm thick) samples poled at given polarising temperature and different fields for Al-Al system.



9 Fig.4.23(c) initial rise plot for (25 μm thick) samples poled at given polarising temperature and different fields for Al-Cu system.

Table 4.1 : Depolarization kinetic data for PVP samples poled at 40°C with various polarizing fields. Sample thickness 20 μm . Al-Al system.

Polarizing Field	α -peak					ρ -peak				
	Peak current (Amp)	Peak Temp. ($^{\circ}\text{C}$)	Activation Energy (eV)	Relaxation time sec (τ_0)	Charge Released Coul. (Q)	Peak current (Amp)	Peak Temp. ($^{\circ}\text{C}$)	Activation Energy (eV)	Relaxation time sec (τ_0)	Charge Released Coul. (Q)
(Ep)										
05	5.0×10^{-12}	95	0.273	3.2×10^6	4.0×10^{-9}	2.0×10^{-11}	170	0.587	8.6×10^6	6.2×10^{-8}
10	7.0×10^{-12}	95	0.282	5.6×10^9	6.2×10^{-9}	3.0×10^{-11}	170	0.589	9.2×10^8	4.2×10^{-7}
25	9.0×10^{-12}	95	0.283	2.4×10^7	9.6×10^{-9}	5.0×10^{-11}	165	0.591	6.7×10^8	6.6×10^{-7}
50	1.2×10^{-11}	95	0.284	3.82×10^6	3.3×10^{-8}	6.0×10^{-11}	165	0.596	5.24×10^7	6.2×10^{-7}
75	1.6×10^{-11}	95	0.291	4.51×10^8	4.6×10^{-8}	8.5×10^{-11}	170	0.599	6.65×10^6	9.4×10^{-7}
100	2.2×10^{-11}	95	0.293	3.2×10^7	5.6×10^{-8}	1.2×10^{-10}	170	0.600	7.65×10^7	1.6×10^{-6}

Table 4.2 : Depolarization kinetic data for PVP samples poled at 50°C with various polarizing fields. Sample thickness 20 μm . Al-Al system.

Polarizing Field	α -peak					ρ -peak				
	Peak current (Amp)	Peak Temp. ($^{\circ}\text{C}$)	Activation Energy (eV)	Relaxation time sec (τ_0)	Charge Released Coul. (Q)	Peak current (Amp)	Peak Temp. ($^{\circ}\text{C}$)	Activation Energy (eV)	Relaxation time sec (τ_0)	Charge Released Coul. (Q)
(Ep)										
05	3.0×10^{-12}	90	0.282	4.6×10^7	5.0×10^{-9}	2.0×10^{-11}	170	0.596	9.2×10^7	7.6×10^{-8}
10	5.0×10^{-12}	90	0.287	4.6×10^8	7.0×10^{-9}	3.2×10^{-11}	170	0.602	1.6×10^8	8.2×10^{-8}
25	8.0×10^{-12}	90	0.291	4.8×10^7	1.2×10^{-8}	7.0×10^{-11}	175	0.607	4.4×10^8	4.4×10^{-8}
50	1.2×10^{-11}	90	0.297	2.83×10^6	4.6×10^{-8}	1.2×10^{-10}	165	0.612	5.6×10^6	1.2×10^{-6}
75	1.8×10^{-11}	90	0.302	1.62×10^7	6.6×10^{-8}	3.0×10^{-10}	170	0.632	4.8×10^7	3.4×10^{-6}
100	3.0×10^{-11}	90	0.309	6.2×10^7	6.8×10^{-8}	5.0×10^{-10}	175	0.633	3.2×10^4	4.2×10^{-6}

Table 4.3 : Depolarization kinetic data for PVP samples poled at 60°C with various polarizing

Polarizing Field	α -peak						ρ -peak			
	Peak current (Amp)	Peak Temp. (°C)	Activation Energy (eV)	Relaxation time sec (τ_0)	Charge Released Coul. (Q)	Peak current (Amp)	Peak Temp. (°C)	Activation Energy (eV)	Relaxation time sec (τ_0)	Charge Released Coul. (Q)
(Ep)										
05	1.0×10^{-11}	100	0.292	4.1×10^3	1.4×10^{-8}	7.0×10^{-11}	175	0.601	4.53×10^4	5.4×10^{-7}
10	2.0×10^{-11}	100	0.297	2.3×10^5	3.2×10^{-8}	1.6×10^{-10}	175	0.606	8.57×10^5	5.8×10^{-7}
25	4.0×10^{-11}	100	0.299	6.4×10^6	4.6×10^{-8}	4.0×10^{-10}	170	0.612	4.7×10^4	7.4×10^{-7}
50	6.0×10^{-11}	100	0.302	8.9×10^7	9.8×10^{-8}	7.0×10^{-10}	175	0.624	2.1×10^5	1.2×10^{-6}
75	8.0×10^{-11}	100	0.314	2.2×10^6	2.2×10^{-7}	9.0×10^{-10}	160	0.632	1.46×10^6	3.41×10^{-6}
100	10.0×10^{-10}	100	0.318	3.6×10^5	3.6×10^{-7}	10.0×10^{-9}	170	0.641	2.66×10^5	5.61×10^{-6}

Table 4.4 : Depolarization kinetic data for PVP samples poled at 70°C with various polarizing fields. Sample thickness 20 μm . Al-Al system.

Polarizing Field	α -peak						ρ -peak			
	Peak current (Amp)	Peak Temp. ($^{\circ}\text{C}$)	Activation Energy (eV)	Relaxation time sec (τ_0)	Charge Released Coul. (Q)	Peak current (Amp)	Peak Temp. ($^{\circ}\text{C}$)	Activation Energy (eV)	Relaxation time sec (τ_0)	Charge Released Coul. (Q)
(Ep)										
05	1.2×10^{-11}	90	0.291	2.4×10^4	4.2×10^{-8}	7.0×10^{-11}	180	0.625	2.62×10^5	6.2×10^{-7}
10	1.6×10^{-11}	90	0.293	1.6×10^5	5.0×10^{-8}	9.0×10^{-11}	180	0.629	8.94×10^6	9.8×10^{-7}
25	2.4×10^{-11}	90	0.296	8.6×10^6	6.8×10^{-8}	1.6×10^{-10}	180	0.630	4.46×10^5	1.4×10^{-6}
50	3.4×10^{-11}	90	0.299	2.14×10^4	1.2×10^{-7}	2.4×10^{-10}	175	0.634	4.34×10^6	3.4×10^{-6}
75	5.0×10^{-11}	90	0.301	7.24×10^6	3.0×10^{-7}	3.6×10^{-10}	180	0.639	4.88×10^5	6.4×10^{-6}
100	6.5×10^{-11}	90	0.312	9.5×10^7	4.2×10^{-7}	5.0×10^{-10}	175	0.640	9.87×10^6	8.4×10^{-6}

Table 4.5 : Depolarization kinetic data for PVP samples poled at 80°C with various polarizing fields. Sample thickness 20 μm . Al-Al system.

Polarizing Field	α -peak						ρ -peak			
	Peak current (Amp)	Peak Temp. ($^{\circ}\text{C}$)	Activation Energy (eV)	Relaxation time sec (τ_0)	Charge Released Coul. (Q)	Peak current (Amp)	Peak Temp. ($^{\circ}\text{C}$)	Activation Energy sec (τ_0)	Relaxation time (τ_0)	Charge Released Coul. (Q)
(Ep)										
05	1.4×10^{-11}	90	0.304	2.6×10^4	5.2×10^{-8}	5.0×10^{-11}	170	0.606	7.84×10^5	3.87×10^{-7}
10	2.0×10^{-11}	90	0.314	4.6×10^5	6.4×10^{-8}	7.0×10^{-11}	170	0.608	4.56×10^4	6.54×10^{-7}
25	2.5×10^{-11}	90	0.318	2.8×10^6	7.2×10^{-8}	1.2×10^{-10}	175	0.612	4.68×10^5	8.64×10^{-7}
50	3.2×10^{-11}	90	0.305	4.8×10^7	8.4×10^{-8}	2.4×10^{-10}	165	0.614	8.48×10^4	9.48×10^{-7}
75	4.0×10^{-11}	90	0.308	6.9×10^6	9.6×10^{-8}	4.0×10^{-10}	170	0.618	4.82×10^5	1.84×10^{-6}
100	5.0×10^{-11}	90	0.316	2.4×10^5	1.2×10^{-7}	9.0×10^{-10}	165	0.616	4.56×10^5	2.54×10^{-6}

Table 4.6 : Depolarization kinetic data for PVP samples poled at 40°C with various polarizing fields. Sample thickness 20 μm .
Ag-Ag system.

Polarizing Field		α -peak						ρ -peak						ρ' -peak					
		Peak current (Amp)	Peak Temp. ($^{\circ}\text{C}$)	Activation Energy (eV)	Relaxation time Sec (τ_0)	Charge Released Coul. (Q)	Peak current (Amp)	Peak Temp. ($^{\circ}\text{C}$)	Activation Energy (eV)	Relaxation time Sec (τ_0)	Charge Released Coul. (Q)	Peak current (Amp)	Peak Temp. ($^{\circ}\text{C}$)	Activation Energy (eV)	Relaxation time Sec (τ_0)	Char Relea Coul.			
(Ep)																			
05		5.0×10^{-10}	90	0.272	7.56×10^6	5.67×10^{-7}	3.0×10^{-9}	150	0.582	2.77×10^5	7.72×10^{-6}	2.4×10^{-8}	205	0.885	5.48×10^6	3.87x			
10		7.0×10^{-10}	90	0.276	8.56×10^5	6.68×10^{-7}	8.0×10^{-9}	150	0.586	5.68×10^5	8.76×10^{-6}	4.0×10^{-6}	200	0.887	7.82×10^5	8.46x			
25		9.0×10^{-10}	90	0.279	3.48×10^4	8.43×10^{-7}	1.2×10^{-8}	145	0.588	7.65×10^5	8.80×10^{-6}	6.5×10^{-8}	205	0.889	8.76×10^4	9.25x			
50		1.2×10^{-9}	90	0.282	8.3×10^6	9.8×10^{-7}	1.6×10^{-8}	150	0.591	2.98×10^5	9.20×10^{-6}	8.0×10^{-8}	200	0.892	9.44×10^5	1.24x			
75		1.6×10^{-9}	90	0.286	6.4×10^5	4.6×10^{-6}	3.0×10^{-8}	145	0.593	6.47×10^5	4.60×10^{-5}	1.4×10^{-7}	205	0.894	1.44×10^6	3.46x			
100		2.4×10^{-9}	90	0.289	4.6×10^6	6.4×10^{-6}	4.5×10^{-8}	150	0.593	2.68×10^4	6.20×10^{-5}	2.2×10^{-7}	210	0.894	3.66×10^7	8.76x			

Table 4.7 : Depolarization kinetic data for PVP samples poled at 60°C with various polarizing fields. Sample thickness 20 μm .
Ag-Ag system.

Polarizing Field	α -peak						ρ -peak						ρ' -peak					
	Peak current (Amp)	Peak Temp. ($^{\circ}\text{C}$)	Activation Energy (eV)	Relaxation time Sec (τ_0)	Charge Released Coul. (Q)	Peak current (Amp)	Peak Temp. ($^{\circ}\text{C}$)	Activation Energy (eV)	Relaxation time Sec (τ_0)	Charge Released Coul. (Q)	Peak current (Amp)	Peak Temp. ($^{\circ}\text{C}$)	Activation Energy (eV)	Relaxation time Sec (τ_0)	Charge Released Coul. (Q)			
(Ep)																		
05	5.0×10^{-10}	80	0.277	7.83×10^4	3.87×10^{-8}	3.0×10^{-5}	145	0.587	7.4×10^4	6.47×10^{-7}	3.6×10^{-8}	215	0.886	7.6×10^5	4.4×10^{-5}			
10	7.0×10^{-10}	80	0.284	5.63×10^5	4.65×10^{-7}	5.0×10^{-5}	150	0.594	8.8×10^5	8.56×10^{-7}	4.5×10^{-8}	210	0.889	8.2×10^5	7.58×10^{-5}			
25	9.0×10^{-10}	80	0.287	6.46×10^5	6.88×10^{-7}	7.0×10^{-5}	145	0.599	9.7×10^5	9.5×10^{-7}	6.5×10^{-8}	210	0.892	2.4×10^6	8.66×10^{-5}			
50	1.2×10^{-9}	80	0.291	3.27×10^6	8.24×10^{-7}	9.0×10^{-5}	150	0.601	1.4×10^6	3.8×10^{-6}	1.2×10^{-7}	210	0.897	5.6×10^6	2.54×10^{-5}			
75	1.6×10^{-9}	80	0.301	8.24×10^5	2.6×10^{-6}	2.0×10^{-6}	150	0.604	3.7×10^6	6.4×10^{-6}	2.0×10^{-7}	215	0.901	8.6×10^5	3.8×10^{-5}			
100	2.0×10^{-9}	80	0.306	1.26×10^6	4.6×10^{-6}	4.6×10^{-6}	155	0.609	8.2×10^6	8.5×10^{-6}	4.0×10^{-7}	210	0.907	9.6×10^5	8.8×10^{-5}			

Table 4.8 : Depolarization kinetic data for PVP samples poled at 80°C with various polarizing fields. Sample thickness 20 μm .
Ag-Ag system.

Polarizing Field	α -peak					ρ -peak					ρ' -peak				
	Peak current (Amp)	Peak Temp. ($^{\circ}\text{C}$)	Activation Energy (eV)	Relaxation time Sec (τ_0)	Charge Released Coul. (Q)	Peak current (Amp)	Peak Temp. ($^{\circ}\text{C}$)	Activation Energy (eV)	Relaxation time Sec (τ_0)	Charge Released Coul. (Q)	Peak current (Amp)	Peak Temp. ($^{\circ}\text{C}$)	Activation Energy (eV)	Relaxation time Sec (τ_0)	Charge Released Coul. (Q)
(Ep)															
05	7.0×10^{-10}	75	0.301	6.4×10^5	4.6×10^{-8}	5.0×10^{-9}	135	0.705	8.52×10^8	5.8×10^{-7}	5.0×10^{-8}	205	0.975	8.76×10^5	5.78×10^{-6}
10	8.5×10^{-10}	75	0.307	8.72×10^5	7.8×10^{-8}	7.0×10^{-9}	140	0.709	6.75×10^6	7.6×10^{-7}	7.0×10^{-6}	210	0.979	7.87×10^7	7.67×10^{-6}
25	1.0×10^{-10}	75	0.309	4.82×10^4	8.4×10^{-8}	1.0×10^{-8}	135	0.712	8.47×10^5	8.8×10^{-7}	1.0×10^{-7}	210	0.979	4.97×10^5	7.94×10^{-6}
50	1.4×10^{-9}	75	0.312	8.97×10^6	9.8×10^{-8}	2.0×10^{-8}	135	0.724	6.97×10^6	9.6×10^{-7}	7.6×10^{-7}	210	0.980	6.8×10^5	5.6×10^{-6}
75	2.2×10^{-9}	75	0.324	8.34×10^5	3.6×10^{-7}	4.5×10^{-8}	140	0.729	5.26×10^7	2.5×10^{-5}	3.0×10^{-7}	210	0.981	4.9×10^5	5.4×10^{-6}
100	3.0×10^{-9}	75	0.322	5.87×10^6	6.4×10^{-7}	8.0×10^{-8}	135	0.725	6.4×10^7	4.6×10^{-5}	5.0×10^{-7}	210	0.982	8.99×10^5	5.8×10^{-6}

Table 4.9 : Depolarization kinetic data for PVP samples poled at 40°C with various polarizing fields. Sample thickness 20 μm .
Cu-Cu system.

Polarizing Field	α -peak						ρ -peak						ρ' -peak					
	Peak current (Amp)	Peak Temp. ($^{\circ}\text{C}$)	Activation Energy (eV)	Relaxation time Sec (τ_0)	Charge Released Coul. (Q)	Peak current (Amp)	Peak Temp. ($^{\circ}\text{C}$)	Activation Energy (eV)	Relaxation time Sec (τ_0)	Charge Released Coul. (Q)	Peak current (Amp)	Peak Temp. ($^{\circ}\text{C}$)	Activation Energy (eV)	Relaxation time Sec (τ_0)	Charge Released Coul. (Q)			
(Ep)																		
05	1.0×10^{-9}	70	0.265	5.65×10^6	5.65×10^{-7}	1.0×10^{-8}	145	0.667	4.68×10^5	5.4×10^{-6}	5.4×10^{-6}	220	0.782	6.57×10^5	8.8×10^{-6}			
10	1.4×10^{-9}	70	0.267	2.47×10^6	7.42×10^{-7}	1.6×10^{-8}	150	0.669	6.87×10^5	8.6×10^{-6}	7.5×10^{-8}	215	0.789	4.24×10^5	9.4×10^{-6}			
25	1.8×10^{-9}	70	0.268	6.68×10^5	8.66×10^{-7}	2.8×10^{-8}	145	0.677	8.9×10^5	9.8×10^{-6}	1.0×10^{-7}	220	0.801	8.86×10^5	2.6×10^{-5}			
50	2.4×10^{-9}	70	0.272	6.49×10^5	9.46×10^{-7}	4.0×10^{-8}	145	0.679	2.57×10^5	2.7×10^{-5}	1.8×10^{-7}	215	0.807	2.47×10^6	4.68×10^{-5}			
75	3.4×10^{-9}	70	0.279	7.58×10^5	3.46×10^{-6}	6.5×10^{-8}	150	0.680	6.65×10^5	3.5×10^{-5}	3.0×10^{-7}	220	0.812	7.87×10^5	7.88×10^{-5}			
100	4.0×10^{-9}	70	0.280	8.77×10^6	4.46×10^{-6}	8.0×10^{-8}	140	0.680	8.85×10^5	6.6×10^{-5}	5.0×10^{-7}	215	0.819	8.87×10^7	7.7×10^{-5}			

Table 4.10 : Depolarization kinetic data for PVP samples poled at 60°C with various polarizing fields. Sample thickness 20 μm .
Cu-Cu system.

Polarizing Field	α -peak						ρ -peak						ρ' -peak			
	Peak current (Amp)	Peak Temp. ($^{\circ}\text{C}$)	Activation Energy (eV)	Relaxation time Sec (τ_0)	Charge Released Coul. (Q)	Peak current (Amp)	Peak Temp. ($^{\circ}\text{C}$)	Activation Energy (eV)	Relaxation time Sec (τ_0)	Charge Released Coul. (Q)	Peak current (Amp)	Peak Temp. ($^{\circ}\text{C}$)	Activation Energy (eV)	Relaxation time Sec (τ_0)	Charge Released Coul. (Q)	
(Ep)																
05	1.2×10^{-9}	80	0.265	8.76×10^5	6.78×10^{-7}	2.0×10^{-8}	140	0.678	6.58×10^6	6.56×10^{-6}	7.0×10^{-8}	205	0.783	7.86×10^5	7.87×10^{-6}	
10	1.6×10^{-9}	80	0.269	6.67×10^5	7.66×10^{-7}	3.0×10^{-8}	145	0.681	7.32×10^5	8.77×10^{-6}	1.0×10^{-7}	210	0.788	4.29×10^6	9.24×10^{-6}	
25	2.0×10^{-9}	80	0.272	4.28×10^5	8.24×10^{-7}	4.0×10^{-8}	140	0.687	7.77×10^5	9.46×10^{-6}	1.2×10^{-7}	205	0.790	5.56×10^5	3.55×10^{-5}	
50	2.6×10^{-9}	80	0.276	2.88×10^7	9.82×10^{-7}	6.0×10^{-8}	145	0.689	8.46×10^6	1.78×10^{-5}	1.8×10^{-7}	200	0.799	6.58×10^5	4.68×10^{-5}	
75	3.0×10^{-9}	80	0.277	3.64×10^7	4.46×10^{-6}	7.0×10^{-8}	140	0.690	9.43×10^5	4.82×10^{-5}	3.0×10^{-7}	205	0.888	8.76×10^6	6.78×10^{-5}	
100	3.8×10^{-9}	80	0.279	4.22×10^7	5.26×10^{-6}	1.0×10^{-7}	145	0.691	9.98×10^5	6.66×10^{-5}	5.0×10^{-7}	200	0.891	8.94×10^5	8.78×10^{-5}	

**Table 4.11 : Depolarization kinetic data for PVP samples poled at 80°C with various polarizing fields. Sample thickness 20 μm .
Cu-Cu system.**

Polarizing Field		α -peak						p -peak						p' -peak					
		Peak current (Amp)	Peak Temp. ($^{\circ}\text{C}$)	Activation Energy (eV)	Relaxation time Sec (τ_0)	Charge Released Coul. (Q)	Peak current (Amp)	Peak Temp. ($^{\circ}\text{C}$)	Activation Energy (eV)	Relaxation time Sec (τ_0)	Charge Released Coul. (Q)	Peak current (Amp)	Peak Temp. ($^{\circ}\text{C}$)	Activation Energy (eV)	Relaxation time Sec (τ_0)	Charge Released Coul. (Q)			
(Ep)																			
05		1.4×10^{-9}	85	0.321	5.66×10^6	6.68×10^{-7}	2.4×10^{-8}	150	0.802	4.43×10^6	1.7×10^{-6}	7.0×10^{-8}	215	0.917	3.3×10^5	2.2×10^{-6}			
10		2.0×10^{-9}	85	0.324	6.66×10^5	8.78×10^{-7}	3.0×10^{-8}	150	0.808	3.74×10^5	2.4×10^{-6}	8.0×10^{-8}	215	0.919	4.7×10^6	2.8×10^{-6}			
25		2.6×10^{-9}	85	0.336	7.59×10^5	9.84×10^{-7}	4.0×10^{-8}	150	0.803	4.22×10^6	3.2×10^{-6}	1.0×10^{-7}	215	0.920	8.7×10^7	3.2×10^{-5}			
50		4.0×10^{-9}	85	0.339	8.69×10^4	1.66×10^{-6}	5.5×10^{-8}	155	0.810	6.54×10^5	4.4×10^{-6}	1.4×10^{-7}	220	0.921	9.2×10^6	4.4×10^{-5}			
75		5.5×10^{-9}	85	0.34	8.97×10^6	3.76×10^{-6}	6.0×10^{-8}	150	0.814	7.25×10^6	7.8×10^{-6}	2.0×10^{-7}	210	0.927	2.4×10^5	4.82×10^{-5}			
100		6.5×10^{-9}	85	0.341	9.24×10^5	8.68×10^{-6}	7.0×10^{-8}	150	0.819	8.22×10^5	9.9×10^{-6}	3.4×10^{-7}	215	0.929	7.2×10^5	6.99×10^{-5}			

Table 4.12 : Depolarization kinetic data for PVP samples poled at 40°C with various polarizing fields. Sample thickness 20 μm .
Sn-Sn system.

Polarizing Field	α -peak					ρ -peak					ρ' -peak				
	Peak current (Amp)	Peak Temp. ($^{\circ}\text{C}$)	Activation Energy (eV)	Relaxation time Sec (τ_0)	Charge Released Coul. (Q)	Peak current (Amp)	Peak Temp. ($^{\circ}\text{C}$)	Activation Energy (eV)	Relaxation time Sec (τ_0)	Charge Released Coul. (Q)	Peak current (Amp)	Peak Temp. ($^{\circ}\text{C}$)	Activation Energy (eV)	Relaxation time Sec (τ_0)	Charge Released Coul. (Q)
(Ep)															
05	7.0×10^{-10}	70	0.267	8.36×10^5	3.38×10^{-8}	2.0×10^{-9}	130	0.685	7.44×10^4	4.47×10^{-7}	3.0×10^{-8}	200	0.872	3.78×10^4	4.78×10^{-6}
10	9.5×10^{-10}	70	0.269	6.24×10^4	4.26×10^{-8}	3.4×10^{-9}	125	0.689	4.56×10^5	6.54×10^{-7}	4.5×10^{-8}	200	0.876	4.66×10^6	6.64×10^{-6}
25	1.2×10^{-9}	70	0.270	6.67×10^5	7.66×10^{-8}	5.0×10^{-9}	125	0.678	2.47×10^6	7.42×10^{-7}	5.5×10^{-8}	205	0.879	5.78×10^6	7.75×10^{-6}
50	1.6×10^{-9}	70	0.279	6.78×10^6	8.78×10^{-8}	9.0×10^{-9}	130	0.686	3.48×10^5	8.43×10^{-7}	8.5×10^{-8}	195	0.880	8.78×10^5	8.2×10^{-6}
75	2.6×10^{-9}	70	0.280	2.97×10^5	9.2×10^{-8}	2.0×10^{-8}	135	0.682	6.59×10^5	9.56×10^{-7}	1.4×10^{-7}	200	0.884	6.66×10^6	8.44×10^{-6}
100	3.6×10^{-9}	70	0.279	4.38×10^6	2.4×10^{-7}	3.0×10^{-8}	140	0.701	6.21×10^5	1.26×10^{-7}	2.4×10^{-7}	205	0.886	7.45×10^5	2.74×10^{-5}

Table 4.13 : Depolarization kinetic data for PVP samples poled at 60°C with various polarizing fields. Sample thickness 20 μm .
Sn-Sn system.

Polarizing Field	α -peak						ρ -peak						ρ' -peak			
	Peak current (Amp)	Peak Temp. (°C)	Activation Energy (eV)	Relaxation time Sec (τ_0)	Charge Released Coul. (Q)	Peak current (Amp)	Peak Temp. (°C)	Activation Energy (eV)	Relaxation time Sec (τ_0)	Charge Released Coul. (Q)	Peak current (Amp)	Peak Temp. (°C)	Activation Energy (eV)	Relaxation time Sec (τ_0)	Charge Released Coul. (Q)	Peak current (Amp)
(Ep)																
05	8.0×10^{-10}	65	0.264	2.57×10^5	7.52×10^{-8}	4.0×10^{-9}	135	0.556	7.38×10^8	3.7×10^{-7}	4.0×10^{-8}	200	0.782	7.4×10^5	4.7×10^{-6}	4.7×10^{-6}
10	1.2×10^{-9}	65	0.267	8.34×10^6	4.38×10^{-7}	6.0×10^{-9}	130	0.565	1.46×10^5	5.4×10^{-7}	6.0×10^{-8}	205	0.757	7.66×10^6	6.67×10^{-6}	6.67×10^{-6}
25	1.8×10^{-9}	65	0.580	8.78×10^5	8.78×10^{-7}	9.0×10^{-9}	135	0.558	5.62×10^6	6.25×10^{-7}	8.0×10^{-8}	200	0.762	5.48×10^5	8.45×10^{-6}	8.45×10^{-6}
50	2.4×10^{-9}	65	0.247	2.29×10^4	2.29×10^{-7}	1.4×10^{-8}	130	0.562	6.27×10^7	7.26×10^{-7}	2.0×10^{-7}	205	0.767	1.29×10^6	9.21×10^{-5}	9.21×10^{-5}
75	3.0×10^{-9}	65	0.266	4.53×10^6	4.53×10^{-6}	3.0×10^{-8}	125	0.567	4.28×10^6	7.56×10^{-7}	3.0×10^{-7}	200	0.769	7.21×10^7	1.27×10^{-5}	1.27×10^{-5}
100	3.6×10^{-9}	60	0.249	7.44×10^6	7.44×10^{-6}	4.5×10^{-8}	130	0.570	5.28×10^7	8.25×10^{-7}	7.0×10^{-7}	210	0.771	6.31×10^6	1.36×10^{-5}	1.36×10^{-5}

Table 4.14 : Depolarization kinetic data for PVP samples poled at 80°C with various polarizing fields. Sample thickness 20 μm .
Sn-Sn system.

Polarizing Field	α -peak					ρ -peak					ρ' -peak				
	Peak current (Amp)	Peak Temp. ($^{\circ}\text{C}$)	Activation Energy (eV)	Relaxation time Sec (τ_0)	Charge Released Coul. (Q)	Peak current (Amp)	Peak Temp. ($^{\circ}\text{C}$)	Activation Energy (eV)	Relaxation time Sec (τ_0)	Charge Released Coul. (Q)	Peak current (Amp)	Peak Temp. ($^{\circ}\text{C}$)	Activation Energy (eV)	Relaxation time Sec (τ_0)	Charge Released Coul. (Q)
(Ep)															
05	1.0×10^{-10}	70	0.282	3.33×10^4	4.4×10^{-7}	1.0×10^{-8}	140	0.614	3.36×10^6	4.4×10^{-6}	5.0×10^{-8}	210	0.787	8.78×10^6	4.78×10^{-6}
10	1.4×10^{-9}	70	0.285	4.47×10^5	5.7×10^{-7}	1.6×10^{-8}	135	0.623	5.57×10^5	5.6×10^{-6}	7.0×10^{-8}	205	0.782	5.88×10^7	6.88×10^{-6}
25	2.0×10^{-9}	70	0.287	8.76×10^6	6.6×10^{-7}	3.0×10^{-8}	140	0.619	9.99×10^6	7.6×10^{-6}	1.0×10^{-7}	210	0.753	9.44×10^6	3.57×10^{-5}
50	2.8×10^{-9}	70	0.289	5.48×10^5	7.6×10^{-7}	4.5×10^{-8}	135	0.621	8.88×10^5	8.2×10^{-6}	1.6×10^{-7}	210	0.776	3.78×10^6	4.65×10^{-5}
75	3.6×10^{-9}	70	0.290	8.77×10^5	8.4×10^{-7}	7.0×10^{-8}	140	0.627	4.48×10^6	8.8×10^{-6}	3.0×10^{-7}	215	0.775	8.48×10^5	6.68×10^{-5}
100	5.0×10^{-9}	70	0.292	9.48×10^5	9.5×10^{-7}	9.0×10^{-8}	140	0.614	3.54×10^5	9.2×10^{-6}	7.0×10^{-7}	210	0.786	3.35×10^4	7.44×10^{-5}

Table 4.15 : Depolarization kinetic data for PVP samples poled at 40°C with various polarizing fields. Sample thickness 20 μm .
Al-Ag system.

Polarizing Field	α -peak						ρ -peak						ρ' -peak			
	Peak current (Amp)	Peak Temp. (°C)	Activation Energy (eV)	Relaxation time Sec (τ_0)	Charge Released Coul. (Q)	Peak current (Amp)	Peak Temp. (°C)	Activation Energy (eV)	Relaxation time Sec (τ_0)	Charge Released Coul. (Q)	Peak current (Amp)	Peak Temp. (°C)	Activation Energy (eV)	Relaxation time Sec (τ_0)	Charge Released Coul. (Q)	Peak current (Amp)
(Ep)																
05	1.0×10^{-11}	80	0.252	4.46×10^6	6.57×10^{-9}	1.0×10^{-11}	160	0.497	9.57×10^6	6.56×10^{-9}	2.0×10^{-9}	200	0.823	6.48×10^6	7.65×10^{-7}	2.0×10^{-9}
10	1.4×10^{-11}	80	0.256	4.87×10^7	7.59×10^{-9}	1.6×10^{-10}	155	0.512	8.86×10^5	7.82×10^{-9}	4.0×10^{-9}	195	0.834	8.46×10^7	8.76×10^{-7}	4.0×10^{-9}
25	2.0×10^{-11}	80	0.258	7.58×10^6	8.24×10^{-9}	3.0×10^{-9}	160	0.517	9.98×10^6	8.94×10^{-9}	8.5×10^{-9}	200	0.836	5.86×10^6	9.82×10^{-7}	8.5×10^{-9}
50	2.8×10^{-10}	80	0.265	8.98×10^7	9.47×10^{-9}	4.5×10^{-9}	160	0.519	8.78×10^5	2.43×10^{-8}	2.0×10^{-8}	195	0.894	8.76×10^5	1.57×10^{-6}	2.0×10^{-8}
75	3.6×10^{-10}	80	0.266	2.44×10^7	2.25×10^{-8}	7.0×10^{-9}	165	0.520	9.98×10^7	5.44×10^{-8}	4.0×10^{-8}	200	0.841	7.89×10^7	2.23×10^{-6}	4.0×10^{-8}
100	5.0×10^{-10}	80	0.268	3.87×10^6	3.45×10^{-8}	9.0×10^{-9}	165	0.521	2.35×10^6	6.66×10^{-8}	1.0×10^{-7}	205	0.847	3.34×10^6	3.35×10^{-6}	1.0×10^{-7}

Table 4.16 : Depolarization kinetic data for PVP samples poled at 60°C with various polarizing fields. Sample thickness 20 μm .
Al-Ag system.

Polarizing Field	α -peak					p-peak					p' -peak				
	Peak current (Amp)	Peak Temp. (°C)	Activation Energy (eV)	Relaxation time Sec (τ_0)	Charge Released Coul. (Q)	Peak current (Amp)	Peak Temp. (°C)	Activation Energy (eV)	Relaxation time Sec (τ_0)	Charge Released Coul. (Q)	Peak current (Amp)	Peak Temp. (°C)	Activation Energy (eV)	Relaxation time Sec (τ_0)	Charge Released Coul. (Q)
(Ep)															
05	4.0×10^{-11}	75	0.265	5.5×10^6	3.37×10^{-9}	1.0×10^{-10}	160	0.502	8.78×10^6	3.78×10^{-5}	2.0×10^{-9}	190	0.512	5.6×10^6	3.37×10^{-7}
10	5.5×10^{-11}	75	0.263	4.32×10^7	4.32×10^9	2.4×10^{-9}	160	0.504	7.77×10^4	7.78×10^{-5}	3.2×10^{-9}	190	0.923	6.4×10^5	4.88×10^{-7}
25	8.0×10^{-11}	75	0.264	7.77×10^6	7.77×10^9	5.5×10^{-9}	160	0.512	8.99×10^6	8.24×10^{-5}	6.0×10^{-9}	195	0.924	8.8×10^6	5.86×10^{-7}
50	9.5×10^{-10}	75	0.267	8.32×10^5	8.32×10^9	1.2×10^{-9}	165	0.525	9.99×10^6	9.21×10^{-5}	3.0×10^{-8}	200	0.929	9.27×10^7	8.88×10^{-5}
75	1.4×10^{-10}	75	0.268	9.67×10^6	9.67×10^9	3.5×10^{-9}	170	0.519	3.33×10^5	2.27×10^{-5}	8.0×10^{-8}	195	0.919	5.88×10^6	9.4×10^{-6}
100	2.0×10^{-10}	75	0.269	2.43×10^5	2.43×10^9	7.0×10^{-9}	165	0.517	4.44×10^6	3.32×10^{-5}	2.0×10^{-7}	195	0.927	8.85×10^4	2.4×10^{-5}

Table 4.17 : Depolarization kinetic data for PVP samples poled at 80°C with various polarizing fields. Sample thickness 20 μm .
Al-Ag system.

Polarizing Field	α -peak						ρ -peak						ρ' -peak			
	Peak current (Amp)	Peak Temp. ($^{\circ}\text{C}$)	Activation Energy (eV)	Relaxation time Sec (τ_0)	Charge Released Coul. (Q)	Peak current (Amp)	Peak Temp. ($^{\circ}\text{C}$)	Activation Energy (eV)	Relaxation time Sec (τ_0)	Charge Released Coul. (Q)	Peak current (Amp)	Peak Temp. ($^{\circ}\text{C}$)	Activation Energy (eV)	Relaxation time Sec (τ_0)	Charge Released Coul. (Q)	Charge Released Coul. (Q)
(Ep)																
05	5.0×10^{-11}	70	0.278	5.5×10^6	3.87×10^{-9}	1.8×10^{-10}	160	0.556	4.4×10^7	4.87×10^{-8}	3.0×10^{-9}	195	0.887	5.7×10^7	5.7×10^{-7}	
10	7.0×10^{-11}	70	0.282	4.32×10^7	7.68×10^9	3.6×10^{-10}	165	0.564	7.7×10^6	6.87×10^{-8}	5.0×10^{-9}	195	0.890	8.7×10^6	6.3×10^{-7}	
25	9.0×10^{-11}	70	0.292	7.77×10^6	8.77×10^9	6.0×10^{-10}	165	0.569	8.8×10^7	8.94×10^{-8}	9.0×10^{-9}	200	0.891	9.4×10^7	7.8×10^{-7}	
50	1.6×10^{-10}	70	0.297	8.32×10^5	9.21×10^9	0.4×10^{-9}	160	0.567	9.9×10^6	9.64×10^{-8}	3.0×10^{-8}	195	0.896	8.8×10^6	8.2×10^{-7}	
75	2.4×10^{-10}	70	0.294	9.67×10^5	2.78×10^8	6.0×10^{-9}	165	0.568	2.4×10^6	2.47×10^{-7}	9.0×10^{-8}	200	0.892	4.4×10^7	2.4×10^{-5}	
100	3.4×10^{-10}	70	0.293	2.43×10^6	3.58×10^8	2.0×10^{-9}	160	0.570	4.4×10^7	3.37×10^{-7}	3.2×10^{-7}	200	0.893	6.6×10^8	3.4×10^{-5}	

Table 4.18 : Depolarization kinetic data for PVP samples poled at 40°C with various polarizing fields. Sample thickness 20 μm .
Al-Cu system.

Polarizing Field	α -peak					ρ -peak					ρ' -peak				
	Peak current (Amp)	Peak Temp. (°C)	Activation Energy (eV)	Relaxation time Sec (τ_0)	Charge Released Coul. (Q)	Peak current (Amp)	Peak Temp. (°C)	Activation Energy (eV)	Relaxation time Sec (τ_0)	Charge Released Coul. (Q)	Peak current (Amp)	Peak Temp. (°C)	Activation Energy (eV)	Relaxation time Sec (τ_0)	Charge Released Coul. (Q)
(Ep)															
05	4.0×10^{-11}	90	0.265	4.5×10^6	2.5×10^{-9}	1.0×10^{-10}	160	0.543	4.6×10^5	4.4×10^{-8}	5.0×10^{-9}	200	0.762	4.7×10^6	4.7×10^{-7}
10	6.0×10^{-11}	90	0.269	6.6×10^7	3.6×10^9	2.0×10^{-10}	165	0.556	4.8×10^4	4.8×10^{-8}	2.0×10^{-8}	200	0.773	8.7×10^5	8.7×10^{-7}
25	8.0×10^{-11}	90	0.268	8.8×10^6	4.2×10^9	3.0×10^{-10}	160	0.563	5.4×10^6	5.4×10^{-8}	3.0×10^{-8}	200	0.782	9.87×10^7	2.5×10^{-6}
50	1.4×10^{-10}	90	0.271	9.4×10^7	9.6×10^9	8.0×10^{-9}	160	0.596	8.8×10^7	8.8×10^{-8}	4.0×10^{-8}	195	0.793	8.66×10^5	3.78×10^{-6}
75	2.2×10^{-10}	90	0.273	2.8×10^8	1.6×10^8	7.8×10^{-9}	165	0.570	3.3×10^6	3.3×10^{-7}	1.2×10^{-7}	195	0.792	7.77×10^6	4.48×10^{-6}
100	3.6×10^{-10}	90	0.276	3.55×10^7	3.6×10^8	4.0×10^{-9}	160	0.572	4.6×10^5	4.6×10^{-7}	2.0×10^{-7}	200	0.795	6.43×10^7	8.86×10^{-6}

Table 4.19 : Depolarization kinetic data for PVP samples poled at 60°C with various polarizing fields. Sample thickness 20 μm .
Al-Cu system.

Polarizing Field		α -peak					ρ -peak					ρ' -peak				
		Peak current (Amp)	Peak Temp. ($^{\circ}\text{C}$)	Activation Energy (eV)	Relaxation time Sec (τ_0)	Charge Released Coul. (Q)	Peak current (Amp)	Peak Temp. ($^{\circ}\text{C}$)	Activation Energy (eV)	Relaxation time Sec (τ_0)	Charge Released Coul. (Q)	Peak current (Amp)	Peak Temp. ($^{\circ}\text{C}$)	Activation Energy (eV)	Relaxation time Sec (τ_0)	Charge Released Coul. (Q)
(Ep)																
	05	6.0×10^{-11}	95	0.274	4.88×10^6	7.7×10^{-9}	2.0×10^{-10}	165	0.617	4.49×10^6	7.4×10^{-8}	1.0×10^{-9}	200	0.885	6.6×10^6	3.37×10^{-7}
	10	8.0×10^{-11}	95	0.279	9.88×10^5	9.82×10^8	3.0×10^{-10}	160	0.623	5.51×10^5	9.6×10^{-8}	2.0×10^{-8}	115	0.889	7.3×10^5	6.65×10^{-7}
	25	1.0×10^{-11}	95	0.282	2.56×10^6	2.78×10^8	5.0×10^{-10}	165	0.624	8.76×10^4	1.2×10^{-7}	3.0×10^{-8}	200	0.891	8.2×10^7	8.8×10^{-6}
	50	1.2×10^{-10}	95	0.280	3.33×10^6	4.56×10^8	8.0×10^{-10}	160	0.625	8.92×10^5	2.4×10^{-7}	5.0×10^{-8}	195	0.899	9.73×10^5	9.2×10^{-6}
	75	1.6×10^{-10}	95	0.287	4.47×10^5	5.66×10^8	3.0×10^{-9}	165	0.634	3.78×10^6	3.6×10^{-7}	1.0×10^{-7}	200	0.901	8.48×10^5	9.8×10^{-6}
	100	2.2×10^{-10}	95	0.286	6.66×10^5	7.64×10^8	1.0×10^{-9}	165	0.617	6.68×10^7	4.6×10^{-7}	2.6×10^{-7}	200	0.909	7.65×10^7	1.4×10^{-6}

Table 4.20 : Depolarization kinetic data for PVP samples poled at 80°C with various polarizing fields. Sample thickness 20 μm .
Al-Sn system.

Polarizing Field	α -peak						ρ -peak						ρ' -peak			
	Peak current (Amp)	Peak Temp. (°C)	Activation Energy (eV)	Relaxation time Sec (τ_0)	Charge Released Coul. (Q)	Peak current (Amp)	Peak Temp. (°C)	Activation Energy (eV)	Relaxation time Sec (τ_0)	Charge Released Coul. (Q)	Peak current (Amp)	Peak Temp. (°C)	Activation Energy (eV)	Relaxation time Sec (τ_0)	Charge Released Coul. (Q)	Peak current (Amp)
(Ep)																
05	8.0×10^{-11}	100	0.288	4.7×10^7	6.6×10^{-9}	3.0×10^{-10}	160	0.601	3.01×10^7	7.7×10^{-8}	1.0×10^{-9}	195	0.915	6.87×10^6	3.78×10^{-7}	3.78×10^{-7}
10	1.2×10^{-10}	100	0.292	8.8×10^6	6.92×10^{-9}	5.5×10^{-10}	160	0.606	3.06×10^6	8.8×10^{-8}	2.0×10^{-8}	190	0.918	7.76×10^7	7.99×10^{-7}	7.99×10^{-7}
25	8.0×10^{-10}	100	0.297	9.3×10^5	7.72×10^{-9}	8.0×10^{-10}	160	0.605	9.85×10^7	9.6×10^{-8}	3.0×10^{-8}	195	0.920	5.56×10^6	3.42×10^{-6}	3.42×10^{-6}
50	2.6×10^{-10}	100	0.299	9.9×10^6	8.88×10^{-9}	1.8×10^{-9}	155	0.607	7.76×10^5	1.48×10^{-7}	5.0×10^{-8}	200	0.919	8.87×10^5	9.07×10^{-6}	9.07×10^{-6}
75	3.2×10^{-10}	100	0.301	3.72×10^7	3.55×10^{-8}	1.8×10^{-9}	155	0.604	8.82×10^5	2.78×10^{-7}	8.0×10^{-7}	200	0.917	7.82×10^6	2.25×10^{-5}	2.25×10^{-5}
100	5.0×10^{-10}	100	0.287	5.24×10^7	6.76×10^{-8}	2.2×10^{-8}	160	0.603	7.59×10^6	3.6×10^{-7}	1.2×10^{-7}	200	0.909	8.23×10^7	4.6×10^{-5}	4.6×10^{-5}

Table 4.21 : Depolarization kinetic data for PVP samples poled at 40°C with various polarizing fields. Sample thickness 20 μm .
Al-Sn system.

Polarizing Field	α -peak						ρ -peak						ρ' -peak			
	Peak current (Amp)	Peak Temp. ($^{\circ}\text{C}$)	Activation Energy (eV)	Relaxation time Sec (τ_0)	Charge Released Coul. (Q)	Peak current (Amp)	Peak Temp. ($^{\circ}\text{C}$)	Activation Energy (eV)	Relaxation time Sec (τ_0)	Charge Released Coul. (Q)	Peak current (Amp)	Peak Temp. ($^{\circ}\text{C}$)	Activation Energy (eV)	Relaxation time Sec (τ_0)	Charge Released Coul. (Q)	Charge Released Coul. (Q)
(Ep)																
05	2.0×10^{-11}	60	0.287	6.77×10^6	7.68×10^{-9}	3.0×10^{-10}	155	0.667	5.4×10^5	6.6×10^{-8}	1.4×10^{-9}	200	0.897	4.4×10^6	3.7×10^{-7}	3.7×10^{-7}
10	3.0×10^{-10}	60	0.288	8.77×10^6	8.8×10^{-9}	4.5×10^{-10}	155	0.669	6.24×10^6	7.4×10^{-8}	2.0×10^{-9}	200	0.902	6.4×10^5	4.7×10^{-7}	4.7×10^{-7}
25	5.0×10^{-11}	60	0.286	9.45×10^6	9.2×10^{-9}	7.0×10^{-10}	150	0.671	7.23×10^5	8.2×10^{-8}	3.6×10^{-9}	195	0.907	7.7×10^7	6.4×10^{-7}	6.4×10^{-7}
50	6.5×10^{-11}	60	0.289	2.44×10^5	1.2×10^{-8}	1.0×10^{-9}	155	0.672	8.45×10^6	1.6×10^{-7}	5.0×10^{-9}	205	0.909	8.2×10^6	7.6×10^{-7}	7.6×10^{-7}
75	8.0×10^{-11}	60	0.288	3.77×10^6	1.6×10^{-7}	1.6×10^{-9}	160	0.673	9.27×10^5	2.4×10^{-7}	1.0×10^{-8}	205	0.906	9.4×10^5	8.4×10^{-7}	8.4×10^{-7}
100	1.2×10^{-11}	60	0.284	8.8×10^6	2.4×10^{-7}	2.0×10^{-8}	155	0.674	2.58×10^7	3.2×10^{-7}	2.0×10^{-8}	205	0.905	2.7×10^5	4.6×10^{-7}	4.6×10^{-7}

Table 4.22 : Depolarization kinetic data for PVP samples poled at 60°C with various polarizing fields. Sample thickness 20 μm .
Al-Sn system.

Polarizing Field		α -peak						ρ -peak								
		Peak current	Peak Temp.	Activation Energy	Relaxation time	Charge Released	Peak current	Peak Temp.	Activation Energy	Relaxation time	Charge Released	Peak current	Peak Temp.	Activation Energy	Relaxation time	Charge Released
(Ep)		(Amp)	(°C)	(eV)	Sec (τ_0)	Coul. (Q)	(Amp)	(°C)	(eV)	Sec (τ_0)	Coul. (Q)	(Amp)	(°C)	(eV)	Sec (τ_0)	Coul. (Q)
05		4.0×10^{-11}	65	0.292	6.6×10^5	3.0×10^{-9}	4.0×10^{-10}	160	0.778	6.7×10^4	7.8×10^{-8}	2.0×10^{-9}	195	0.947	4.7×10^5	6.56×10^{-7}
10		5.0×10^{-10}	65	0.297	7.4×10^5	6.0×10^{-9}	6.0×10^{-10}	155	0.772	7.8×10^5	8.2×10^{-8}	4.5×10^{-9}	200	0.956	6.68×10^6	7.76×10^{-7}
25		6.5×10^{-11}	65	0.301	8.7×10^6	7.4×10^{-9}	1.0×10^{-9}	160	0.776	8.7×10^4	8.8×10^{-8}	7.0×10^{-9}	195	0.961	7.43×10^6	8.68×10^{-7}
50		8.0×10^{-11}	65	0.307	9.2×10^5	8.2×10^{-9}	2.0×10^{-9}	165	0.781	9.7×10^6	1.4×10^{-7}	1.0×10^{-8}	200	0.959	8.42×10^5	9.54×10^{-6}
75		1.0×10^{-10}	65	0.306	8.7×10^6	9.7×10^{-9}	2.6×10^{-8}	165	0.762	1.72×10^7	2.6×10^{-7}	2.0×10^{-8}	200	0.958	9.21×10^4	8.78×10^{-6}
100		1.4×10^{-10}	65	0.305	1.78×10^7	1.88×10^{-8}	4.0×10^{-8}	155	0.785	2.45×10^6	4.8×10^{-7}	3.5×10^{-8}	195	0.956	7.76×10^5	6.68×10^{-6}

Table 4.23 : Depolarization kinetic data for PVP samples poled at 80°C with various polarizing fields. Sample thickness 20 μm . Al-Sn system.

Polarizing Field	α -peak					ρ -peak					ρ' -peak				
	Peak current (Amp)	Peak Temp. ($^{\circ}\text{C}$)	Activation Energy (eV)	Relaxation time Sec (τ_0)	Charge Released Coul. (Q)	Peak current (Amp)	Peak Temp. ($^{\circ}\text{C}$)	Activation Energy (eV)	Relaxation time Sec (τ_0)	Charge Released Coul. (Q)	Peak current (Amp)	Peak Temp. ($^{\circ}\text{C}$)	Activation Energy (eV)	Relaxation time Sec (τ_0)	Charge Released Coul. (Q)
(Ep)															
05	6.0×10^{-11}	70	0.323	4.78×10^5	6.0×10^{-9}	6.0×10^{-10}	150	0.745	2.27×10^6	3.3×10^{-8}	3.0×10^{-9}	205	0.934	4.7×10^6	6.7×10^{-7}
10	8.0×10^{-10}	70	0.317	6.33×10^5	8.0×10^{-9}	8.0×10^{-10}	145	0.756	3.34×10^5	4.6×10^{-8}	5.0×10^{-9}	205	0.934	8.7×10^5	8.4×10^{-7}
25	1.0×10^{-11}	70	0.315	4.78×10^5	2.4×10^{-8}	2.4×10^{-9}	150	0.759	4.27×10^6	6.6×10^{-8}	7.0×10^{-9}	205	0.947	9.41×10^6	9.6×10^{-7}
50	1.2×10^{-11}	70	0.313	9.23×10^5	3.5×10^{-8}	3.5×10^{-9}	155	0.753	6.63×10^5	8.7×10^{-8}	2.0×10^{-8}	200	0.956	7.82×10^6	1.4×10^{-6}
75	1.6×10^{-10}	70	0.321	3.44×10^5	5.0×10^{-8}	5.0×10^{-9}	150	0.750	7.24×10^6	9.4×10^{-8}	4.0×10^{-8}	195	0.957	6.52×10^6	2.8×10^{-6}
100	2.2×10^{-10}	70	0.316	7.65×10^5	8.0×10^{-8}	8.0×10^{-9}	155	0.751	8.8×10^5	1.4×10^{-7}	7.0×10^{-8}	200	0.962	7.82×10^6	4.2×10^{-6}

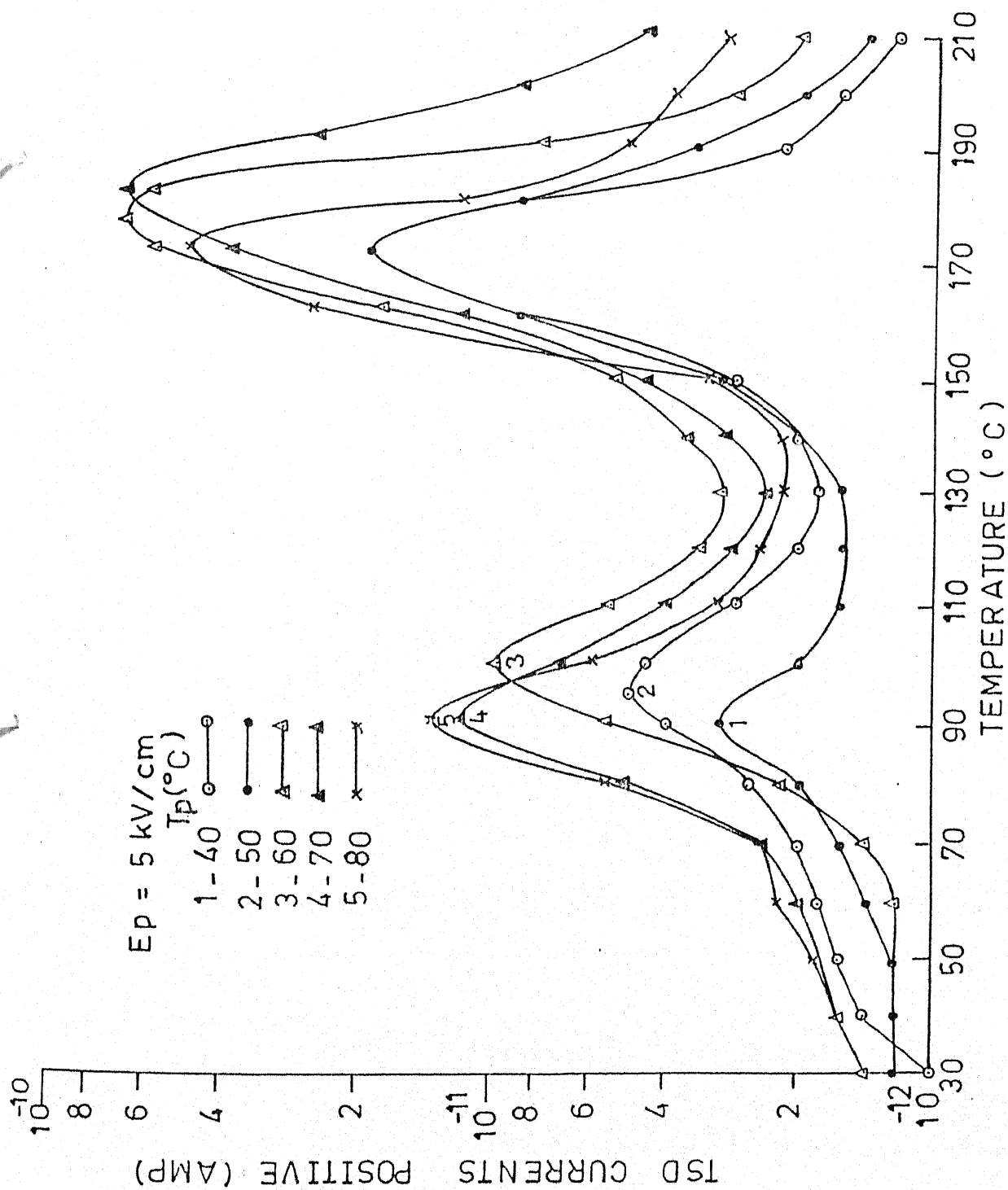


Fig. 4.24 Effect of various polarising temperatures on TSD thermograms of (20 μm thick) samples for given field with Al-Al system.

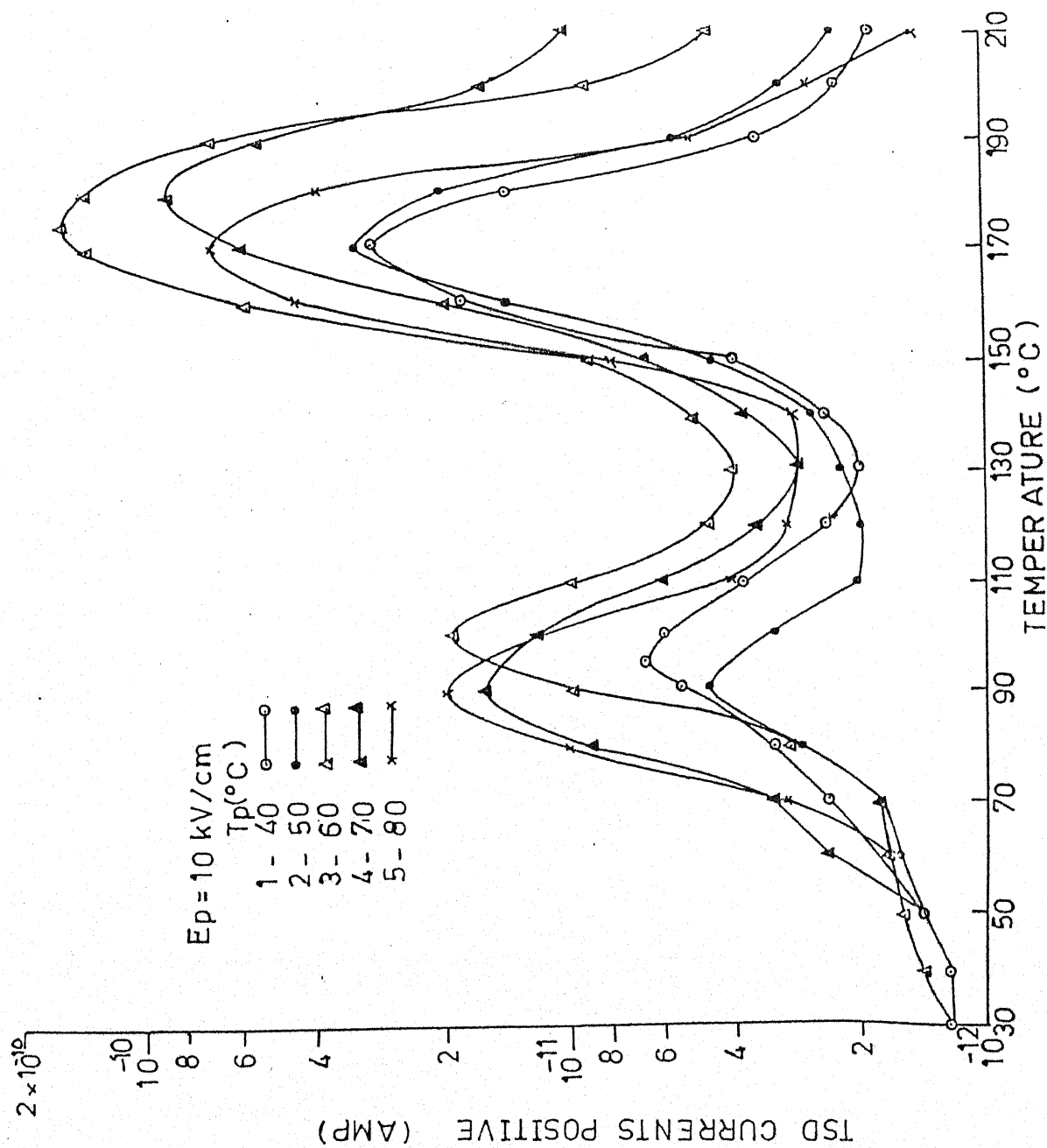


Fig. 4.25 Effect of various polarising temperatures on TSD thermograms of (20 μm thick) samples. for given field with Al-Al system.

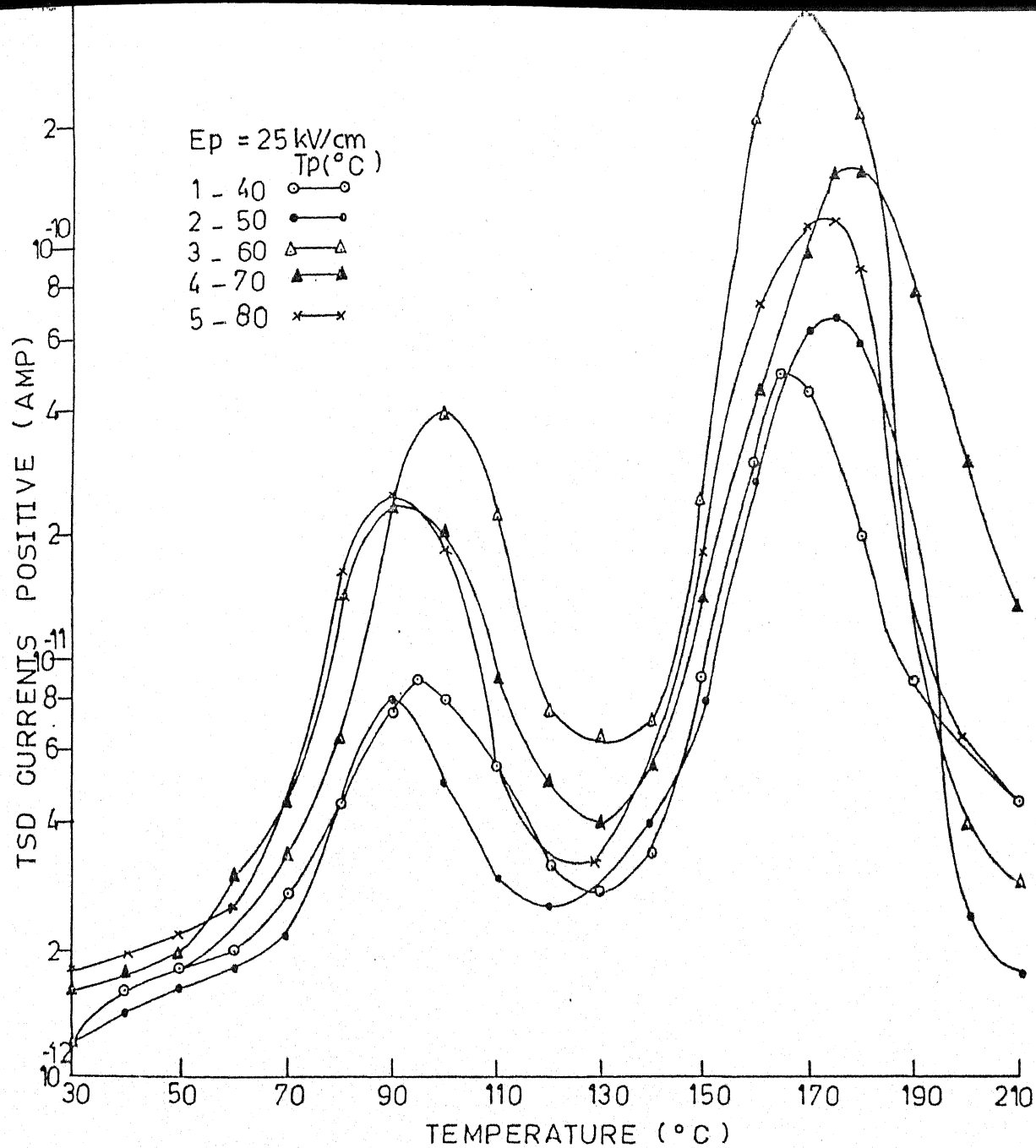


Fig. 4.26 Effect of various polarising temperatures on TSDC thermograms of (20 μ m thick) samples for given field with Al-Al system.

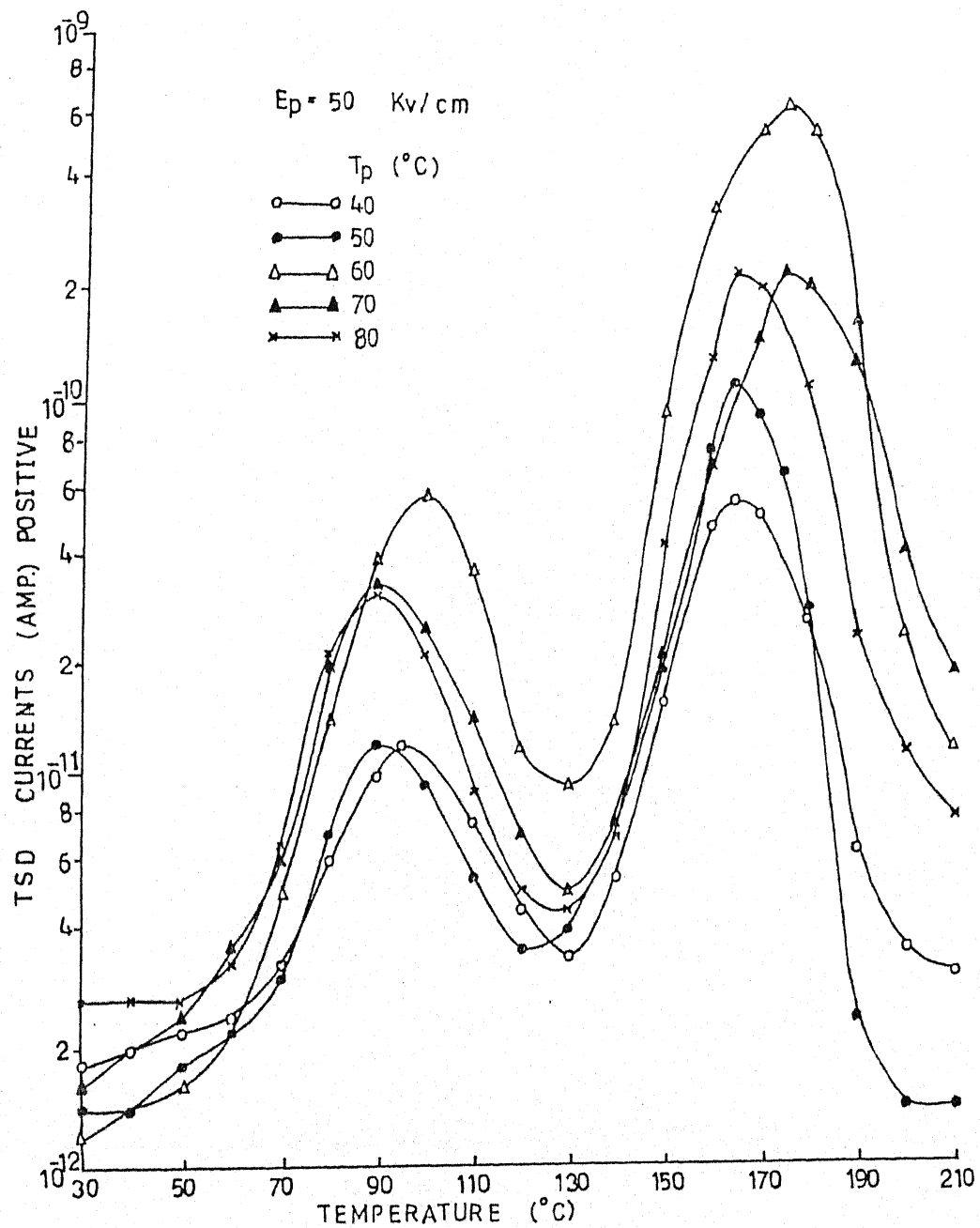


Fig. 4.27 Effect of various polarising temperatures on TSDC thermograms of (20 μm thick) samples for given field with Al-Al system.

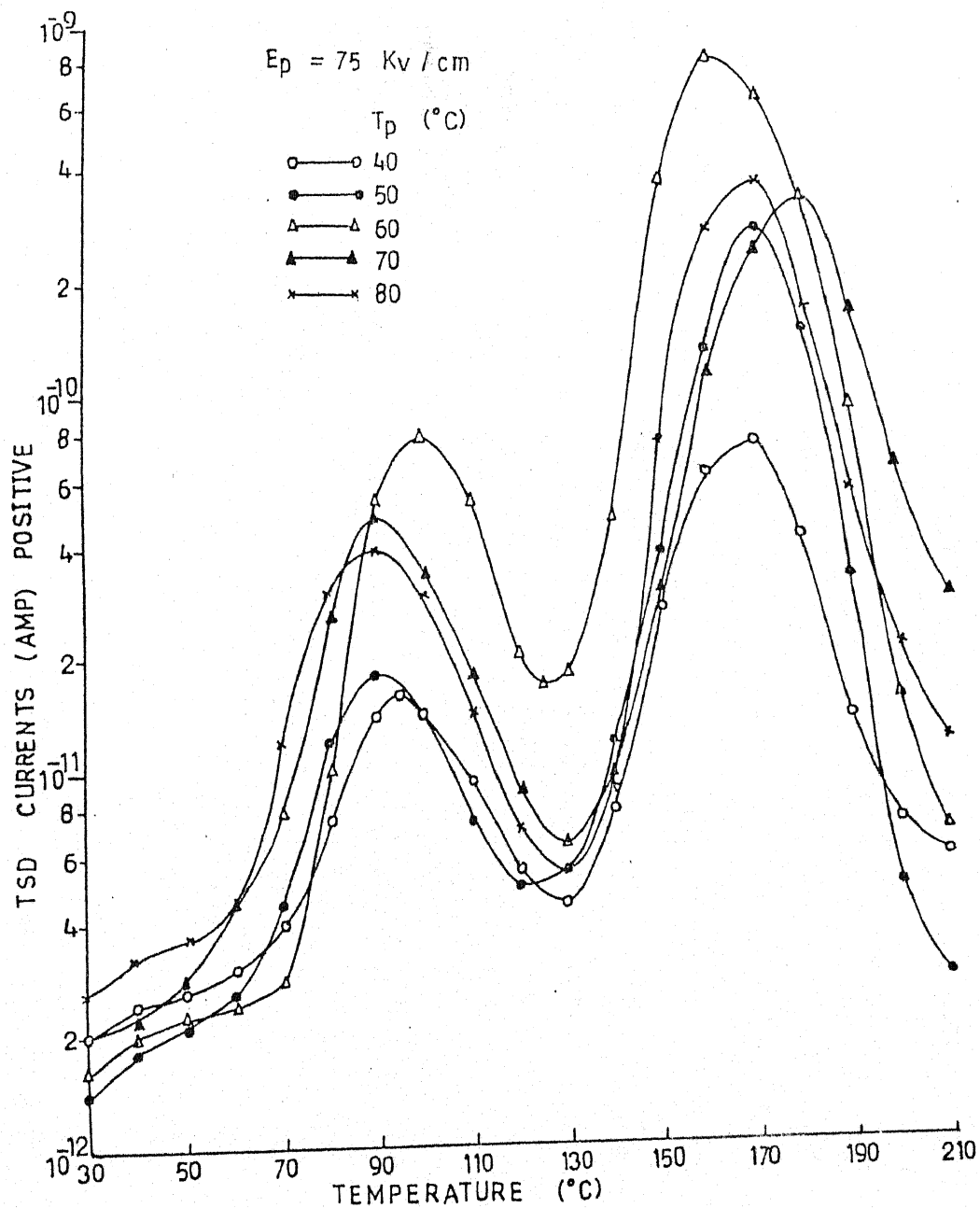


Fig. 4.28 Effect of various polarising temperatures on TSDC thermograms of ($20 \mu\text{m}$ thick) samples for given field with Al-Al system.

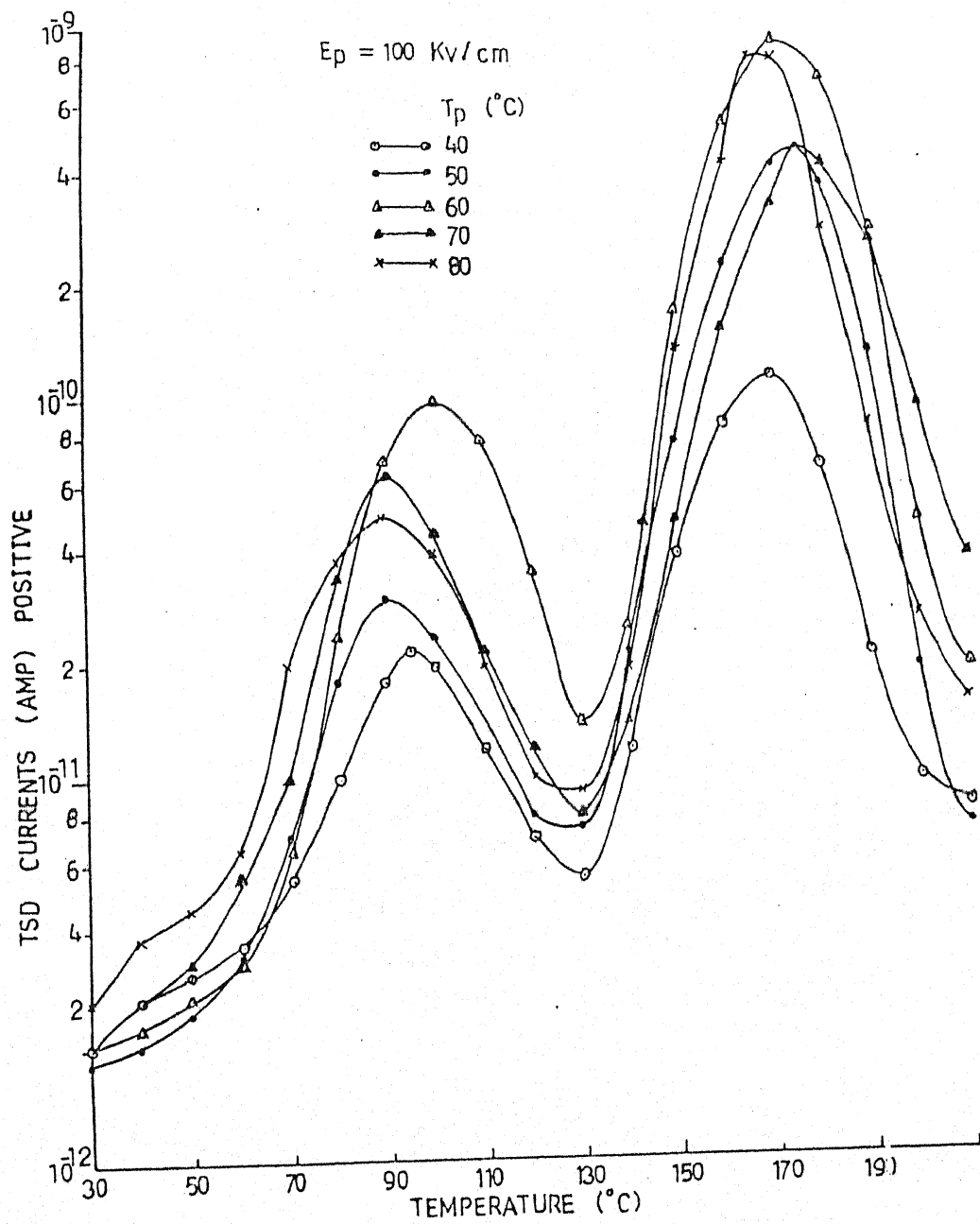


Fig. 4.29 Effect of various polarising temperatures on TSDC thermograms of (20 μm thick) samples for given field with Al-Al system.

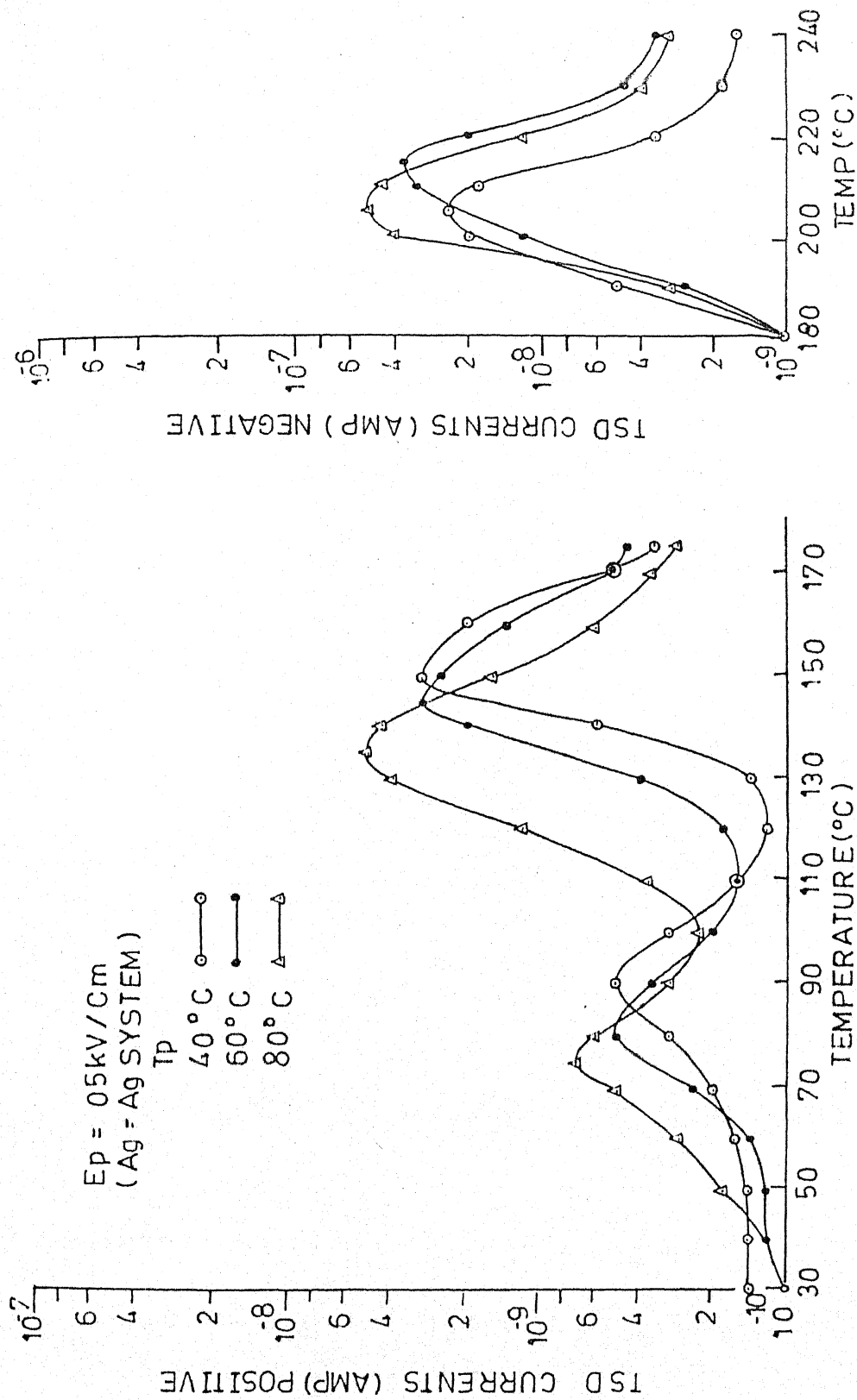


Fig. 4.30 Effect of various polarising temperatures on TSDC thermograms of $(20 \mu\text{m})$ thick) for given field with Ag-Ag system.

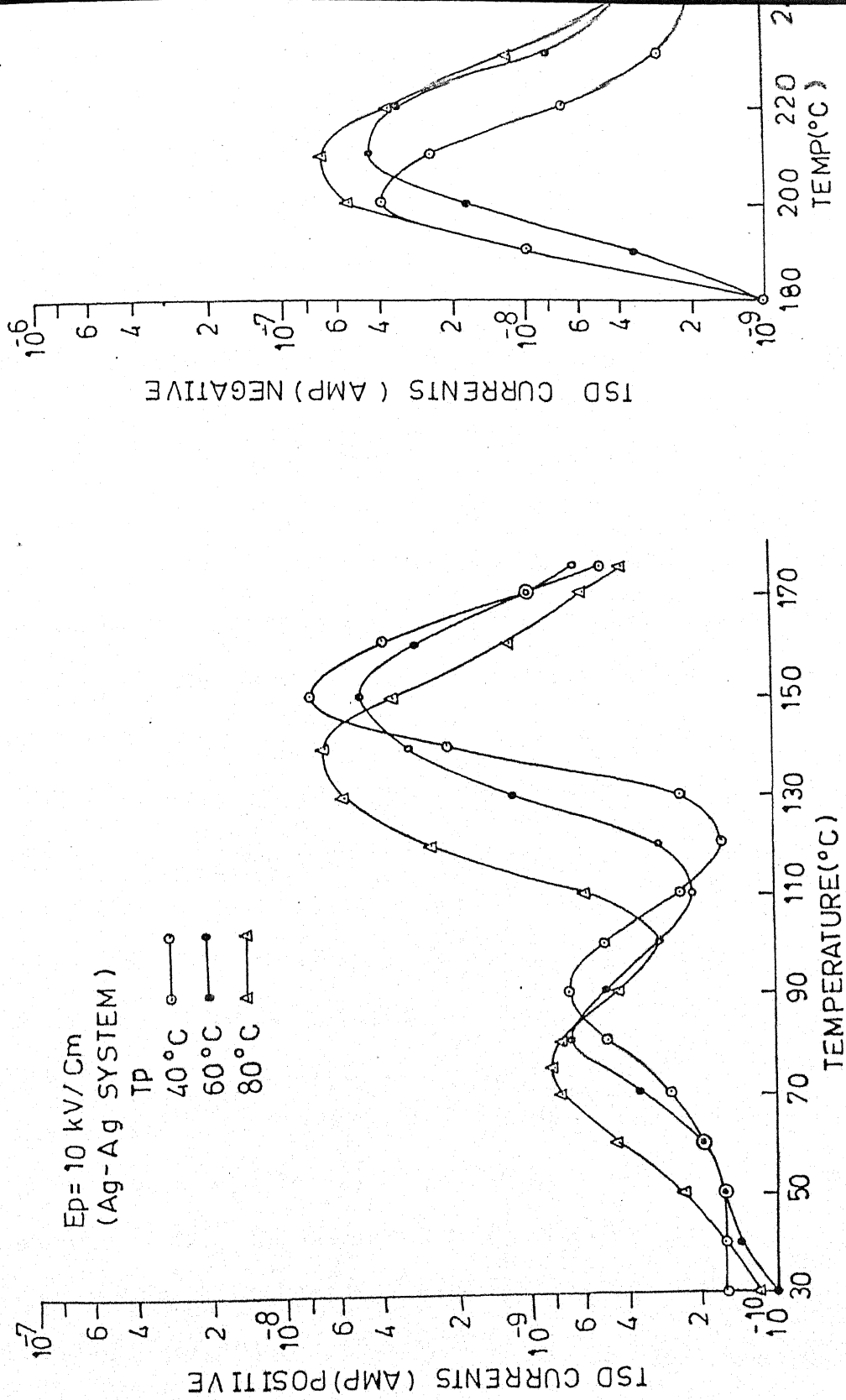


Fig. 4.31 Effect of various polarising temperatures on TSDC thermograms of
 (20 μm thick) samples for given field with Ag-Ag system.

fashion. Peak current is plotted against polarising field (not shown) and the relationship is found to be nearly linear.

Figs. 4.32 to 4.37 show TSDC thermograms for the samples prepared by incorporating other similar electrode system of Ag-Ag for different polarising temperatures T_p (= 40, 60 and 80°C) at constant polarising fields E_p . The values of E_p taken are the same as for Al-Al system. The α and ρ peaks have been found in a similar manner as observed in Al-Al system (Fig.4.24) whereas, additional current peak (ρ') has been found around $205 \pm 5^\circ\text{C}$ in a direction which is opposite to both the peaks. There is no shift in the positions of three peaks for different polarising temperatures. The height of α current peak is almost unaffected with the increase in polarising temperature while for ρ and ρ' peaks, there is no systematic variation of current peak height with rise in T_p . A similar type of behaviour is also observed for Cu-Cu configuration shown in Figs. 4.36 to 4.41 and for Sn-Sn electrode system shown in Figs. 4.42 to 4.47 for the same T_p and E_p under identical conditions. Different tables of depolarisation kinetic data show that relaxation parameters together with positions of current peaks varies with the rise of different similar electrode systems.

Effect of different polarising temperature is also observed on TSDC thermograms of PVP foil electrets for samples prepared using dissimilar electrode combinations. For Al-Ag configuration, results are shown in Figs. 4.48 to 4.53 for the

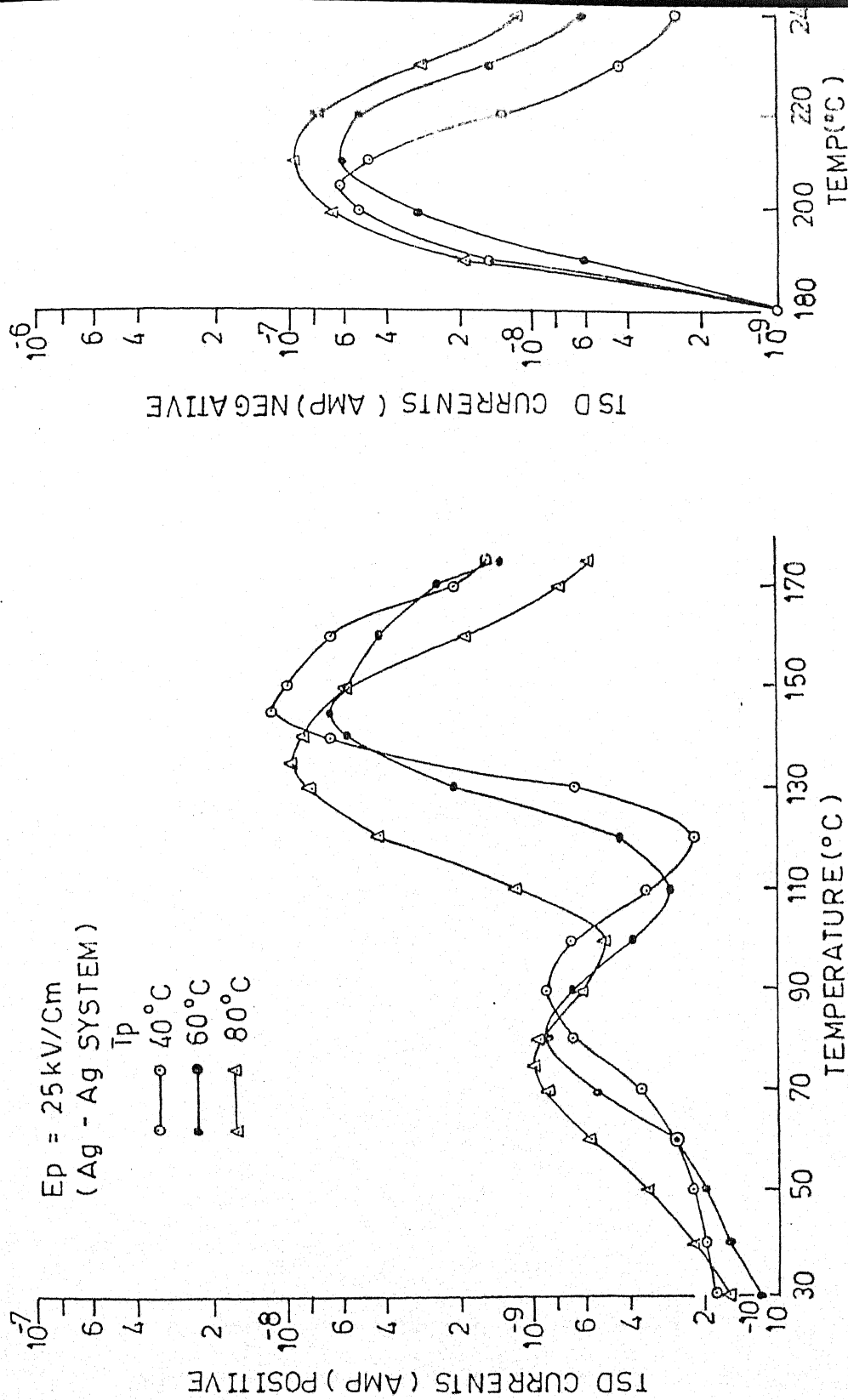


Fig. 4.32 Effect of various polarising temperatures on TSDC thermograms of
 (20 μm thick) samples for given field with Ag-Ag system.

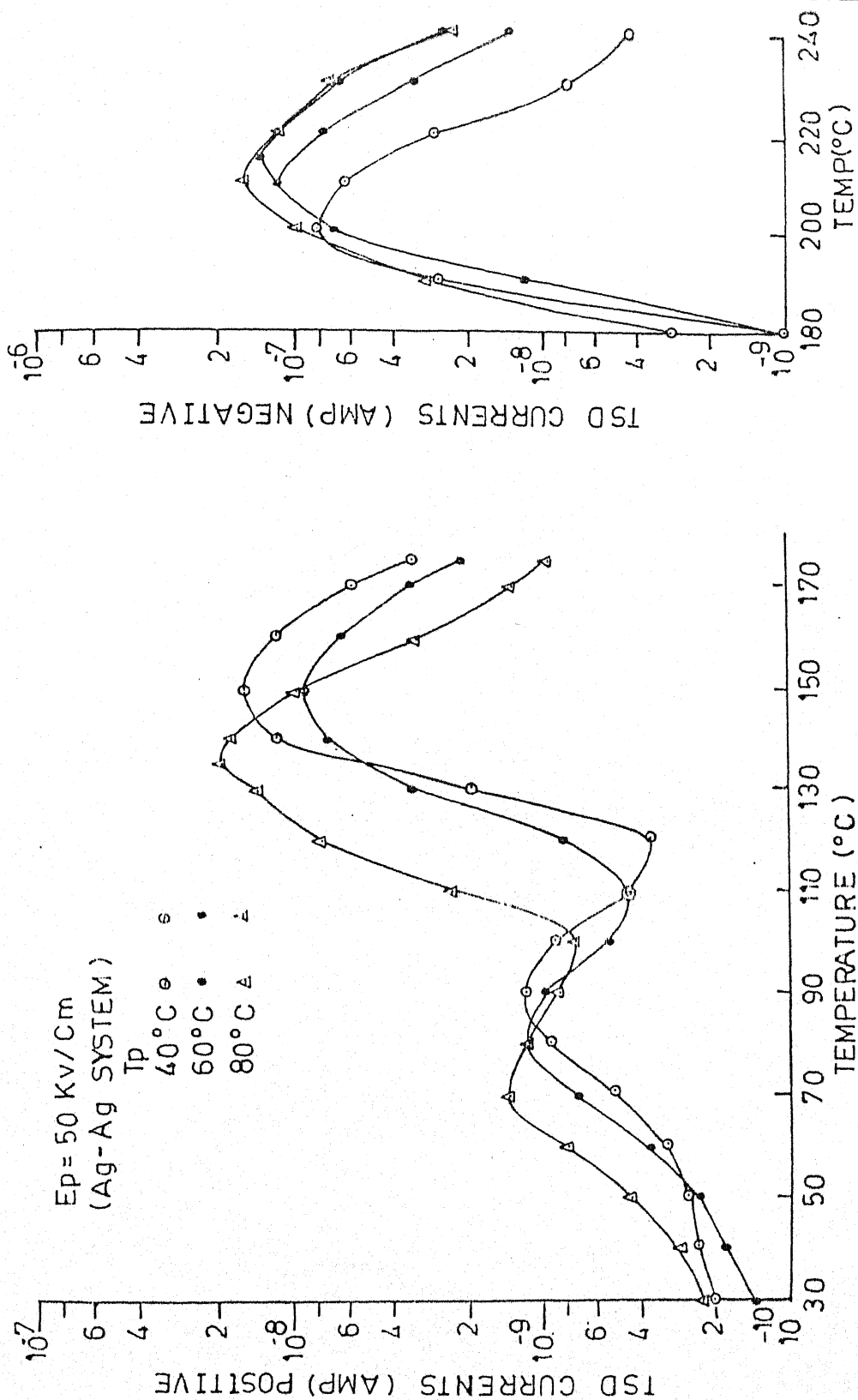


Fig. 4.33 Effect of various polarising temperatures on TSDC thermograms of
 (20 μm thick) samples for given field with Ag-Ag system.

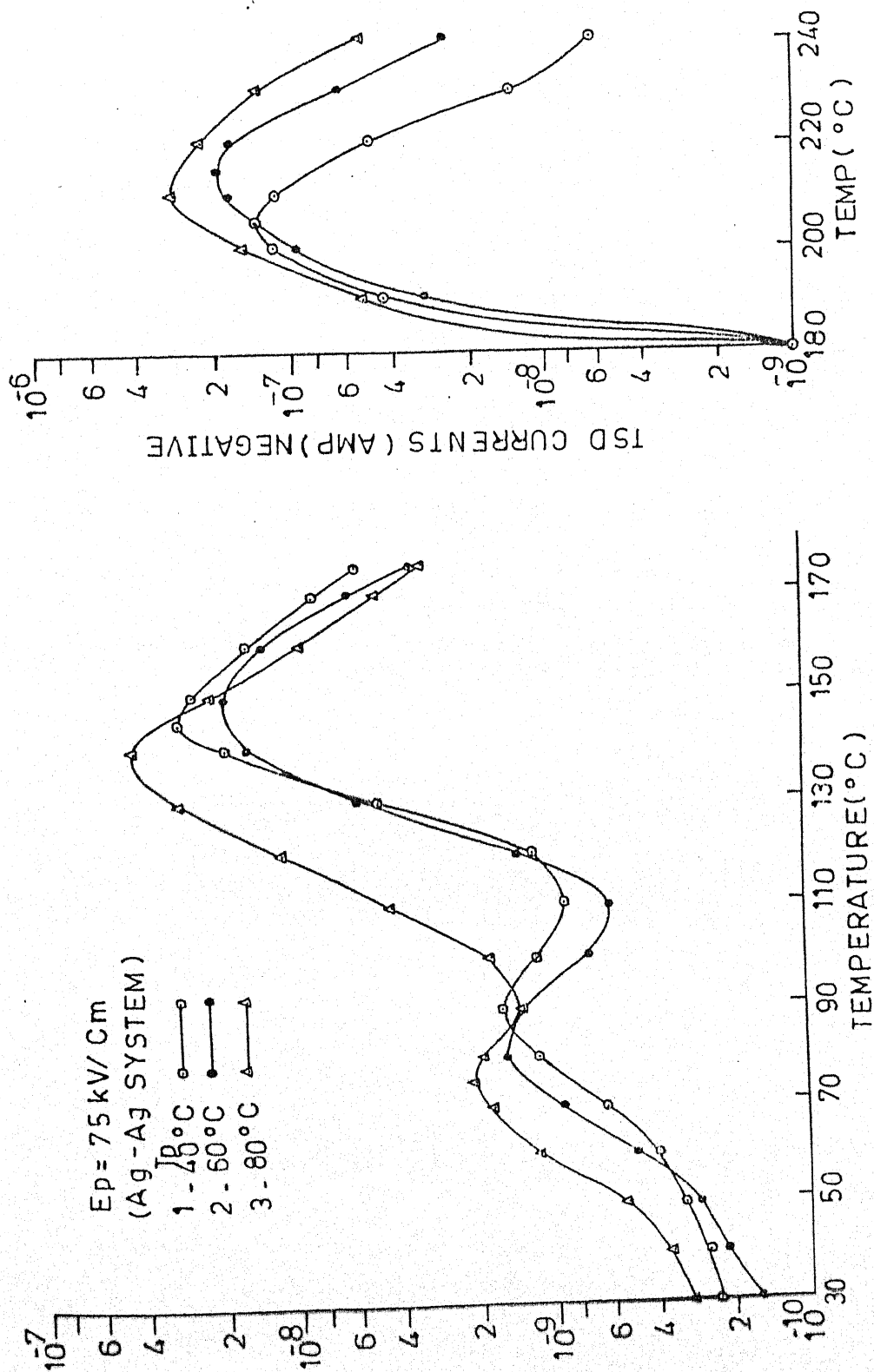


Fig. 4.34 Effect of various polarising temperatures on TSDC thermograms of
 (20 μm thick) samples for given field with Ag-Ag system.

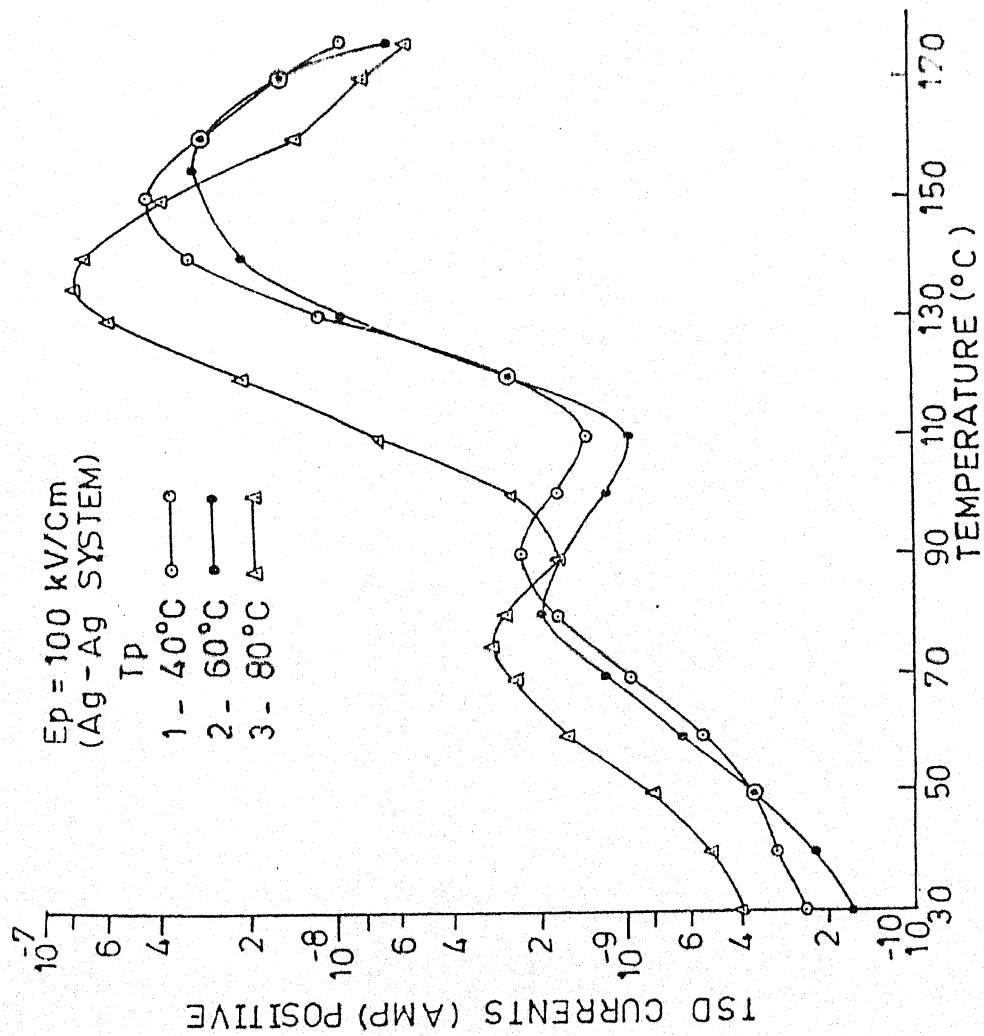


Fig. 4.35 Effect of various polarising temperatures on TSDC thermograms of
 (20 μm thick) samples for given field with Ag-Ag system.

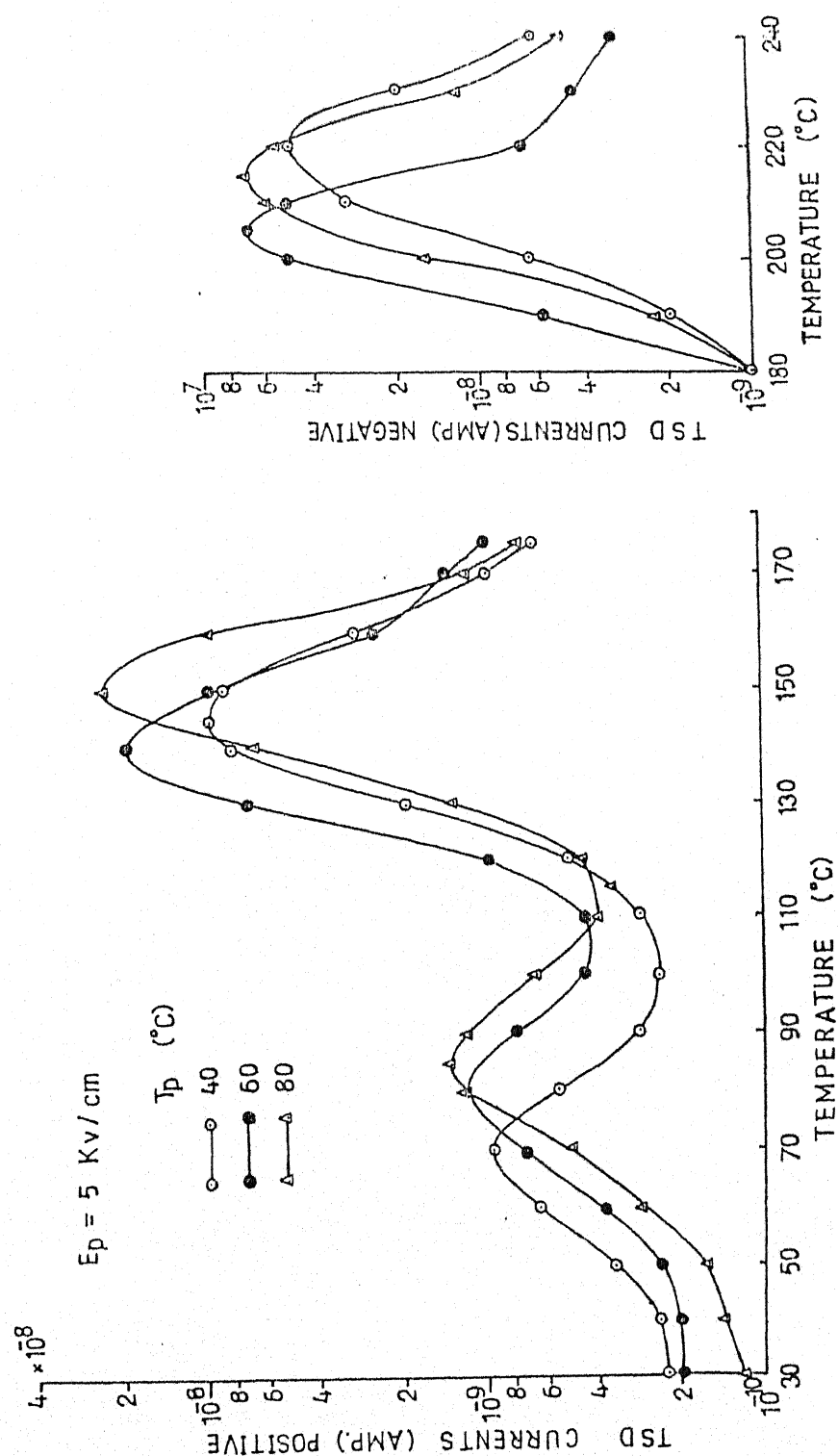


Fig. 4.36 Effect of various polarising temperatures on TSDC thermograms of (20 μm thick) samples for given field with Cu-Cu system.

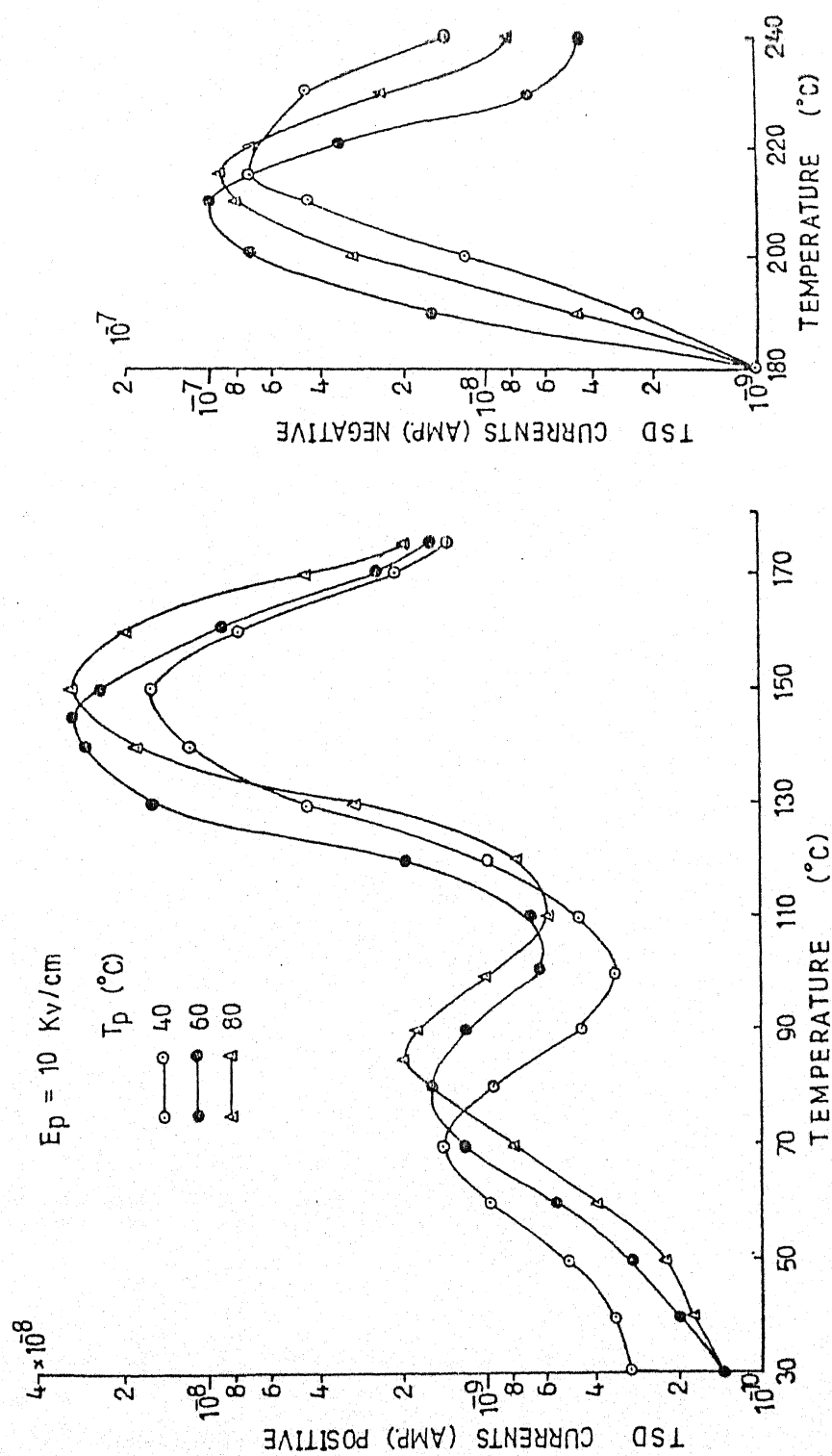


Fig. 4.37 Effect of various polarising temperatures on TSDC thermograms of (20 μm thick) samples for given field with Cu-Cu system.

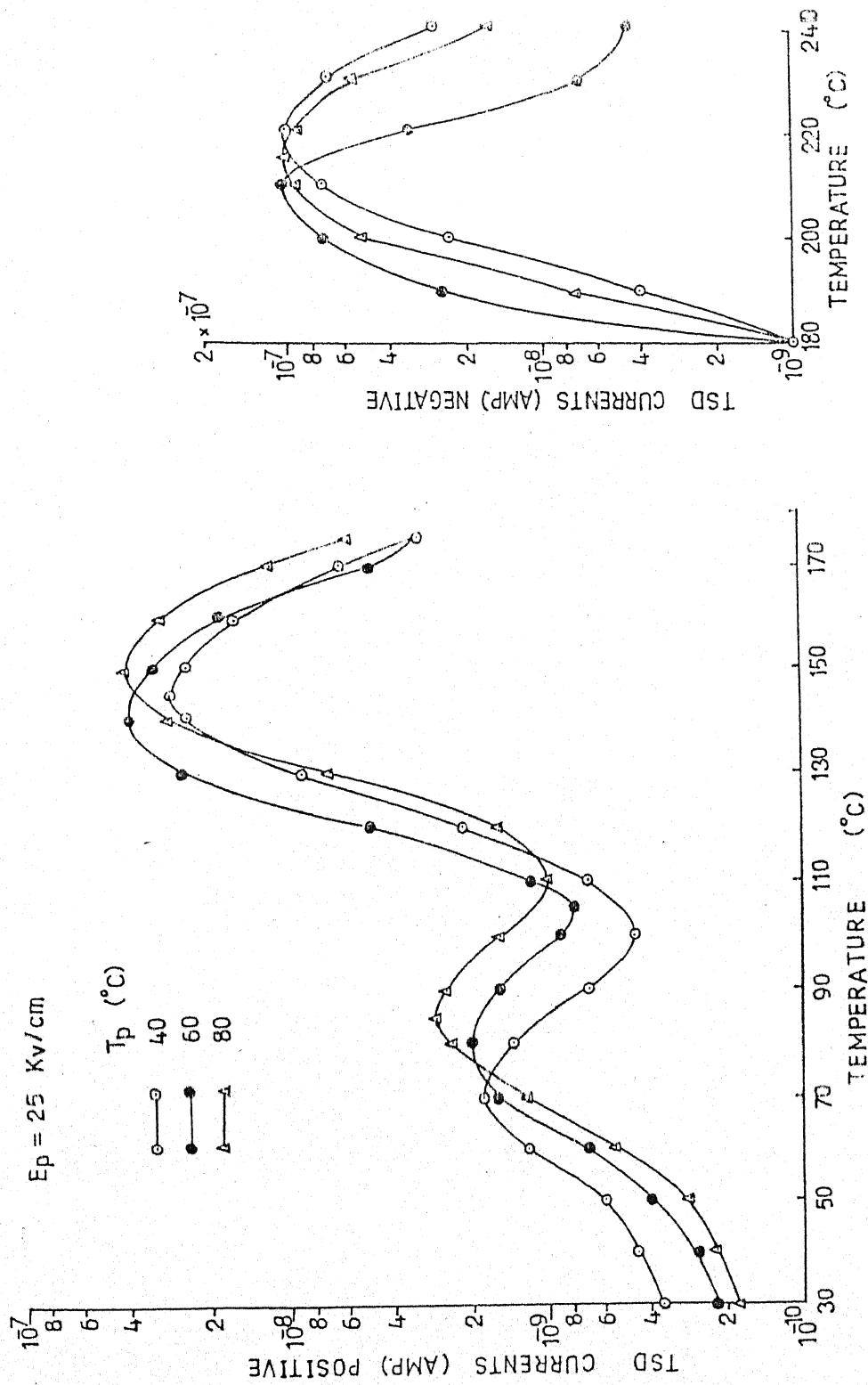


Fig. 4.38 Effect of various polarising temperatures on TSDC thermograms of (20 μm thick) samples for given field with Cu-Cu system.

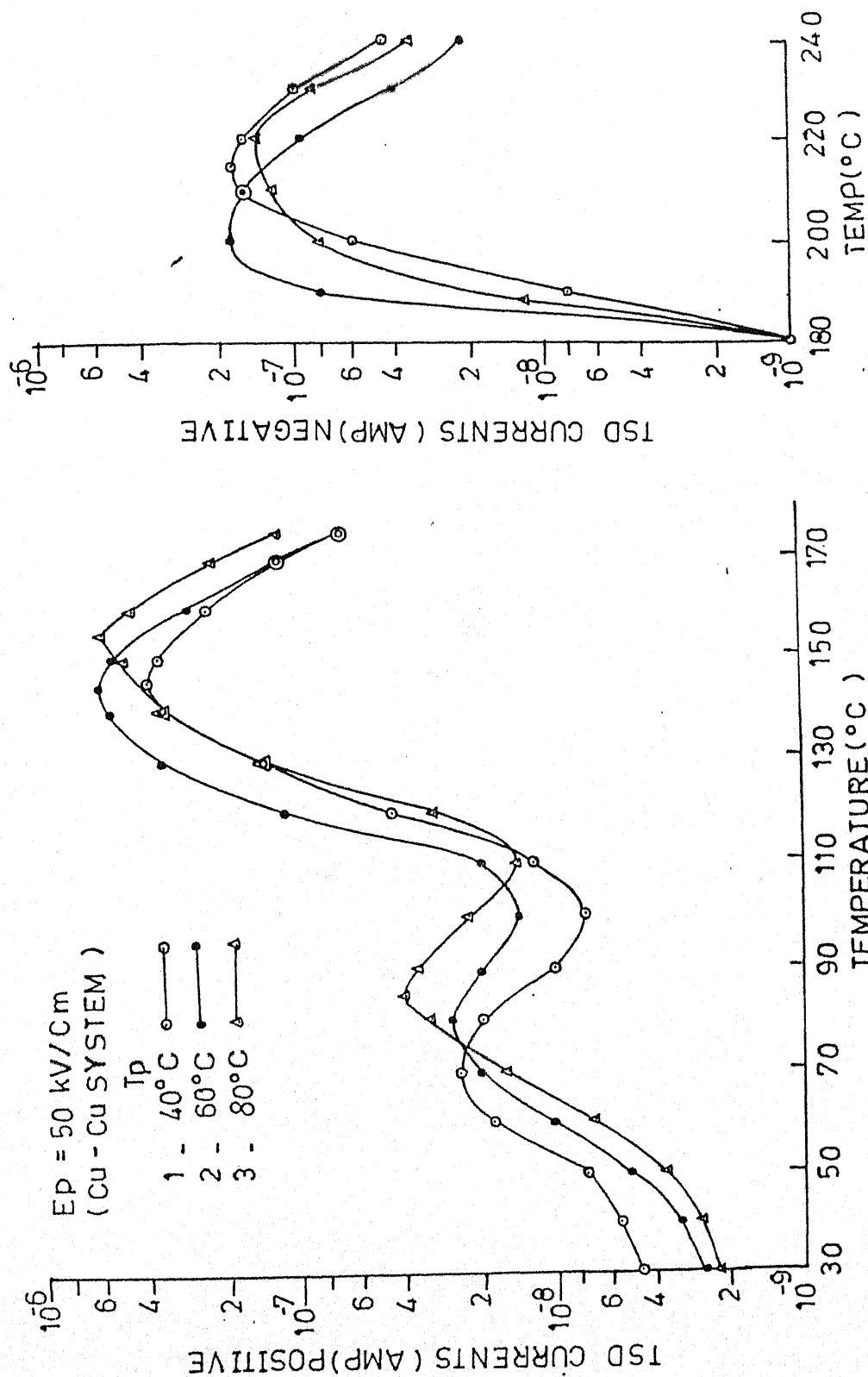


Fig. 4.39 Effect of various polarising temperatures on TSDC thermograms of (20 μ m thick) samples for given field with Cu-Cu system.

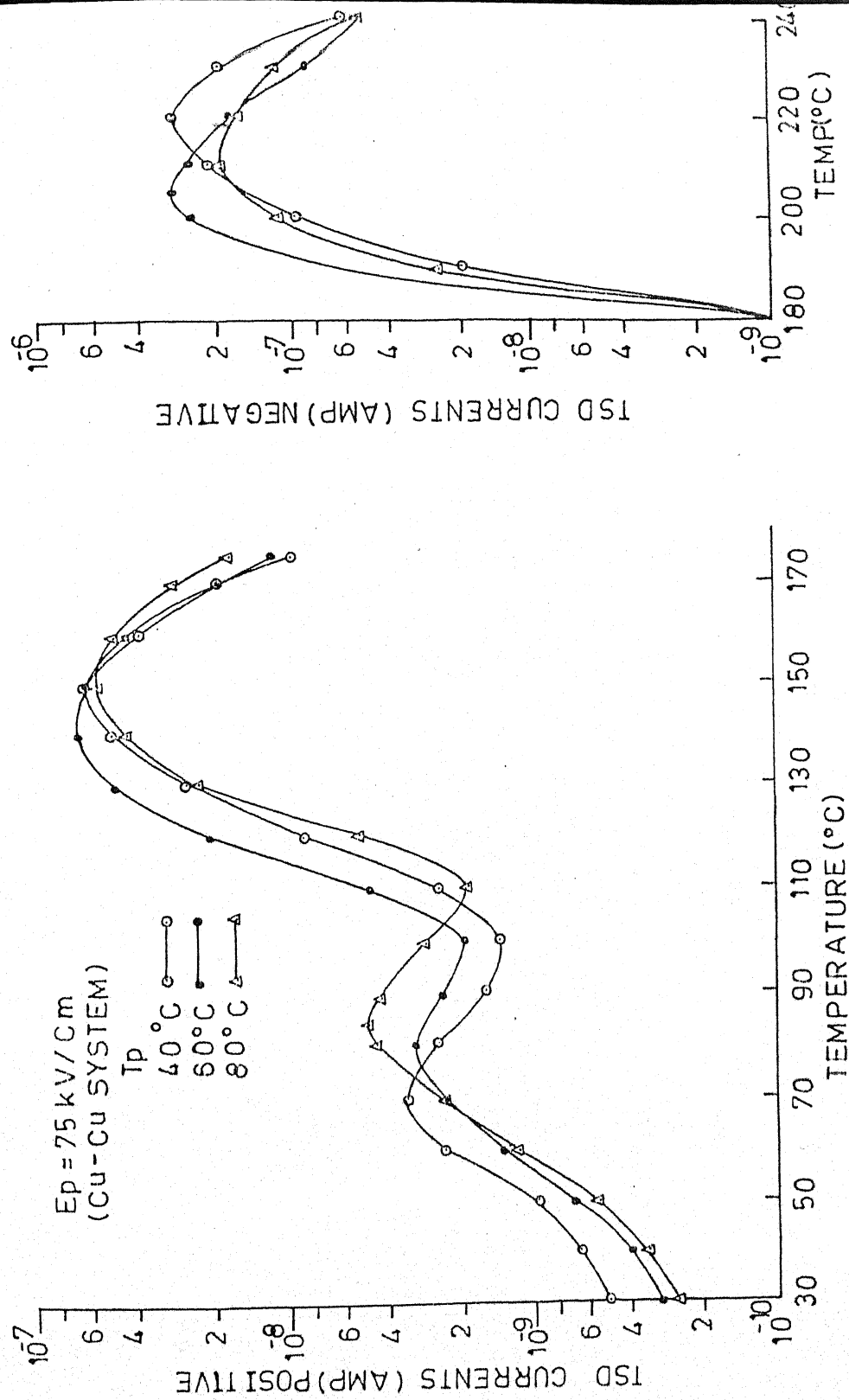


Fig 4.40 Effect of various polarising temperatures on TSDC thermograms of
 ($20 \mu\text{m}$ thick) samples for given field with Cu-Cu system.

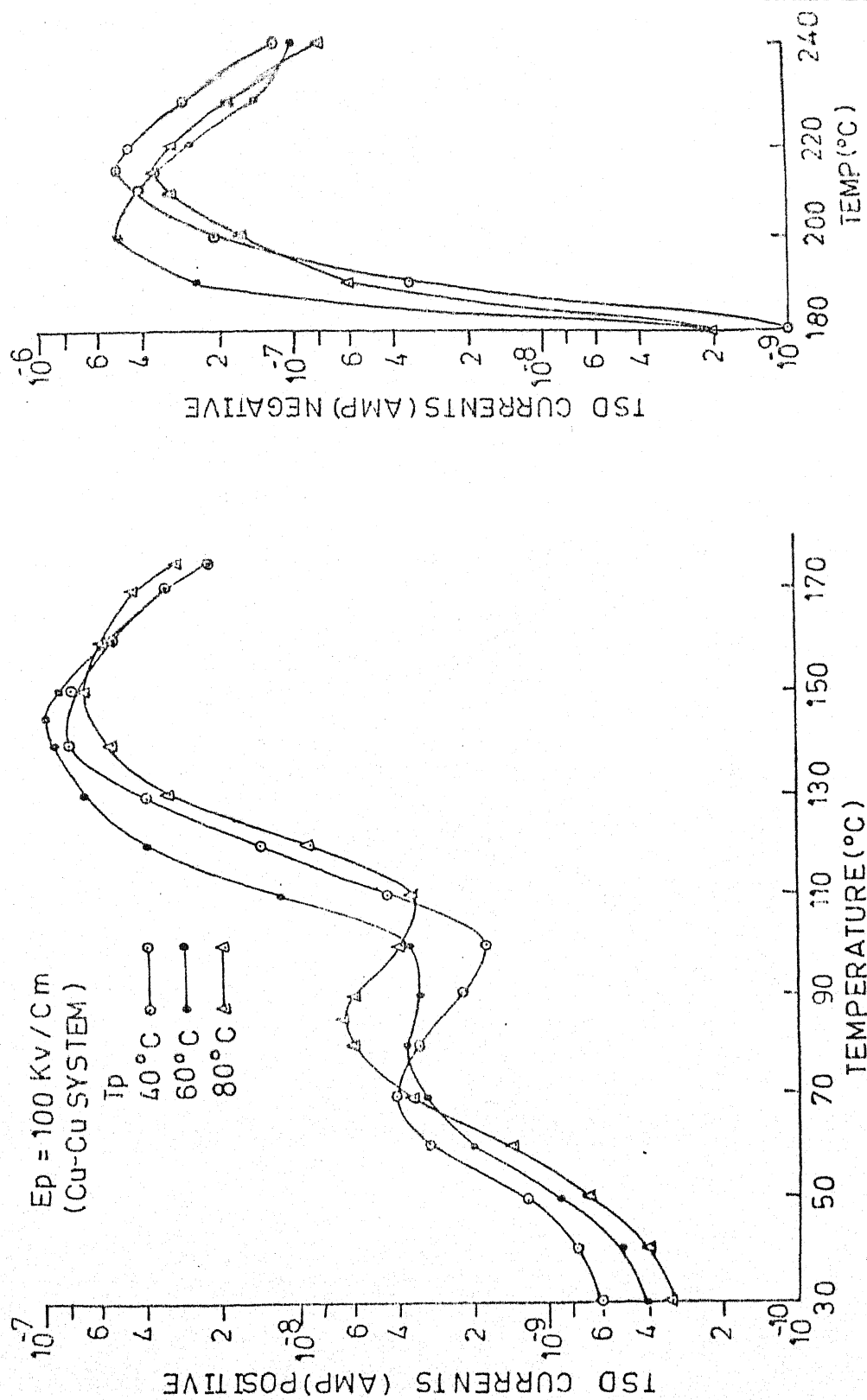


Fig. 4.41 Effect of various polarising temperatures on TSDC thermograms of
 (20 μm thick) samples for given field with Cu-Cu system.

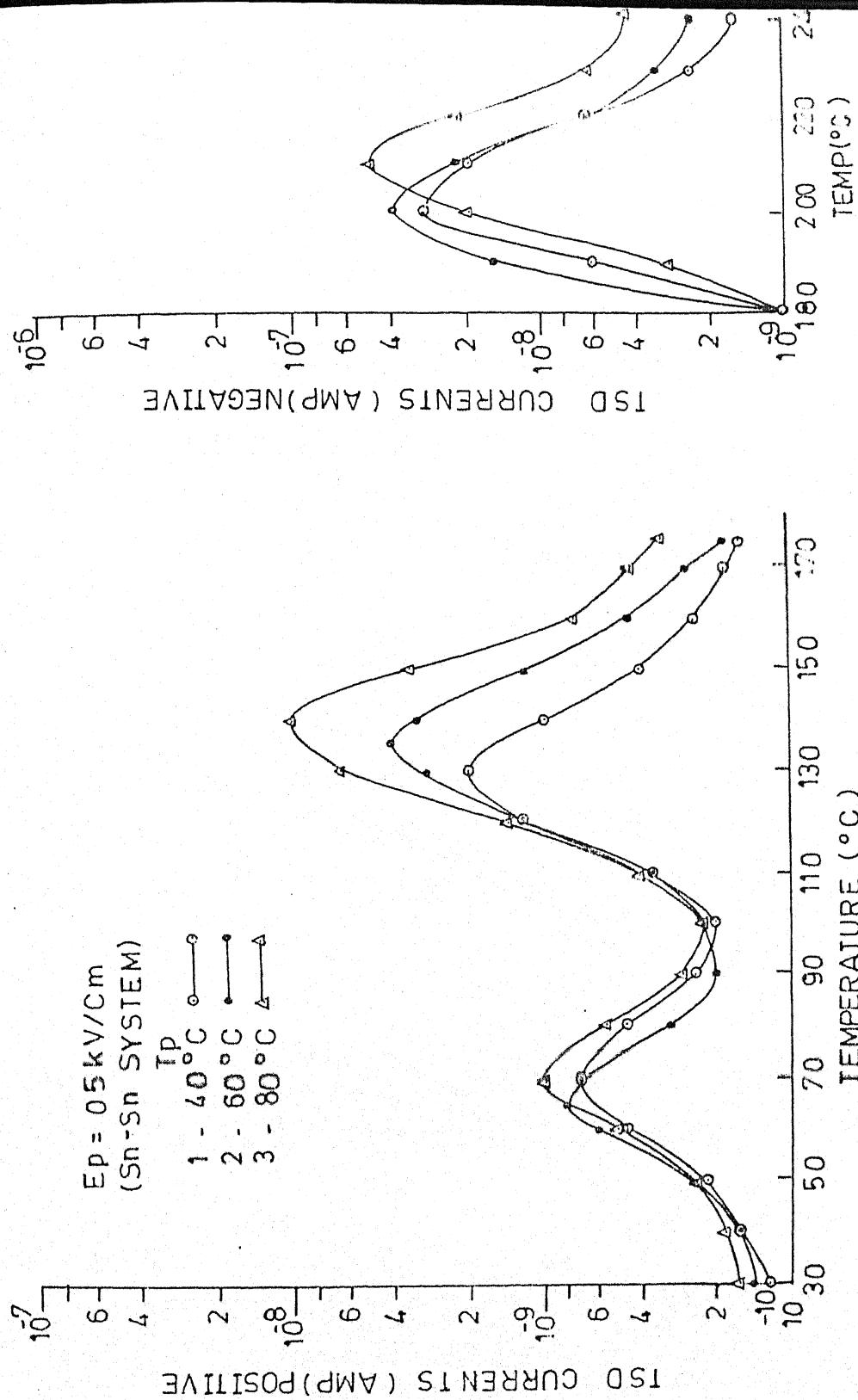


Fig. 4.42 Effect of various polarising temperatures on TSDC thermograms of
 ($20 \mu\text{m}$ thick) samples for given field with Sn-Sn system.

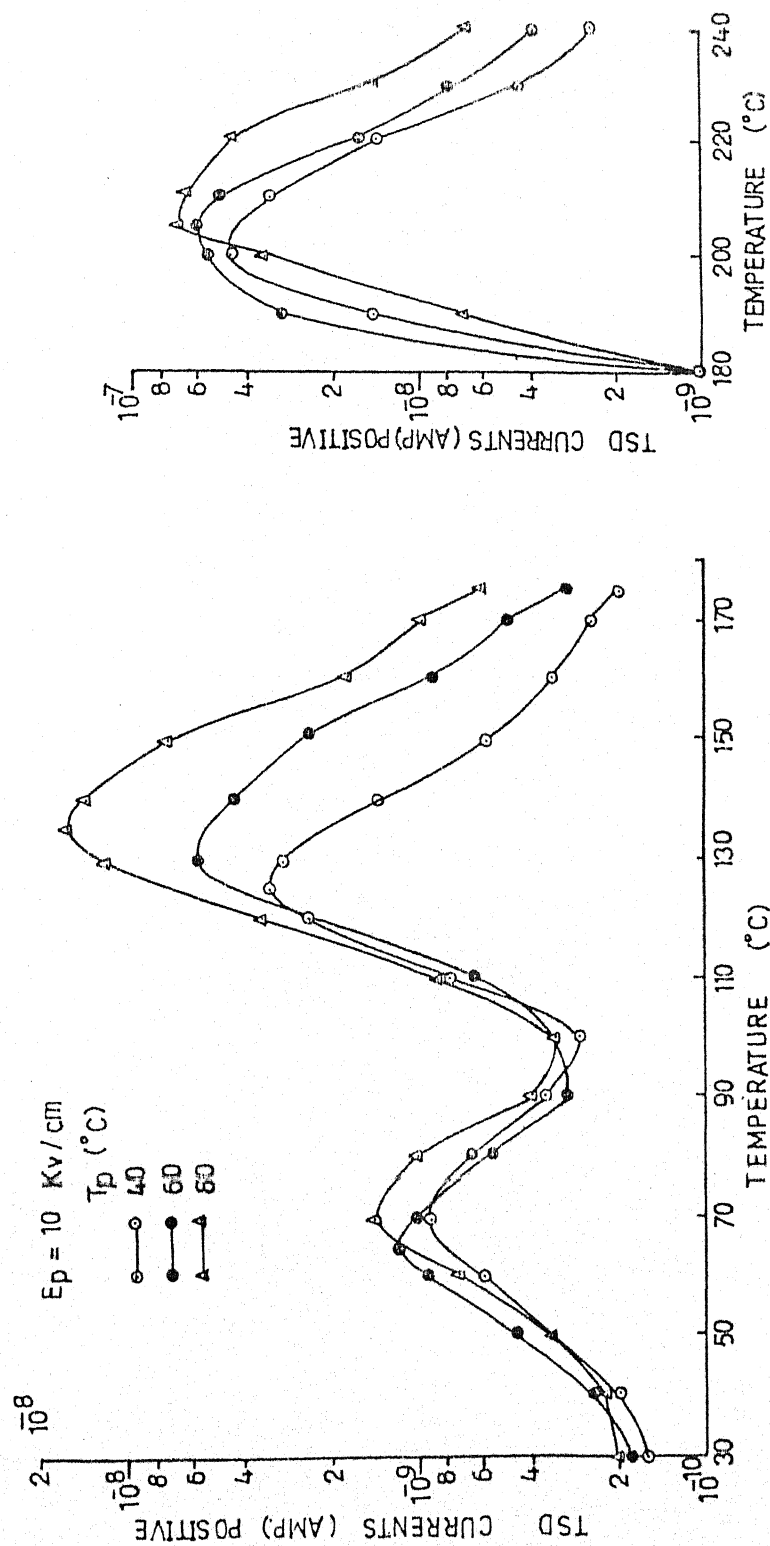


Fig. 4.43 Effect of various polarising temperatures on TSDC thermograms of
 (20 μm thick) samples for given field with Sn-Sn system.

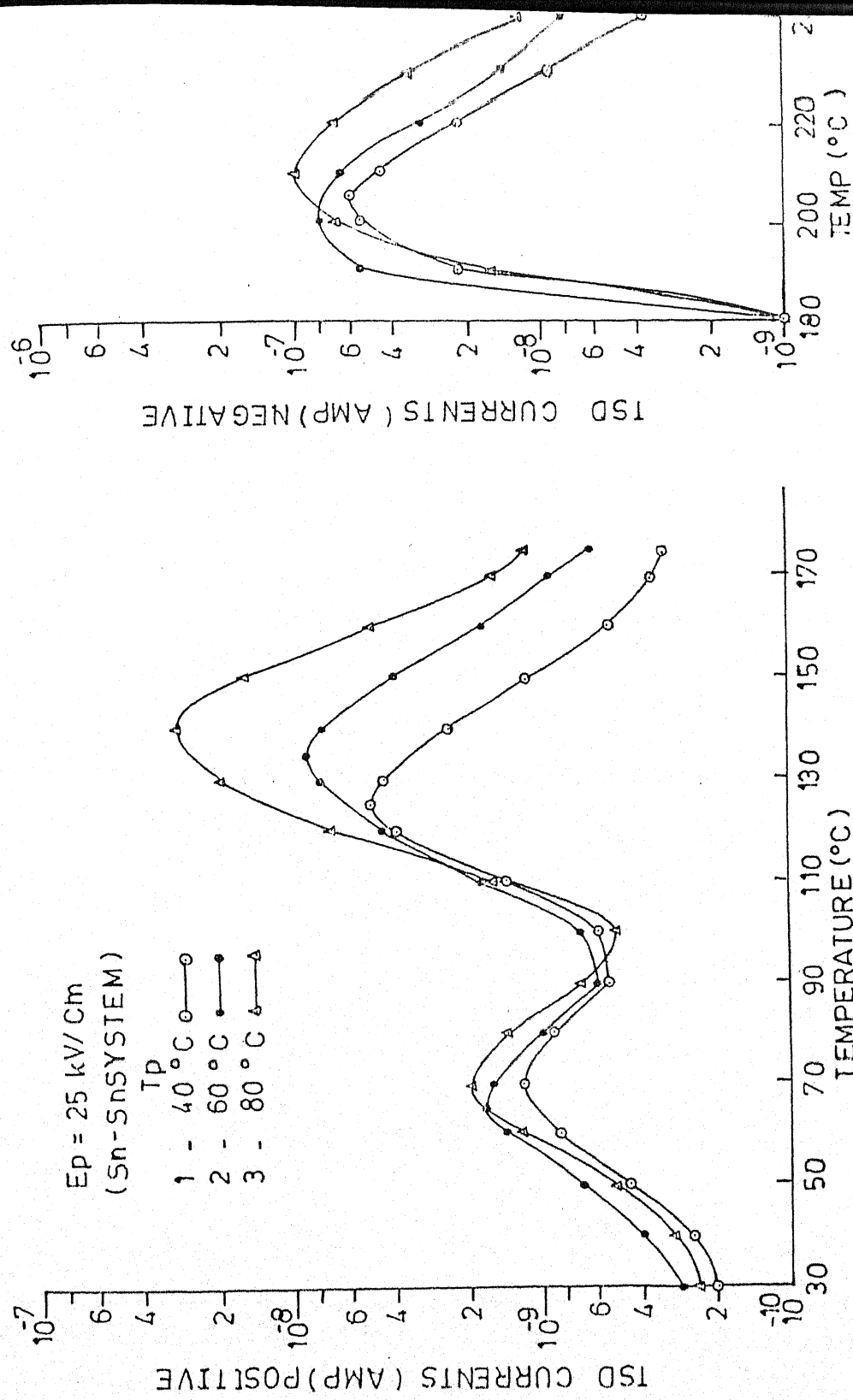


Fig. 4.44 Effect of various polarising temperatures on TSDC thermograms of
 ($20 \mu\text{m}$ thick) samples for given field with Sn-Sn system.

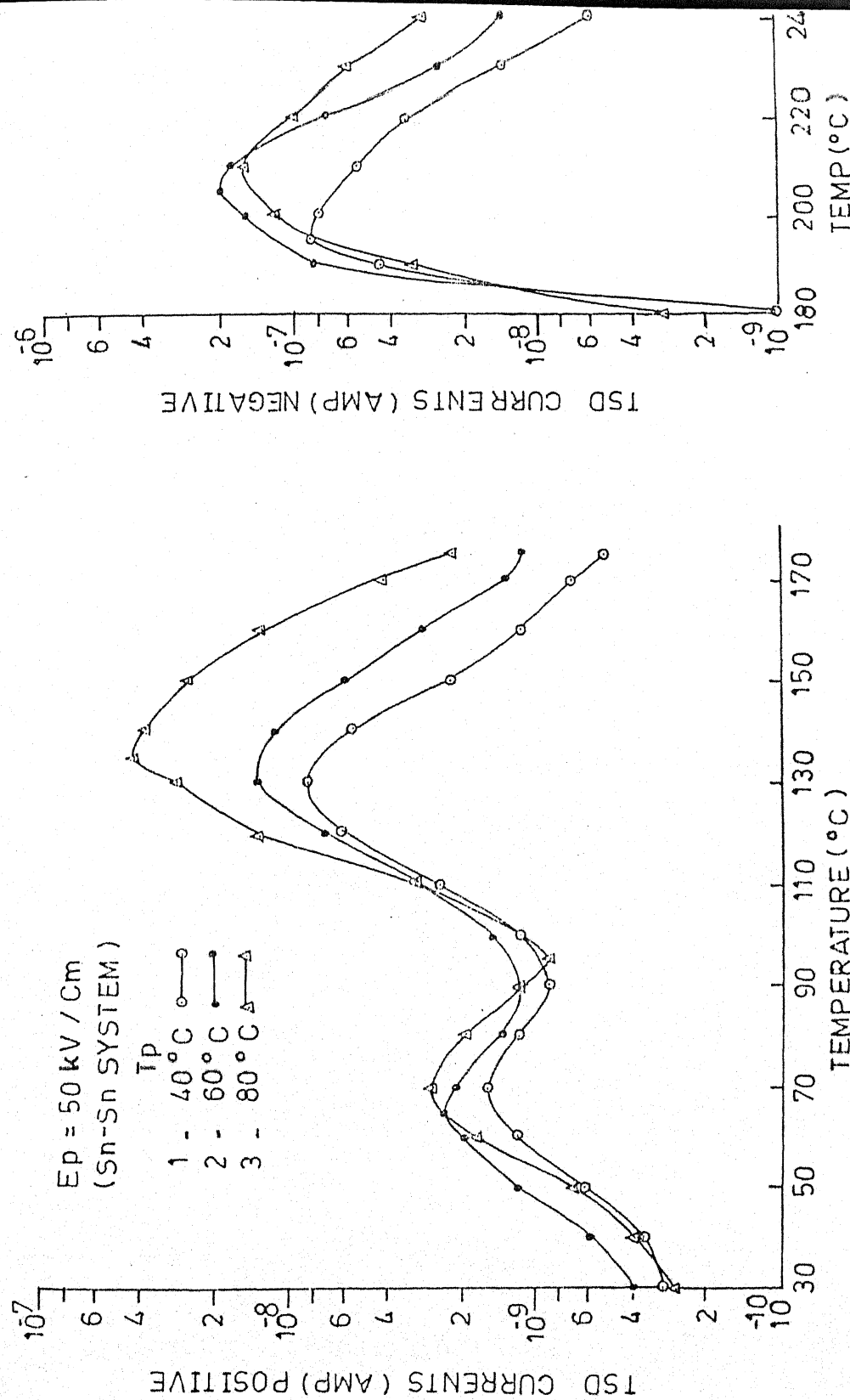


Fig. 4.45 Effect of various polarising temperatures on TSDC thermograms of
(20 μ m thick) samples for given field with Sn-Sn system.

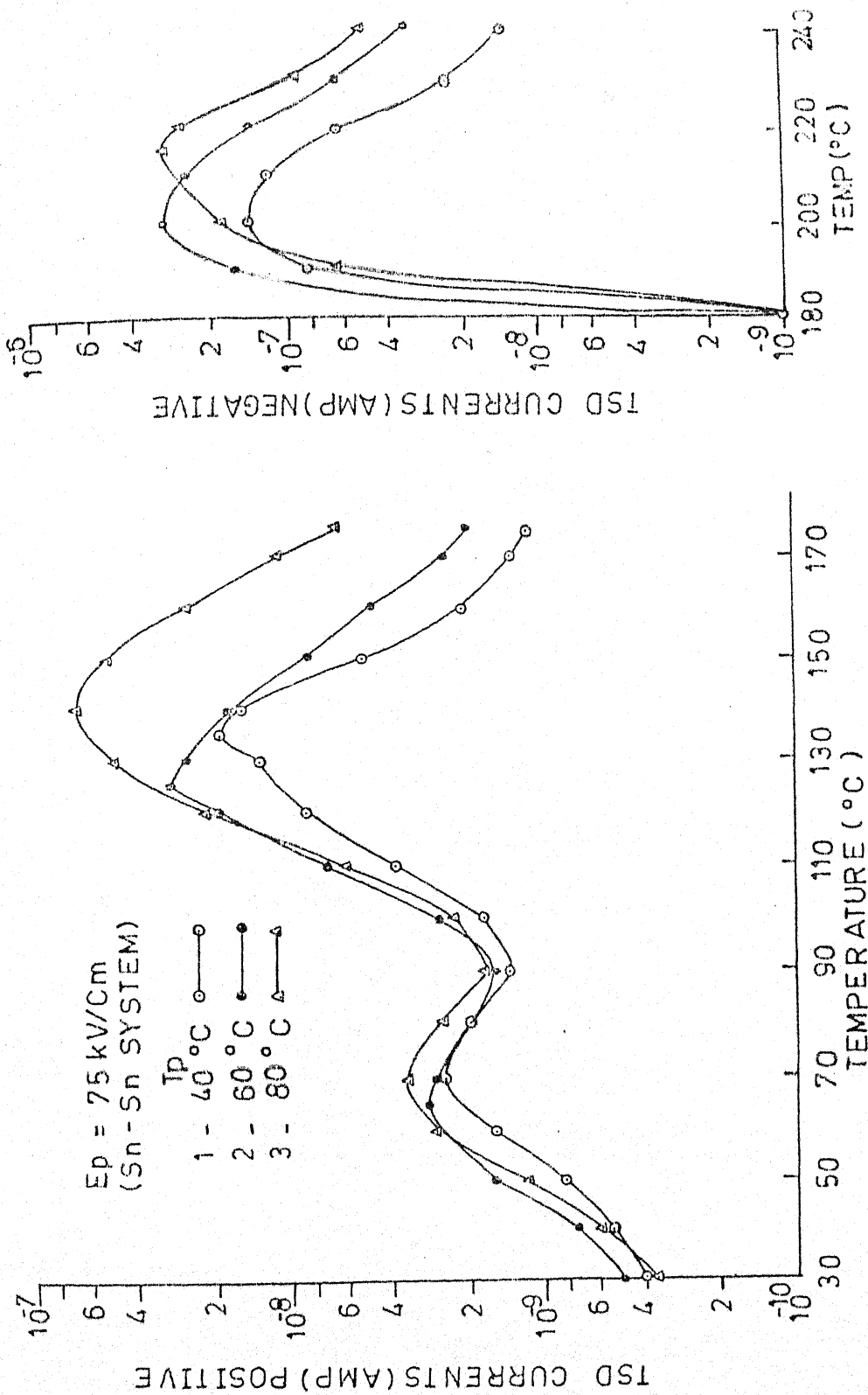


Fig. 4.46 Effect of various polarising temperatures on TSDC thermograms of
 (20 μm thick) samples for given field with Sn-Sn system.

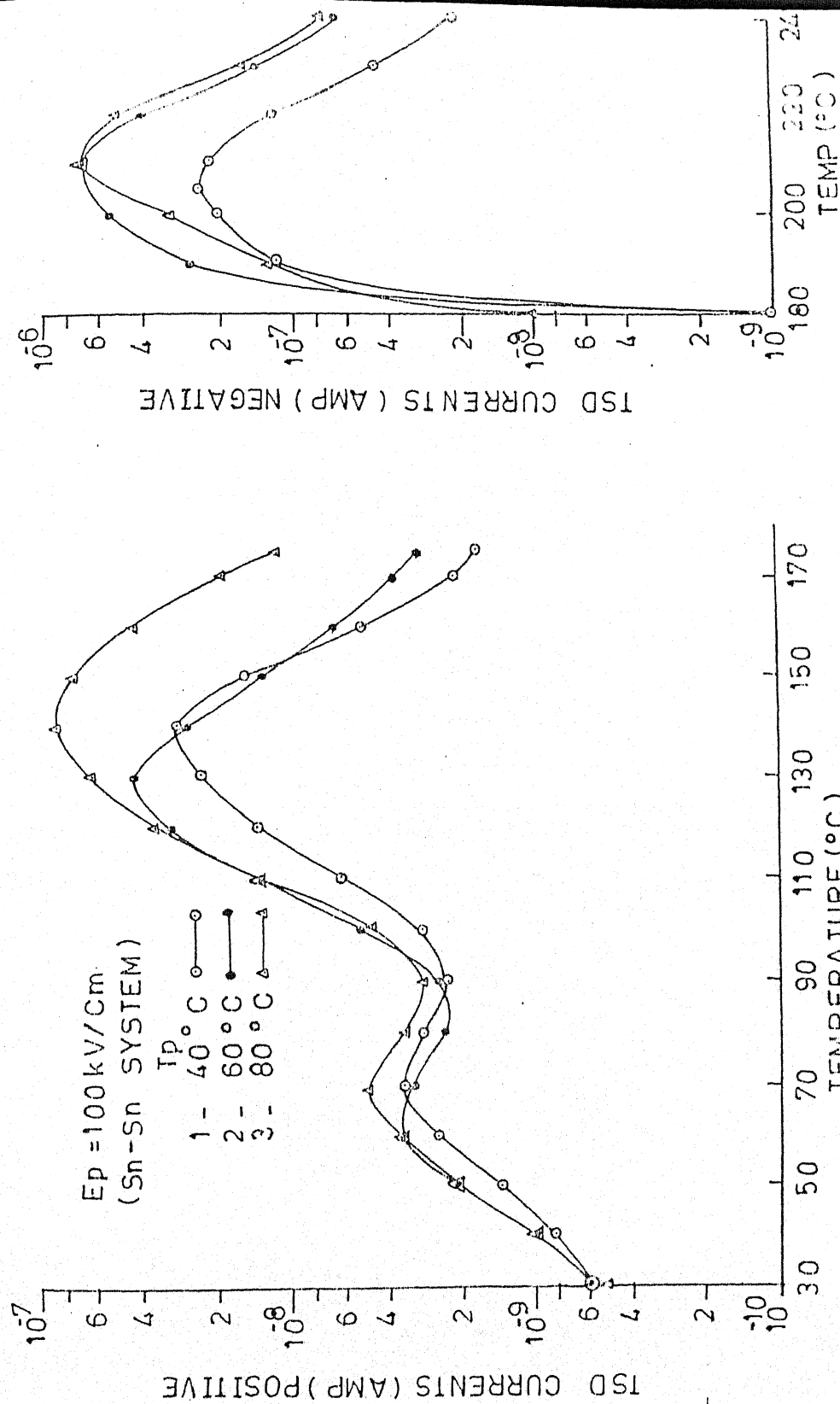


Fig. 4.47 Effect of various polarising temperatures on TSDC thermograms of
 (20 μm thick) samples for given field with Sn-Sn system.

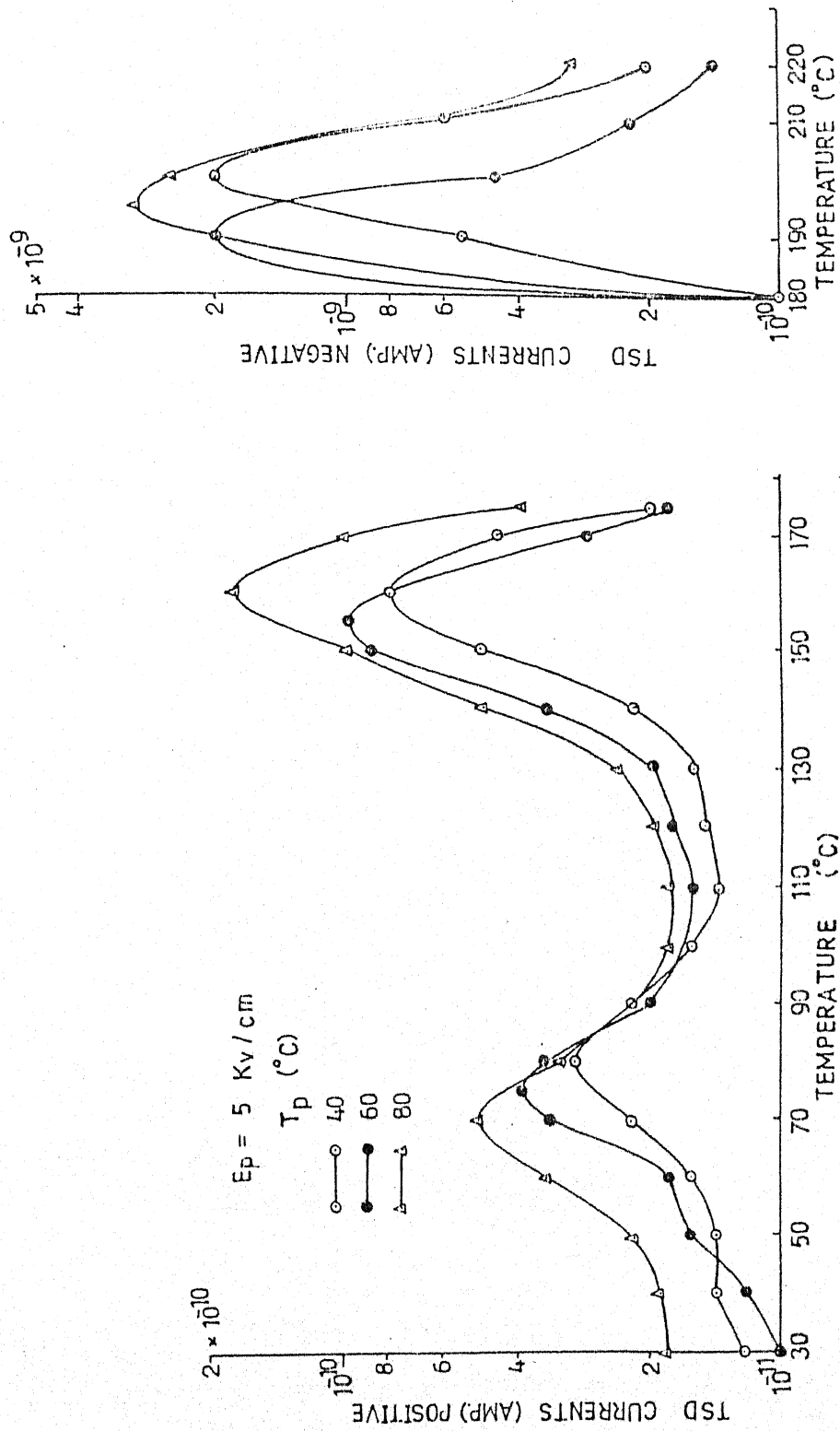


Fig. 4.48 Effect of various polarising temperatures on TSDC thermograms of
 (20 μm thick) samples for given field with Al-Ag system.

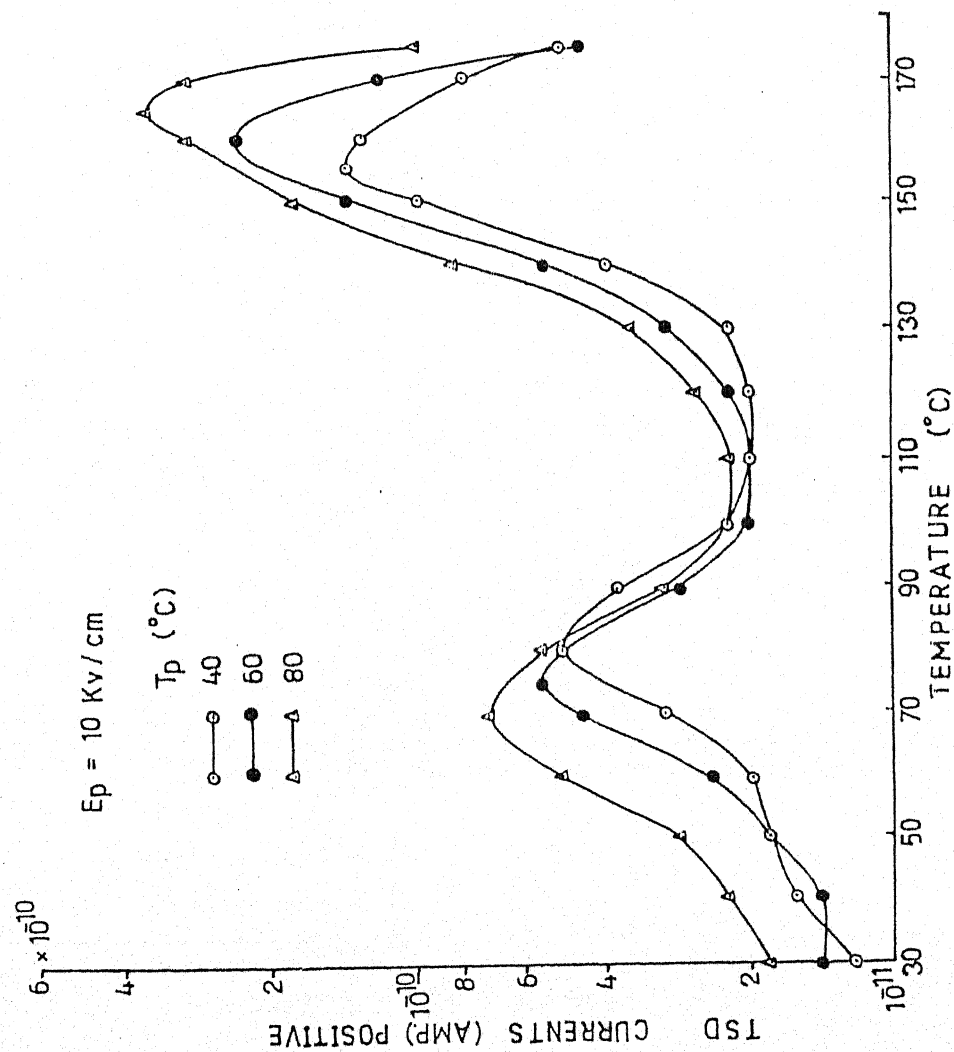


Fig. 4.49 Effect of various polarising temperatures on TSDC thermograms of (20 μm thick) samples for given field with Al-Ag system.

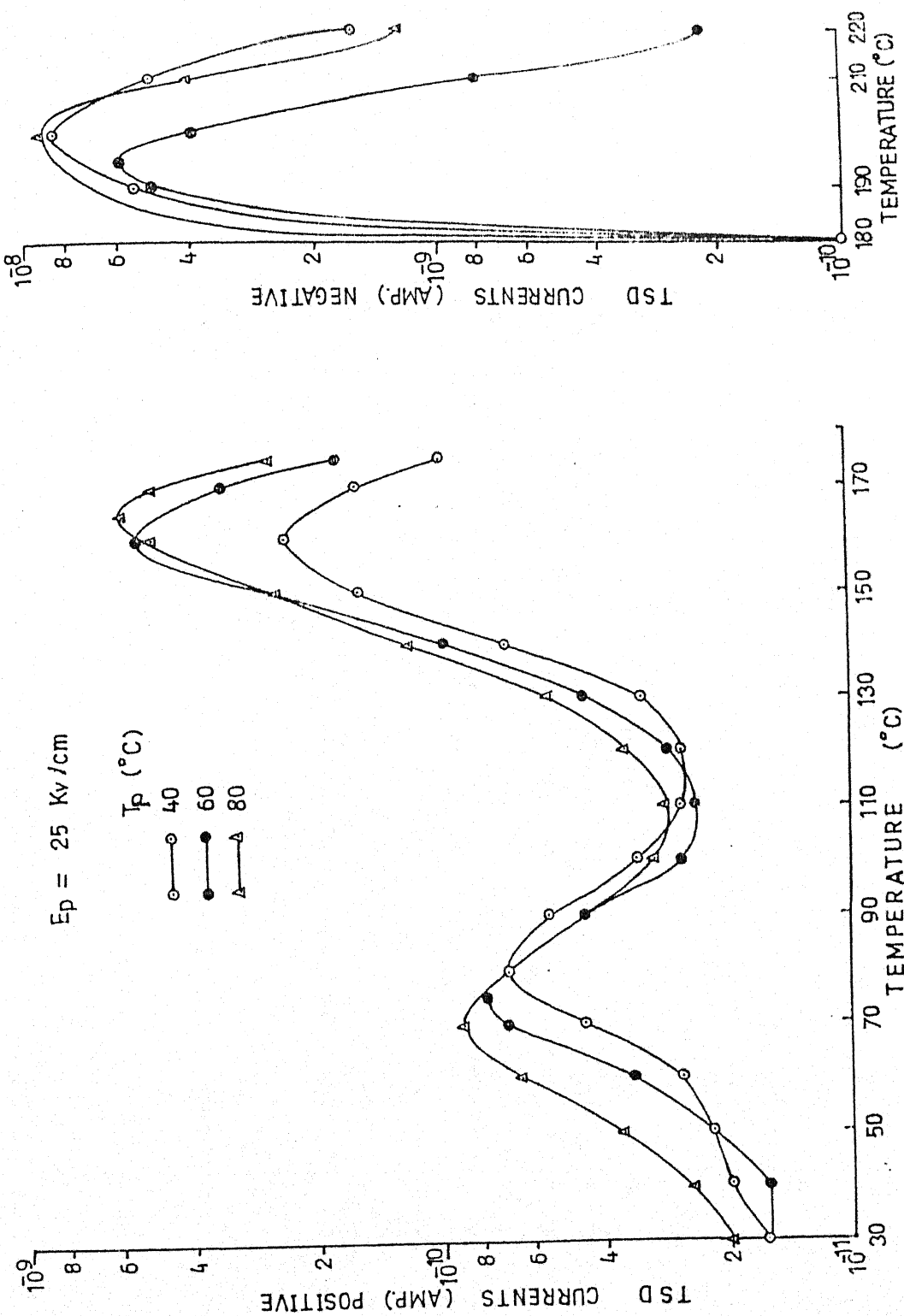


Fig. 4.50 Effect of various polarising temperatures on TSDC thermograms of (20 μm thick) samples for given field with Al-Ag system.

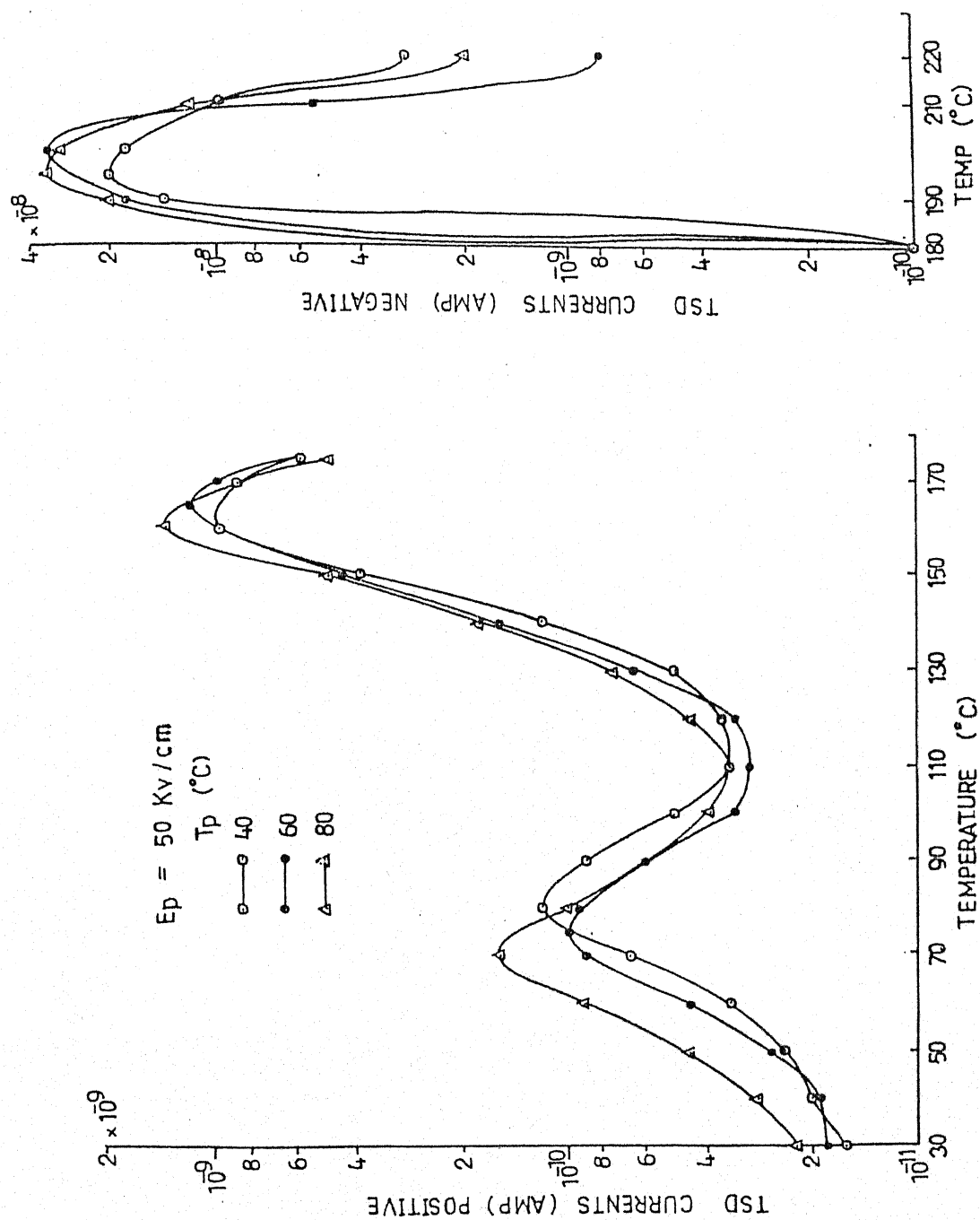


Fig. 4.51 Effect of various polarising temperatures on TSDC thermograms of
 (20 μm thick) samples for given field with Al-Ag system.

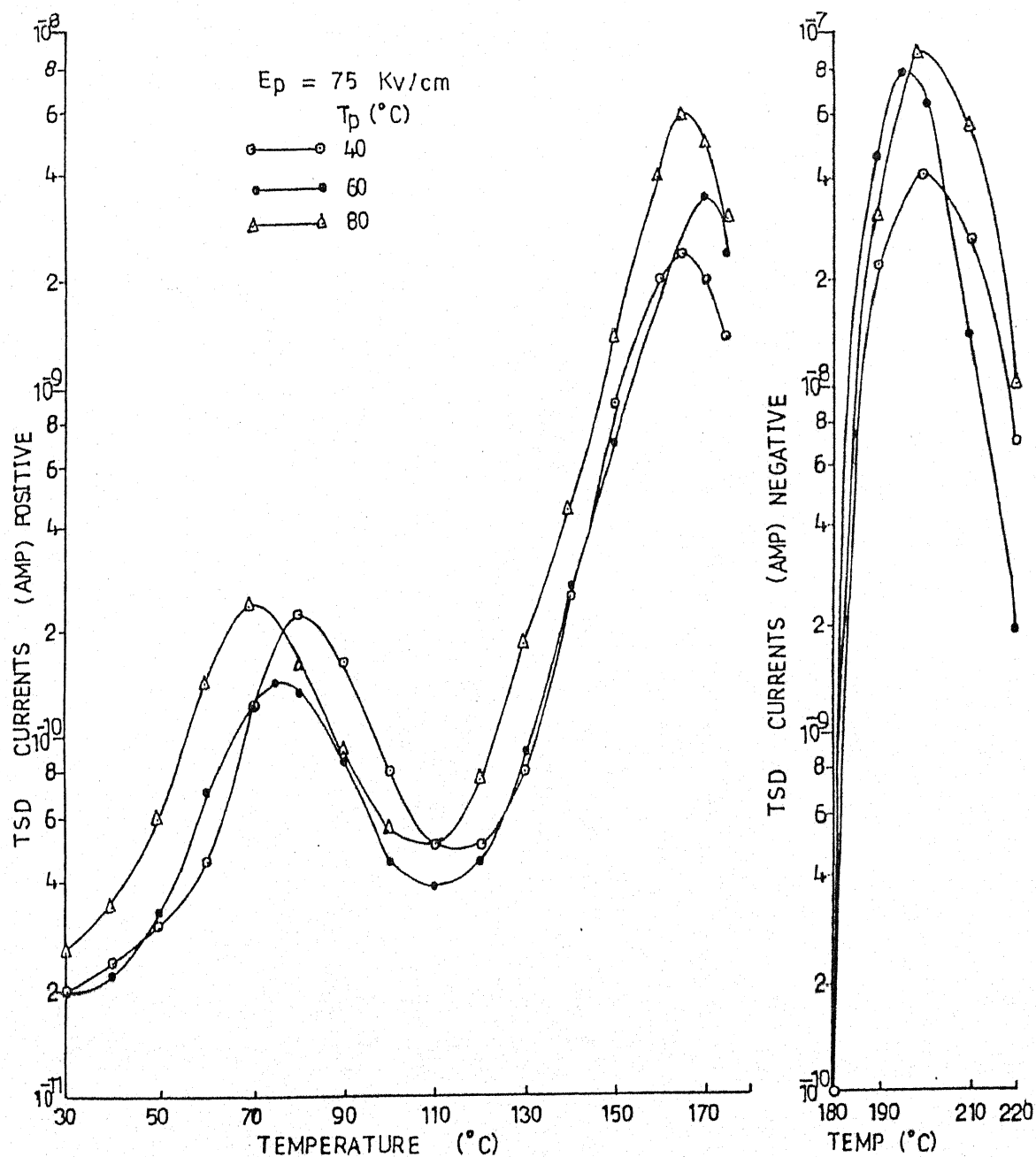


Fig. 4.52 Effect of various polarising temperatures on TSDC thermograms of (20 μm thick) samples for gi field with Al-Ag system.

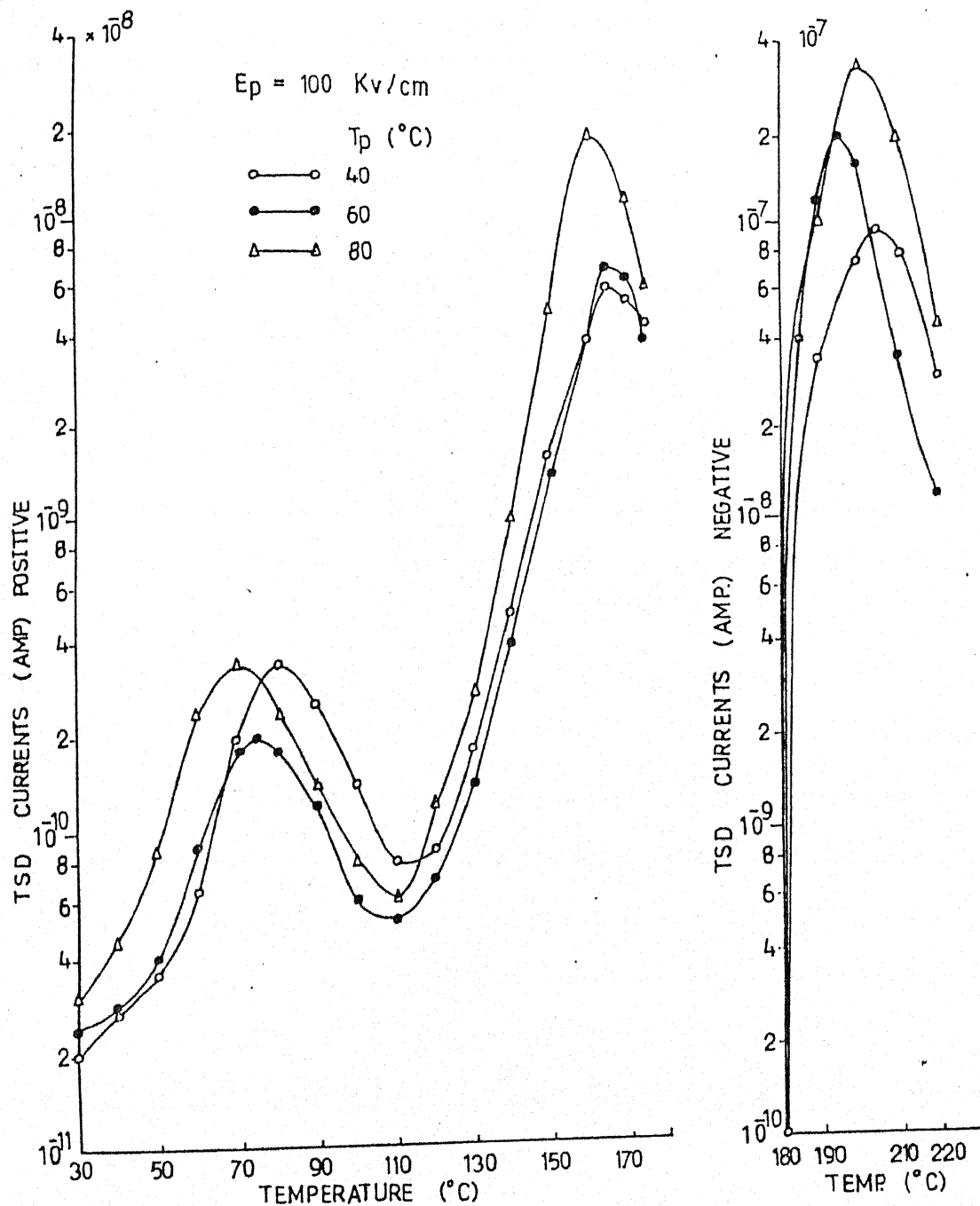


Fig. 4.53 Effect of various polarising temperatures on TSDC thermograms of (20 μm thick) samples for given field with Al-Ag system.

same T_p and E_p as in similar electrode system. In this case also, all the thermograms show three current peaks which occur at temperatures 75 ± 5 , 160 ± 5 , $200 \pm 5^\circ\text{C}$ and designated as α , ρ and ρ' peaks respectively. The nature of three peaks is found to be same as observed in Ag-Ag, Cu-Cu and Sn-Sn systems (Figs. 4.30 to 4.47). For the ρ peak depolarising current is higher than for α peak, while for ρ' peak, depolarising current is further higher than for α and ρ peaks. The height of all the three peaks is found to increase in magnitude with the increase in T_p . A similar type of behaviour is also found for other dissimilar electrode combination, viz. Al-Cu shown in Figs. 4.54 to 4.59. For Al-Sn system, TSDC thermograms are shown in Figs. 4.60 to 4.65 which differ from thermograms of Figs. 4.48 to 4.59 for Al-Ag and Al-Cu system, in the sense that the values of ρ' peak current is here found to be lower in magnitude than that of ρ peak. Other behaviour is similar. The peak current is found to vary almost linearly with the polarising fields (not shown) for similar as well as dissimilar electrode systems.

Figs. 4.66 to 4.72 exhibit the effect of film thickness on TSDC thermograms of PVP foil electrets for different electrode configurations, for samples poled at 60°C by using field of 100 kV/cm. All the curves show decrease in peak current when film thickness is increased and shifts the α peak by $\pm 10^\circ\text{C}$ and ρ peak by $\pm 5^\circ\text{C}$, i.e. shift is more for α peak. The depolarization kinetic data for 5 μm , 25 μm thick film for

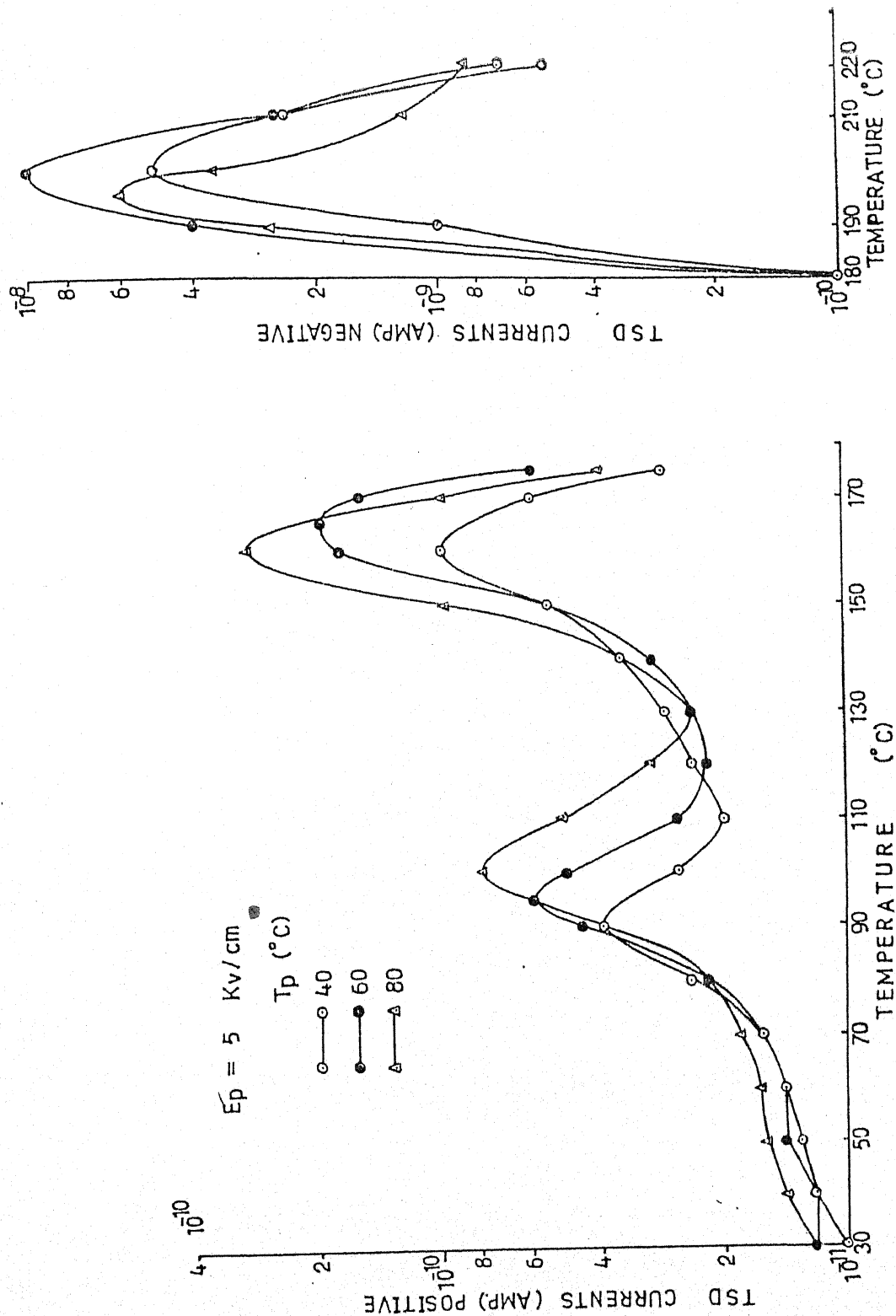


Fig. 4.54 Effect of various polarising temperatures on TSDC thermograms of
 (20 μm thick) samples for given field with Al-Cu system.

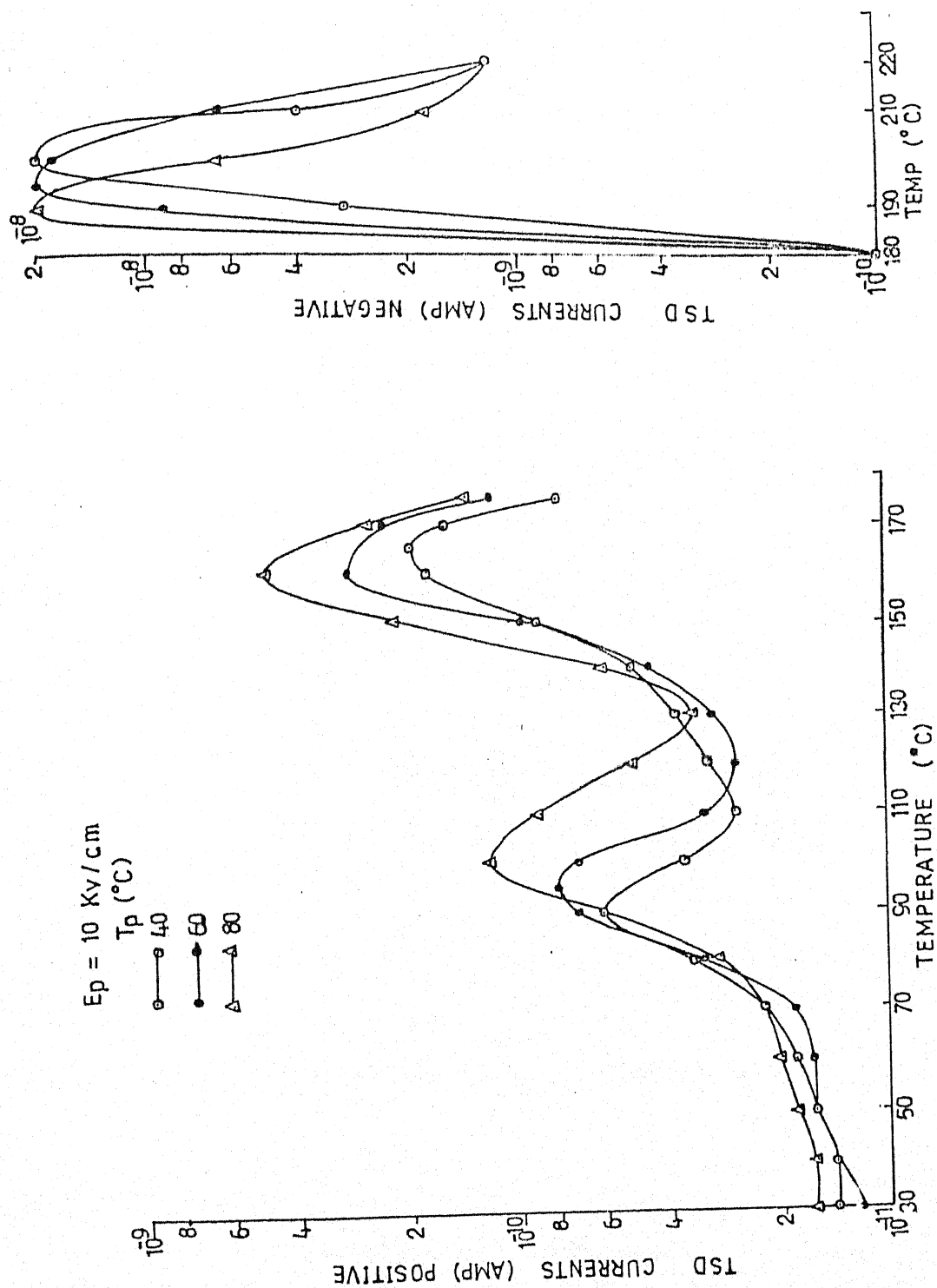


Fig. 4.55 Effect of various polarising temperatures on TSDC thermograms of (20 μm thick) samples for given field with Al-Cu system.

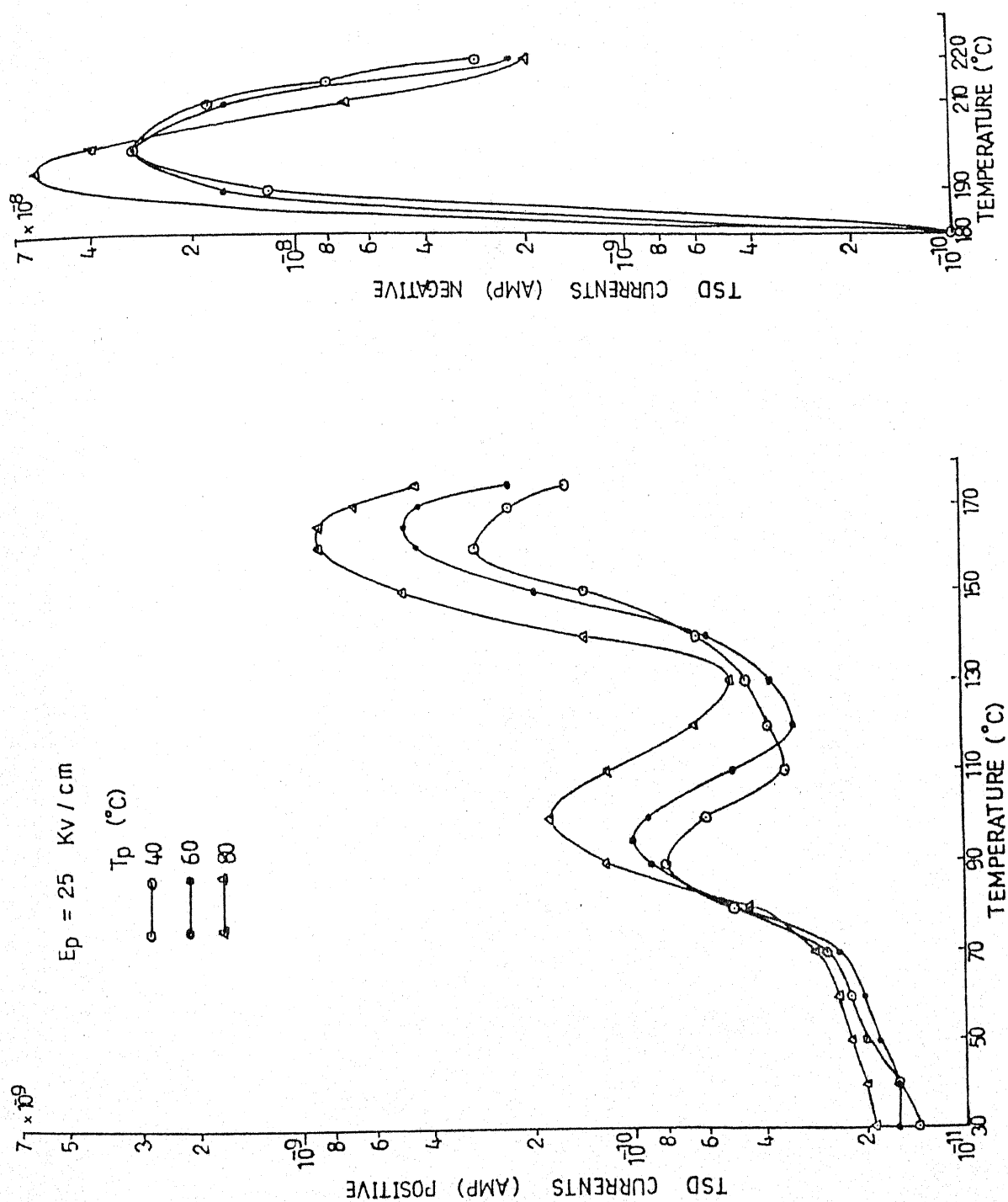


Fig. 4.56 Effect of various polarising temperatures on TSDC thermograms of
 (20 μm thick) samples for given field with Al-Cu system.

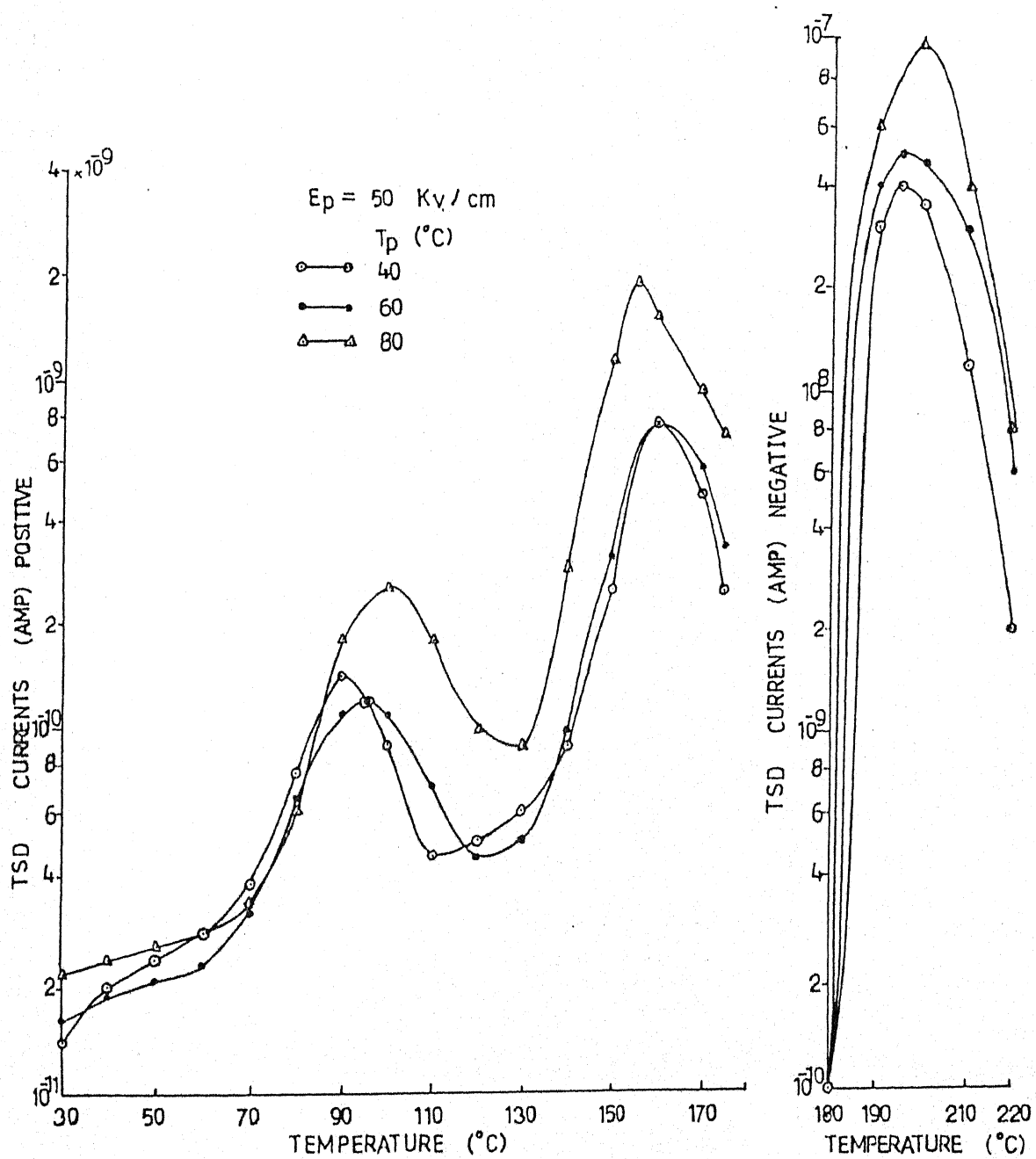


Fig. 4.57 Effect of various polarising temperatures on TSDC thermograms of (20 μm thick) samples for given field with Al-Cu system.

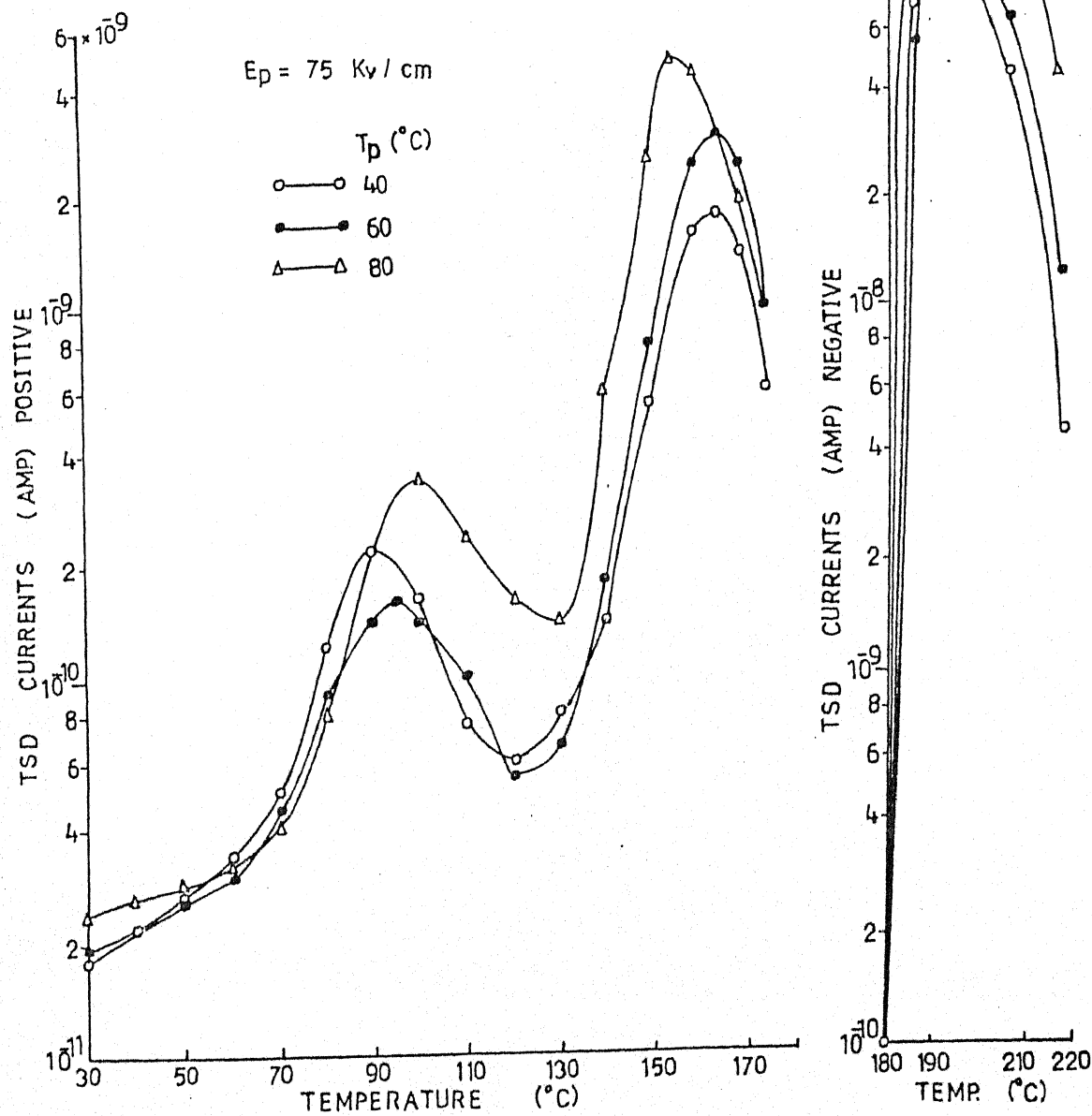


Fig. 4.58 Effect of various polarising temperatures on TSDC thermograms of (20 μ m thick) samples for given field with Al-Cu system.

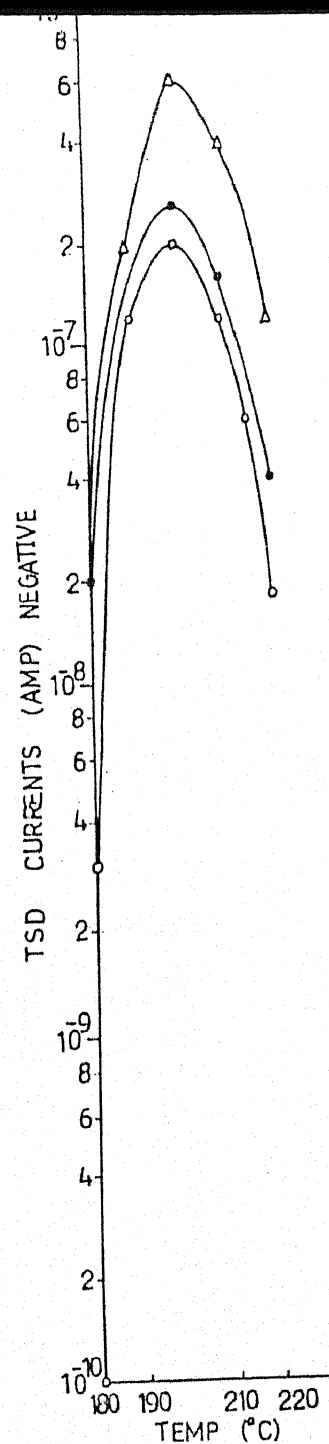
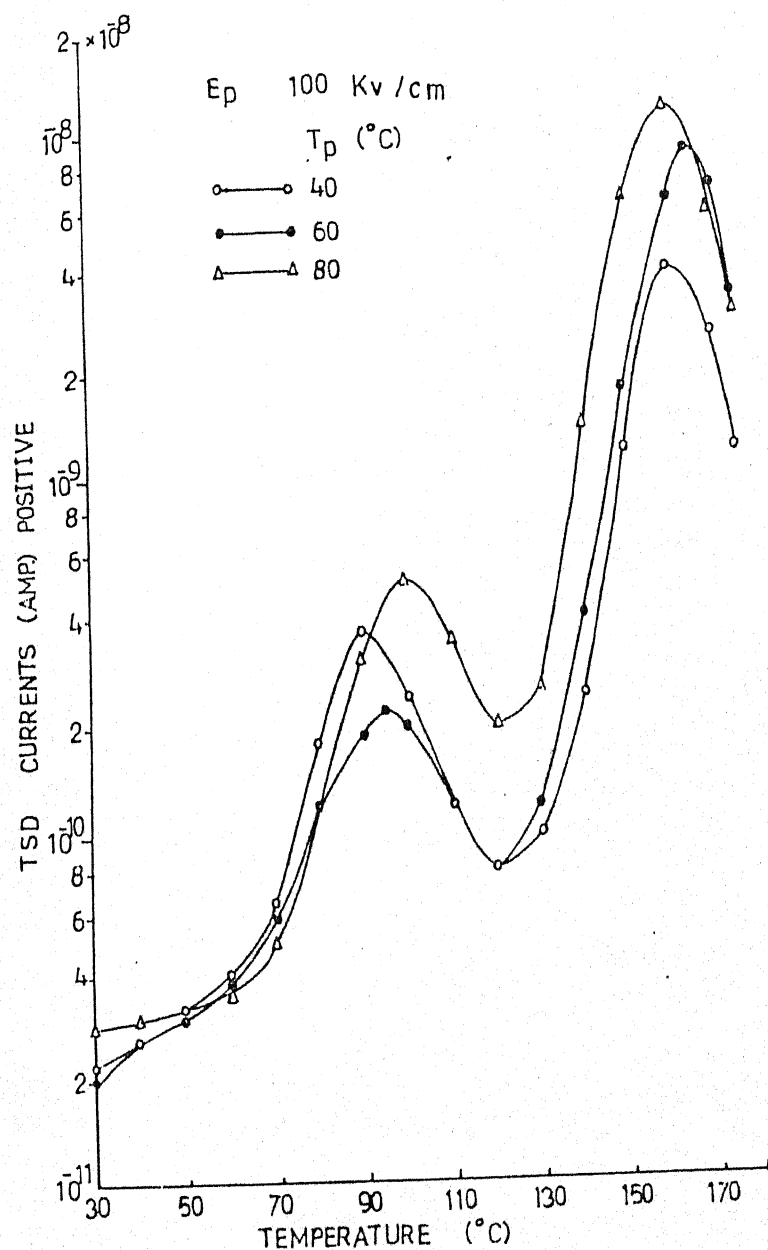


Fig. 4.59 Effect of various polarising temperatures on TSDC thermograms of (20 μm thick) samples for given field with Al-Cu system.

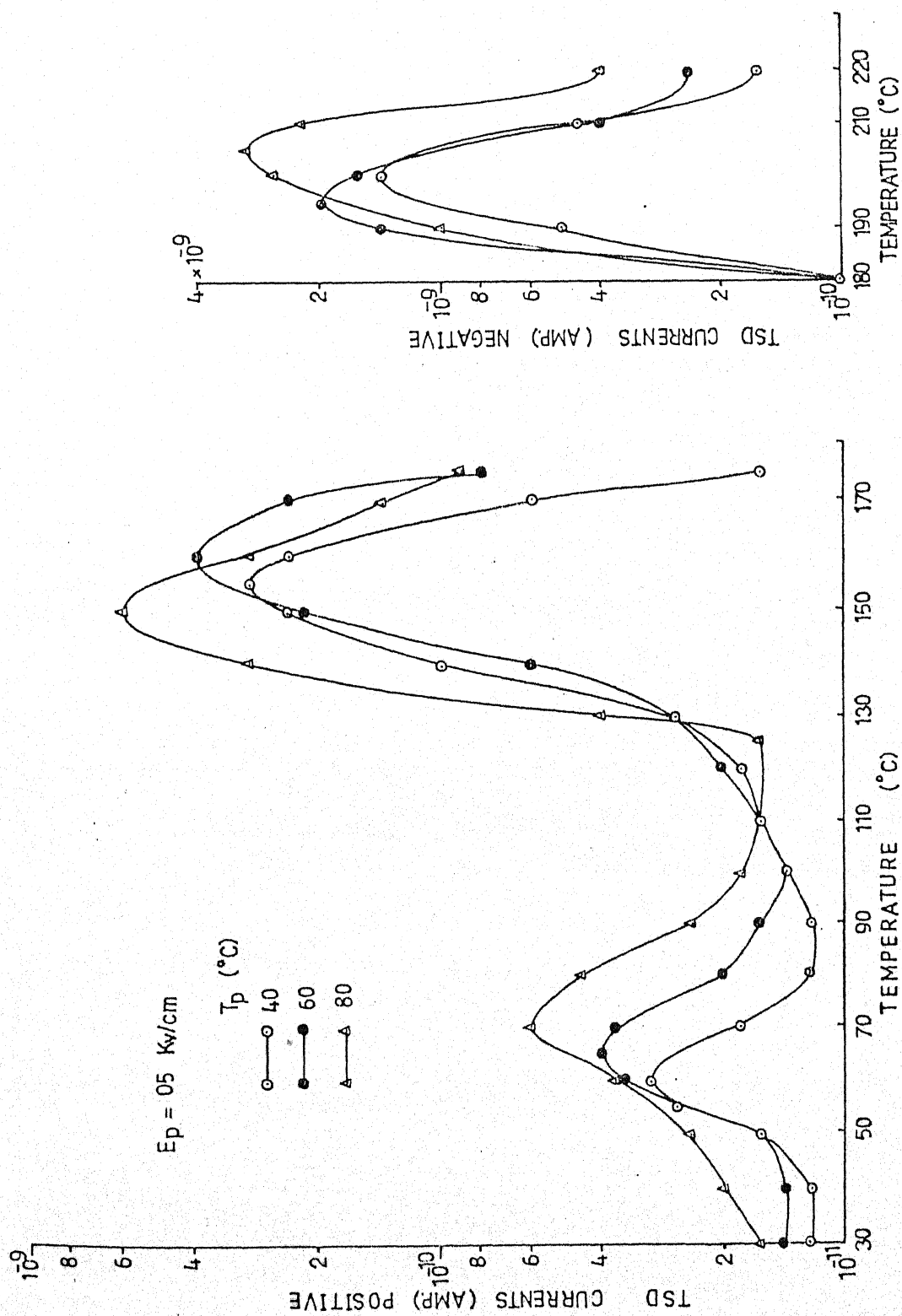


Fig. 4.60 Effect of various polarising temperatures on TSDC thermograms of (20 μm thick) samples for given field with Al-Sn system.

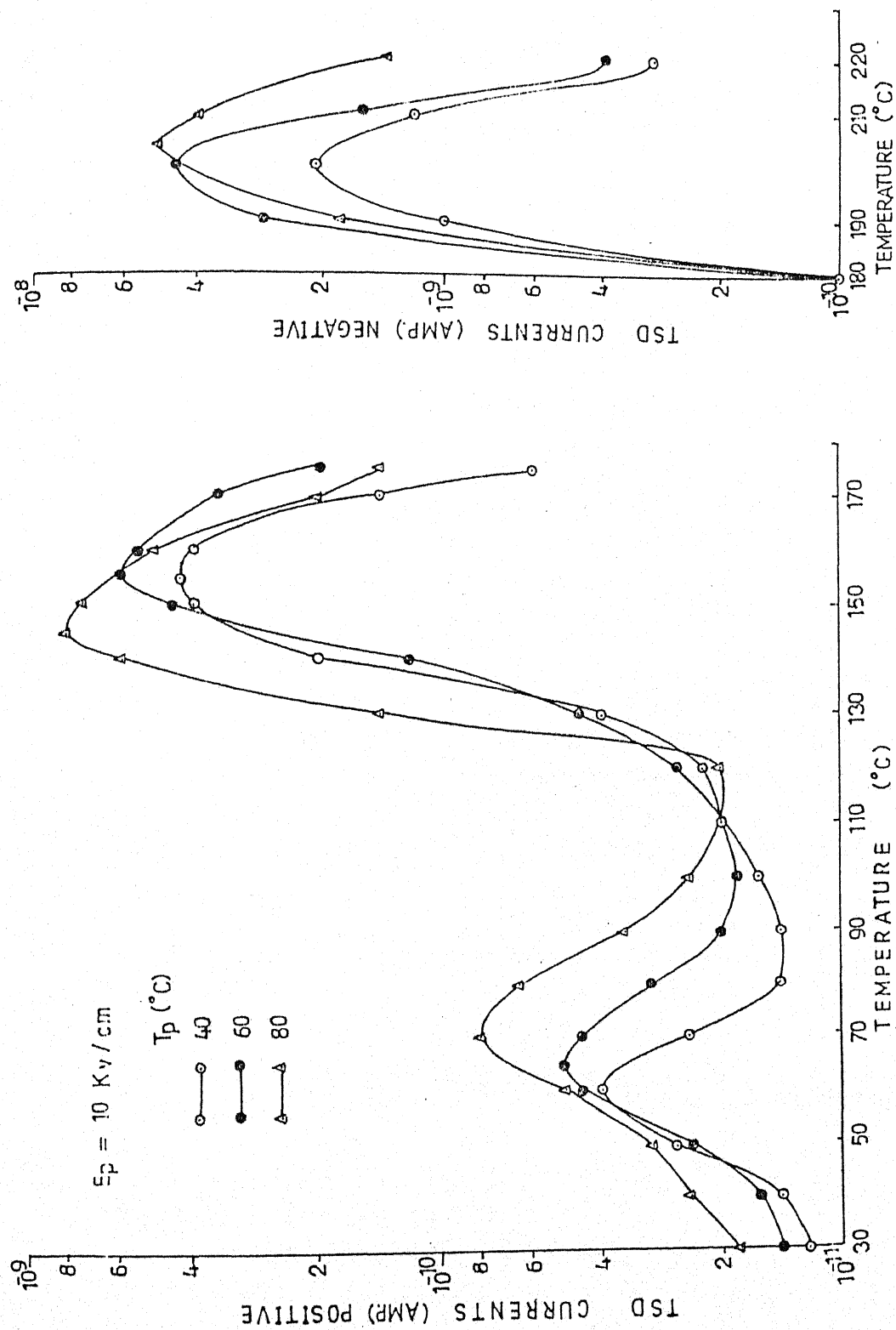


Fig. 4.61 Effect of various polarising temperatures on TSDC thermograms of (20 μm thick) samples for given field with Al-sn system.

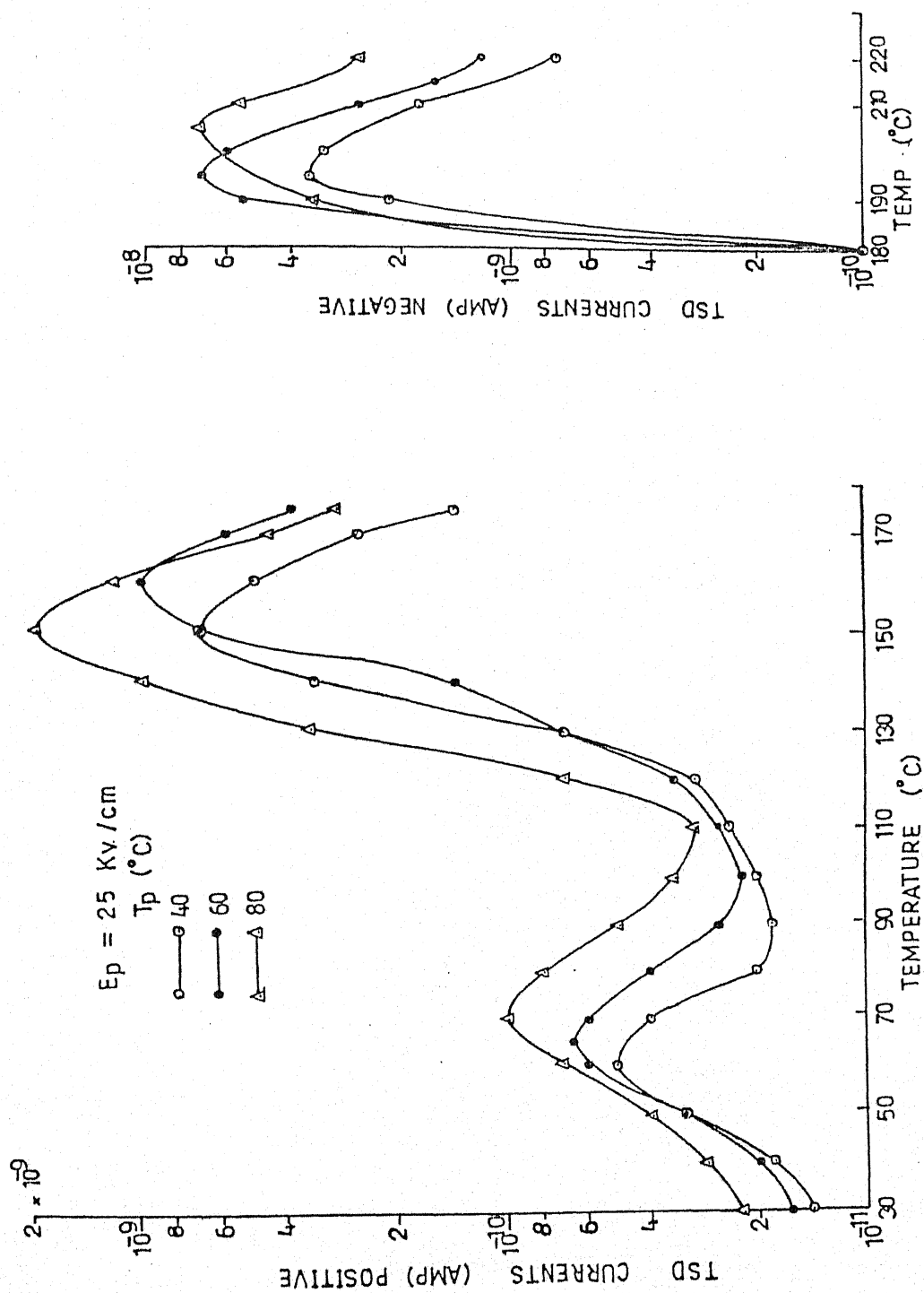


Fig. #.62 Effect of various polarising temperatures on TSDC thermograms of
 (20 μm thick) samples for given field with Al-Sn system.

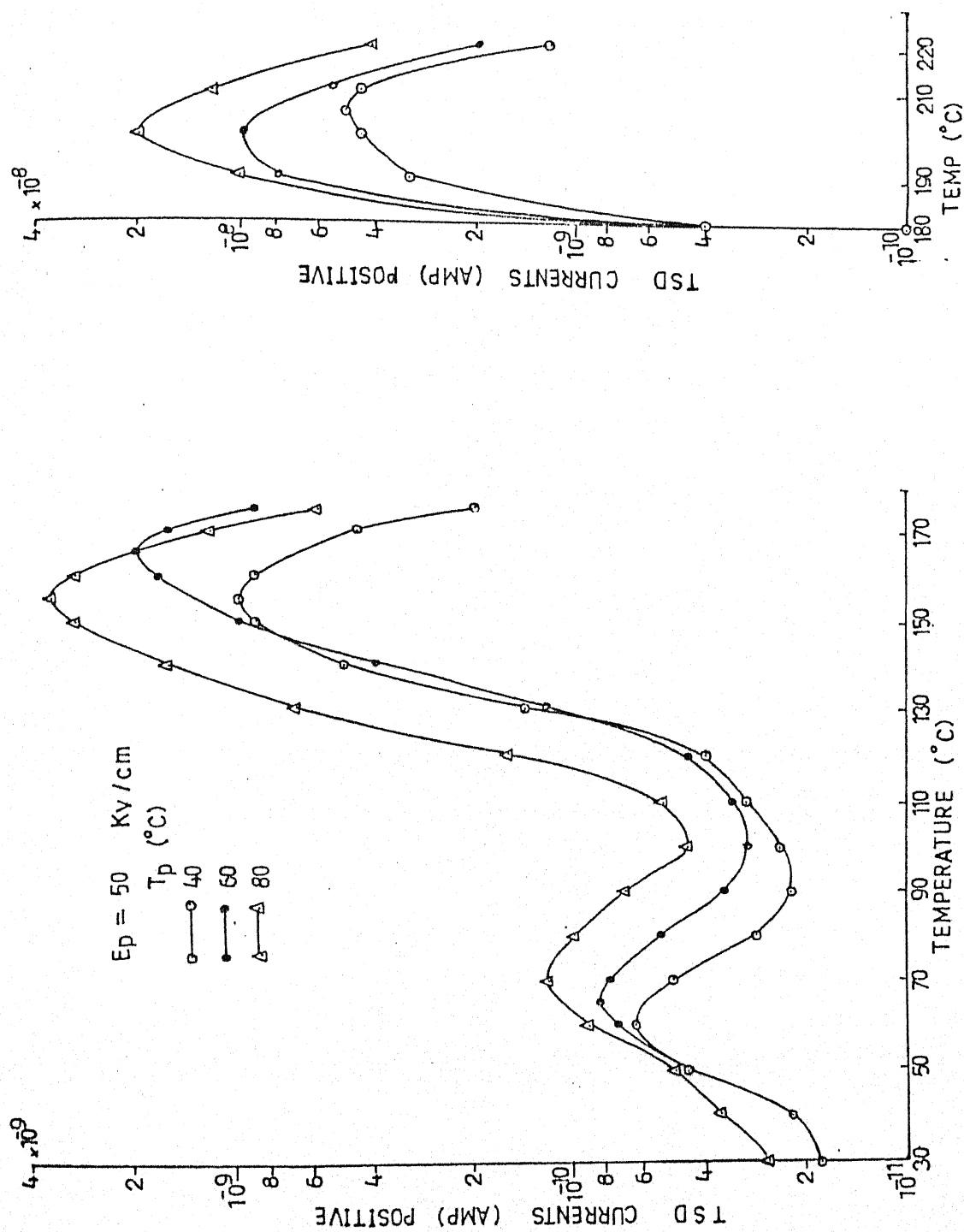


Fig. 4.63 Effect of various polarising temperatures on TSDC thermograms of (20 μm thick) samples for given field with Al-Sn system.

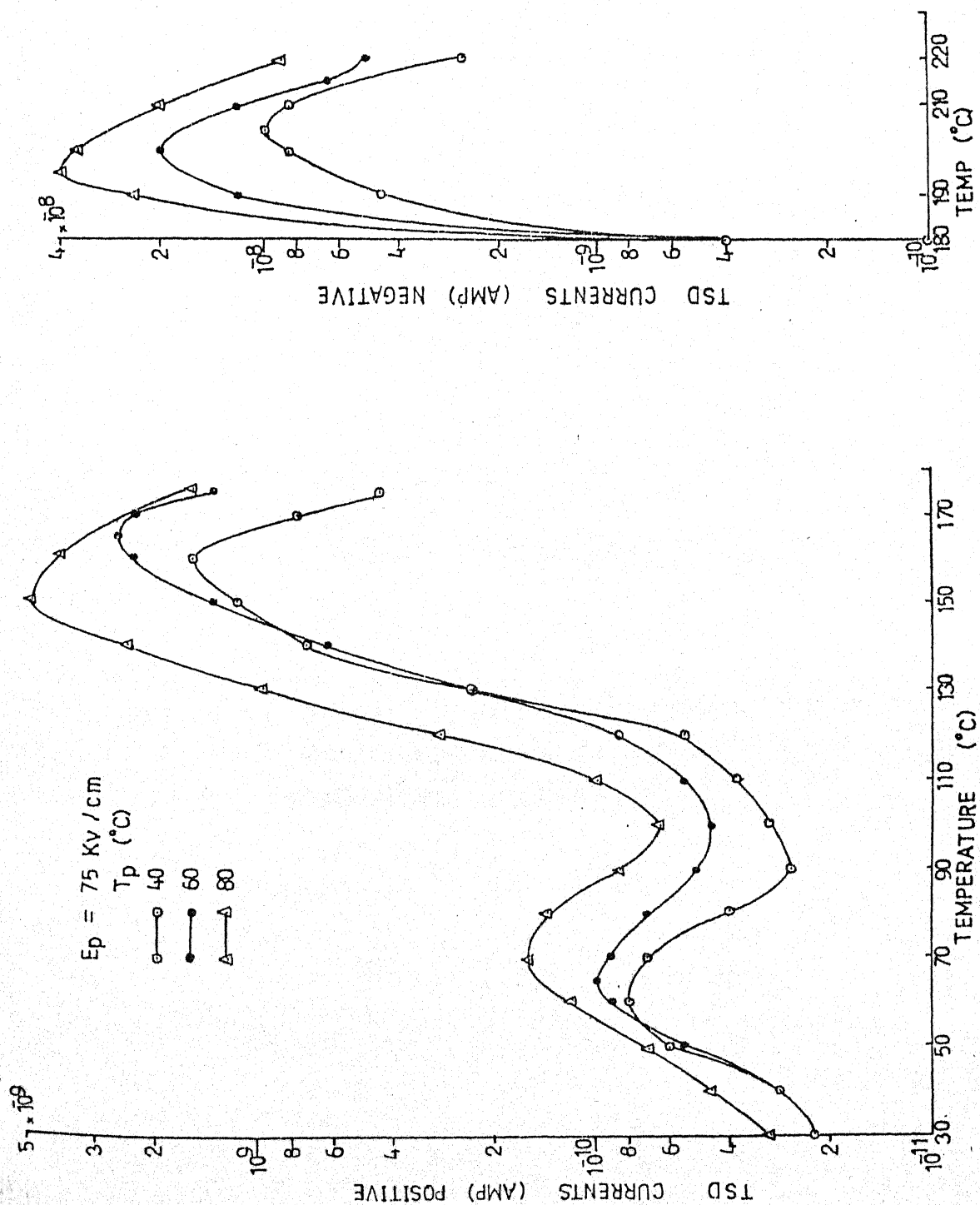


Fig. 4.64 Effect of various polarising temperatures on TSDC thermograms of (20 μm thick) samples for given field with Al-Sn system.

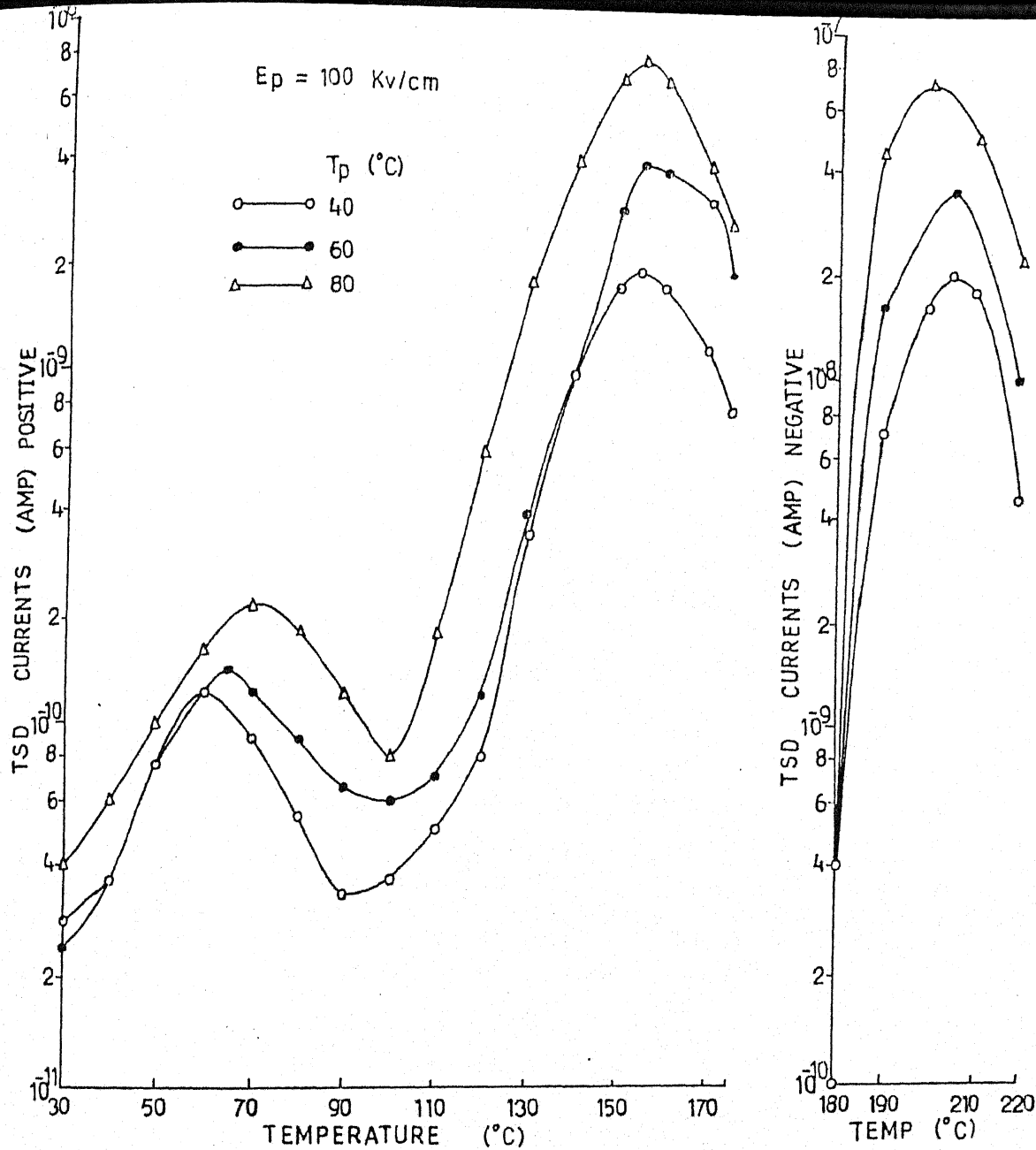


Fig. 4.65 Effect of various polarising temperatures on TSDC thermograms of (20 μm thick) samples for given field with Al-Sn system.

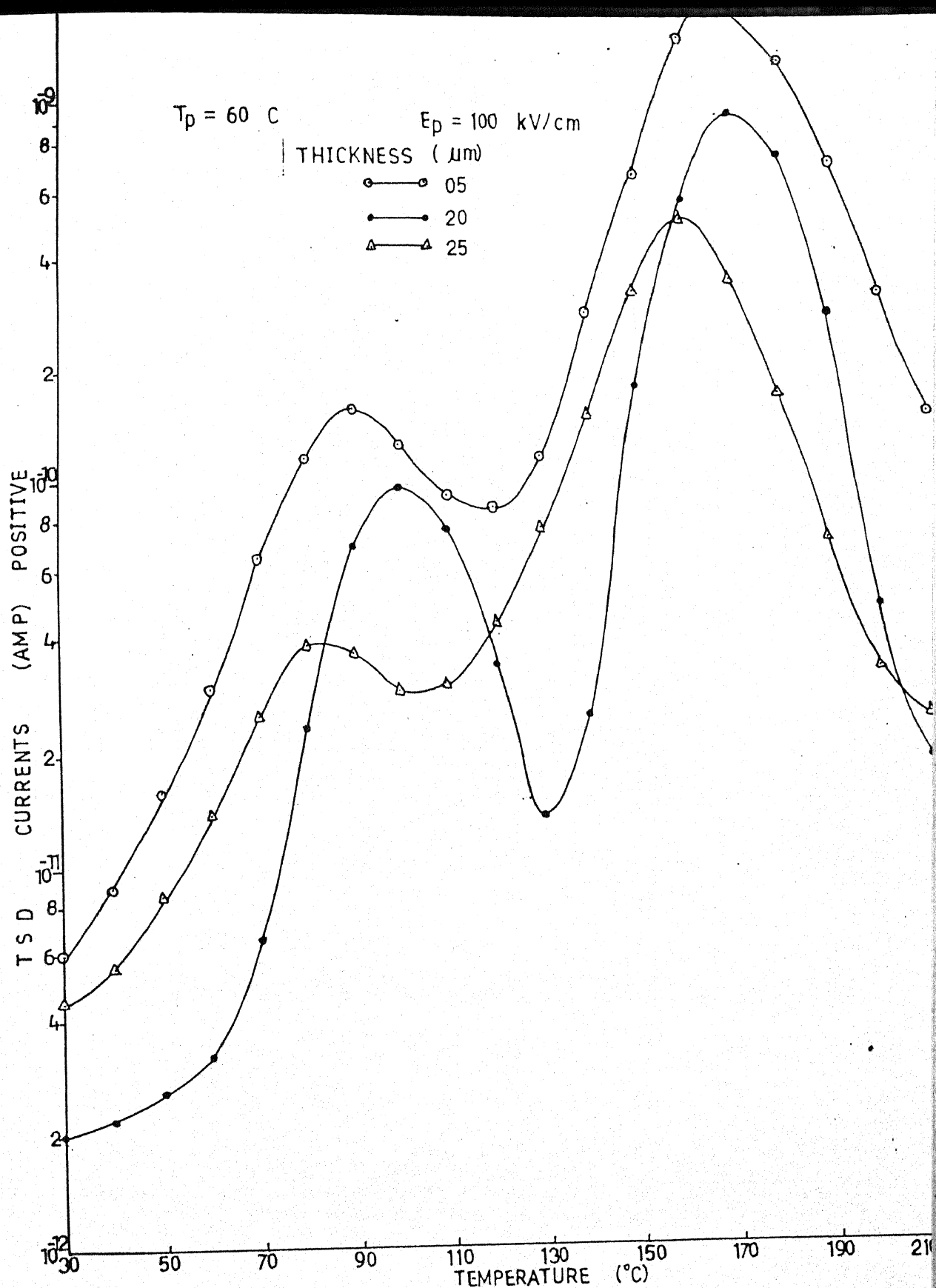


Fig : 4.66 : Effect of film thickness on TSDC thermograms of the samples poled at the given temperature and field with Al-Al system

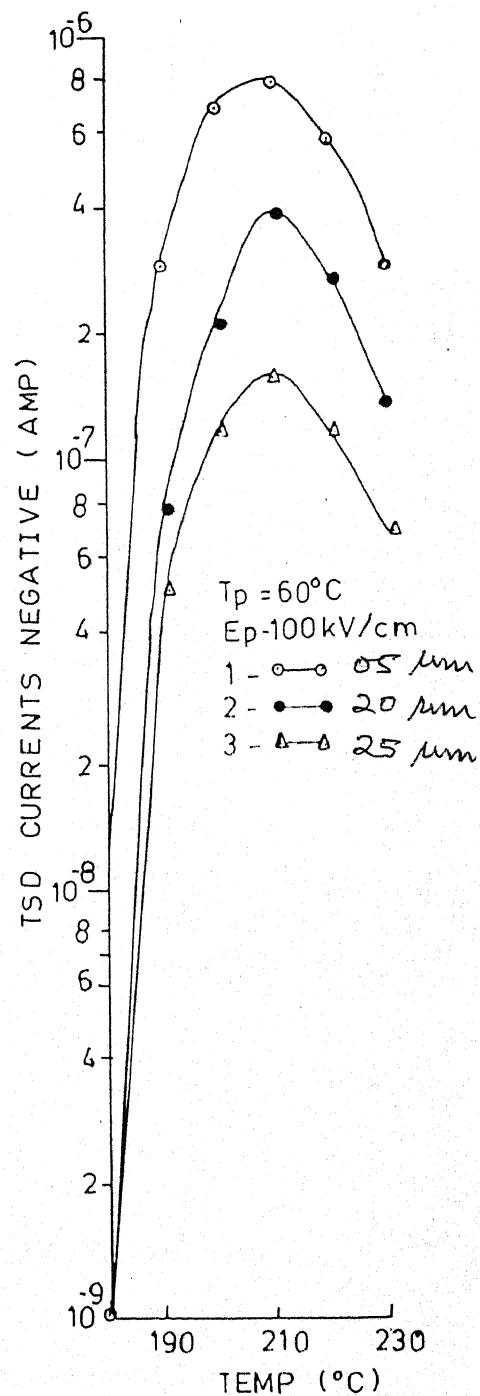
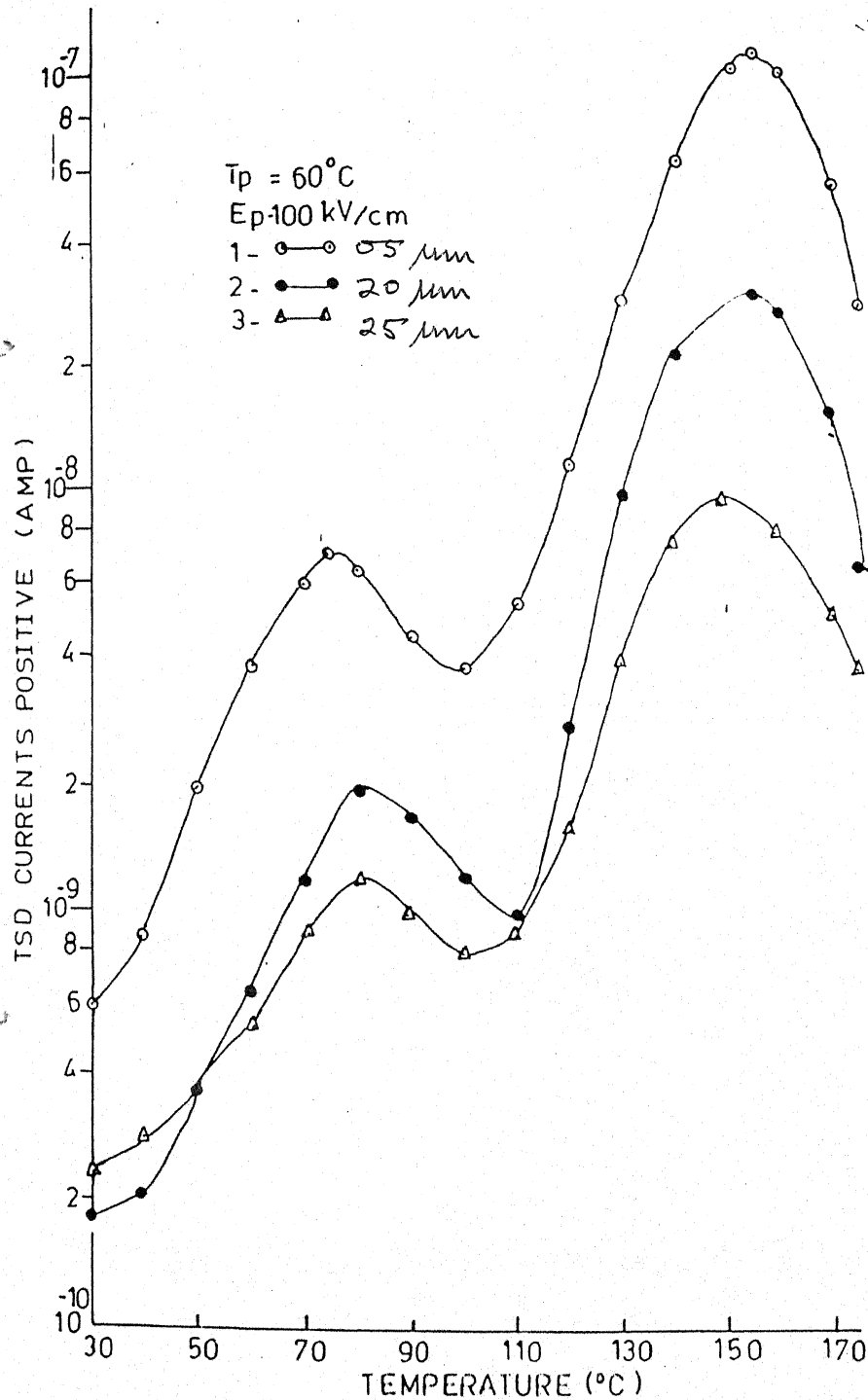


Fig. 4.67 Effect of film thickness on TSDC thermograms of the samples poled at given temperature and field with Ag-Ag System.

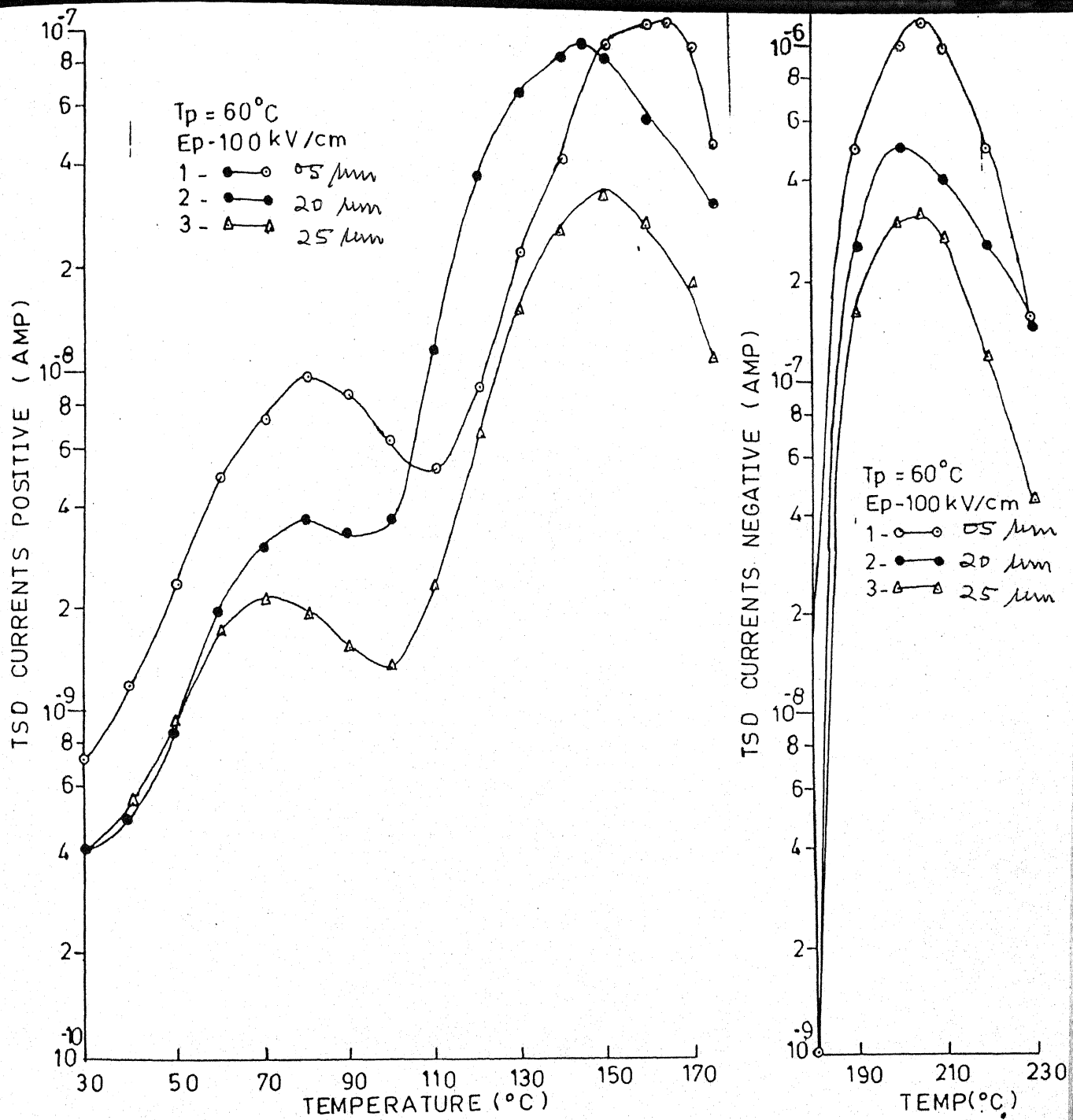


Fig.4.68 Effect of film thickness on TSDC thermograms of the samples poled at given temperature field with Cu-Cu System.

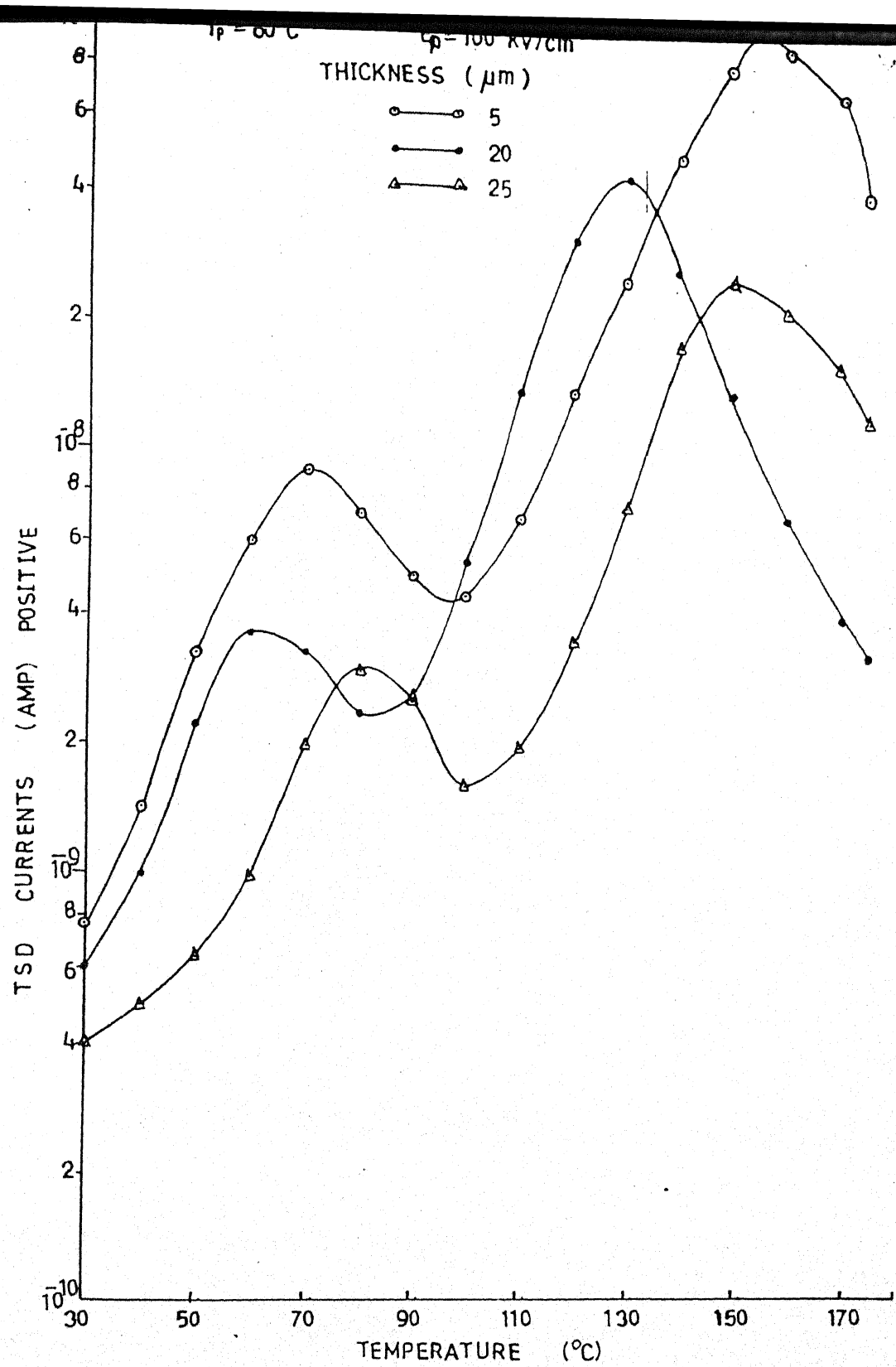


Fig 4.69 : Effect of film thickness on TSDC thermograms of the samples poled at the given temperature and field with Sn-Sn system

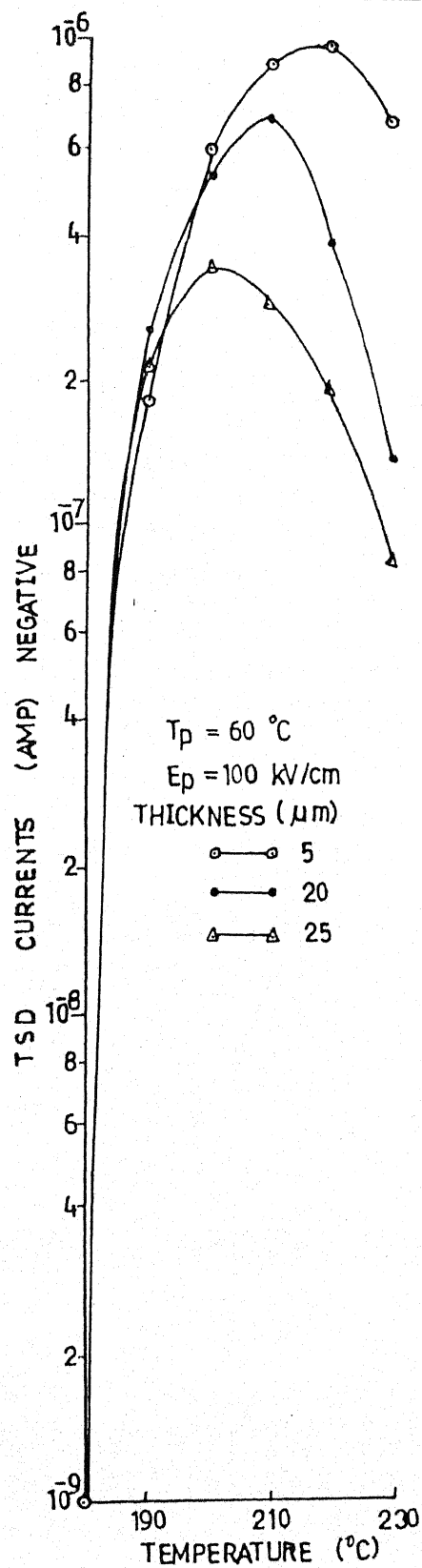


Fig 4.69 : Effect of film thickness on TSDC thermograms of the samples poled at the given temperature and field with Sn-Sn system (remaining part)

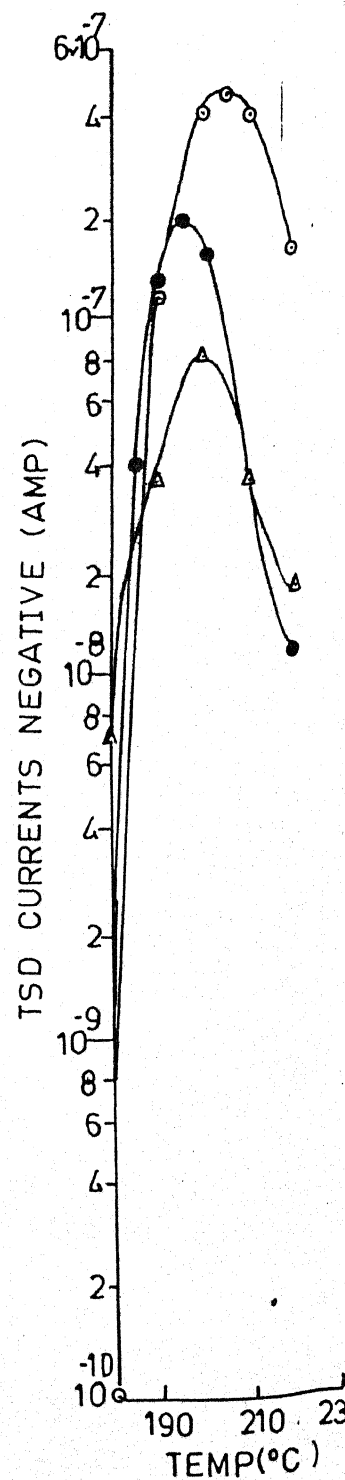
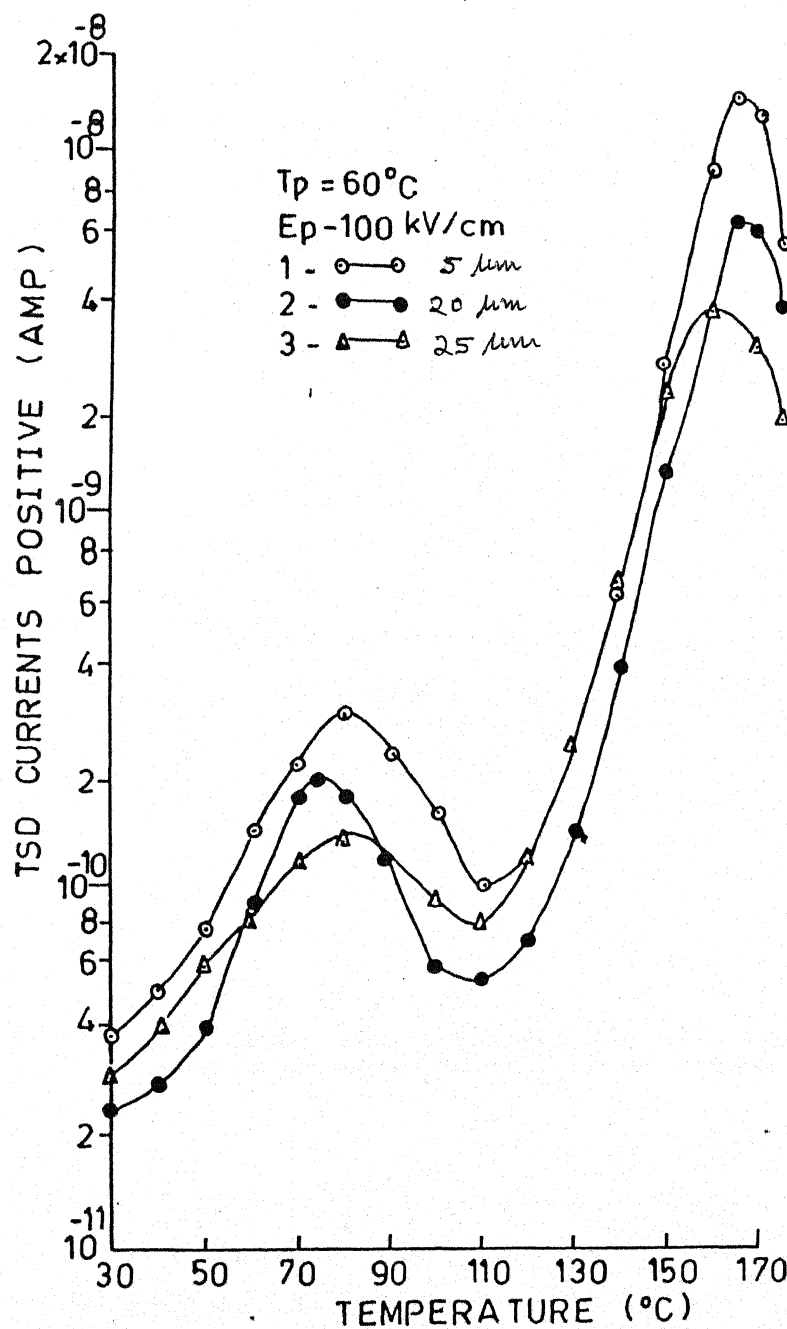


Fig.4.70 Effect of film thickness on TSDC thermograms of the samples poled at given temperature field with Al-Ag System.

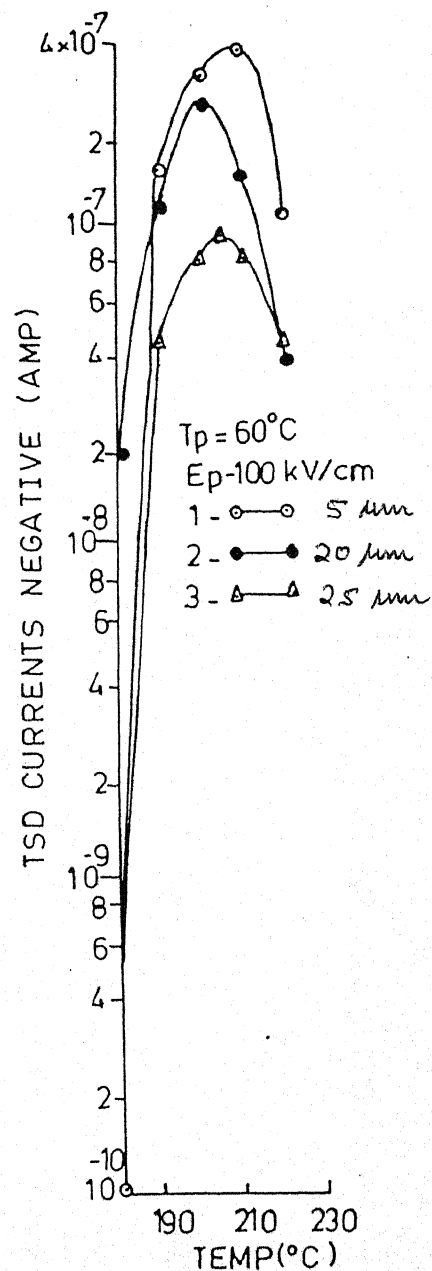
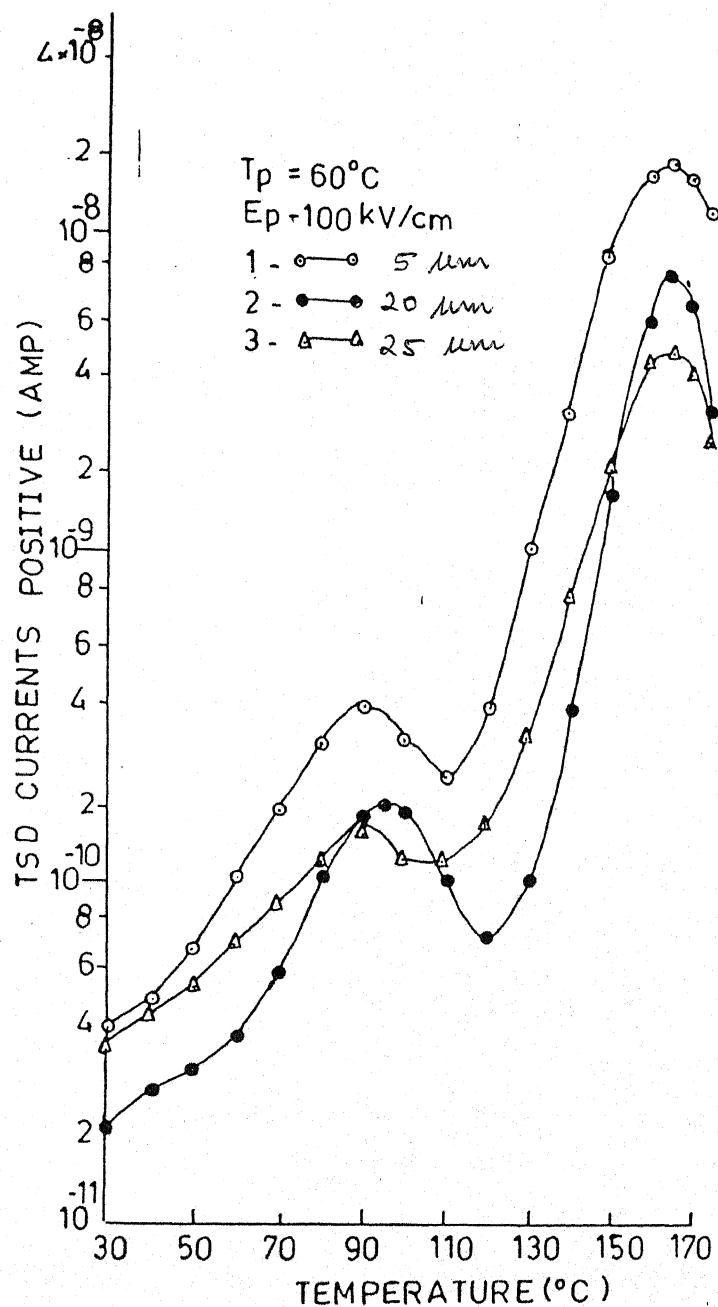


Fig.4.71 Effect of film thickness on TSDC thermograms of the samples poled at given temperature and field with Al-Cu System.

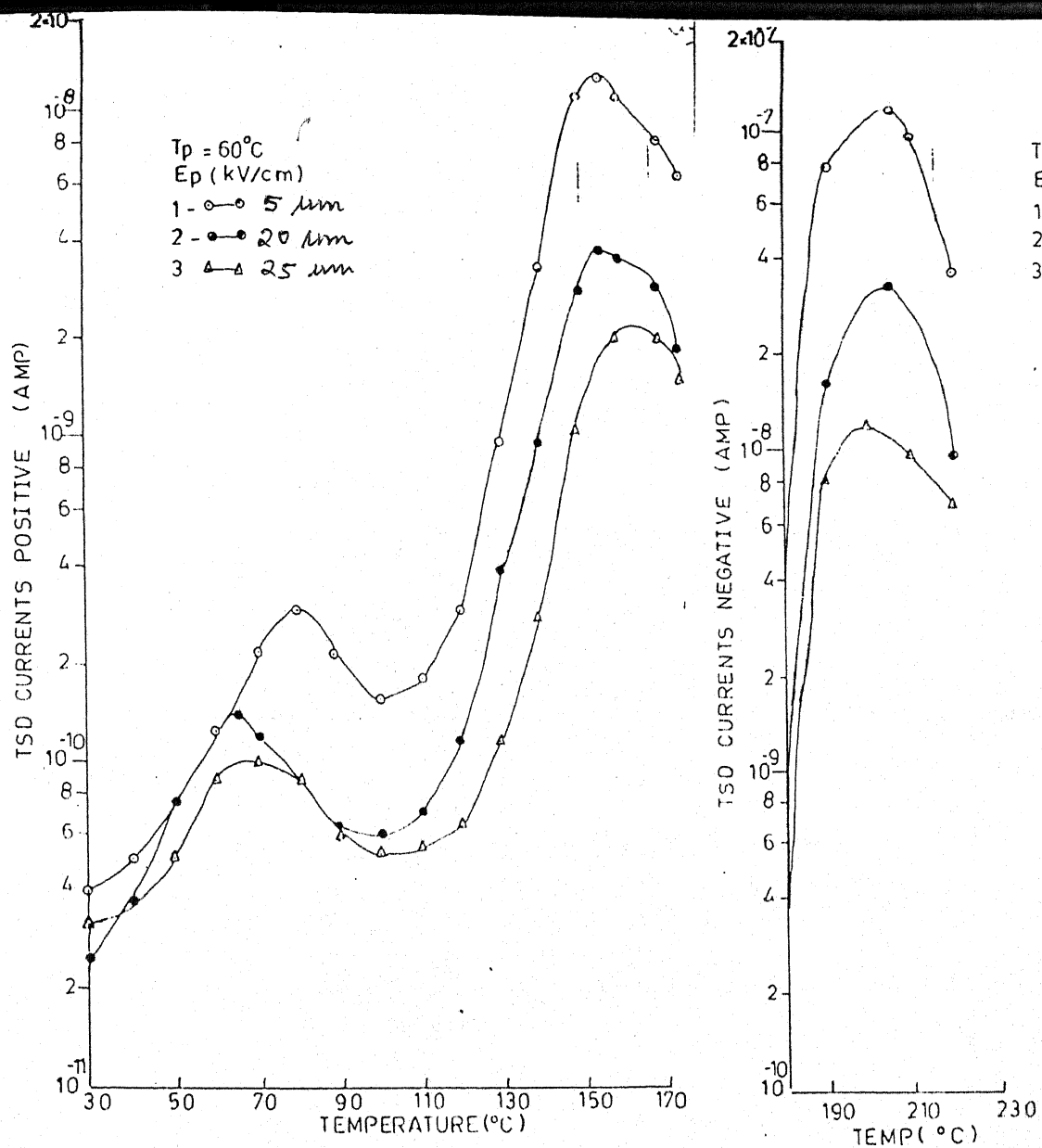


Fig.4.72 Effect of film thickness on TSDC thermograms of the samples poled at given temperature and field with Al-Sn System.

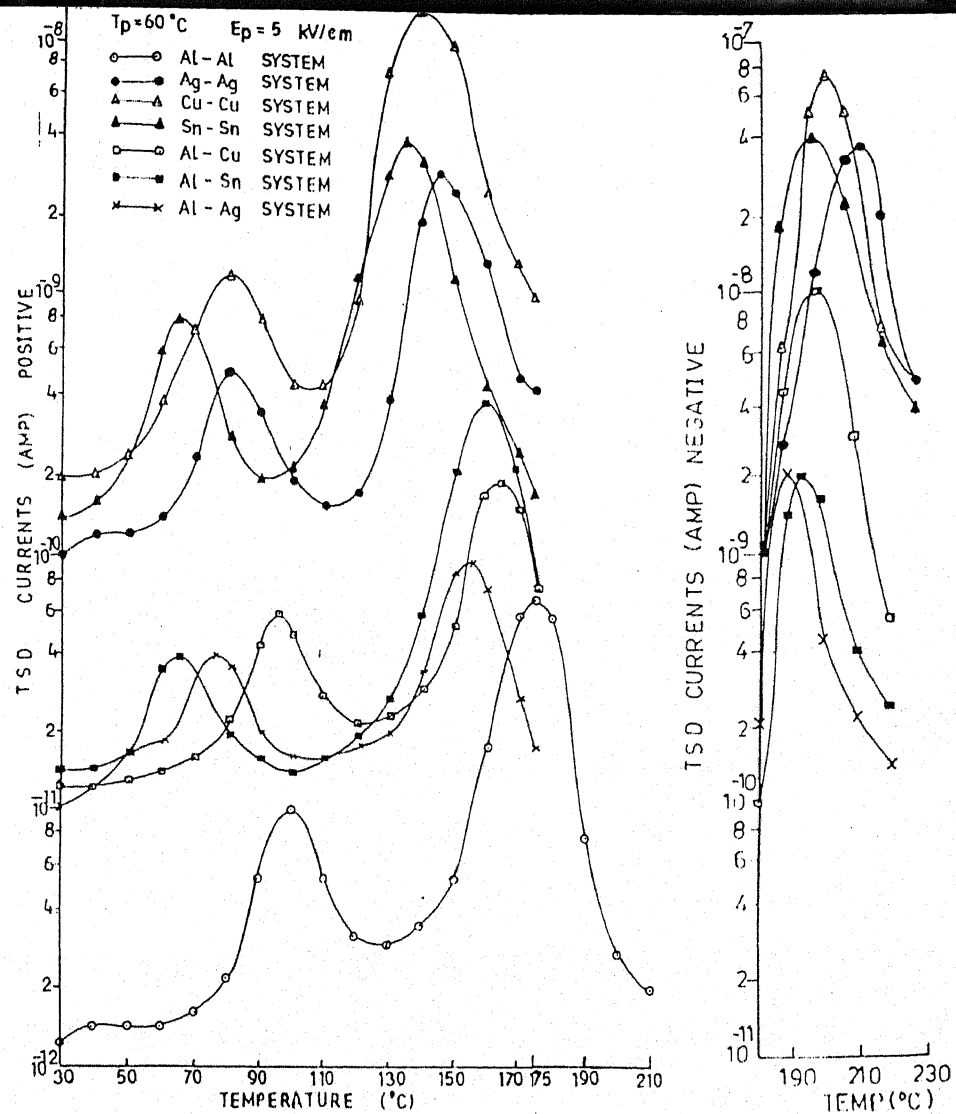


Fig.4.73 Effect of different electrode material. on TSDC thermograms of samples poled at 60°C by field of 5 kV/cm

samples poled at 60°C by 100 kV/cm field are shown in Tables 4.24 to 4.37 for various electrode configurations.

To see the effect of the nature of different metal electrodes used for polarisation on TSDC thermograms, samples are prepared under identical conditions, poled at 60°C by using field of 5 kV/cm and using different metals like Al, Sn, Ag and Cu for which work functions are 3.38 eV, 4.09 eV, 4.31 eV and 4.46 eV respectively. The TSDC thermograms are shown in Fig. 4.73. The curve reveals that maximum polarisation in PVP foil electrets can be brought about by contacting the film with Cu-Cu configuration whereas, minimum polarisation is found for Al-Al system. Intermediate polarisation can be obtained to PVP foil electrets by forming the samples, with dissimilar electrode combinations. Another point to be noticed is that α and ρ peak shift towards the lower temperature, as the work function of the electrode material is increased. Shift in peak temperature with work function is more for ρ peak than α peak. However, the shape of all curves is identical. The values of E_a , I_m , T_m and Q for different electrode series, are given in Tables 4.1 to 4.23.

The electrification of the polymers takes place due to one or more than one of the following mechanisms operative simultaneously when it is subjected to dynamical, mechanical or thermal treatment with or without static electric fields -

Table 4.24 : Depolarization kinetic data for PVP samples poled at 60°C with various polarizing fields. Sample thickness 05 μm . Al-Al system.

Polarizing Field	α -peak						ρ -peak			
	Peak current (Amp)	Peak Temp. (°C)	Activation Energy (eV)	Relaxation time sec (τ_0)	Charge Released Coul. (Q)	Peak current (Amp)	Peak Temp. (°C)	Activation Energy (eV)	Relaxation time sec (τ_0)	Charge Released Coul. (Q)
(Ep)										
05	2.0×10^{-11}	90	0.265	6.5×10^4	3.78×10^{-9}	1.2×10^{-10}	170	0.254	7.5×10^6	6.7×10^{-8}
10	3.0×10^{-11}	90	0.267	6.8×10^5	4.65×10^{-9}	2.0×10^{-10}	165	0.256	6.5×10^5	7.6×10^{-8}
25	5.0×10^{-11}	90	0.269	7.26×10^4	5.46×10^{-9}	3.5×10^{-10}	170	0.245	7.8×10^4	8.4×10^{-8}
50	7.0×10^{-11}	90	0.270	9.33×10^6	6.77×10^{-9}	7.0×10^{-10}	165	0.253	6.93×10^5	9.8×10^{-8}
75	9.0×10^{-11}	90	0.272	4.62×10^6	8.77×10^{-9}	1.2×10^{-8}	170	0.257	7.78×10^6	1.4×10^{-7}
100	1.6×10^{-10}	90	0.271	7.52×10^4	9.6×10^{-9}	2.0×10^{-8}	165	0.259	8.47×10^5	3.7×10^{-7}

Table 4.25 : Depolarization kinetic data for PVP samples poled at 60°C with various polarizing fields. Sample thickness 05 μm . Al-Cu system.

Polarizing Field	α -peak					ρ -peak					ρ' -peak				
	Peak current (Amp)	Peak Temp. (°C)	Activation Energy (eV)	Relaxation time Sec (τ_0)	Charge Released Coul. (Q)	Peak current (Amp)	Peak Temp. (°C)	Activation Energy (eV)	Relaxation time Sec (τ_0)	Charge Released Coul. (Q)	Peak current (Amp)	Peak Temp. (°C)	Activation Energy (eV)	Relaxation time Sec (τ_0)	Charge Released Coul. (Q)
(Ep)															
05	8.0×10^{-11}	90	0.267	7.8×10^5	4.45×10^{-9}	3.0×10^{-10}	160	0.665	2.27×10^7	7.7×10^{-8}	2.0×10^{-8}	200	0.985	4.7×10^5	6.62×10^{-8}
10	1.2×10^{-10}	90	0.271	8.4×10^5	4.98×10^{-9}	4.5×10^{-10}	155	0.669	3.34×10^6	8.7×10^{-8}	3.5×10^{-8}	205	0.988	8.6×10^6	7.82×10^{-8}
25	1.6×10^{-10}	90	0.272	9.6×10^4	6.0×10^{-9}	2.2×10^{-9}	160	0.667	4.27×10^5	9.7×10^{-8}	7.0×10^{-8}	205	0.987	5.4×10^7	9.89×10^{-8}
50	2.2×10^{-10}	90	0.274	3.34×10^6	7.4×10^{-9}	3.0×10^{-9}	155	0.665	6.63×10^6	1.6×10^{-7}	1.4×10^{-7}	200	0.986	6.4×10^6	1.46×10^{-7}
75	3.2×10^{-10}	90	0.275	7.56×10^7	8.0×10^{-8}	1.4×10^{-8}	165	0.662	8.2×10^6	7.6×10^{-7}	2.4×10^{-7}	200	0.985	7.4×10^7	2.36×10^{-7}
100	4.0×10^{-10}	90	0.274	8.44×10^6	1.6×10^{-8}	2.0×10^{-8}	165	0.663	5.6×10^5	9.4×10^{-7}	4.0×10^{-7}	200	0.977	8.4×10^6	2.98×10^{-7}

Table 4.26 : Depolarization kinetic data for PVP samples poled at 60°C with various polarizing fields. Sample thickness 25 μm . Al-Al system.

Polarizing Field	α -peak					ρ -peak				
	Peak current (Amp)	Peak Temp. ($^{\circ}\text{C}$)	Activation Energy (eV)	Relaxation time sec (τ_0)	Charge Released Coul. (Q)	Peak current (Amp)	Peak Temp. ($^{\circ}\text{C}$)	Activation Energy (eV)	Relaxation time sec (τ_0)	Charge Released Coul. (Q)
05	7.0×10^{-12}	85	0.275	5.4×10^5	6.88×10^{-9}	5.0×10^{-11}	180	0.641	4.8×10^8	7.6×10^{-9}
10	9.0×10^{-12}	85	0.272	6.78×10^4	8.78×10^{-9}	7.0×10^{-11}	155	0.645	5.7×10^7	8.4×10^{-9}
25	1.2×10^{-11}	85	0.273	9.85×10^6	9.6×10^{-9}	9.5×10^{-11}	160	0.648	7.6×10^6	1.24×10^{-8}
50	2.0×10^{-11}	85	0.274	7.88×10^3	3.45×10^{-8}	1.6×10^{-10}	155	0.646	8.7×10^5	4.48×10^{-8}
75	3.0×10^{-11}	85	0.276	8.54×10^4	7.78×10^{-8}	3.0×10^{-10}	160	0.647	6.4×10^6	8.76×10^{-8}
100	4.0×10^{-11}	85	0.278	8.59×10^6	8.43×10^{-8}	5.5×10^{-10}	160	0.657	9.6×10^4	9.87×10^{-8}

Table 4.27 : Depolarization kinetic data for PVP samples poled at 60°C with various polarizing fields. Sample thickness 25 μm .
Al-Cu system.

Polarizing Field	α -peak					ρ -peak					ρ' -peak				
	Peak current (Amp)	Peak Temp. (°C)	Activation Energy (eV)	Relaxation time Sec (τ_0)	Charge Released Coul. (Q)	Peak current (Amp)	Peak Temp. (°C)	Activation Energy (eV)	Relaxation time Sec (τ_0)	Charge Released Coul. (Q)	Peak current (Amp)	Peak Temp. (°C)	Activation Energy (eV)	Relaxation time Sec (τ_0)	Charge Released Coul. (Q)
(Ep)															
05	4.0×10^{-11}	90	0.282	6.4×10^4	7.6×10^{-9}	1.0×10^{-10}	160	0.617	7.5×10^6	6.4×10^{-8}	4.0×10^{-9}	200	0.887	4.7×10^5	7.8×10^{-7}
10	5.5×10^{-11}	90	0.285	7.6×10^5	8.2×10^{-9}	1.4×10^{-10}	155	0.623	4.7×10^5	8.9×10^{-8}	6.5×10^{-9}	195	0.891	5.4×10^5	7.8×10^{-7}
25	8.5×10^{-11}	90	0.286	8.4×10^6	9.4×10^{-9}	5.0×10^{-10}	160	0.633	8.7×10^6	9.4×10^{-8}	1.2×10^{-8}	200	0.886	7.8×10^4	4.6×10^{-5}
50	1.2×10^{-10}	90	0.284	9.78×10^6	4.6×10^{-8}	1.4×10^{-9}	165	0.634	9.4×10^5	2.6×10^{-7}	2.6×10^{-8}	205	0.887	1.87×10^6	7.8×10^{-5}
75	1.4×10^{-10}	90	0.283	8.66×10^4	7.6×10^{-8}	2.0×10^{-9}	160	0.628	8.78×10^6	3.4×10^{-7}	6.0×10^{-8}	200	0.886	4.87×10^5	8.75×10^{-5}
100	1.8×10^{-10}	90	0.287	7.65×10^5	8.2×10^{-8}	5.0×10^{-9}	160	0.625	9.47×10^5	4.6×10^{-7}	1.0×10^{-7}	205	0.885	6.54×10^5	9.87×10^{-5}

Table 4.28 : Depolarization kinetic data for PVP samples poled at 60°C with various polarizing fields. Sample thickness 05 μm .
Cu-Cu system.

Polarizing Field	α -peak					ρ -peak					ρ' -peak				
	Peak current (Amp)	Peak Temp. (°C)	Activation Energy (eV)	Relaxation time Sec (τ_0)	Charge Released Coul. (Q)	Peak current (Amp)	Peak Temp. (°C)	Activation Energy (eV)	Relaxation time Sec (τ_0)	Charge Released Coul. (Q)	Peak current (Amp)	Peak Temp. (°C)	Activation Energy (eV)	Relaxation time Sec (τ_0)	Charge Released Coul. (Q)
(Ep)															
05	2.0×10^{-9}	80	0.287	5.7×10^6	3.4×10^{-9}	7.0×10^{-9}	160	0.678	4.72×10^5	6.5×10^{-7}	7.0×10^{-8}	200	0.982	4.7×10^6	6.84×10^{-6}
10	3.0×10^{-9}	80	0.283	9.7×10^5	4.81×10^{-9}	1.0×10^{-8}	155	0.669	9.85×10^4	7.4×10^{-6}	1.2×10^{-7}	205	0.987	3.87×10^5	9.87×10^{-6}
25	4.0×10^{-9}	80	0.285	8.78×10^6	7.87×10^{-9}	2.0×10^{-8}	150	0.665	4.47×10^6	8.35×10^{-6}	2.0×10^{-7}	200	0.989	4.91×10^6	8.78×10^{-5}
50	5.0×10^{-9}	80	0.286	4.56×10^7	9.0×10^{-9}	3.0×10^{-8}	150	0.667	7.81×10^5	9.98×10^{-6}	4.0×10^{-7}	205	0.986	5.87×10^5	9.98×10^{-5}
75	8.0×10^{-9}	80	0.284	8.78×10^6	1.67×10^{-8}	9.0×10^{-8}	160	0.666	8.94×10^5	4.88×10^{-5}	7.0×10^{-7}	200	0.989	8.45×10^6	3.58×10^{-5}
100	1.0×10^{-8}	80	0.282	9.52×10^5	3.85×10^{-8}	1.2×10^{-7}	160	0.663	9.37×10^5	9.88×10^{-5}	1.2×10^{-6}	205	0.981	9.78×10^5	8.78×10^{-5}

Table 4.29 : Depolarization kinetic data for PVP samples poled at 60°C with various polarizing fields. Sample thickness 25 μm .
Cu-Cu system.

Polarizing Field	α -peak					ρ -peak					ρ' -peak				
	Peak current (Amp)	Peak Temp. ($^{\circ}\text{C}$)	Activation Energy (eV)	Relaxation time Sec (τ_0)	Charge Released Coul. (Q)	Peak current (Amp)	Peak Temp. ($^{\circ}\text{C}$)	Activation Energy (eV)	Relaxation time Sec (τ_0)	Charge Released Coul. (Q)	Peak current (Amp)	Peak Temp. ($^{\circ}\text{C}$)	Activation Energy (eV)	Relaxation time Sec (τ_0)	Charge Released Coul. (Q)
(Ep)															
05	2.0×10^{-10}	70	0.285	4.9×10^8	2.29×10^{-9}	6.0×10^{-5}	150	0.678	4.7×10^6	6.5×10^{-7}	7.68×10^{-7}	200	0.987	4.7×10^5	8.54×10^{-5}
10	3.0×10^{-10}	70	0.286	4.7×10^8	7.29×10^{-9}	9.0×10^{-8}	155	0.673	9.81×10^5	7.4×10^{-6}	8.86×10^{-7}	200	0.986	6.7×10^6	9.97×10^{-6}
25	4.0×10^{-9}	70	0.287	9.56×10^8	9.27×10^{-9}	1.2×10^{-8}	150	0.675	3.37×10^6	8.35×10^{-6}	8.67×10^{-7}	205	0.985	3.8×10^7	2.58×10^{-6}
50	5.0×10^{-9}	70	0.288	4.83×10^7	7.29×10^{-8}	2.0×10^{-8}	150	0.674	4.48×10^5	9.98×10^{-6}	2.54×10^{-6}	200	0.984	7.8×10^7	3.88×10^{-5}
75	8.0×10^{-9}	70	0.286	8.85×10^7	8.43×10^{-8}	2.6×10^{-8}	155	0.676	8.78×10^6	4.88×10^{-5}	6.66×10^{-6}	200	0.986	6.5×10^6	8.76×10^{-5}
100	1.0×10^{-9}	70	0.285	9.78×10^7	9.78×10^{-8}	3.6×10^{-7}	150	0.675	9.82×10^6	9.88×10^{-5}	7.87×10^{-6}	205	0.989	9.8×10^6	9.32×10^{-3}

Table 4.30 : Depolarization kinetic data for PVP samples poled at 60°C with various polarizing fields. Sample thickness 05 μm .
Ag-Ag system.

Polarizing Field	α -peak					p-peak					p'-peak				
	Peak current (Amp)	Peak Temp. ($^{\circ}\text{C}$)	Activation Energy (eV)	Relaxation time Sec (τ_0)	Charge Released Coul. (Q)	Peak current (Amp)	Peak Temp. ($^{\circ}\text{C}$)	Activation Energy (eV)	Relaxation time Sec (τ_0)	Charge Released Coul. (Q)	Peak current (Amp)	Peak Temp. ($^{\circ}\text{C}$)	Activation Energy (eV)	Relaxation time Sec (τ_0)	Charge Released Coul. (Q)
(Ep)															
05	1.2×10^{-9}	75	0.275	4.6×10^5	2.78×10^{-7}	6.0×10^{-9}	150	0.665	4.8×10^7	3.71×10^{-7}	5.0×10^{-8}	205	0.975	8.81×10^6	3.9×10^{-6}
10	1.6×10^{-9}	75	0.269	8.7×10^6	5.66×10^{-7}	1.0×10^{-8}	145	0.678	6.7×10^8	4.82×10^{-7}	7.0×10^{-8}	210	0.977	9.54×10^5	4.85×10^{-6}
25	2.0×10^{-9}	75	0.268	3.4×10^6	7.68×10^{-7}	1.4×10^{-8}	145	0.669	6.85×10^8	7.66×10^{-6}	1.4×10^{-7}	210	0.978	8.78×10^4	8.8×10^{-6}
50	3.0×10^{-9}	75	0.276	9.75×10^7	8.76×10^{-7}	2.0×10^{-8}	145	0.675	3.78×10^7	5.44×10^{-6}	3.0×10^{-7}	205	0.973	3.35×10^6	9.4×10^{-5}
75	5.0×10^{-9}	75	0.277	3.64×10^6	9.88×10^{-7}	5.5×10^{-8}	150	0.676	4.48×10^7	7.98×10^{-6}	6.0×10^{-7}	200	0.974	9.91×10^7	3.78×10^{-5}
100	7.0×10^{-9}	75	0.278	4.48×10^8	3.88×10^{-6}	1.4×10^{-7}	155	0.677	3.85×10^5	8.88×10^{-6}	6.0×10^{-7}	210	0.977	2.84×10^6	6.67×10^{-5}

Table 4.31 : Depolarization kinetic data for PVP samples poled at 60°C with various polarizing fields. Sample thickness 25 μm .
Ag-Ag system.

Polarizing Field	α -peak					ρ -peak					ρ' -peak				
	Peak current (Amp)	Peak Temp. ($^{\circ}\text{C}$)	Activation Energy (eV)	Relaxation time Sec (τ_0)	Charge Released Coul. (Q)	Peak current (Amp)	Peak Temp. ($^{\circ}\text{C}$)	Activation Energy (eV)	Relaxation time Sec (τ_0)	Charge Released Coul. (Q)	Peak current (Amp)	Peak Temp. ($^{\circ}\text{C}$)	Activation Energy (eV)	Relaxation time Sec (τ_0)	Charge Released Coul. (Q)
50	3.0×10^{-10}	80	0.287	4.78×10^4	4.78×10^{-8}	1.4×10^{-9}	150	0.693	3.57×10^4	5.5×10^{-7}	2.0×10^{-8}	210	1.03	4.7×10^6	4.4×10^{-5}
75	4.0×10^{-10}	80	0.283	5.66×10^5	5.66×10^{-8}	2.0×10^{-9}	145	0.697	4.78×10^5	6.64×10^{-7}	3.2×10^{-8}	210	1.01	6.7×10^5	9.4×10^{-6}
100	5.0×10^{-10}	80	0.284	6.66×10^6	6.66×10^{-8}	4.0×10^{-9}	155	0.696	9.78×10^5	8.59×10^{-7}	5.0×10^{-8}	205	1.00	9.87×10^6	3.2×10^{-5}
125	7.5×10^{-9}	80	0.285	7.67×10^5	7.67×10^{-8}	6.0×10^{-9}	155	0.695	3.78×10^5	9.58×10^{-7}	9.0×10^{-8}	215	1.04	10.87×10^5	4.7×10^{-5}
150	1.0×10^{-9}	80	0.286	8.88×10^4	8.88×10^{-8}	7.0×10^{-9}	150	0.698	4.46×10^6	2.27×10^{-6}	1.2×10^{-7}	210	1.02	4.37×10^6	6.65×10^{-5}
200	1.2×10^{-9}	80	0.284	9.46×10^6	9.46×10^{-8}	1.0×10^{-9}	150	0.694	6.61×10^4	3.57×10^{-6}	1.6×10^{-7}	210	1.00	6.65×10^5	8.87×10^{-5}

Table 4.32 : Depolarization kinetic data for PVP samples poled at 60°C with various polarizing fields. Sample thickness 05 μm .
Sn-Sn system.

Polarizing Field	α -peak					ρ -peak					ρ' -peak				
	Peak current (Amp)	Peak Temp. ($^{\circ}\text{C}$)	Activation Energy (eV)	Relaxation time Sec (τ_0)	Charge Released Coul. (Q)	Peak current (Amp)	Peak Temp. ($^{\circ}\text{C}$)	Activation Energy (eV)	Relaxation time Sec (τ_0)	Charge Released Coul. (Q)	Peak current (Amp)	Peak Temp. ($^{\circ}\text{C}$)	Activation Energy (eV)	Relaxation time Sec (τ_0)	Charge Released Coul. (Q)
Ep															
05	9.5×10^{-10}	70	287	6.6×10^3	3.87×10^{-8}	6.0×10^{-9}	150	0.755	3.8×10^6	3.38×10^{-7}	7.0×10^{-8}	210	1.080	4.6×10^4	4.48×10^{-5}
10	1.4×10^{-9}	70	0.295	9.85×10^4	6.65×10^{-7}	1.2×10^{-8}	155	0.752	4.81×10^5	8.46×10^{-6}	1.2×10^{-7}	215	1.000	6.41×10^5	6.78×10^{-5}
25	2.4×10^{-9}	70	0.294	7.88×10^3	7.47×10^{-7}	2.0×10^{-8}	160	0.753	5.86×10^6	7.56×10^{-6}	3.0×10^{-7}	220	1.060	1.68×10^7	8.96×10^{-5}
50	3.8×10^{-9}	70	0.296	8.46×10^4	6.65×10^{-7}	4.0×10^{-8}	150	0.754	6.65×10^7	9.55×10^{-6}	5.0×10^{-7}	210	1.070	8.64×10^6	9.97×10^{-5}
75	6.0×10^{-9}	70	0.297	8.54×10^5	7.85×10^{-7}	7.0×10^{-8}	160	0.751	7.78×10^6	2.47×10^{-5}	7.0×10^{-7}	210	1.060	9.47×10^5	3.48×10^{-5}
100	9.0×10^{-9}	70	0.298	9.97×10^6	9.98×10^{-7}	1.0×10^{-8}	155	0.755	9.91×10^4	3.38×10^{-5}	1.0×10^{-6}	220	1.050	3.38×10^6	4.47×10^{-5}

Table 4.33 : Depolarization kinetic data for PVP samples poled at 60°C with various polarizing fields. Sample thickness 25 μm . Sn-Sn system.

Polarizing Field	α -peak					ρ -peak					ρ' -peak				
	Peak current (Amp)	Peak Temp. ($^{\circ}\text{C}$)	Activation Energy (eV)	Relaxation time Sec (τ_0)	Charge Released Coul. (Q)	Peak current (Amp)	Peak Temp. ($^{\circ}\text{C}$)	Activation Energy (eV)	Relaxation time Sec (τ_0)	Charge Released Coul. (Q)	Peak current (Amp)	Peak Temp. ($^{\circ}\text{C}$)	Activation Energy (eV)	Relaxation time Sec (τ_0)	Charge Released Coul. (Q)
(Ep)															
05	4.0×10^{-10}	80	0.297	4.46×10^6	7.77×10^{-5}	3.0×10^{-5}	150	0.747	8.78×10^5	4.78×10^{-7}	3.0×10^{-8}	200	0.987	1.87×10^6	6.67×10^{-6}
10	6.0×10^{-10}	80	0.268	4.78×10^6	8.76×10^{-6}	4.5×10^{-5}	150	0.697	9.48×10^6	7.78×10^{-7}	5.0×10^{-8}	210	0.978	8.78×10^5	5.58×10^{-6}
25	9.0×10^{-10}	80	0.275	5.58×10^5	9.43×10^{-5}	8.0×10^{-5}	155	0.691	1.51×10^5	8.47×10^{-7}	7.0×10^{-8}	205	0.979	9.88×10^6	6.65×10^{-6}
50	1.2×10^{-9}	80	0.285	6.64×10^6	10.11×10^{-6}	1.4×10^{-5}	160	0.698	10.49×10^6	3.57×10^{-6}	1.4×10^{-7}	210	0.985	3.24×10^5	5.66×10^{-6}
75	2.0×10^{-9}	80	0.277	7.74×10^5	11.14×10^{-5}	1.6×10^{-5}	155	0.701	11.81×10^7	8.67×10^{-6}	2.4×10^{-7}	205	0.986	4.44×10^7	2.46×10^{-5}
100	3.0×10^{-9}	80	0.286	8.74×10^6	8.76×10^{-7}	2.6×10^{-5}	150	0.721	6.48×10^6	9.32×10^{-6}	3.4×10^{-7}	200	0.995	7.64×10^6	3.47×10^{-5}

Table 4.34 : Depolarization kinetic data for PVP samples poled at 60°C with various polarizing fields. Sample thickness 05 μm .
Al-Ag system.

Polarizing Field	α -peak					ρ -peak					ρ' -peak				
	Peak current (Amp)	Peak Temp. (°C)	Activation Energy (eV)	Relaxation time Sec (τ_0)	Charge Released Coul. (Q)	Peak current (Amp)	Peak Temp. (°C)	Activation Energy (eV)	Relaxation time Sec (τ_0)	Charge Released Coul. (Q)	Peak current (Amp)	Peak Temp. (°C)	Activation Energy (eV)	Relaxation time Sec (τ_0)	Charge Released Coul. (Q)
(Ep)															
05	7.0×10^{-11}	80	0.265	4.5×10^6	3.68×10^{-9}	2.0×10^{-10}	160	0.672	3.35×10^4	5.87×10^{-9}	3.0×10^{-9}	205	1.010	2.78×10^6	7.78×10^{-7}
10	9.0×10^{-11}	80	0.267	6.5×10^5	8.63×10^{-9}	4.0×10^{-10}	165	0.670	4.48×10^5	6.99×10^{-9}	8.0×10^{-9}	205	1.000	5.46×10^7	9.87×10^{-7}
25	1.4×10^{-10}	80	0.265	5.8×10^6	9.68×10^{-9}	1.0×10^{-9}	160	0.671	6.56×10^5	8.24×10^{-9}	3.0×10^{-8}	200	1.020	6.64×10^6	2.56×10^{-6}
50	1.8×10^{-10}	80	0.268	9.81×10^7	2.54×10^{-8}	2.0×10^{-9}	165	0.677	7.66×10^5	9.35×10^{-8}	1.0×10^{-7}	210	1.050	9.65×10^7	3.65×10^{-6}
75	2.2×10^{-10}	80	0.271	3.85×10^6	3.38×10^{-8}	7.0×10^{-9}	165	0.679	8.761×10^5	2.75×10^{-7}	2.0×10^{-7}	205	1.060	8.72×10^5	6.78×10^{-6}
100	3.0×10^{-10}	80	0.270	4.48×10^4	4.68×10^{-8}	1.6×10^{-8}	165	0.673	9.76×10^5	3.36×10^{-7}	4.5×10^{-7}	205	1.040	6.43×10^5	8.76×10^{-6}

Table 4.35 : Depolarization kinetic data for PVP samples poled at 60°C with various polarizing fields. Sample thickness 05 μm .
Al-Sn system.

Polarizing Field	α -peak					ρ -peak					ρ' -peak				
	Peak current (Amp)	Peak Temp. (°C)	Activation Energy (eV)	Relaxation time Sec (τ_0)	Charge Released Coul. (Q)	Peak current (Amp)	Peak Temp. (°C)	Activation Energy (eV)	Relaxation time Sec (τ_0)	Charge Released Coul. (Q)	Peak current (Amp)	Peak Temp. (°C)	Activation Energy (eV)	Relaxation time Sec (τ_0)	Charge Released Coul. (Q)
(Ep)															
05	6.0×10^{-11}	80	0.281	3.2×10^4	5.4×10^{-9}	5.0×10^{-10}	160	0.712	4.7×10^6	7.7×10^{-8}	3.0×10^{-9}	195	1.110	5.64×10^6	4.67×10^{-7}
10	8.0×10^{-11}	80	0.287	4.7×10^6	6.54×10^{-9}	8.0×10^{-10}	165	0.718	3.2×10^5	9.8×10^{-8}	1.0×10^{-8}	200	1.060	6.54×10^5	5.57×10^{-7}
25	1.0×10^{-10}	80	0.289	8.7×10^5	7.84×10^{-9}	2.0×10^{-9}	155	0.719	4.8×10^6	2.4×10^{-7}	3.0×10^{-8}	205	1.070	7.77×10^6	6.68×10^{-7}
50	1.4×10^{-10}	80	0.284	9.9×10^6	2.74×10^{-8}	5.0×10^{-9}	160	0.721	7.8×10^7	4.67×10^{-7}	7.0×10^{-8}	195	1.090	8.74×10^4	9.32×10^{-7}
75	2.0×10^{-10}	80	0.285	8.7×10^5	3.05×10^{-8}	9.0×10^{-9}	160	0.725	8.4×10^6	7.64×10^{-7}	9.0×10^{-8}	200	1.010	9.88×10^3	1.45×10^{-6}
100	3.0×10^{-10}	80	0.286	6.6×10^4	8.66×10^{-8}	1.4×10^{-8}	155	0.726	9.9×10^6	8.88×10^{-7}	1.2×10^{-7}	205	1.080	10.02×10^4	2.22×10^{-6}

Table 4.36 : Depolarization kinetic data for PVP samples poled at 60°C with various polarizing fields. Sample thickness 25 μm .
Al-Ag system.

Polarizing Field	α -peak						ρ -peak						ρ' -peak			
	Peak current (Amp)	Peak Temp. ($^{\circ}\text{C}$)	Activation Energy (eV)	Relaxation time Sec (τ_0)	Charge Released Coul. (Q)	Peak current (Amp)	Peak Temp. ($^{\circ}\text{C}$)	Activation Energy (eV)	Relaxation time Sec (τ_0)	Charge Released Coul. (Q)	Peak current (Amp)	Peak Temp. ($^{\circ}\text{C}$)	Activation Energy (eV)	Relaxation time Sec (τ_0)	Charge Released Coul. (Q)	Peak current (Amp)
(Ep)																
05	3.0×10^{-11}	80	0.295	4.7×10^4	4.7×10^{-5}	8.0×10^{-11}	160	0.735	6.4×10^5	7.7×10^{-8}	1.4×10^{-9}	195	1.090	3.78×10^6	5.4×10^{-7}	5.4×10^{-7}
10	4.5×10^{-11}	80	0.294	6.8×10^5	6.8×10^{-6}	1.8×10^{-10}	160	0.736	8.4×10^6	9.8×10^{-8}	3.6×10^{-9}	200	1.000	8.54×10^5	6.54×10^{-7}	6.54×10^{-7}
25	6.5×10^{-11}	80	0.297	8.8×10^4	8.8×10^{-6}	7.0×10^{-9}	165	0.739	8.7×10^7	2.4×10^{-7}	1.0×10^{-8}	200	1.010	9.46×10^6	8.54×10^{-7}	8.54×10^{-7}
50	9.5×10^{-11}	80	0.296	9.4×10^5	9.4×10^{-6}	2.0×10^{-9}	165	0.742	8.92×10^6	4.67×10^{-7}	2.0×10^{-8}	195	1.040	8.44×10^4	9.22×10^{-7}	9.22×10^{-7}
75	1.2×10^{-10}	80	0.298	3.7×10^6	3.7×10^{-7}	2.6×10^{-9}	155	0.729	9.28×10^5	7.64×10^{-7}	3.6×10^{-8}	200	1.060	7.77×10^6	2.78×10^{-7}	2.78×10^{-7}
100	1.4×10^{-10}	80	0.299	4.7×10^5	4.7×10^{-7}	4.0×10^{-9}	160	0.748	7.85×10^6	8.88×10^{-7}	7.0×10^{-8}	200	1.070	9.82×10^4	3.58×10^{-7}	3.58×10^{-7}

Table 4.37 : Depolarization kinetic data for PVP samples poled at 60°C with various polarizing fields. Sample thickness 25 μm . Al-Sn system.

Polarizing Field		α-peak					ρ-peak					ρ'-peak				
		Peak current (Amp)	Peak Temp. (°C)	Activation Energy (eV)	Relaxation time Sec (τ _o)	Charge Released Coul. (Q)	Peak current (Amp)	Peak Temp. (°C)	Activation Energy (eV)	Relaxation time Sec (τ _o)	Charge Released Coul. (Q)	Peak current (Amp)	Peak Temp. (°C)	Activation Energy (eV)	Relaxation time Sec (τ _o)	Charge Released Coul. (Q)
(Ep)																
05		3.0x10 ⁻¹¹	70	0.301	4.9x10 ³	7.6x10 ⁻⁶	3.0x10 ⁻¹⁰	160	0.776	9.3x10 ⁴	4.65x10 ⁻⁸	1.0x10 ⁻⁹	200	1.080	4.12x10 ⁶	3.2x10 ⁻⁷
10		4.5x10 ⁻¹¹	70	0.302	9.43x10 ²	8.43x10 ⁻⁶	5.5x10 ⁻¹⁰	165	0.765	4.7x10 ⁵	4.7x10 ⁻⁶	2.0x10 ⁻⁹	200	1.030	6.68x10 ⁶	5.7x10 ⁻⁷
25		7.0x10 ⁻¹¹	70	0.298	5.88x10 ⁶	9.66x10 ⁻⁶	8.0x10 ⁻¹⁰	160	0.769	6.5x10 ⁶	9.01x10 ⁻⁸	3.0x10 ⁻⁹	195	1.040	9.85x10 ⁴	8.6x10 ⁻⁶
50		8.0x10 ⁻¹¹	70	0.298	8.55x10 ⁵	1.33x10 ⁻⁶	1.8x10 ⁻⁹	165	0.773	7.7x10 ⁷	9.08x10 ⁻⁸	5.0x10 ⁻⁹	205	1.060	3.78x10 ⁵	9.0x10 ⁻⁶
75		9.0x10 ⁻¹¹	70	0.297	9.11x10 ⁴	5.43x10 ⁻⁶	1.8x10 ⁻⁹	160	0.747	8.4x10 ⁶	2.78x10 ⁻⁷	8.0x10 ⁻⁹	205	1.050	5.88x10 ⁶	2.0x10 ⁻⁵
100		1.0x10 ⁻¹⁰	70	0.303	3.78x10 ⁵	8.87x10 ⁻⁶	2.2x10 ⁻⁹	160	0.765	9.5x10 ⁵	2.84x10 ⁻⁷	1.2x10 ⁻⁸	200	1.040	6.12x10 ⁷	8.6x10 ⁻⁵

- (i) Space charge injected into the dielectric by surface breakdown between the dielectric and the electrode.
- (ii) Space charge injected from the electrodes.
- (iii) Space charge caused by migration of charge carriers over macroscopic distances.
- (iv) Electronic or ionic dipoles caused by migration of charges over microscopic distances, and
- (v) Orientation of permanent dipoles.

Generally, polymers contain a small number of free charge carriers, i.e. ions, electrons or both [30]. During electret formation, the carriers move comparatively free in the direction of the applied field over microscopic distances before they fall into deep traps from which they can be released only on receiving sufficient energy. PVP is a polar polymer, the contribution to the polarization may be due to alignment of the dipoles under the effect of the electric field.

It is well established [31,32] that the two relaxation processes α and ρ exist in bulk PVP and they have been attributed to the molecular motion of permanent dipoles/orientation of the main chains from polarised state to their equilibrium state with large activation energy. The

process having small energy is due to relaxation of the side chain or small polar group from polarised state to the equilibrium state. An additional observed relaxation on ρ' peak process could be associated with the space charge polarisation [33].

The TSDC thermograms of PVP foil electrets show two well resolved peaks at $95 \pm 5^\circ\text{C}$ and $175 \pm 5^\circ\text{C}$ in case of Al-Al system in the ascending order of temperature. The first peak (α) is attributed to disorientation of polar side groups. The polar side group pyrrolidone ring in PVP has carbonyl group of double bond. This group is attached to the main chain with an amide bond. Here, the pyrrolidone group may have different possible orientations/rotations with respect to the main chain of the polymer and thus a distributed energy is associated with TSDC results. The value of activation energy (E) associated with this peak is found to be 0.51 eV and is related to disorientation of polar groups of PVP. The second peak (ρ) is associated with the primary relaxation process which occurred in the temperature range $175 \pm 5^\circ\text{C}$ of glass transition of PVP. The value of E calculated for ρ -peak is found to be of the order of 1.03 eV which suggests the possibility of ionic processes [34], and is related to charge carriers of ionic nature. PVP exhibits the properties of solid free radical, probably at the temperature of the phase transition. Hence, the ionic and other charges may certainly be present during polarisation of the sample. In PVP the

different charge/ions are due to the presence of different active groups [35]. All types of dissociated ions are possible, including opposite charge carriers, at T_g . The releasing of the carriers/ions from the polarised state seems to be possible at the ρ -peak temperature. The structure also gets loosened to some extent. In this way, all types of charge carriers/ions are released, giving rise to a peak (ρ) in higher temperature region. This is in agreement with the earlier finding [36].

The α -peak is a dipolar peak and may be attributed to disorientation of polar side groups. The polar side group moiety, pyrrolidone ring in PVP has carbonyl group of double bond. The group is attached to main chain with an amide bond. The value of activation energy associated with this peak is found to be nearly 0.35 eV and is related to disorientation of polar groups of PVP. The ρ -peak is associated with the primary relaxation process which occurred in the temperature range of rubber-glass transition of PVP (around 175°C). The value of E calculated for this peak is found to be of the order of 0.83 eV suggests the possibility of ionic processes. PVP exhibits the properties of solid free radical, probably at the temperature of phase transition; hence the ionic and other electronic charges may certainly be present during polarisation of the sample associated with ρ -peak. This agrees with the earlier findings [36].

Due to high resistivity of polymers at temperature lower than T_g , the mobility of the molecules/dipoles is low [37] so that they do not get polarised under the influence of applied field. Hence, a small current is observed which may be due to the depolarisation of some loosely bound side groups/chains. While at the temperature higher than T_g , the mobility of molecules/dipoles is high and they get polarised easily.

Under the influence of electric field the irregularly distributed dipoles of side chains are mobilised/oriented in a certain direction. Thermal activation at a constant rate cause the release of charges due to their mobilisation giving a peak at the site of maximum release of charge. The increase in current magnitude with electric field may be attributed to the increase in mobility of charge carriers.

There is a linear dependence of the released charge on the polarisation field strength. This relationship favours an uniform polarisation process. In PVP which is a polar material, the possibility of permanent dipole alignment cannot be ruled out because uniform polarisation is a characteristic of dipole orientation process.

The TSDC spectra are characterised by various peaks, due to the dissipation of charges arising because of polarization during charging process. The polarisation of the material may arise due to various mechanisms, the important of which are

dipole orientation, charge displacement molecular and domain structures, macro/microscopic displacement of ions with subsequent trapping, surface and space charge polarisation, etc. The processes mentioned above other than the last two are considered always to give rise to the TSDC of polarity opposite to the charging current. But in the case of surface and space charge polarisation, TSDC of opposite or the same polarity that of charging current may be found depending upon the distribution of the space charge in the bulk of sample. If the zero field point in the case of space and surface charge polarisation is nearer to the electrode than the centre of the bulk, the observed current is supposed to be of the polarity opposite to the charging current otherwise the observed current will be of the same polarity as that of the charging current. This can be the explanation for the appearance of additional current peak (ρ') around $205 \pm 3^\circ\text{C}$ in a direction opposite to both α and ρ peaks, in case of samples prepared by using similar electrodes configurations of Ag-Ag; Cu-Cu and Sn-Sn. Turnhout [38] and Venderschueren [39] have observed a similar peak. According to Perlman [40] TSDC peaks have the same temperature dependence, if the polarisation is uniform and are either due to depolarisation process or migration of charge carriers. The second and third peaks in our experiment correspond to different types of carriers/ions released in the primary relaxation process.

The homo charges injected from electrode during polarisation may not necessarily be discharging at their respective electrodes during the depolarisation and in that case, the current reversal in the external circuit may be observed due to the motion of the zero-field-plane as suggested by Gross and Perlman [41]. Therefore, behaviour of the depolarising current corresponding to ρ' will mainly depend on the concentration and the type of the injected charge carriers in addition to the concentration of the included charge carriers which form the space charge. Gubkin and Skanavi [42] have also suggested that there is an accumulation of charge at the interface of the two different materials and these charges penetrate in the dielectric and get trapped into the available traps, thus forming the space-charge. TSDC thermograms for pure PVP foil samples with dissimilar electrode combinations (Al-Ag; Al-Cu and Al-Sn) show that the magnitude of current is higher as compared to Al-Al electrode system. The difference in the work functions of the electrodes used in the sandwiched system gives higher TSD current at elevated temperature. The peak value of the current seems to be controlled by the effective work function for metal-insulator-metal interfaces. The difference between the work function of metal (1) and metal (2) will control the magnitude of current, but for Al-Al system the characteristics of the polymer may prevail as the net contribution of current from charge injected from electrode would then be zero [43]. A

marked electrode effect has been observed for the ρ' peak. The slightly different peak positions in dissimilar electrode metal combination have been observed. These results suggest that the liberated opposite pair of ions and carriers may be affected by the work function difference of the electrode metals and a possibility also seems to be present that the internal field of PVP may get modified by work function of different electrode materials. The high value of activation energy (~ 1.23 eV) is associated with ρ' -peak suggests the possibility of space charge mechanism produced by injected space carriers from the electrodes. This high value of activation energy is in favour of self motion of charge carriers/injected charge carriers (or ions) to some atomic distances towards opposite electrodes. Alternatively, there is also a possibility of homocharges due to air breakdown between dielectric and electrode interfaces but it can be ruled out in this case since the vacuum deposited electrodes are used during the studies. These charges of external origin are injected from the injecting nature of electrodes (metal) and some of these may get trapped in different trap levels, hence another possibility of detrapping of trapped charge carriers is possible. Space charge may also be affected by the neutralization process of charge carriers/near the electrode-dielectric interfaces. This phenomenon of neutralization of charge carriers/ions is the usual phenomenon at higher temperatures.

The values of E_a , I_m , T_m and Q for the electrode series are given in Table 4.1 to 4.23. All these values are different for samples prepared with different electrodes. Such electrode dependence has also been found by quite few workers [44-46]. Table reveals a close relationship between the surface charge and TSD currents of PVP foil electrets on the metal electrodes. The results support the Gross's theory [47] of homocharge which attributes it either to electrode dielectric interface breakdown (ruled out in our case due to experimental arrangement used) or to the charge injection from the electrodes. The electrons and holes migrate from the electrodes on to the surface of the dielectric [44,48]. When the polymer is polarized under identical conditions of polarisation with electrodes (Al, Sn, Ag, Cu) of different work function determined by contact potential method [49], but less than that of PVP, the metal with higher work function injects a large number of charge carriers than that with lower work functions [45]. Since the injection of charge carriers from the electrodes to the polymers results in a reduction of the contribution of the heterocharge (due to the charge carriers present in the bulk of the material) so the charge released to the external circuit and the magnitude of the peak current I_m , should decrease with the work function of the metal. The present observations tend to behave similarly (for Sn, Ag, and Cu) electrodes. The behaviour of Al is ambiguously different which cannot be explained with the present

framework, as reported by Grepsted *et al.* [50] in case of PVC thermoelectrets.

Slight difference in peak positions for different metal-electrode-metal combinations were observed (Fig. 4.78). These results suggest that the liberated opposite part of ions and carriers may be slightly affected by the work function difference of different combinations. In these results, a possibility seems to be present, that the internal field of PVP may get modified by the difference in the work function of different electrodes. Peak value of the currents seems to be controlled effectively by the work function for metal-insulator-metal interfaces.

TSDC thermograms of pure PVP foil samples prepared with different similar and dissimilar electrode combinations show that the α -peak position is independent of polarisation field and the linear relation between peak current and polarisation field suggests uniform polarisation and the activation energies of the order of 0.35 eV supports that the peak corresponds to dipolar mechanism. The height of the α -peak is found to increase with the rise in field values. This may be due to the fact that as the field is increased, dipole orientation increases and more and more dipoles get themselves arranged in a definite direction with respect to the field, giving rise to increase in peak magnitude with the field. This is quite in conformity with the theory of increase in polarisation with polarisation field.

The effect of polarisation temperature T_p on the TSDC thermograms of PVP foil electrets with different electrode configuration show that an increase in T_p enhances the height of all the three peaks and this enhancement has been relatively more pronounced in case of ρ' -peak. The values of activation energy for all the relaxations increase linearly with T_p . At lower T_p , the conduction is slow so that fewer carriers are available to accumulate and this reduces the height of the peak. Moreover, at low values of T_p , only the fast sub-polarisations could be operative but as T_p is raised, more sub-polarisations (with longer relaxation times) would be activated [51,52], thereby enhancing the peak magnitudes. When all the subpolarisations are filled, the current maxima appear at transition temperatures. Infact, the values of activation energy for the corresponding decay processes increase with the increase in T_p implies that α , ρ and ρ' -relaxations in the present case are due to a distribution of relaxation times in which both the activation energy and the pre-exponential factor are distributed.

For homoelectrets, poling temperature mainly influences the penetration depth of the injected carriers [53]. By changing the polarity of injection voltage, negative or positive carriers can be injected which can have different drift mobilities, retrapping and recombination rates. Decay of positive carriers is faster than negative carriers. Only the negative carriers and not the positive ones can be injected at

room temperature. This make it likely that electrons contribute significantly in a negative injection. At low temperature, the conductivity is low and the fewer carriers are available to accumulate, which weakens the space charge peak. The values of activation energy for poling temperatures 40 to 80°C are calculated to be 0.247 to 1.11 eV. Thus, activation energy increases with the increase in poling temperature. This fact, combined with the magnitude of activation energy associated with the peak, lead to conclude that the trapping site is being destroyed due to increased molecular motion [54].

The trapping in polymers is not an unusual phenomenon. Several concepts of traps in organic polymers such as those created due to the difference in energy levels between the amorphous and crystalline regions or due to the line and point defect and the association of these lattice defects with the molecular etc. have been proposed [55]. Therefore, it is possible that the charge carriers injected from the electrodes are captured in traps available to them.

On heating the foil electrets to 100°C, the polarised volume charge relax to their equilibrium position as a result of which a current is observed and up to this temperature the space charge remains practically frozen but with further increase in temperature the traps start releasing the charge carriers and thus the current due to space charge ρ -peak is observed.

Figs. 4.66 to 4.72 show the effect of thickness variation on the TSDC thermograms of PVP foil electrets poling at 60°C by field 100 kV/cm using different electrode configurations. All the curves show peak current I_m decreases as the thickness of foil increases; the sharpness of the peak also diminishes. These observations can be attributed to ion migration, because for a given polarising field, when ion migration takes place, I_m decreases. The value of activation energy given in Tables 4.1 to 4.23 show that the charge carriers are ionic [42]. The decrease in I_m with the thickness may also be attributed to the fact that the excess charges have to move through a longer distance to be neutralized on reaching the electrodes [56]. This is also supported by the increased activation energy with thickness (Tables 4.1 to 4.23).

REFERENCES

1. Frei, H. and Groetzinger, G., Physik Z. **37**, 720 (1936).
2. Altheim, Von, Ann. d. Phys. **35**, 417 (1939).
3. Bucci, C. and Fieshi, R., Ionic thermocurrent in dielectric Phys. Rev. **148**, 816 (1966).
4. Hino, T., Jap. J. Appl. Phys. **12**, 611 (1973).
5. Chatain, D. et al., Phys. Stat. Sol.A **13**, 303 (1972).
6. Fischer, P. and Rohl, P., Annual Report Conf. on Electrical Insulation and Dielectric Phenomena, NAS, Washington (USA) (1975).
7. Blake, A.E. et al., J. Phys. D. Appl. Phys. **7**, 759 (1974).
8. Nishitani, T. and Yoshino, K., Jap. J. Appl. Phys. **14**, 721 (1975).
9. Perlman, M.M. et al. J. Appl. Phys. **50**, 3622 (1979).
10. Cantaloube, B. and Dryfus, C., J. Polym. Sci. Polym. Phys. **17**, 95 (1975).
11. Singh, R. and Dutt, S.C., J. Electrostat (Netherland) **8**, 279 (1980).
12. Ohara, K., J. Electrostat. **8**, 299 (1980).
13. Mahendru, P.C. and Chand, S., Ind. J. Pure Appl. Phys. **18**, 183 (1980).
14. Lacabnne, C. and Chatain, D., J. Appl. Phys. **50**, 2723 (1979).
15. Jain, K. and Mahendru, P.C., Nhooo Cimento B (Italy) **55B**, 123 (1980).
16. Lilly, A.C. et al., J. Appl. Phys. **41**, 2001 (1970).
17. Stupp, S.I. and Caro, S.H., J. Appl. Phys. **46**, 120 (1975).
18. Guillet, J. and Seytre, G., J. Polym. Sci. Poly. Phys. Ed. **15**, 541 (1977).
19. Takeda, S. and Naito, M., 3rd Intern. Conf. Solid Surfaces, Vienna, 2007 (1977).

20. Sessler, G.M. and West J.E., Phys. Rev. B **10**, 4488 (1974).
21. Fischer, P. and Rohl, P., J. Polym. Sci. Poly Phys. (Ed.) **14**, 543 (1976).
22. Hino, T., J. Appl. Phys. **46**, 1956 (1975).
23. Kessler, A., J. Electrochem. Sol. **123**, 1236 (1976).
24. Takamatsu, T. and Fukada, E., Electrets charge storage and transport in dielectrics, Electrochem. Soc. Inc., New York (1973).
25. Gupta, C.L. and Tyagi, R.C., Ind. J. Pure & Appl. Phys. **16**, 428 (1978).
26. Kulshreshtha, Y.K. and Srivastava, A.P., Polymer J. Japan **11**, 515 (1979).
27. Mahendru, P.C., Jain, K. and Chopra, V.K., J. Phys. D. Appl. Phys. **8**, 305 (1975).
28. Mahendru, P.C. and Mahendru, P., J. Phys. D. Appl. Phys. **9**, 83 (1976).
29. Garlic, G.F.J. and Gibson, A.F., Proc. Phys. Soc. **60**, 574 (1948).
30. Garlic, G.F.J. and Gibson, A.F., Proc. Phys. Soc. **60**, 574 (1948).
31. Ishida, Y., Matsuo, M. and Yama Fuji, Kolloid Z. **180**, 108 (1962).
32. Yama Fuji, K., J. Phys. Soc. Japan **15**, 2295 (1960).
33. Gubkin, A.N. and Matsonashvili, Fiz. Tverd. Tela **4**, 1196 (1962).
34. Mahendru, P.C., Agarwal, J.P. and Jain, Kamlesh, Thin Solid Films **71**, L-5 (1980).
35. Chatterjee, S.K. and Sethi, K.R., J. Polym. Sci. Polym. Phys. **21**, 1045 (1983).
36. Khare, P.K. and Srivastava, A.P., Indian J. Pure & Appl. Phys. **30**, 131 (1992).
37. Reiser, A., Lock, MWV Knight, Research Laboratory Kodak Ltd., Middlesex (1969).
38. Turnhout, J. Van, Thermally Stimulated Discharge of Polymer Electrets (Elsevier, Amsterdam) (1975).

39. Vanderschueren, J., Bull. Sci. AIM (Lige) **4**, 291 (1974).
40. Perlman, M.M., J. Appl. Phys. (USA) **42**, 2645 (1971).
41. Gross, B. and Perlman, M.M., J. Appl. Phys. (USA) **43**, 853 (1972).
42. Gubkin, A.M. and Skanavi, G.I., Izvest. Akad. Nauk. SSR Ser. Fiz. **22**, 330 (1958).
43. Khare, P.K., Surendra, P. and Srivastava, A.P., Ind. J. Pure & Appl. Phys. **30**, 165 (1992).
44. Srivastava, S.K., Ranade, J.D. and Srivastava, A.P., Phys. Lett. **72A**, 185 (1979).
45. Gupta, N.P., Jain, K. and Mahendru, P.C., Thin Solid Films **61**, 297 (1979).
46. Srivastava, S.K., Ranade, J.D. and Srivastava, A.P., Jap. J. Appl. Phys. **18**, 2303 (1979).
47. Talwar, I.M., Ph.D. Thesis, University of Sagar, Sagar (1968).
48. Bogroditskii, N.P., Tairova, D.A. et al., Fizika Tverad. Tela **6**, 2301 (1954).
49. American Institute of Physics Handbook, New York : McGraw Hill Book Co., p.9-14 (1965).
50. Grepstad, J.K., Gartland, P.O. and Slagsvold, B.J., Surf. Sci. **57**, 348 (1976).
51. Turnhout, J. Van, Thermally stimulated discharge of polymer electrets (Elsevier; Amsterdam), 1975.
52. Solunov, H. and Vassilev, T., J. Polym. Sci. Polym. Phys. **12**, 1273 (1974).
53. Kessler, A., J. Elec. Chem. Soc. **123**, 1236 (1976).
54. Perlman, M.M., J. Elec. Chem. Soc. **119**, 7 (1972).
55. Van Roggan, A., Ann. Rep. Konf. Elect. Insul. Nat. Res. Council Puv. **1356**, 3-12 (1965).
56. Turnhout, J. Van, Thermally stimulated discharge of polymer electrets (Elsevier, Amsterdam), 1975.

CHAPTER V

TRANSIENT CURRENTS
IN CHARGING AND
DISCHARGING MODES
AND
STEADY STATE
ELECTRICAL CONDUCTION
IN PURE
POLYVINYL PYRROLIDONE
(PVP)
FOIL ELECTRET

5.1 INTRODUCTION

If we take a polymeric sample and apply a step field to it, the field interacts with the bound and free charge causing their motion. The motion of charges manifests itself as a current flow in the external circuit. Generally, this current known as absorption or charging current, depends on the time elapsed after the application of potential to the electrodes; usually it falls off at first and then becomes steady. After the step voltage has been removed, there is still a current flowing in the external circuit, which is called desorption or discharging current. We find that under isothermal conditions both absorption as well as desorption currents decay approximately in most of the cases as t^{-n} , where t is the time elapsed after the application of the step voltage and 'n' is an exponent whose value may be greater or less than 1, depending upon the properties of the material chosen and the experimental conditions [1-12]. The discharge current may be the mirror image of the charging current except that a steady state current is not reached. The isothermal desorption current decays for a long time, depending upon the internal phenomena taking place irrespective of the steady state current level.

Desorption currents can yield much useful information about the charging process even when the corresponding absorption current is masked by the conduction current during charging. The analysis of the experimental conditions can lead

to a quantitative as well as a qualitative idea of the mechanisms. The results can be compared with some other studies like thermally stimulated discharge current (TSDC), etc., to arrive at coherent and cogent conclusion. Transient current measurements are tedious - on being carried out over a long time is not a regular study but nevertheless it is a very useful one, giving far more consistent results than the others. This being so on account of electrical and other perturbing influences affecting the charging process far less than in other experiments involving decay processes.

In past several years, a good amount of work has been reported on electrical conduction in polymeric materials and various mechanisms such as ionic conduction [13,14], Schottky emission [15-17], space charge limited conduction [18,19], Tunnelling [20], Poole-Frenkel mechanism [21], charge hopping [22] and Polaron mechanism [23] have been proposed to explain the experimental results.

The fact that electronic conduction plays a role in polymers has been established experimentally by Seanor [24]. To discuss electronic condition, it is necessary to investigate the generation of free carriers and their transport through the material. Several reviews [25-29] deal with the problem of carrier generation. Three mechanisms of current flow may be distinguished. Schottky emissions [15-17] occur in the low field high temperature limit. Tunnelling [30,31] occurs in the high field low temperature limits.

Thermal field emission occurs when the dominant contribution to the observed currents arises from the tunnelling of thermally activated electrons.

In polymers at low temperature, the density of free charge carriers is extremely low and with an electric field, non-equilibrium conditions can be achieved, which can be easily enhanced by injecting a charge through an ohmic contact. Current-voltage curves is generally non-linear on account of two basic causes. At high fields the charges are accumulated between the electrodes. The density, energy distribution and nature of the traps have a determining influence on current-voltage characteristics which also depends on type of charges involved in the conduction process.

Trapping sites exert strong influence on the current flow, i.e. the concentration of free carriers and their mobility if the activation energy values are low 0.2 to 0.3 eV, hopping is contacted with charge jumps brought about by motion of chain elements while great values (0.5 eV) the so-called trap hopping mechanism is involved.

5.2 EXPERIMENTAL DETAILS

In the present investigation samples were thermally poled with fields 05 to 100 kV/cm at various temperatures (ranging from 40-80°C) for 180 min. during which the transient currents in the charge mode was observed 2 min after the

application of the field. The current was also observed in the discharge mode for the same period of time, 2 min after the removal of the field. The polarization was carried out by connecting a dc power supply (EC-HV 4800 D) in series with an electrometer which was carefully shielded and grounded to avoid ground loops and extraneous electrical noise.

After making proper electrical connections, the sandwiched sample mounted on electrode assembly was placed inside the thermostat and allowed to attain required temperature. It took about 1.5 hrs. When the sample attained the desired temperature, a dc voltage was applied. A sudden burst of current observed in the beginning decreases with time. Its initial as well as steady value was recorded. At lower voltages and temperatures, it took longer period to reach the steady state while at higher voltages and temperatures, steady state was obtained in considerable low period. The effect of voltage variation in current was noted by increasing the voltage at fixed temperatures while temperature variation was measured keeping voltage constant and increasing the temperature. A fresh sample is used for each set of observation.

5.3 RESULTS

The general characteristics of the observed results on transient currents in charging and discharging modes, are :

5.3-1 TIME DEPENDENCE

The time dependence of the charging and discharging transient currents in PVP foils has been investigated over a period of time $0.1-10^2$ minutes. Figs. 5.1(a) to (c) show typical $\log I$ vs $\log t$ plots for charging mode, charged at temperatures from 40 to 80°C with fields of 5, 10, 25, 50, 75 and 100 kV/cm, respectively for Al-PVP-Al configuration. Discharging modes are shown in 5.1 (A) to (C) under the same temperatures, fields, configuration conditions. In both the cases, PVP film of 20 μm thickness is used. These graphs show that the current decays at a faster rate for the first few minutes and then the decay rate slows down to reach the steady value. The transients are observed to obey the Curie Von Schweilder relationship.

$$I(t) = A(T) t^{-n}$$

where t is the time after the application or removal of the field, $A(T)$ is a temperature dependent factor and n is the decay constant.

The charging and discharging currents are mirror image of each other, in most of the cases.

A similar type of charging and discharging currents behaviour is also observed for the PVP samples of same thickness poled at same temperatures and field conditions for Ag-PVP-Ag, Cu-PVP-Cu and Sn-PVP-Sn configurations, as shown in Figs. 5.2, 5.3 and 5.4, respectively. No appreciable change in behaviour of charging and discharging currents is noticed when

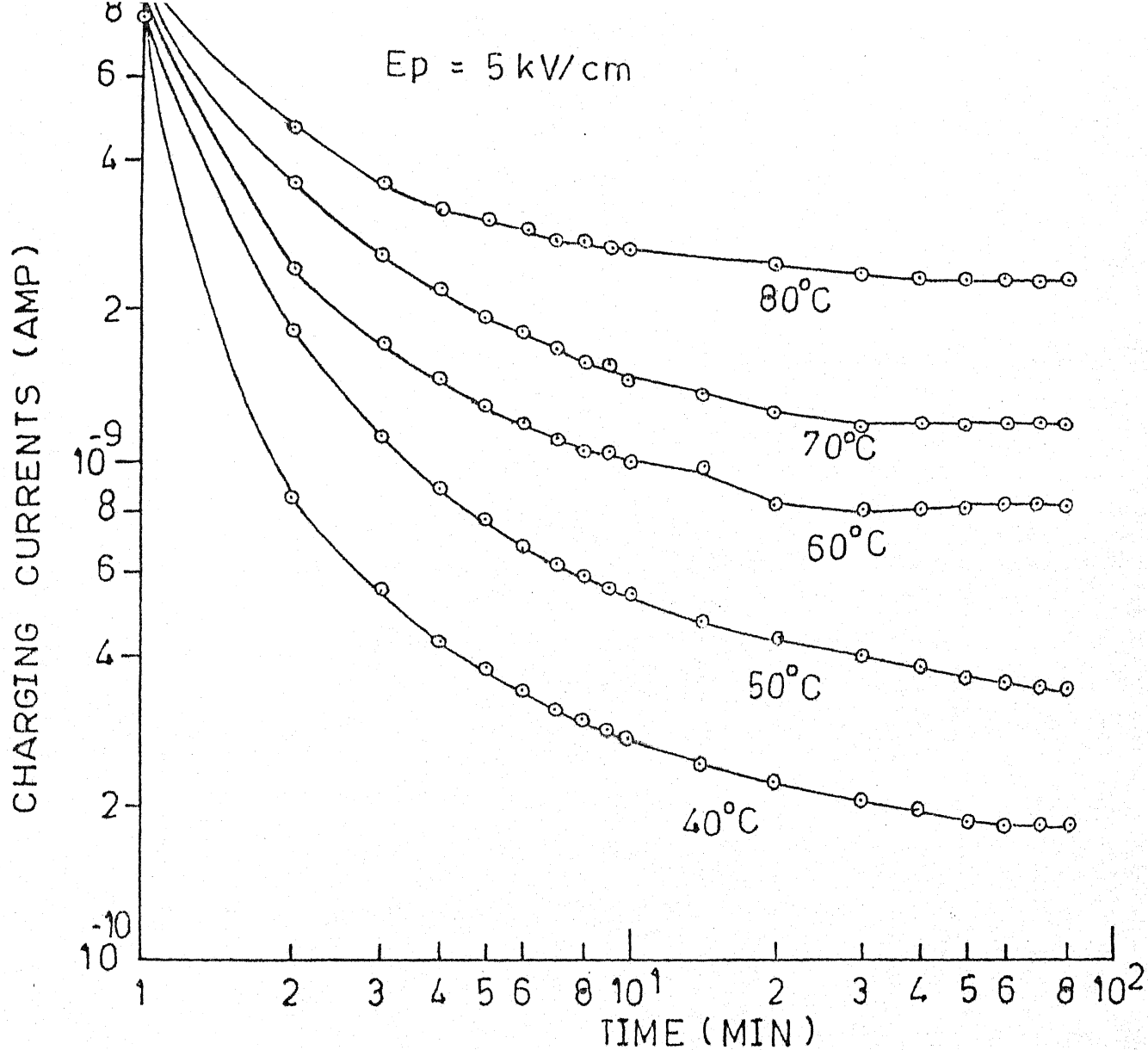


Fig. 5.1 (a) Transient current curves for charging mode at polarising field and temperatures as mentioned, with Al-Al system.

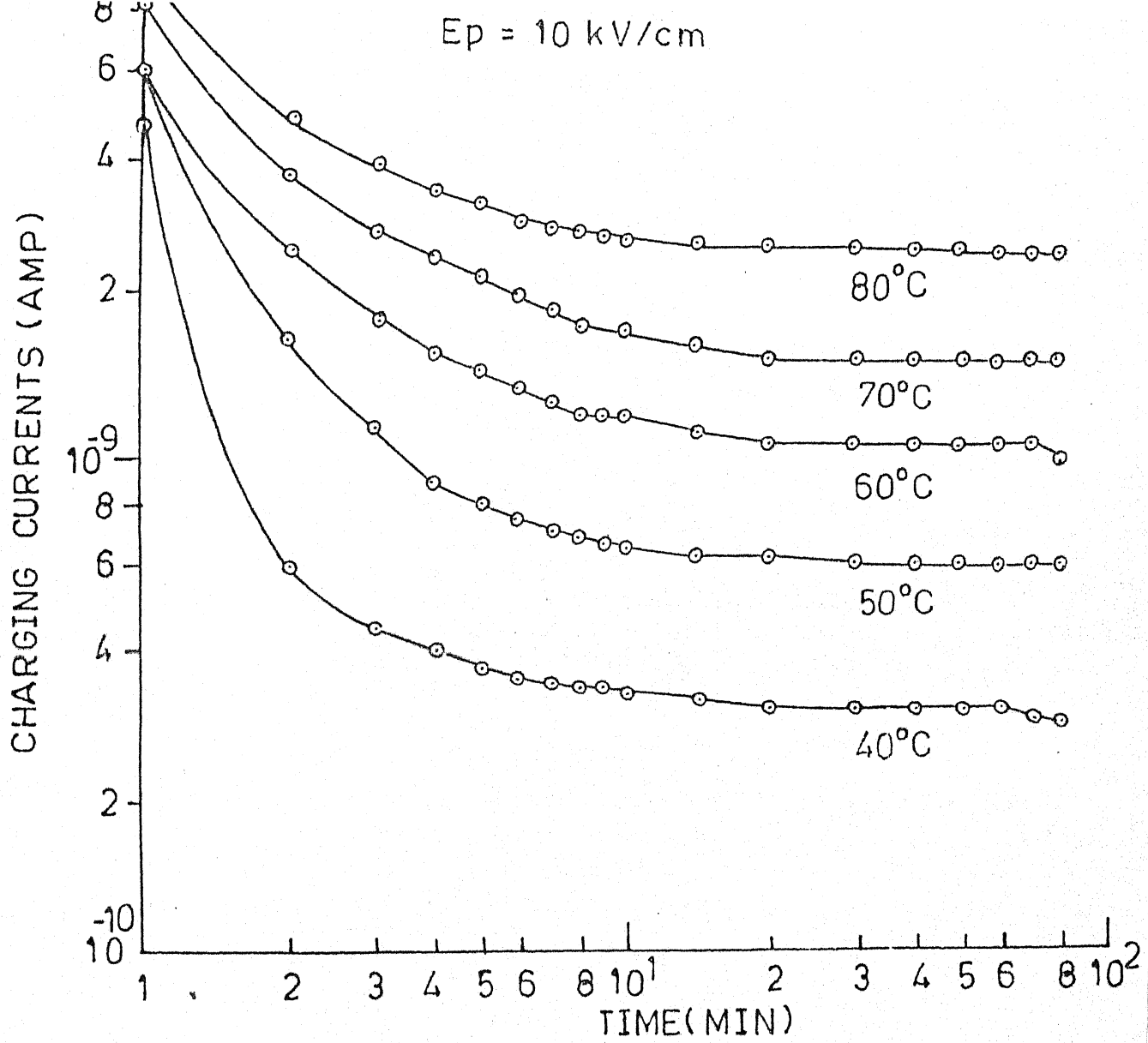


Fig.5.1 (a) Transient current curves for charging mode at polarising field and temperatures as mentioned, with Al-Al system.

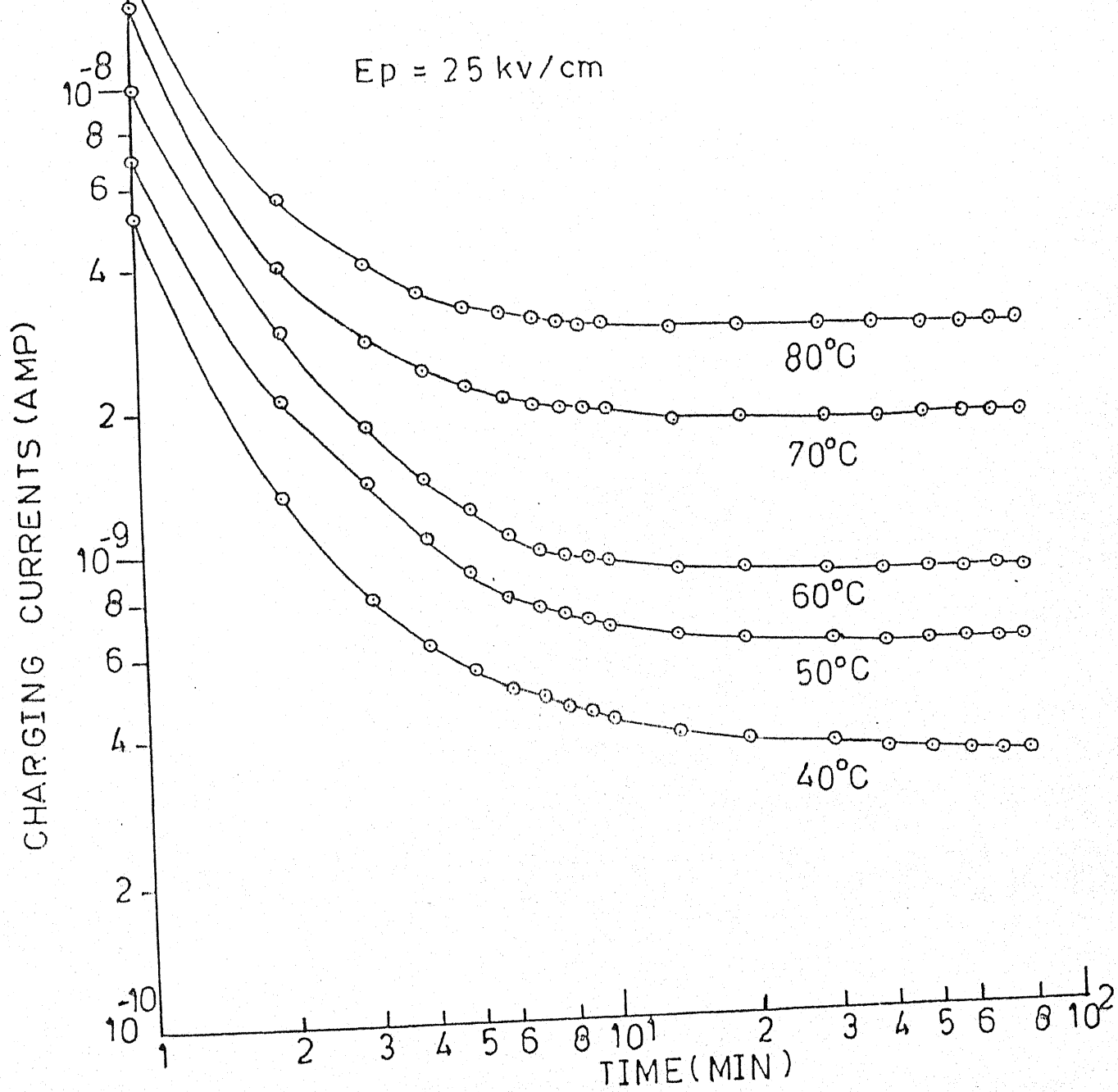


Fig. 5.1 (b) Transient current curves for charging mode at polarising field and temperatures as mentioned, with Al-Al system.

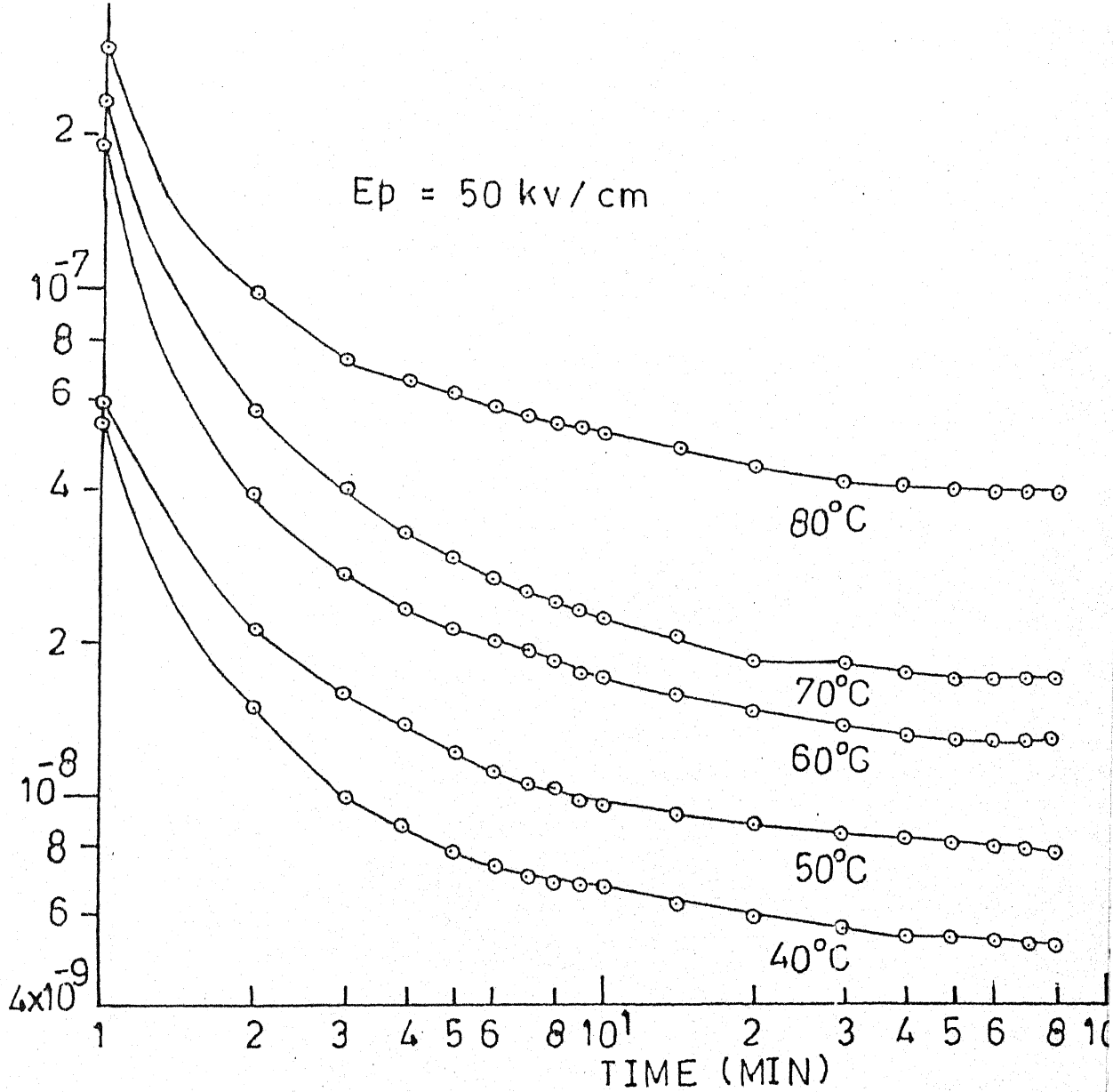


Fig.5.1 (b) Transient current curves for charging mode at polarising field and temperatures as mentioned, with Al-Al system.

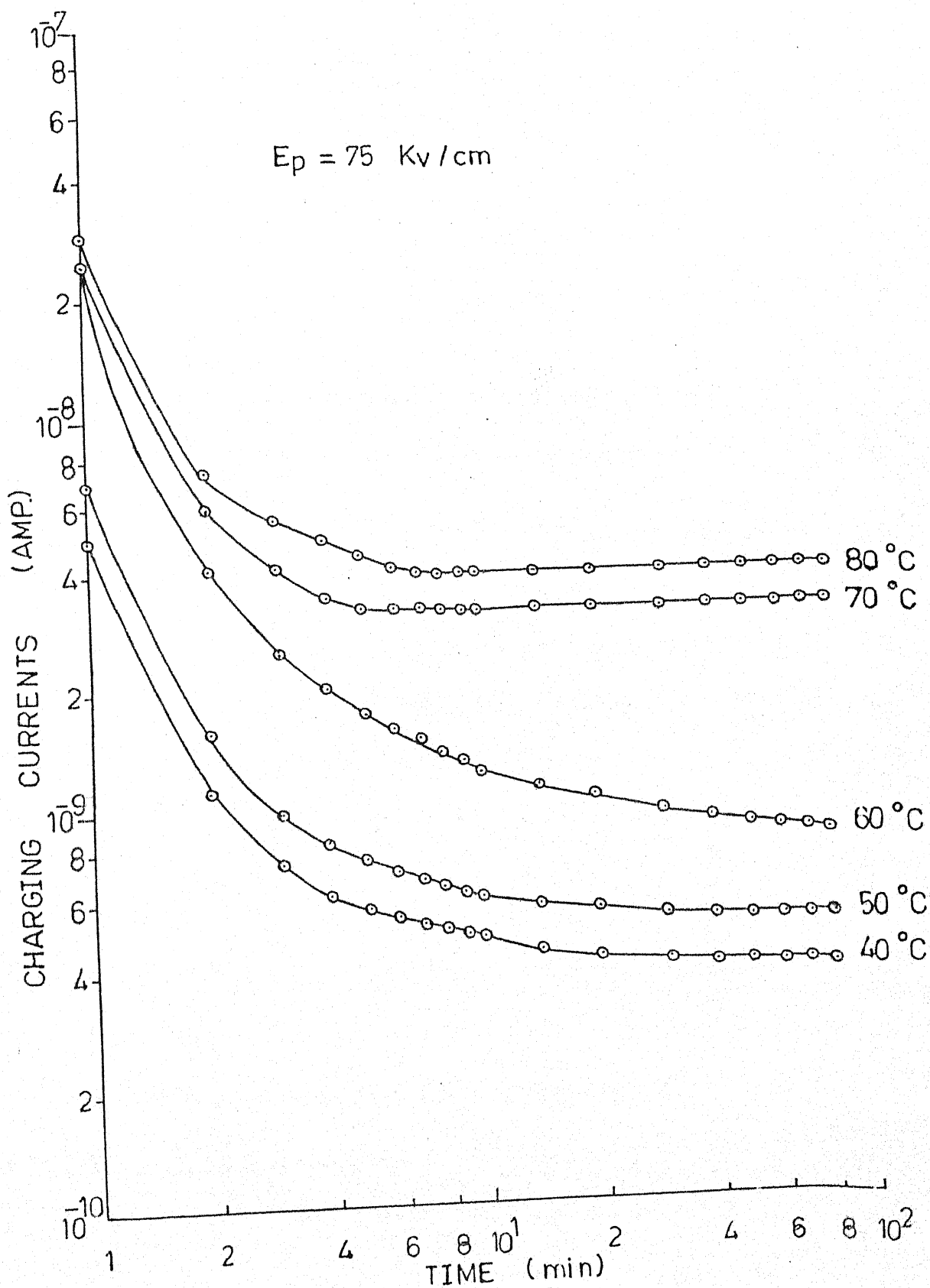


Fig. 5.1 (c) Transient current curves for charging mode at polarising field and temperatures as mentioned, with Al-Al system.

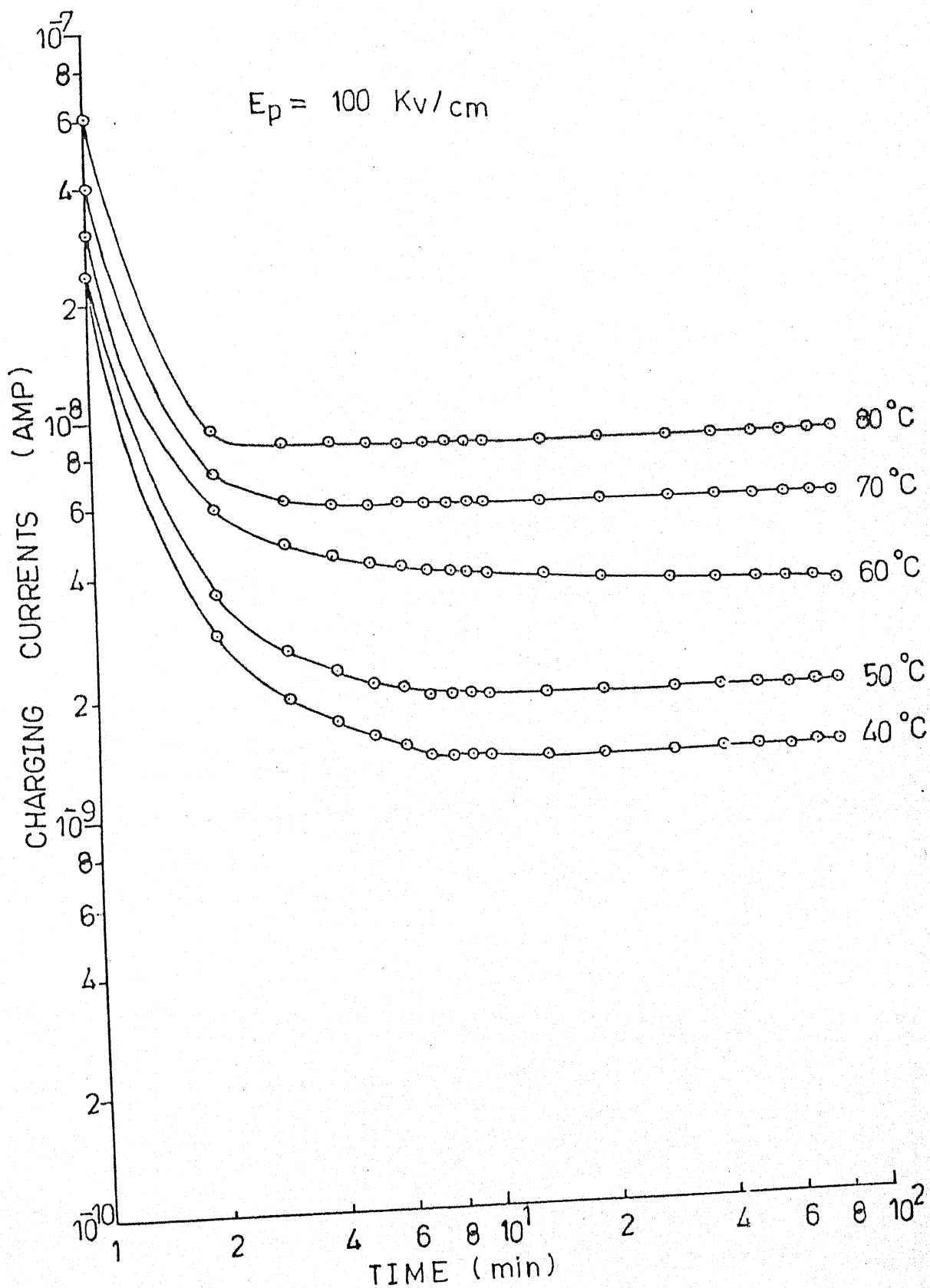


Fig.5.1 (c) Transient current curves for charging mode at polarising field and temperatures as mentioned, with Al-Al system.

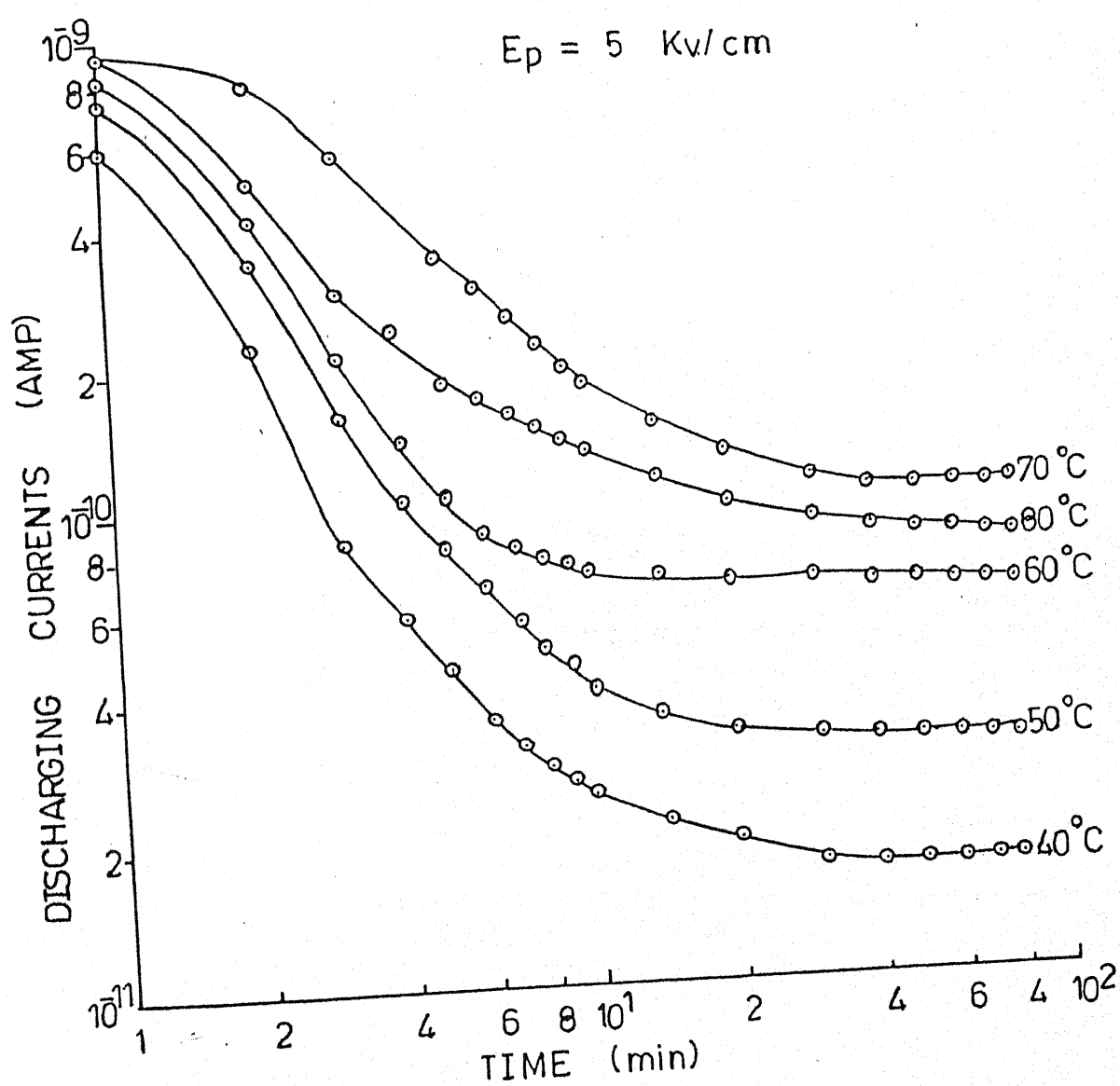


Fig.5.1 (A) Transient current curves for discharging mode at polarising field and temperatures as mentioned, with Al-Al system.

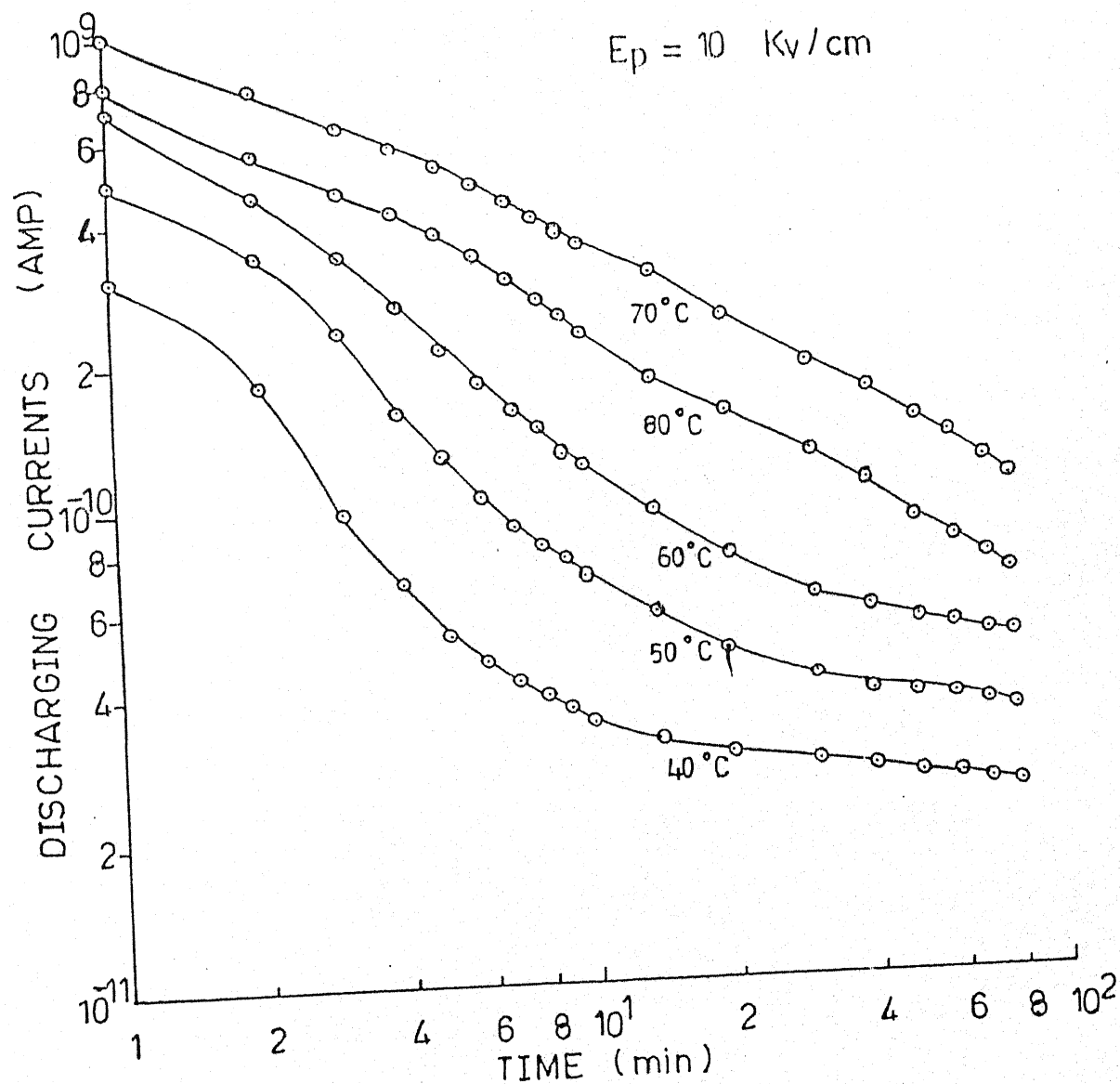


Fig.5.1 (A)

Transient current curves for discharging mode at polarising field and temperatures as mentioned, with Al-Al system.

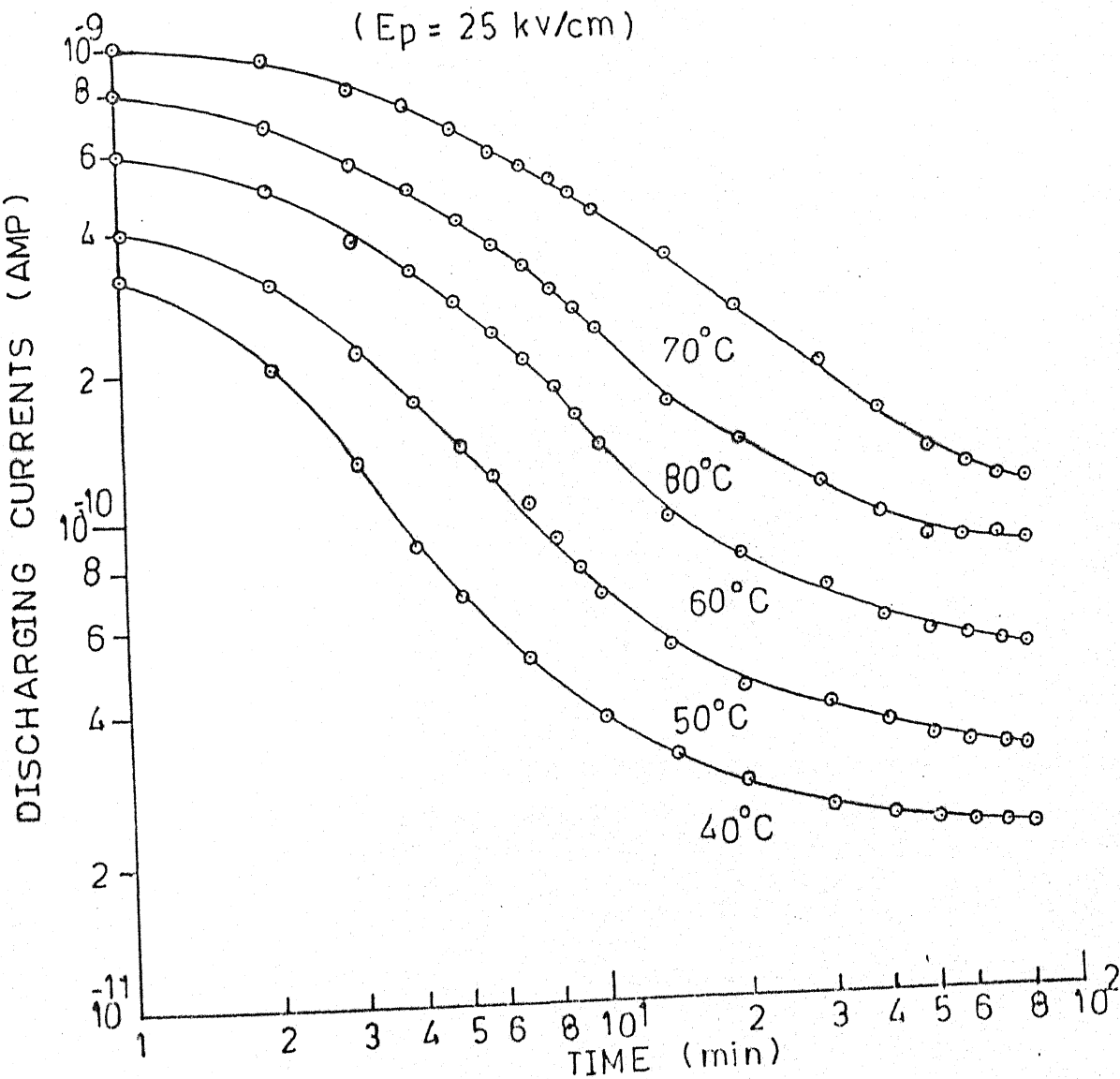


Fig.5.1 (B) Transient current curves for discharging mode at polarising field and temperatures as mentioned, with Al-Al system.

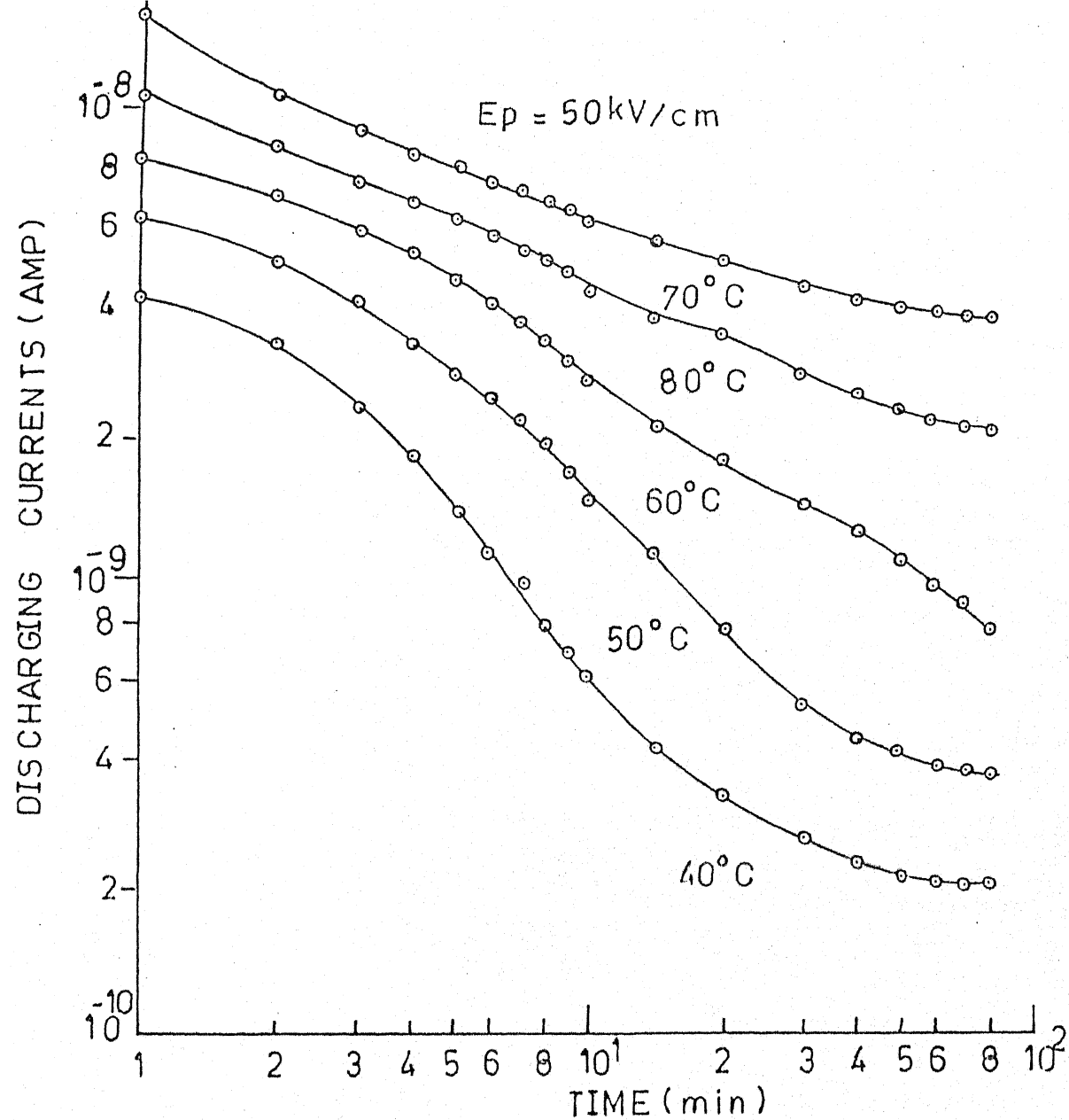


Fig.5.1 (B) Transient current curves for discharging mode at polarising field and temperatures as mentioned, with Al-Al system.

$$E_p = 75 \text{ Kv / cm}$$

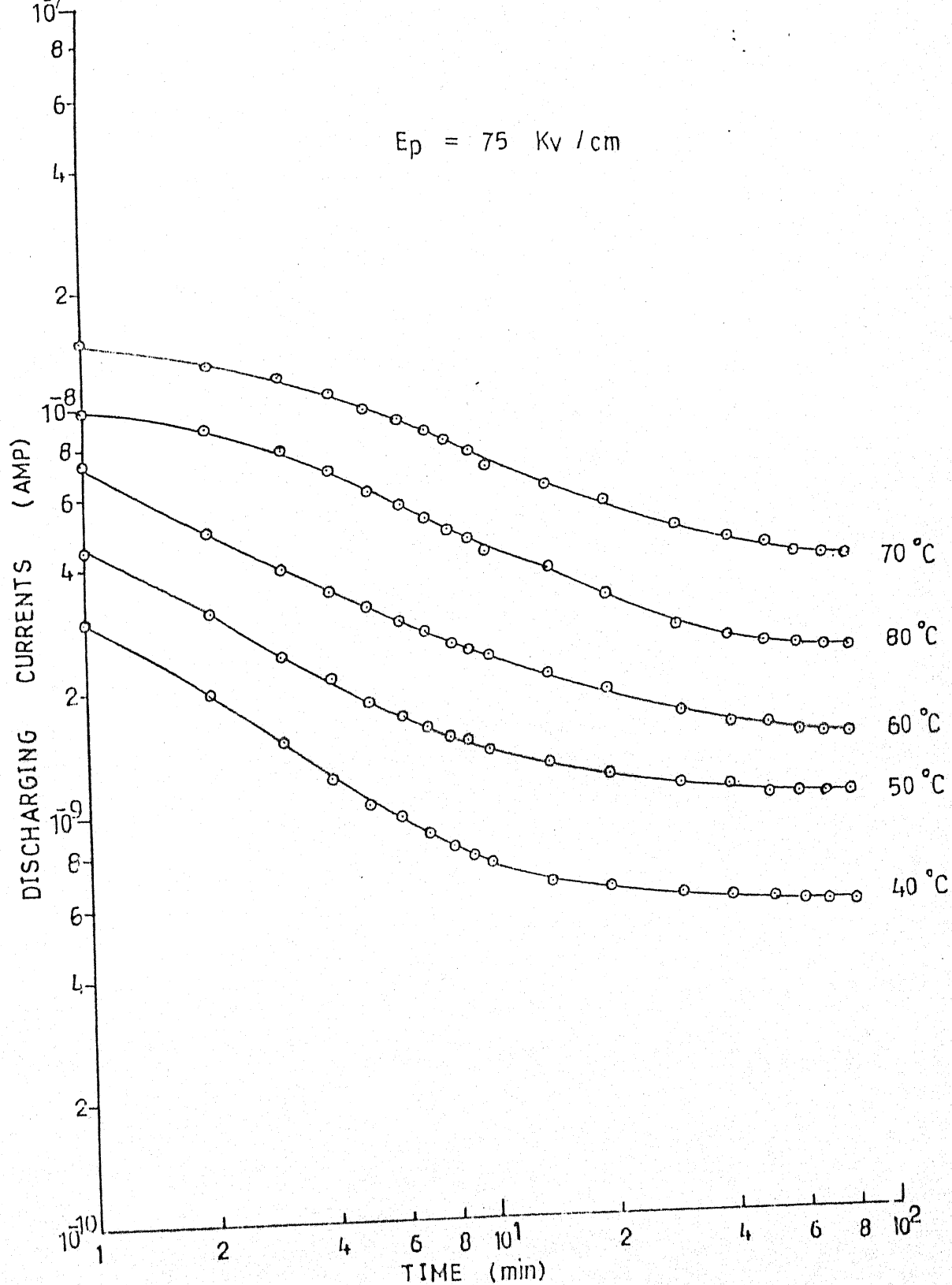


Fig.5.1 (C) Transient current curves for discharging mode at polarising field and temperatures as mentioned, with Al-Al system.

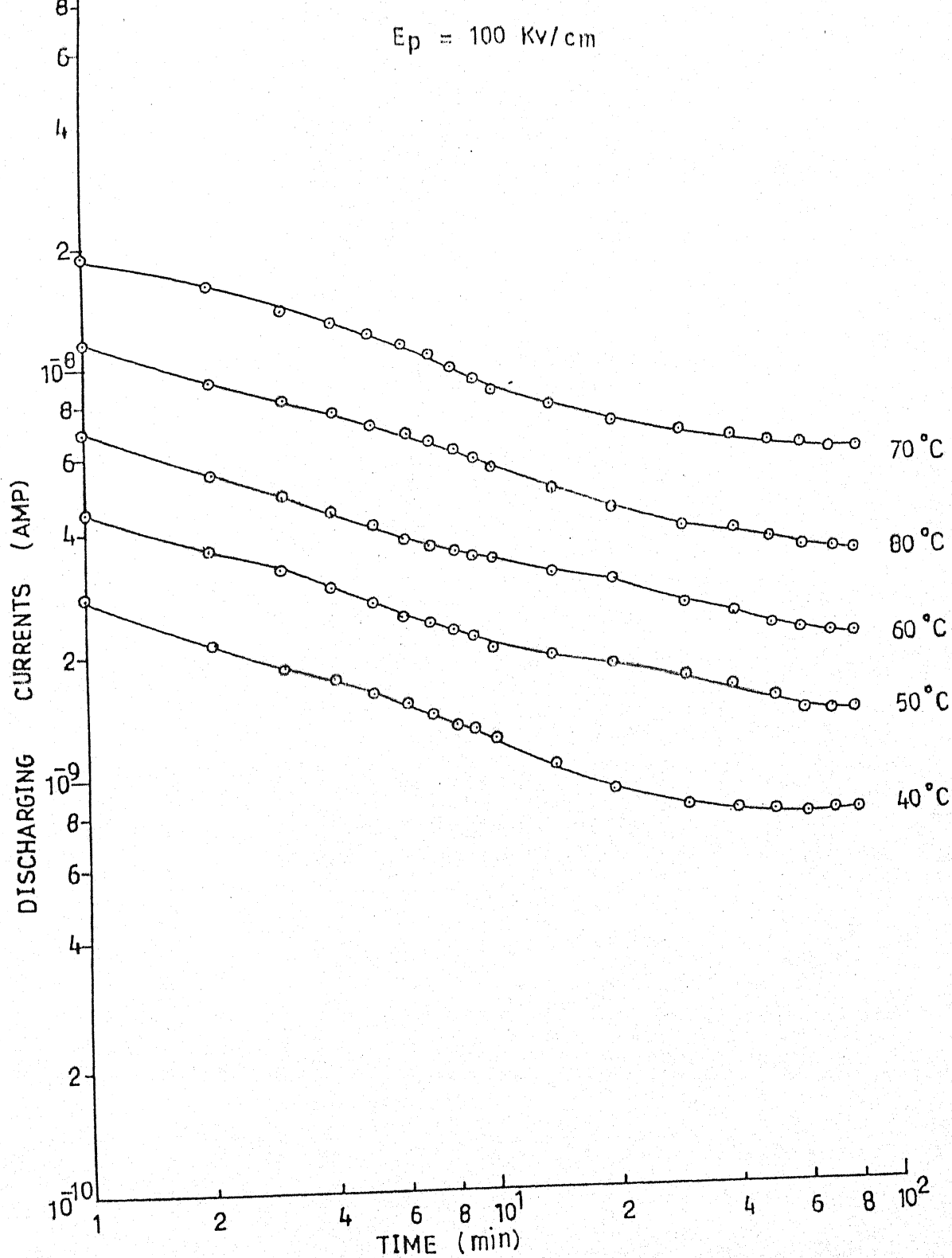


Fig.5.1 (C) Transient current curves for discharging mode at polarising field and temperatures as mentioned, with Al-Al system.

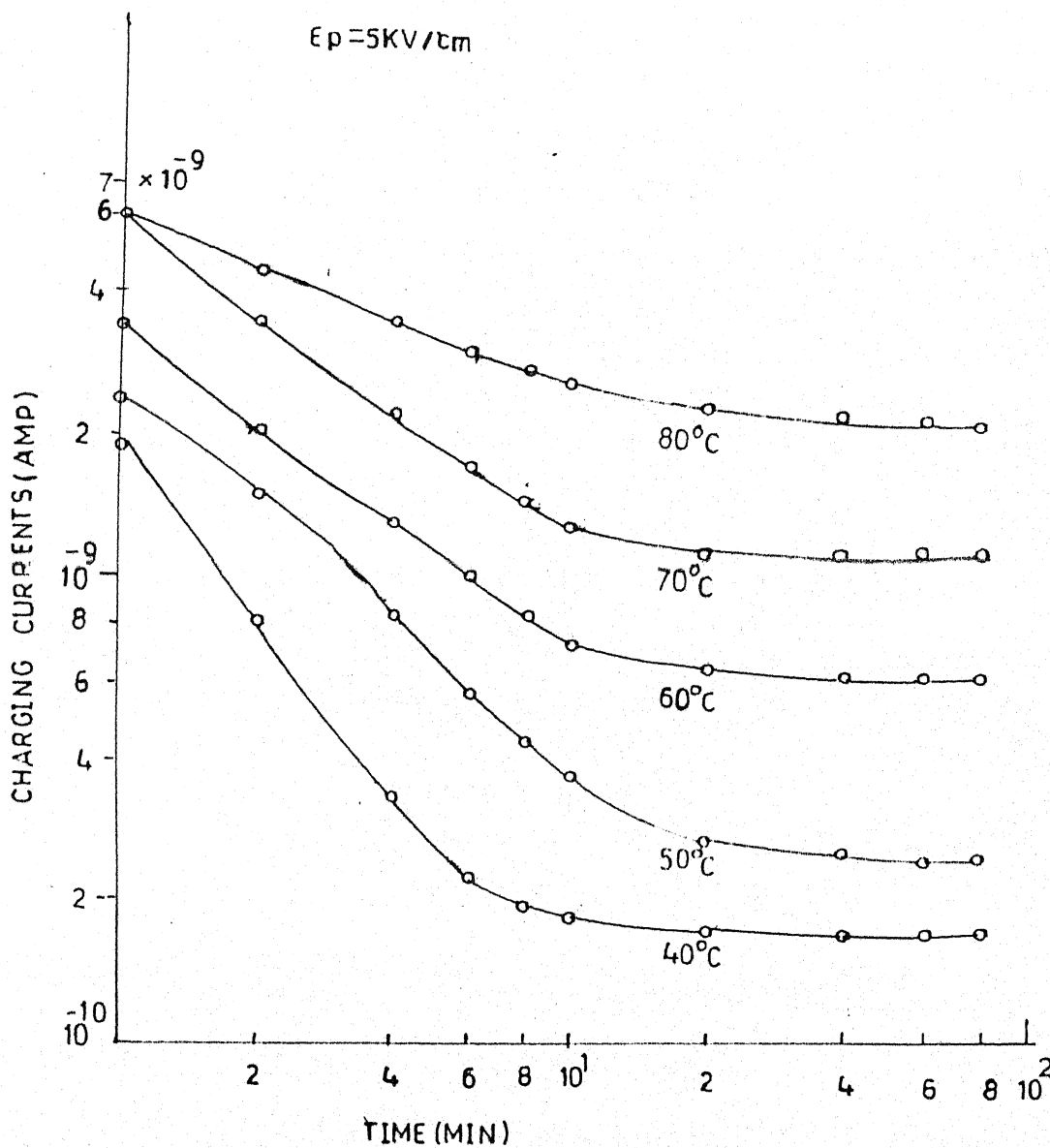


Fig 5.2(a) Transient current curves for charging mode at given polarising field and different temperatures with Ag-Ag system.

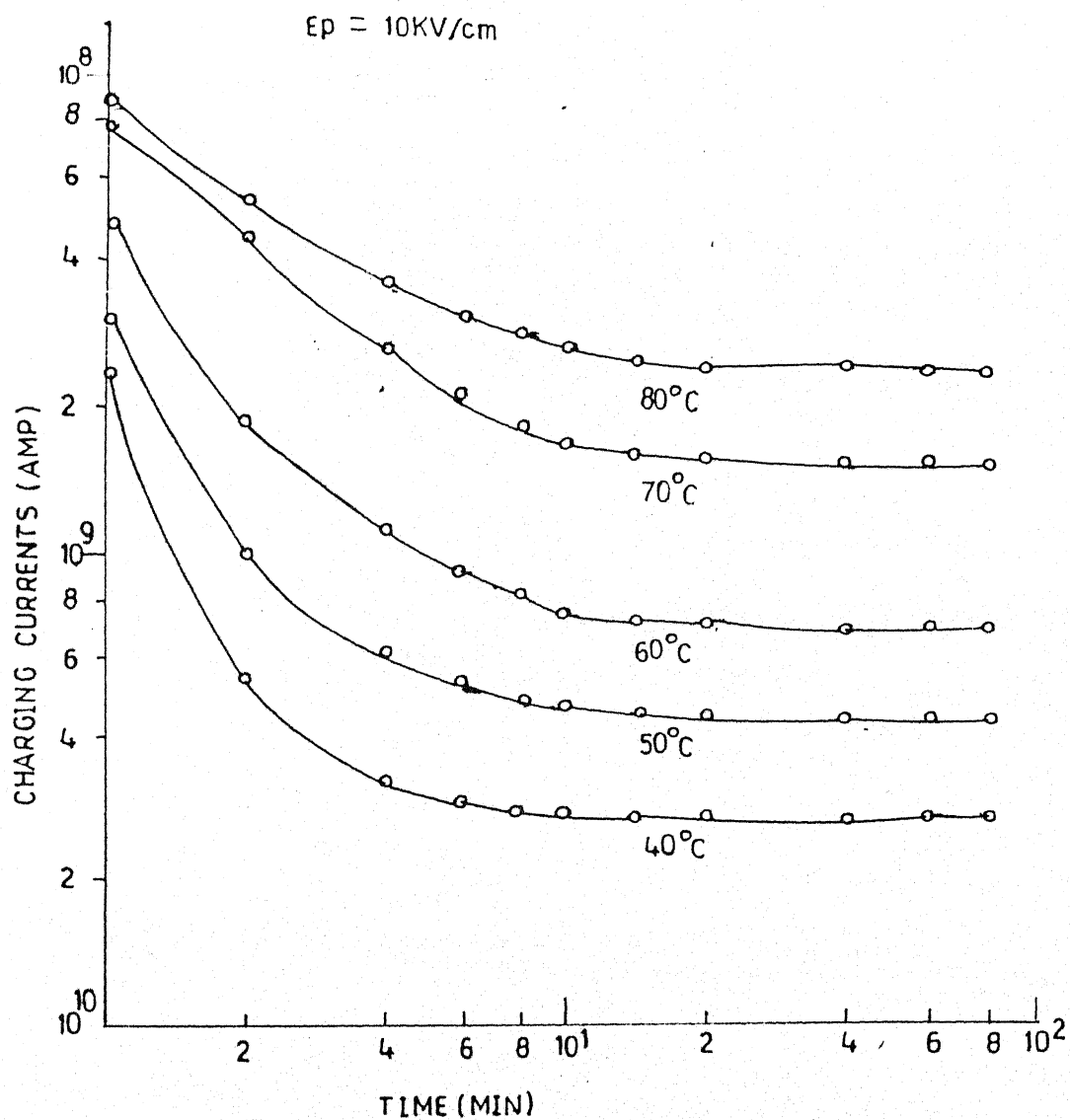


Fig 5.2(a) : Transient current curves for charging mode at given polarising field and different temperatures with Ag-Ag system.

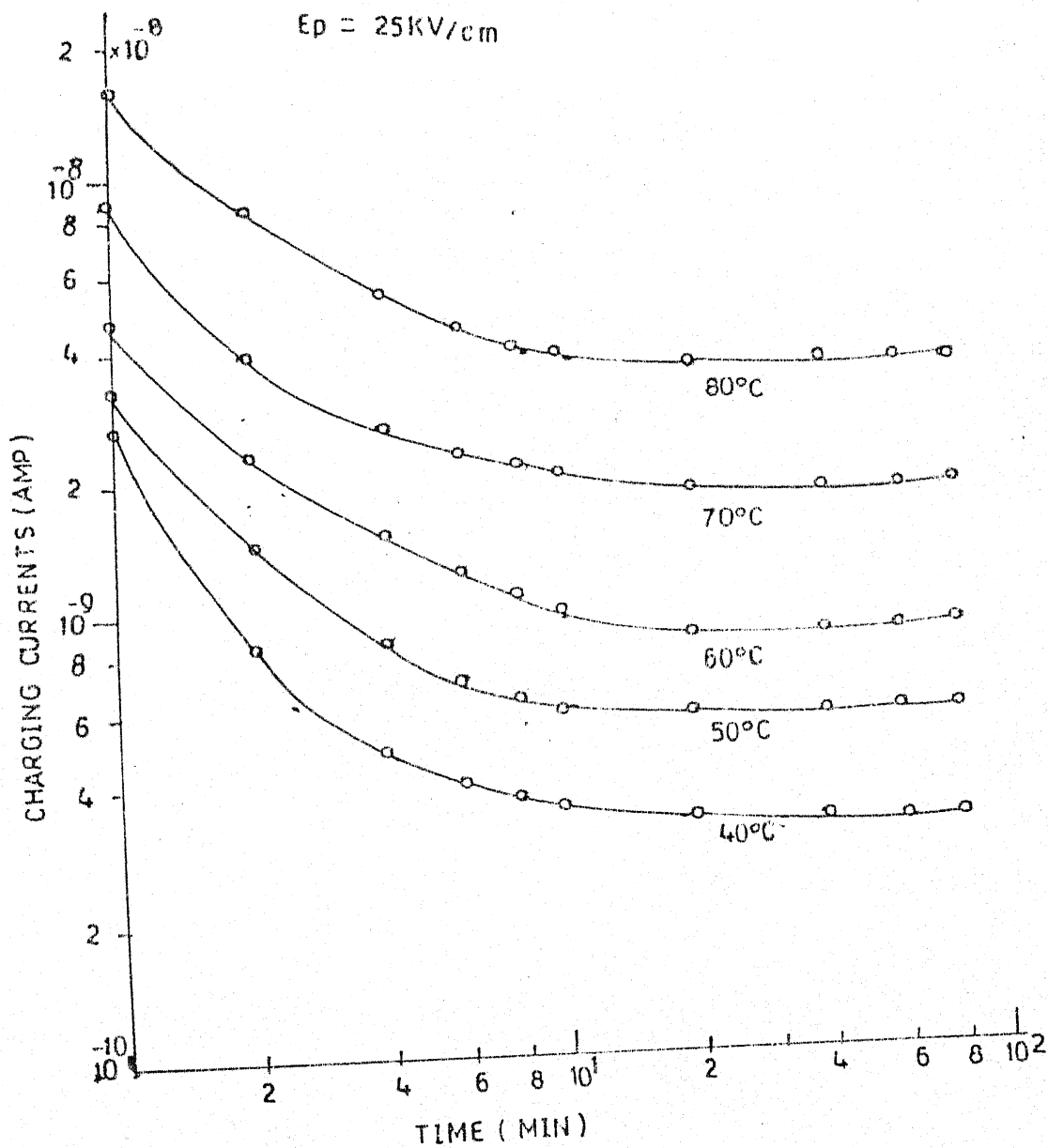


Fig 5.2(b) : Transient current curves for charging mode at given polarising field and different temperatures with Ag-Ag system.

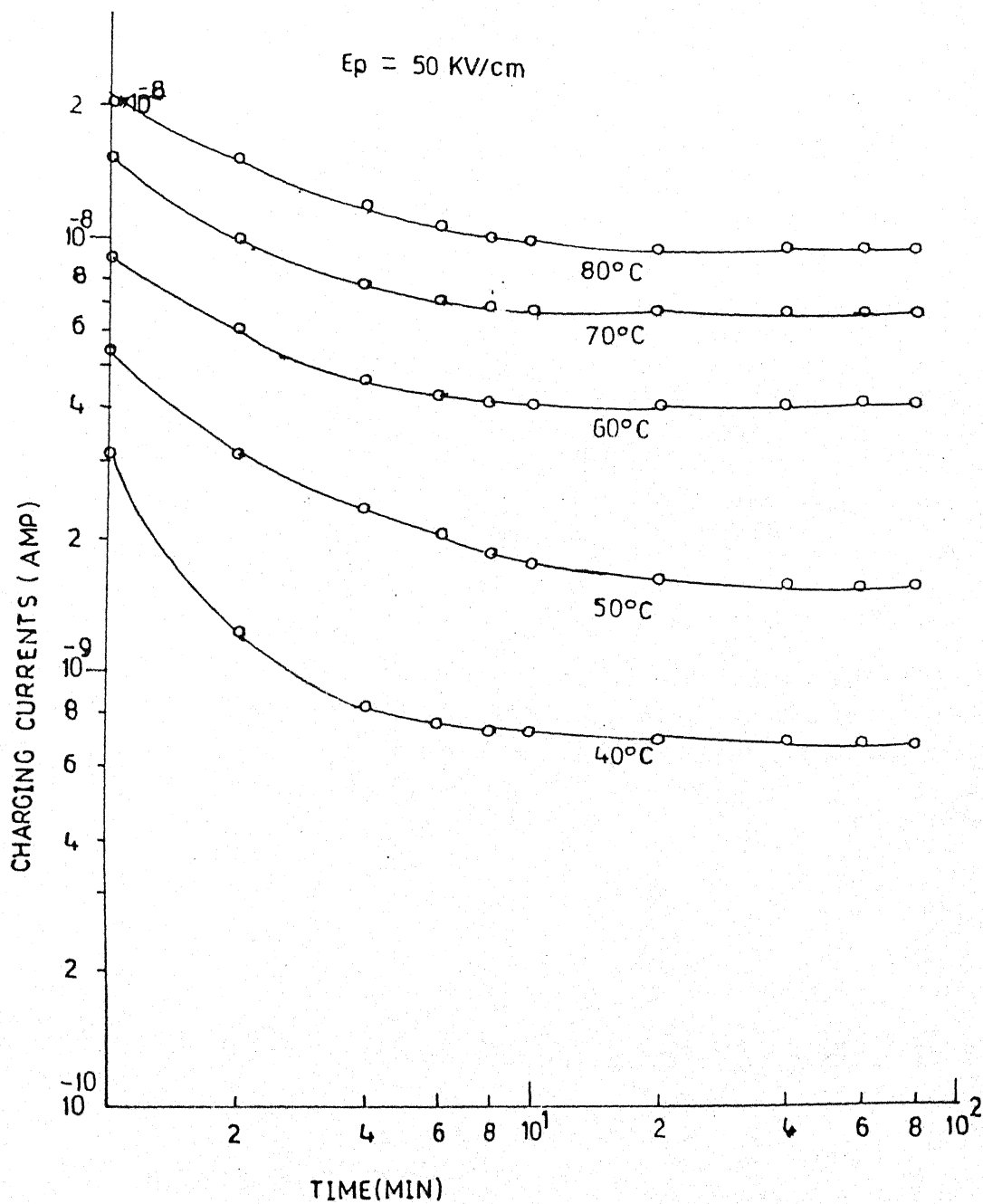


Fig 5.2(b) : Transient current curves for charging mode at given polarising field and different temperatures with Ag-Ag system.

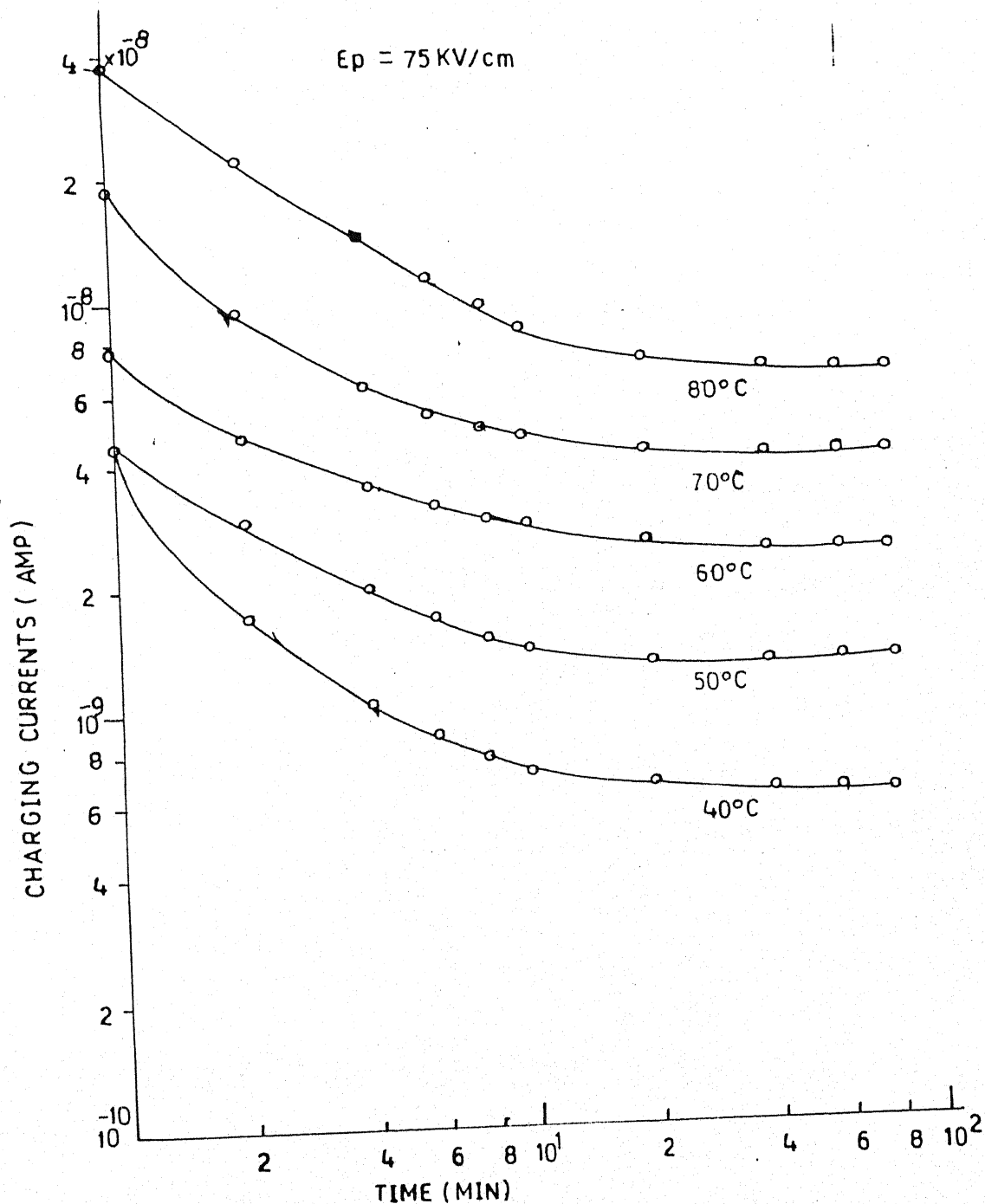


Fig 5.2(c) : Transient current curves for charging at given polarising field and different temperatures with Ag-Ag system.

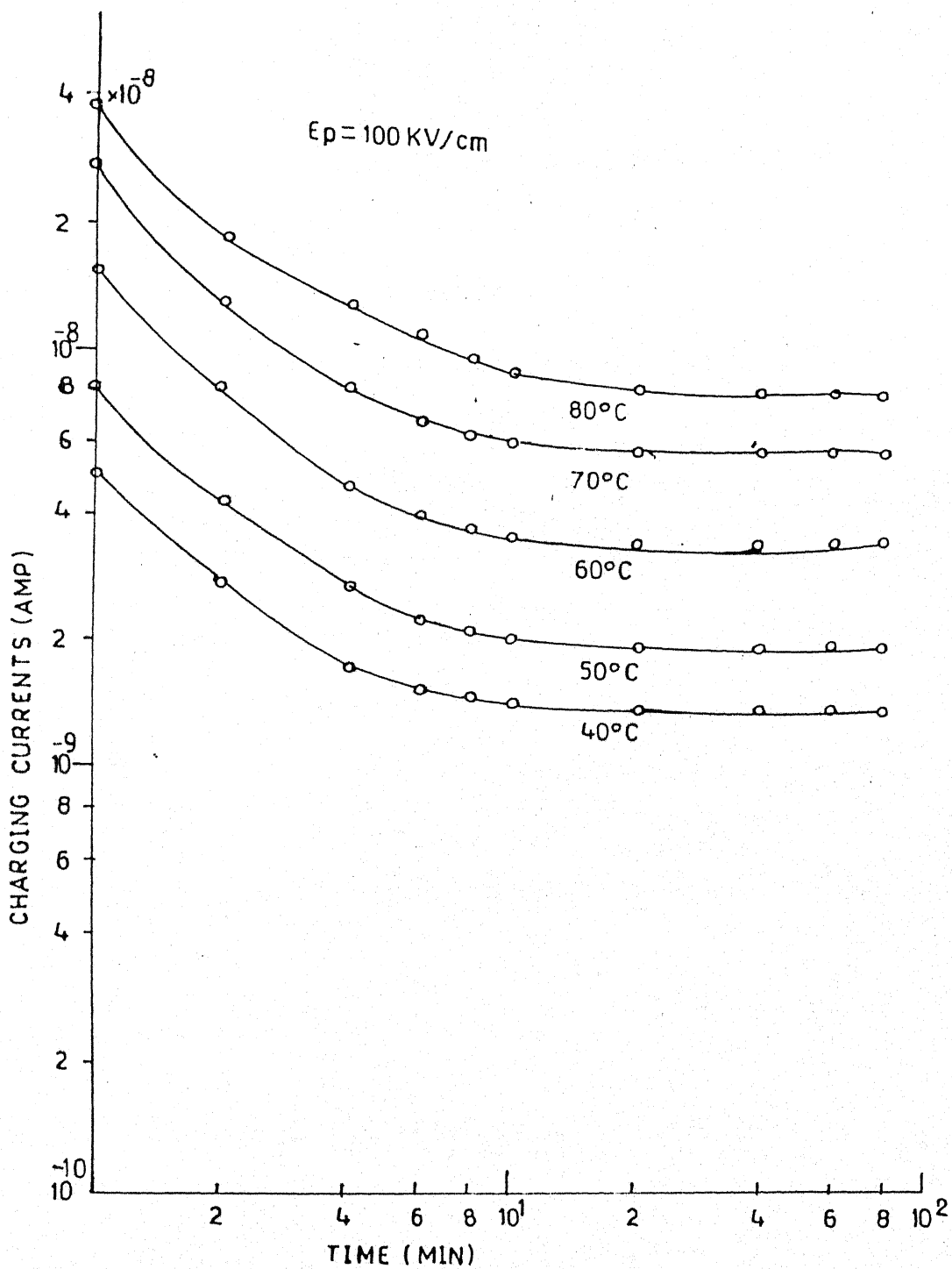


Fig 5.2(c) : Transient current curves for charging ^{mode} at given polarising field and different temperatures with Ag-Ag system

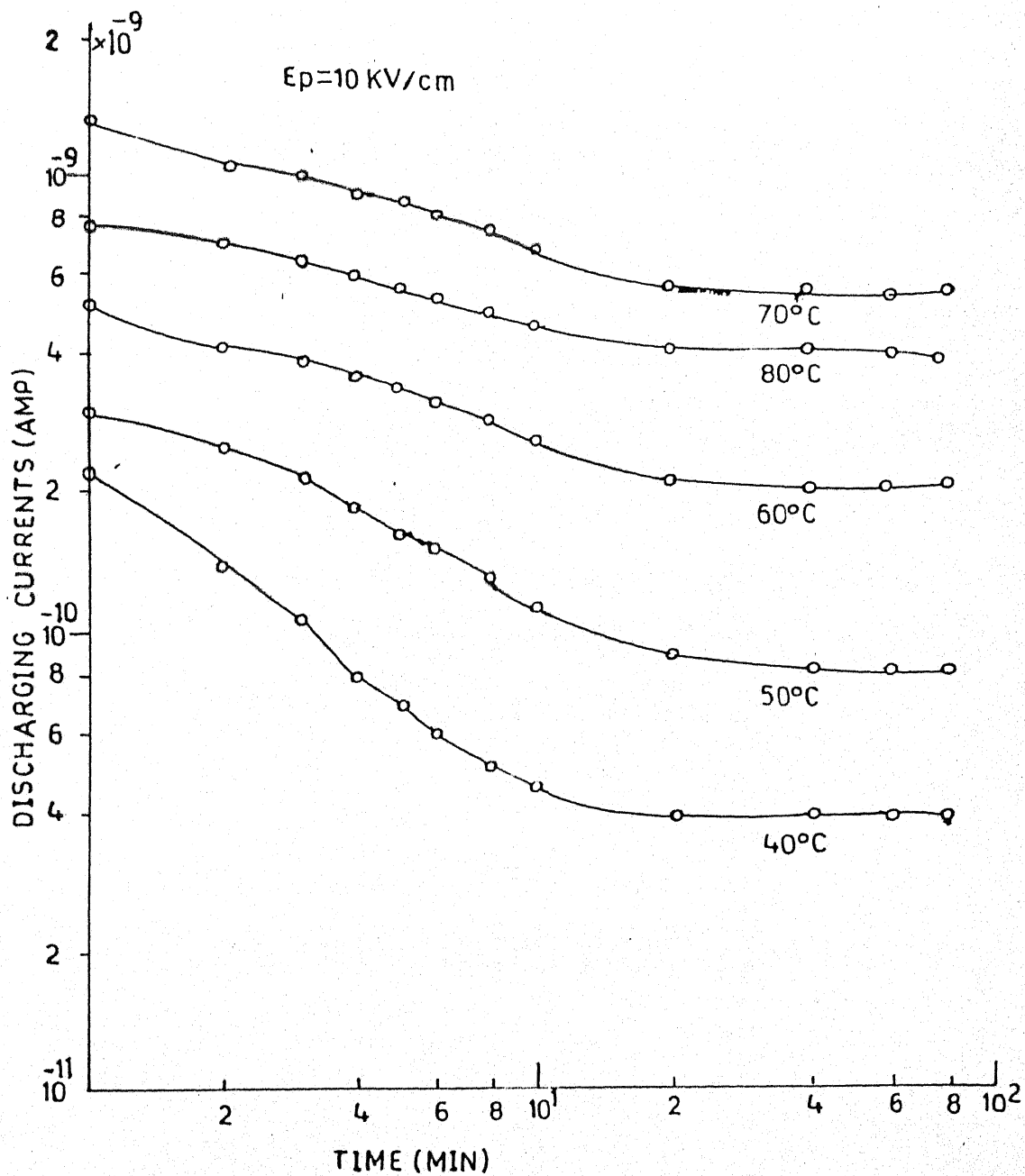


Fig 5.2(A): Transient current curves for discharging mode at given polarising field and different temperatures with Ag-Ag system

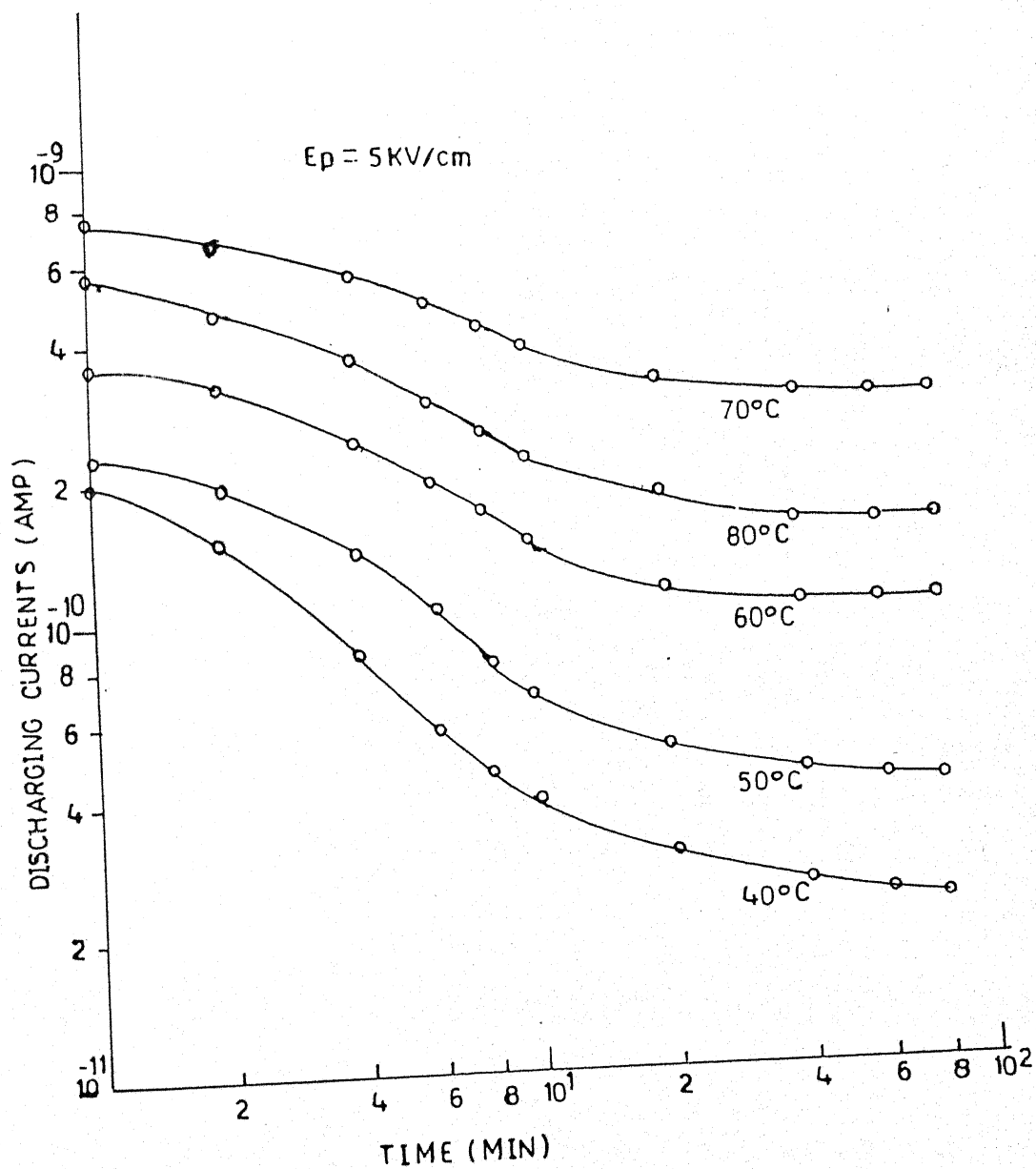


Fig 5.2(A) : Transient current curves for discharging mod given polarising field and different temperatures with Ag-Ag system

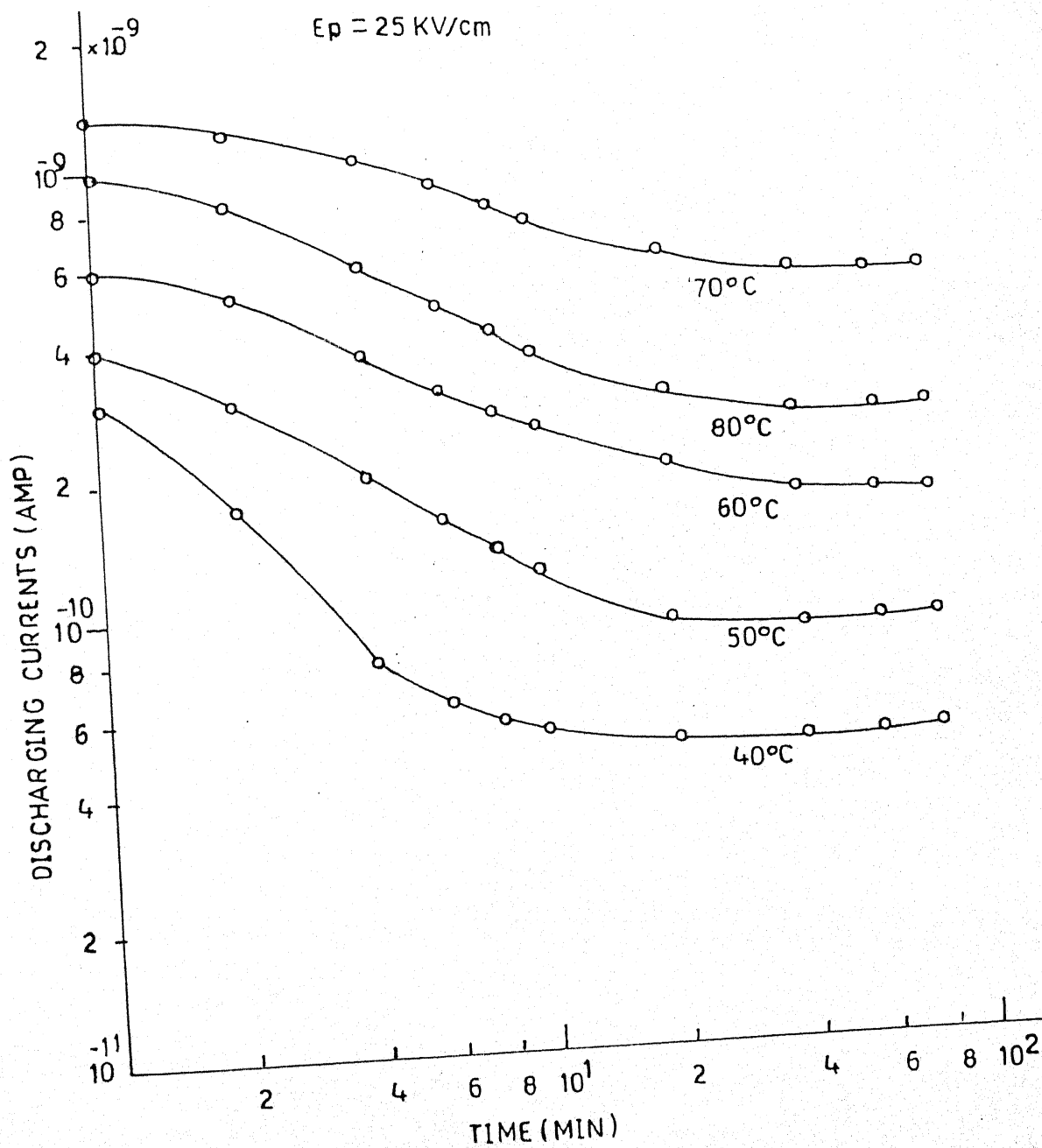


Fig 5.2(B): Transient current curves for discharging mode at given polarising field and different temperatures with Ag-Ag system

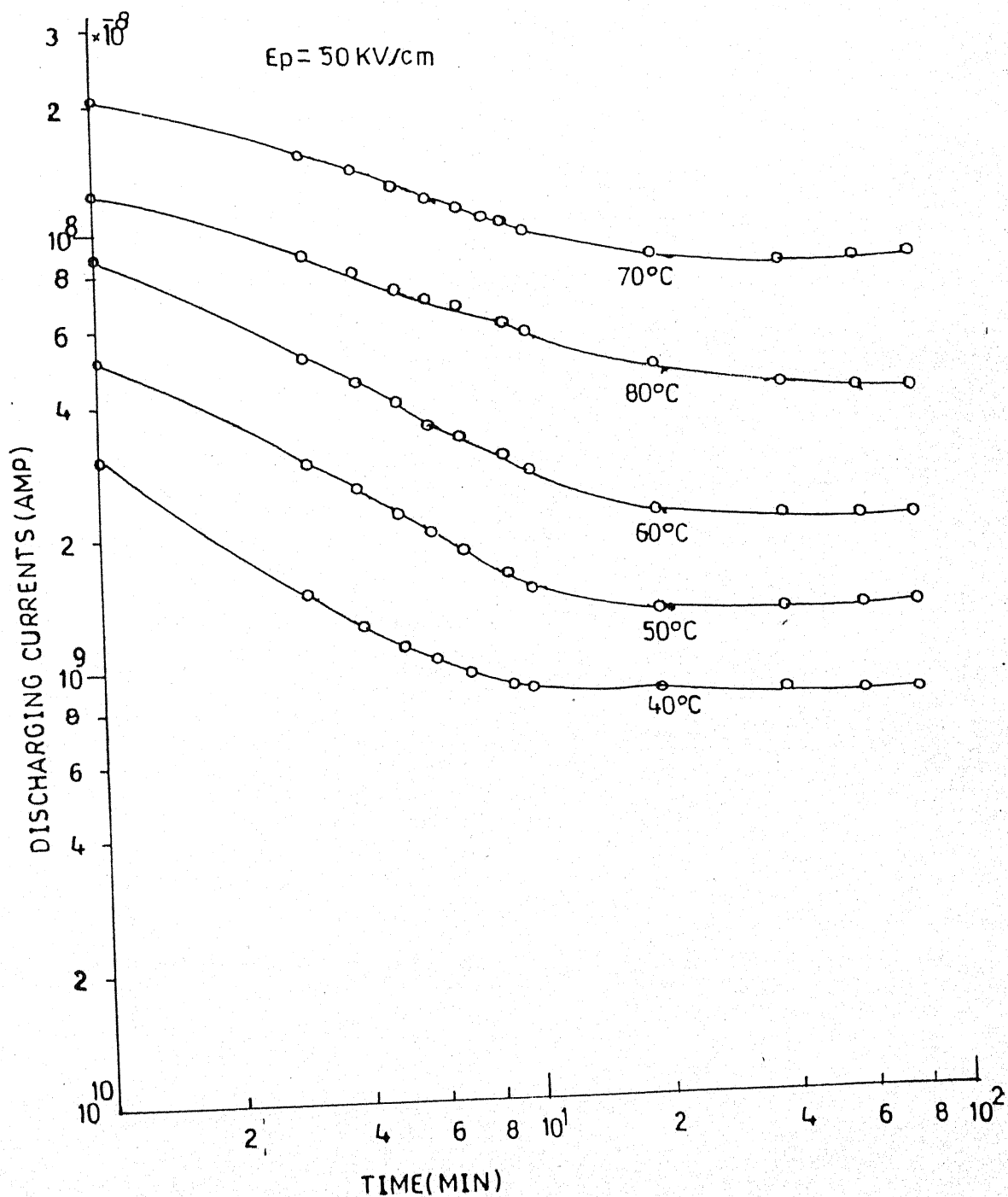


Fig 5.2(B): Transient current curves for discharging mode at given polarising field and different temperatures with Ag-Ag system

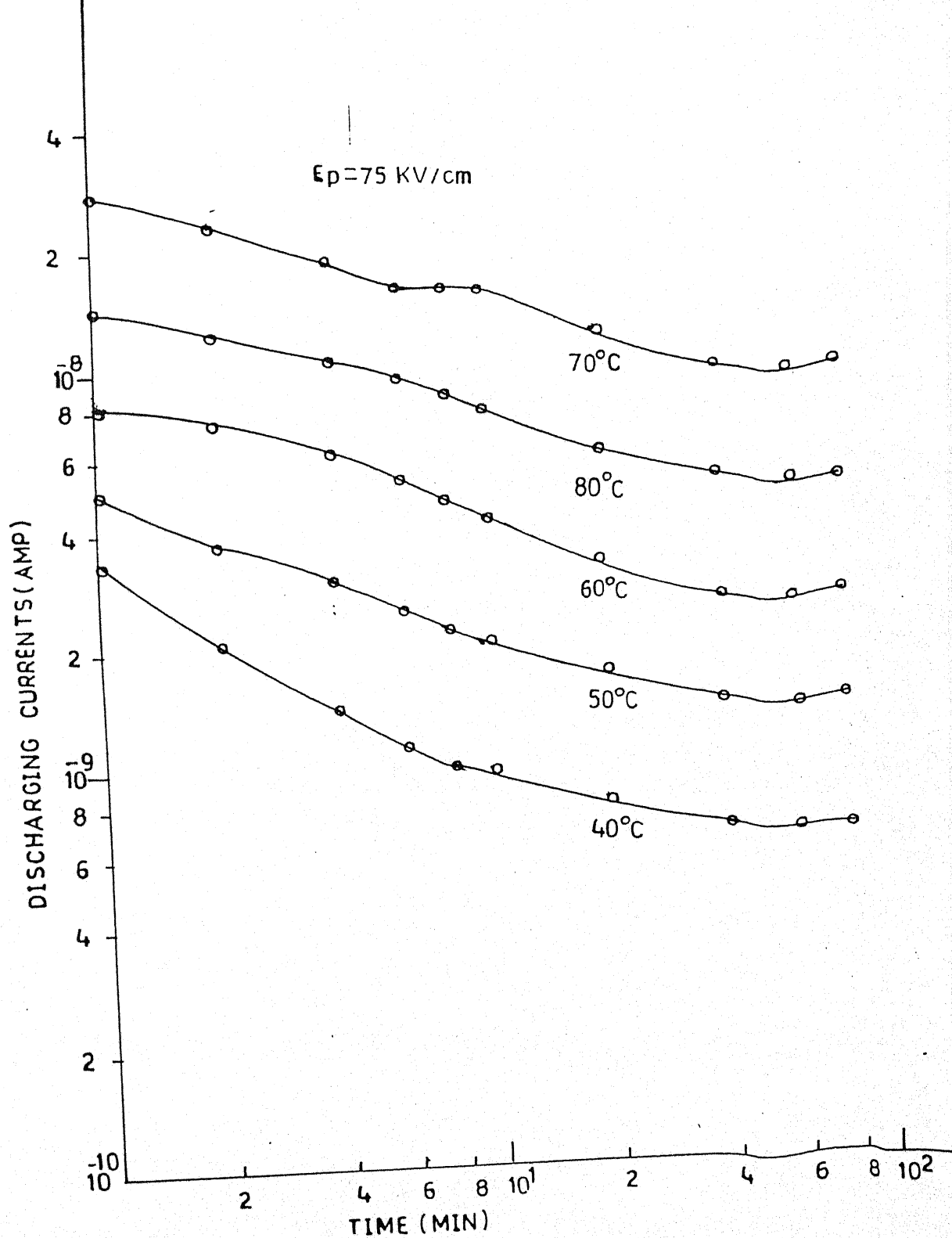


Fig 5.2(C): Transient current curves for discharging mode at given polarising field and different temperatures with Ag-Ag system

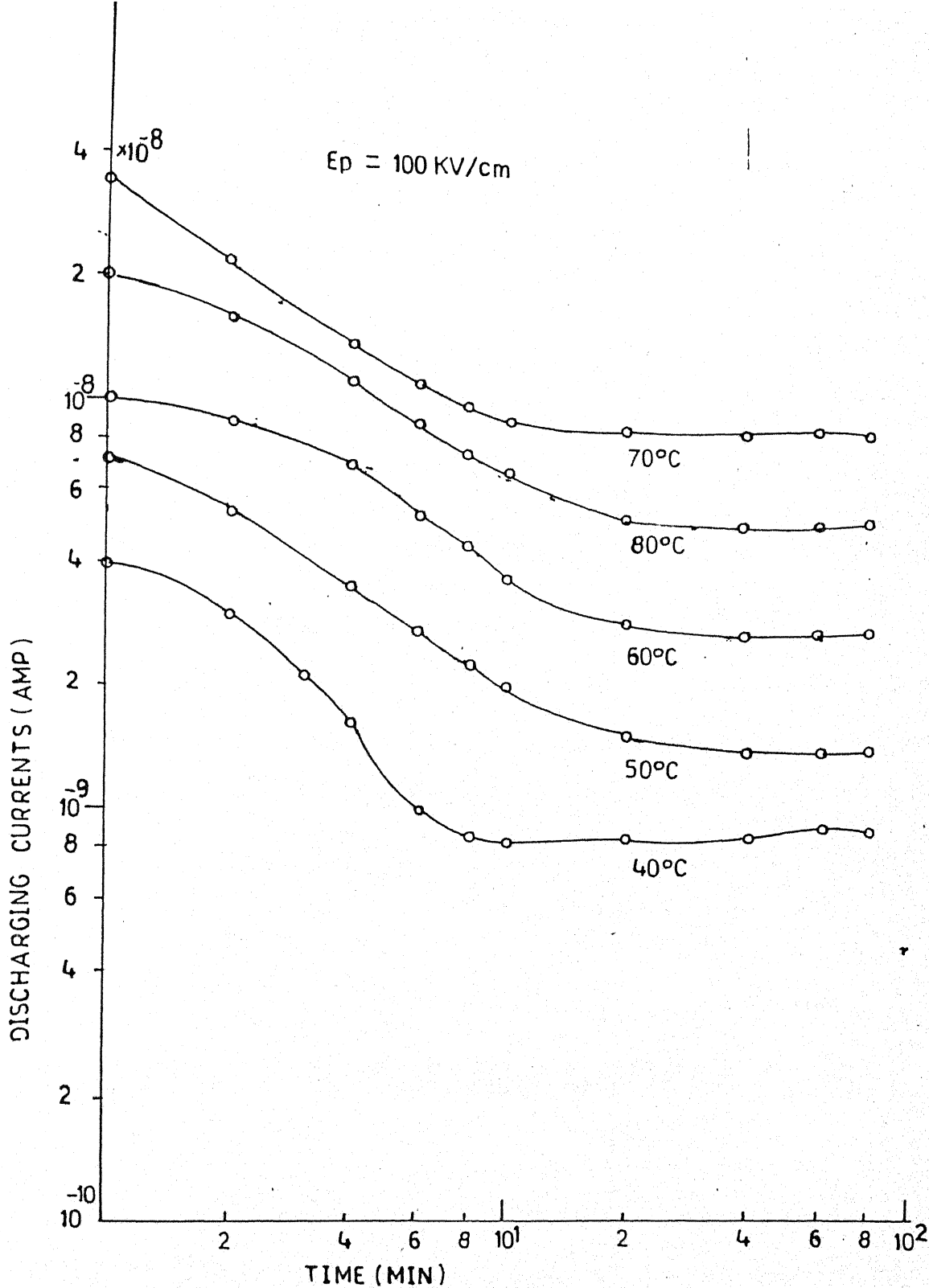


Fig 5.2(C): Transient current curves for discharging mode at given polarising field and different temperatures with Ag-Ag system

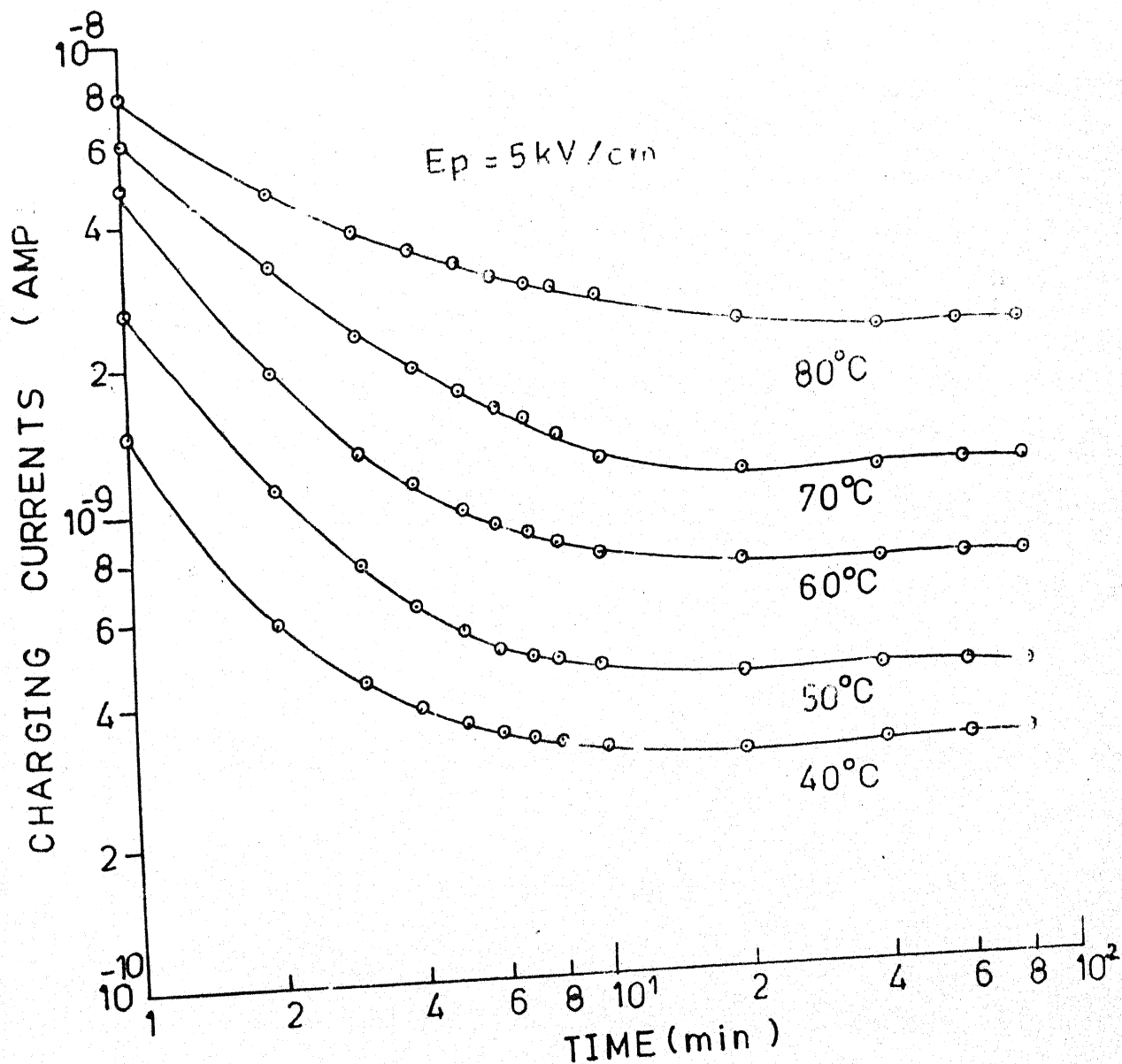


Fig. 5.3 (a) Transient current curves for charging mode at polarising field and different temperatures with Cu-Cu system.

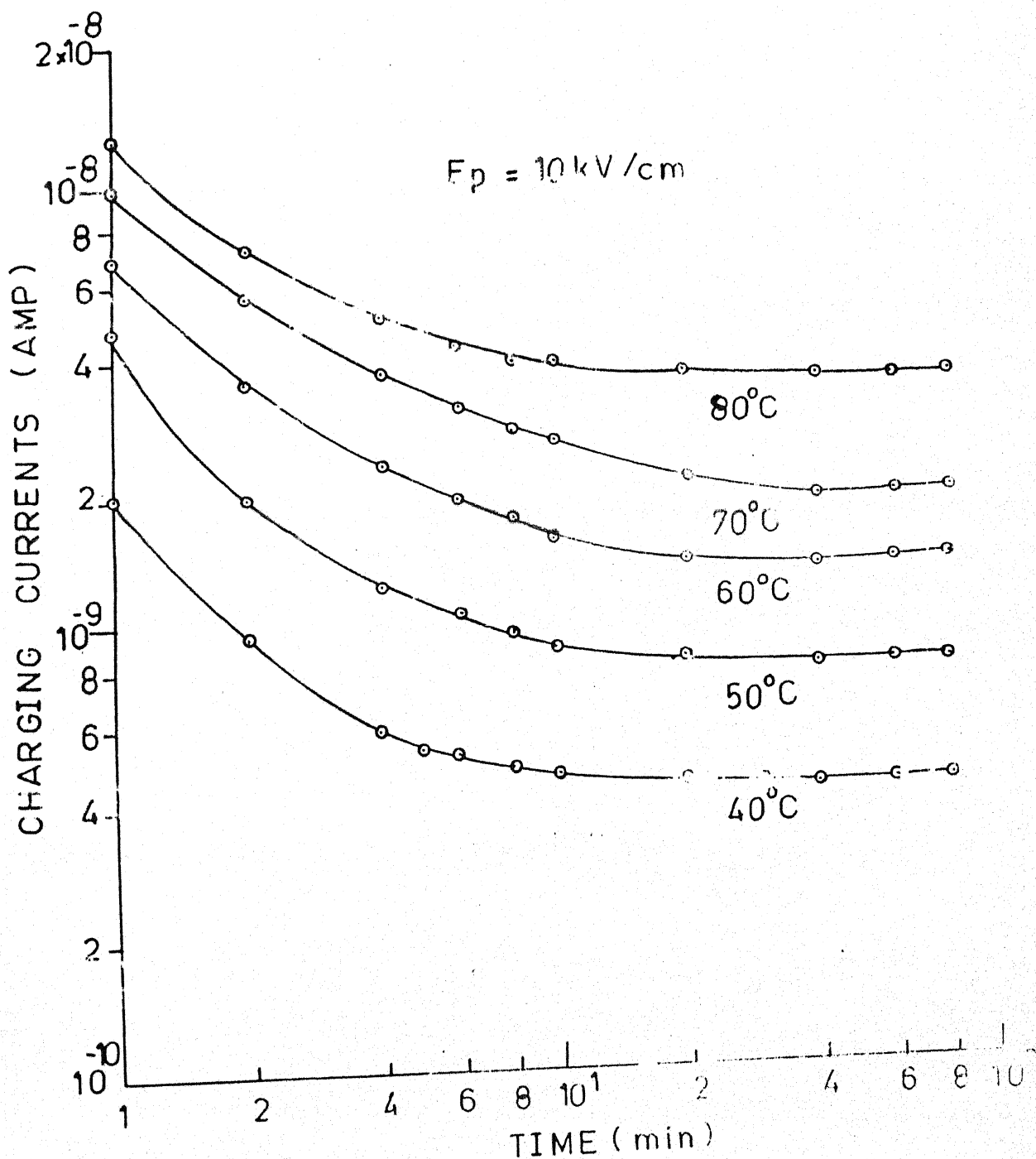


Fig. 5.3 (a) Transient current curves for charging mode at polarising field and different temperatures with Cu-Cu system.

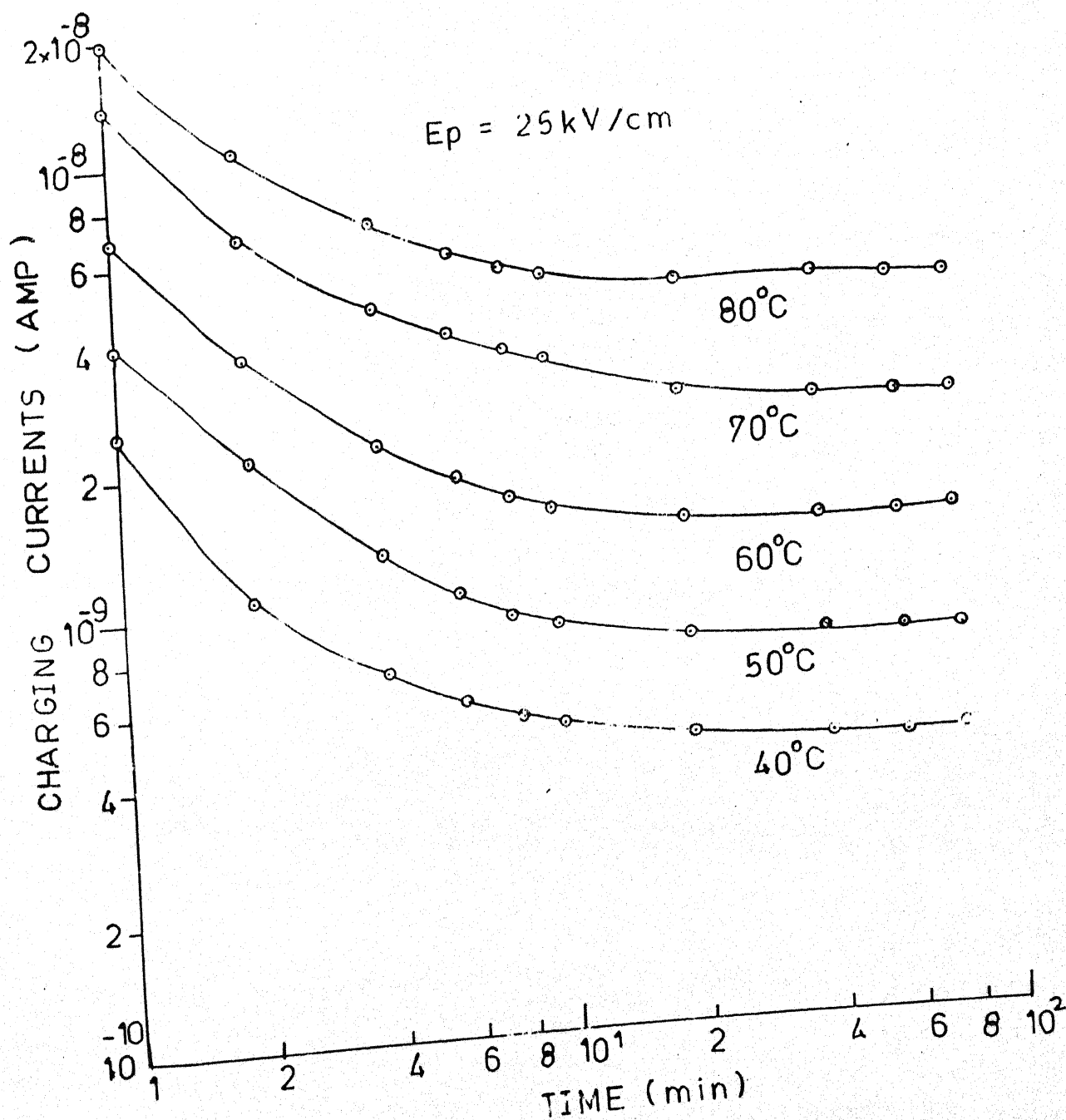


Fig. 5.3 (b) Tansient current curves for charging mode at polarising field and different temperatures with Cu-Cu system.

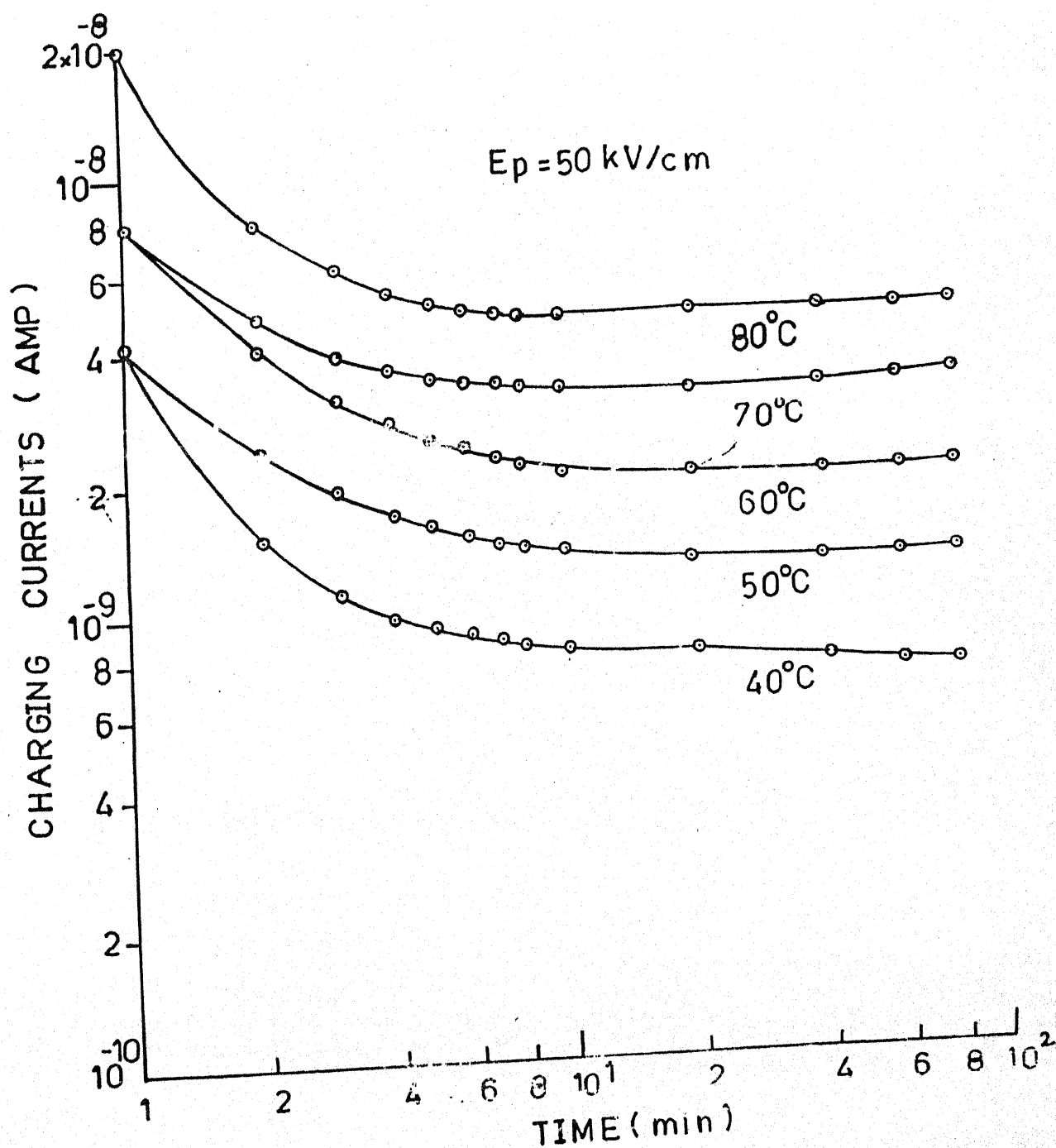


Fig. 5.3 (b) Tansient current curves for charging mode at polarising field and different temperatures with Cu-Cu system.

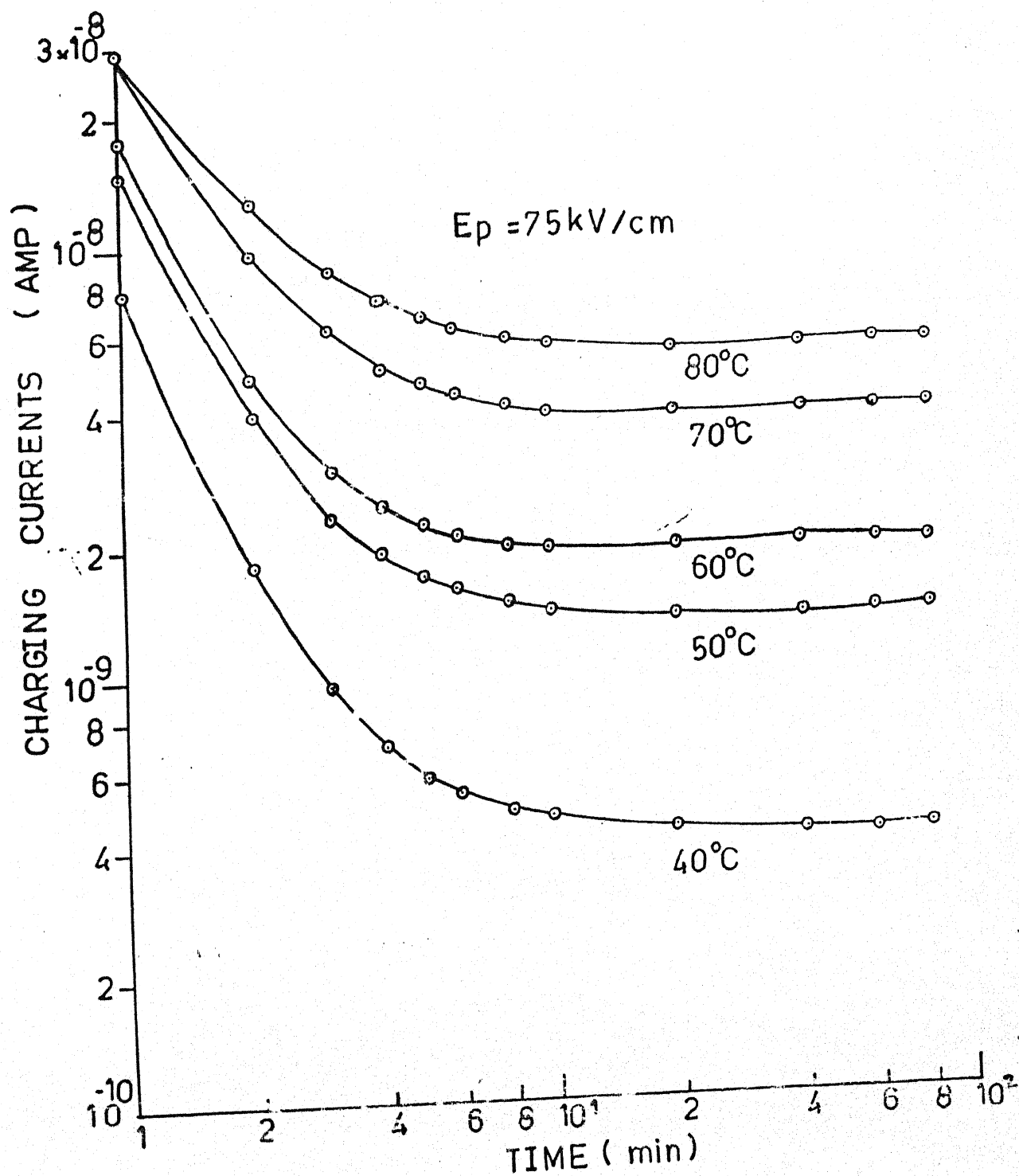


Fig. 5.3 (c) Transient current curves for charging mode at polarising field and different temperatures with Cu-Cu system.

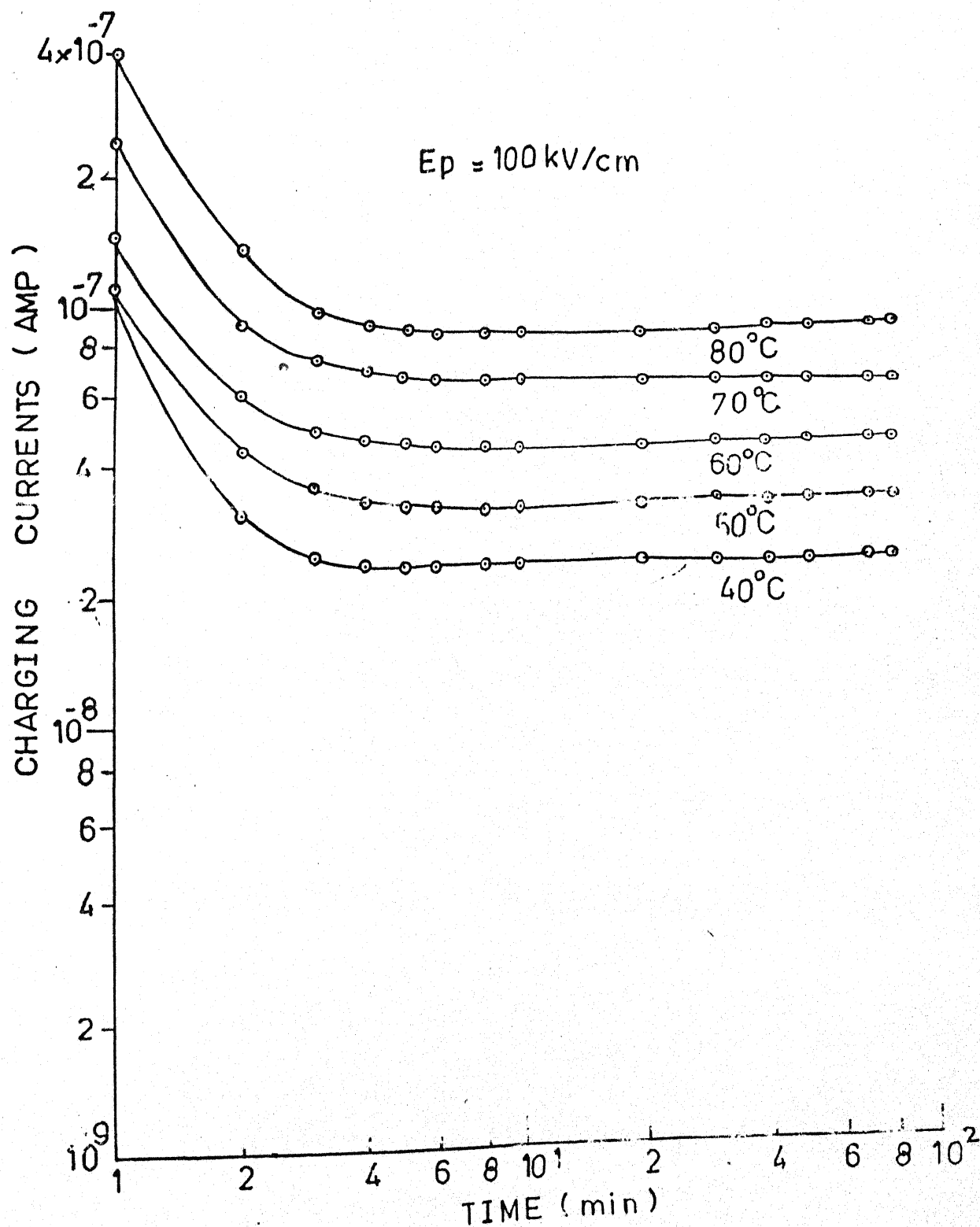


Fig. 5.3 (c) Tansient current curves for charging mode at polarising field and different temperatures with Cu-Cu system.

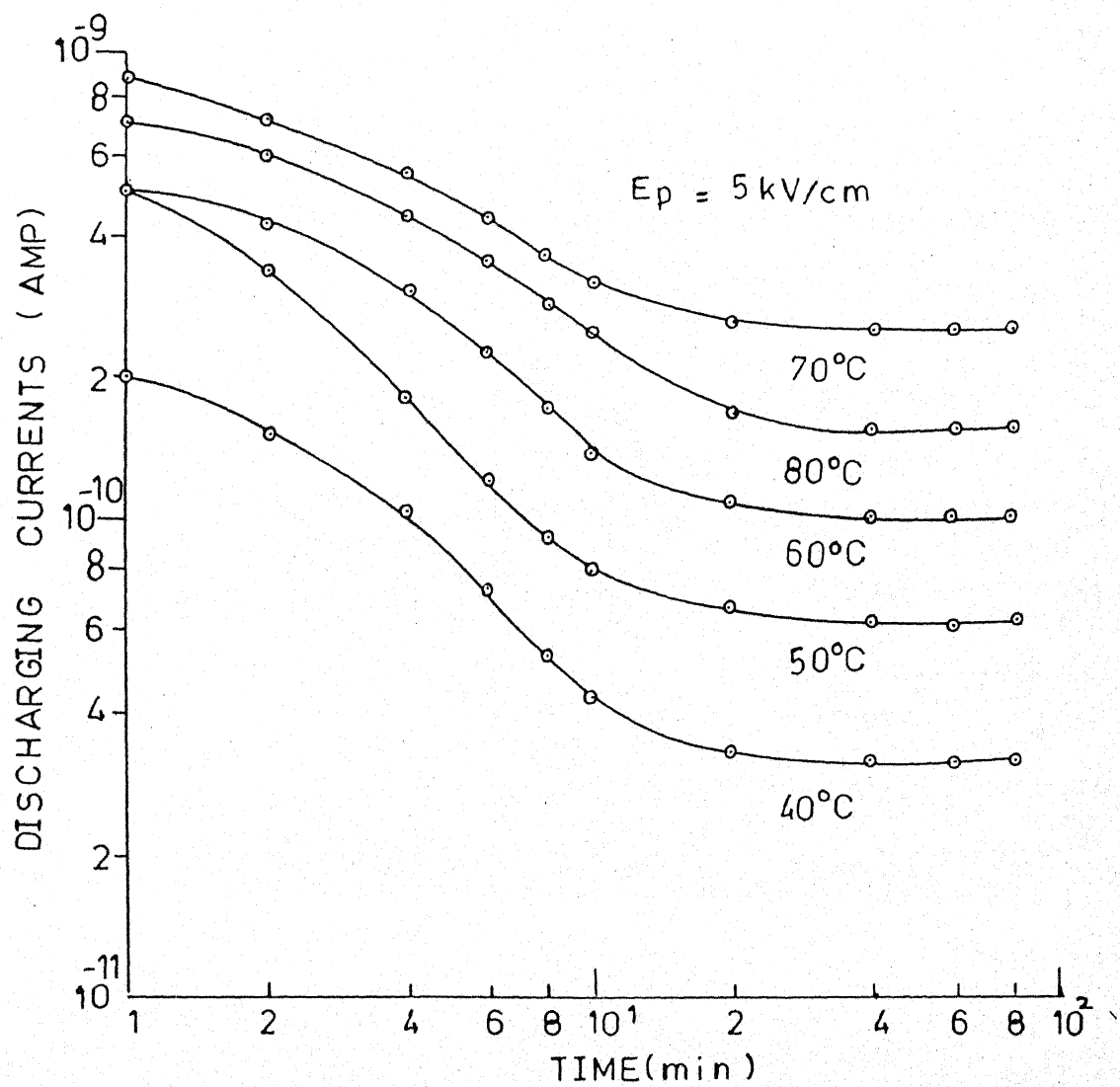


Fig 5.3(A) : Transient current curves for discharging mode at given polarising field and different temperatures with Cu-Cu system

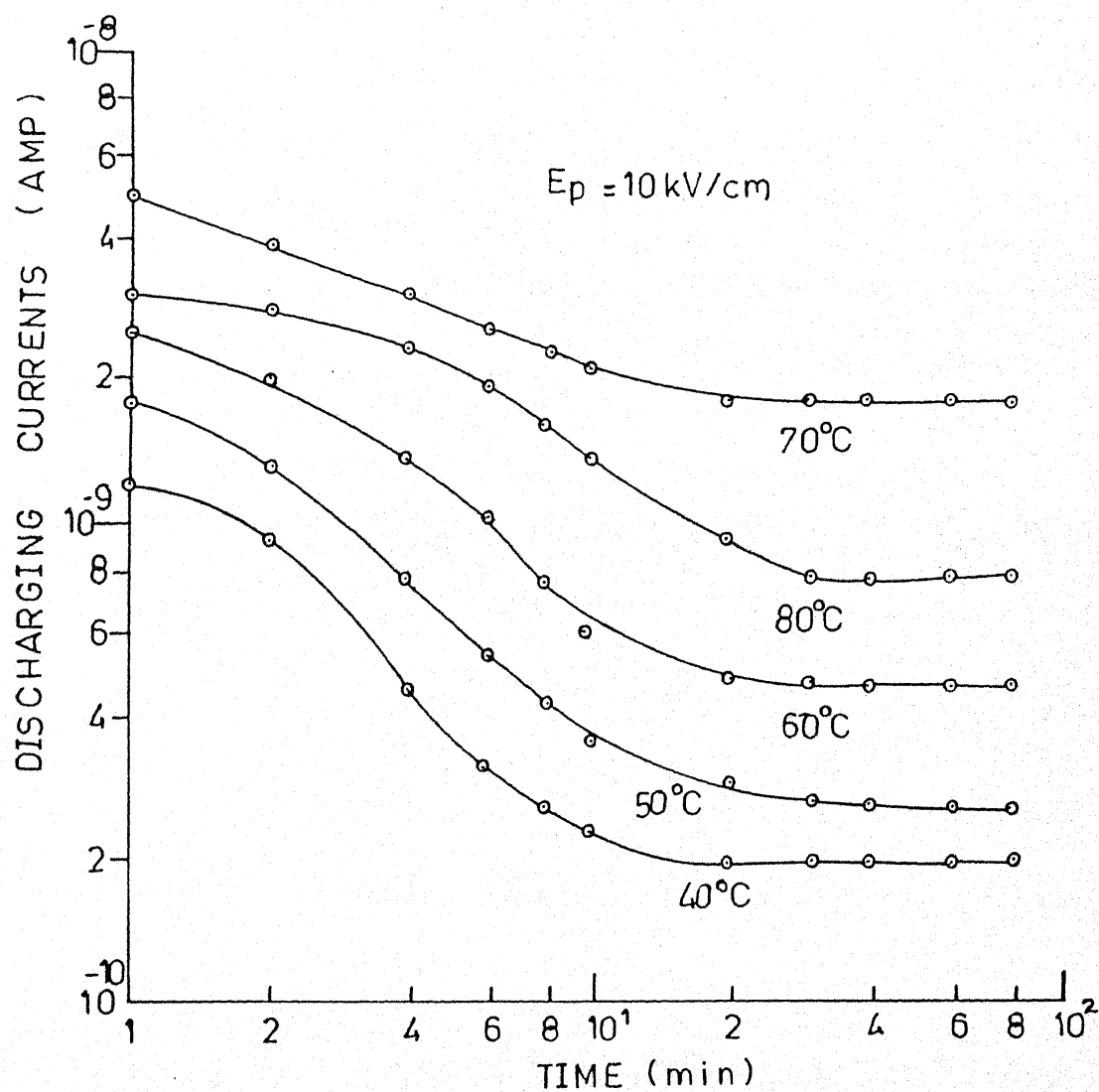


Fig 5.3(A) : Transient current curves for discharging mode at given polarising field and different temperatures with Cu-Cu system

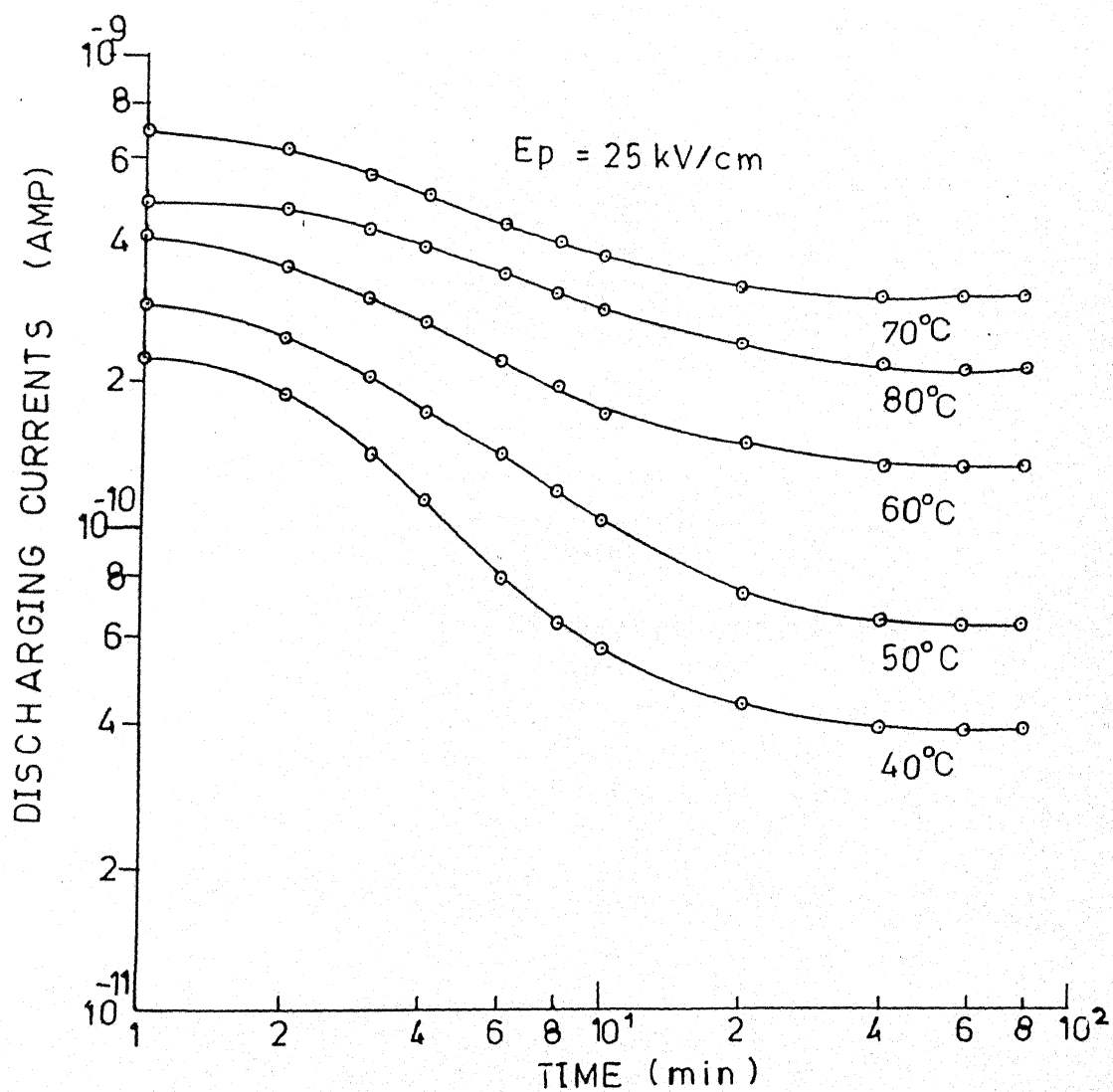


Fig 5.3 (B) : Transient current curves for discharging mode at given polarising field and different temperatures with Cu-Cu system.

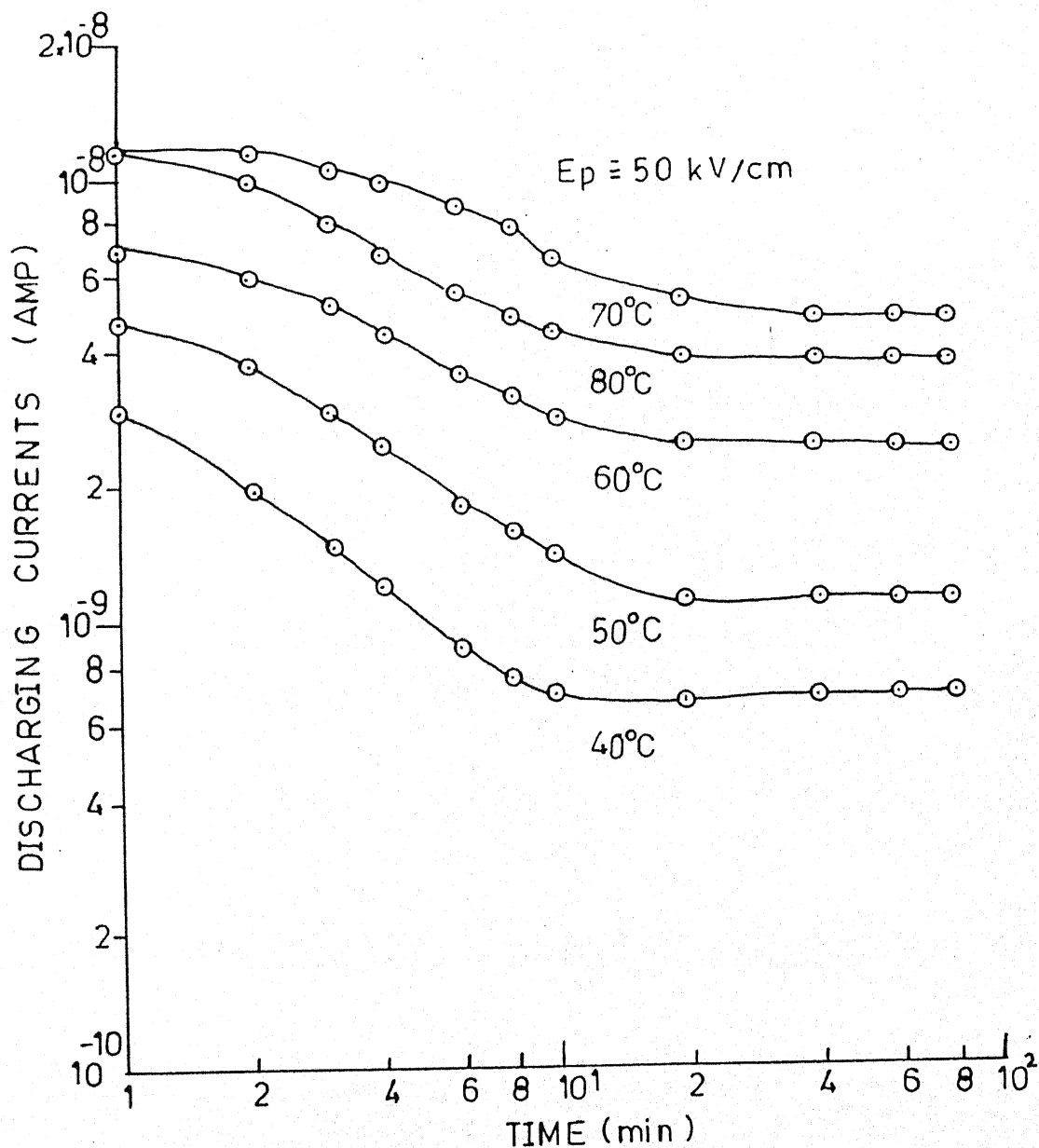


Fig 5.3 (B) : Transient current curves for discharging mode at given polarising field and different temperatures with Cu-Cu system.

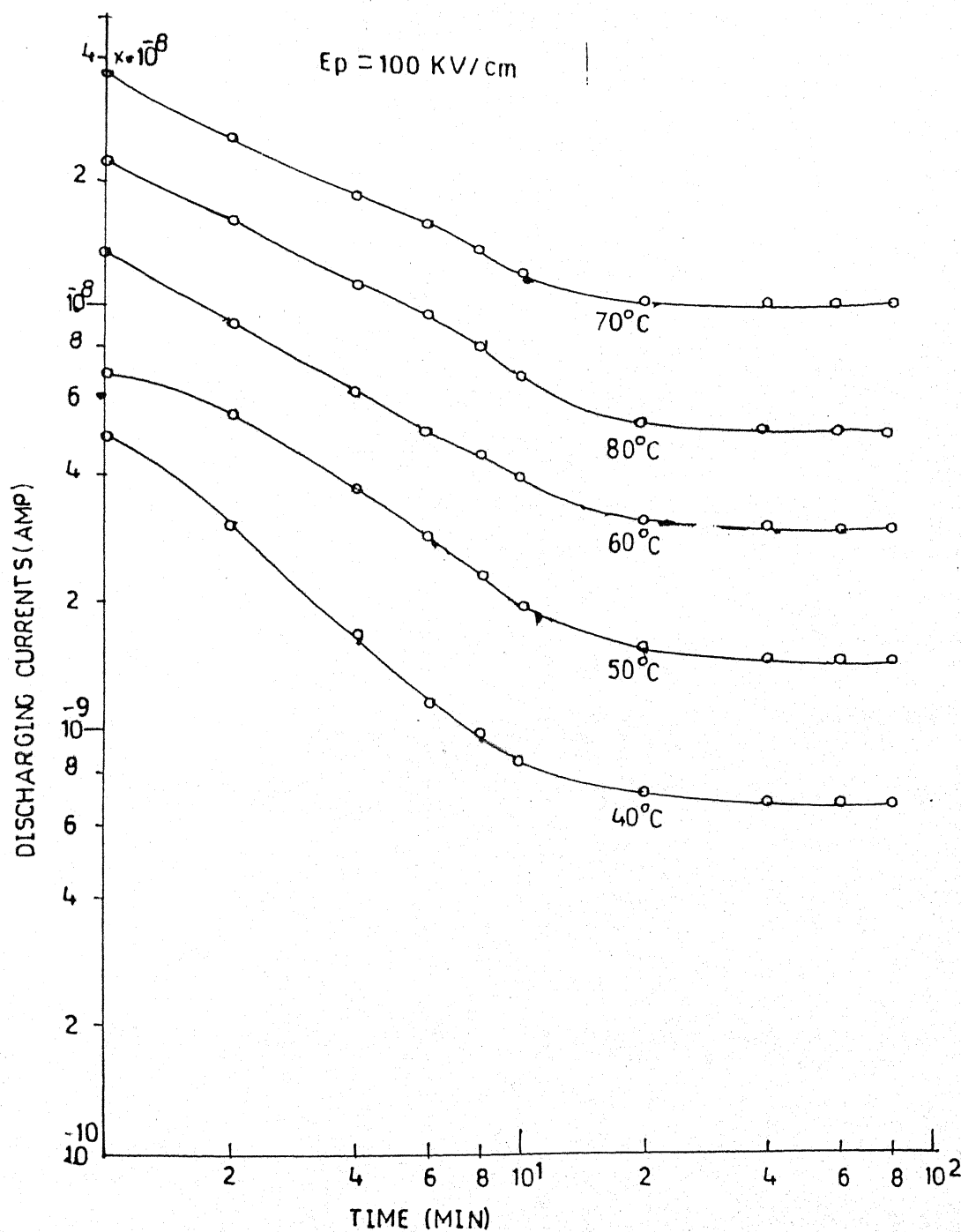


Fig 5.3(C) : Transient current curves for discharging mode at given polarising field and different temperatures with Cu-Cu system.

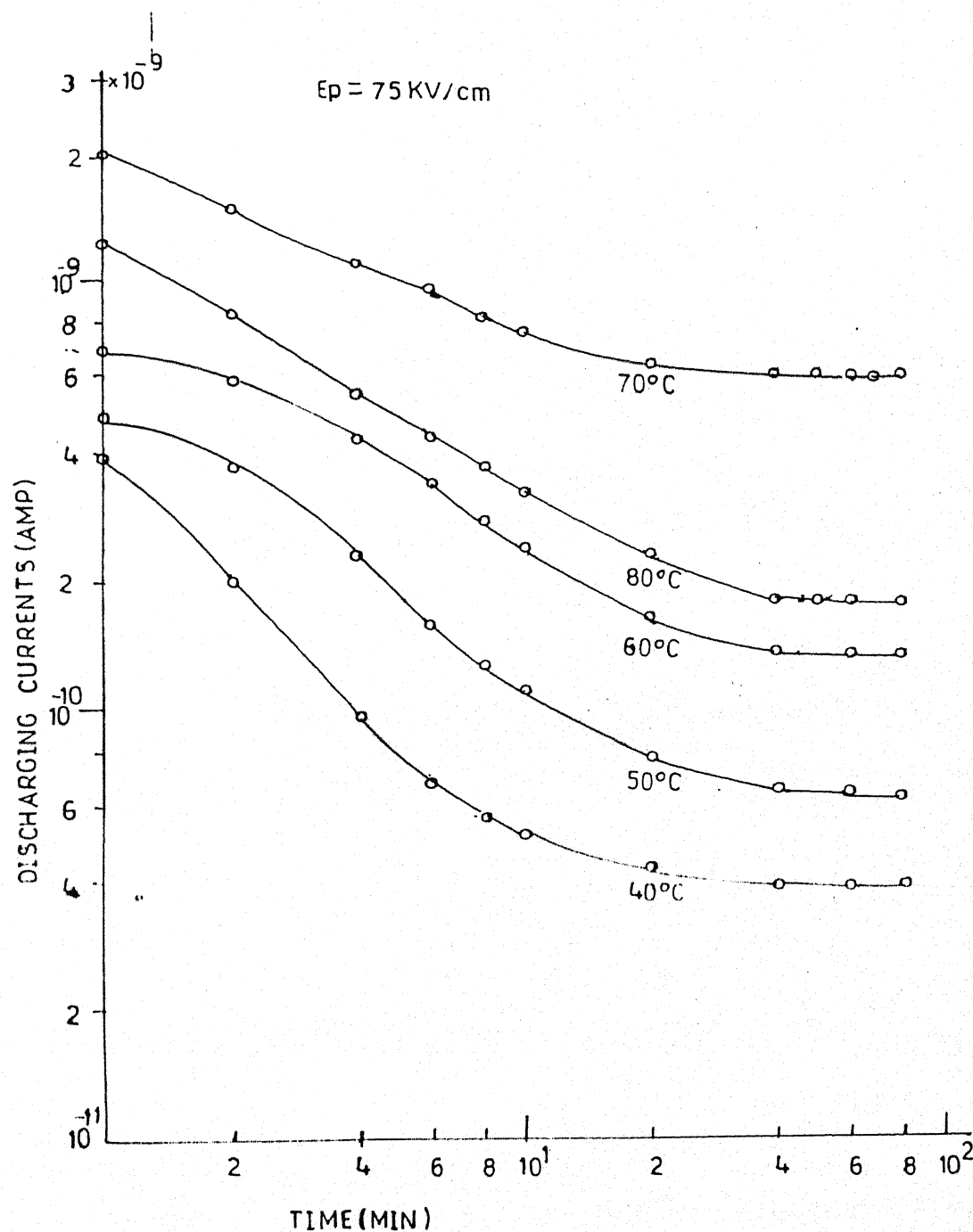


Fig 5.3(C) : Transient current curves for discharging mode at given polarising field and different temperatures with Cu-Cu system.

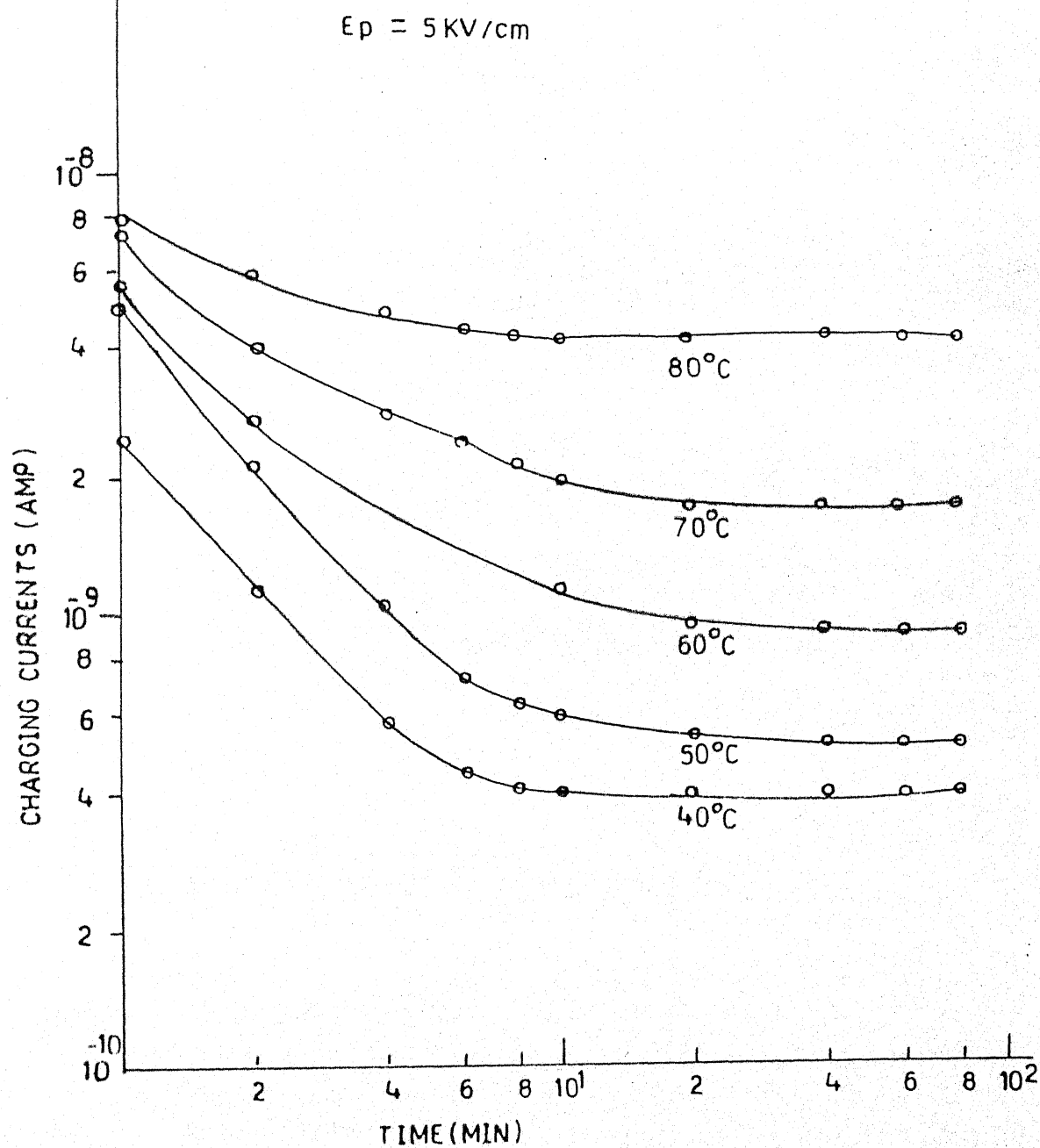


Fig 5.4(a): Transient current curves for charging mode at given polarising field and different temperatures with Sn-Sn system

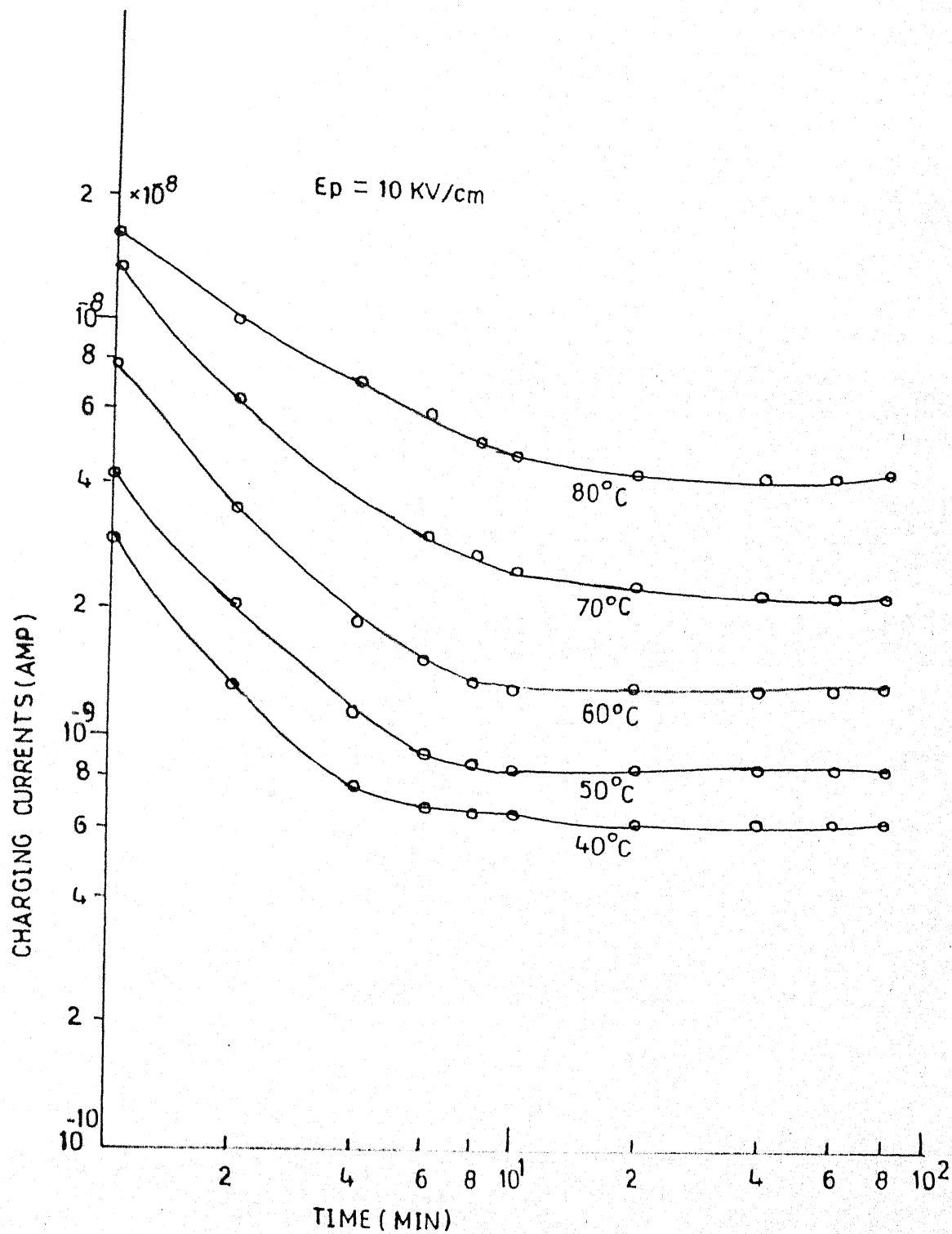


Fig 5.4(a): Transient current curves for charging mode at given polarising field and different temperatures with Sn-Sn system

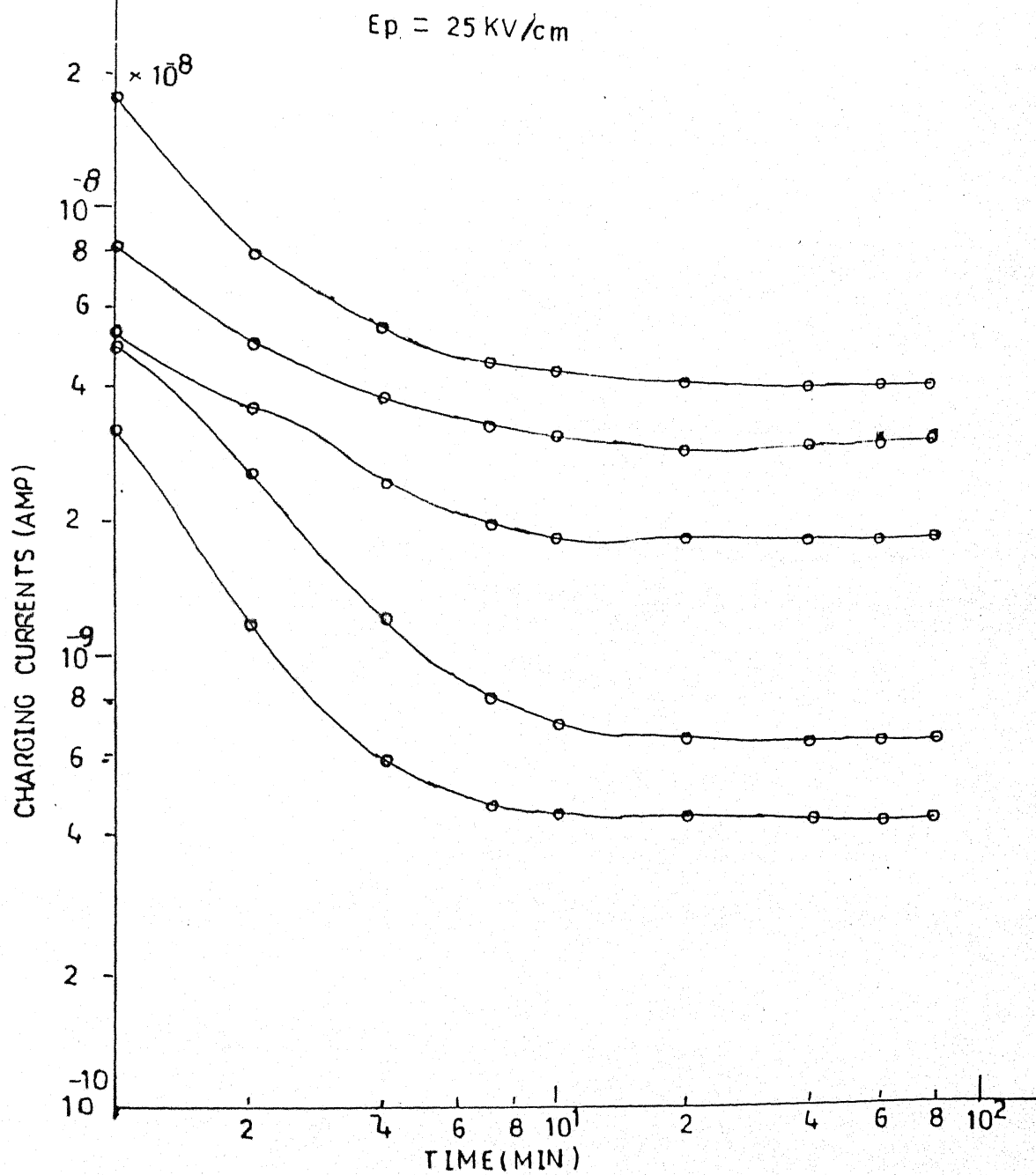


Fig 5.4(b): Transient current curves for charging mode at given polarising field and different temperatures with Sn-Sn system

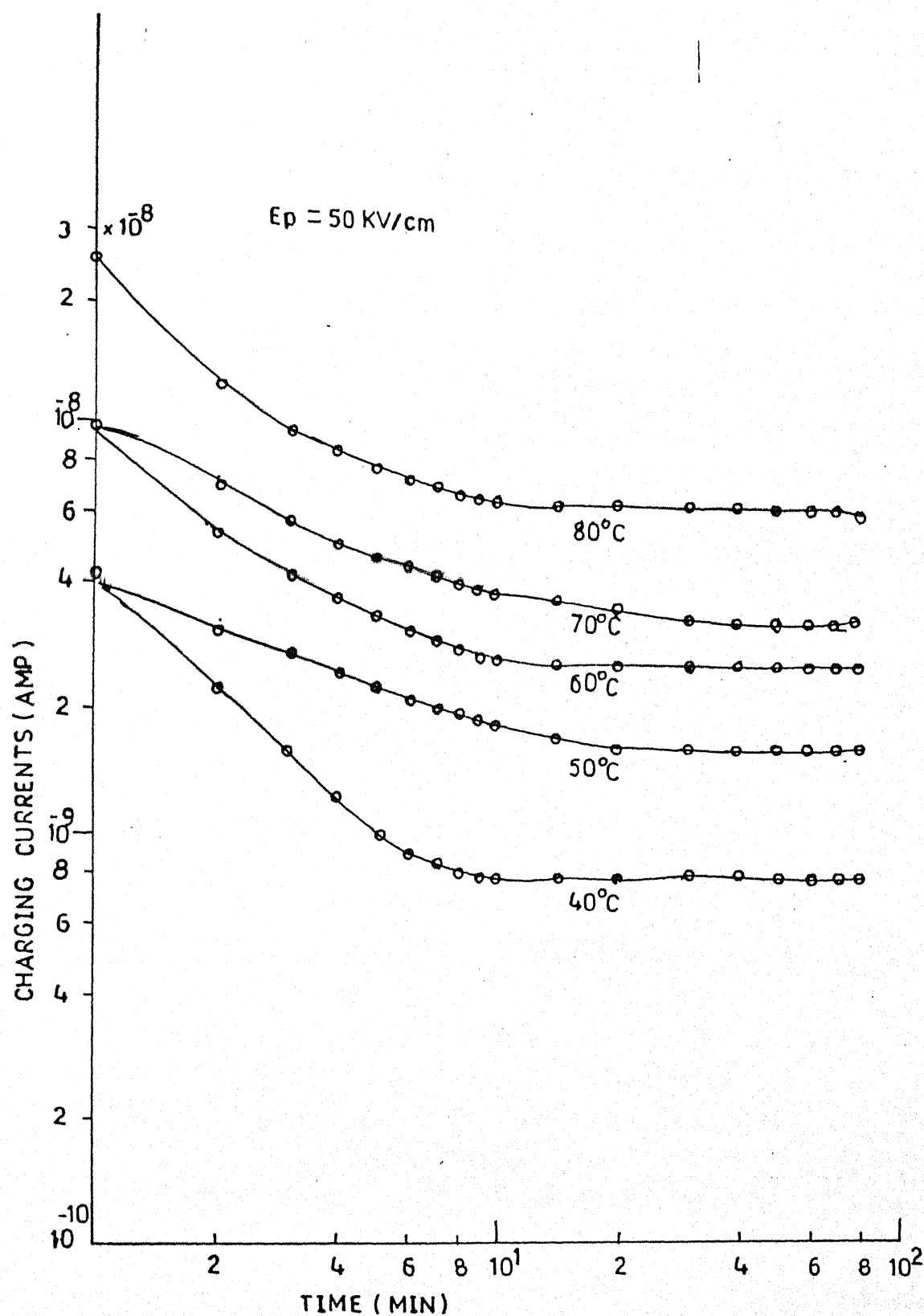


Fig 5.4(b): Transient current curves for charging mode at given polarising field and different temperatures with Sn-Sn system

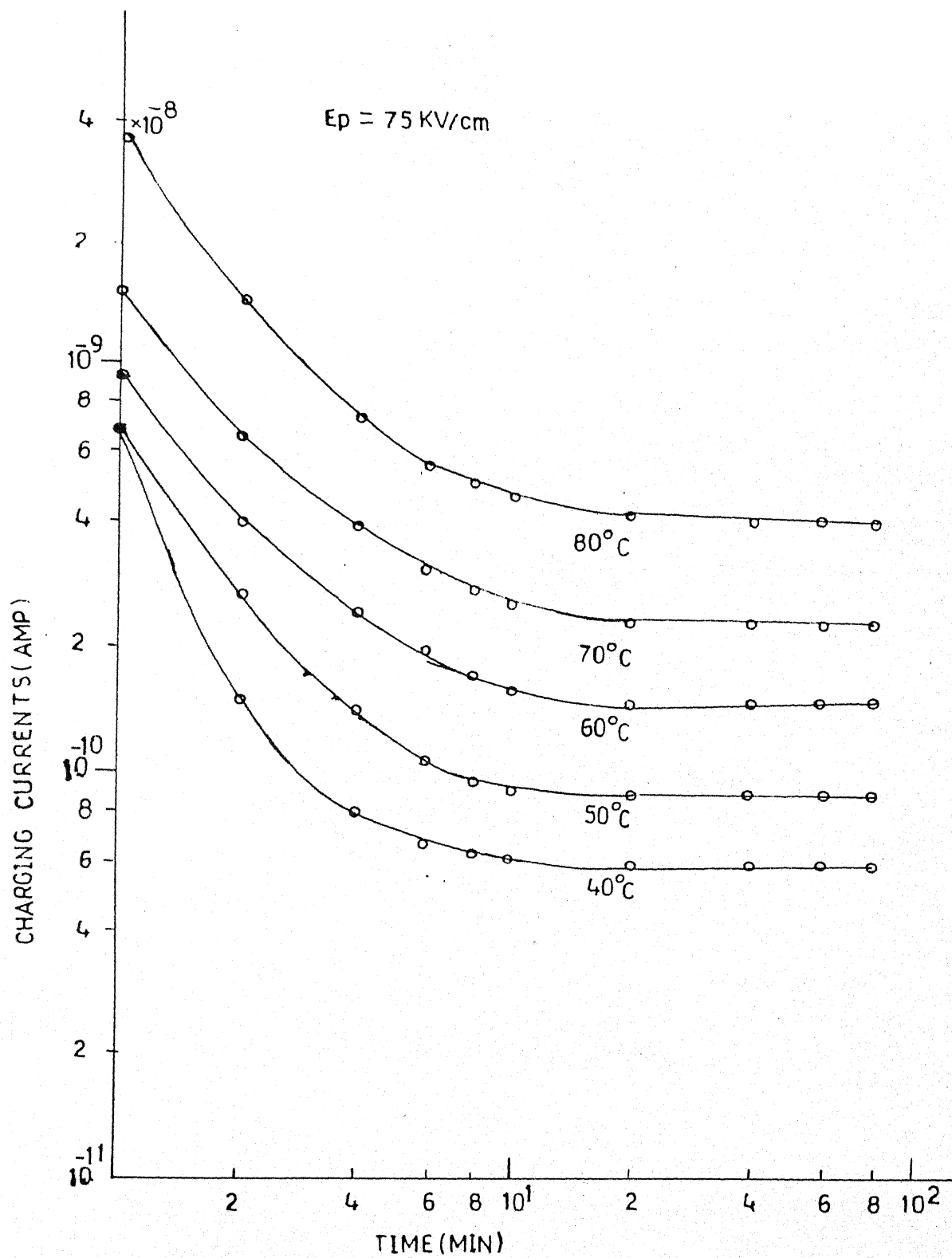


Fig 5.4(c): Transient current curves for charging mode at given polarising field and different temperatures with Sn-Sn system

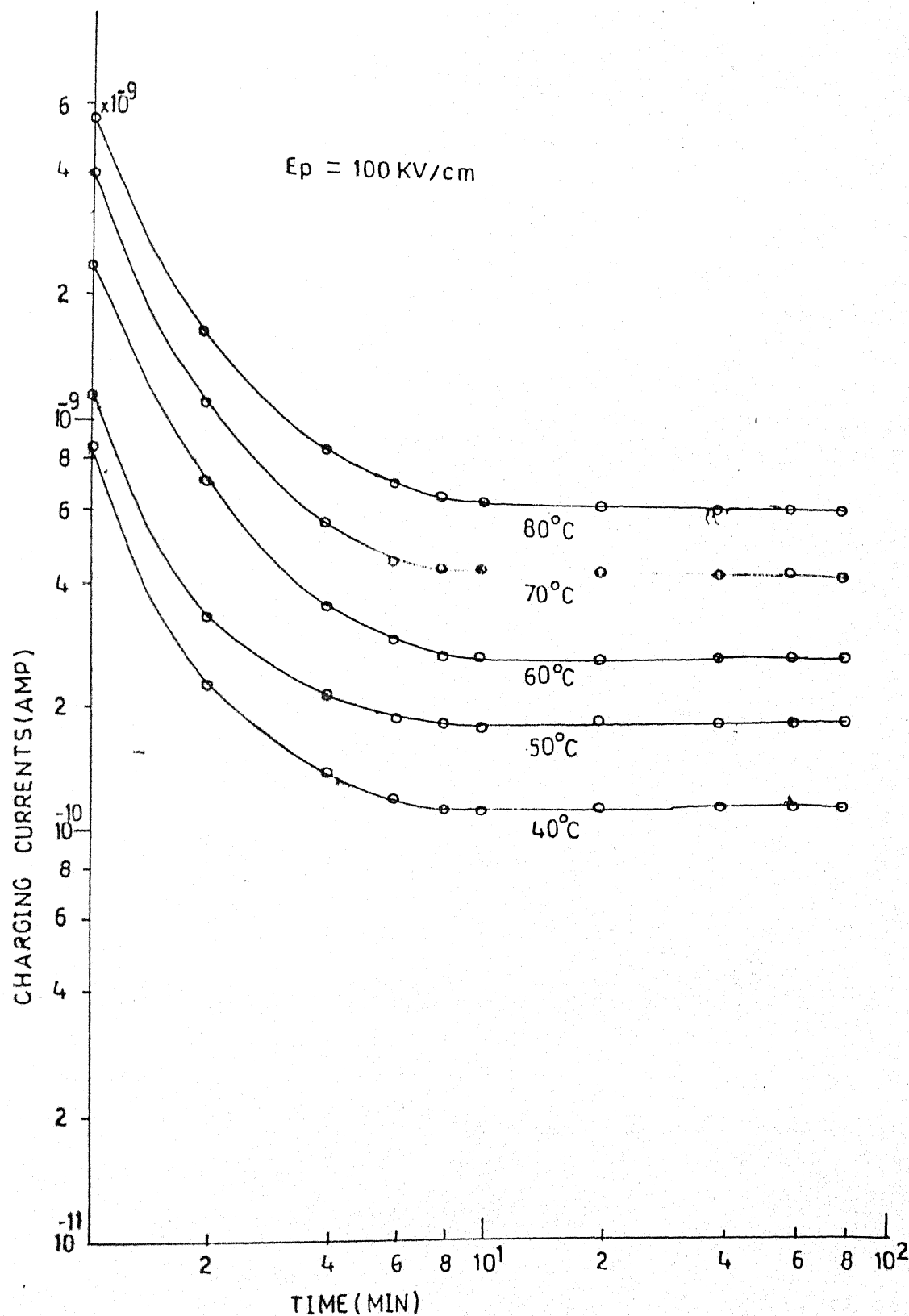


Fig 5.4(c): Transient current curves for charging mode at given polarising field and different temperatures with Sn-Sn system

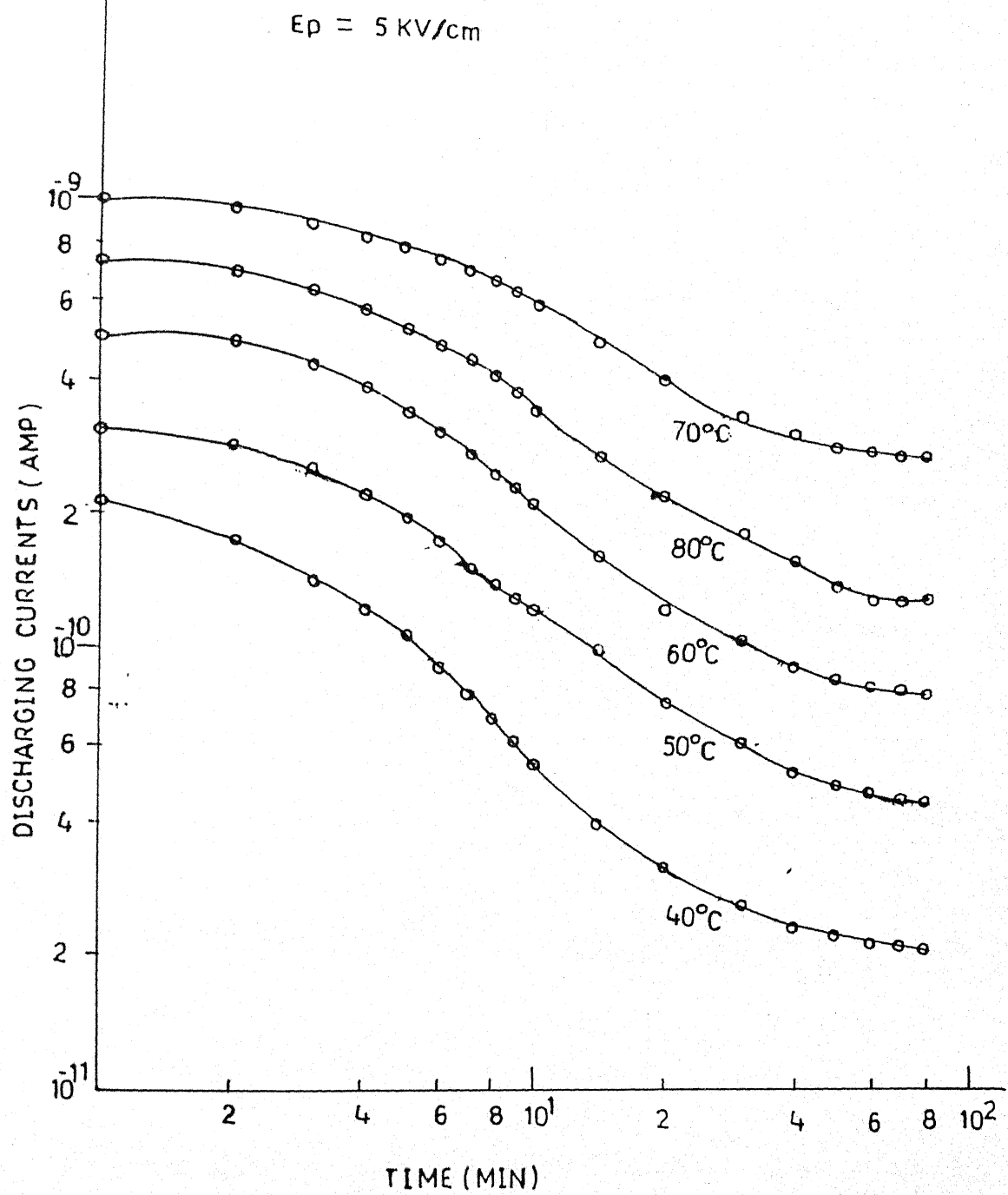


Fig 5.4(A): Transient current curves for discharging mode at given polarising field and different temperatures with Sn-Sn system

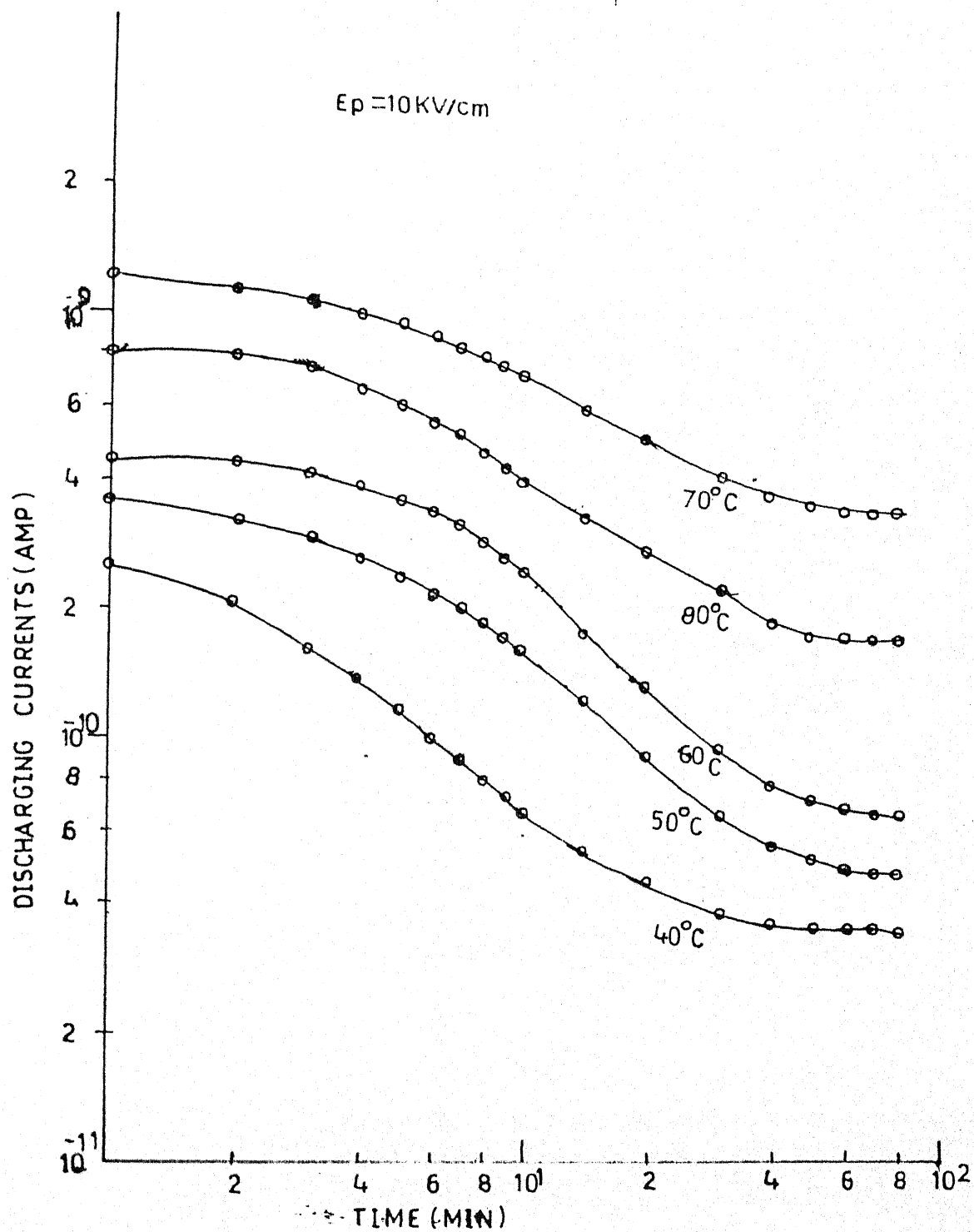


Fig 5.4(A): Transient current curves for discharging mode at given polarising field and different temperatures with Sn-Sn system

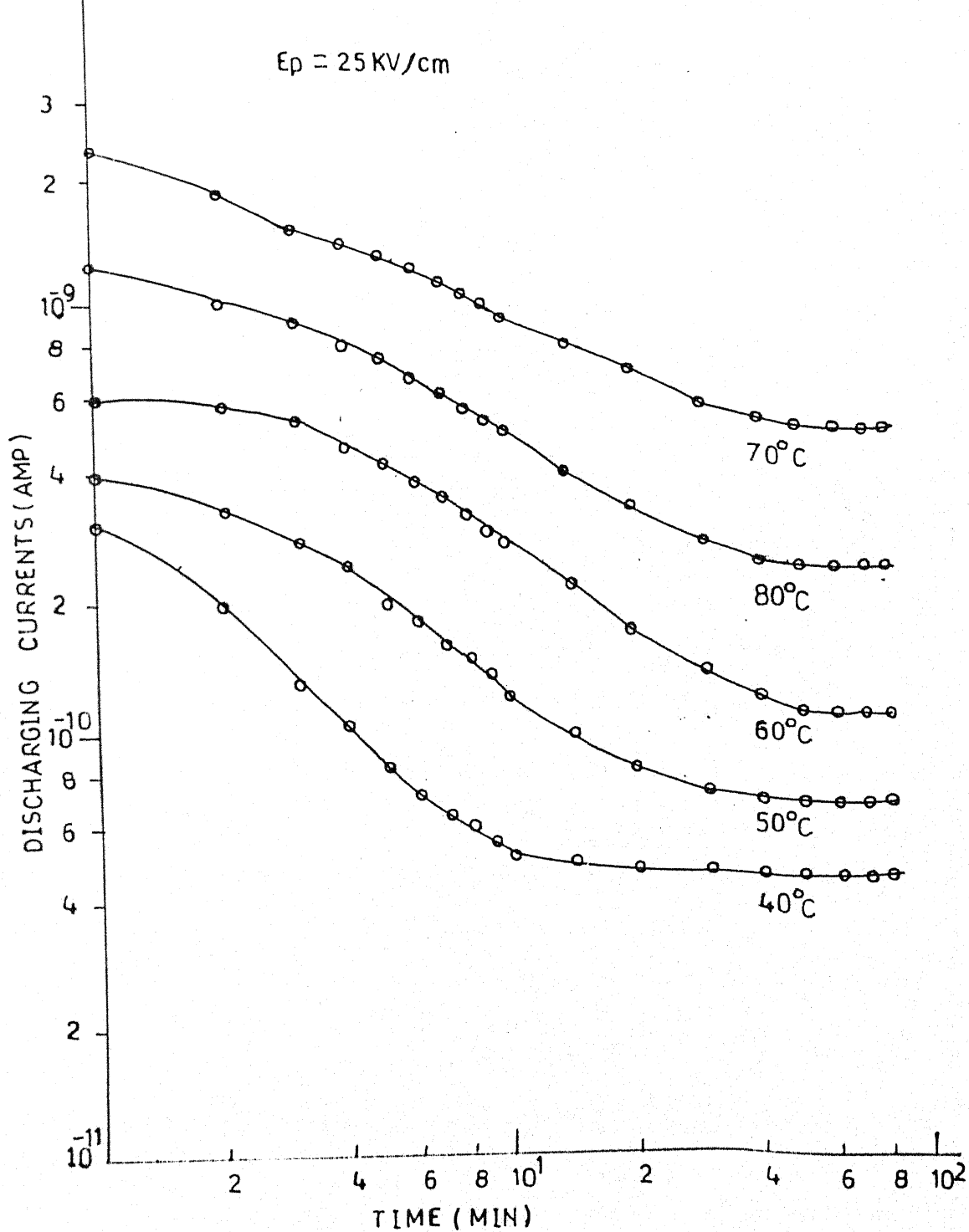


Fig 5.4(B): Transient current curves for discharging mode at given polarising field and different temperatures with Sn-Sn system

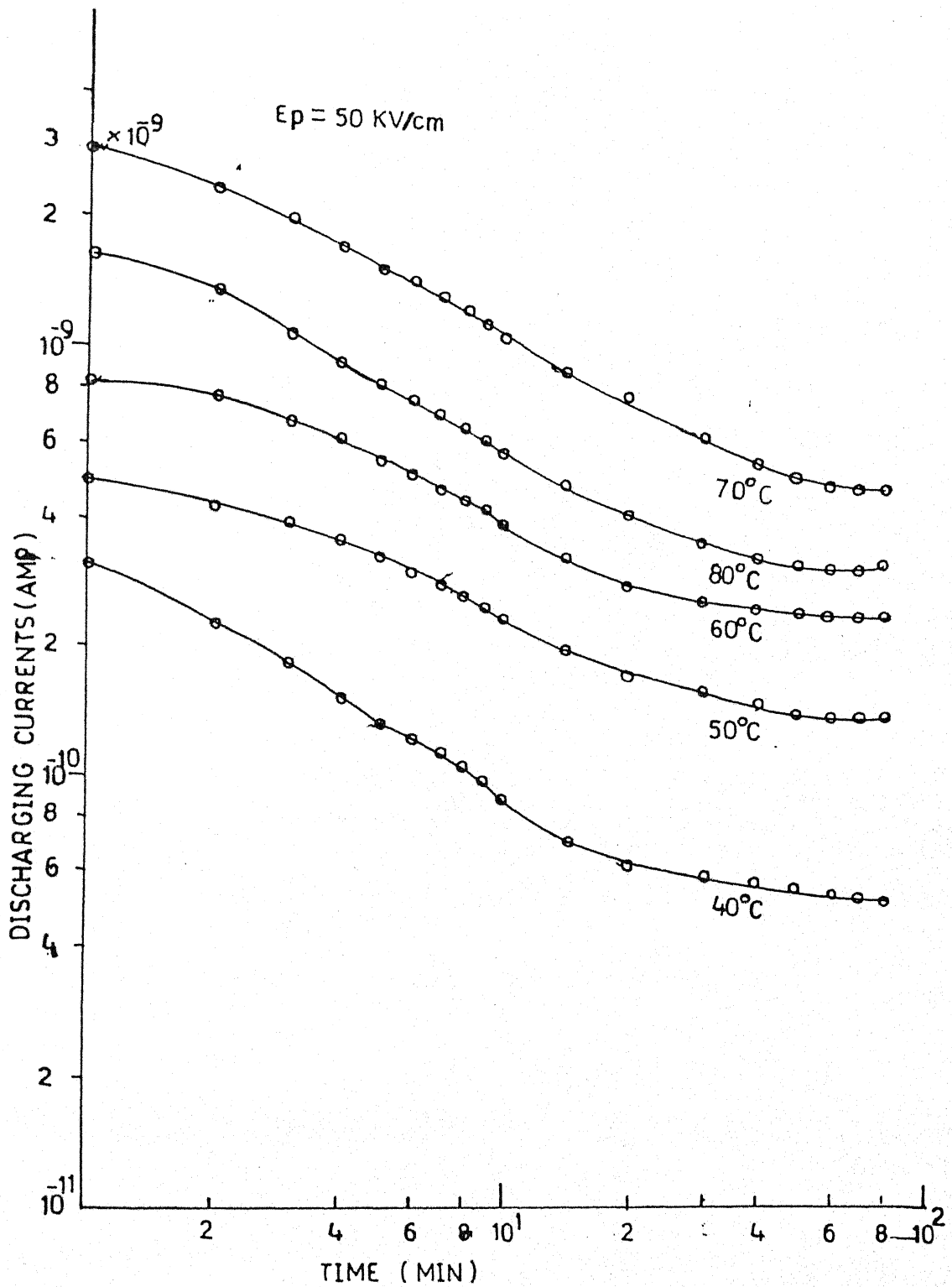


Fig 5.4(B): Transient current curves for discharging mode at given polarising field and different temperatures with Sn-Sn system

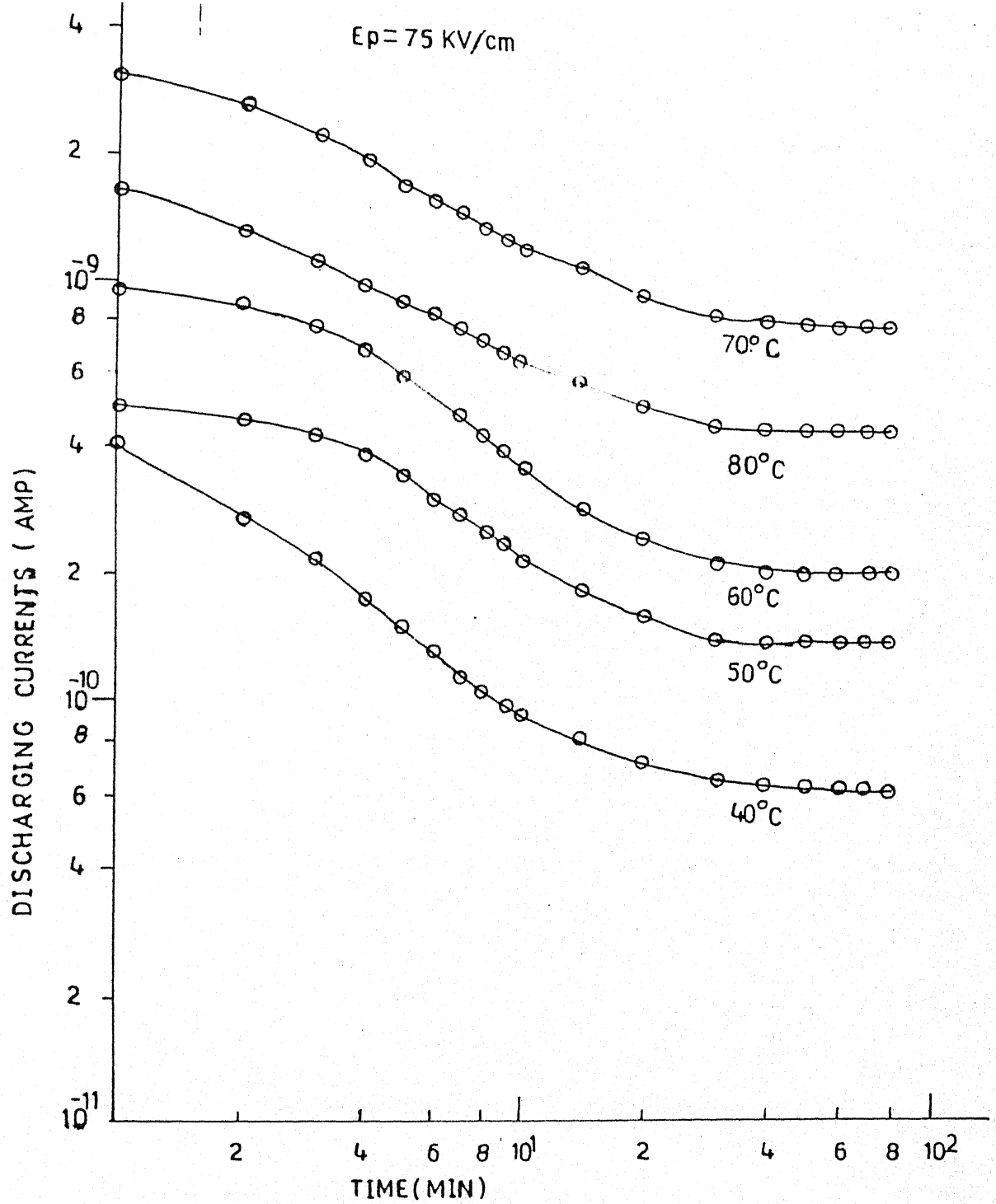


Fig 5.4(C): Transient current curves for discharging mode at given polarising field and different temperatures with Sn-Sn system

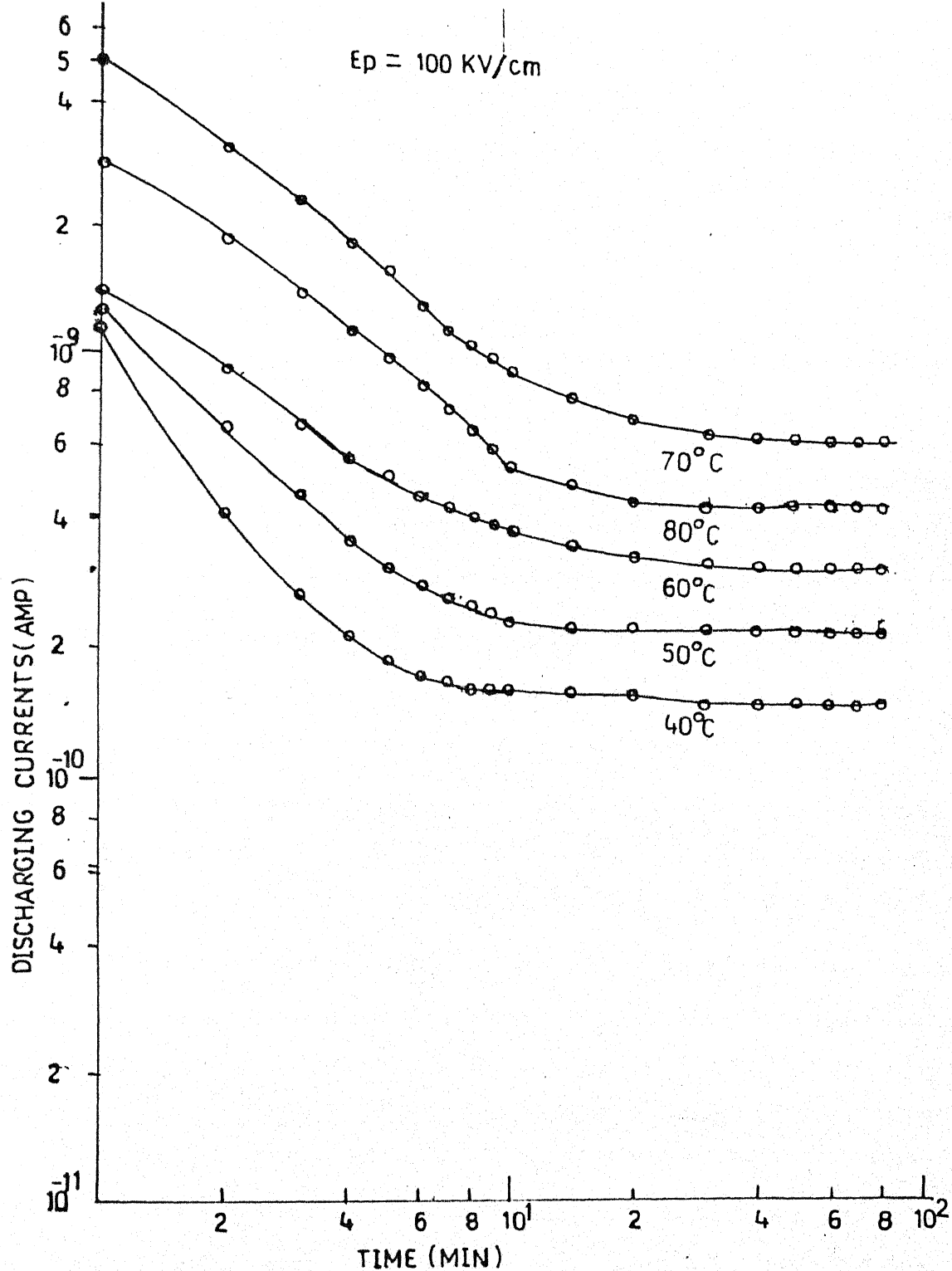


Fig 5.4(C): Transient current curves for discharging mode at given polarising field and different temperatures with Sn-Sn system

we use configuration of dissimilar contacts, viz., Al-PVP-Ag, Al-PVP-Cu, Al-PVP-Sn, shown in Figs. 5.5, 5.6 and 5.7, respectively.

5.3-2 TEMPERATURE DEPENDENCE

The charging and discharging transient observed for samples charged with fields of 5, 10, 25, 50, 75 and 100 kV/cm at different temperatures are shown in Figs. 5.1 to 5.7. Figs. (a) to (c) are for charging modes while (A) to (C) for discharging modes. The curves exhibit t^{-n} dependence. The temperature dependence of the observed transients can be expressed more conveniently by plotting currents observed at various constant times (isochronals) against temperature. Such isochronals have been constructed for various constant fields for fixed times 02, 05, 10, 20 and 40 min. From these plots it is evident that the current shows thermal dependence. Figs. 5.8 to 5.14 are isochronals for Al-Al, Ag-Ag, Cu-Cu, Sn-Sn, Al-Ag, Al-Cu and Al-Sn different electrode configurations respectively.

The isochronals are characterised by a peak located at 70°C for discharging mode. A careful observation reveals that the isochronal profile tends to shift towards high temperature, which suggests the presence of a thermal activated process.

The values of the activation energy are calculated from slopes of $\log I$ vs $10^3/T$ plots (not shown). In general, the

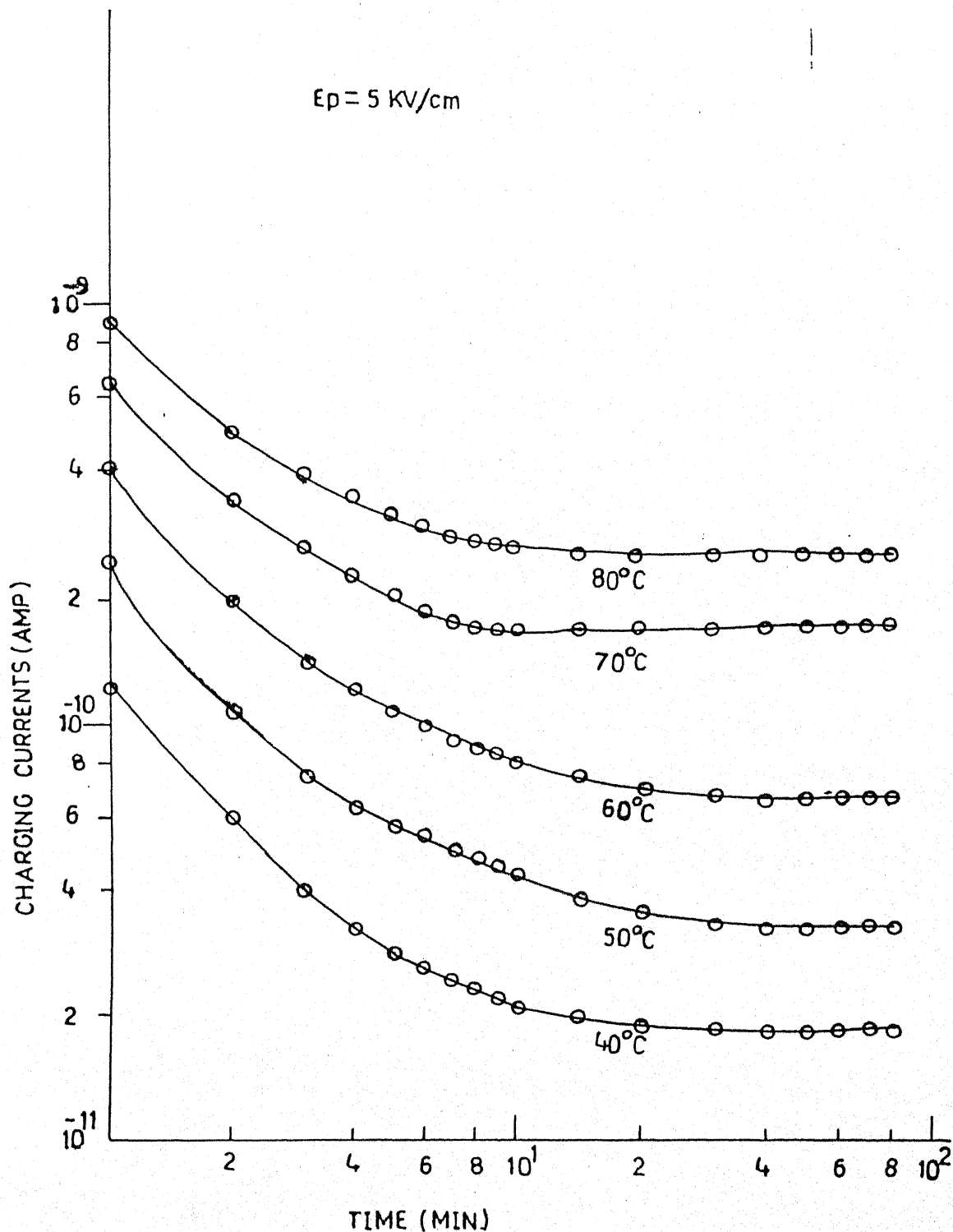


Fig 5.5(a): Transient current curves for charging mode at given polarising field and different temperatures with Al-Ag system

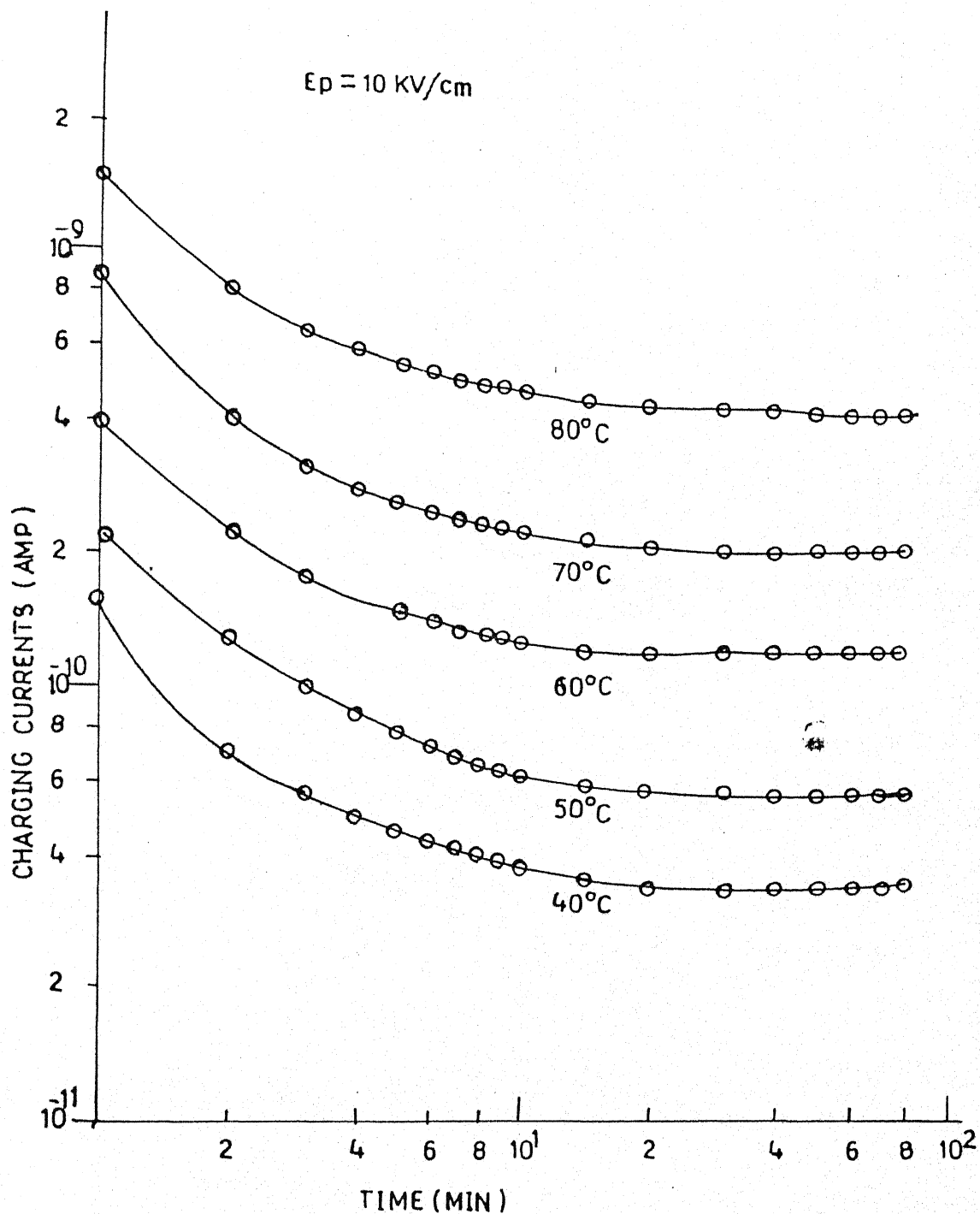


Fig 5.5(a): Transient current curves for charging mode at given polarising field and different temperatures with Al-Ag system

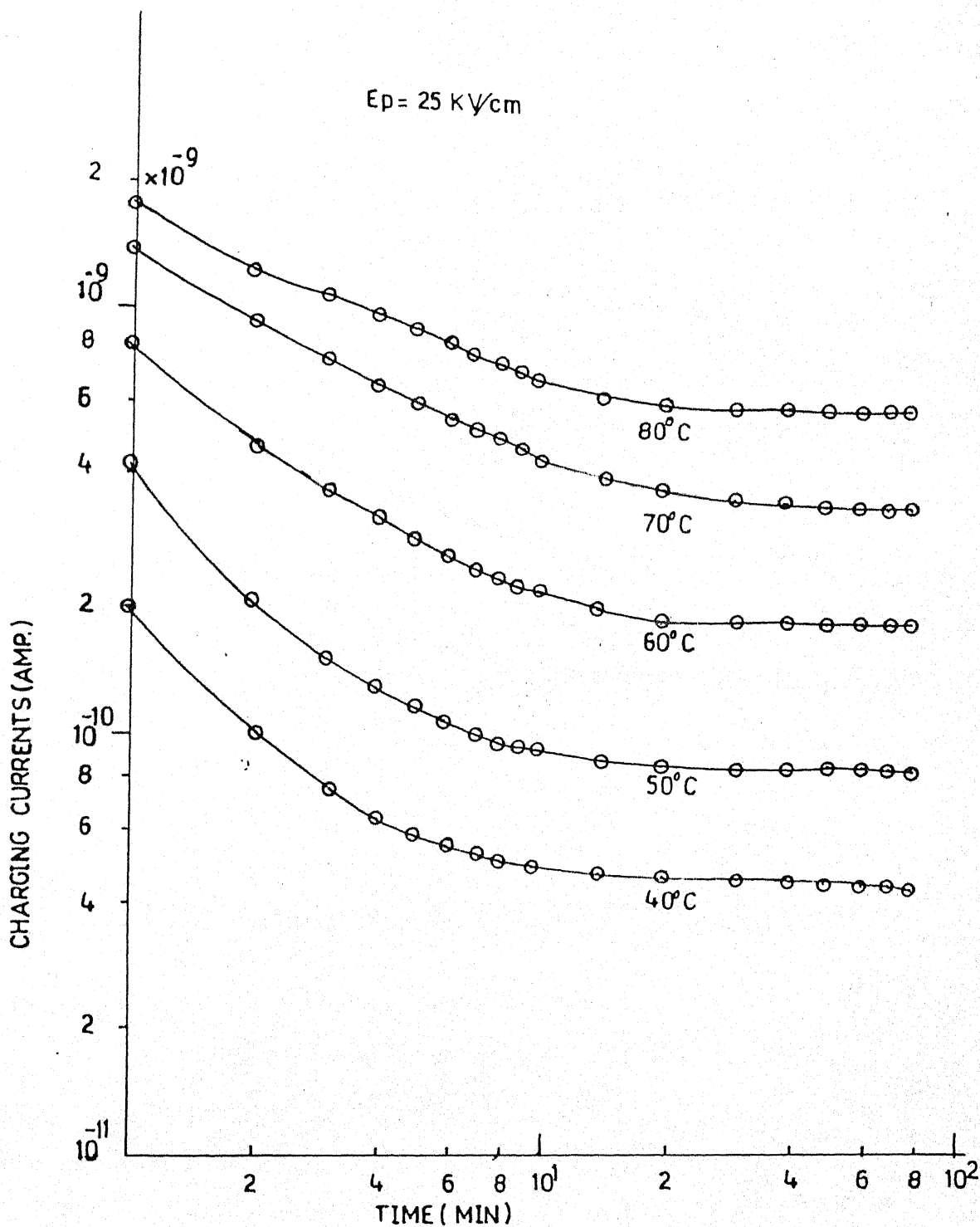


Fig 5.5(b): Transient current curves for charging mode at given polarising field and different temperatures with Al-Ag system

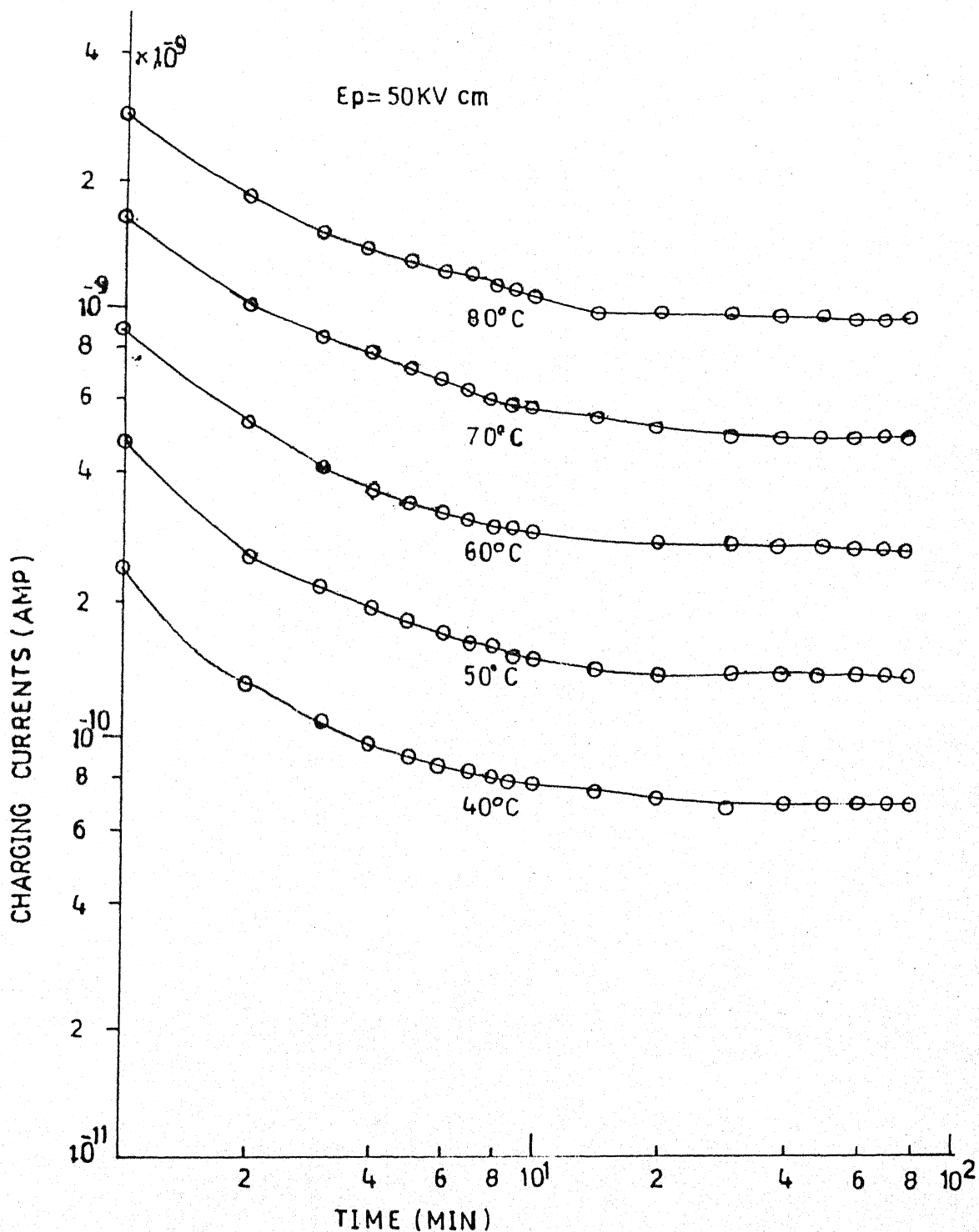


Fig 5.5(b): Transient current curves for charging mode at given polarising field and different temperatures with Al-Ag system

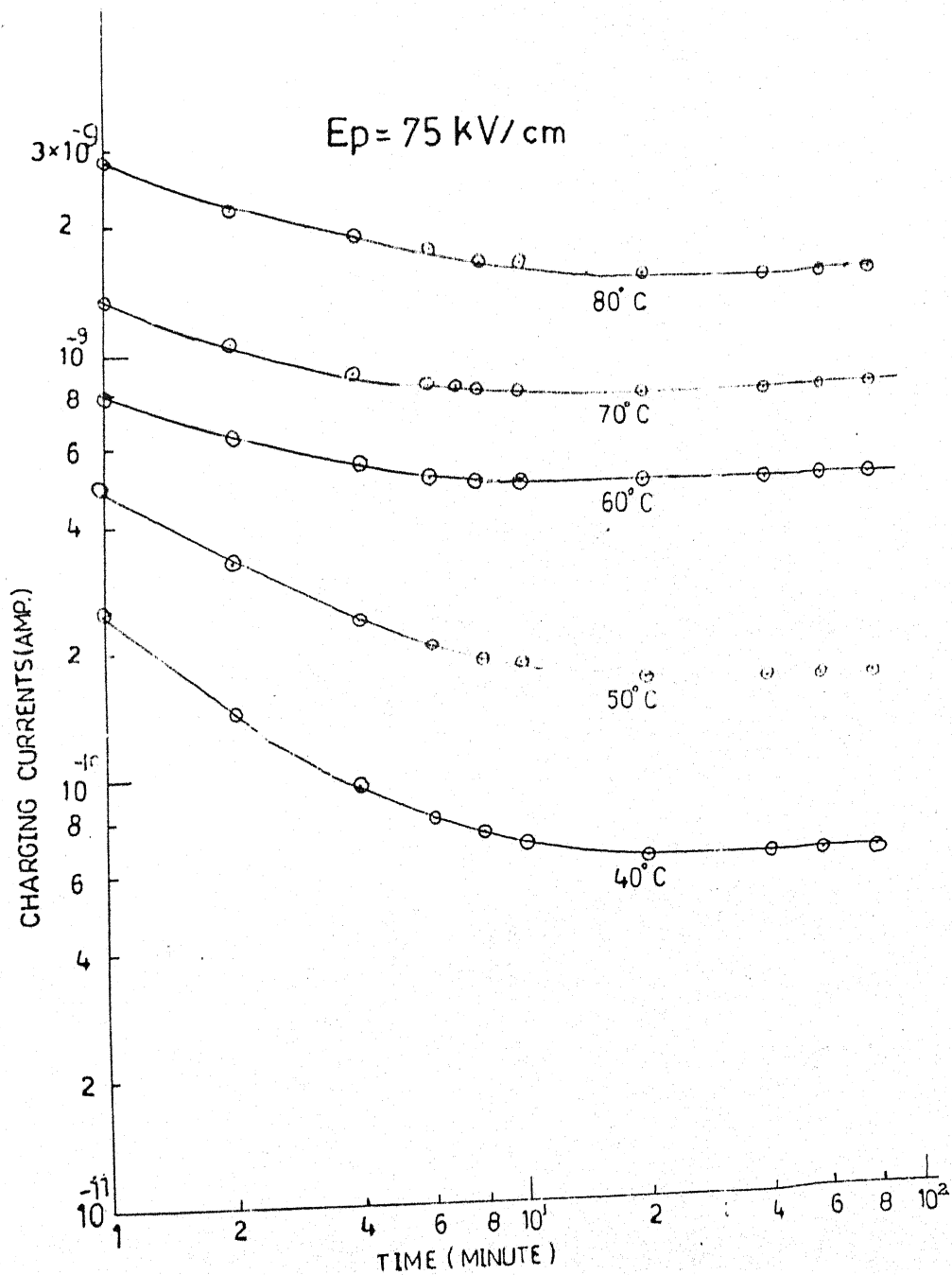


Fig. 5.5 (c) Transient current curves for charging mode at polarising field different temperatures with Al-Ag system.

$$E_p = 100 \text{ kV/cm}$$

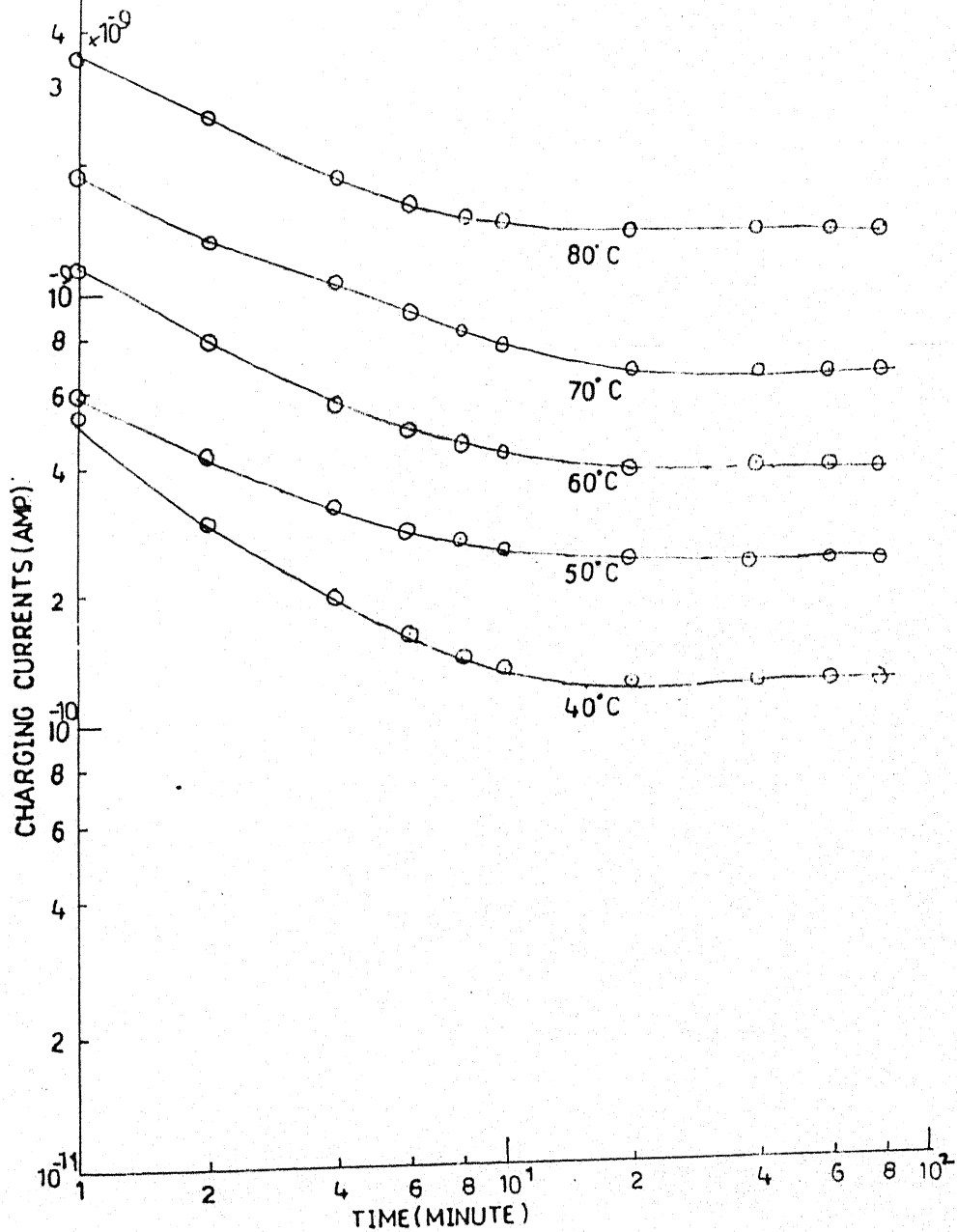


Fig. 5.5 (c) Transient current curves for charging mode at polarising field different temperatures with Al-Ag system.

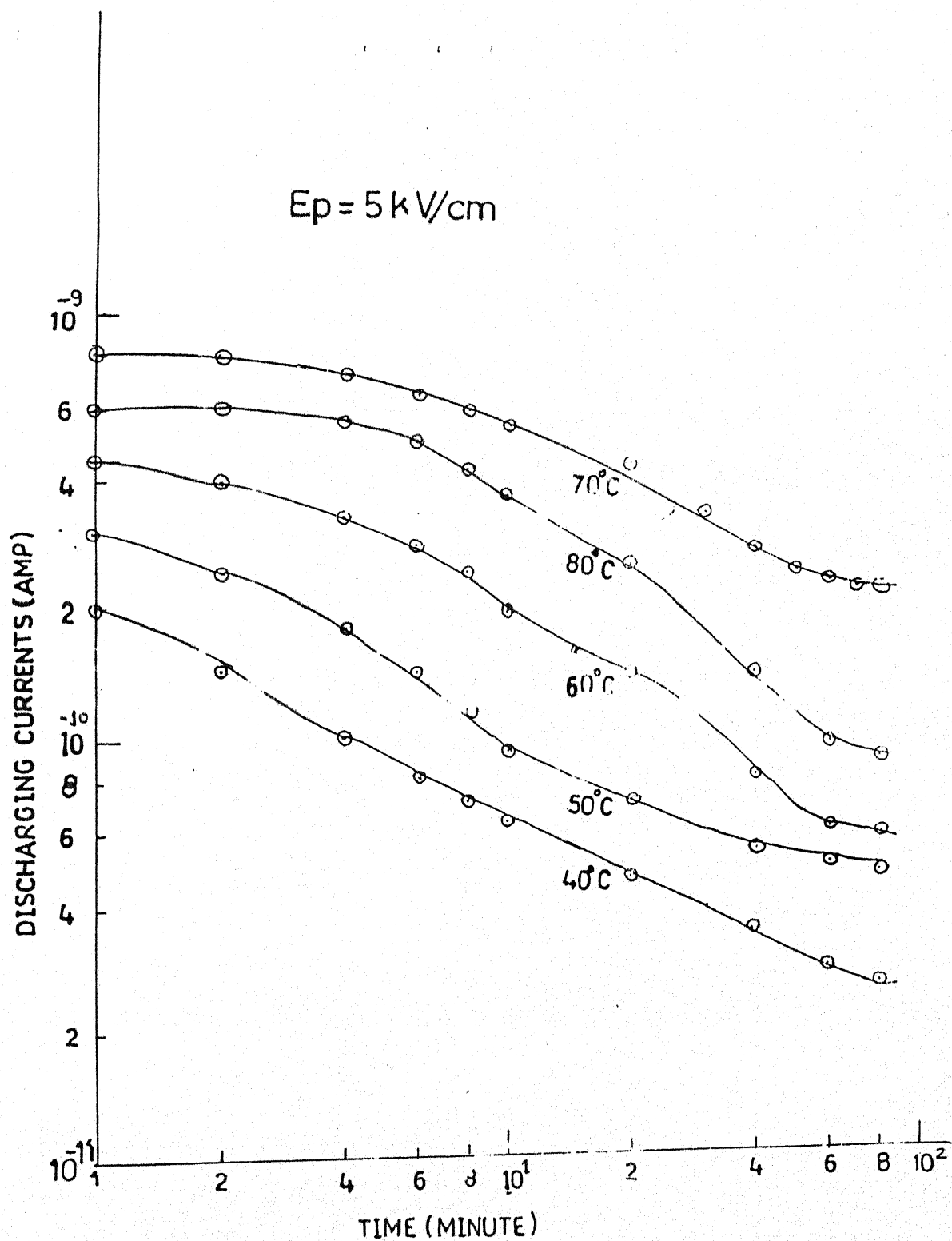


Fig. 5.5 (A) Transient current curves for discharging mode at polarising field and different temperatures with Al-Ag system.

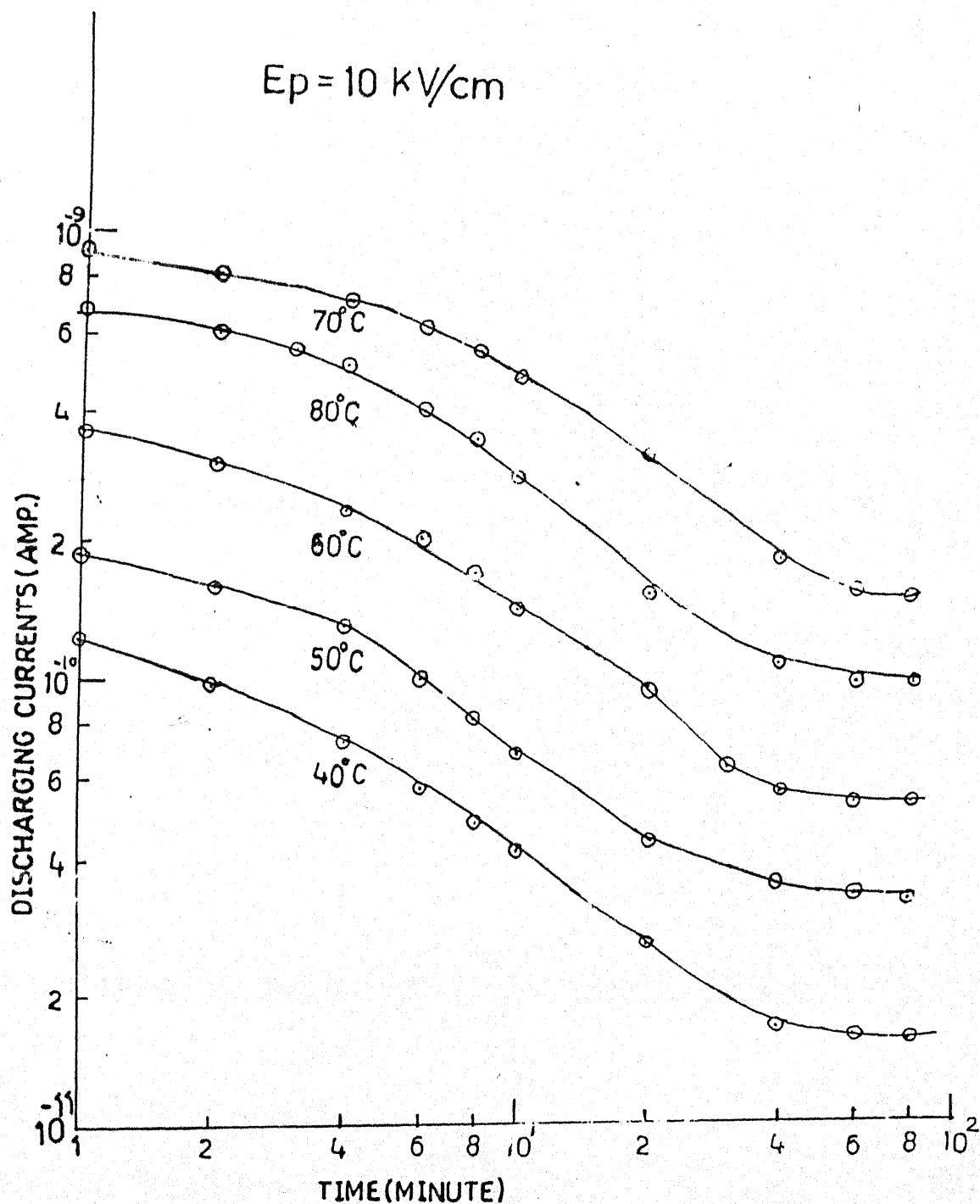


Fig. 5.5 (A) Transient current curves for discharging mode at polarising field and different temperatures with Al-Ag system.

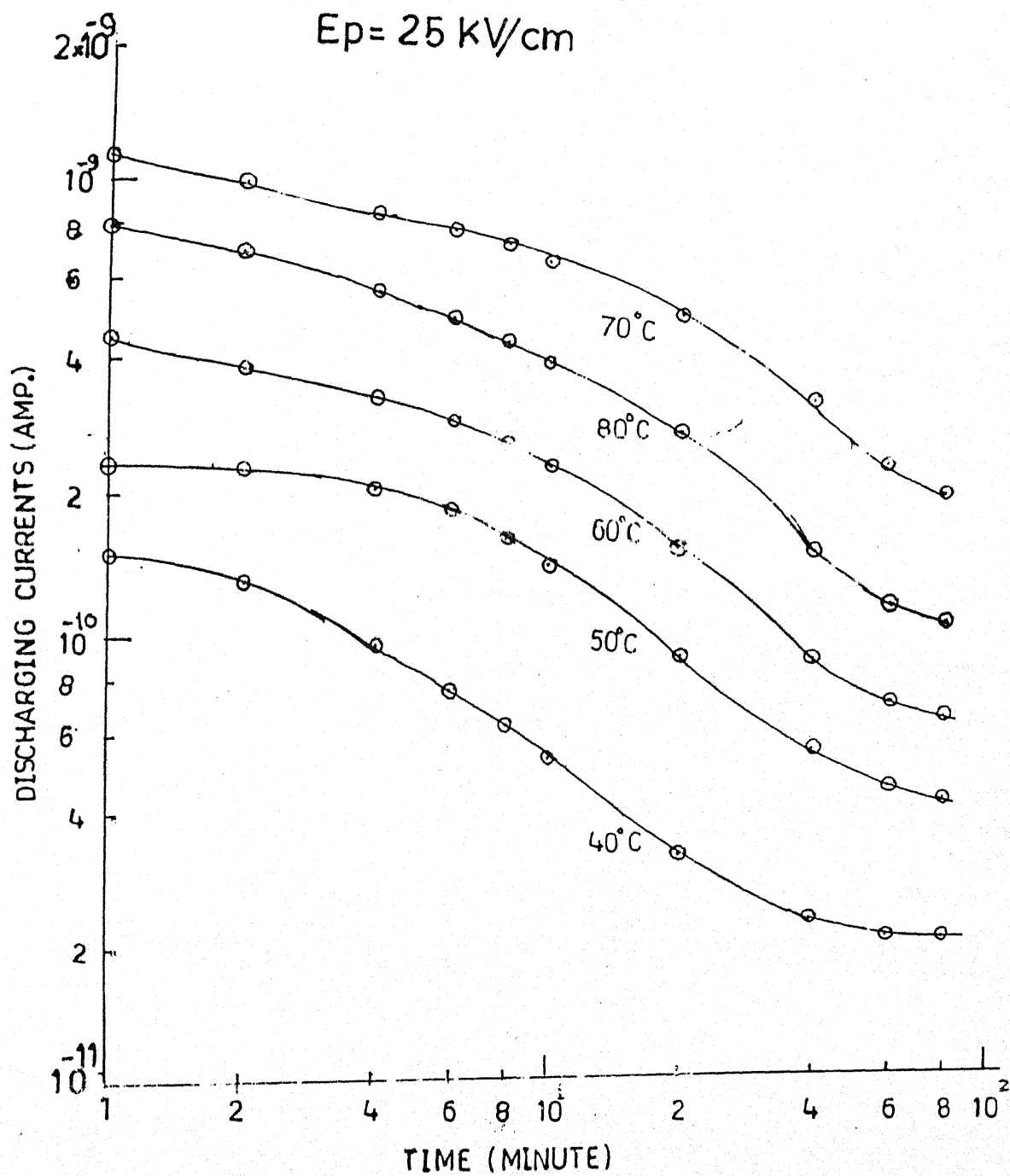


Fig. 5.5 (B) Transient current curves for discharging mode at polarising field and different temperatures with Al-Ag system.

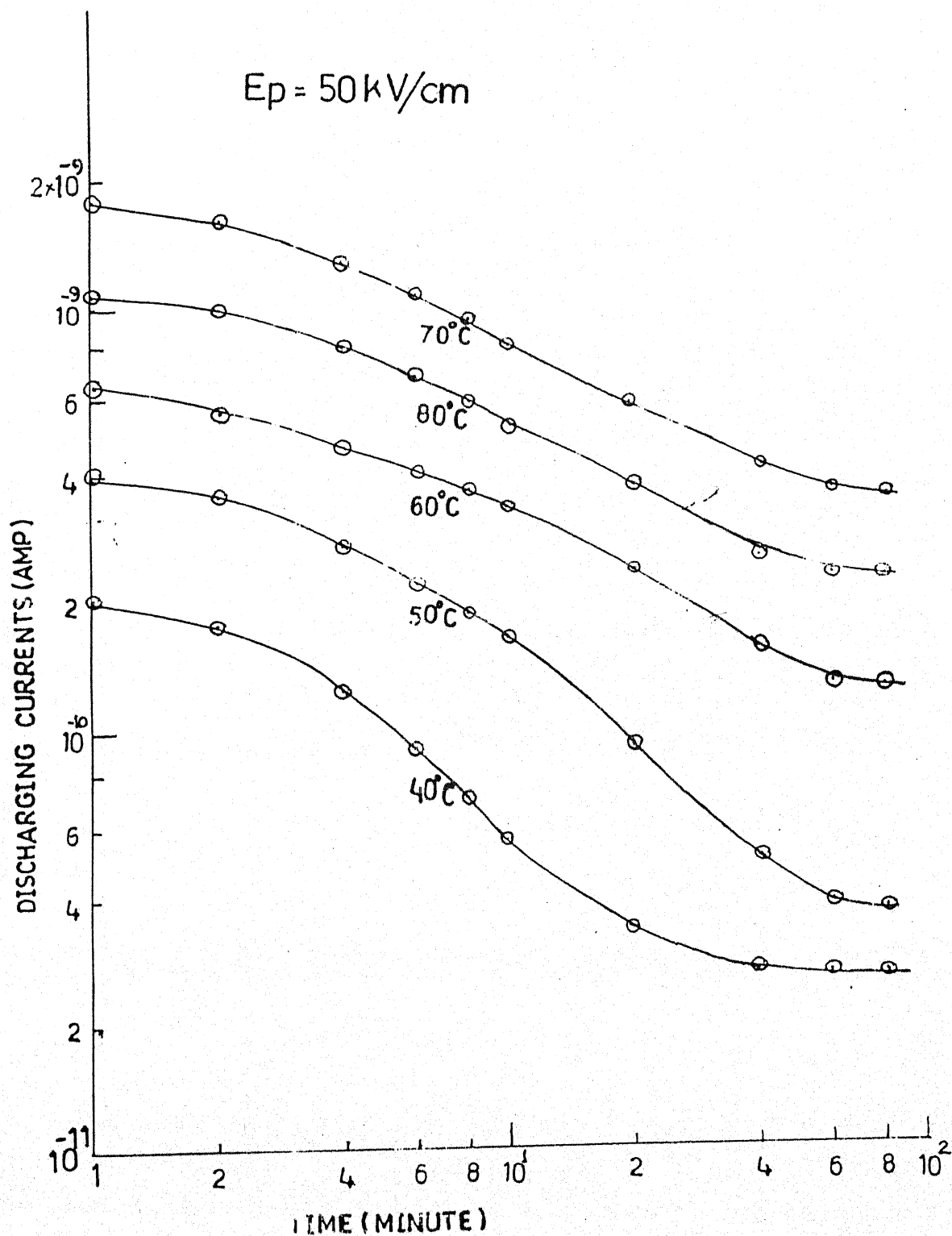


Fig. 5.5 (B) Transient current curves for discharging mode at polarising field and different temperatures with Al-Ag system.

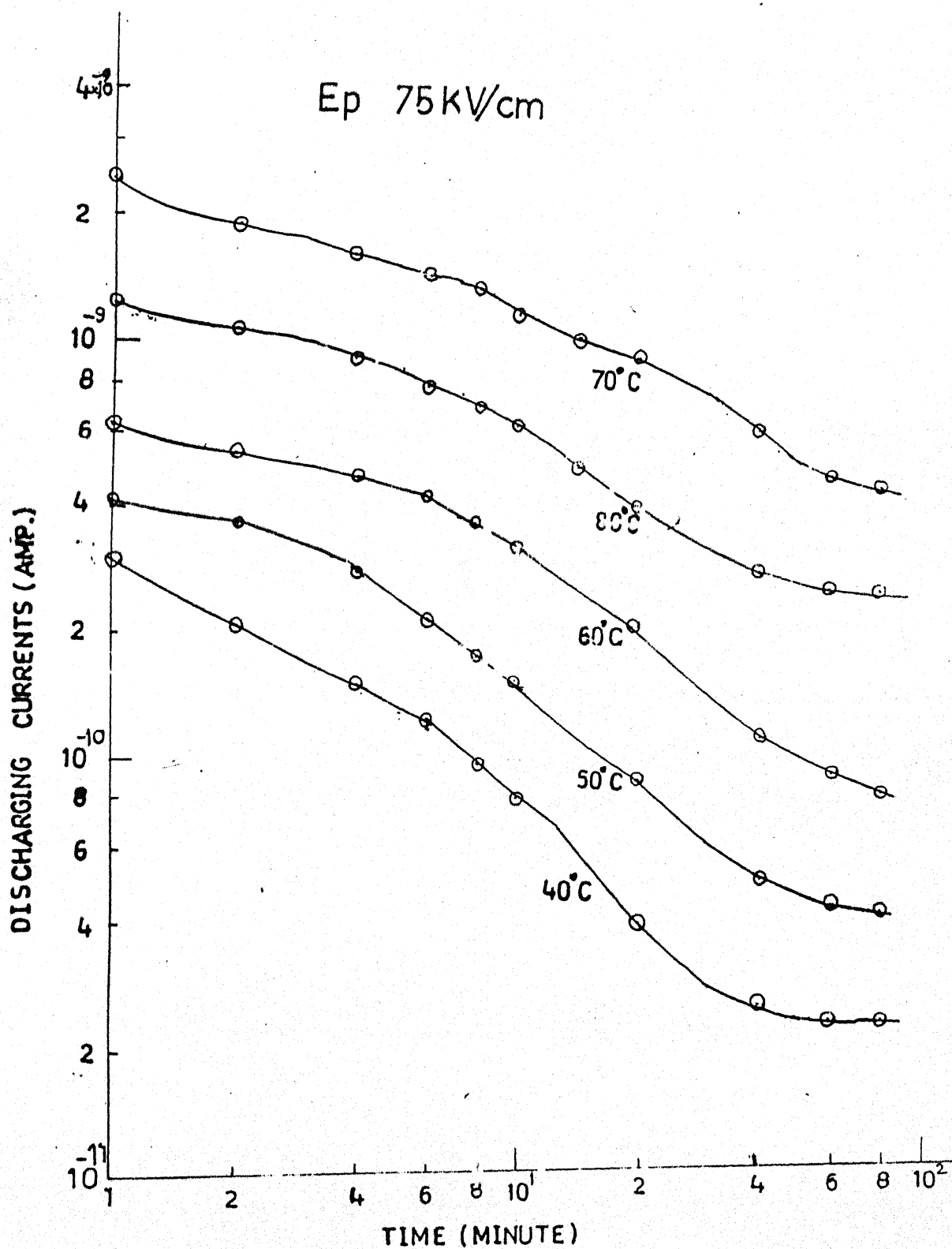


Fig. 5.5 (C) Transient current curves for discharging mode at polarising field and different temperatures with Al-Ag system.

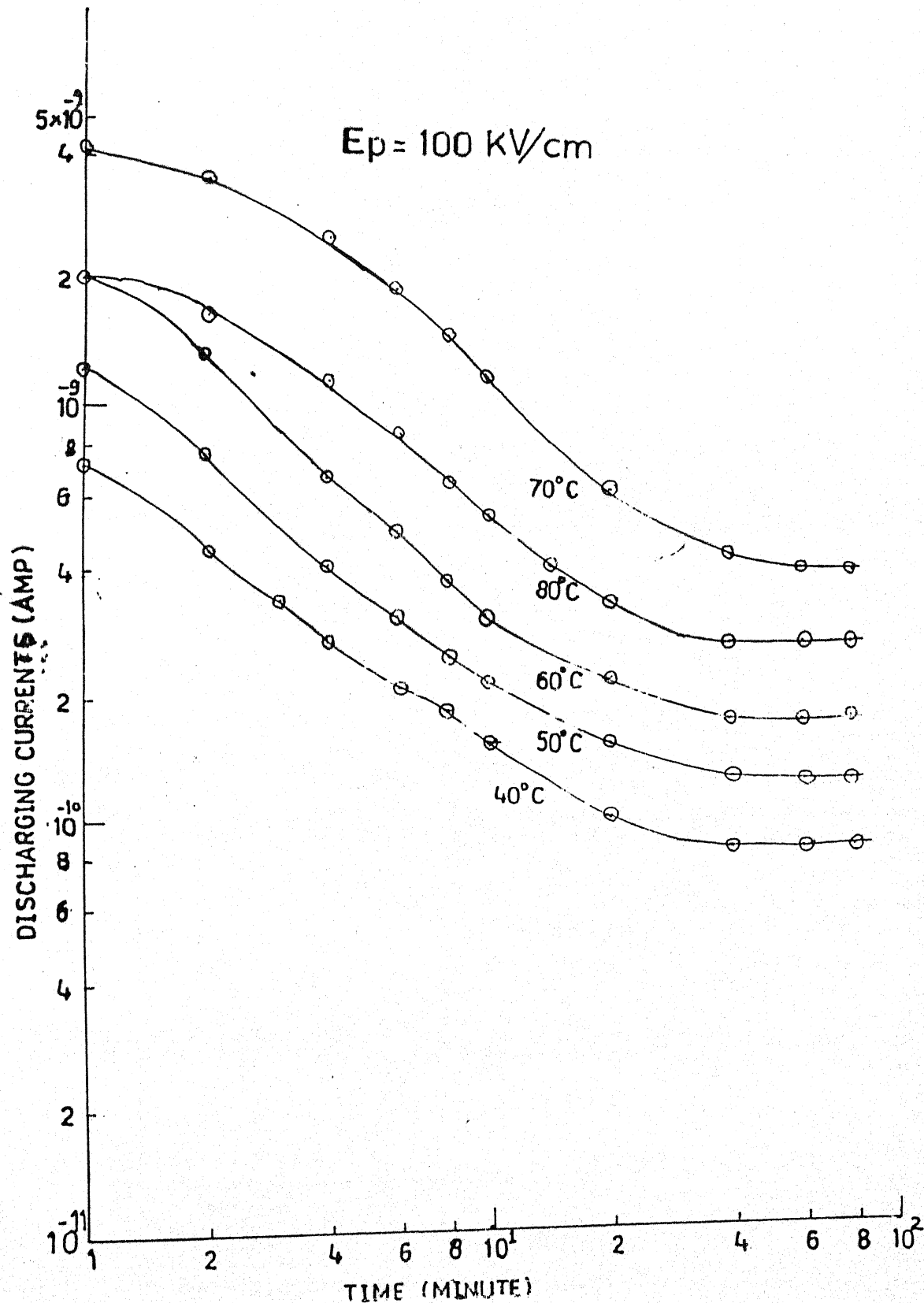


Fig. 5.5 (C) Transient current curves for discharging mode at polarising field and different temperatures with Al-Ag system.

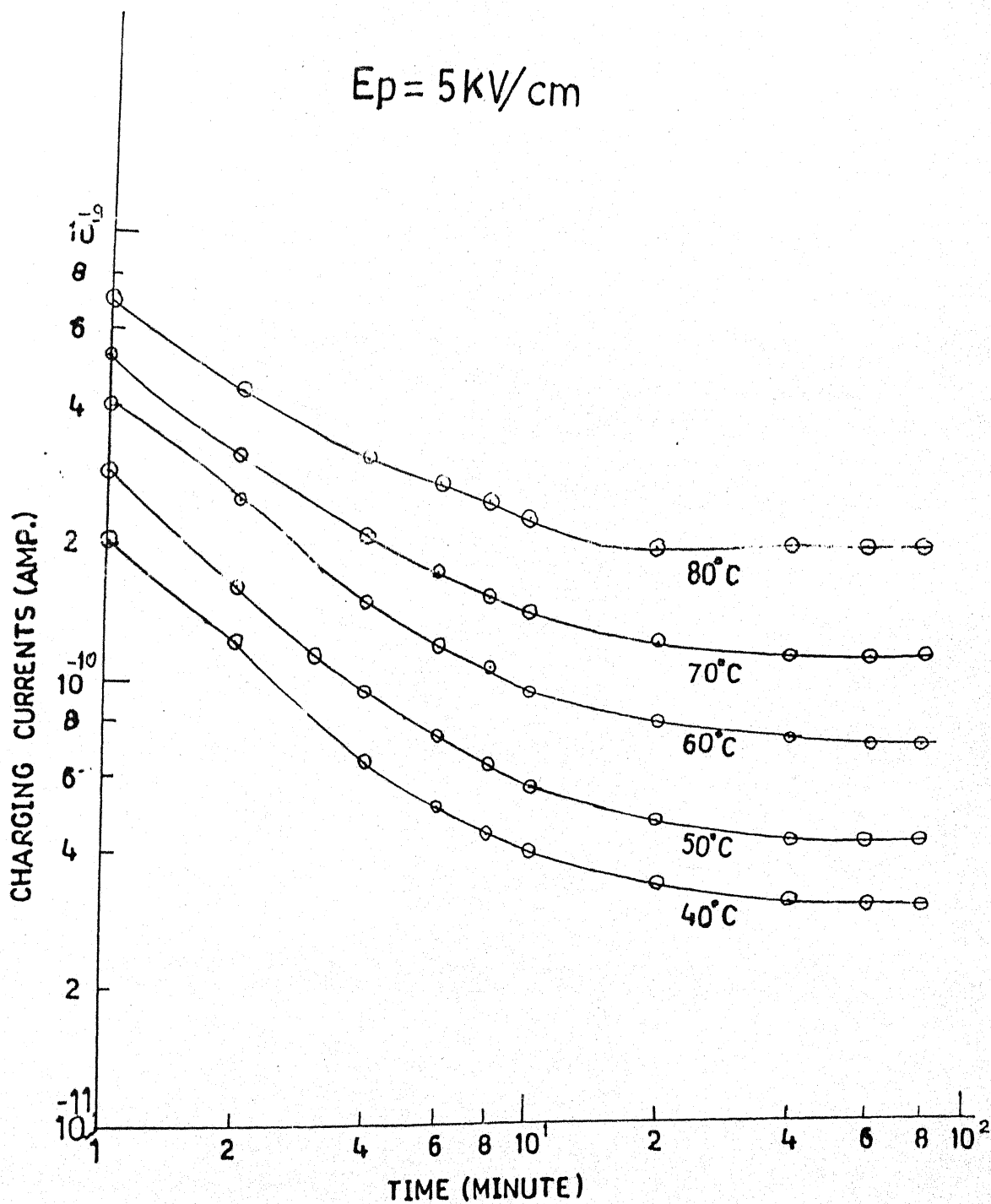


Fig. 5.6 (a) Transient current curves for charging mode at polarising field and different temperatures with Al-Cu system.

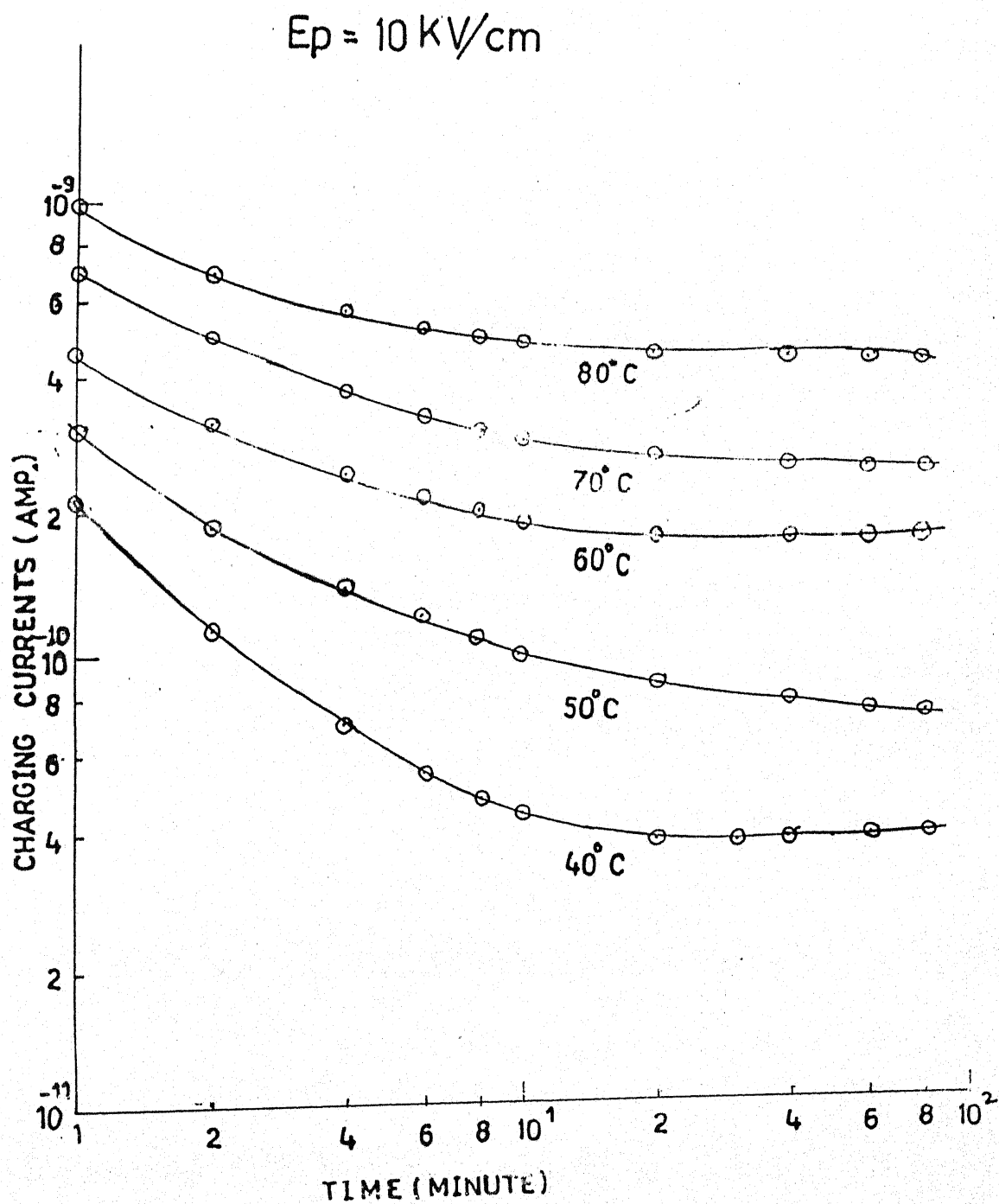


Fig. 5.6 (a) Transient current curves for charging mode at polarising field and different temperatures with Al-Cu system.

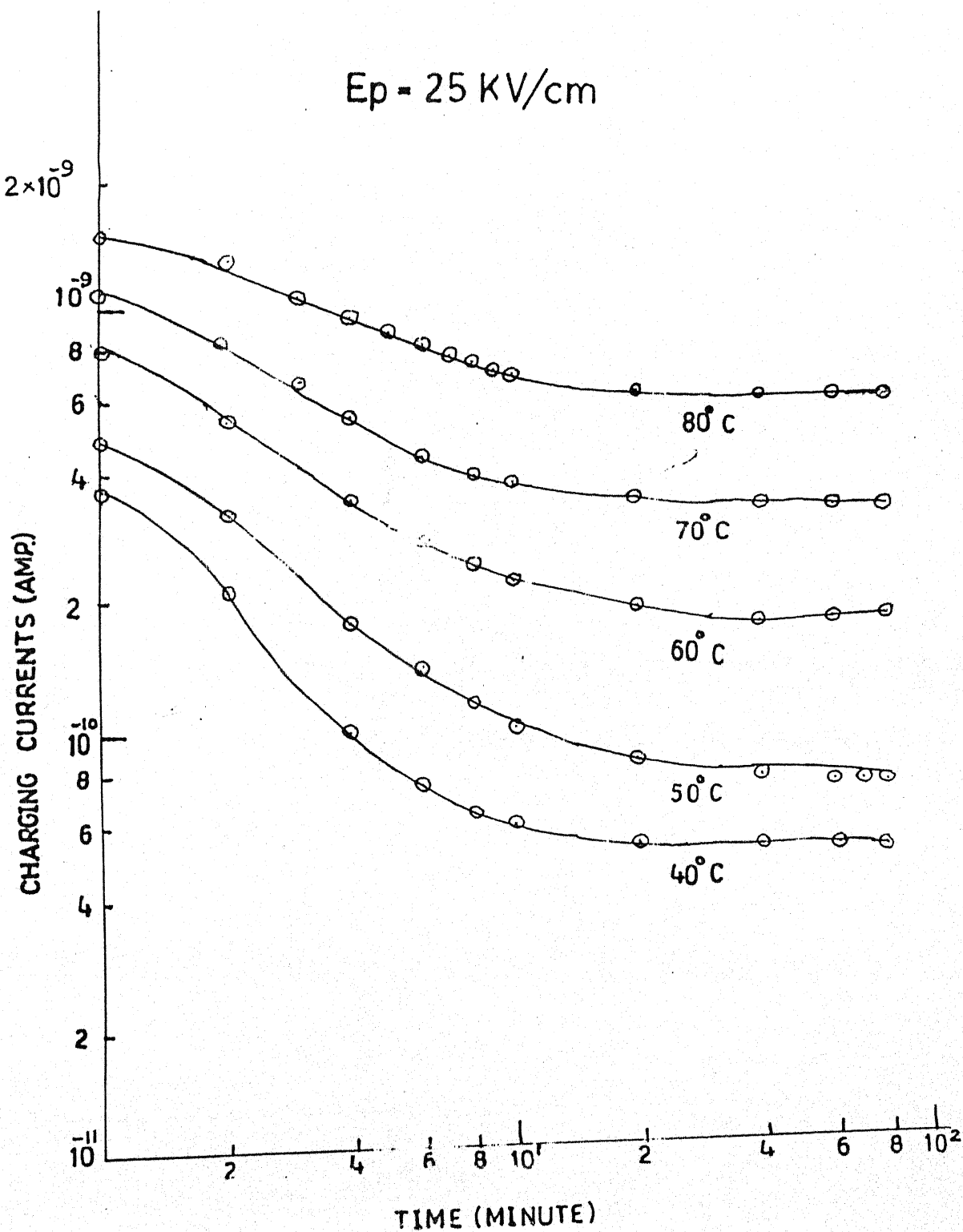


Fig. 5.6 (b) Transient current curves for charging mode at polarising field and different temperatures with Al-Cu system.

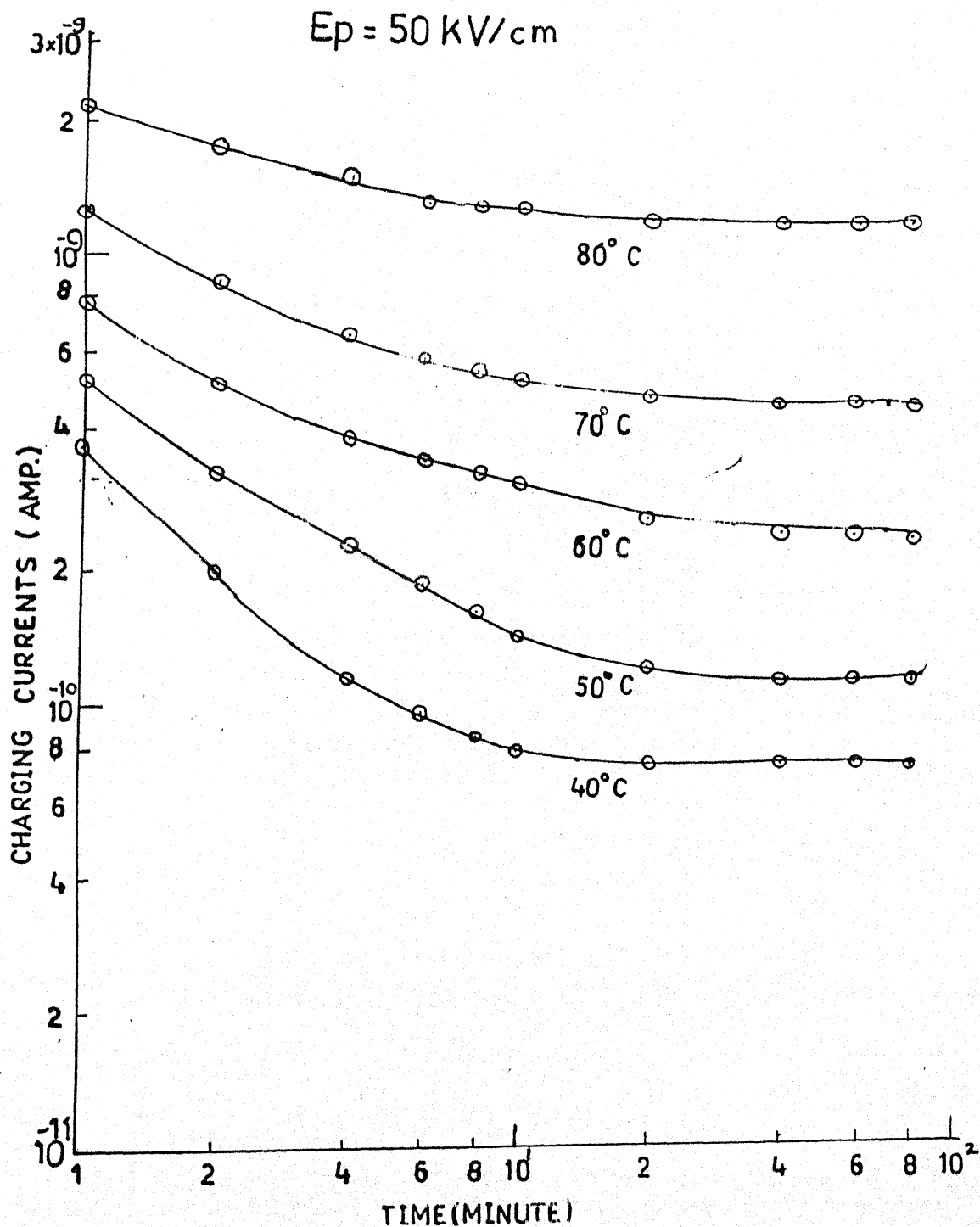


Fig. 5.6 (b) Transient current curves for charging mode at polarising field and different temperatures with Al-Cu system.

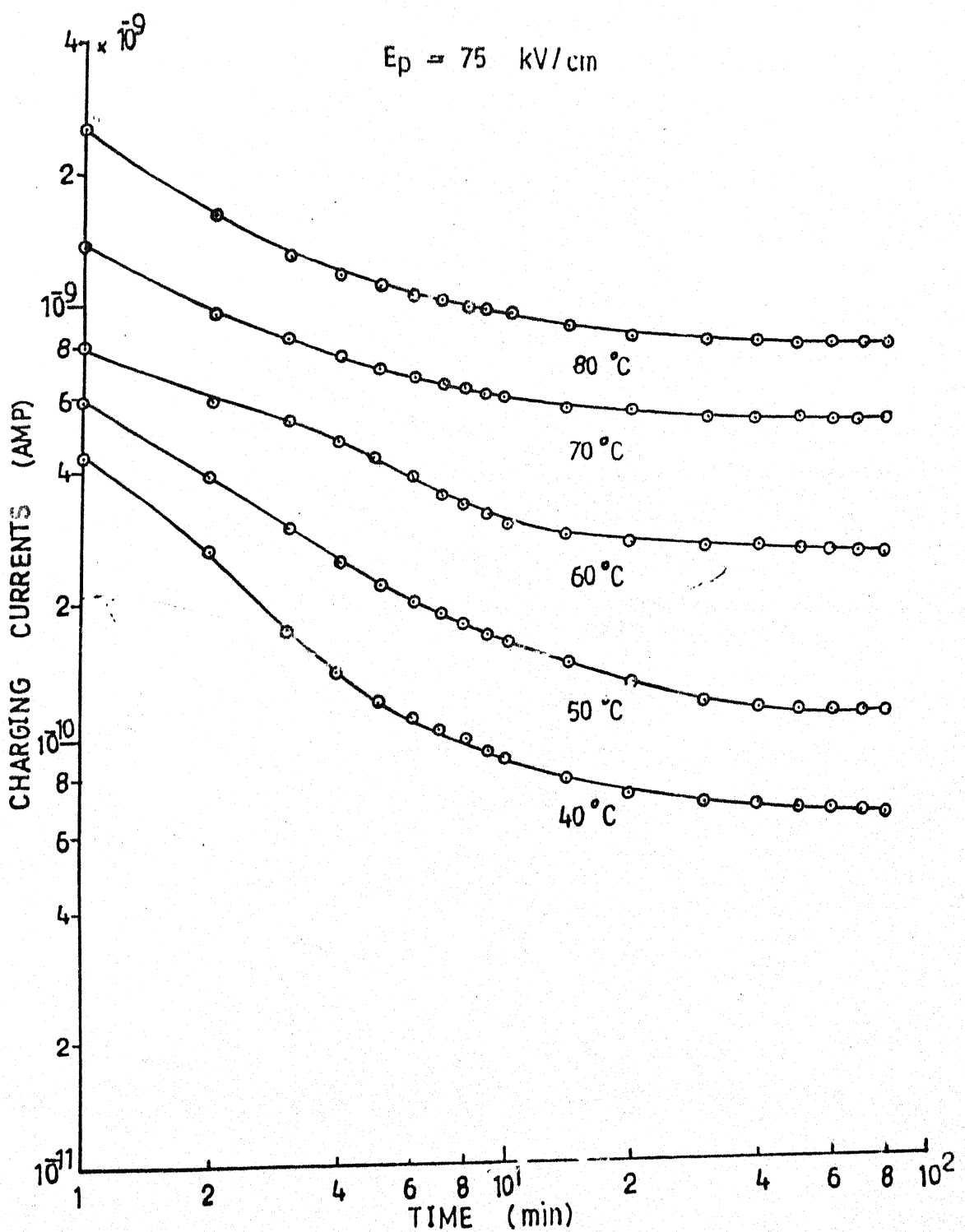


Fig. 5.6 (c) Transient current curves for charging mode at polarising field and different temperatures with Al-Cu system.

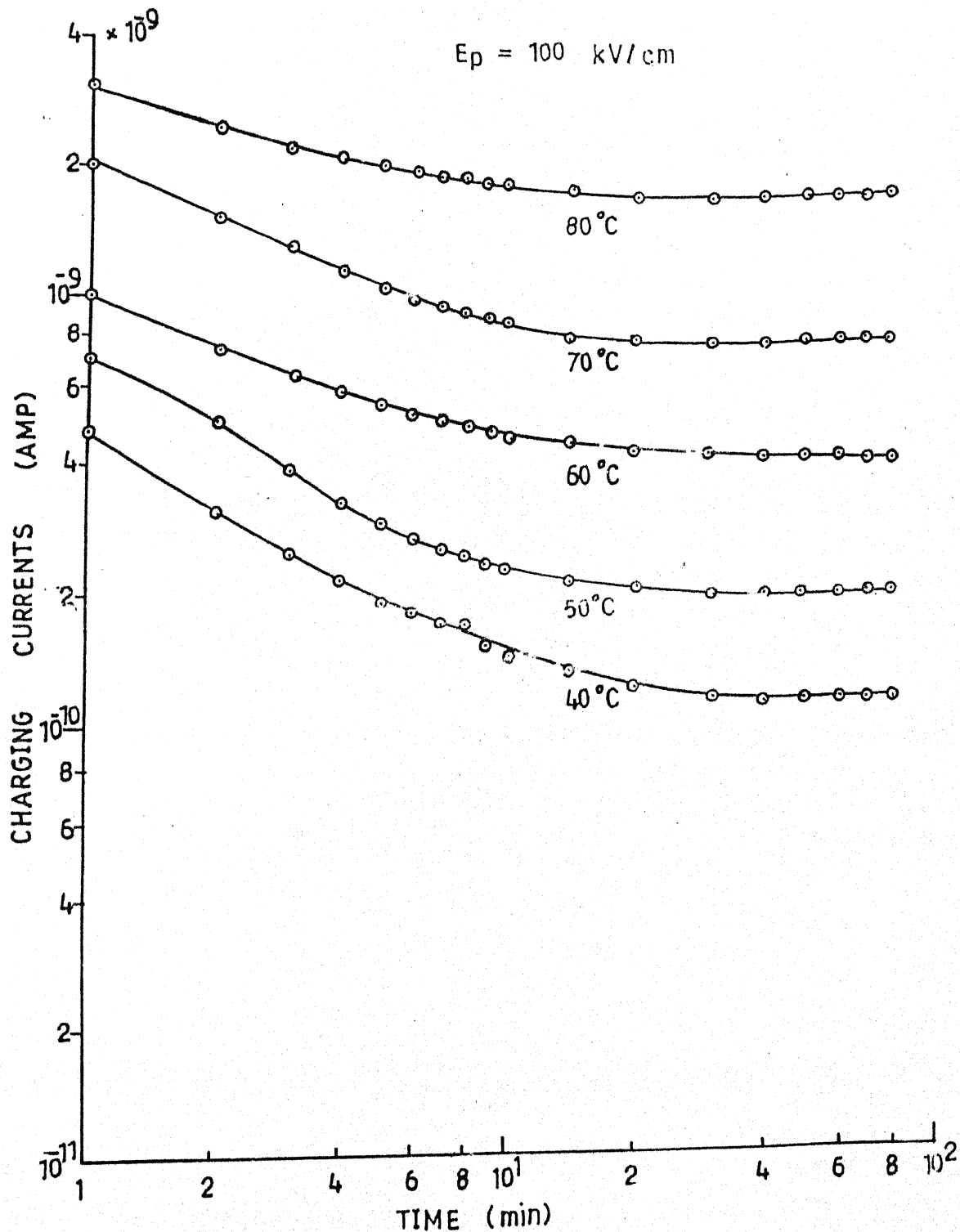


Fig. 5.6 (c) Transient current curves for charging mode at polarising field and different temperatures with Al-Cu system.

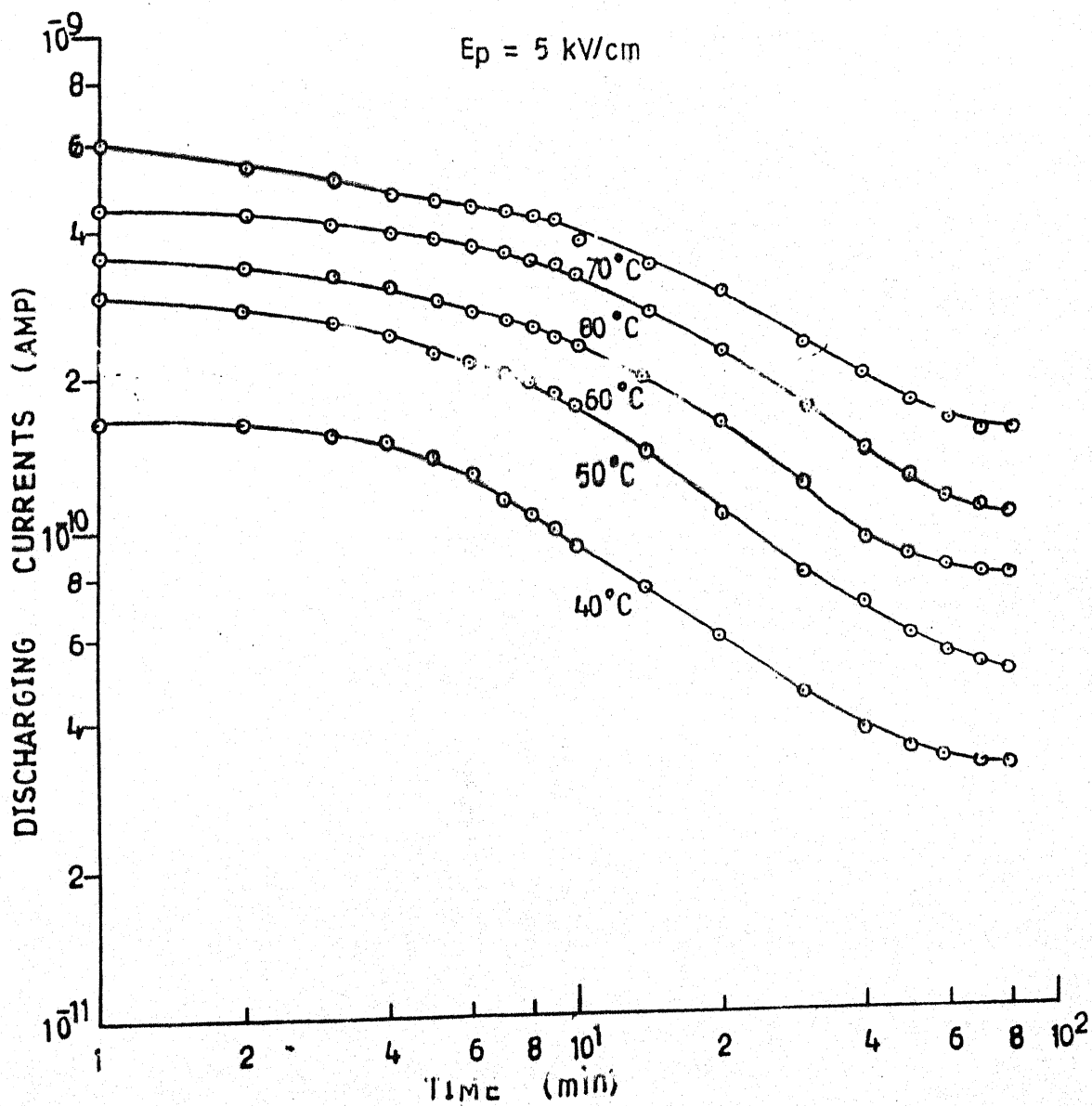


Fig. 5.6 (A) Tansient current curves for discharging mode at polarising field and different temperatures with Al-Cu system.

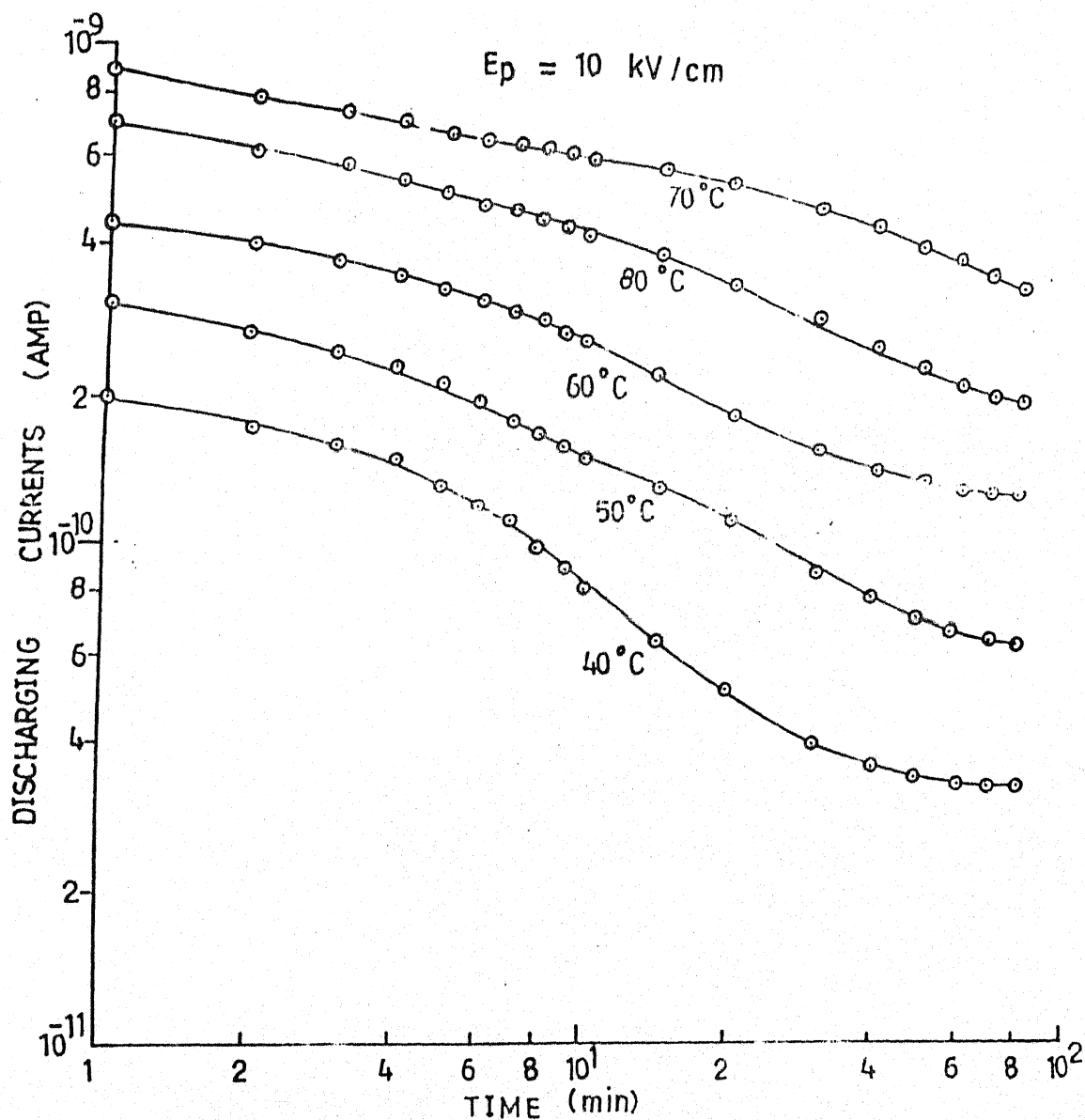


Fig. 5.6 (A) Tansient current curves for discharging mode at polarising field and different temperatures with Al-Cu system.

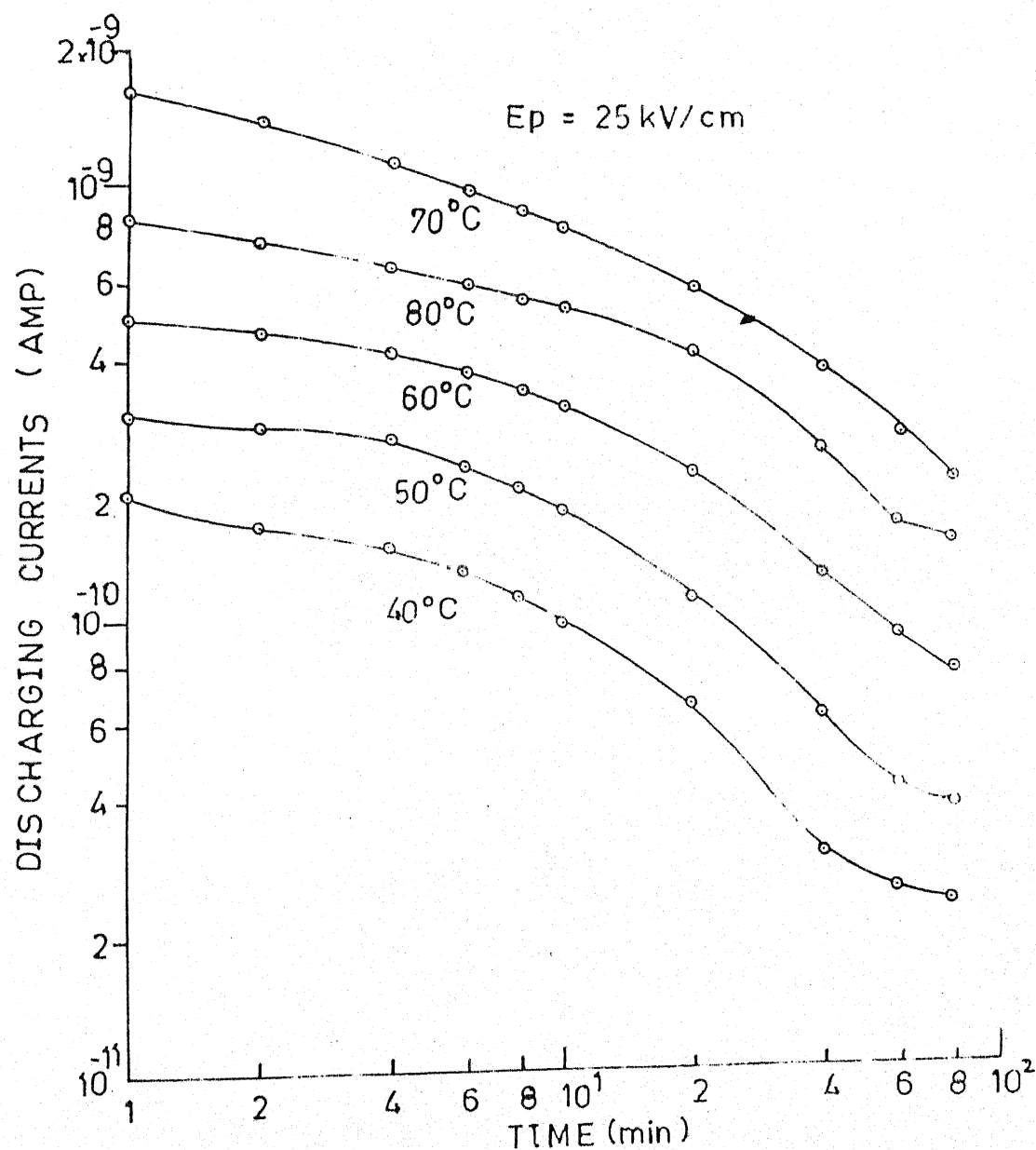


Fig. 5.6 (B) Tansient current curves for discharging mode at polarising field and different temperatures with Al-Cu system.

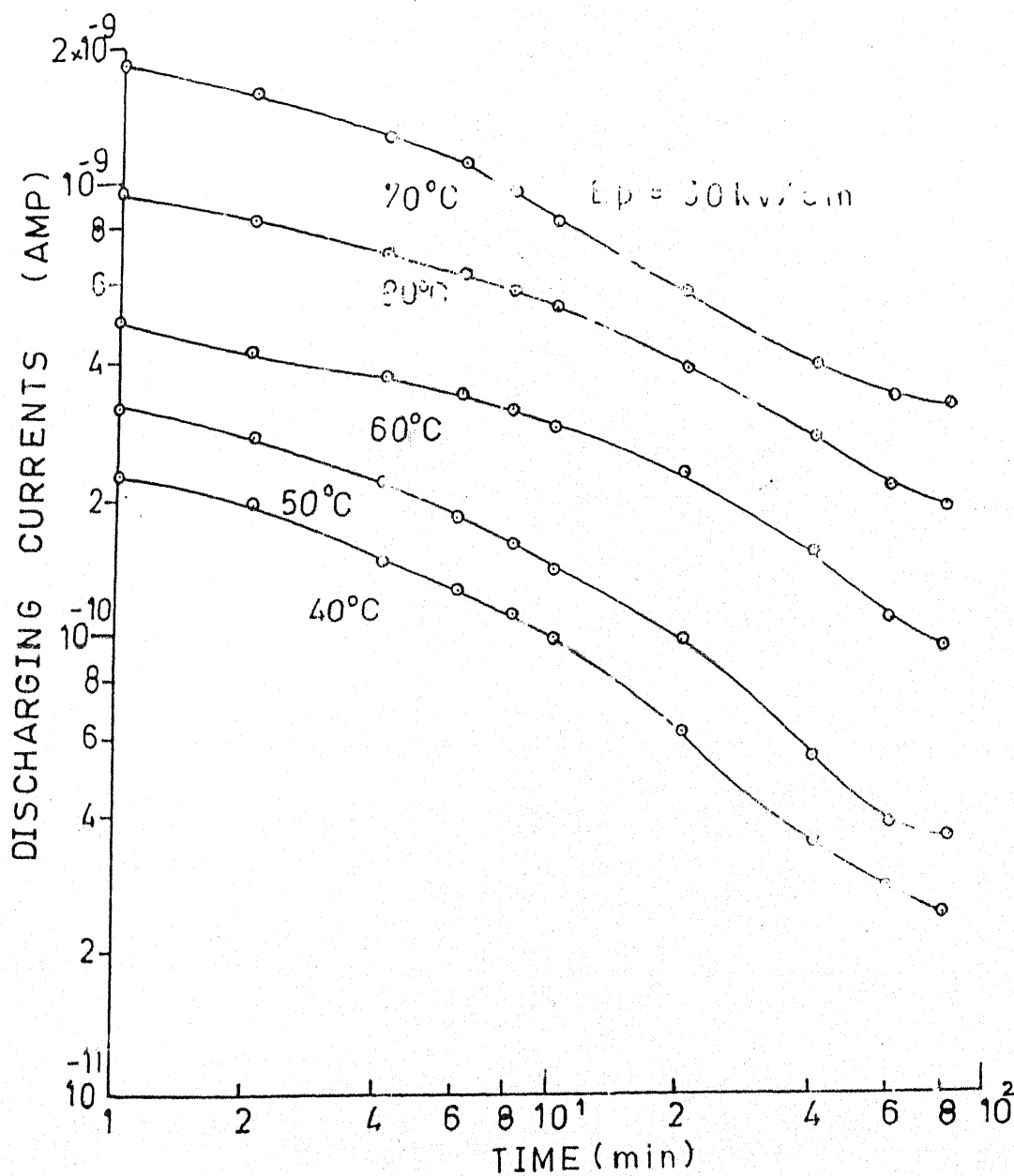


Fig. 5.6 (B) Tansient current curves for discharging mode at polarising field and different temperatures with Al-Cu system.

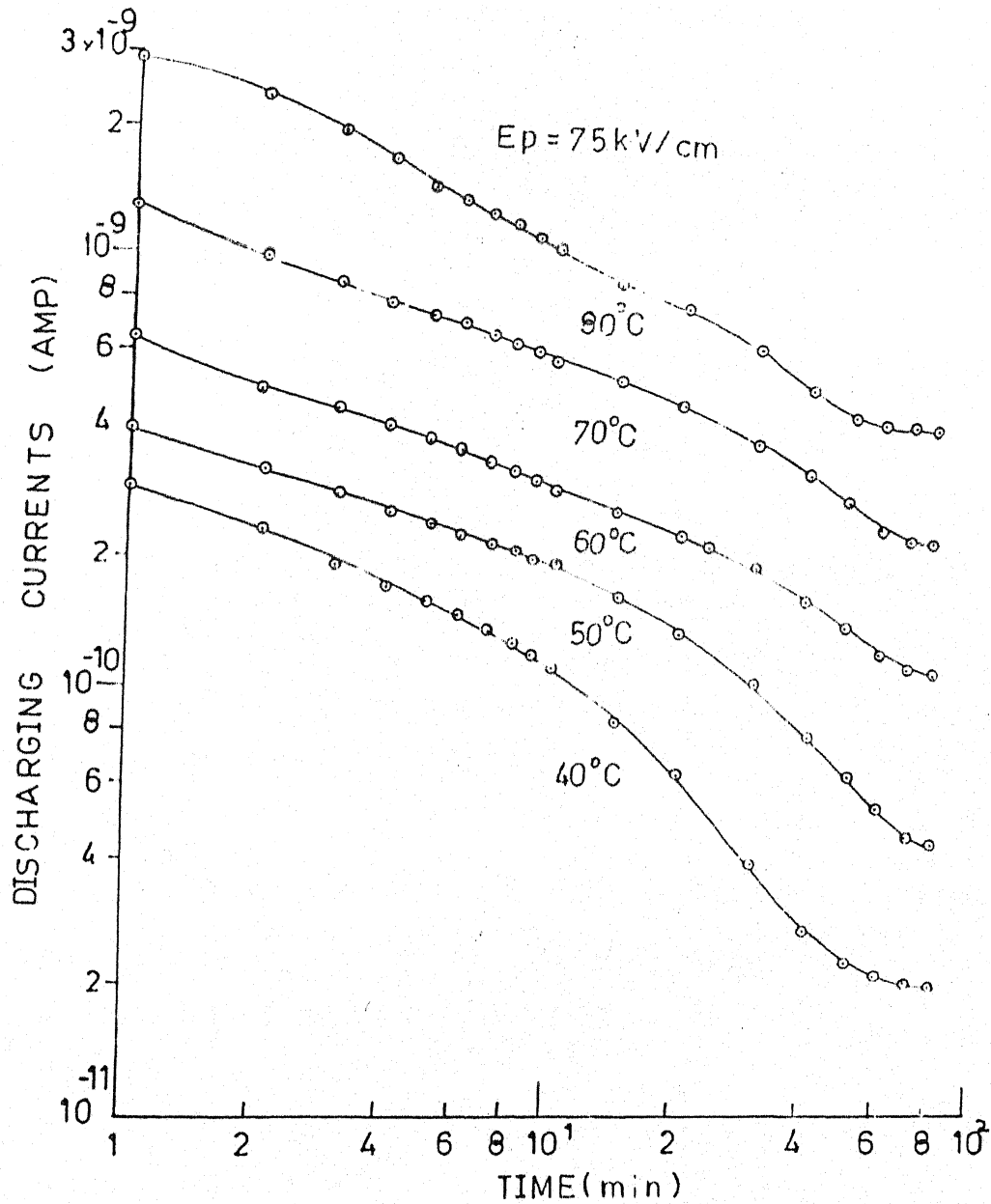


Fig. 5.6 (C) Tansient current curves for discharging mode at polarising field and different temperatures with Al-Cu system.

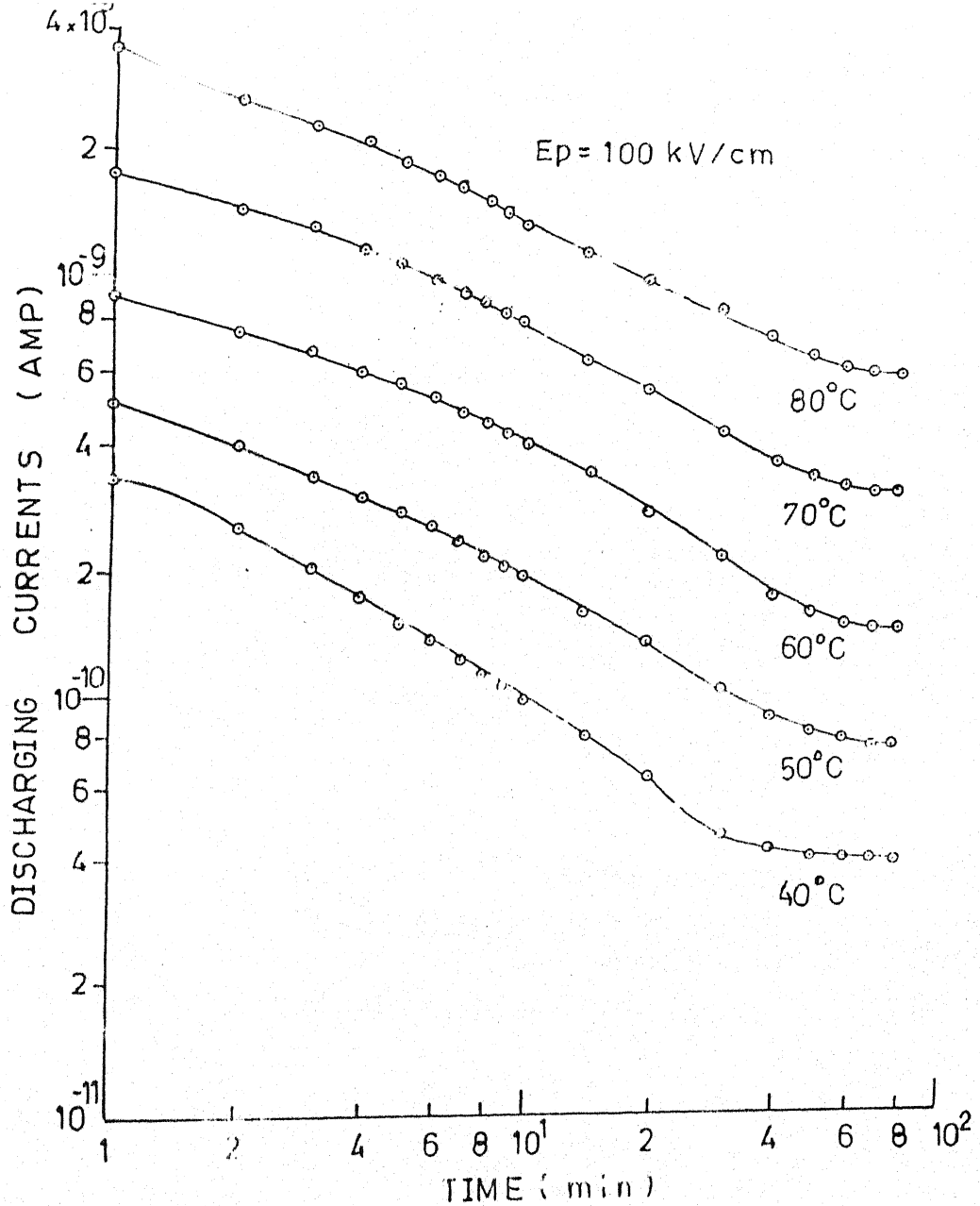


Fig. 5.6 (C) Tansient current curves for discharging mode at polarising field and different temperatures with Al-Cu system.

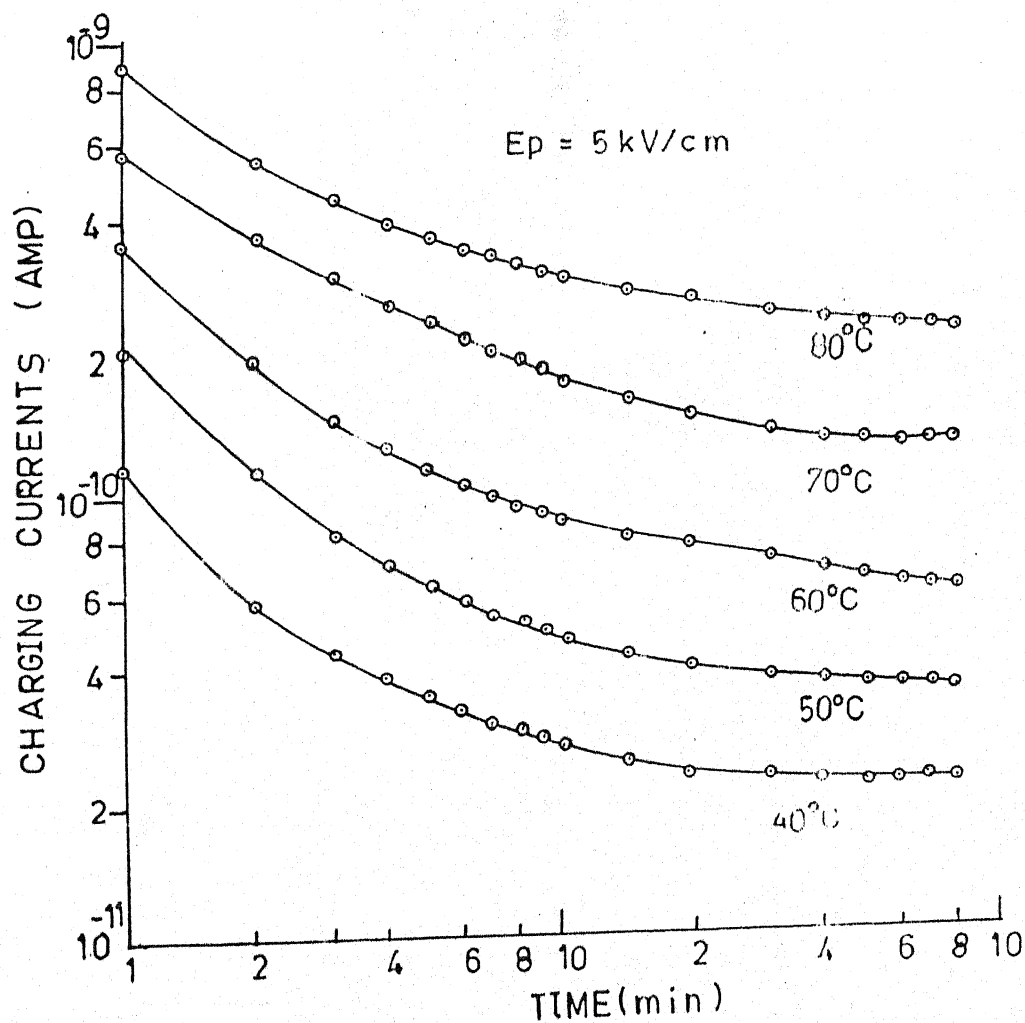


Fig. 5.7 (a) Transient current curves for charging mode at polarising field and different temperatures with Al-Sn system.

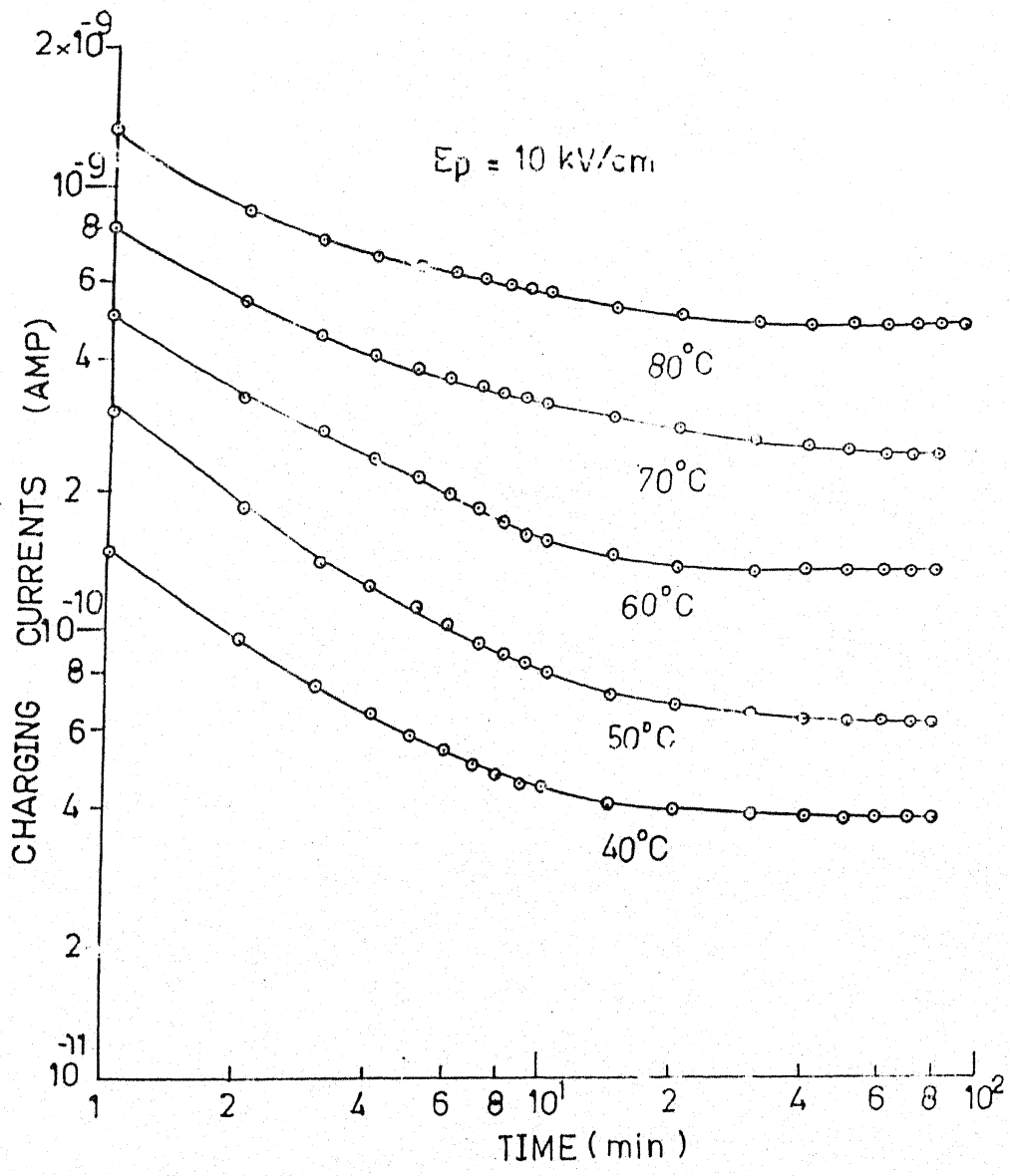


Fig. 5.7 (a) Tansient current curves for charging mode at polarising field and different temperatures with Al-Sn system.

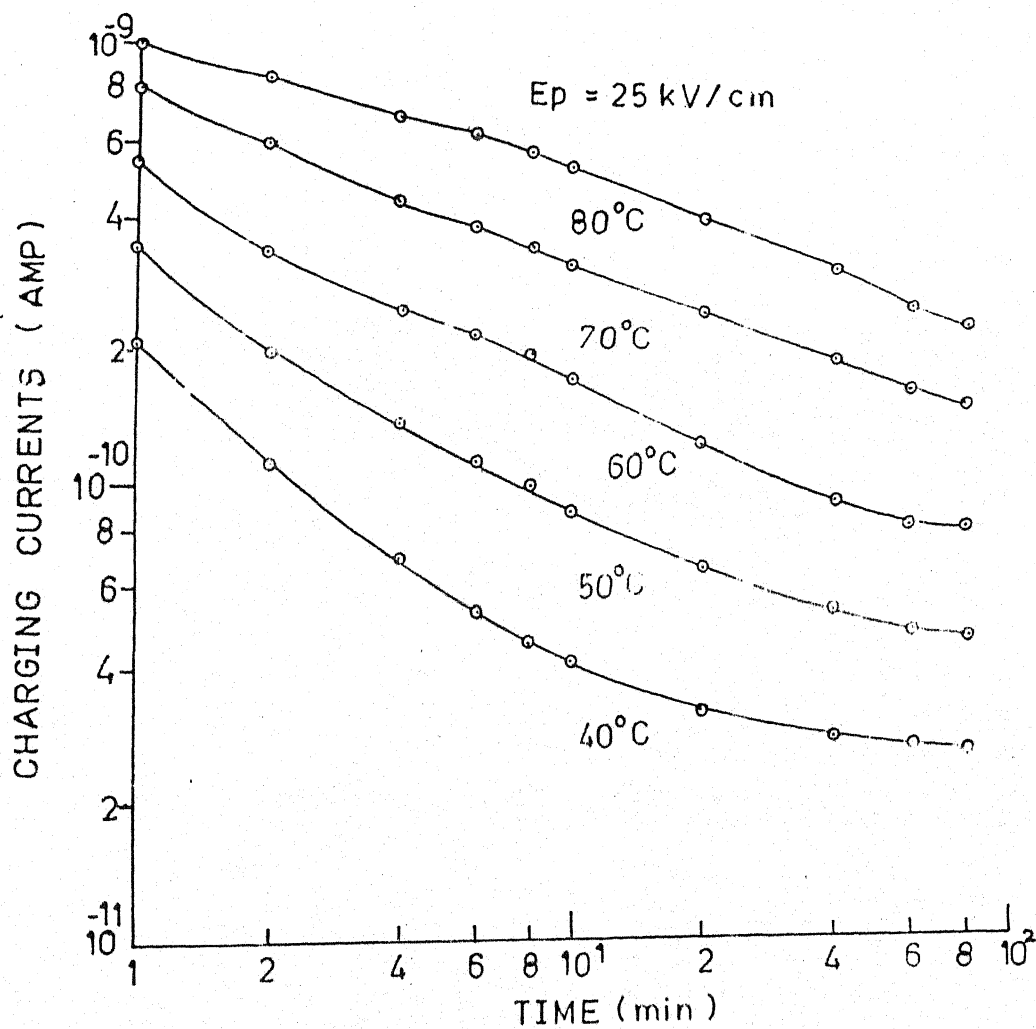


Fig. 5.7 (b) Tansient current curves for charging mode at polarising field and different temperatures with Al-Sn system.

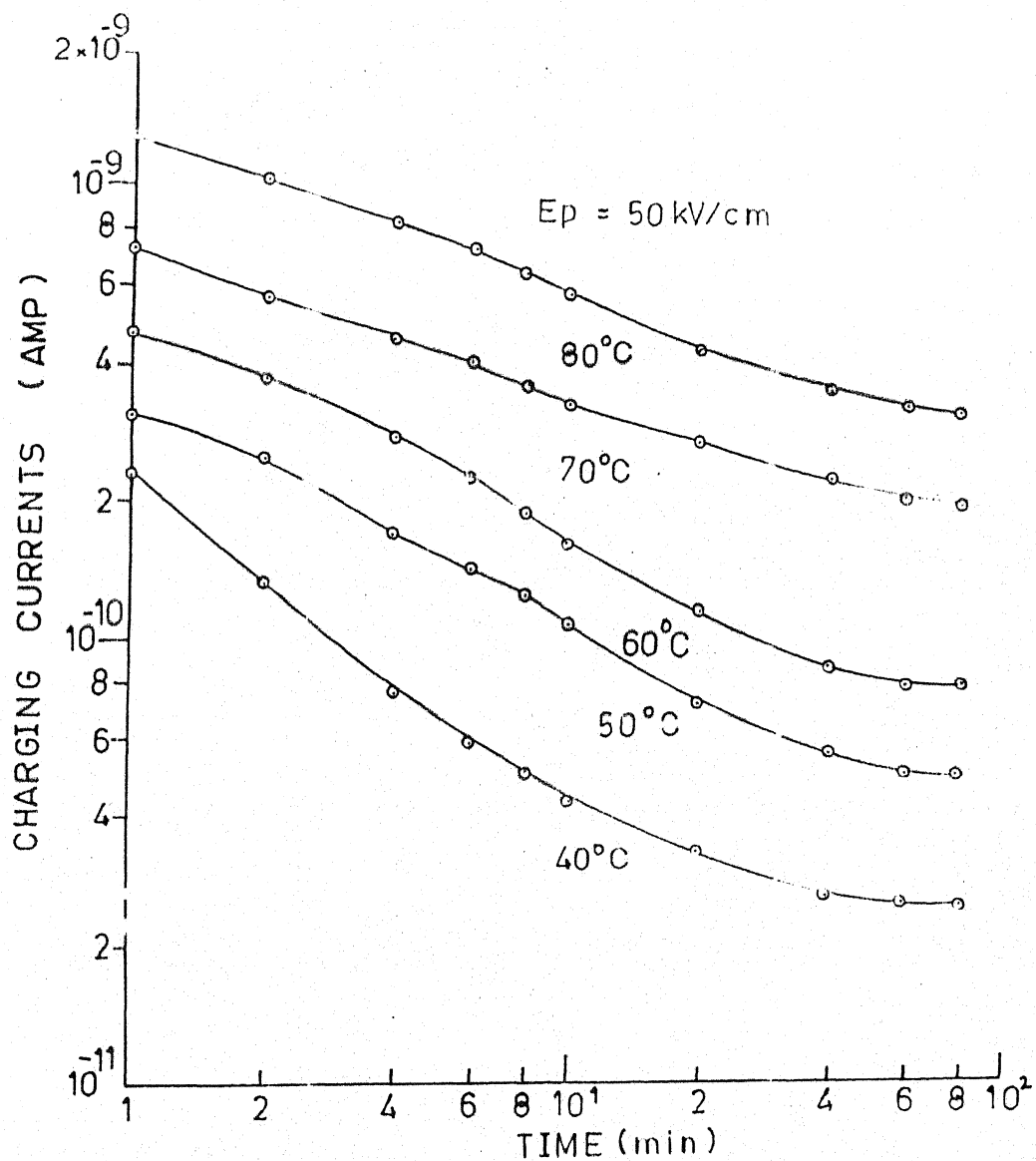


Fig. 5.7 (b) Tansient current curves for charging mode at polarising field and different temperatures with Al-Sn system.

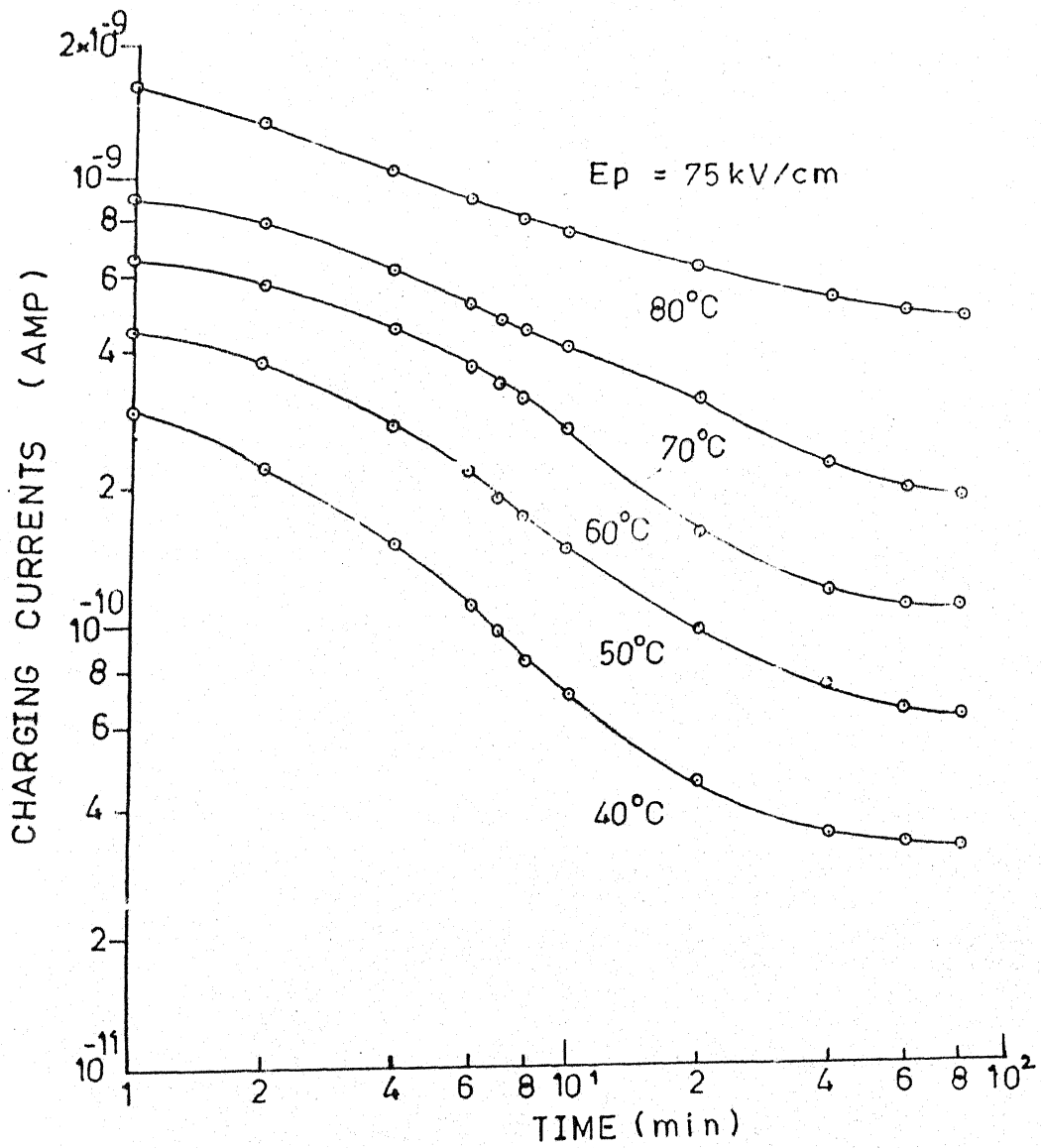


Fig. 5.7 (c) Tansient current curves for charging mode at polarising field and different temperatures with Al-Sn system.

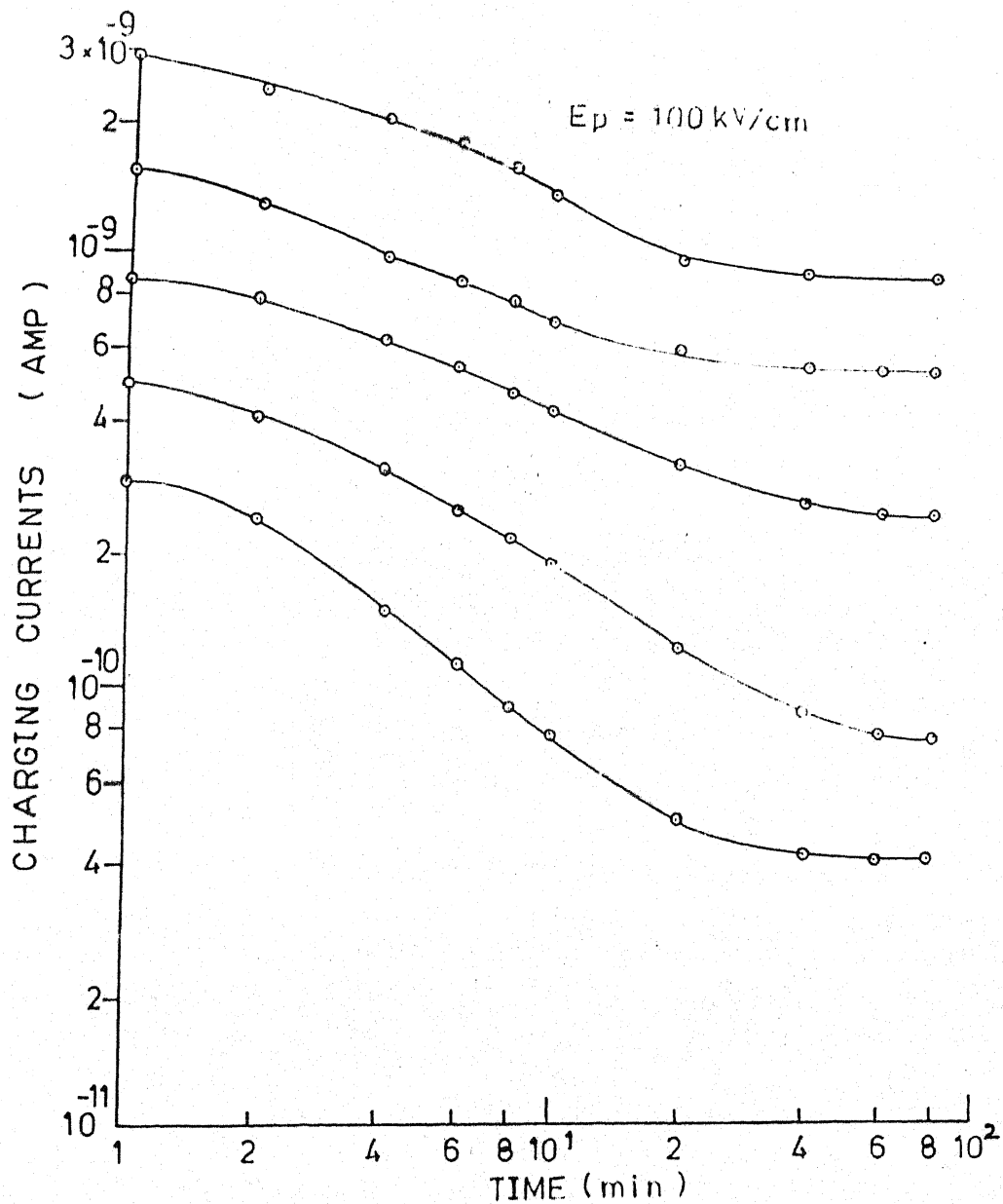


Fig. 5.7 (c) Transient current curves for charging mode at polarising field and different temperatures with Al-Sn system.

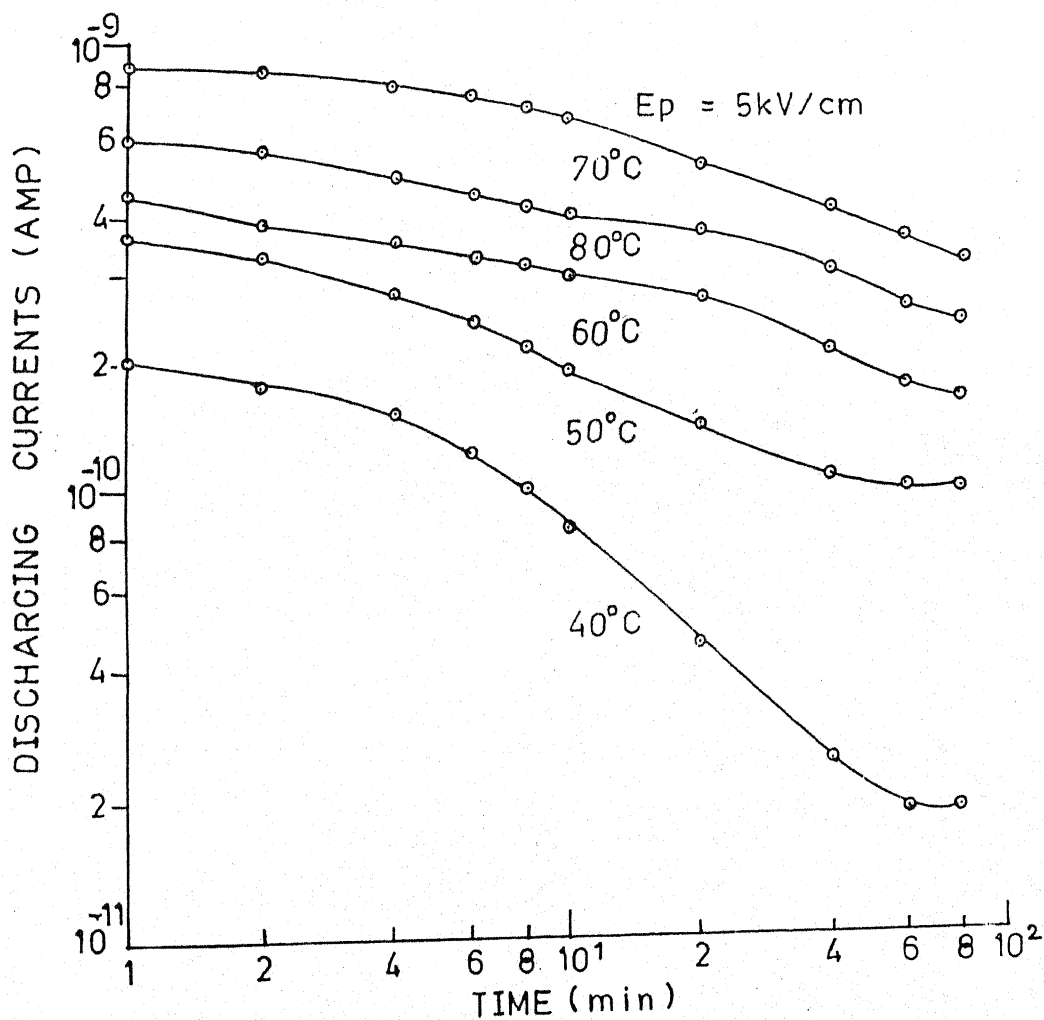


Fig. 5.7 (A) Tansient current curves for discharging mode at polarising field and different temperatures with Al-Sn system.

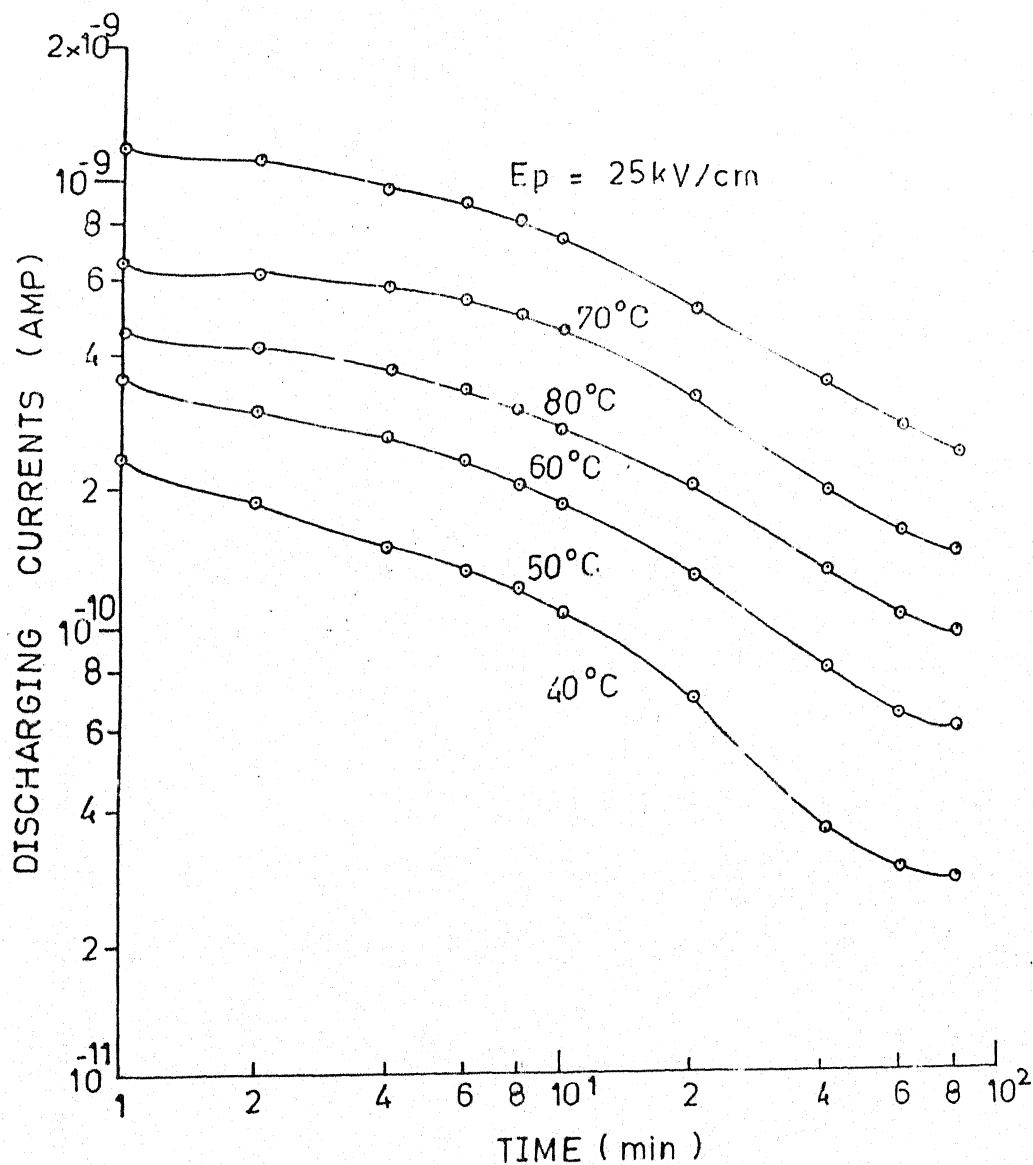


Fig. 5.7 (B) Transient current curves for discharging mode at polarising field and different temperatures with Al-Sn system.

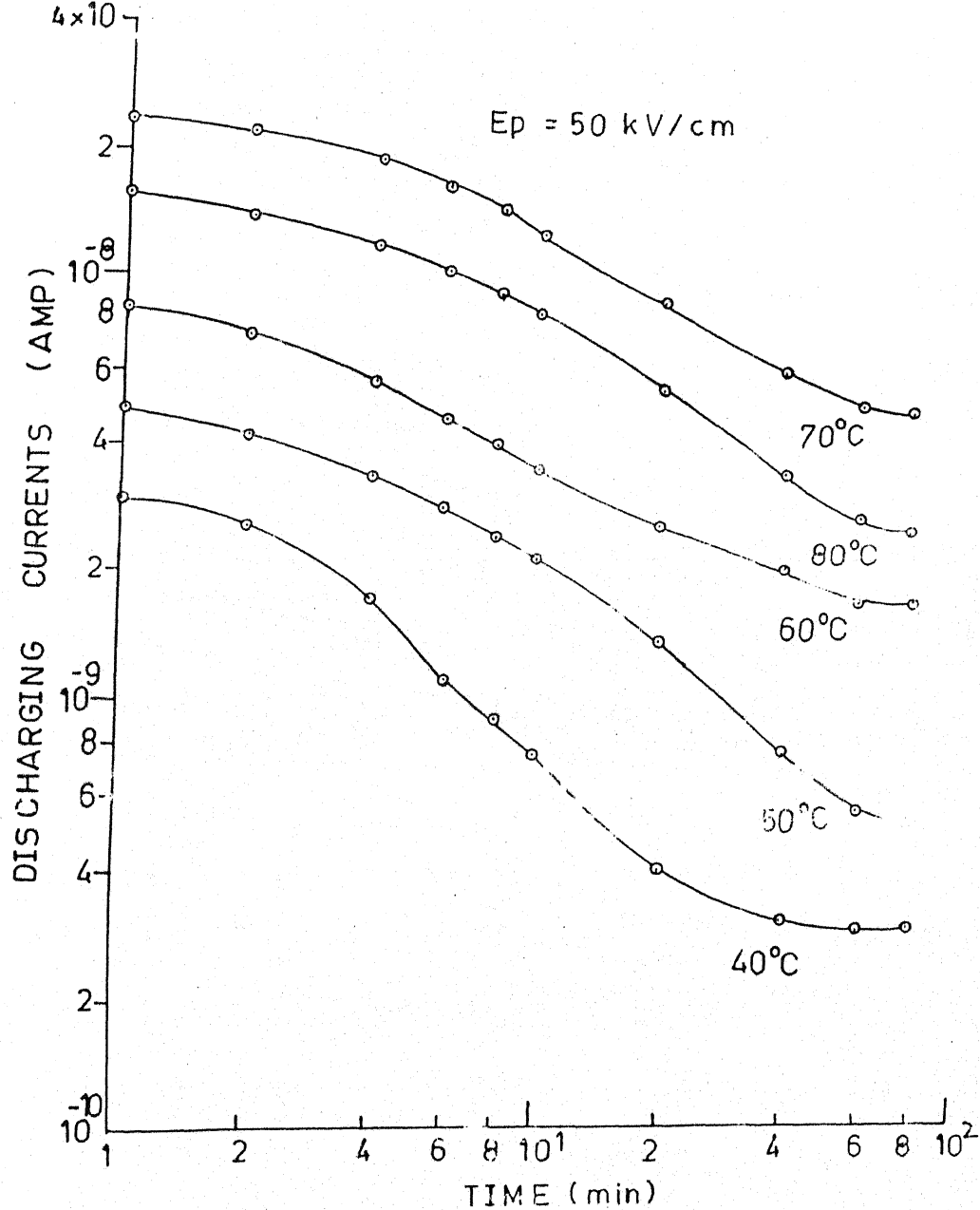


Fig. 5.7 (B) Tansient current curves for discharging mode at polarising field and different temperatures with Al-Sn system.

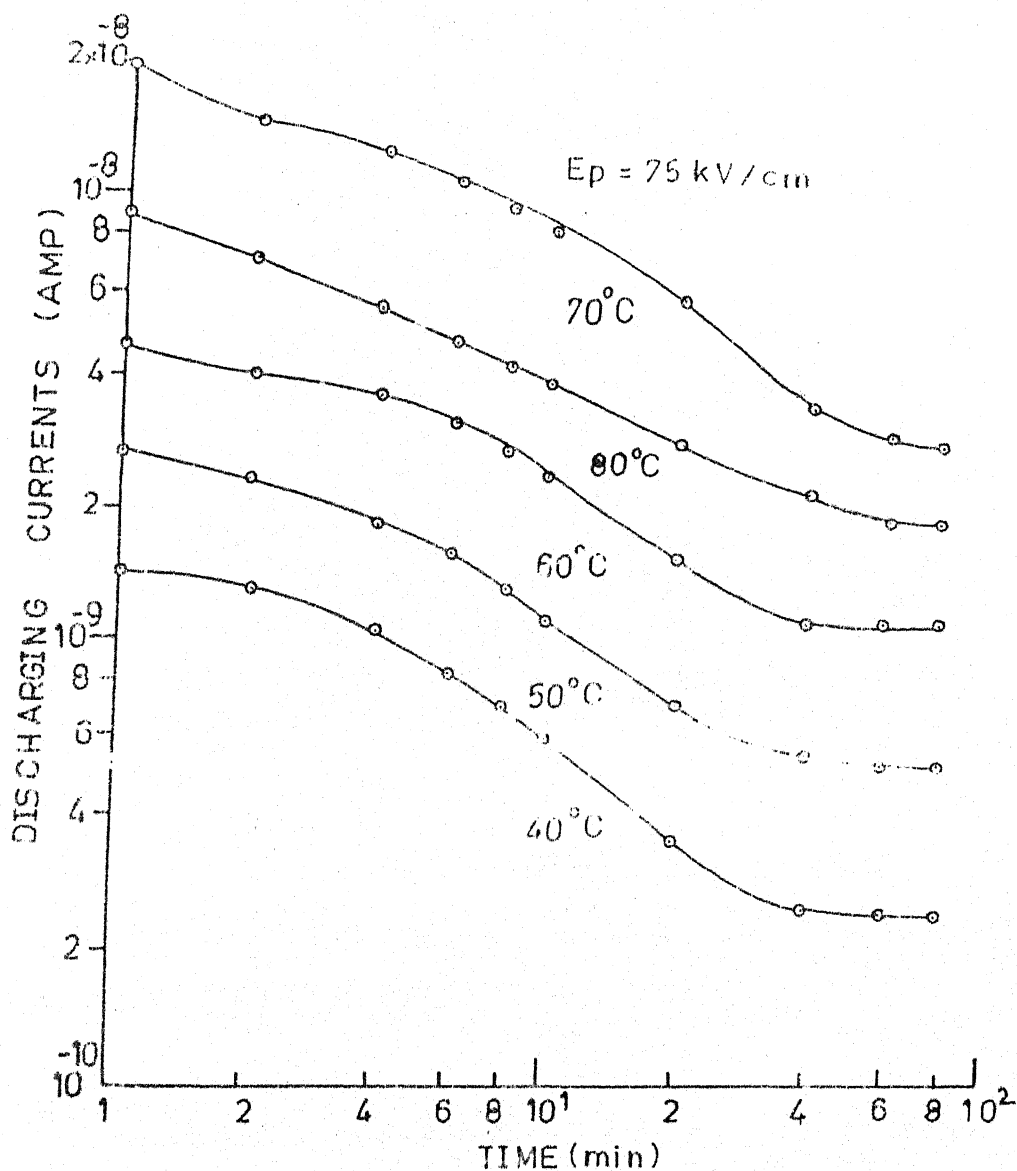


Fig. 5.7 (C) Tansient current curves for discharging mode at polarising field and different temperatures with Al-Sn system.

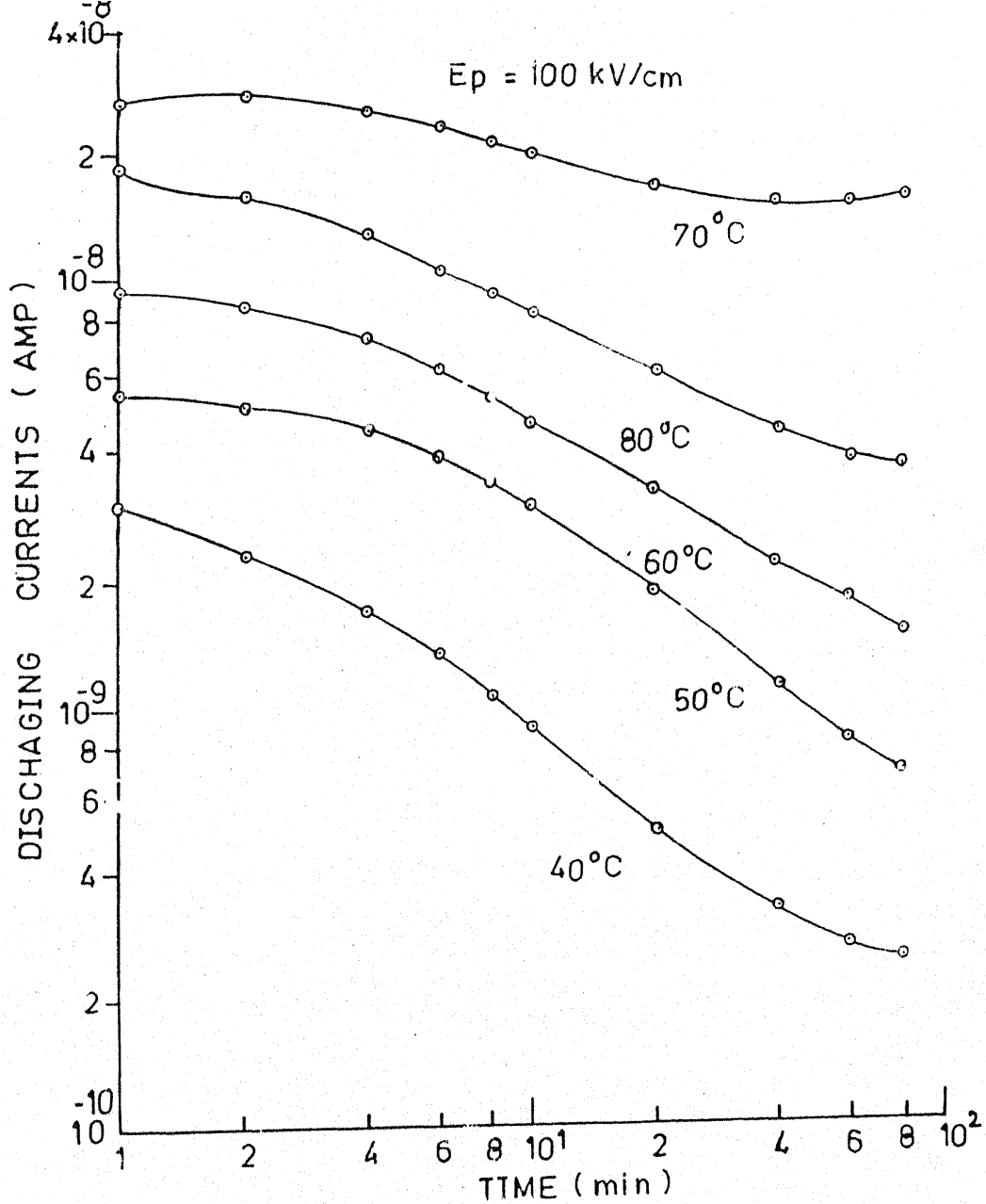


Fig. 5.7 (C) Tansient current curves for discharging mode at polarising field and different temperatures with Al-Sn system.

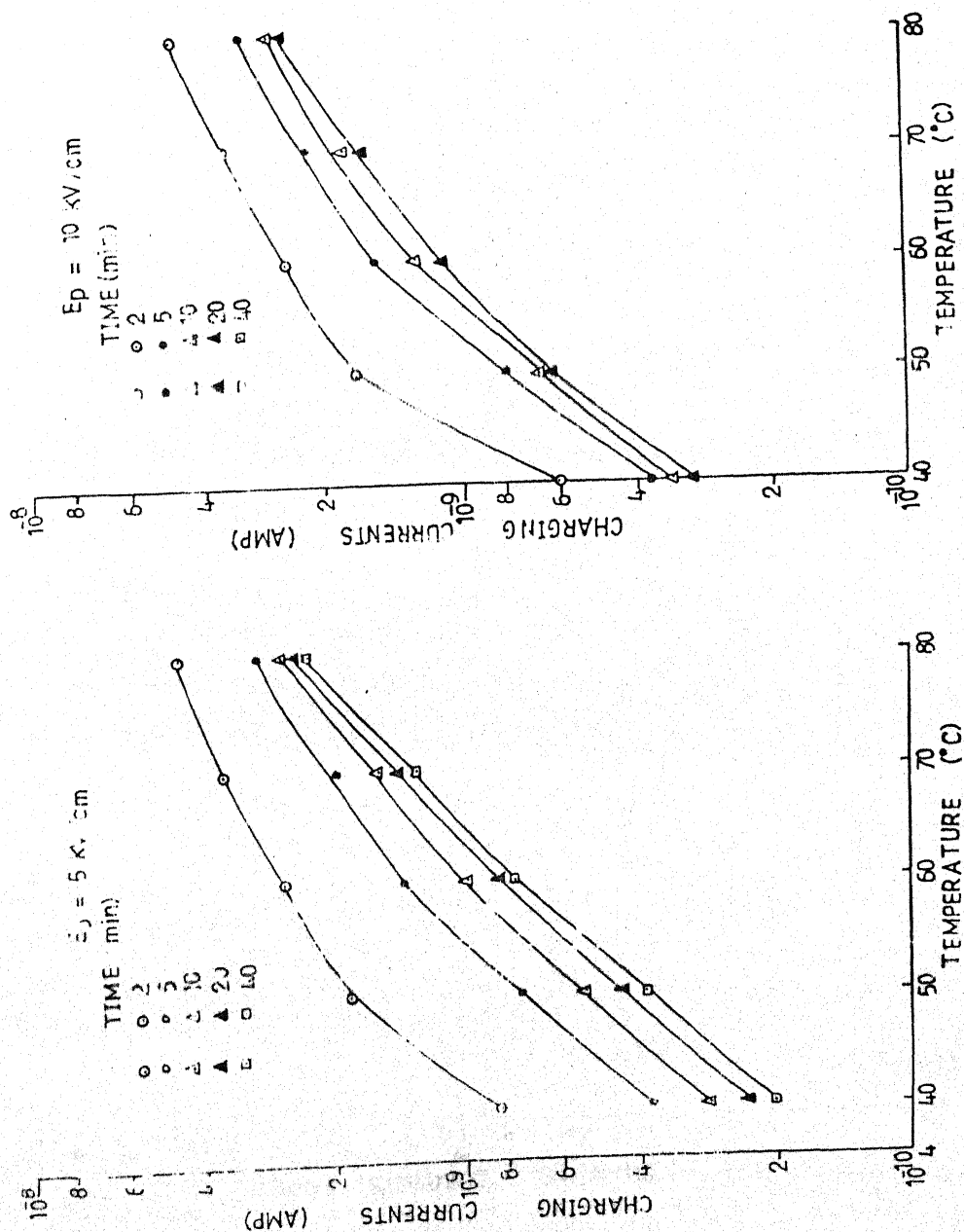


Fig. 5.8 (a) Isochronal current versus temperature plots for charging mode at mentioned field and different constant times, with Al-Al system.

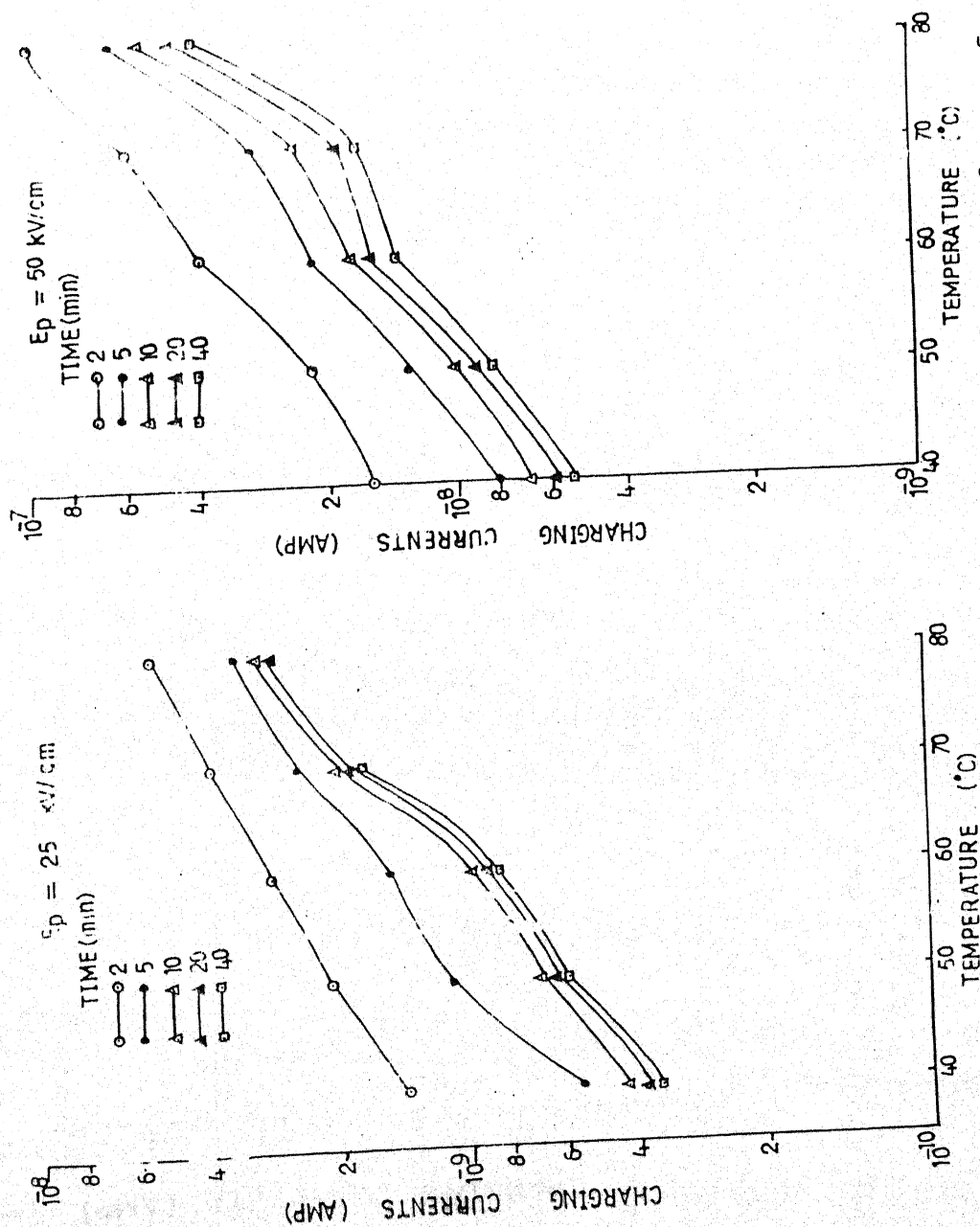


Fig. 5.8 (b) Isochronal current versus temperature plots of charging mode at mentioned field and different constant times, with Al-Al system.

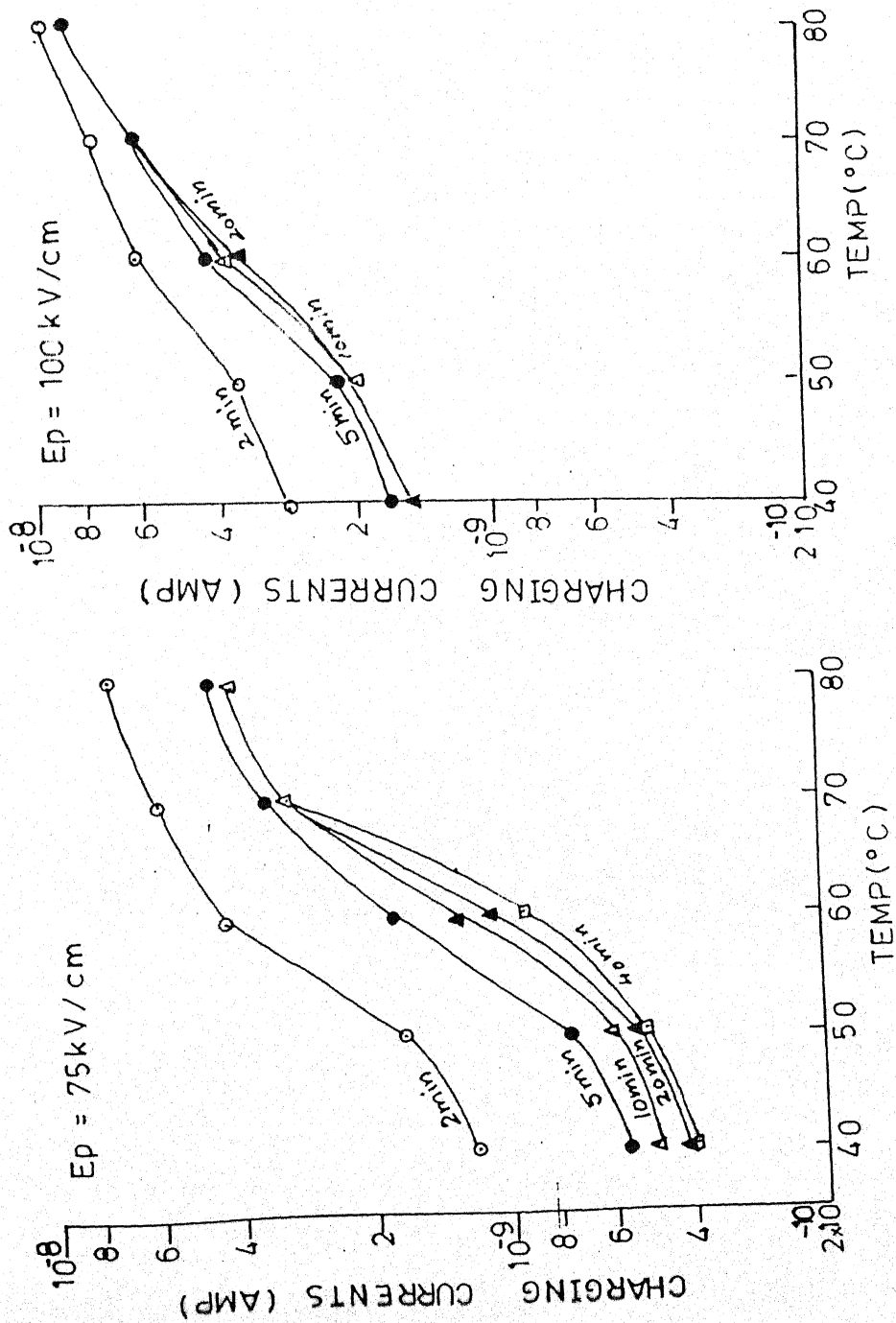


Fig.5.8(c) Isochronal current versus temperatures plots for charging mode at mentioned field and different constant time with Al-Al System.

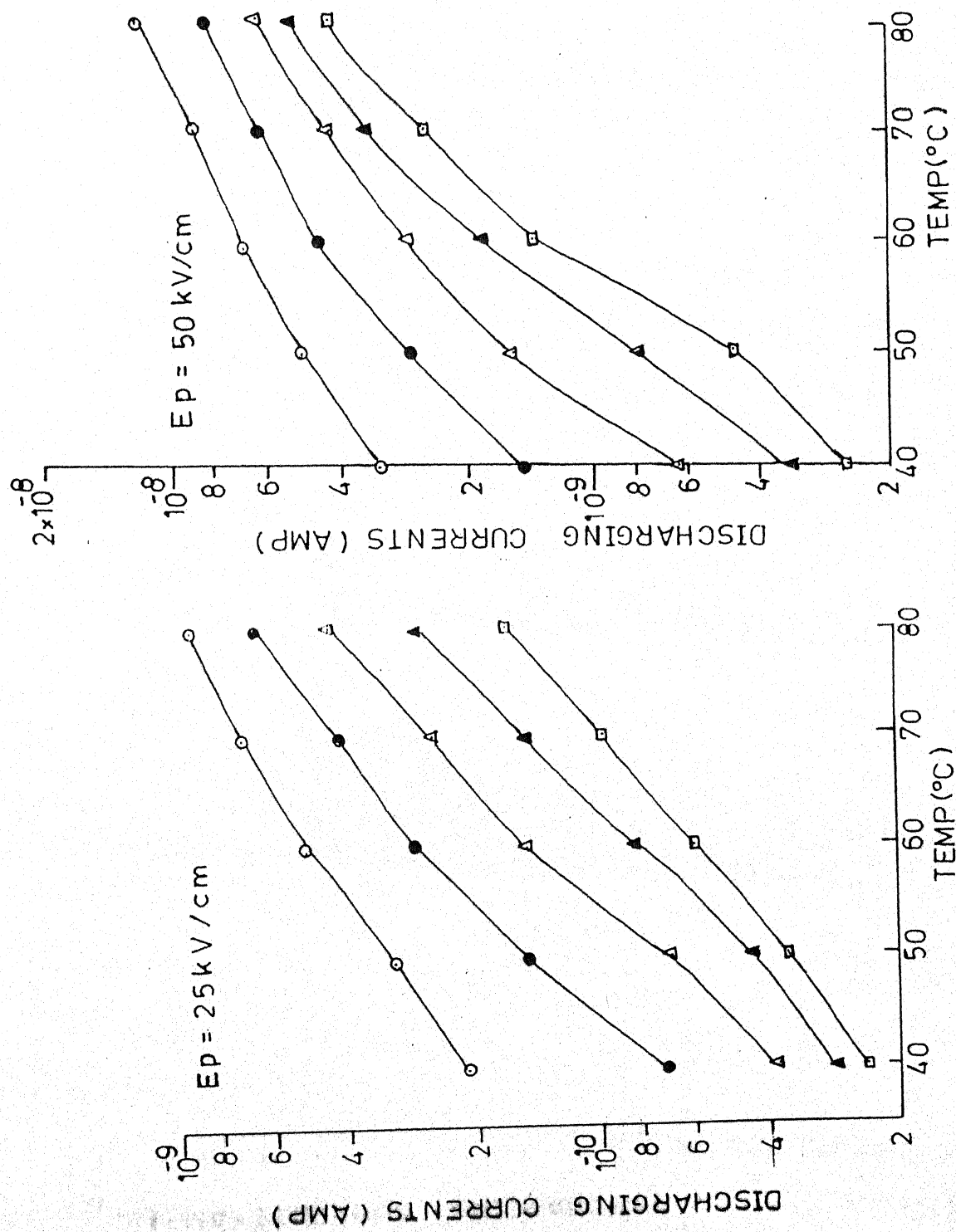


Fig 5.8(B): Isochronal current versus temperature plots for discharging mode at given field and different constant times with Al-Al system.

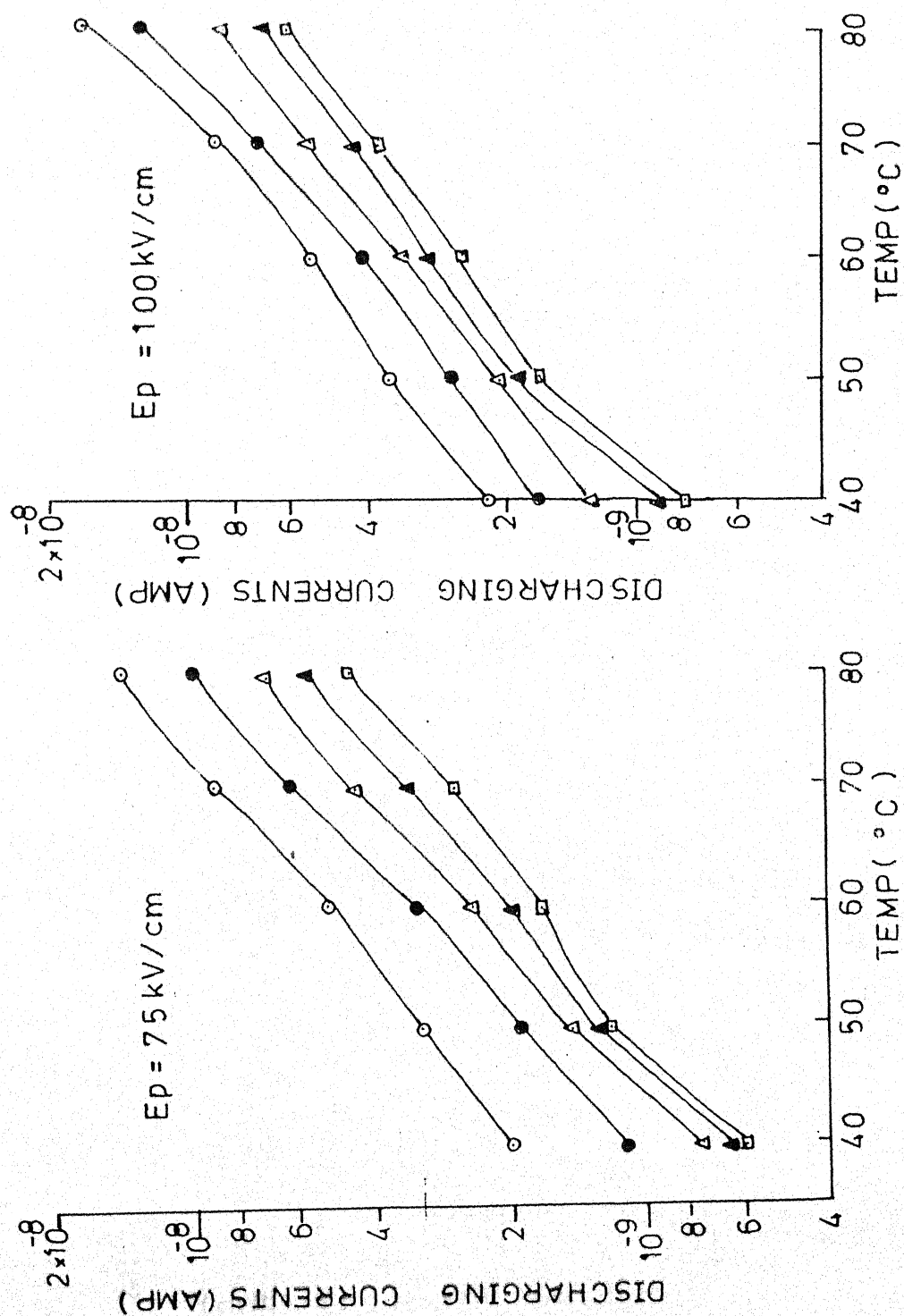


Fig 5.8(c): Isochronal current versus temperature plots for discharging mode at given field and different constant times with Al-Al system.

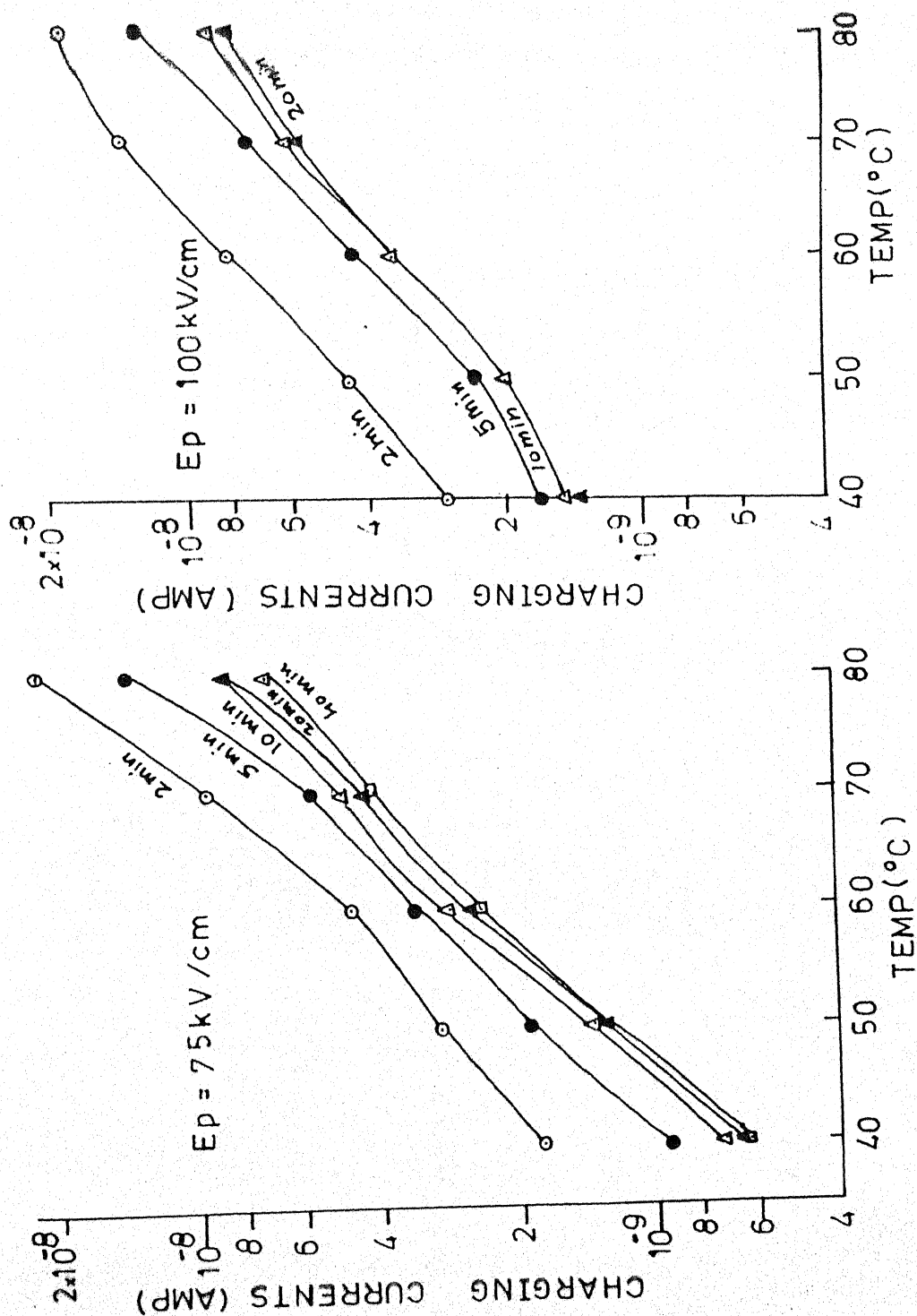


Fig 5.9(c): Isochronal current versus temperature plots for charging mode at given field and different constant times with Ag-Ag system.

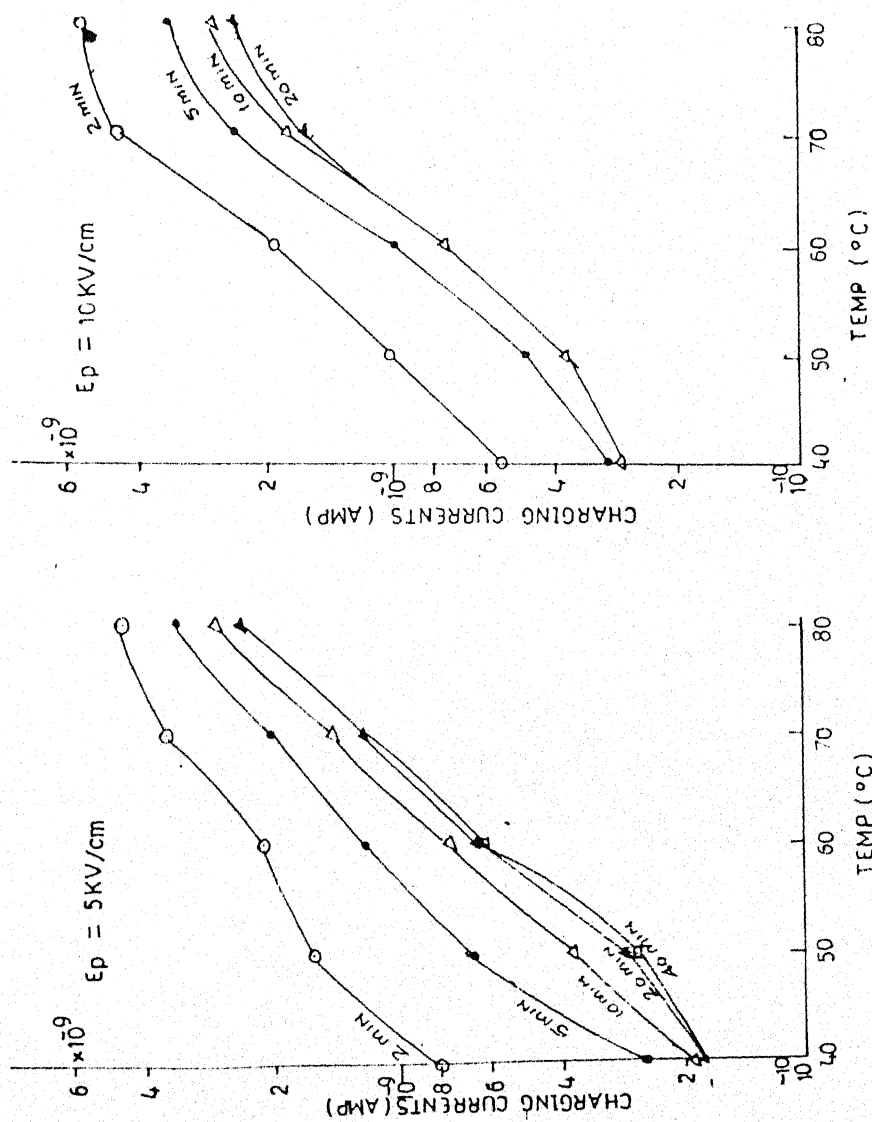


Fig.5.9(a) Isochronal current versus temperatures plots for charging mode at mentioned field and different constant time with Ag-Ag System.

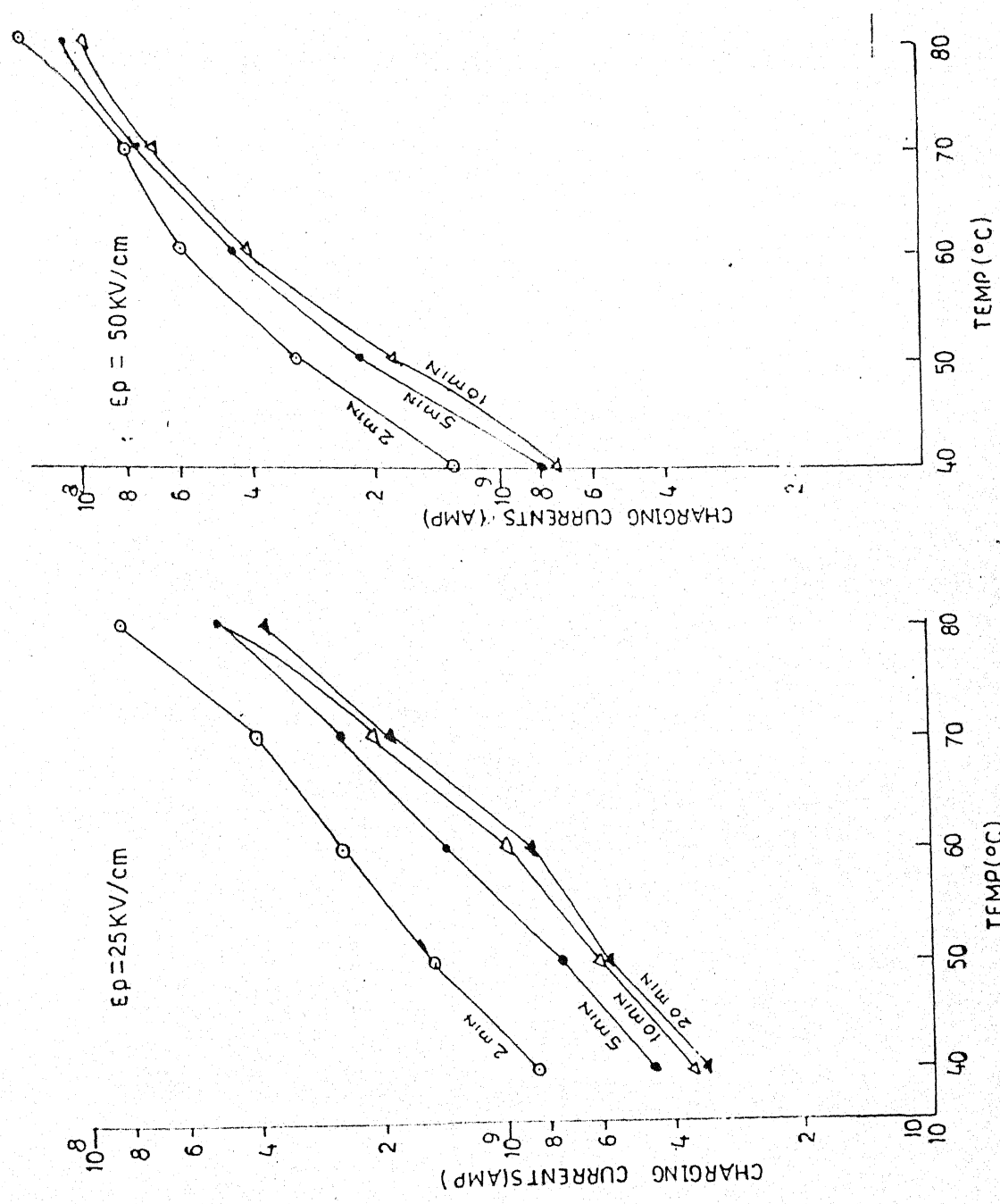


Fig.5.9(b) Isochronal current versus temperatures plots for charging mode at mentioned field an constant time with Ag-Ag system.

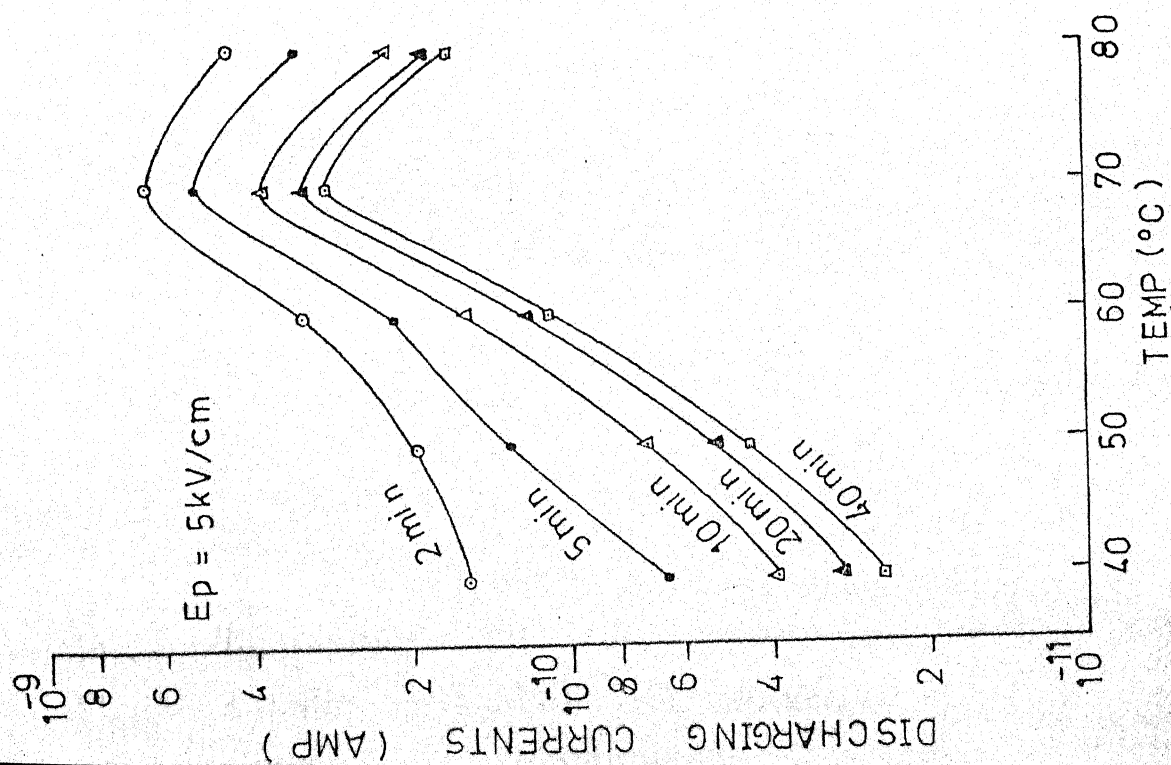
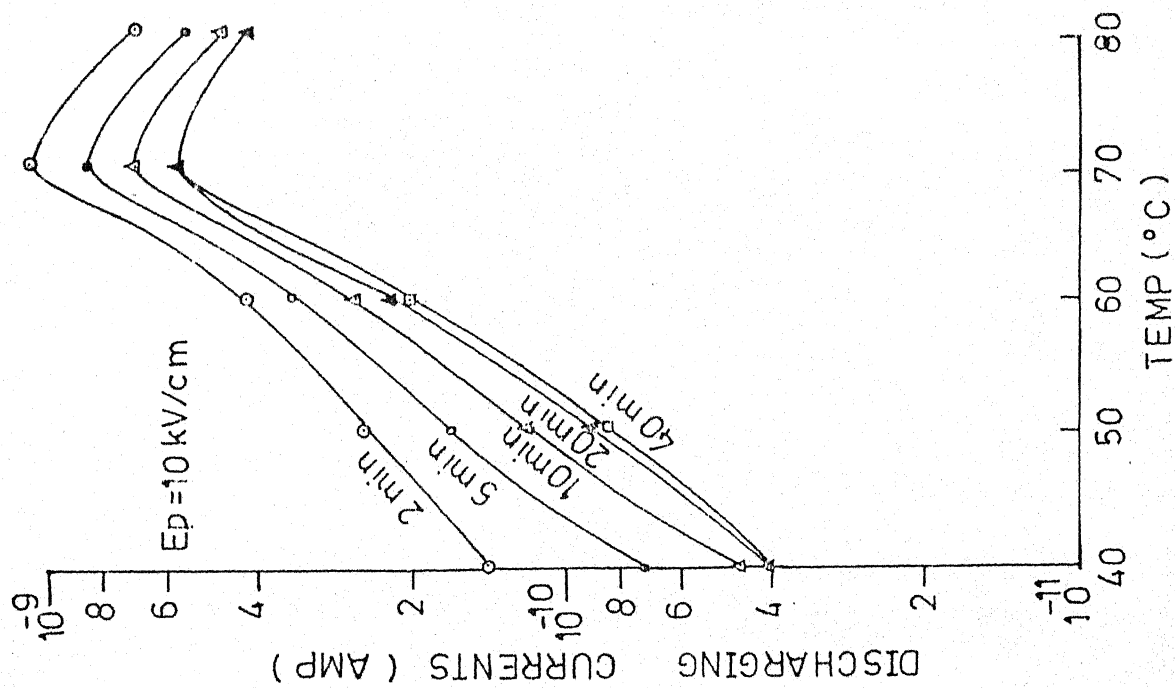


Fig. 5.9 (A) Isochronal current versus temperature plots for discharging mode at mentioned field and constant times, with Ag-Ag system.

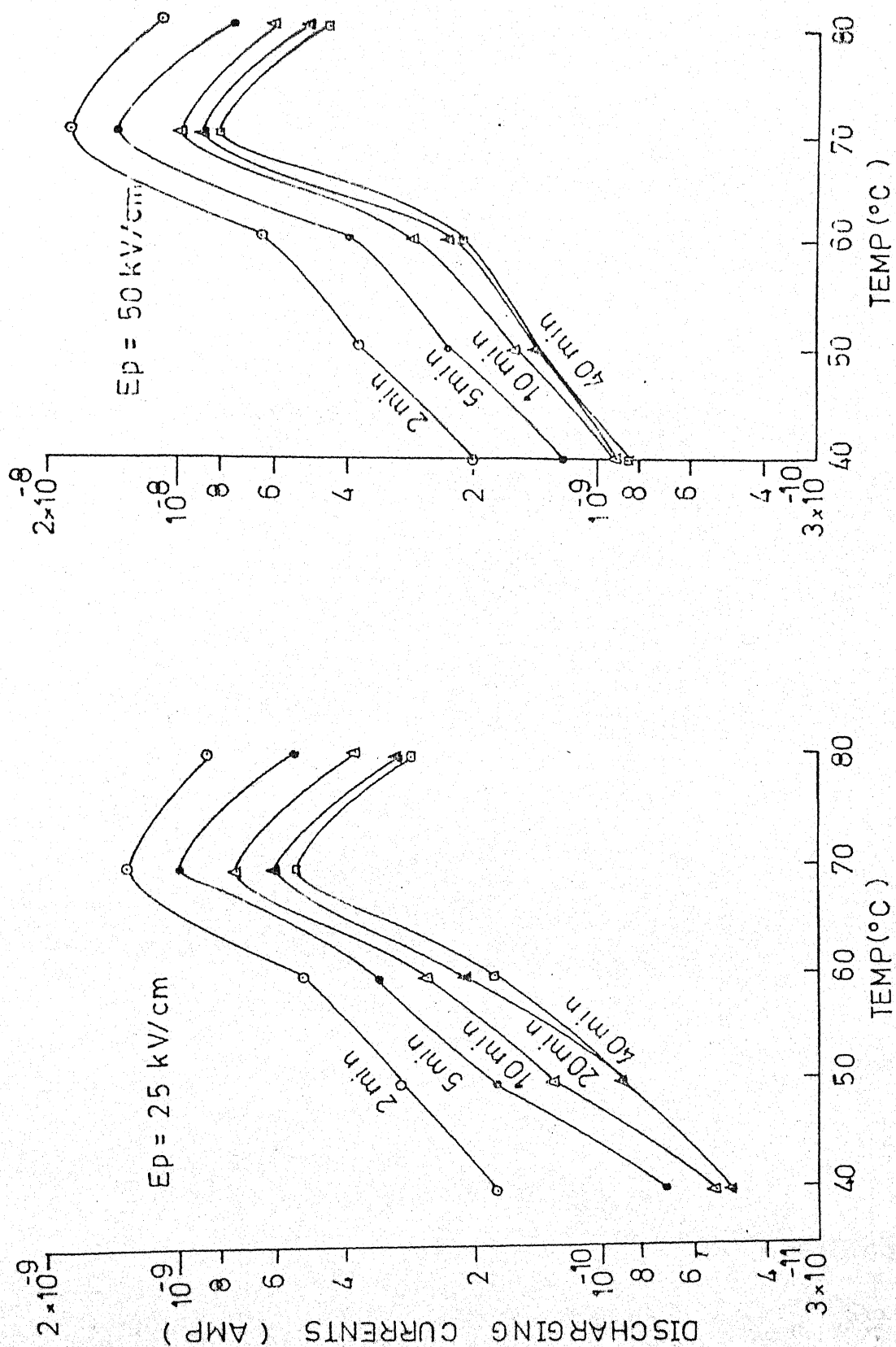


Fig. 5.9 (B) Isochronal current versus temperature plots for discharging mode at mentioned field and different constant times, with Ag-Ag system.

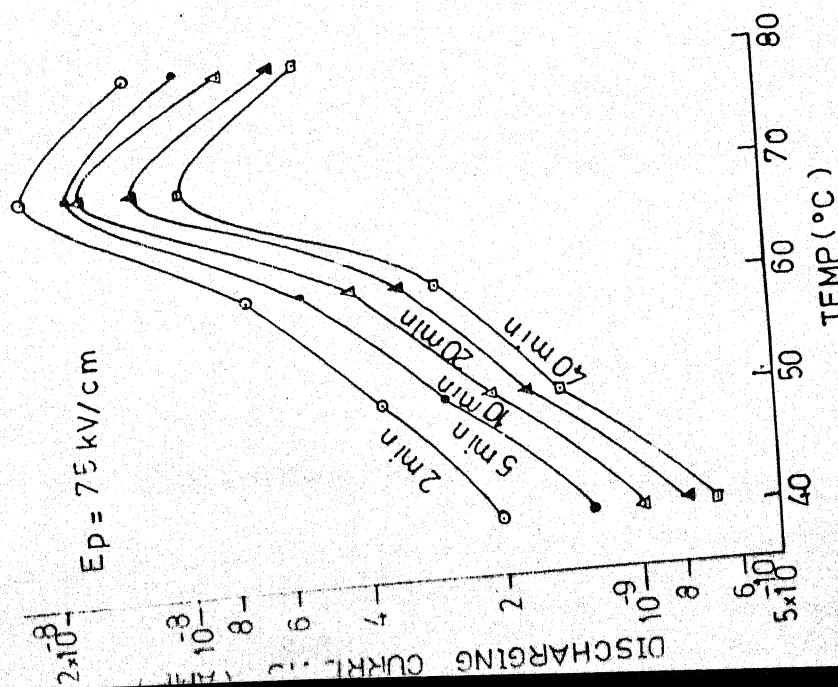
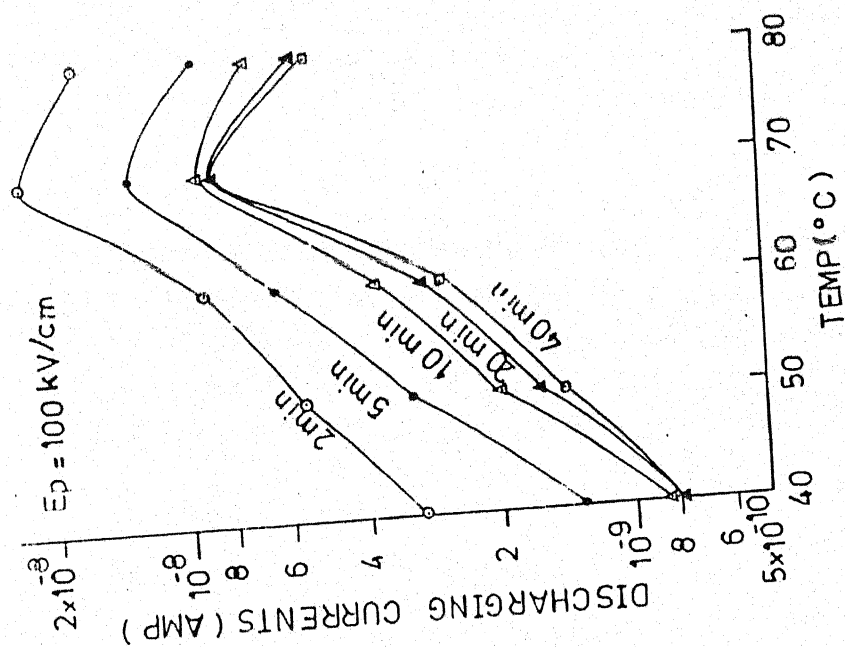


Fig. 5.9 (C) Isochronal current versus temperature plots for discharging mode at mentioned field and different constant times with Ag-Ag system.

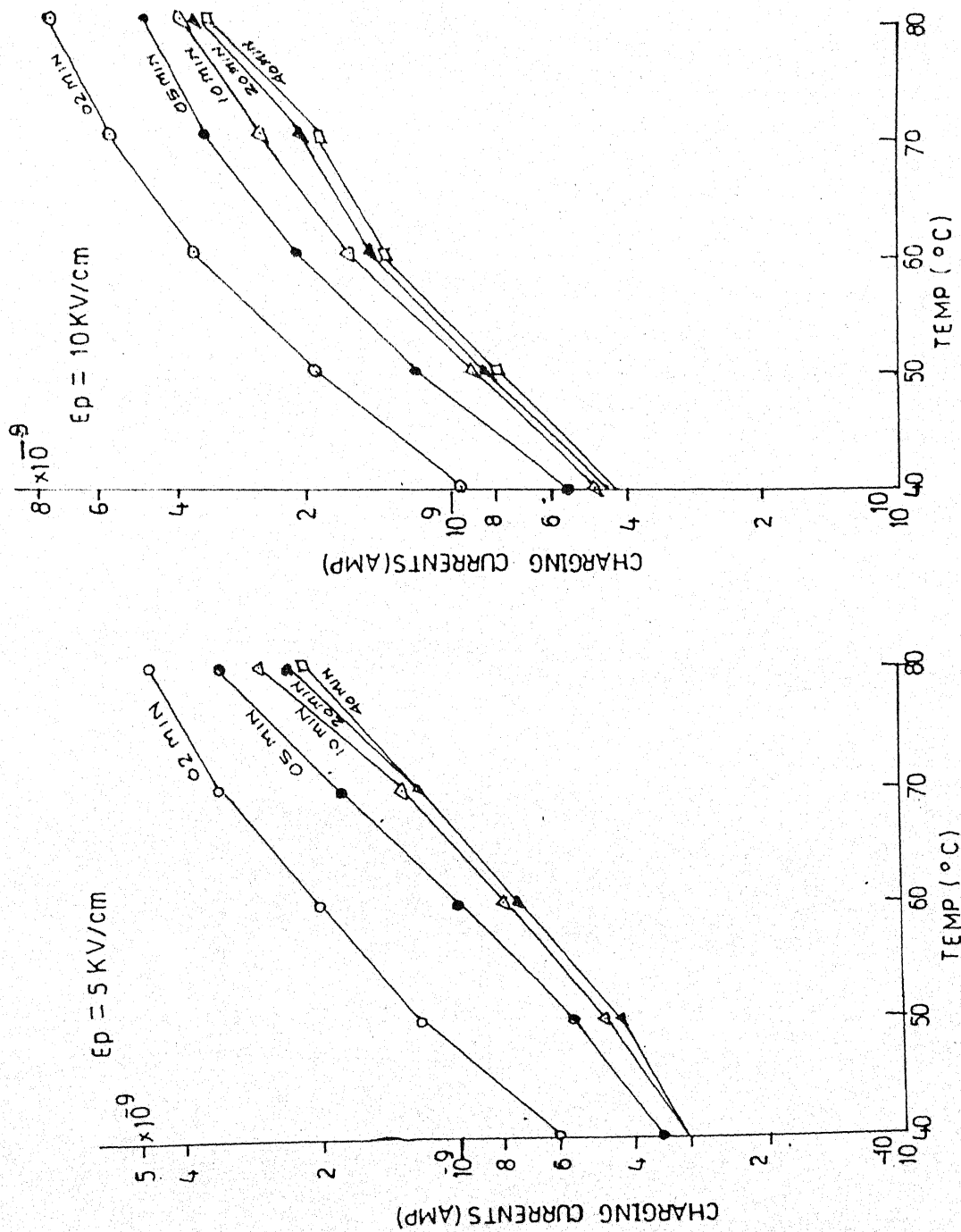


Fig 5.10(a): Isochronal current versus temperature plots for charging mode at given field and different constant times with Cu-Cu system.

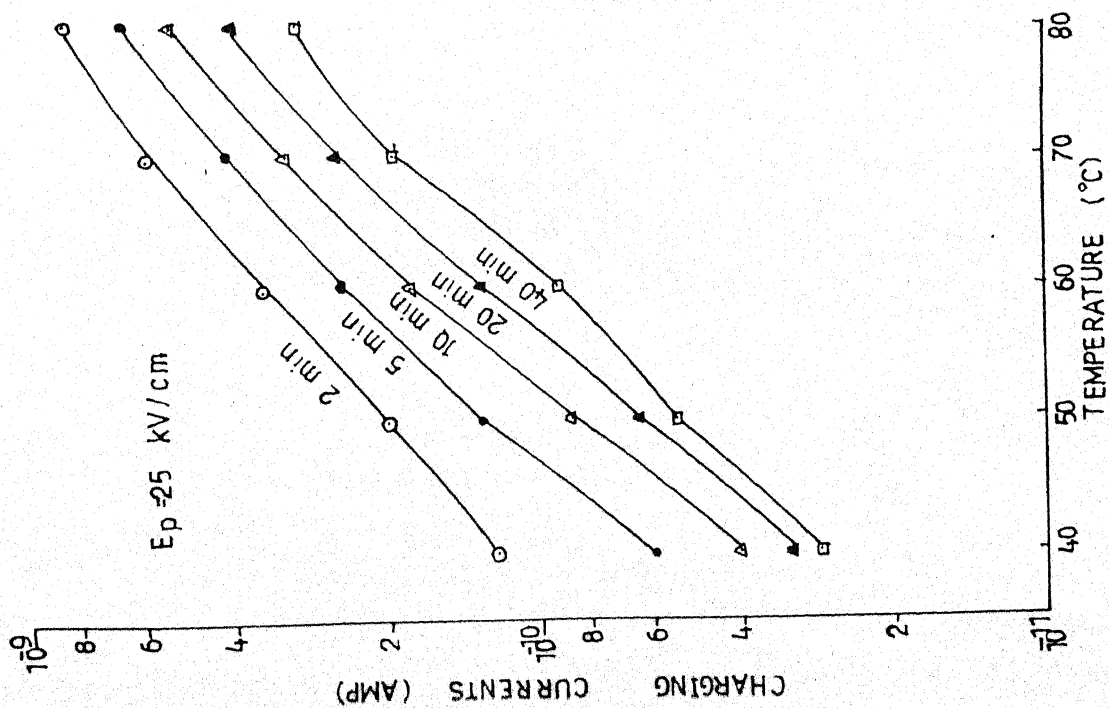
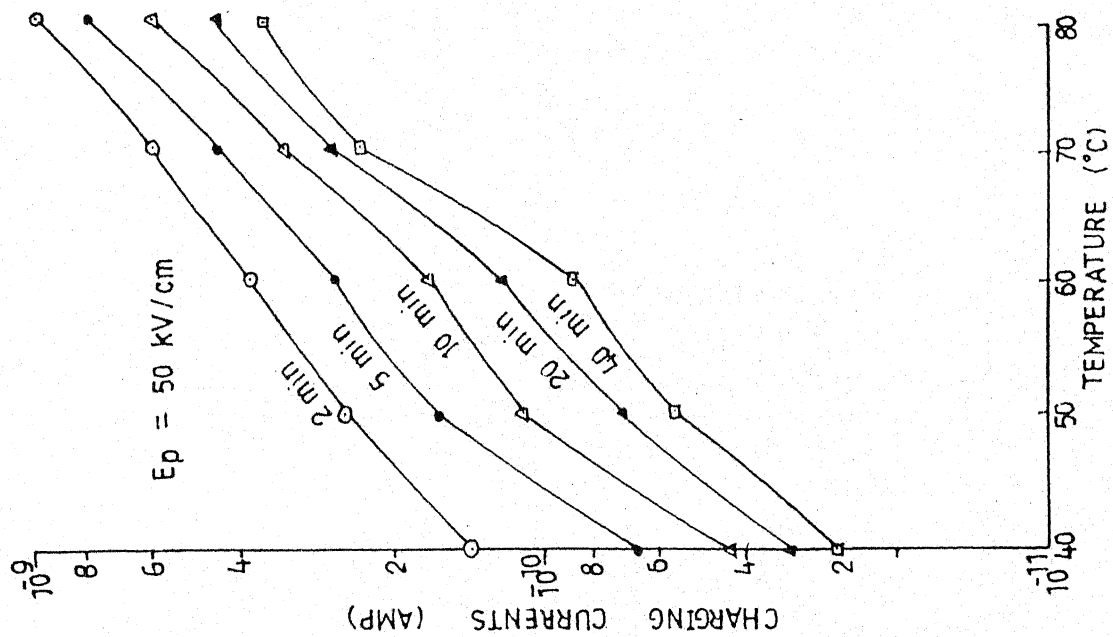


Fig 5.10(b): Isochronal current versus temperature plots for charging mode at given field and different constant times with Cu-Cu system.

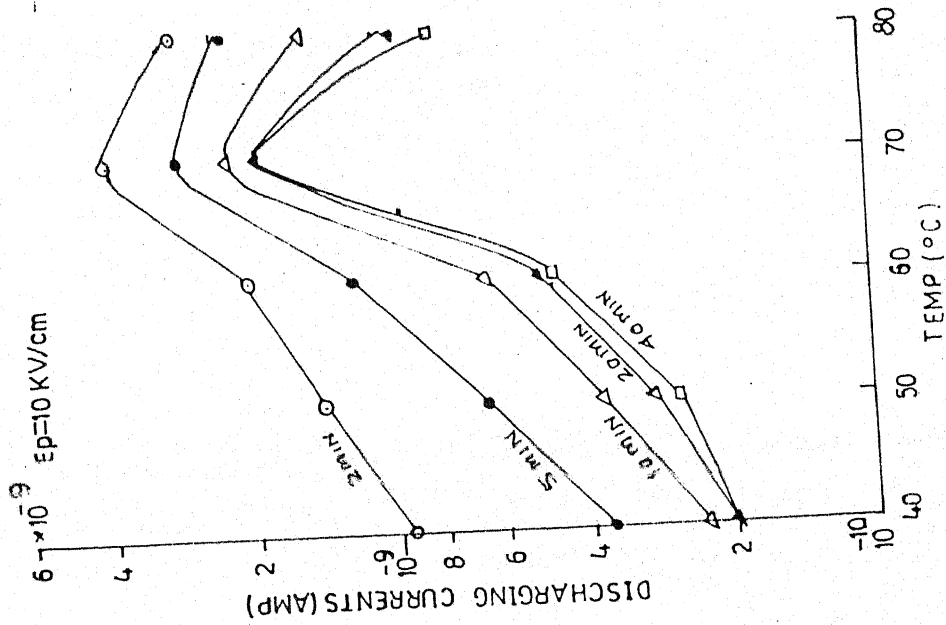
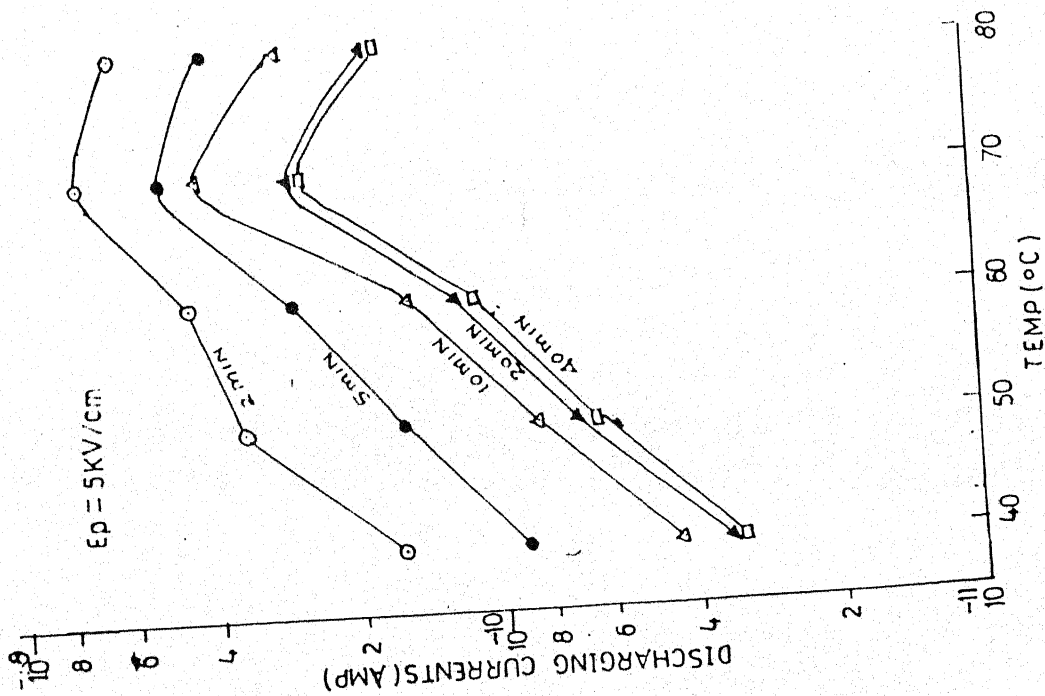


Fig.5.10(A) Isochronal current versus temperatures plots for discharging mode at mentioned field and different constant times with Cu-Cu System.

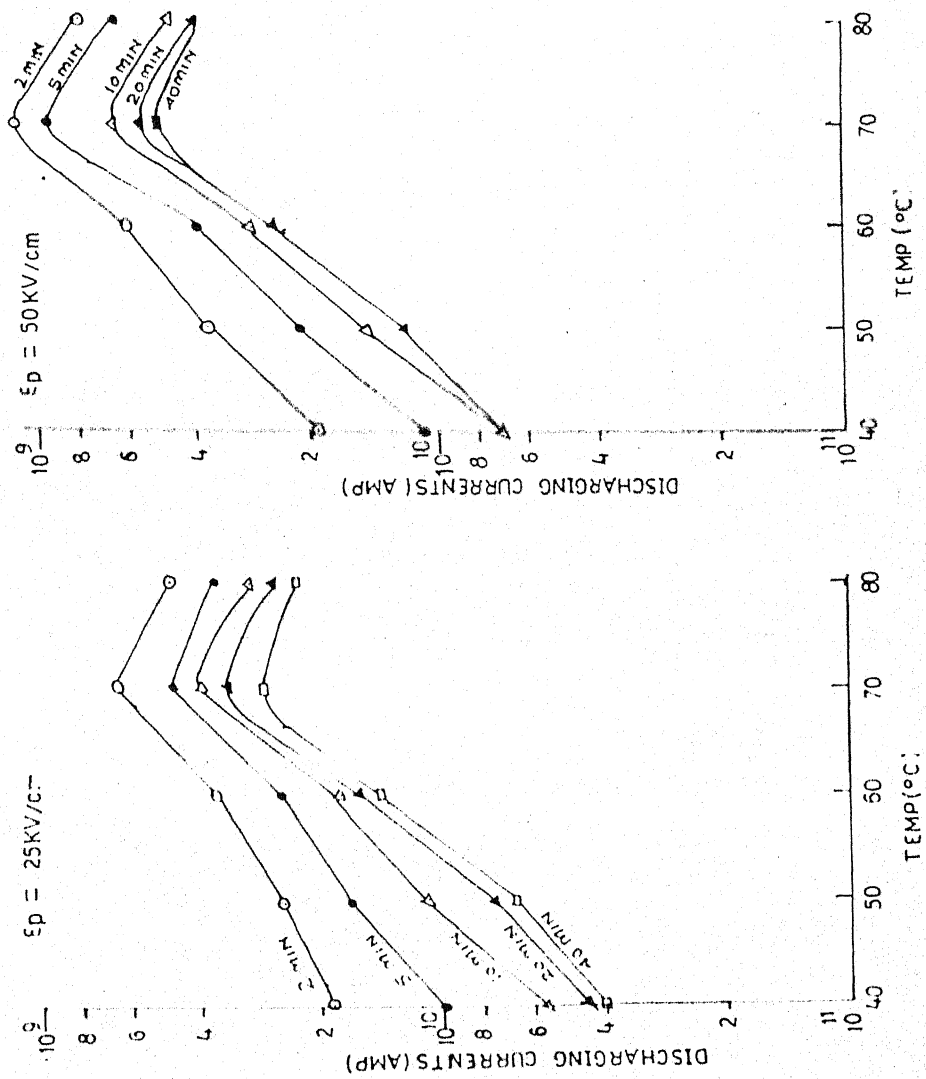


Fig. 5.10(B)

Isochronal current versus temperatures plots for discharging mode at mention field and different constant times with Cu-Cu System.

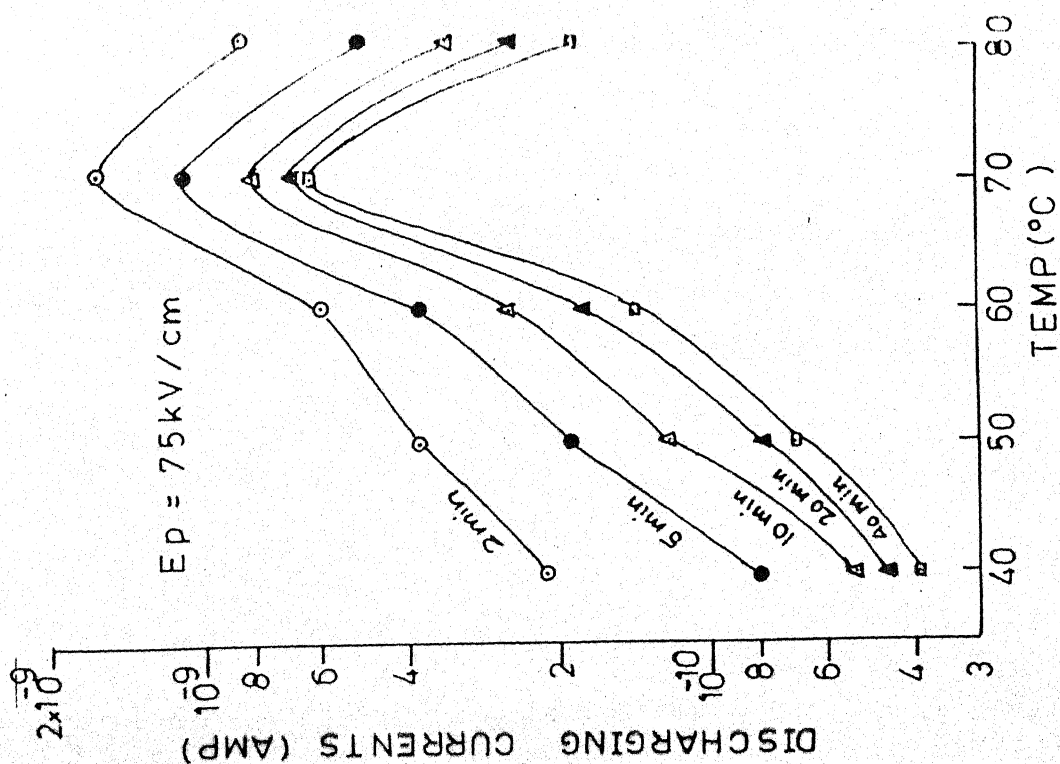
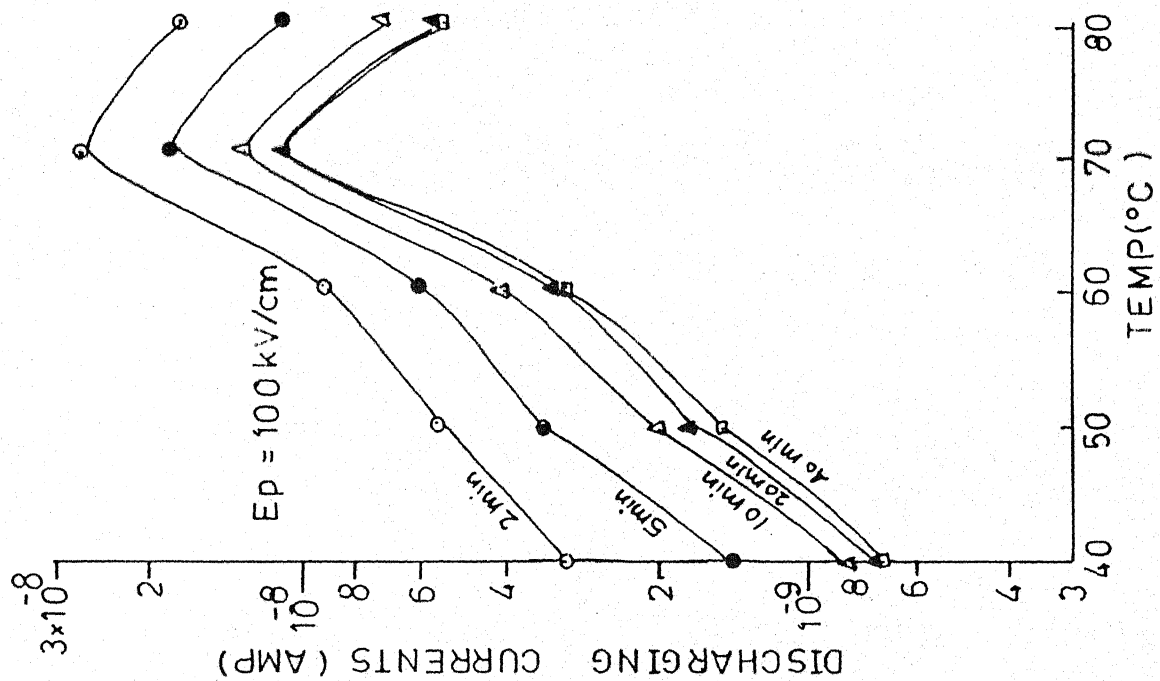


Fig 5.10(C): Isochronal current versus temperature plots for discharging mode at given field and different constant times with Cu-Cu system.

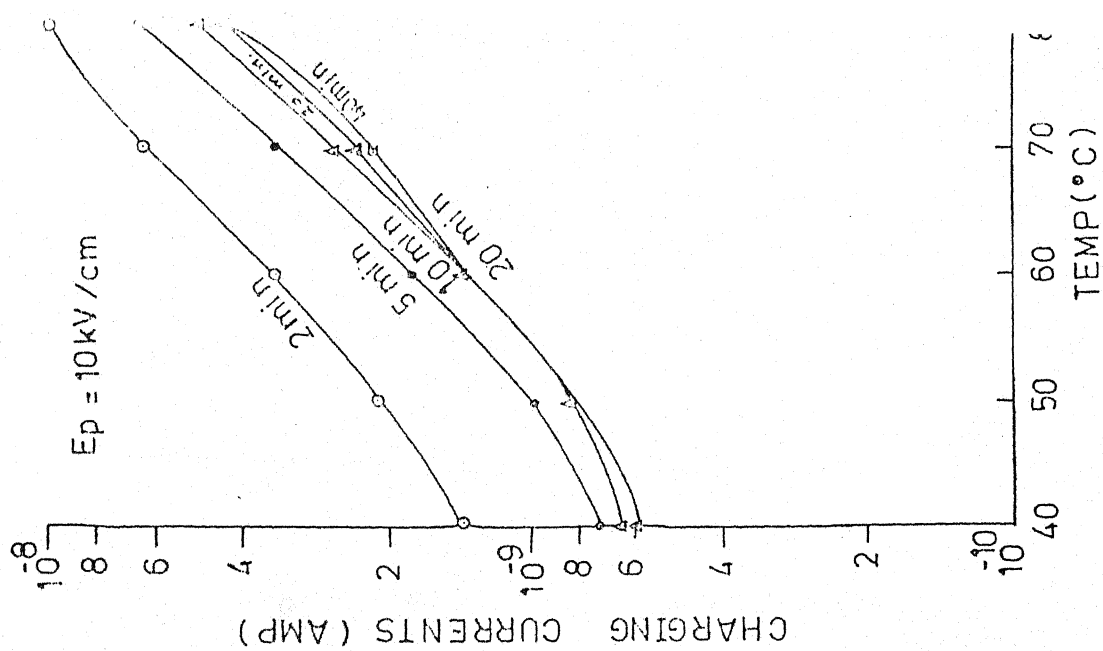
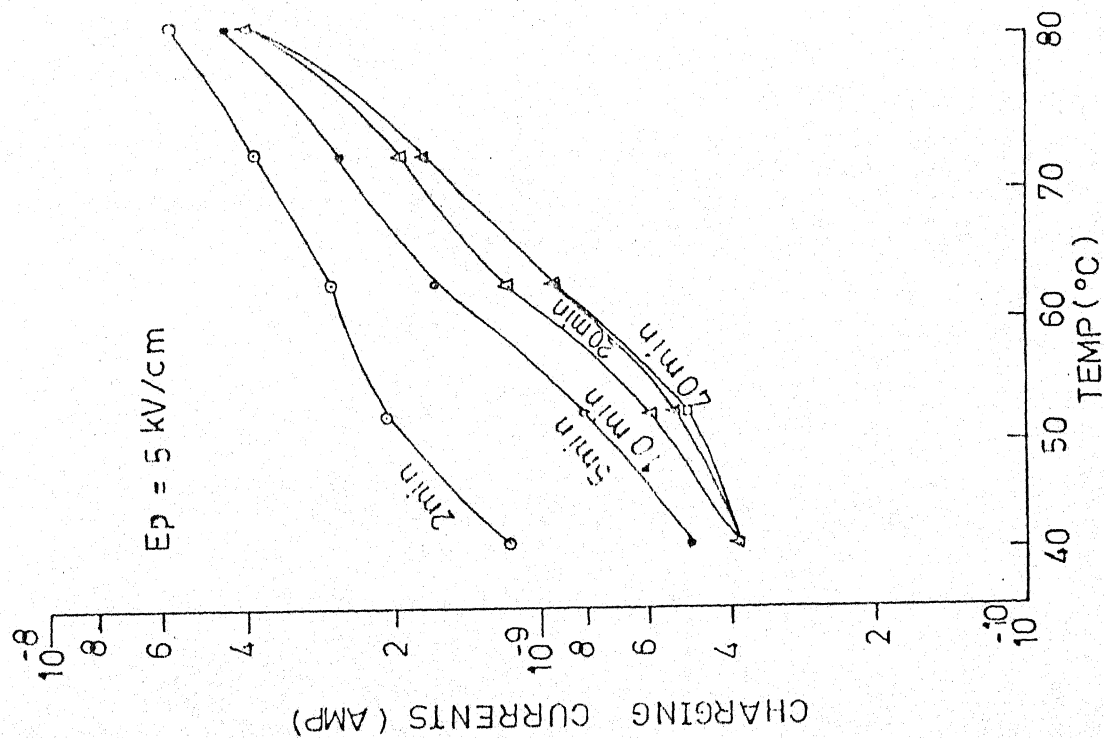


Fig. 5.11 (a) Isochronal current versus temperature plots for charging mode at mentioned field and different constant times, with Sn-Sn system.

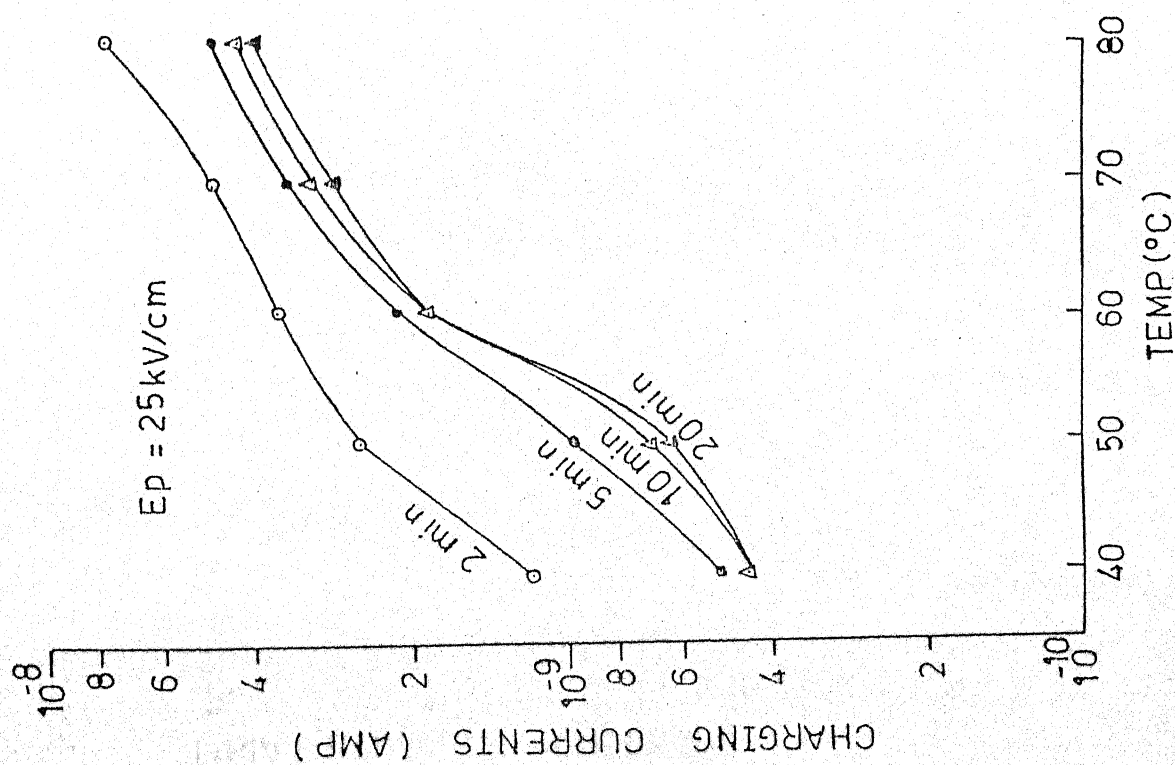
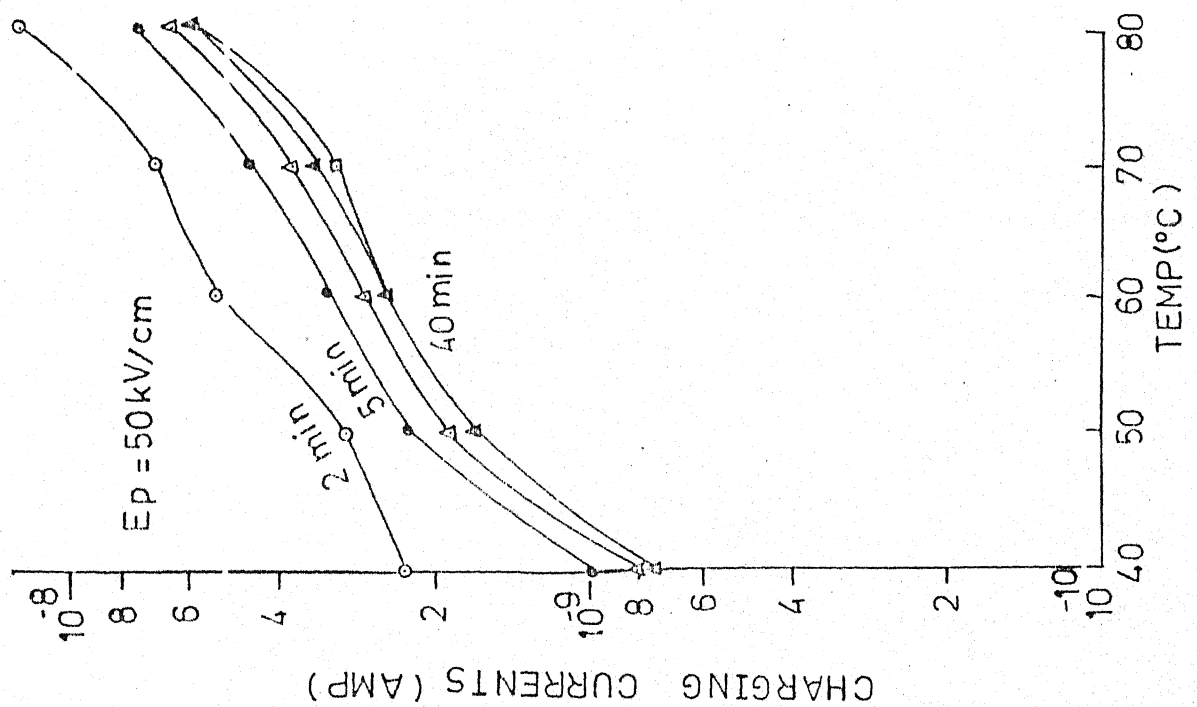


Fig. 5.11 (b) Isochronal current versus temperature plots for charging mode at mentioned field and different constant times with Sn-Sn system.

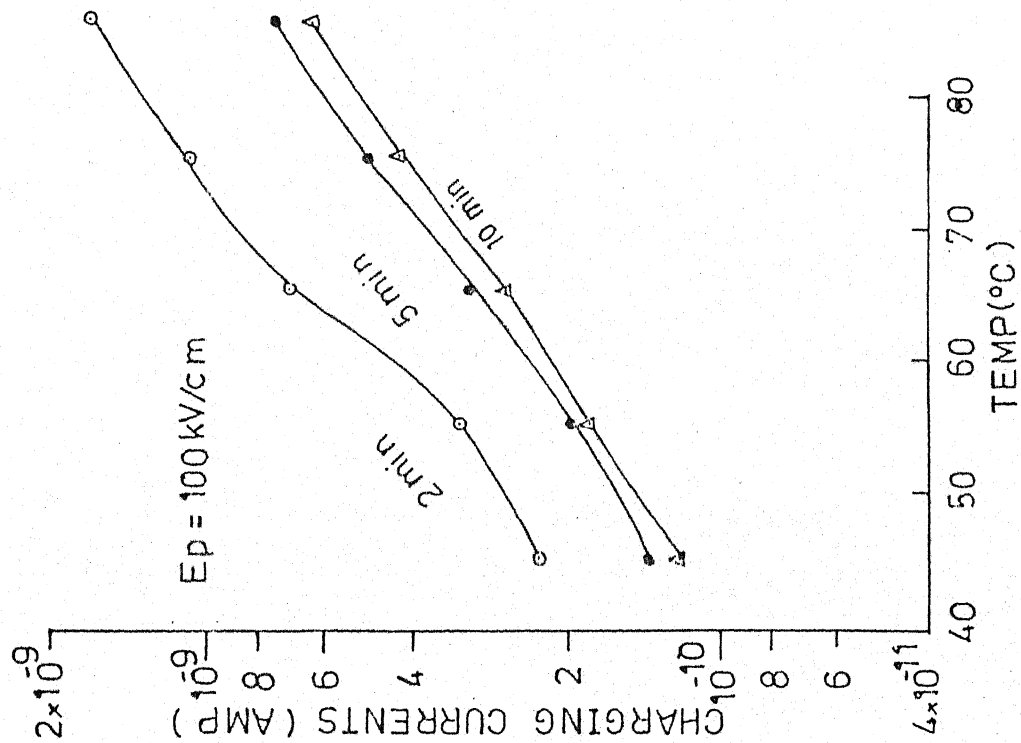
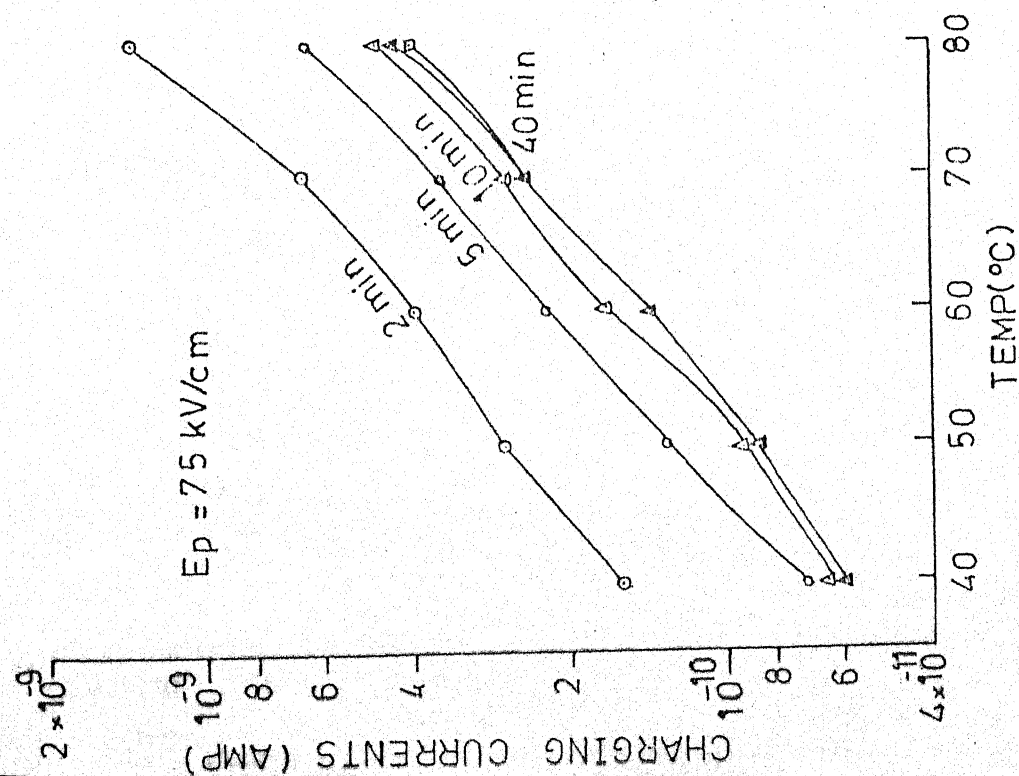


Fig. 5.11 (c) Isochronal current versus temperature plots for charging mode at mentioned field and different constant times with Sn-Sn system.

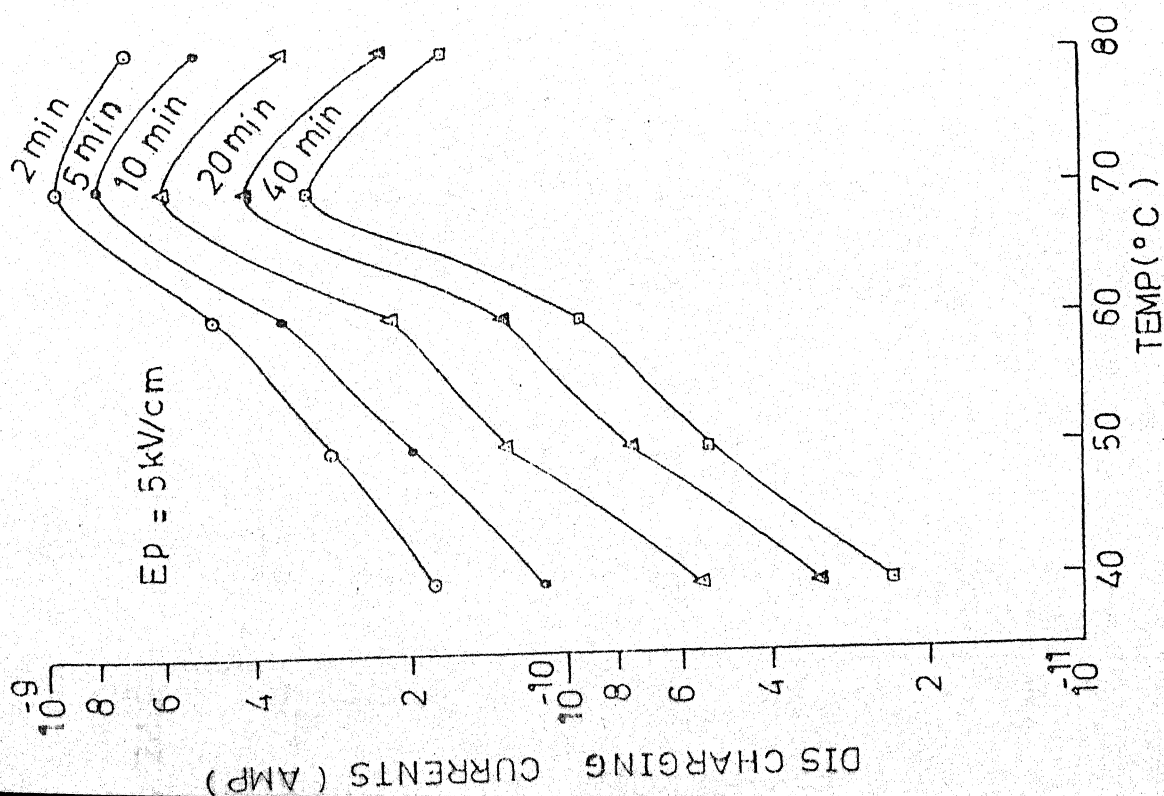
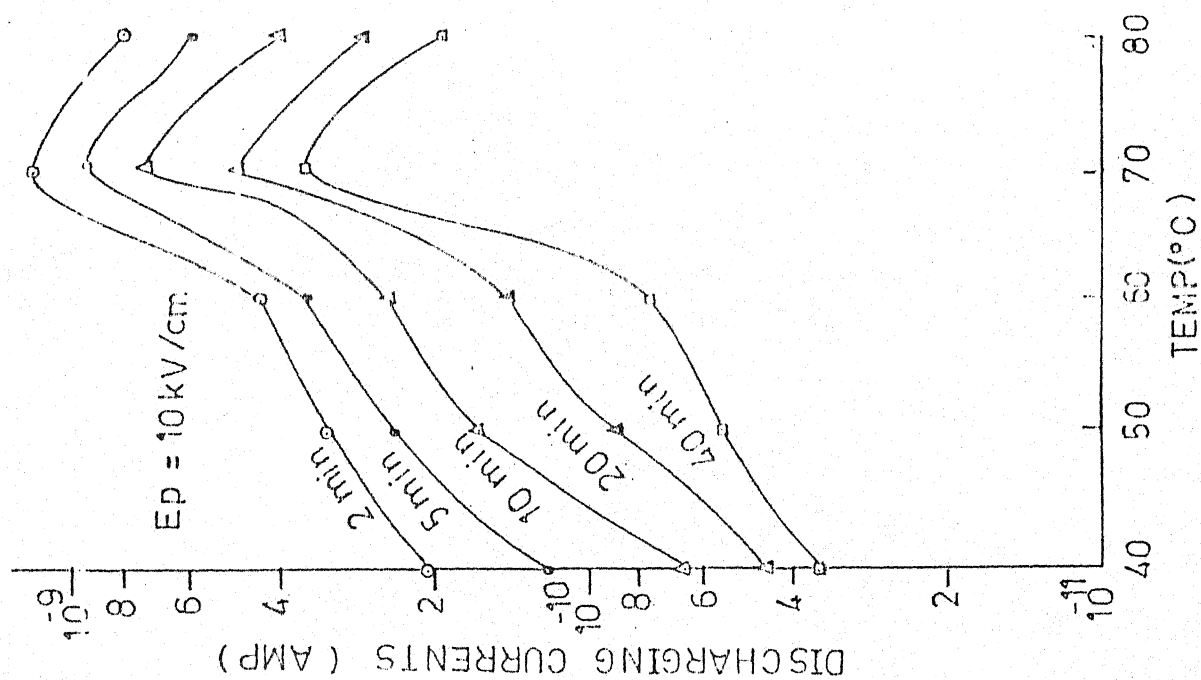


Fig5.11 (A) Isochronal current versus temperature plots for discharging mode at mentioned time and field, with Sn-Sn system.

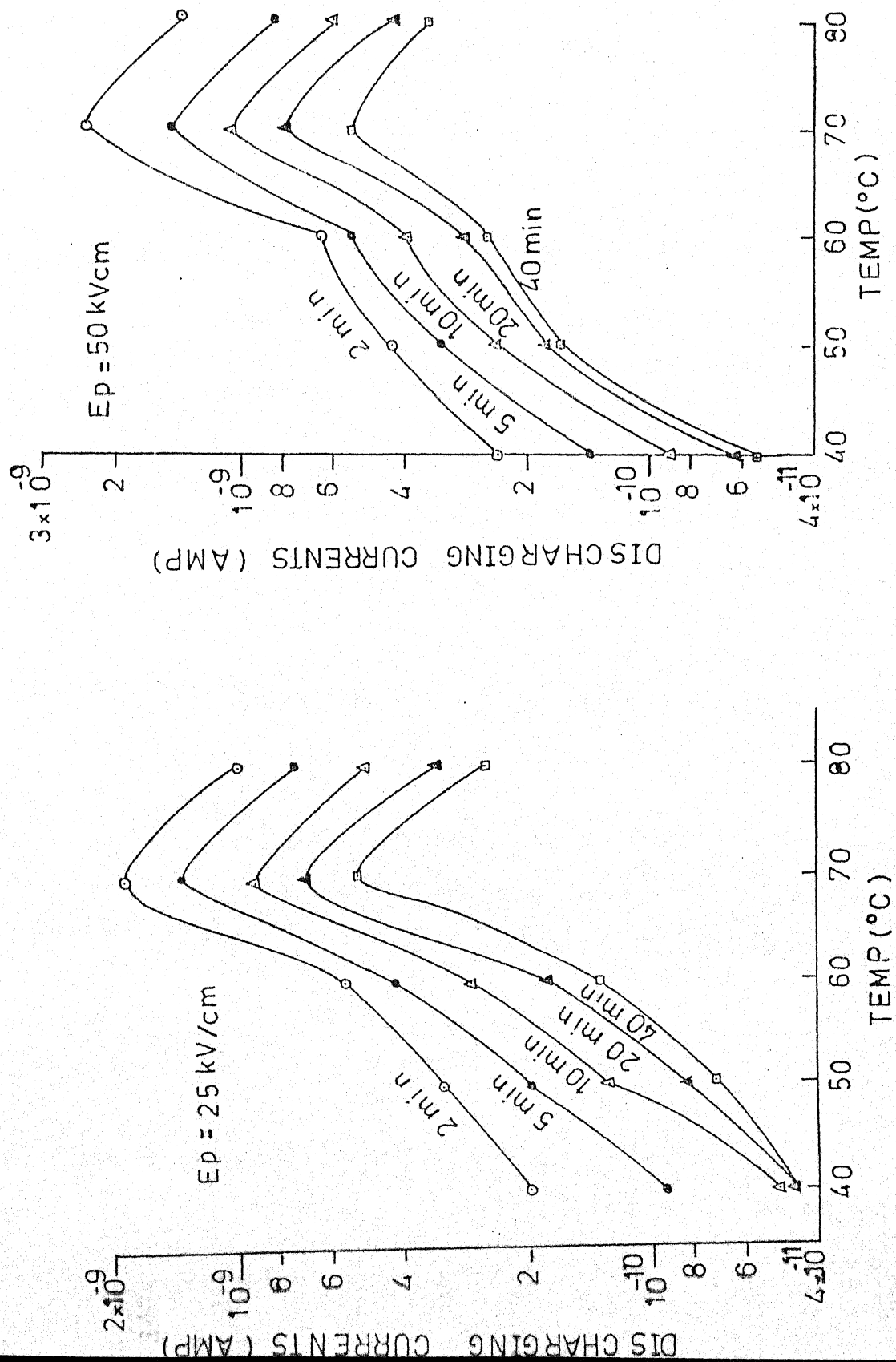


Fig.5.11 (B) Isochronal current versus temperature plots for discharging mode at mentioned field and constant times, with Sn-Sn system.

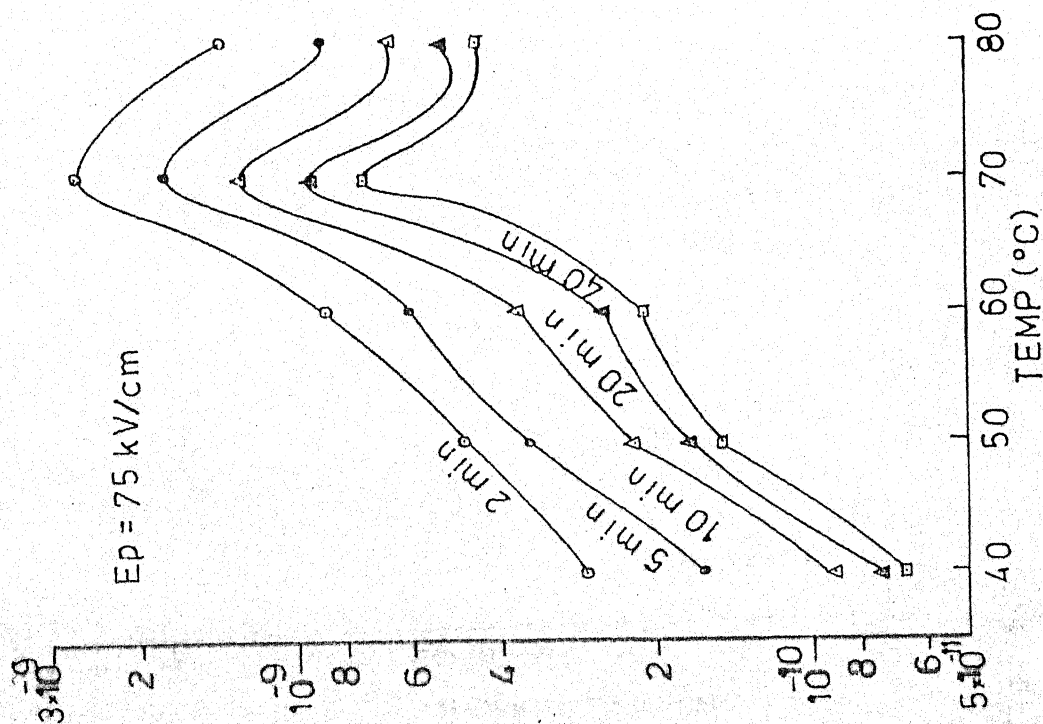
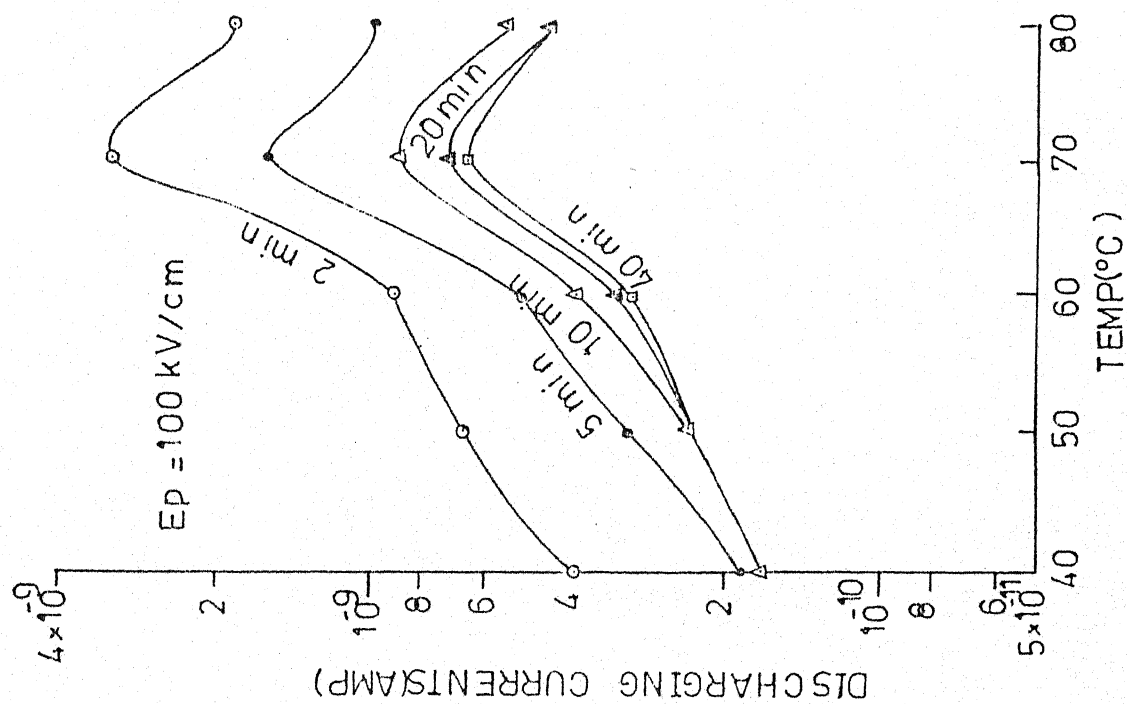


Fig.5.11 (C) Isochronal current versus temperature plots for discharging mode at mentioned field and constant times with Sn-Sn system.

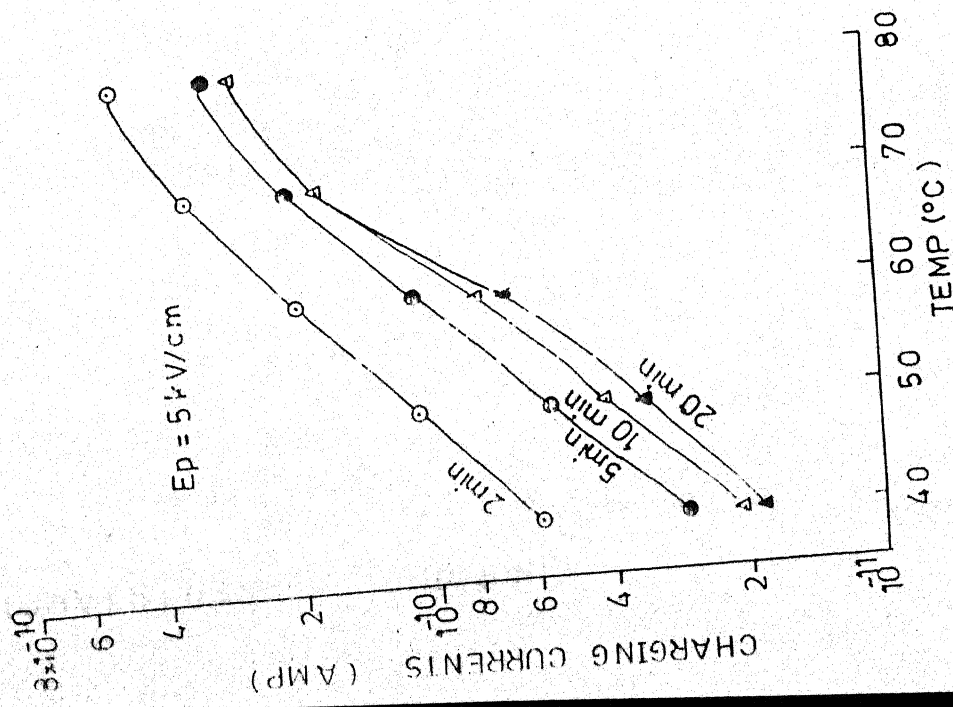


Fig. 5.12 (a) Isochronal current versus temperature plots of charging mode at mentioned field and different constant times, with Al-Ag system.

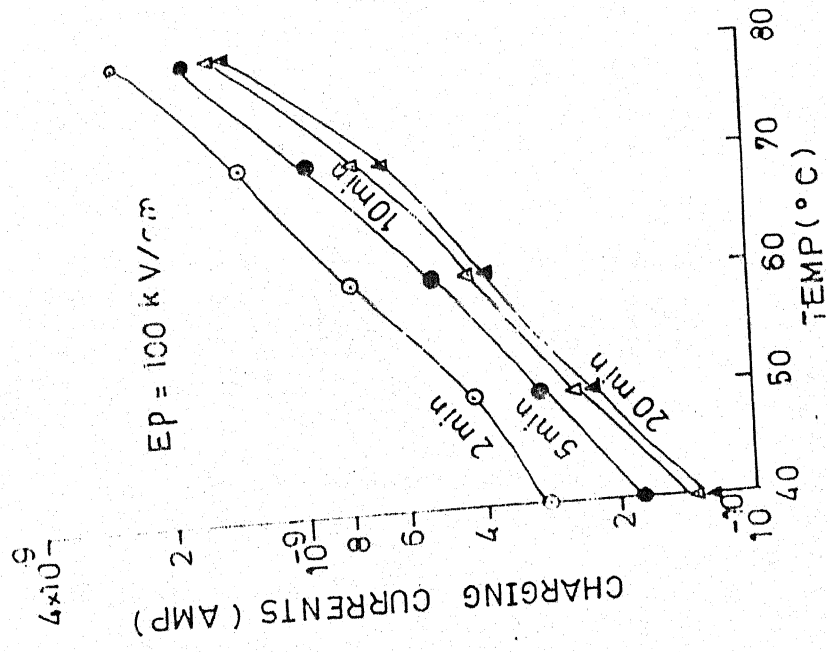


Fig. 5.12 (c) Isochronal current versus temperature plots of charging mode at mentioned field and different constant times, with Al-Ag system.

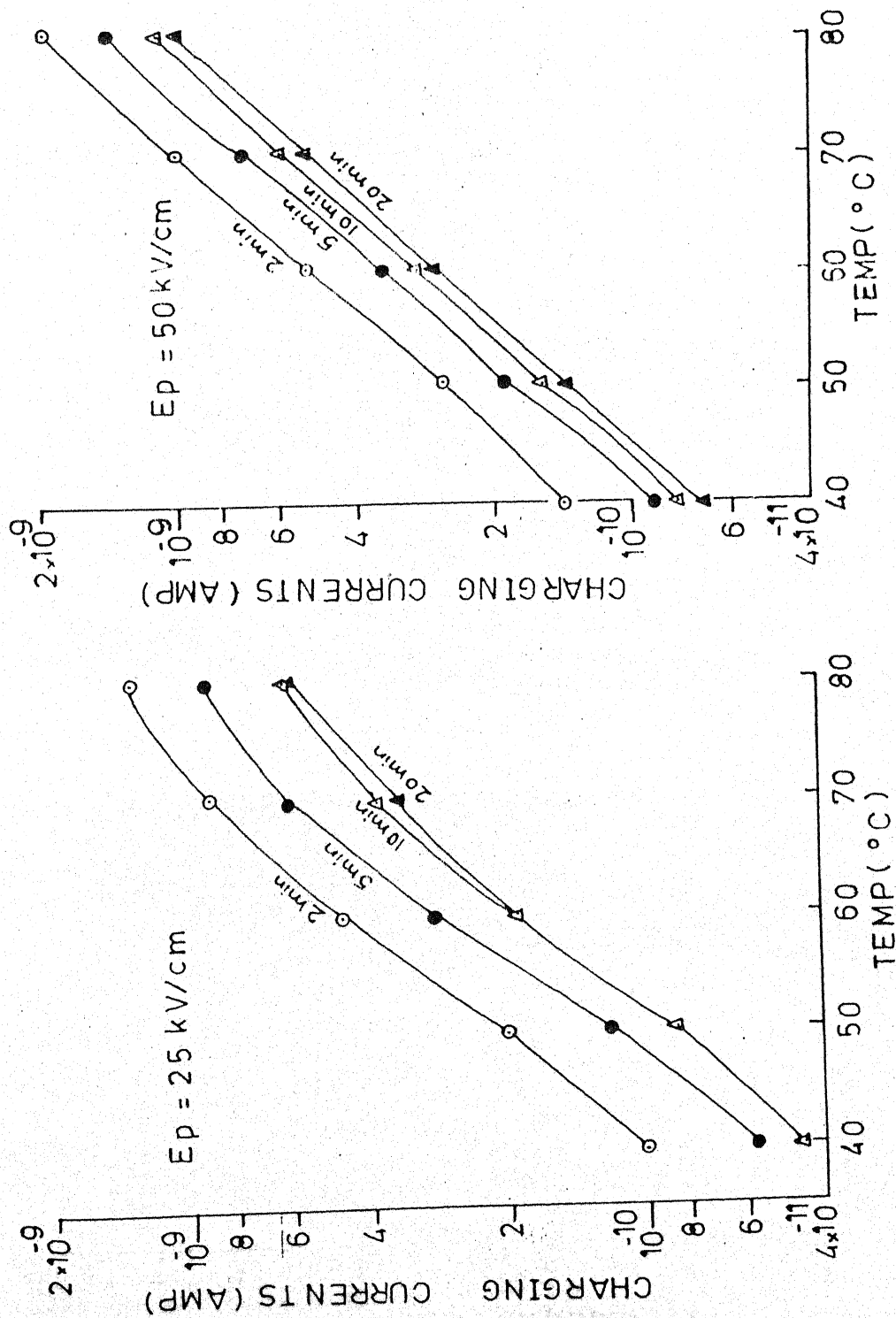


Fig 5.12(b): Isochronal current versus temperature plots for charging mode at given field and different constant times with Al-Ag system.

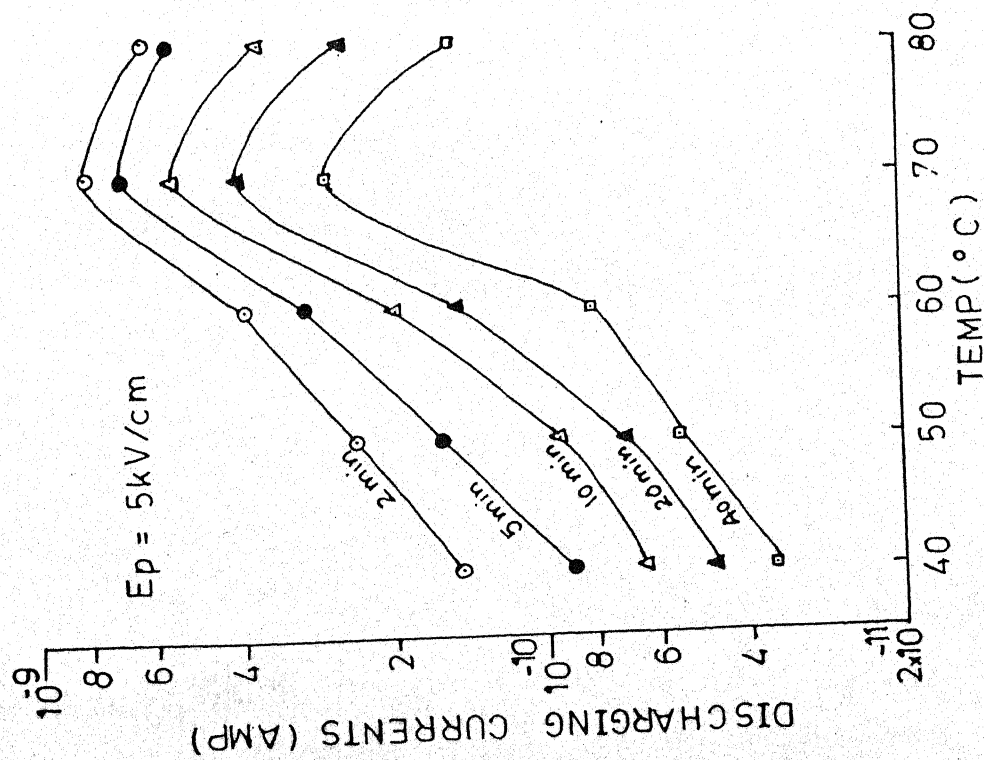


Fig 5.12(A): Isochronal current versus temperature plots for discharging mode at given field and different constant times with Al-Ag system.

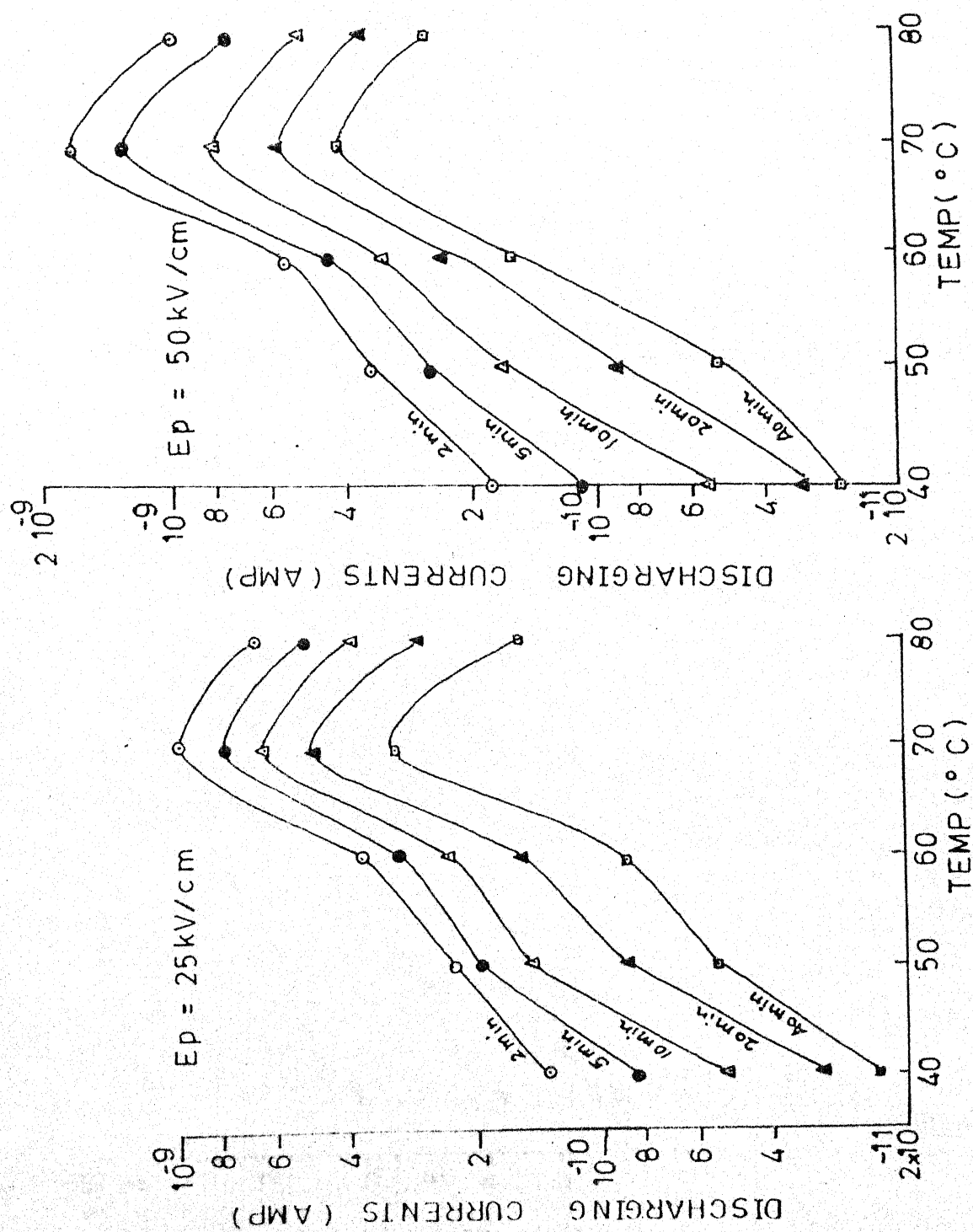


Fig 5.12(B): Isochronal current versus temperature plots for discharging mode at given field and different constant times with Al-Ag system.

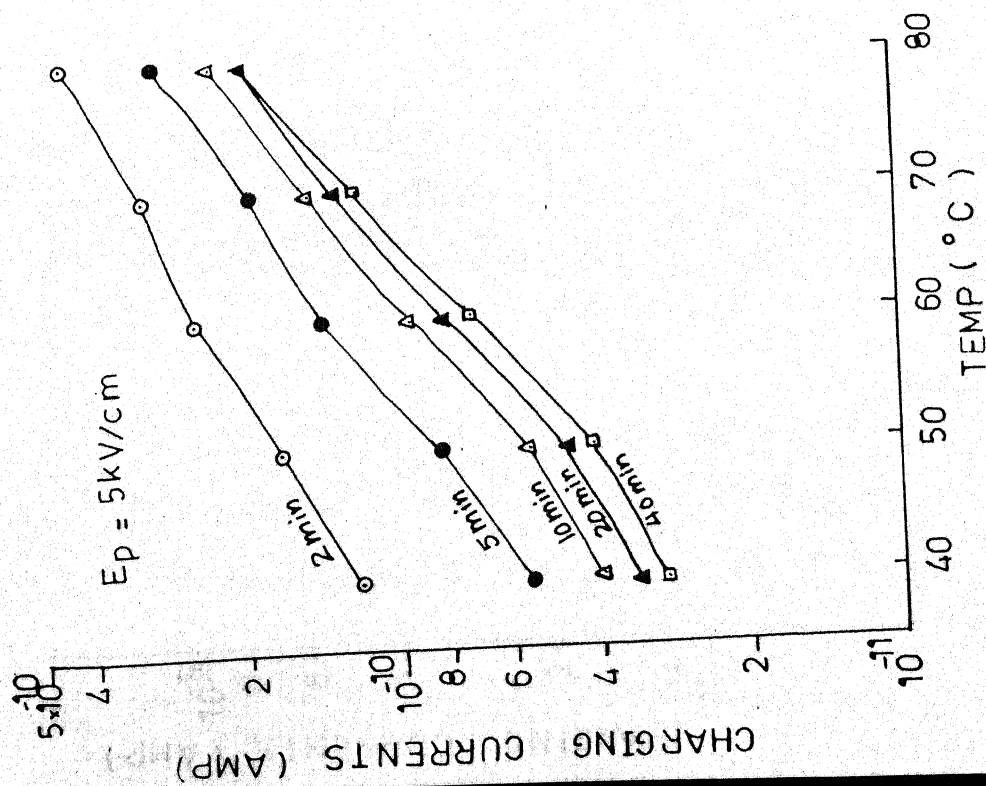


Fig 5.13(a): Isochronal current versus temperatures plots for charging mode at given field and different constant times with Al-Cu system

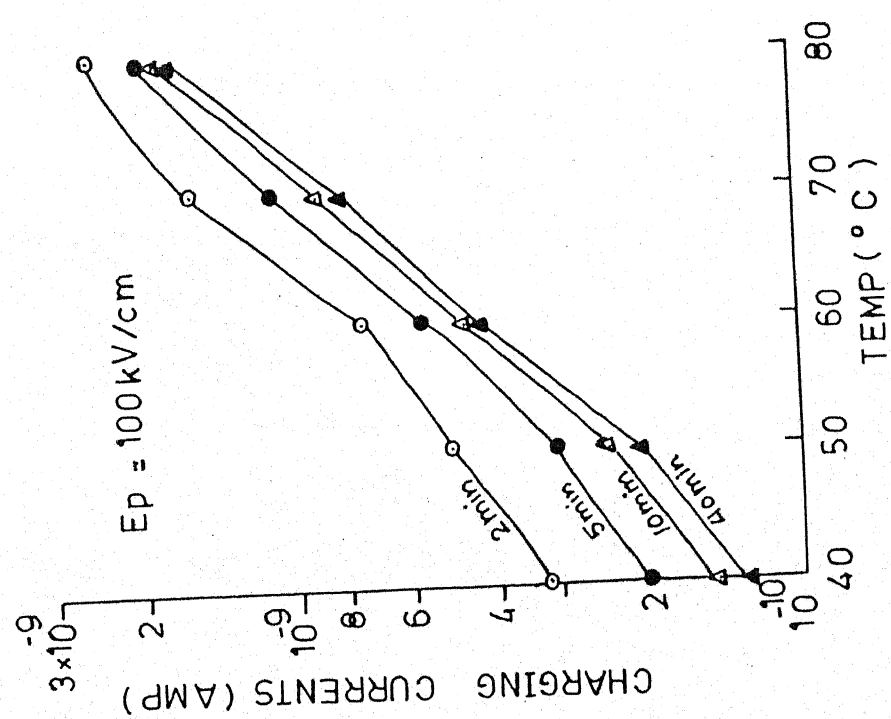


fig 5.13(c) Isochronal current versus temperatures plots for charging mode at given field and different constant times with Al-Cu system.

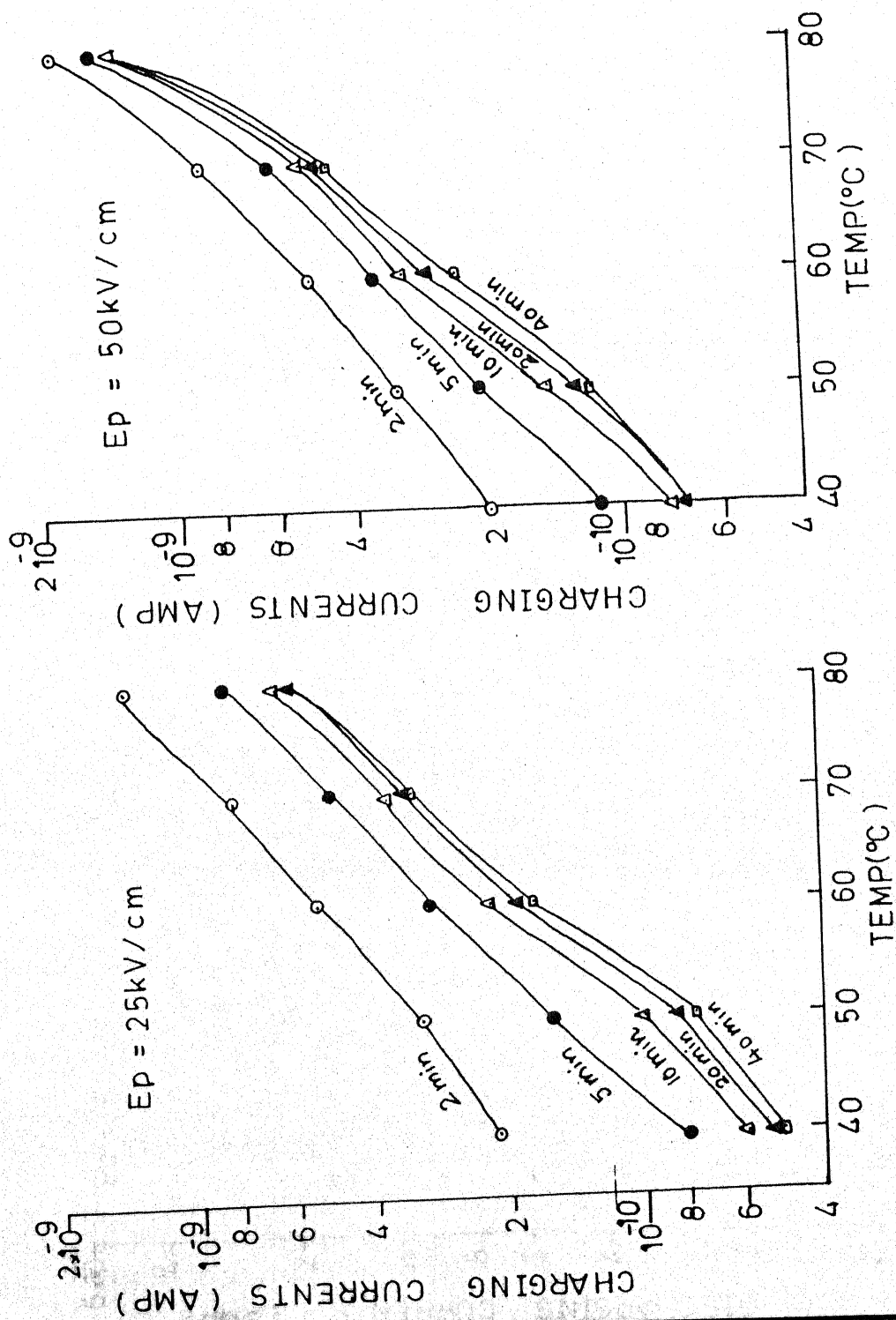


Fig 5.13(b): Isochronal current versus temperature plots for charging mode at given field and different constant times with Al-Cu system.

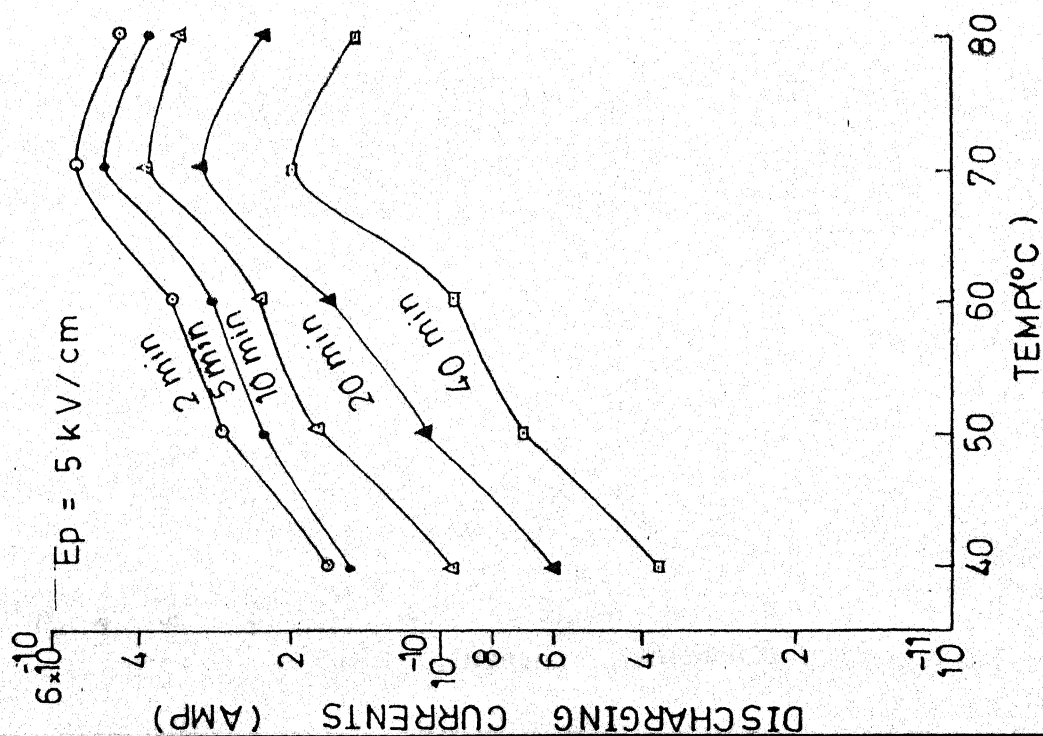
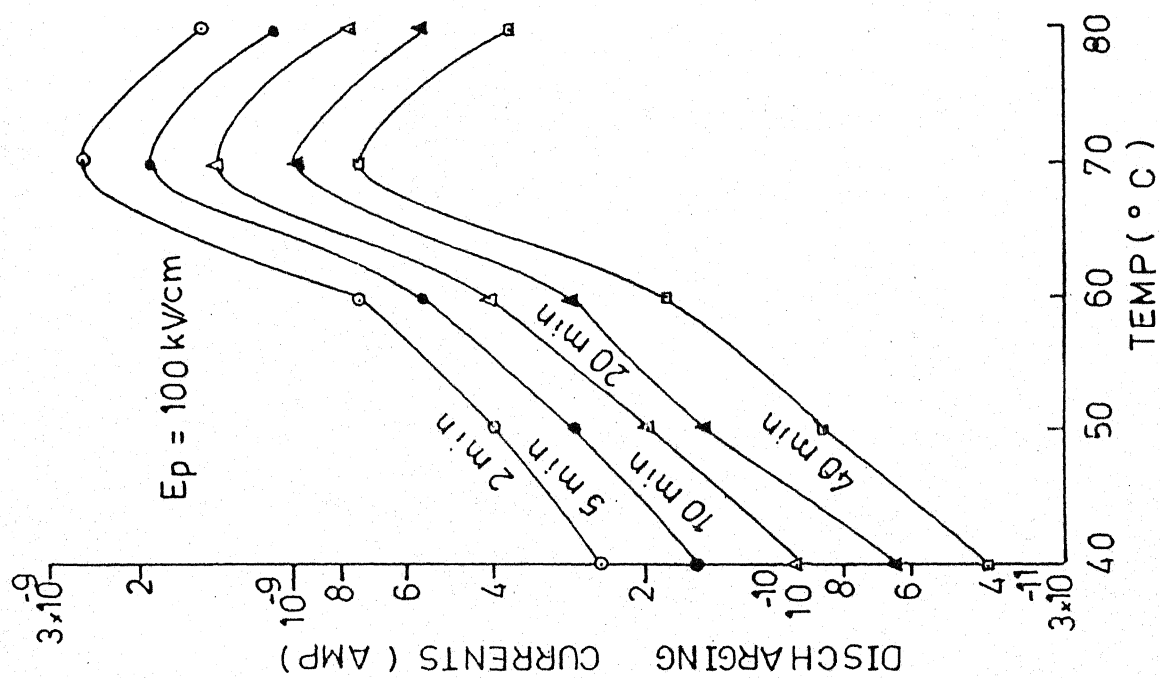


Fig 5.13(A) : Isochronal current versus temperature plot for discharging mode at given field and given constant times with Al-Cu system.

Fig 5.13(C) : Isochronal current versus temperature for discharging mode at given field and given constant times with Al-Cu system.

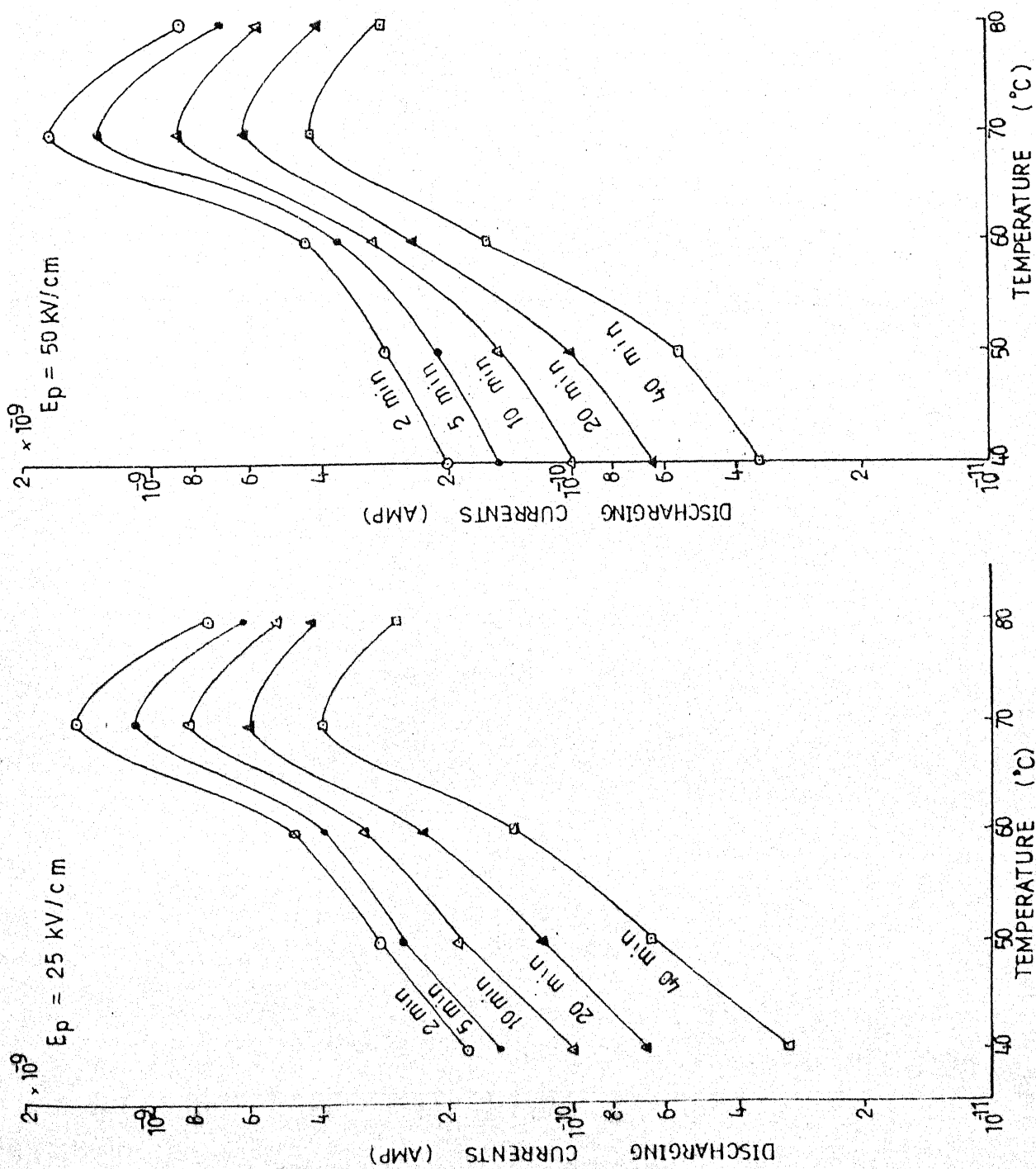
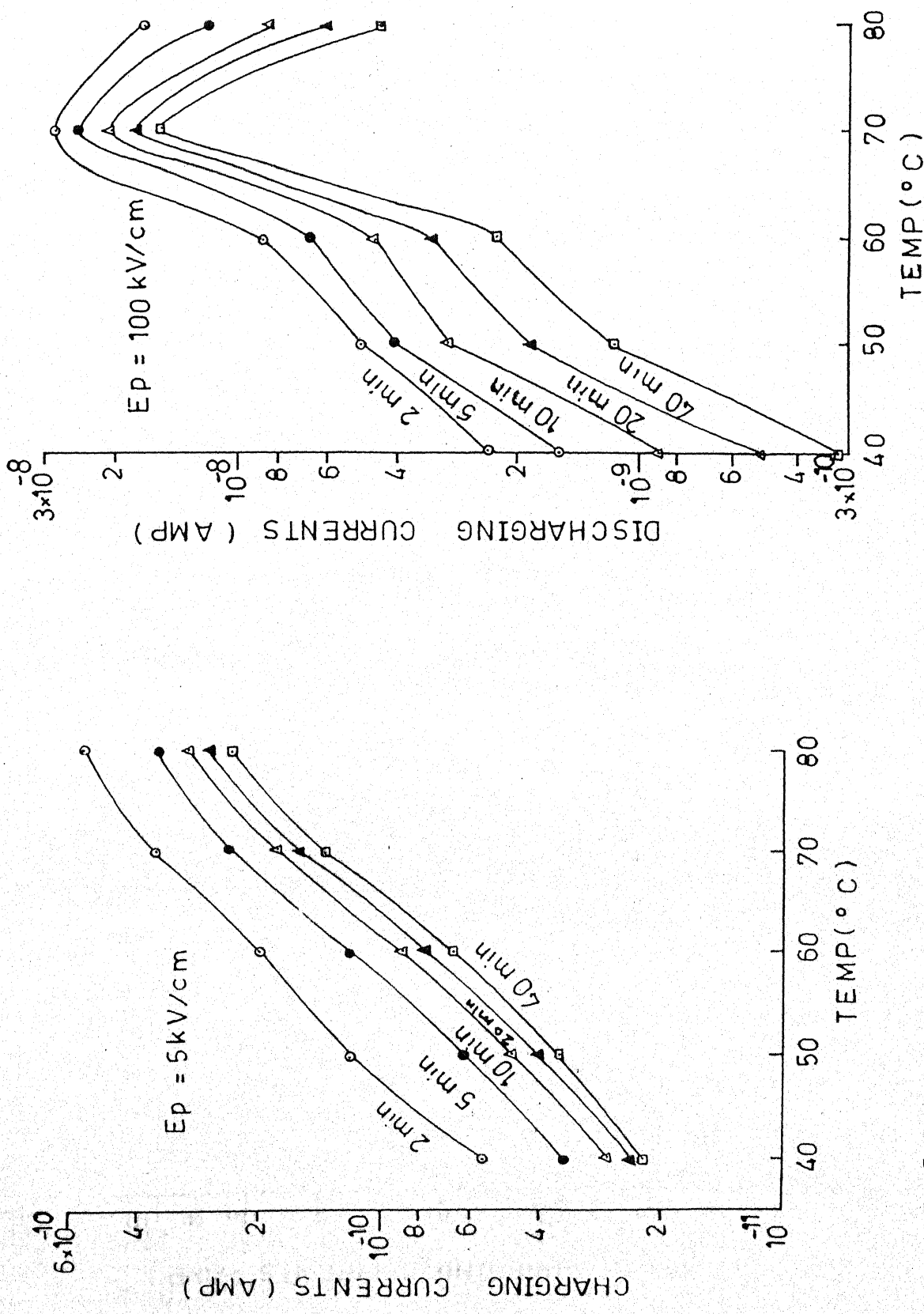


Fig 5.13(B): Isochronal current versus temperature plots for discharging mode at given field and different constant times with Al-Cu system.



Fg 5.14(a): Isochronal current versus temperature plot for charging mode at given field and constant times with Al-Sn system

fig 4.14(c) Isochronal current versus temperature p for discharging mode at given field and constant times with Al-Sn

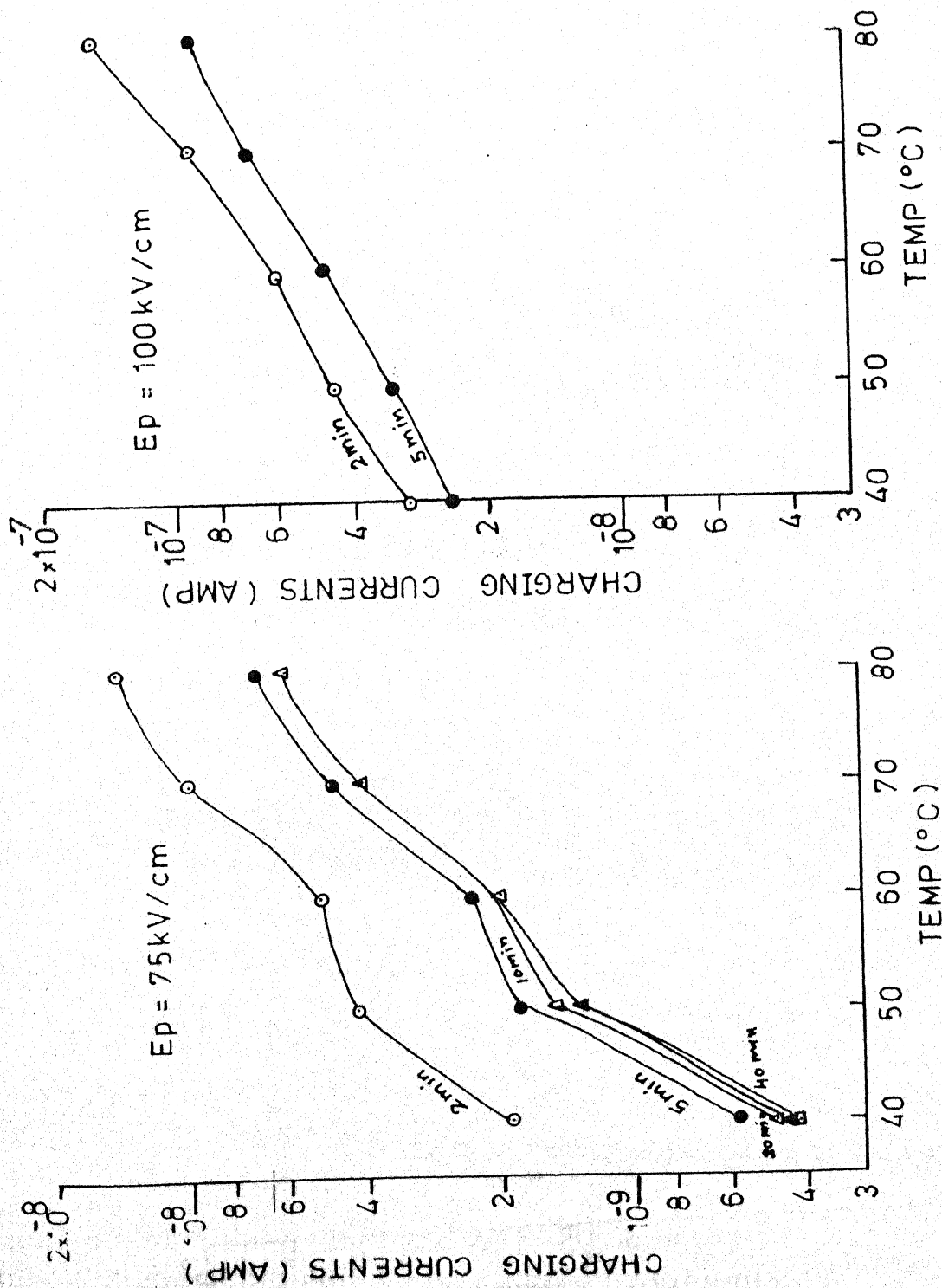


Fig 5.14(c): Isochronal current versus temperature plots for charging mode at given field and different constant times with Al-Sn system.

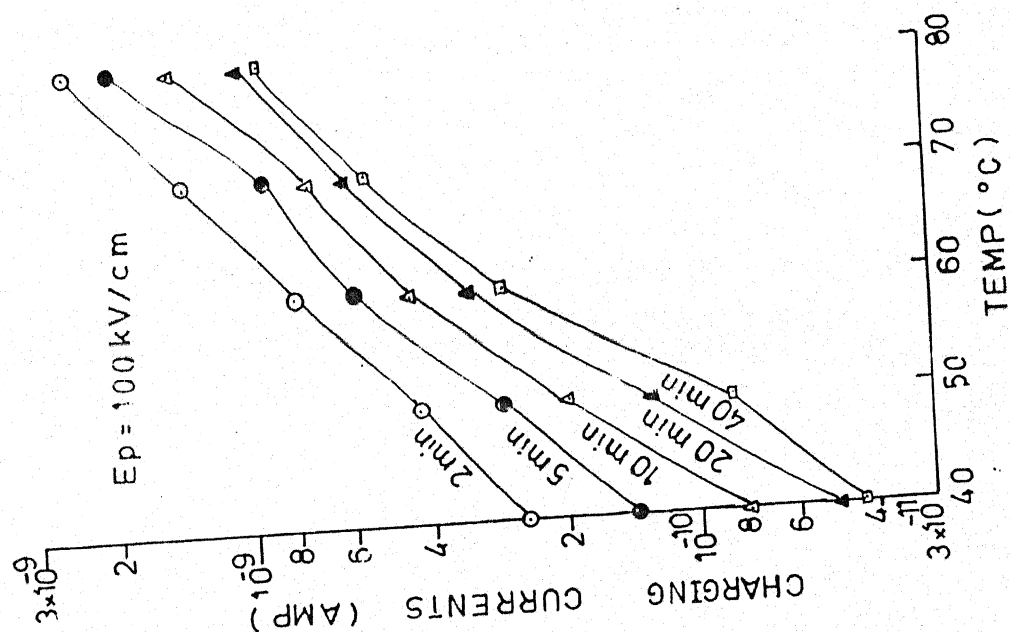


Fig. 5.14 (c) Isochronal current versus temperature plots for charging mode at mentioned field and different constant times, with Al-Sn system.

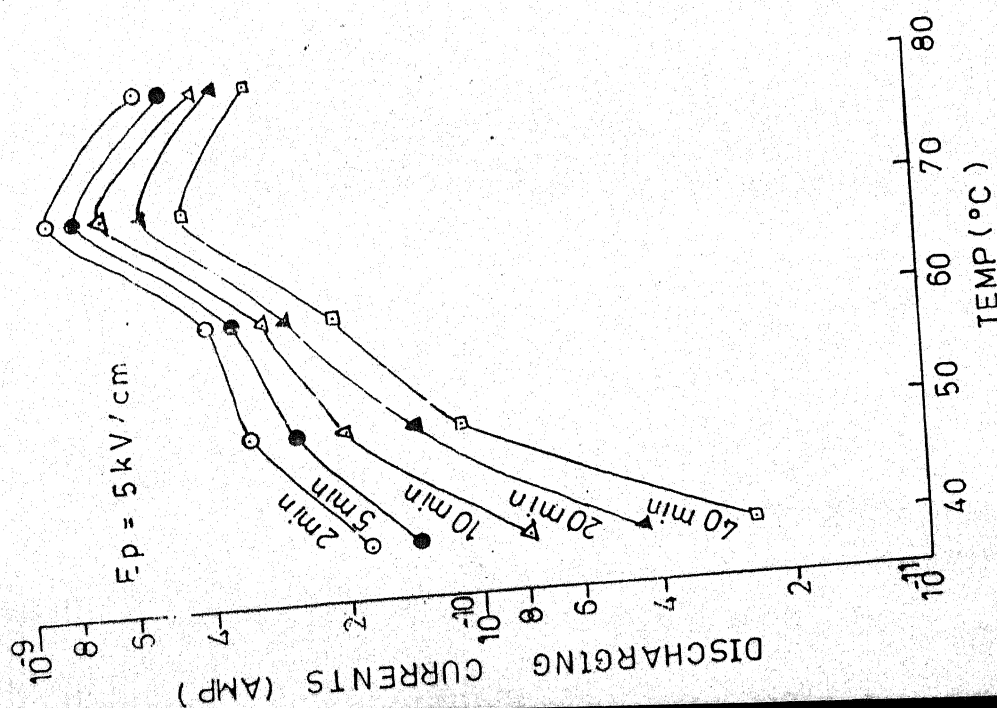


Fig. 5.14 (A) Isochronal current versus temperature plots for discharging mode at mentioned field and different constant times, with Al-Sn system.

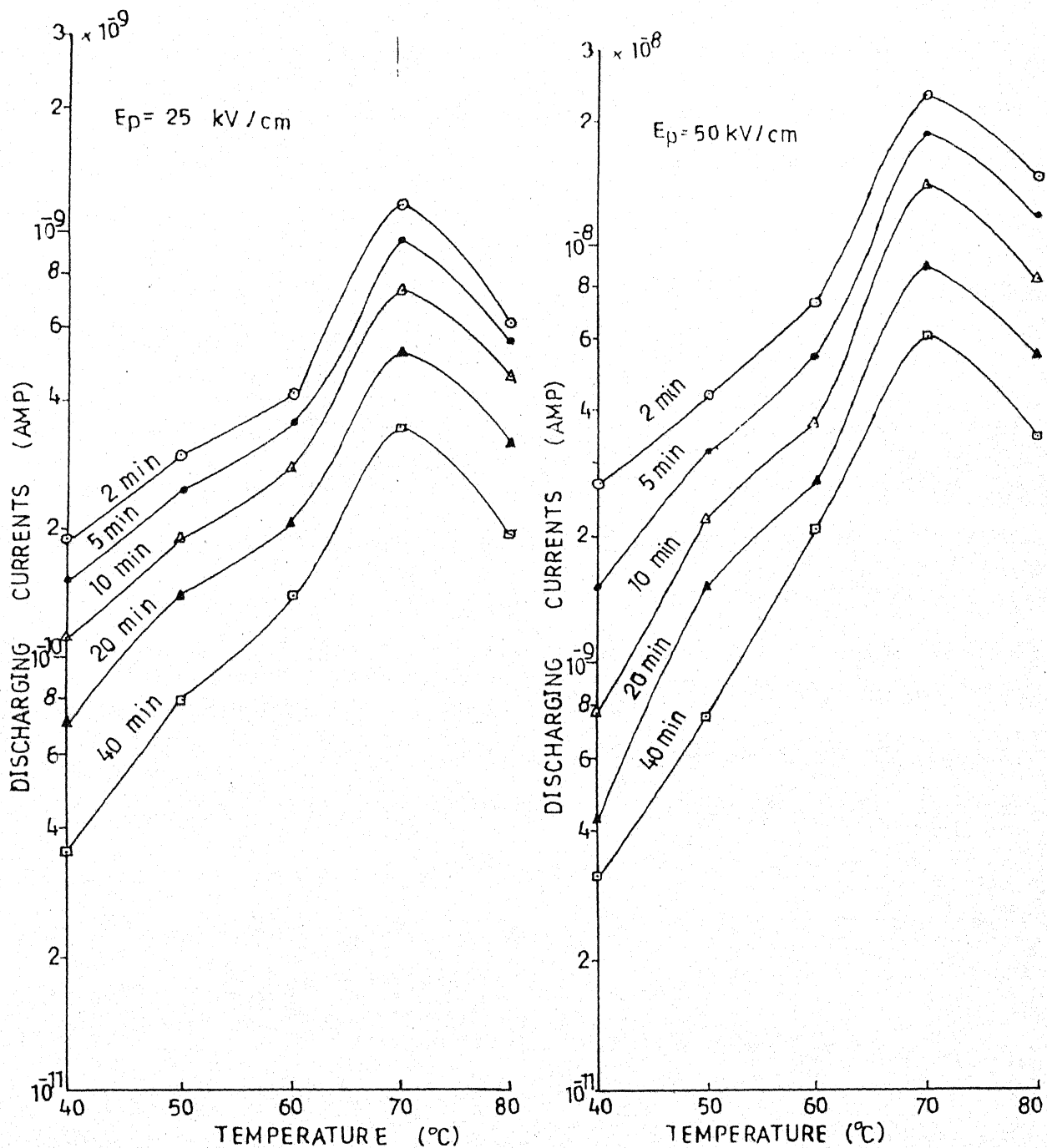


Fig 5.14(B): Isochronal current versus temperature plots for discharging mode at given field and different constant times with Al-Sn system.

value of activation energy increases with increase in the time of observation. Further, the values of activation energy are higher in the case of dissimilar configuration. However, no regular pattern in variation of activation energy with field is observed.

5.3-3 FIELD DEPENDENCE

Figs. 5.15 to 5.18 illustrate the variation of transients with polarising fields at constant times of measurements. Figs. 5.15 to 5.16 are for similar Al-Al system and Figs. 5.17 to 5.18 for dissimilar Al-Ag combinations. From these plots, it can be observed that the current exhibits a complex dependence on the polarising field for dissimilar electrode combination. The current increase with field and shows a broad peak located at 50 kV/cm field value for charging mode and at 45 kV/cm for discharging mode for Al-Al similar electrode system. Finally, the current increases again for higher field values.

5.3-4 ELECTRODE MATERIALS DEPENDENCE

Two sets of electrode material systems are considered, i.e., similar electrode system like Al Al, Ag Ag, Cu Cu and Sn-Sn and dissimilar electrode combinations like Al-Ag, Al-Cu and Al-Sn. It has been observed that, in general, the current values are higher by one order of magnitude in similar electrode system over that of dissimilar electrode combinations.

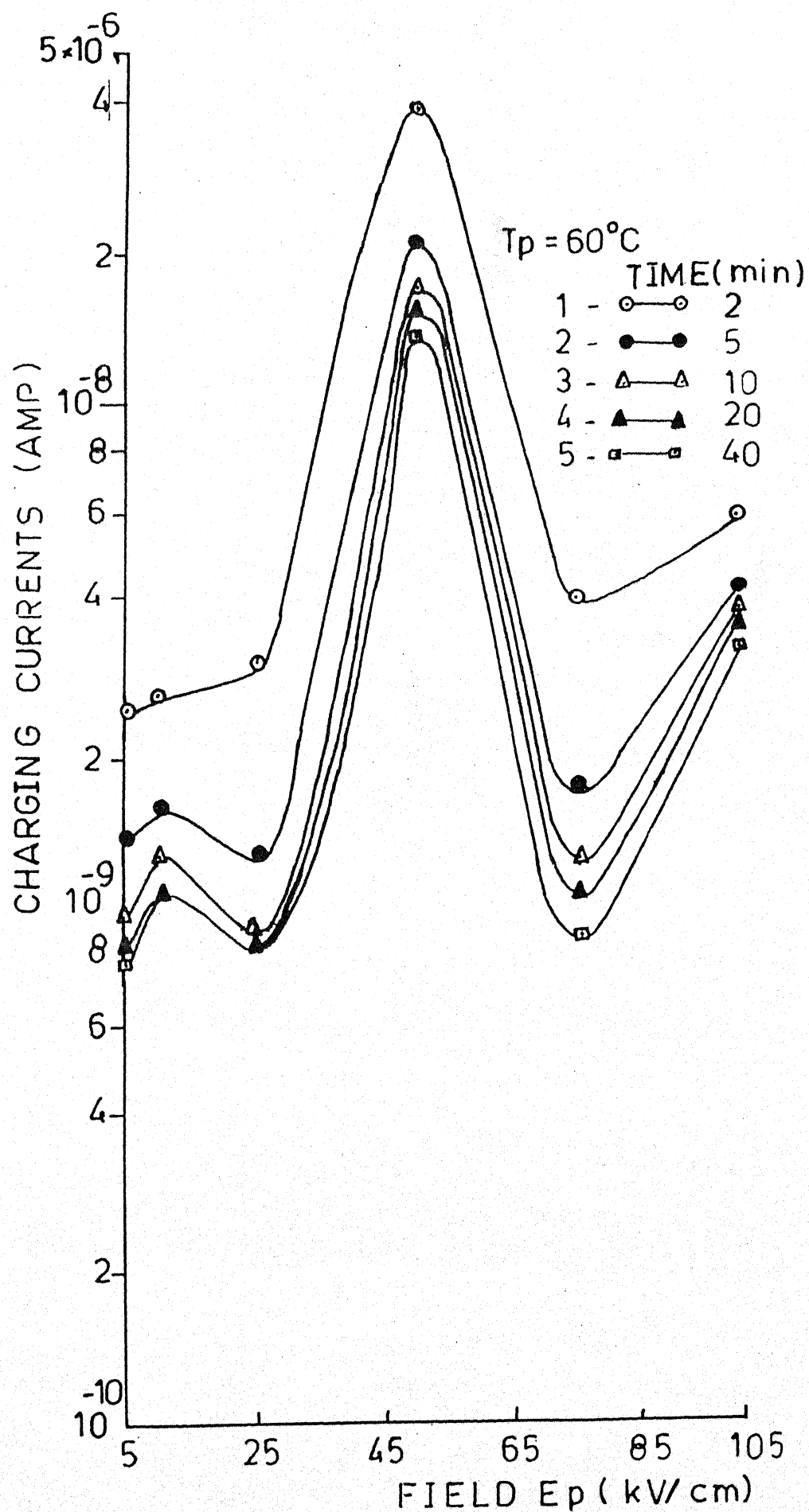


Fig.5.15 Variation of transient currents for charging mode with Polarising field at different constant times for Al-Al System.

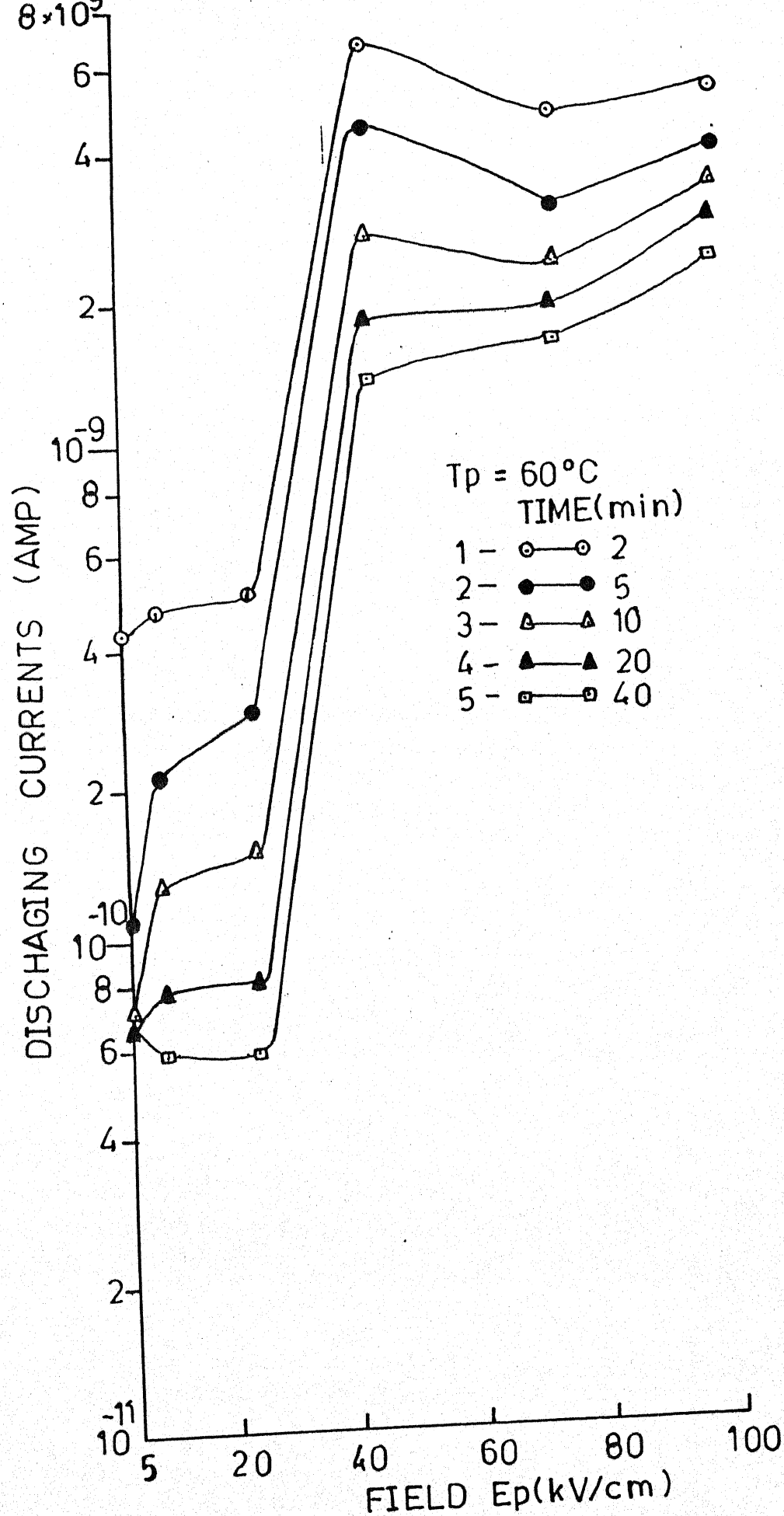


Fig.5.16 Variation of transient current for discharging mode with Polarising field at different constant times for Al-Al System.

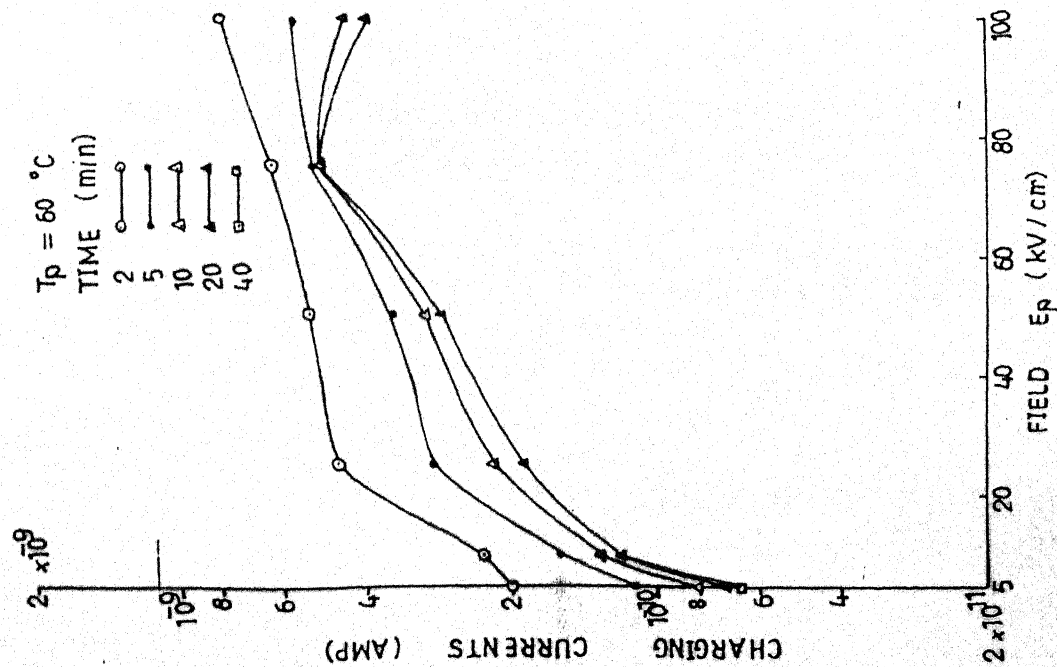


Fig.5.17 Variation of transient currents for charging mode with Polarising field at different constant times for Al-Ag System.

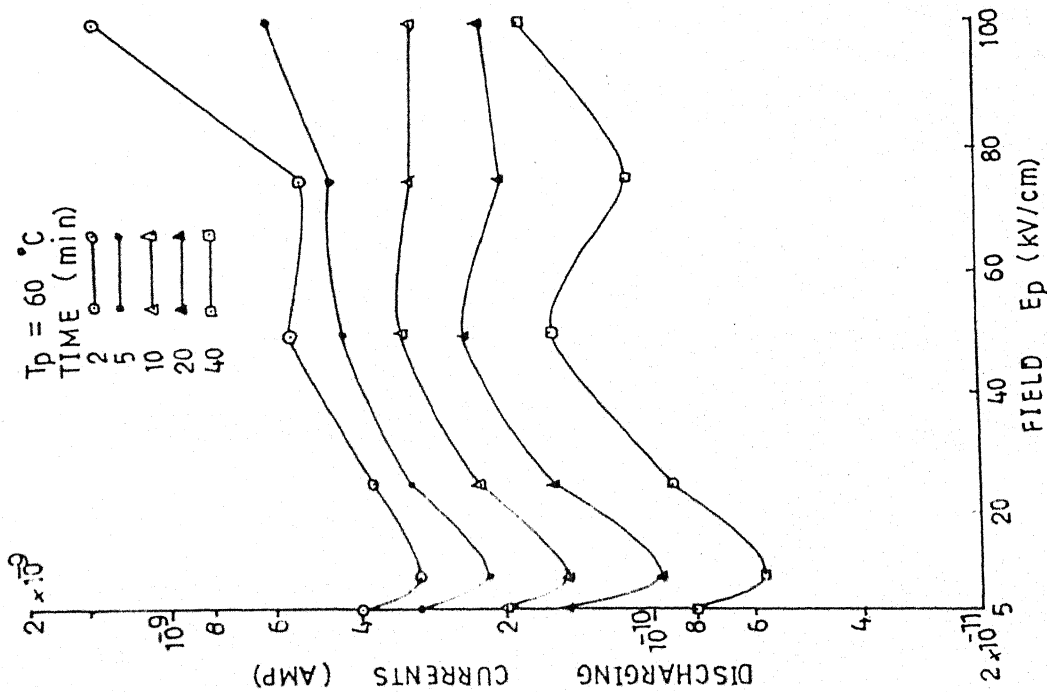


Fig.5.18 Variation of transient current for discharging mode with Polarising field at different constant times for Al-Ag System.

5.3-5 GENERAL CHARACTERISTICS OF THE CURVES

- (i) The transient current polarity is found to be positive in both the cases of charging and discharging modes and observed current approaches stable value in relatively short period under high fields.
- (ii) Curves illustrating the time dependence of charging as well as discharging transients are characterised by two regions, which are designated as short time and long time regions, respectively.
- (iii) Curves illustrating the temperature dependence of charging and discharging transients at various constant times (isochronals) are characterised by a peak at 70°C for discharging mode.
- (iv) Isochronal currents at various constant times show a non linear field dependence characterised with a maximum at a certain field value for a particular temperature for charging mode.
- (v) The activation energy, in general, show an increase with increasing field also with the time of observation. By comparing the values of activation energy for different configuration, it is evident that the value of activation energy are, in general, much higher in the case of

dissimilar electrode combination than for similar configuration.

Figs. 5.19-5.25 represent the isothermal current (I) - voltage (V) characteristics (plotted in the form of $\log I - \log V$ curves) of 5, 20, 30 μm thick polyvinyl pyrrolidone foils at 40, 50, 60, 70 and 80°C using different electrode configurations Al-Al; Cu-Cu; Ag-Ag; Sn-Sn; Al-Sn; Al-Cu and Al Ag combinations, respectively. The increment in the current is approximately the same for whole range of temperatures. The nature of the thermograms is non-linear but similar for all temperatures. The curves show two distinct regions with different slopes, have a knee at a point. Thinnest (5 μm) foil exhibit more current than thick (30 μm) foils. The magnitude of the current has been found to be higher in dissimilar electrode combinations (Al-Sn; Al-Cu; Al-Ag) than similar electrode (Al-Al; Cu-Cu; Ag-Ag; Sn-Sn) systems.

The Schottky plots of PVP foils show the variation of current with field in the form of $\log I$ versus \sqrt{E} (Figs. 5.26-5.28) for 5 μm ; 20 μm and 30 μm thick foils, respectively. The Figures also indicate $\log I$ versus \sqrt{E} isotherms for different electrode combinations (Al-Al; Cu-Cu, Ag-Ag, Sn-Sn, Al-Sn, Al-Cu and Al-Ag).

The isothermal I-V characteristics for PVP foils, in temperature range 40-80°C (Figs. 5.19-5.25) reveal almost ohmic behaviour ($I \propto V$) initially in a limited field region,

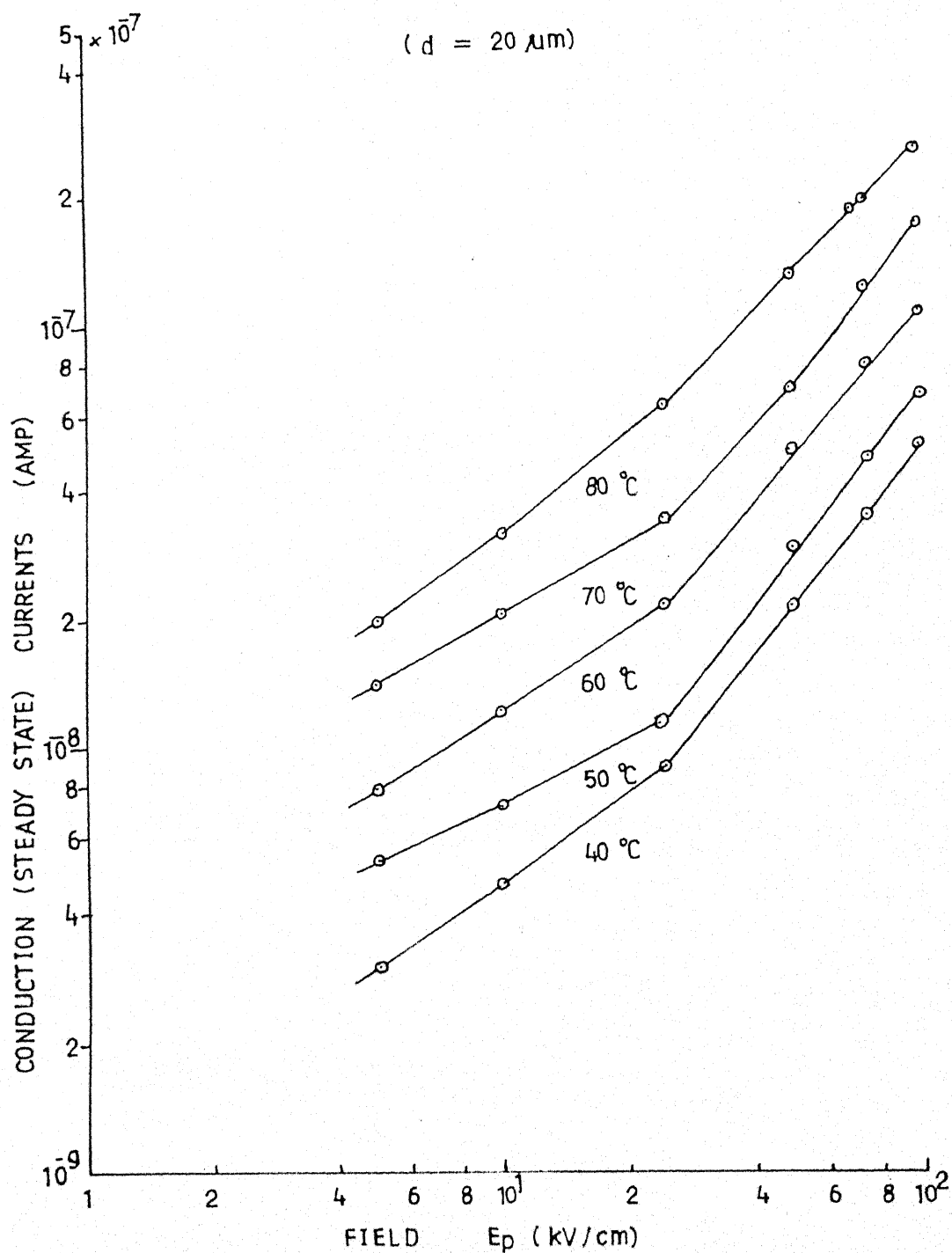


Fig 5.19 : Current -Voltage characteristics of pure PVP as a function of given thickness at different constant temperature with Al-Al system.

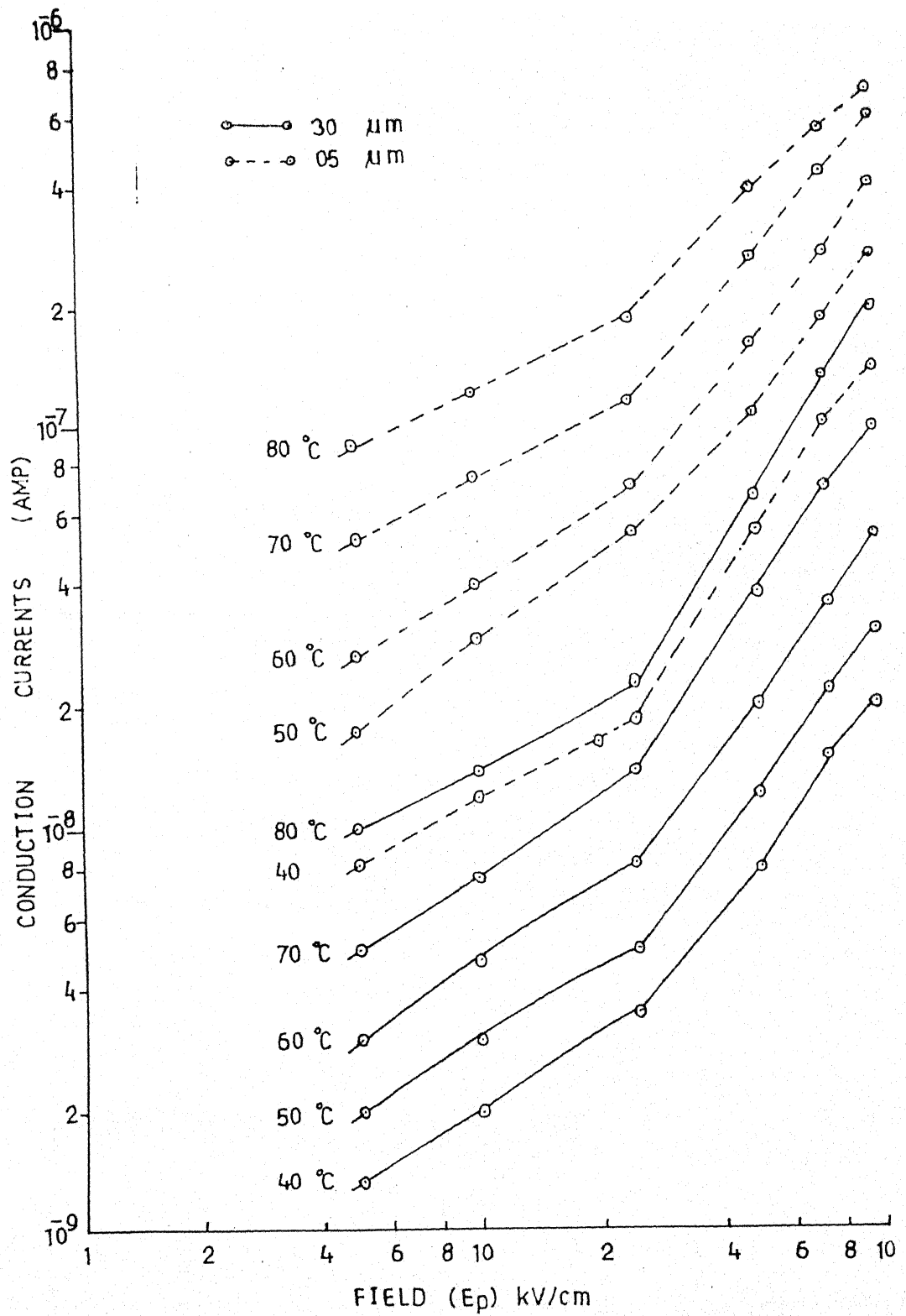


Fig 5.19 : Current - Voltage characteristics of pure PVP as a function of given thickness at different constant temperature with Al-Al system.

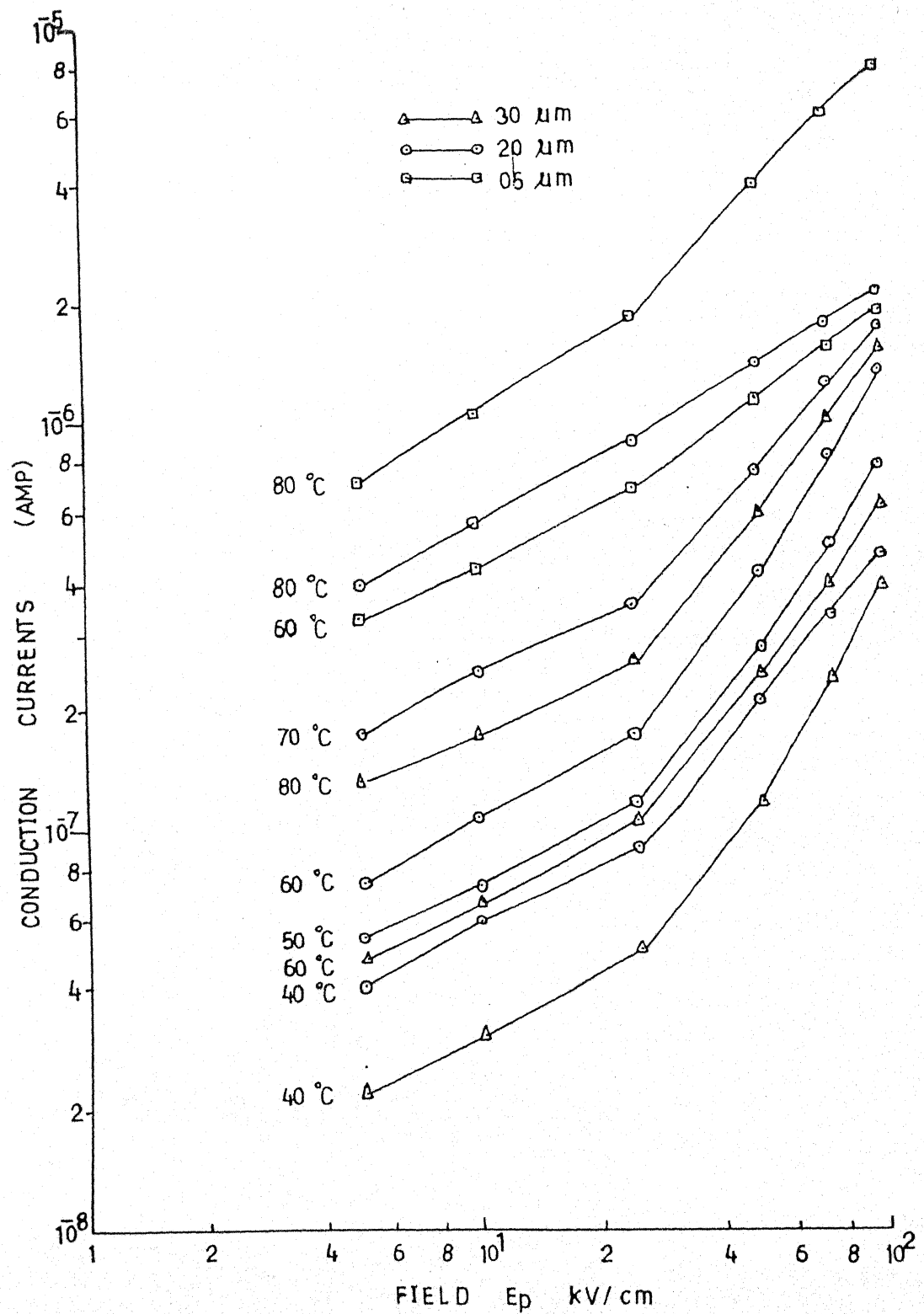


Fig 5.20 : Current-Voltage characteristics of pure PVP as a function of given thickness at different constant temperature with Ag-Ag system.

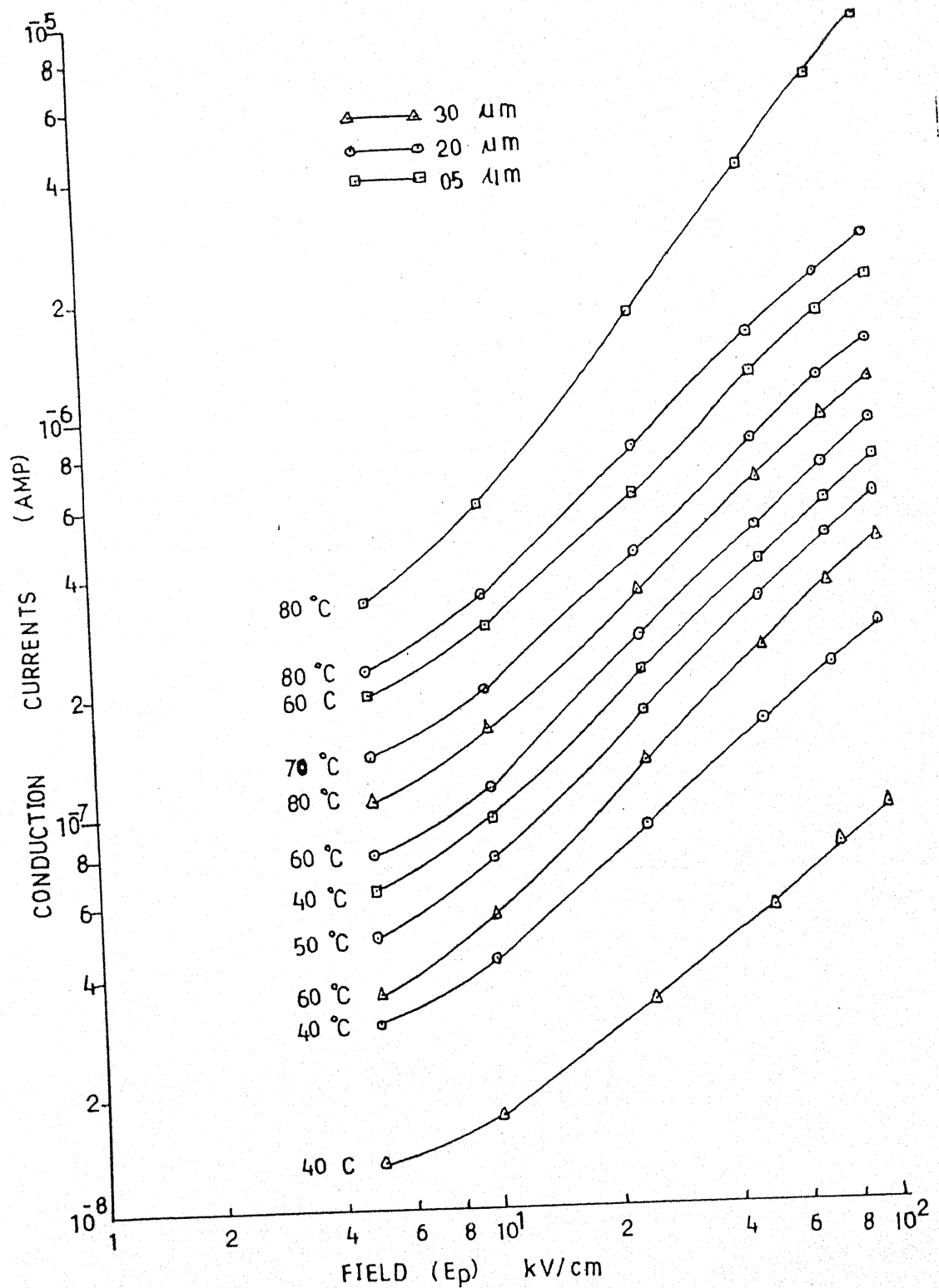


Fig 5.21 : Current-Voltage characteristics of pure PVP as a function of given thickness at different constant temperatures with Cu-Cu system.

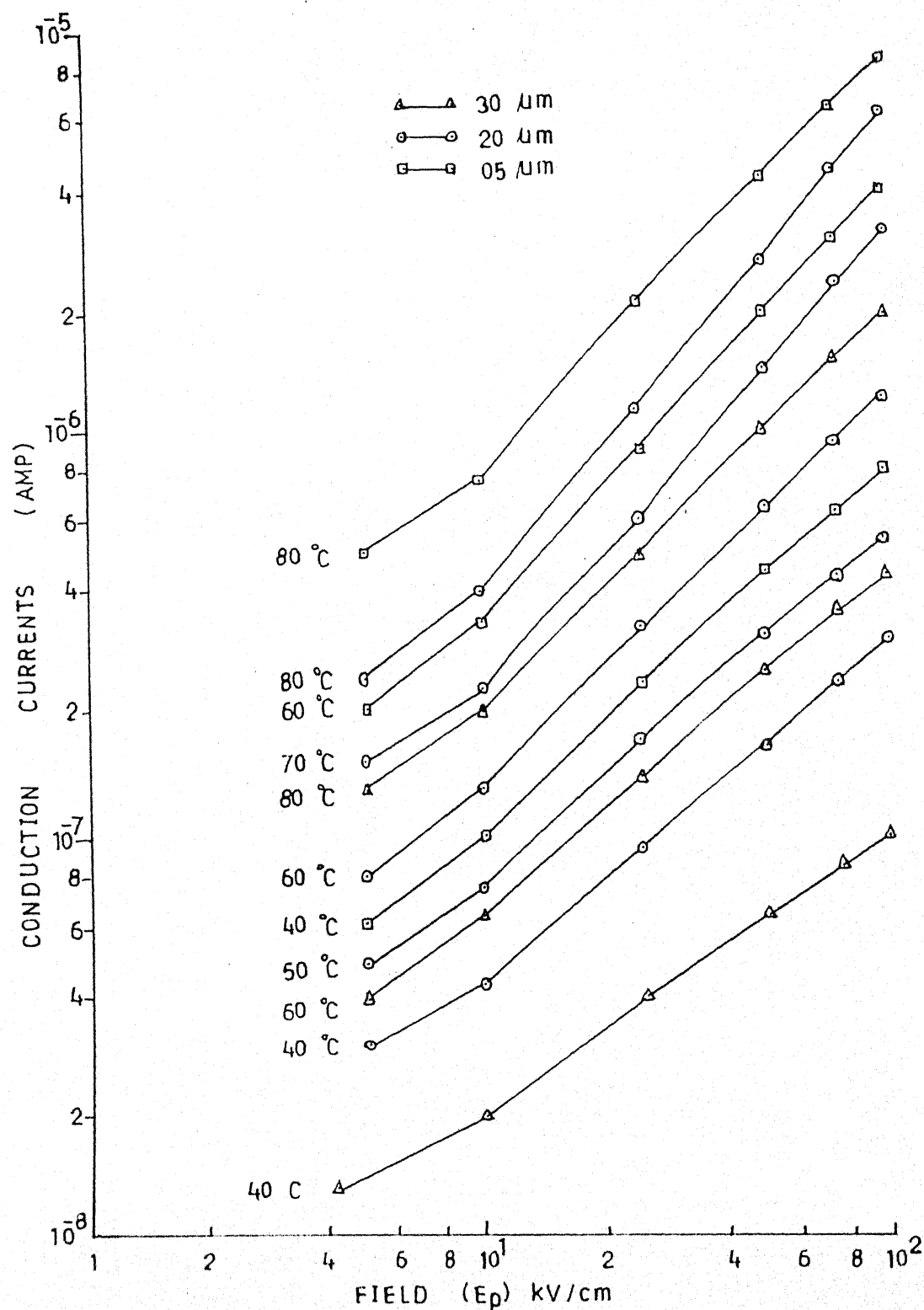


Fig 5.22 : Current-Voltage characteristics of pure PVP as a function of given thickness at different constant temperature with Sn-Sn system.

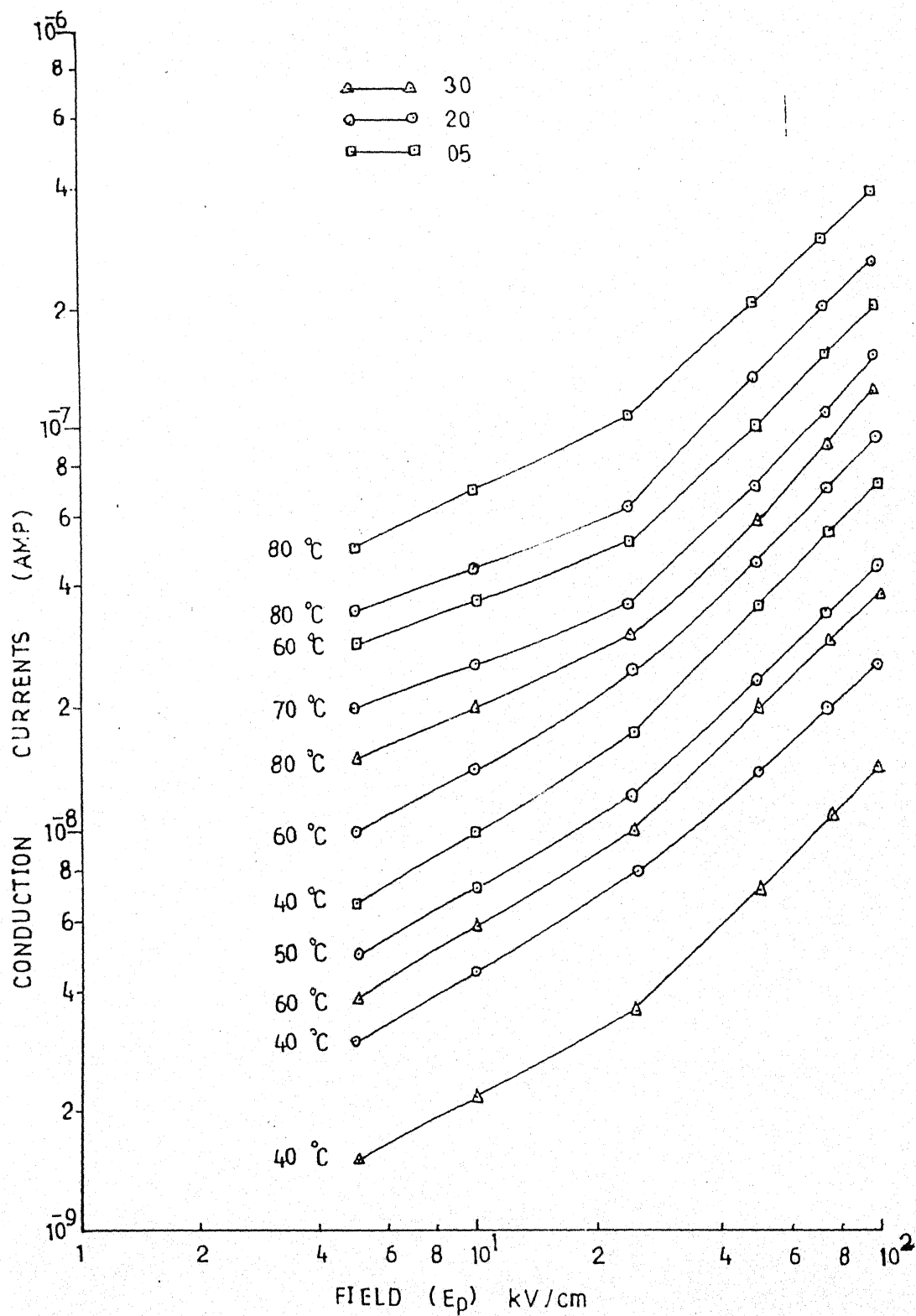


Fig 5.23 : Current-Voltage characteristics of pure PVP as a function of given thickness at different constant temperatures with Al-Ag system.

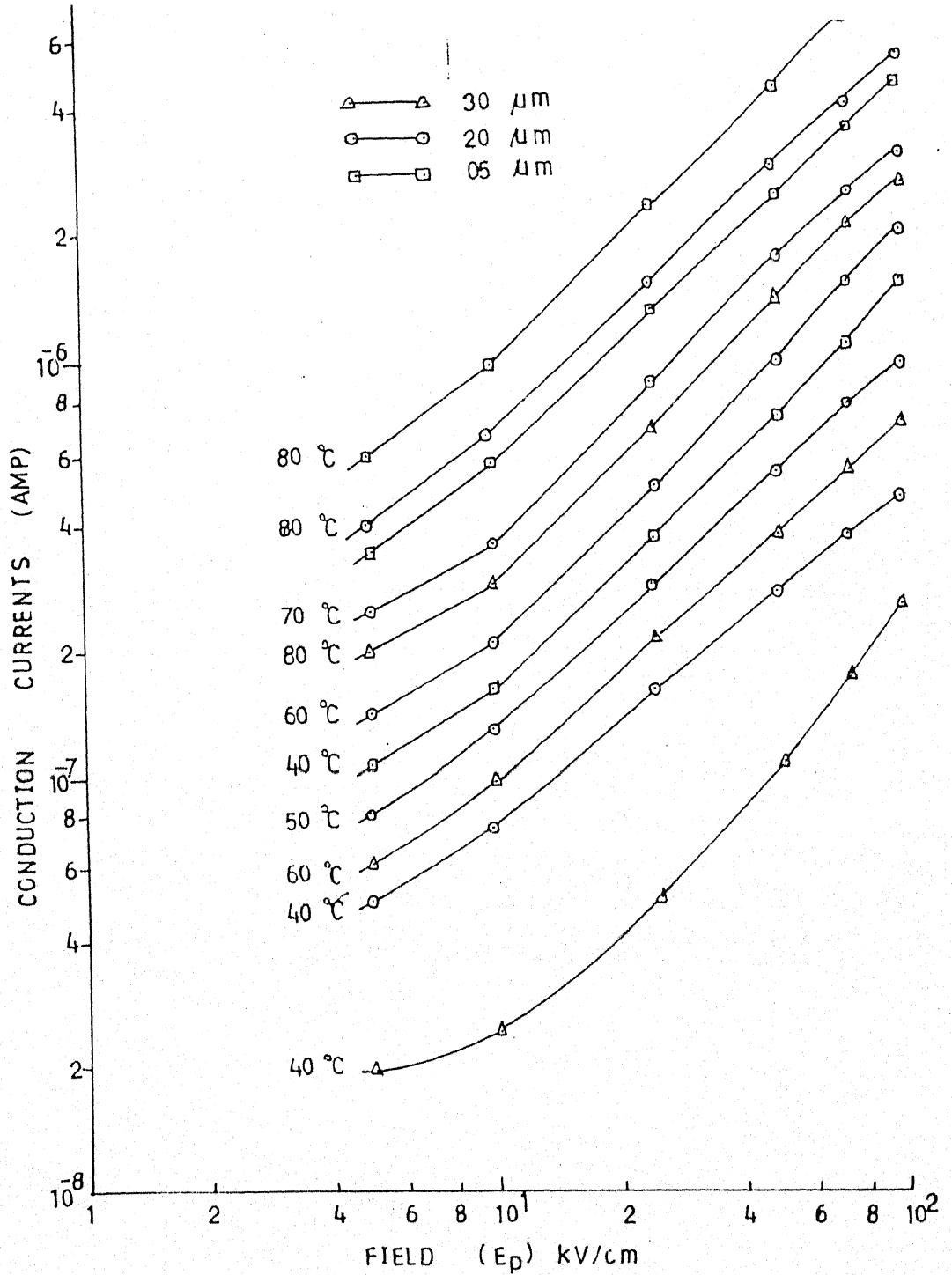


Fig 5.24 : Current-Voltage characteristics of pure PVP as a function of given thickness at different constant temperatures with Al-Cu system.

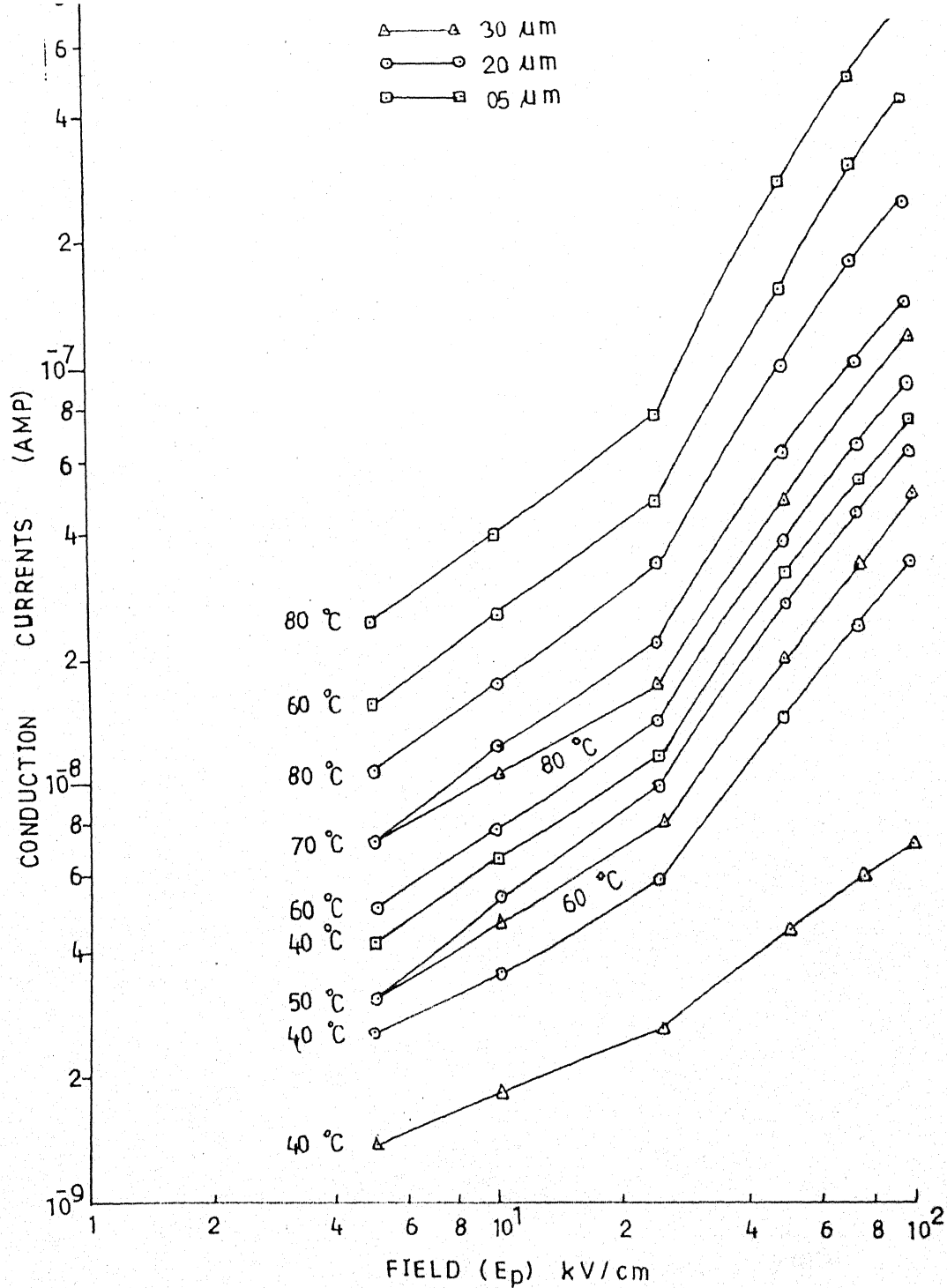


Fig 5.25 :Current-Voltage characteristics of pure PVP as a function of given thickness at different constant temperatures with Al-Sn system.

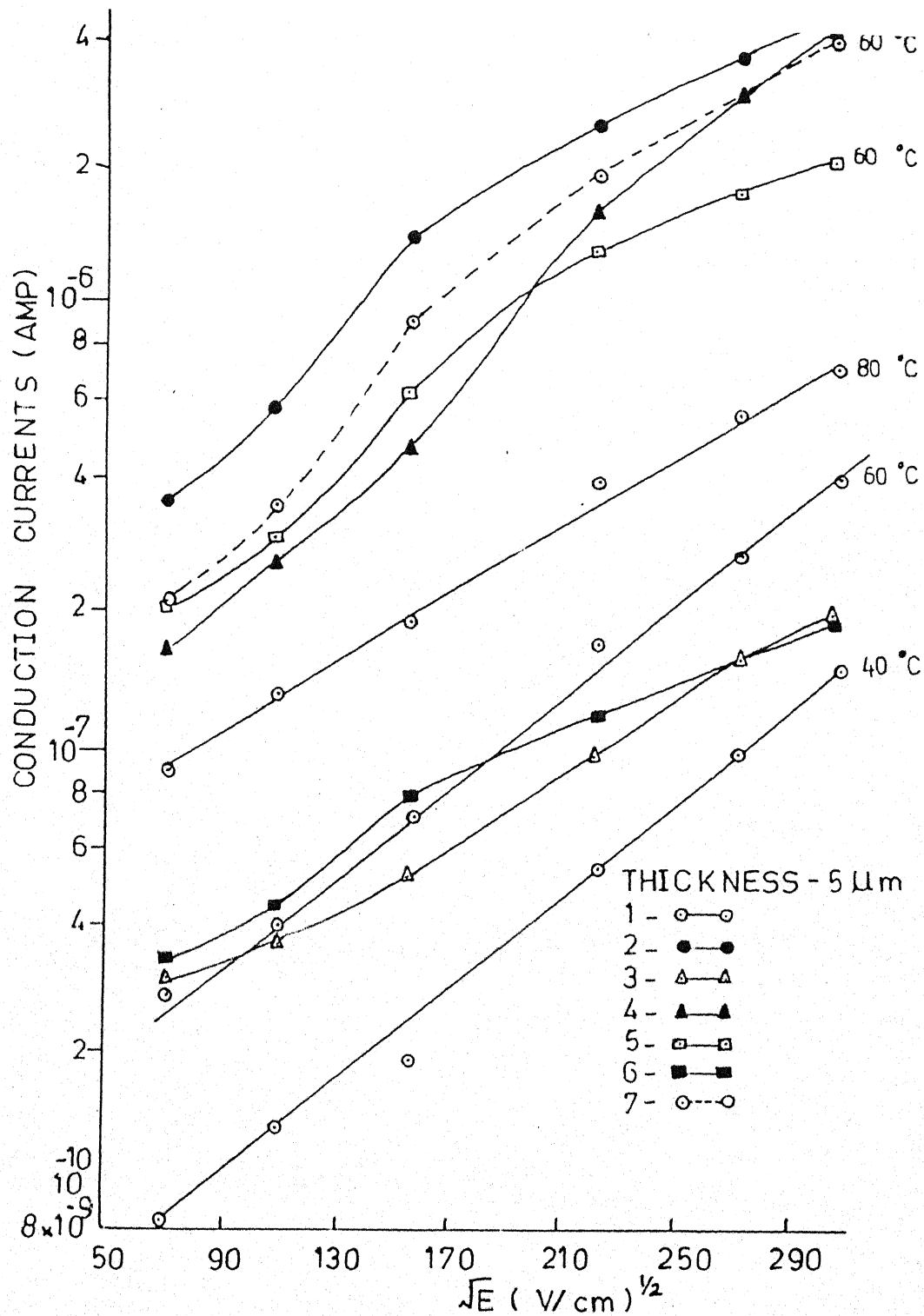


Fig 5.26 : Conduction current versus square root of voltage of 5 μ m thick pure PVP foils at different constant temperatures with various electrodes system.

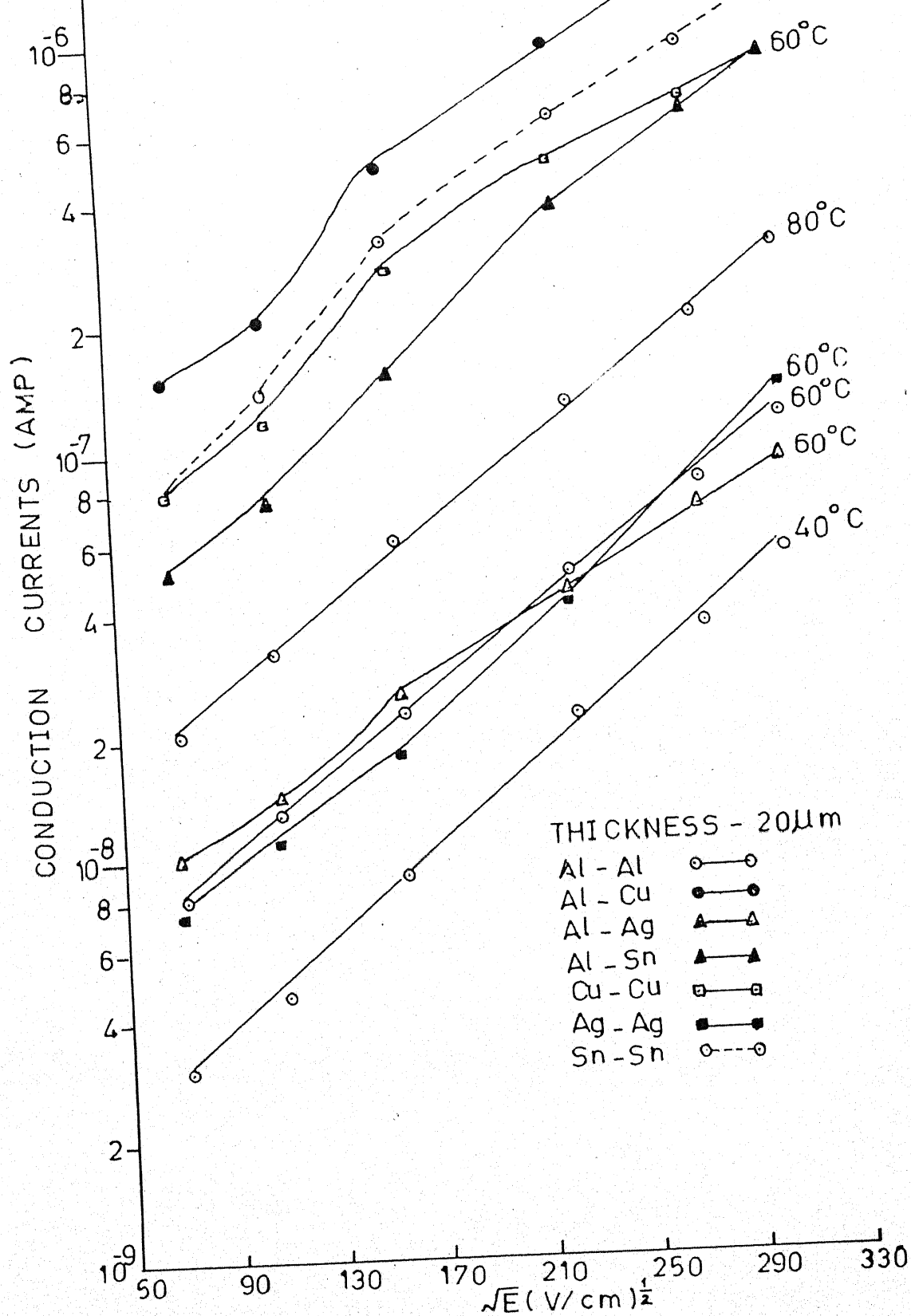


Fig 5.27 : Conduction current versus square root of voltage of 20 μm thick pure PVP foils at different constant temperatures with various electrodes system.

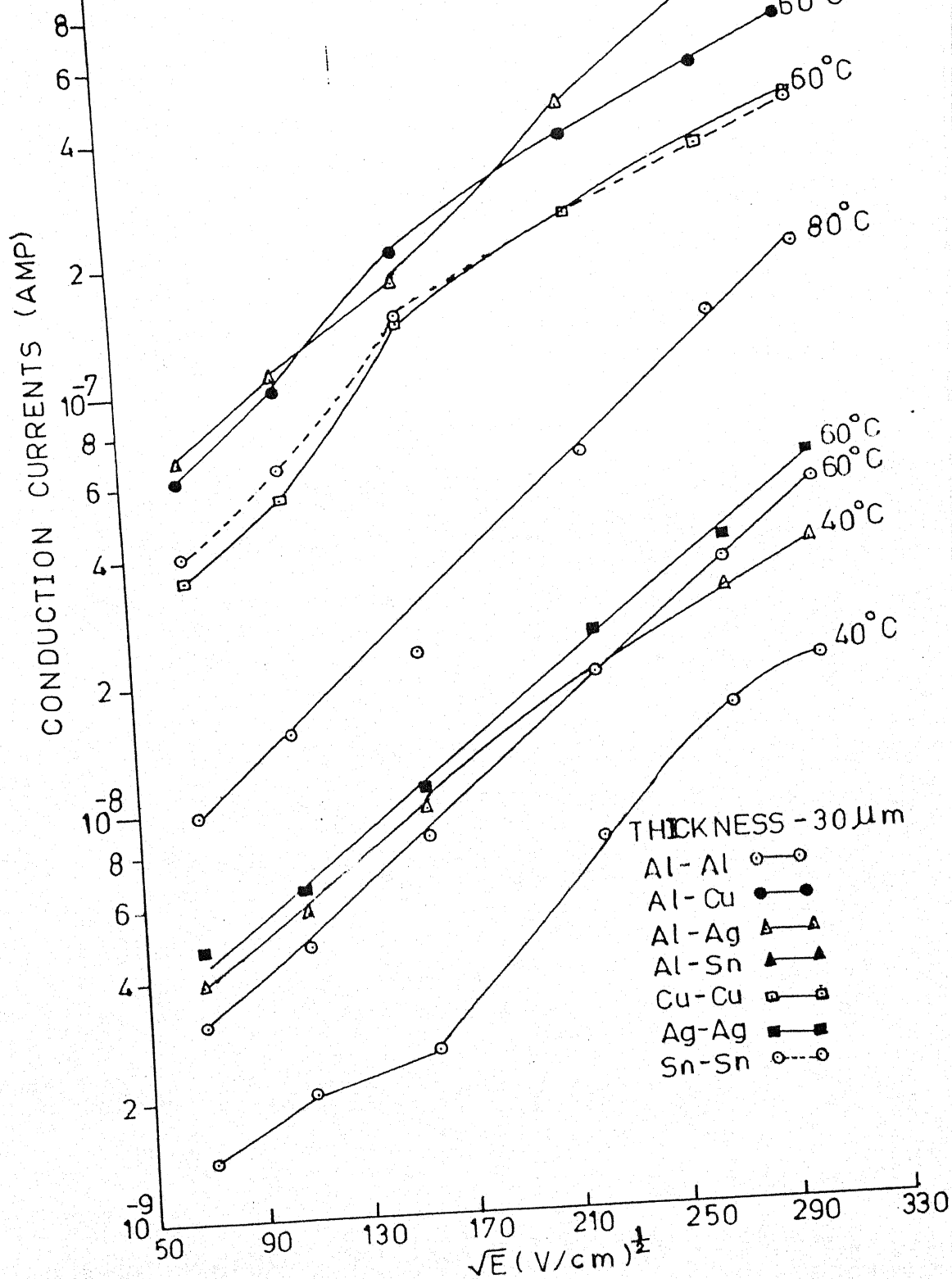


Fig 5.28 : Conduction current versus square root of voltage of 30 μm thick pure PVP foils at different constant temperature with various electrodes system.

which gradually becomes non-ohmic; above a field of 2.5×10^4 V/cm. The slope values (m) in lower field region lie between 0.48 to 0.68. The ohmic behaviour can be understood on the basis of the reasonable assumption that at low voltages there is negligible injection of carriers from the contact and the initial current is governed by the intrinsic free carriers in the material. The current will be ohmic until the injected free carrier density becomes comparable with the thermally created carrier density. To resolve the two mechanisms, a graph of $\log I$ vs \sqrt{E} has been plotted (Figs. 5.26-5.28) for different foils thicknesses and electrode combinations. Separate lines are obtained for Al-Al, Cu-Cu, Ag-Ag, Sn-Sn, Al-Cu, Al-Sn and Al-Ag combinations. This is sufficient to cast doubt on the applicability of PF mechanism.

5.4 DISCUSSION

From the above characteristics, it is evident that at least two distinct mechanisms shall be responsible for the current decay. One mechanism is operative in the range of short time giving rise to a straight line on $\log I$ vs $\log t$ plot with a particular value of decay constant, n_1 , and the other mechanism is operative in the range of long times giving rise to another straight line in $\log I$ vs $\log t$ plot with a decay constant, n_2 , of higher value.

The main mechanisms that have been put forward in order to interpret the transient current decay flowing through a

dielectric are already discussed in Chapter III. We now try to analyse the observed results in the light of the existing models, i.e., dipolar relaxation, tunnelling to empty traps, charge injection leading to space charge effects and electrode polarisation considering the variation of such currents with time, temperature, field and electrode materials.

In the case of tunnelling to empty traps, it is well established that the tunnelling current should be independent of temperature and proportional to the field at moderate fields. However, in the present case, charging and discharging transients at fixed times show thermal dependence and exhibit a complex dependence on the electric field. Thus, it seems that tunnelling to empty traps can be ruled out as a possible mechanism for the observed transients.

In the case of electrode polarisation, the transient currents are reported to be proportional to t^{-n} with the value of decay constant $n = 0$ at short times, and $n > 1$ at longer times. However, in the present case, at short times the value of n is found to vary from 0.43 to 0.62 for similar electrode system and from 0.78 to 0.98 for dissimilar electrode combinations. These observations show that the process of electrode polarisation is unlikely to be dominant in the present case.

Analysing the experimental results further, we know that dipolar relaxation [32,33] can also account for t^{-n} type of

time dependence. However, it has to be borne in mind that, as a general rule, dipolar processes involved in polymer are characterised by a distribution in relaxation times, and that overlapping of several processes are likely to be present. This also implies that the Curie law can only be considered more or less a rough approximation of the real time dependence and can only depict the transient phenomena over short periods of time. Keeping this in mind, the following points may be considered in favour of this model.

The existence of three main relaxations in PVP which are labelled as α , ρ and ρ' in ascending order of temperature. The relaxation involving local motions of the side carbonyl group occurs around 90°C . The ρ relaxation is associated with the conformational motions of the main chain segments and takes place near the glass transition temperature, 170°C . The third relaxation labelled ρ' is reported to result from the ionic space charge polarisation and occurs at 200°C , well above the glass transition temperature.

In the present case transient current at fixed times show an isochronal peak localised at 70°C . Further, the charging and discharging currents are mirror images of each other over most of the temperature range. Thus, it seems likely that the dipolar relaxation process in PVP could be responsible for the transient component of charging and discharging current. It may be noted here that linear dependence on field as expected of a dipolar process has been

observed in polymers only when current are measured at temperatures sufficiently lower than the glass transition temperatures. It seems that at shorter times only dipoles with short relaxation times are oriented/reoriented resulting in a smaller value of decay constant, n_1 . However, at longer time dipoles with longer values of relaxation time also start orienting/reorienting resulting in a current that decays/changes at a faster rate resulting in a higher value of n_2 .

It has been observed that current shows a complex field dependence. Further, the activation energy has been found to increase with the time of observation. Thus, it can be concluded that the observed current may have contribution from charge carriers hopping amongst localized states. The presence of amorphous regions in PVP entails existence of localized states in the band gap.

In fact, systems dominated by hopping of ionic and electronic charge carriers, generally, show a transient decay divided into two successive domains. With the aid of two site models, Lewis [34] has derived an expression for transient behaviour which allows only value of n , i.e. there is no restriction on the value of n . The model assumes that the localized states which are distributed in energy and charge carriers undergo limited transitions to adjacent sites. The observed increase in the value of activation energy at longer times may be explained by the hopping mechanism which requires

the existence of such localized states distributed in energy. Thus, it seems that hopping of charge carriers may also be a possible mechanism for the observed transient.

The increase in the value of activation energy at longer times may adequately be explained in the light of transients controlled by space charge formation in the bulk of the sample. The following observed characteristics are in support of the space charge mechanism :

- (i) The complex dependence of the isochronal transients on the field strength, supports the contention that the field at the electrode (cathode or anode) is modified by the space charge, and
- (ii) isochronal current peak shifts towards higher fields at shorter times, thus suggesting the presence of space charges.

Charges can be injected directly from the electrodes leading to space charge formation inside the dielectric. These charges may get trapped at various trap levels. The faster decay of current corresponding to a higher value of constant n_2 in the long time region for different samples indicates the existence of energetically distributed localized trap levels. It seems that at shorter times, only shallow trap levels get filled/emptied contributing to a charging/discharging current that changes at a slower rate. However, at longer times deeper traps capture/release the charges due to which current decays at the observed faster rate and the observed activation energy value is greater [35-37].

It has been observed in the present investigation that the magnitude of the transient current is generally higher in case of similar electrode system. This can be understood in the light of interfacial polarisation. It seems that due to the higher conductivity of PVP, more interfacial charge is localised on PVP during charging using similar electrode configuration, giving a higher value of charging transients. Similarly, during discharging a higher conduction current will flow in PVP resulting in a higher value of the discharging current.

The complex nature of field dependence may be explained in the manner that the internal field created by the interfacial polarisation decreases the external applied field. The effect of the internal field would be to decrease the apparent charge carrier mobility. The interfacial charge is thus expected to exhibit a maximum at a certain field value. However, the internal field due to interfacial polarisation becomes nearly constant at higher polarising fields. The effect of the internal field may then decrease relative to the applied external field so that the apparent mobility of charge carriers again increases. The interfacial space charge shall, therefore, again increase for higher polarising fields.

Stmik [38] has shown that solid like polymers are not in thermodynamic equilibrium at temperatures below their glass transition. For such materials, free-volume enthalpy and

entropy values are greater than they would be in equilibrium state. The gradual approach to equilibrium affects many properties, e.g., the free-volume of the polymer may decrease. The decrease in free volume lowers the mobility of chain segments and also charge carriers. The decrease in mobility may be expected to reduce conductivity. At higher electric fields, a change in mobility may take place faster than at lower fields and also recombination of charge carriers may be more. This may be responsible to make the observed current in the present case to approach a stable value in relatively shorter periods under high fields.

The field dominant behaviour, more so at lower polarising temperatures (Figs. 5.1-5.7) hints at the initial current being controlled by the bulk phenomena such as polarisation effects and/or ionic currents. The dipolar relaxation seems to be the major contributor to the transient current, particularly at lower polarising temperatures. The role of dipolar relaxation has also been confirmed in PVP by the authors, through thermally stimulated discharge current studies reported in Chapter IV.

From the I-V curve, two distinct regions corresponding to different types of conduction; region I with a slope less than 2 at low or moderate fields and region II with a slope about 2 at high fields are observed. In region I, the I-V data are further found to obey a linear $\log I$ versus \sqrt{E} relation. The values of activation energy have been plotted against the

square root of applied voltages (not shown). A straight line is obtained.

The value of m for higher field region is 2, indicating a possibility of SCL conduction. The value of current is thickness dependent (Fig.5.19-5.25). Vinyl derivatives are prominent species among high polymers containing a lot of structural disorders and impurities within them. The values of slope coefficient ~ 2 of I-V characteristics are the typical proofs for the continuous trap level distribution in the band gap of semi insulating PVP. The defects and impurities can govern the conduction mechanism and also act as trapping centres and get populated by injected charge carriers from the electrodes. Charge carriers from these localized levels are thermally excited to their respective transport bands causing thermally activated ohmic conduction. Depending upon the population of these levels and their respective transport bands, the conduction may change from ohmic to Schottky emission.

The extrinsic electrical conduction in semi-insulating material corresponds to the charge carriers originating from the electrodes and sub-surface levels and the intrinsic one corresponds to the charge carriers originating in the bulk. The Schottky emission, Poole-Frenkel mechanism and tunnelling are the different possible mechanisms associated with the injection of charge carriers from outside the bulk of the samples under study. Schottky emission is analogous to

thermionic emission as it involves charge emission from metal with a difference that the barrier height is lowered by the reduction in the metal insulator work function due to applied electric field.

To identify the probable mechanism, out of Richardson-Schottky and Poole-Frenkel in present investigation, $I-E^{1/2}$ characteristics have been drawn (Figs. 5.26-5.28) by taking Al, Ag, Cu and Sn as upper electrode while the lower electrode has been of Al metal in each configuration and are having different slopes, i.e. they are assymetric to each other. They are straight in high field region while a slight deviation from the relation $I-E^{1/2}$ has been observed in the lower field region. The restoring force in R-S and P-F effects is due to Coulomb interaction between the escaping electron and positive charge.

The proper way of distinguishing between the P-F and R-S mechanisms has been suggested by Jonscher and Ansari. The effect of electrode materials namely aluminium, copper, silver and tin having different work functions 3.38, 4.46, 4.31 and 4.09 eV, respectively on the I-V characteristics has to be considered for deciding conduction mechanism.

The current through the sample differs when the upper electrode aluminium is replaced by silver, copper and tin electrode. The magnitude of current has been found to be higher in dissimilar electrode combinations (Al-Cu, Al-Ag and

Al-Sn) than similar electrode Al-Al, Cu-Cu, Ag-Ag and Sn-Sn systems. This shows the effect of the material of the electrodes on the current of the sample sandwiched between them. The values of current seem to be controlled by the effective work function for metal-insulator-metal interfaces. The difference between the work function of metal (1) and metal (2) will control the magnitude of current but for similar electrodes Al-Al, Ag-Ag, Cu-Cu and Sn-Sn systems, the characteristics of polymer may prevail as the net contribution of current from charge, injected from electrode, would then be zero. The work function of the polymer must be taken to lie above those of metals. So the difference of resultant barrier height between polymer-metal (1), i.e. aluminium, is sufficiently higher than the effective barrier height of polymer-metal (2), i.e., Cu/Ag/Sn interfaces. Their difference will control the magnitude of current. Different lines are obtained for dissimilar electrode combinations. These observations are consistent with the proposed R-S mechanism and suggest that in the higher field regions, the conduction is governed by R-S effect in which the carriers are injected over the field dependent polymer electrode interfacial barrier. The increase in current with increasing metal work function has been interpreted to show that the hole injection is the dominant mechanism.

REFERENCES

1. Dayies, D.K., J. Phys. **D6**, 1017 (1973).
2. Wintle, H.J., J. Non Cryst. Solids **15**, 471 (1974).
3. Das Gupta, D.K. and Joyner, K., J. Phys. D. Appl. Phys. **9**, 829 (1976).
4. Thielen, A. et al. (I) & (II), J. Appl. Phys. **75**, 8 (1994).
5. Vanderschueren, J. and Linkens, A., J. Appl. Phys. **49**, 7 (1978).
6. Maiman, S. and Schacham, S.E., J. Appl. Phys. **75**, 4 (1994).
7. Murata, Y. and Koizumi, N., IEEE, Trans. Elect. Insul. **24**, 3, 449 (1989).
8. Ikeda, S. et al., J. Appl. Phys. **64**, 4, 2026 (1988).
9. Nagashima, H.N. and Farai, R.M., J. Appl. Phys. **75**, 5 (1994).
10. Leal Ferreira, G.F. and Morena, R.A., J. Appl. Phys. **75** (1991) 1.
11. Golden Blum, A. et al., J. Appl. Phys. **75**, 10 (1994).
12. Cole, K.S. and Cole, R.H., J. Chem. Phys. **90**, 341 (1941).
13. Oster, A., Z. Angew. Phys. **23**, 120 (1967).
14. Kosaki, M., Ohshima, H. and Ieda, M., J. Phys. Soc. Japan **4**, 1012 (1970).
15. Lengyel, G., J. Appl. Phys. **37**, 807 (1966).
16. Mann, H., J. Appl. Phys. **35**, 2173 (1964).
17. Vodenicharov, H., Vodenicharov, M. and Shopov, I., C. R. Acad. Bulg. Sci. **24**, 1939 (1971).
18. Caserta, G., Rispoli, B. and Serva, A., Phys. Stat. Sol. **35**, 237 (1969).
19. Patora, J., Piotrowski, J., Kryszewski, M. and Szymanski, A., J. Polym. Sci. Polym. Lett. **10**, 23 (1972).

20. Connell, R.A. and Gregor, L.V., J. Electrochem. Soc. **112**, 1198 (1965).
21. Kulshrestha, Y.K. and Srivastava, A.P., Thin Solid Films **69**, 269 (1980).
22. Pearson, J.A., Am. Chem. Soc. Polym. Prepr. **12**, 68 (1971).
23. Williams, D.J., Am. Chem. Soc. Polym. Prepr. **14**, 83 (1973).
24. Seanor, D.A., J. Polym. Sci. **A-2**, **6**, 463 (1968).
25. Gross, B., Charge Storage in Solid Dielectrics, Elsevier, Amsterdam (1964).
26. Scher, H., Photoconductivity and Related Phenomena, Am. Elsevier, New York (1976).
27. Gill, W.D., Amorphous and Liquid Semiconductors, Taylor and Francis, London (1974).
28. Enck, R. and Pfister, G., Photoconductivity and Related Phenomena, Am. Elsevier, New York (1976).
29. Burnett, G.M., North, A.M. and Sherwood, J.N., Transfer and Storage of Energy by Molecules, John Wiley, New York (1974).
30. Schottky, W., Z. Physik. **15**, 872 (1914).
31. Nordheim, L.K., Proc. Roy. Soc. **A121**, 626 (1928).
32. Lindmayer, J., J. Appl. Phys. **36**, 196 (1965).
33. Dasgupta, D.K. and Joyner, K., J. Phys. D. Appl. Phys. **9**, 829 (1976).
34. Lewis, T.J., "Polymer Surface", D.T. Clark, W.F. Feast, Willey, New York (1979).
35. Khare, P.K., Keller, J.M., Gaur, M.S., Singh, R. and Dutt, S., Polymer International **39**, 303 (1996).
36. Khare, P.K. and Singh Ranjeet, Polymer International **34**, 407 (1994).
37. Khare, P.K., Ph.D. Thesis, Saugor (1989).
38. Struik, L.C.E., Physical aging in amorphous polymers (Elsevier, Amsterdam) (1978).

CHAPTER VI

DIELECTRIC PROPERTIES
IN PURE
POLYVINYL PYRROLIDONE (PVP)
FOIL ELECTRETS

6.1 INTRODUCTION

The dielectric behaviour of polymeric films is of direct interest to both the basic studies of electrical conduction through such films and their applications in capacitors for micro-electronics. To obtain high values of capacitance, the dielectric constant should be high and the thickness be small. Due to the difficulty of obtaining structurally continuous and stable ultrathin films, capacitor applications are generally limited to thick films.

The evaluation of dielectric properties of insulator films [1-5] is carried out by measuring simultaneously the capacitance and the dissipation factor over a wide range of frequencies and temperatures. As all the other electrical parameters of dielectrics, the permittivity depends on the changeably external factors such as the frequency of voltage application, temperature, pressure, humidity, etc. In a number of cases, these dependences are of great practical importance.

Recently, dielectric properties of several polymers [6-12] polar and non-polar have been investigated. Some general relations between dielectric properties have been discussed, distinguishing between resonance phenomena that commonly occur in the optical region and relaxation phenomena which occur in polymers at the lower frequency regions. It has been shown how the real and imaginary parts of the complex dielectric constant are related. In nonpolar polymers, the

dielectric constant depends primarily on the density, but little is known regarding the nature of the dielectric loss. Attention has also been paid to polar polymers. After some preliminary remarks on the nature of dielectric dispersions, some phenomenological notions of dielectric dispersions have been considered. Attempts have been made to relate theory and practice. The topics, such as phase transitions, anisotropy and in homogeneity, have been dealt with.

Dielectric relaxations in polyvinylidene fluoride were studied by Sasabe *et al.* [8]. They observed three distinct absorption peaks (α_c , α_a and β) in the frequency range from 0.1 to 300 Hz in the temperature range -66 to 100°C. The α_c absorption is related to molecular motion in the crystalline region. The α_a absorption can be interpreted as due to the micro-Brownian motion of the amorphous main chains. The β absorption is attributed to local oscillations of the frozen main chains. Kakutani and Ashina [9] studied low-temperature absorption of polyvinyl chloride and concluded that β_1 and β_2 processes are the results of molecular motion in crystalline and amorphous regions of the polymer respectively. Low temperature dielectric relaxation in polyethylene and related hydrocarbon polymers was investigated by Phillips [13]. He uses a simple quantum mechanical model of relaxation process to explain the experimental results. According to this process, a particle in a double potential well tunnels from one well to the other with emission or absorption. Kulshrestha

and Srivastava [14] doped PS with choranyl and Srivastava et al [15] with copper phthalocyanine and observed interfacial polarisation in the measurement of dielectric losses of polymers.

Investigation of dielectric properties is also one of the most convenient and sensitive methods for studying polymer structure. It is, therefore, important that their dielectric behaviour is full understood. This involves complete knowledge of variation of the complex dielectric constant, i.e., capacitance and losses over a wide range of frequencies and temperatures. Whenever a dielectric is subjected to an electric field, dissipation of power depends on the voltage and frequency. These losses of power in a dielectric are commonly known as dielectric losses. Dielectric properties also depend on the type of substance polar or non-polar [16-18], temperature [19,20], frequency [21], structural changes [22], fields [23] and humidity [24].

Mechanism of dielectric properties is given in Chapter 3 together with last decade's work which reveals that no work has been done on dielectric properties of pure or doped PVP. Therefore, it is thought worthwhile to carry out investigations to understand the dielectric behaviour of polyvinyl pyrrolidone foils.

6.2 PRESENT INVESTIGATION

The present investigation is intended to get an insight into various molecular relaxation processes which occur in PVP under the influence of alternating field. This chapter describes the dielectric and loss variation of pure PVP foils as a function of frequency and temperature. Field is also one of the important parameters, particularly in case of polar polymers. Chatterji and Bhadra [25], McMohan [26], Elgard [27] and other [28,29] have observed isotropic increase in dielectric constant with field but no satisfactory interpretation has been given for this effect.

In the present investigation, attention has been paid to audio frequencies and temperature range (40-220°C). Frequency range selected is from 0.5 to 30 kHz.

6.3 FOIL PREPARATION

Foils of PVP (20 μm thick) are grown from solution, geometry of foil and electrode in sandwich configuration is same as described in Chapter II in detail. They are sandwiched between vacuum deposited electrodes of about 1.33 cm^2 .

6.4 EXPERIMENTAL PROCEDURE

The following procedure has been adopted to measure the dielectric properties of PVP foils as a function of frequency and temperature. The temperature of the sample is recorded

with the help of a copper-constantan thermo-couple placed close to the sample. A direct reading potentiometer has been used for the determination of thermo emf. Before starting the measurements, the samples are allowed to attain the equilibrium temperature for a sufficiently long time. The oscillator has been set for the desired frequency and the null detector is tuned to it. The bridge balance has been done by repeated adjustment of capacity selector, capacity and dissipation knobs till the null detector indicated the least deflection. The oscillator then has been set for the next frequency and the bridge has been again balanced in a similar manner. After covering the entire frequency range, the temperature is changed and the measurements have been repeated over the entire frequency range and so on. Two loss maxima at ~ 90 and $\sim 180^{\circ}\text{C}$ are observed.

6.5 RESULTS AND DISCUSSION

Dielectric properties of polymers are investigated by measuring simultaneously the capacitance and the loss factor at regularly varying temperatures and frequencies. Figs. 6.1-6.7 show the capacitance as a function of temperature at fixed frequencies of 0.5, 2, 10, 15, 20 and 30 kHz for different electrode configurations of Al-Al, Ag-Ag, Cu-Cu, Sn-Sn, Al-Ag, Al-Cu and Al-Sn, respectively for pure polyvinyl pyrrolidone foils, 20 μm thick. As the temperature is increased, the capacitances of pure foils are increased. This

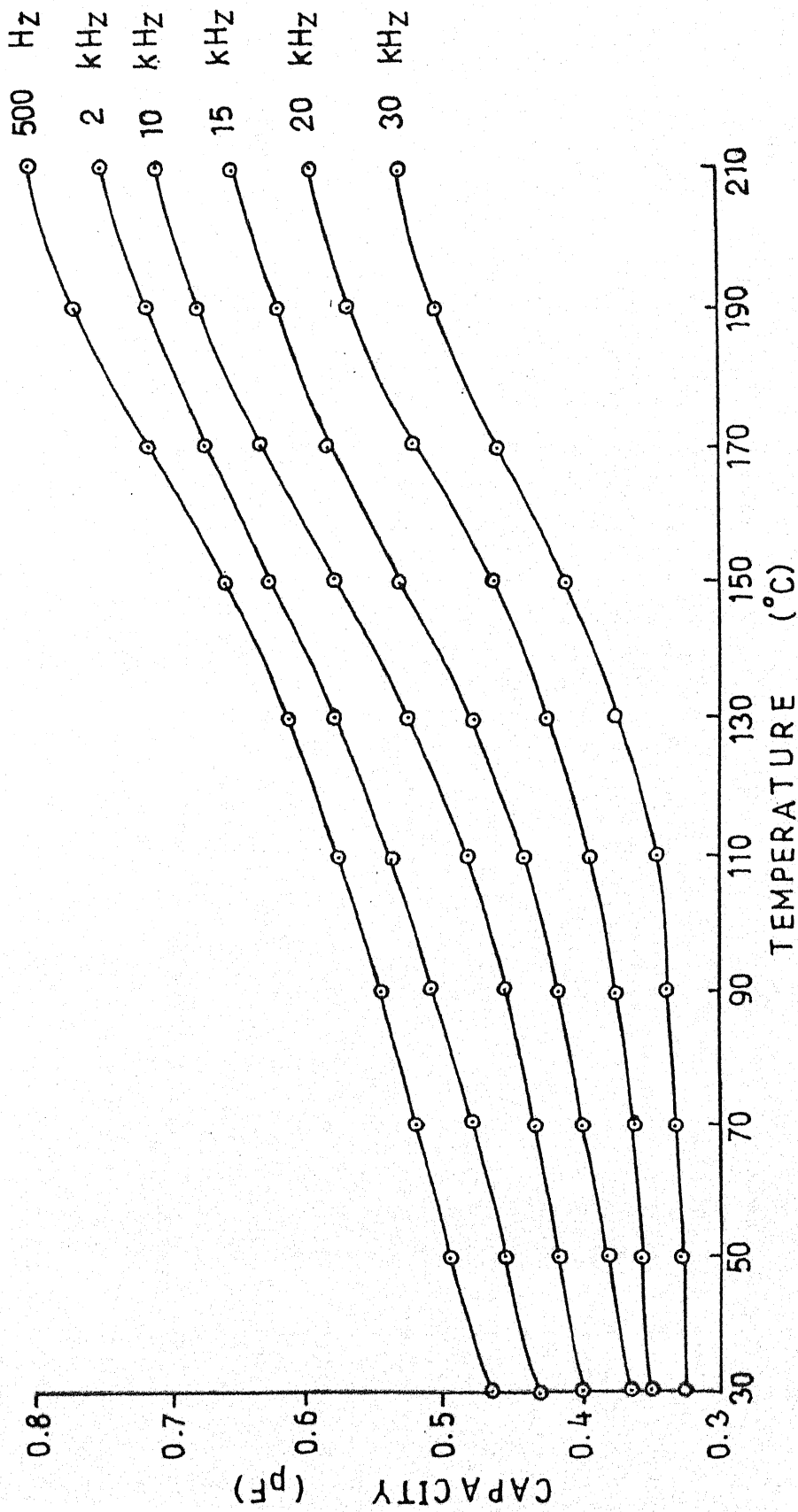


Fig.6.1 Variation of capacity with temperature at different constant frequencies for Al-Al System.

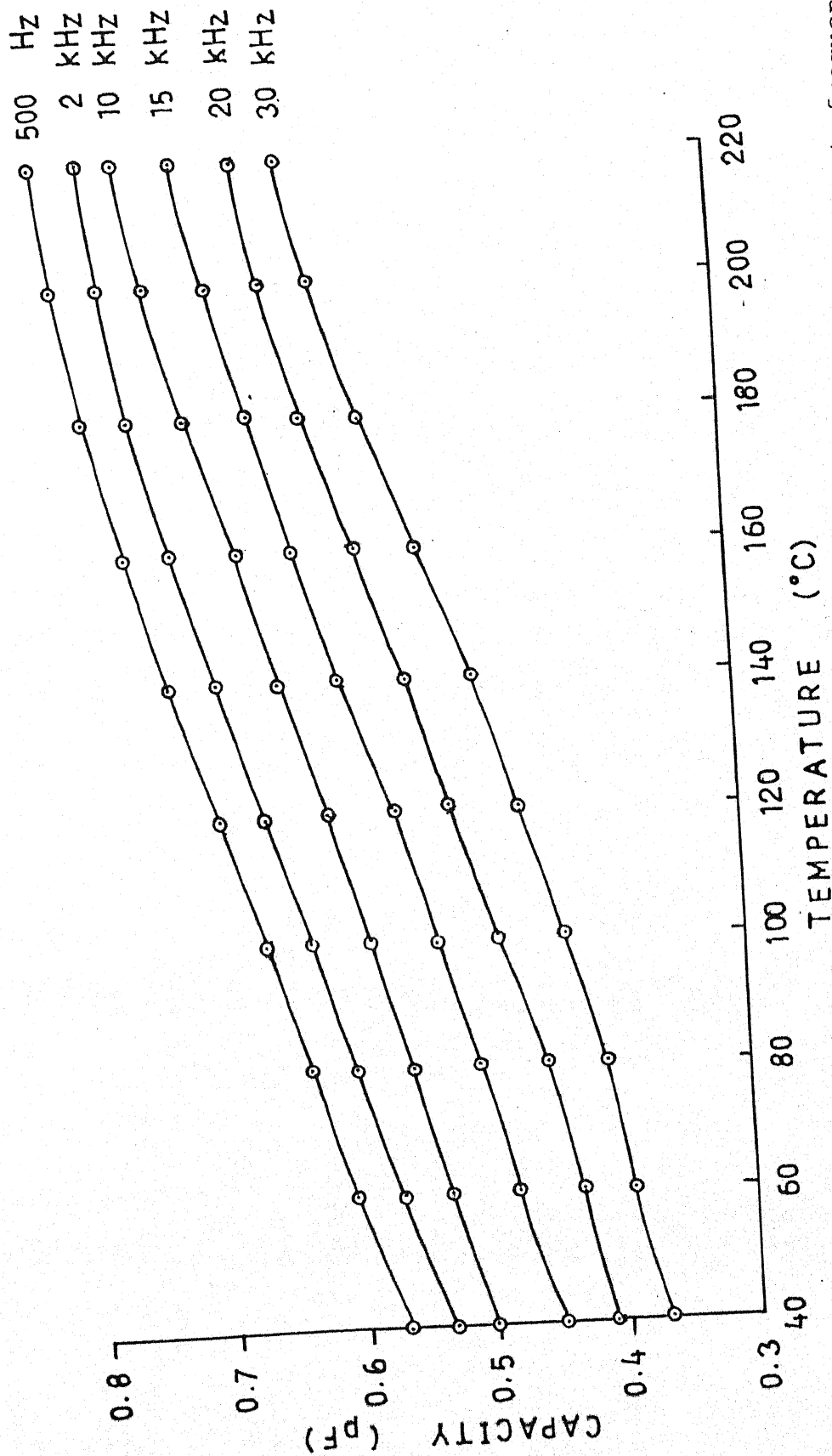


Fig.6.2 Variation of capacity with temperature at different constant frequencies for Ag-Ag System.

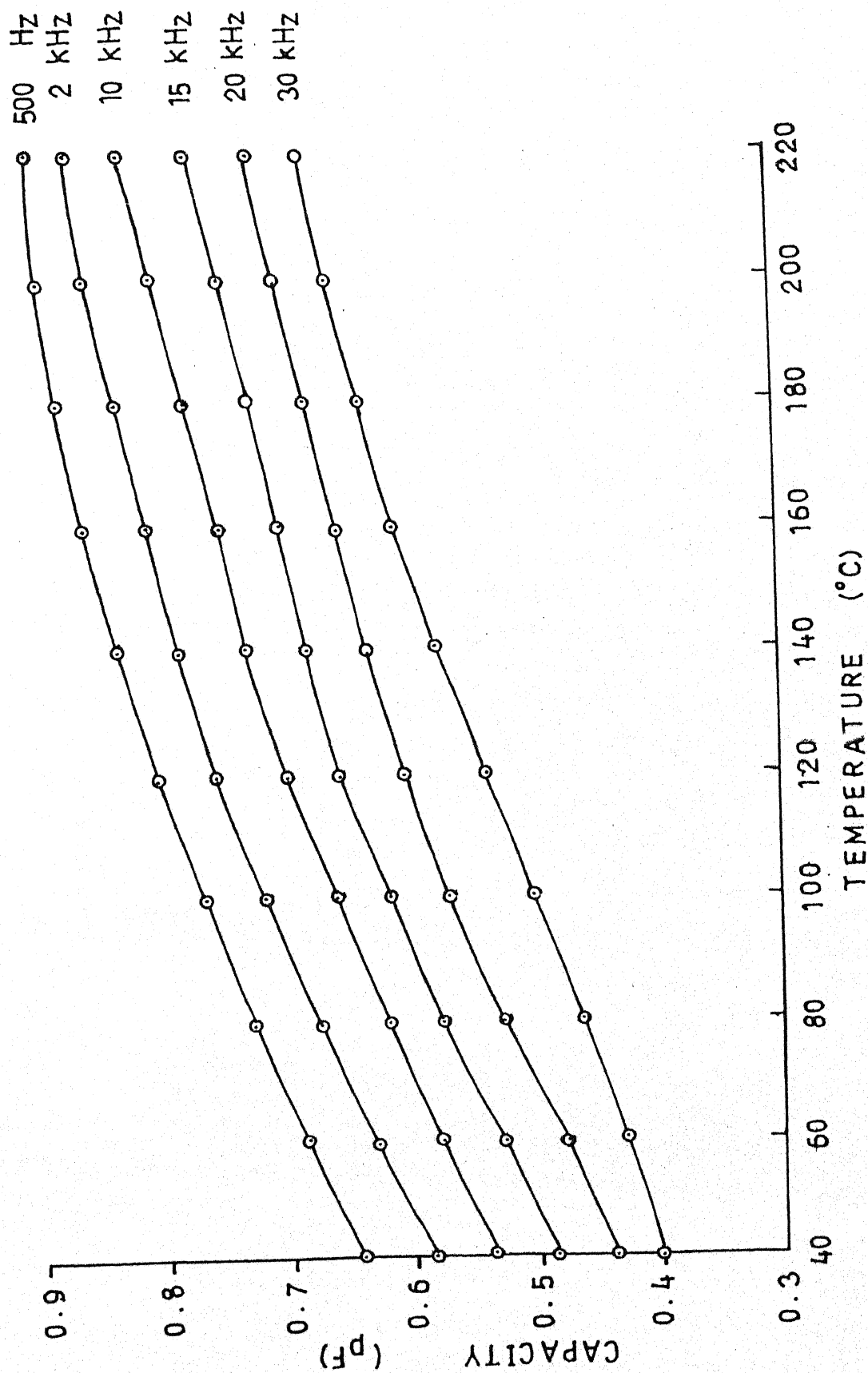


Fig.6.3 Variation of capacity with temperature at different constant frequencies for Cu-Cu System.

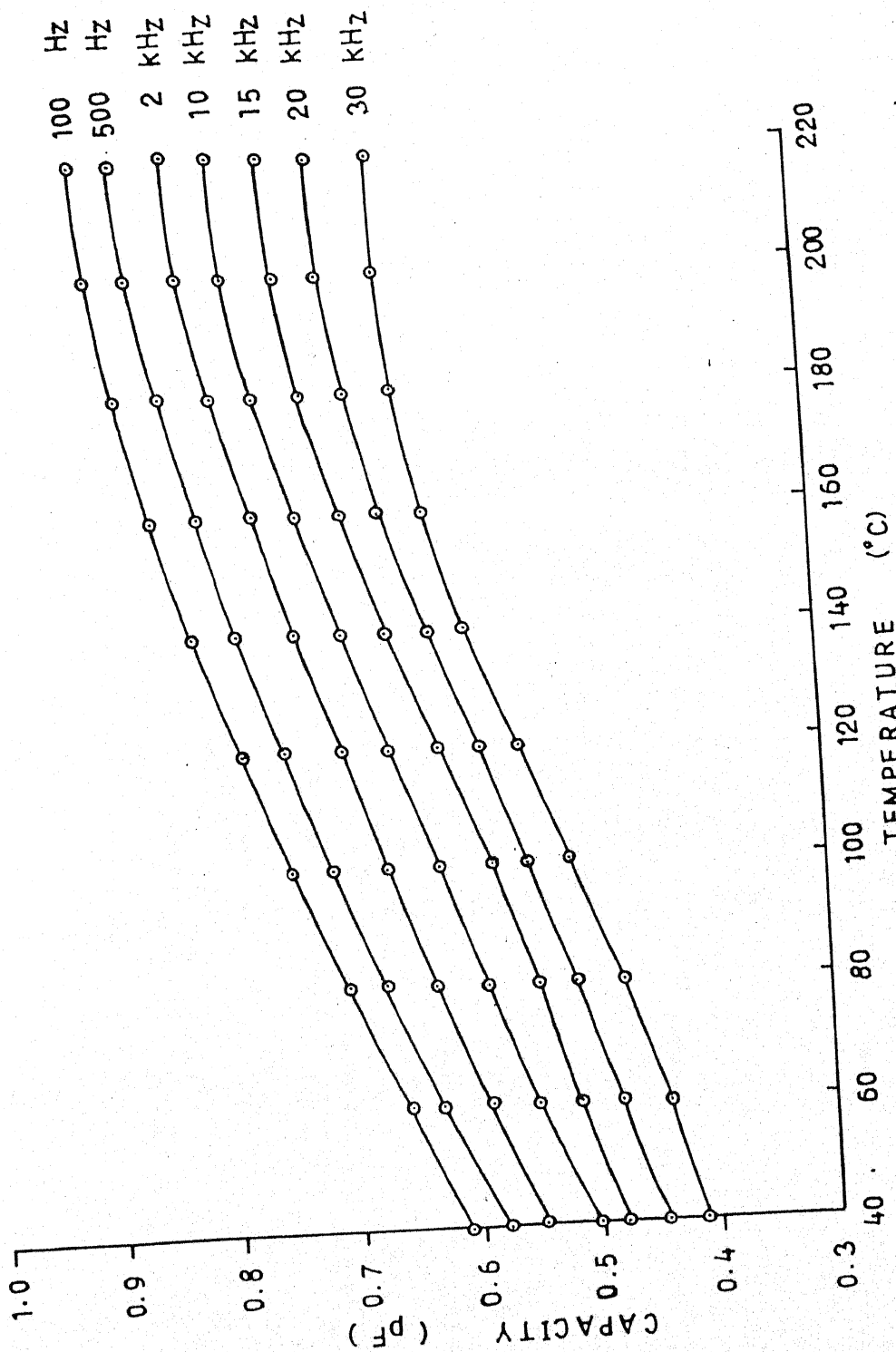


Fig.6.4 Variation of capacity with temperature at different constant frequencies for Sn-Sn system.

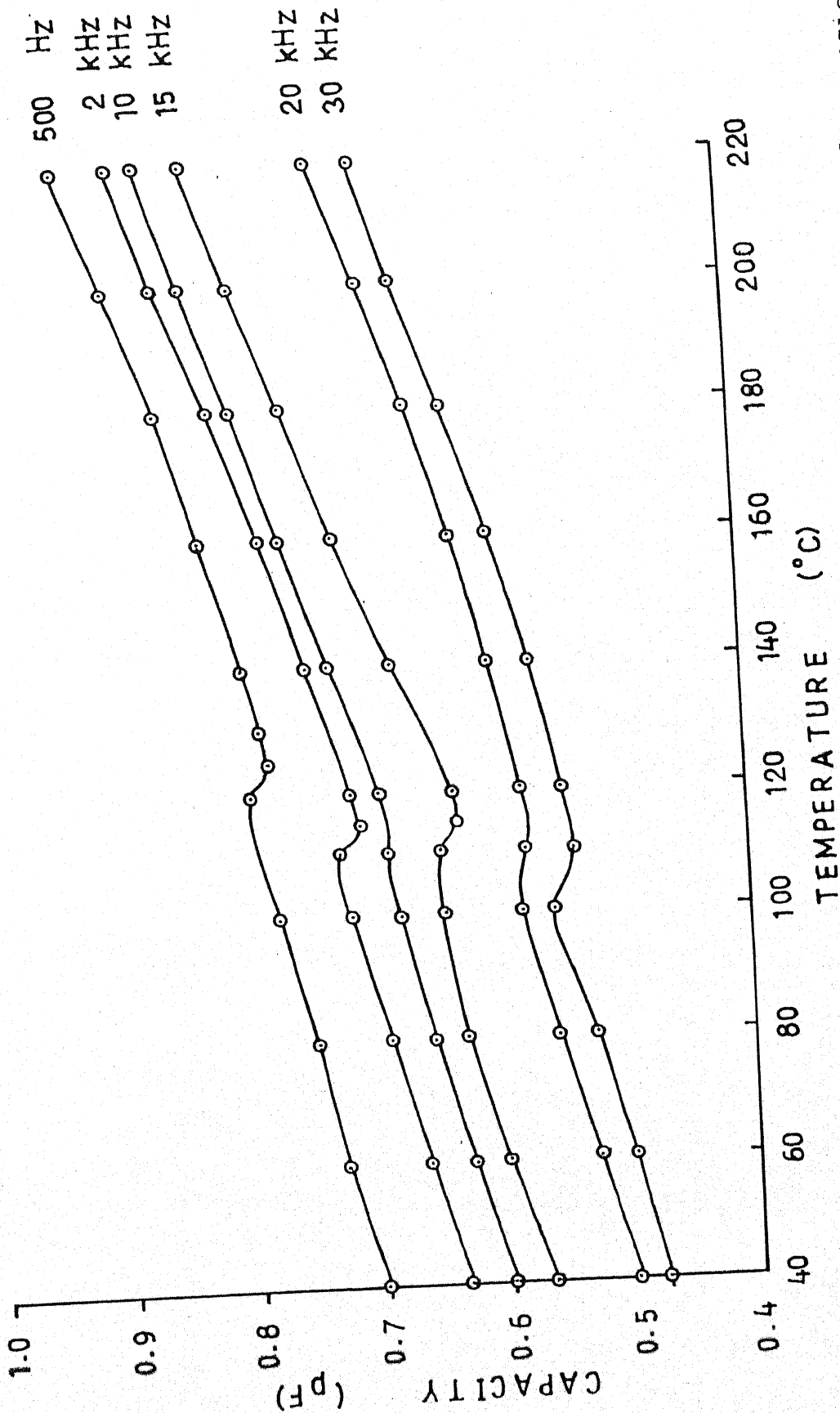


Fig.6.5 Variation of capacity with temperature at different constant frequencies for Al-Ag syst.

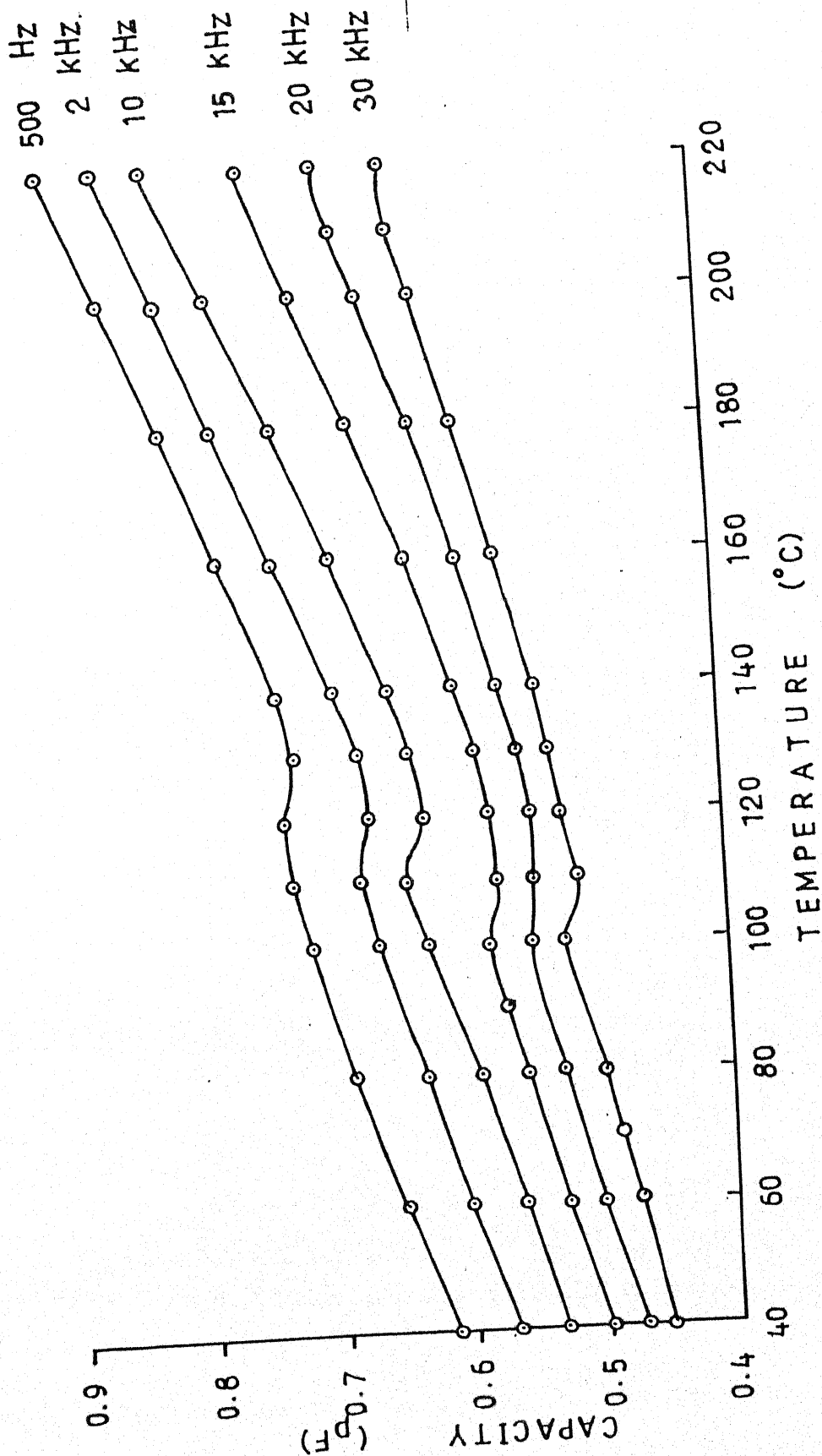


Fig.6.6 Variation of capacity with temperature at different constant frequencies for Al-Cu System.

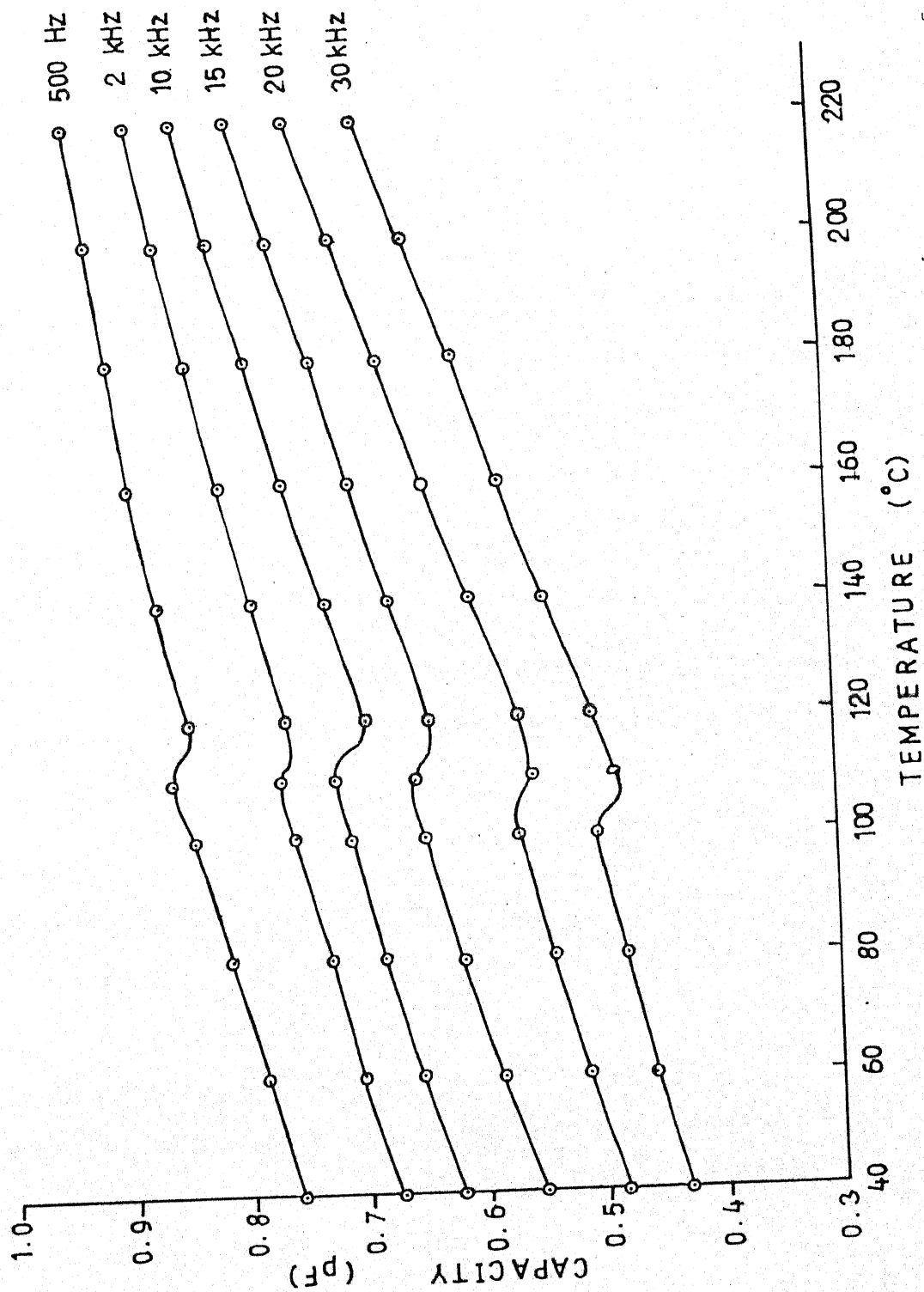


Fig.6.7

Variation of capacity with temperature at different constant frequencies for Al-Sn System.

increase in capacitance is less in the temperature range 30-90°C than the corresponding one in the temperature range 90-210°C. Thus, it may be inferred that increase in capacitance is more above its glass transition temperature T_g (~100°C). This behaviour is found to be same for all similar electrodes configurations. However, in case of dissimilar electrode combinations, in general, a peak is found ~ 105±5°C and remaining variations are the same, as found in case of similar electrode systems. The capacitance is found to be maximum for lowest frequency of measurement and then decreases with the increase of frequency and assumes a minimum value at the highest frequency, at all the temperatures. The rate of fall of capacitance with frequency is largest at the highest temperature and as temperature is decreased, this rate of fall, also decreases almost for all electrode configurations.

Figs. 6.8-6.14 exhibit the variation of loss factor with temperature at different fixed frequencies 0.5, 2, 10, 20 and 30 kHz for different electrode configurations, as mentioned above, for pure polyvinyl pyrrolidone foils of same thickness. All the curves show two loss maxima, one below the glass transition temperature T_g (~100°C) and one above. Lower temperature loss maxima occur at 90±10°C while higher temperature loss maxima occur at 180±10°C, and are designated as α and ρ peaks, respectively. Both the loss maxima shifts to lower temperature as the frequency is decreased. Both the maxima show nearly same amount of shift. Beyond 190°C, the

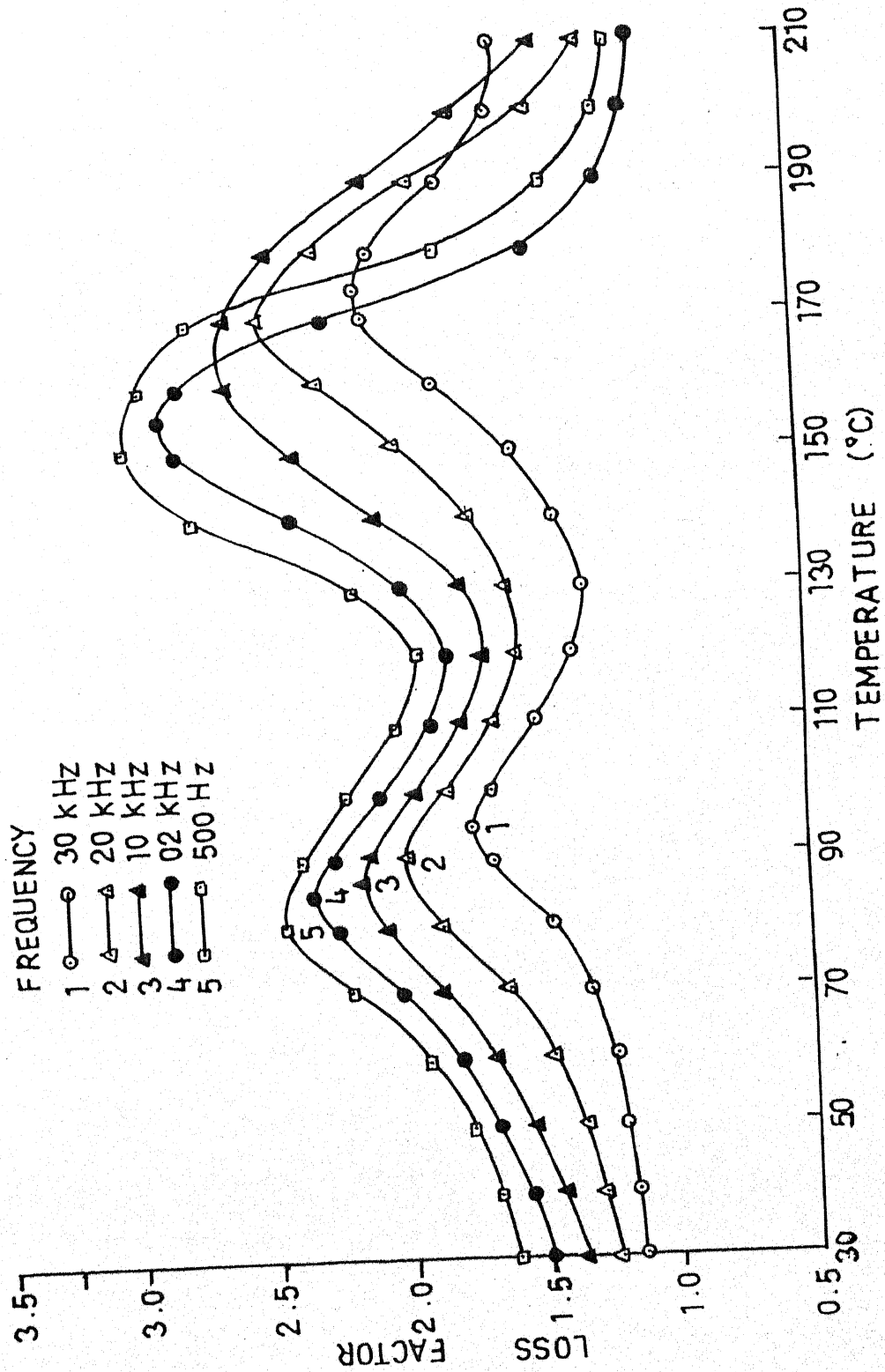


Fig.6.8 Variation of Loss factor with temperatures at different frequencies with Al-Al System.

constant

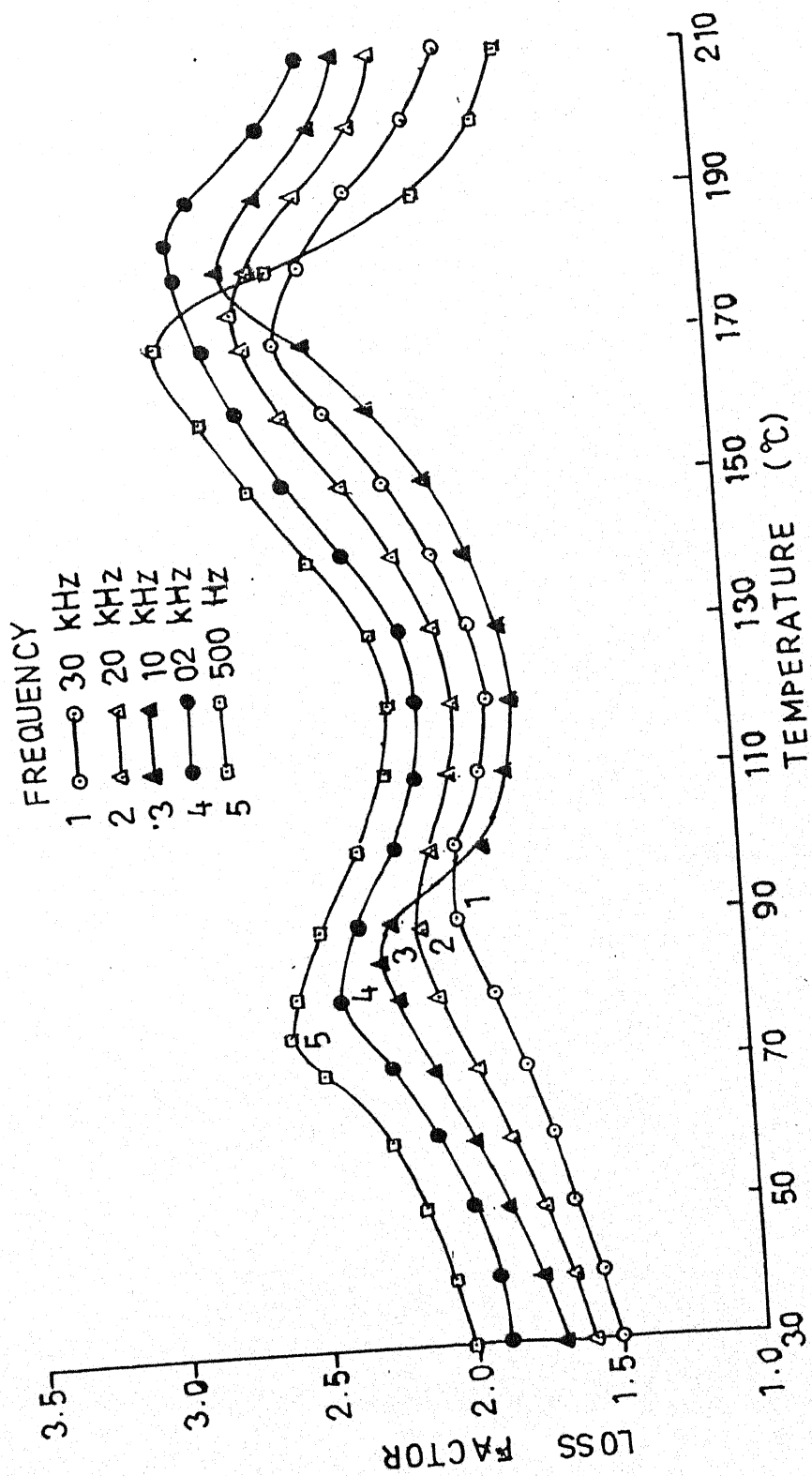


Fig.6.9 Variation of Loss factor with temperatures at different constant frequencies with Ag-Ag System.

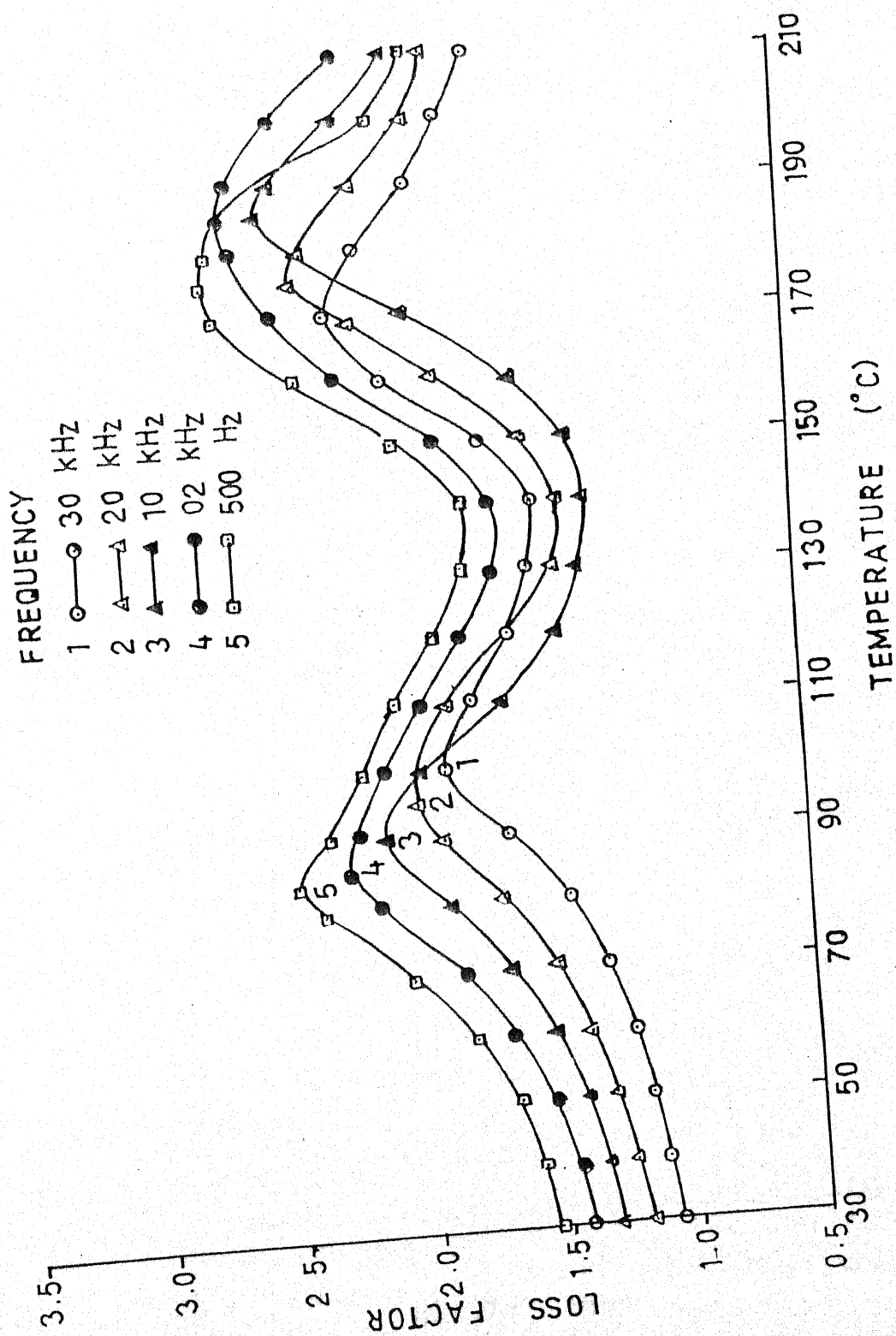


Fig.6.10 Variation of Loss factor with temperatures at different constant frequencies with Cu-Cu System.

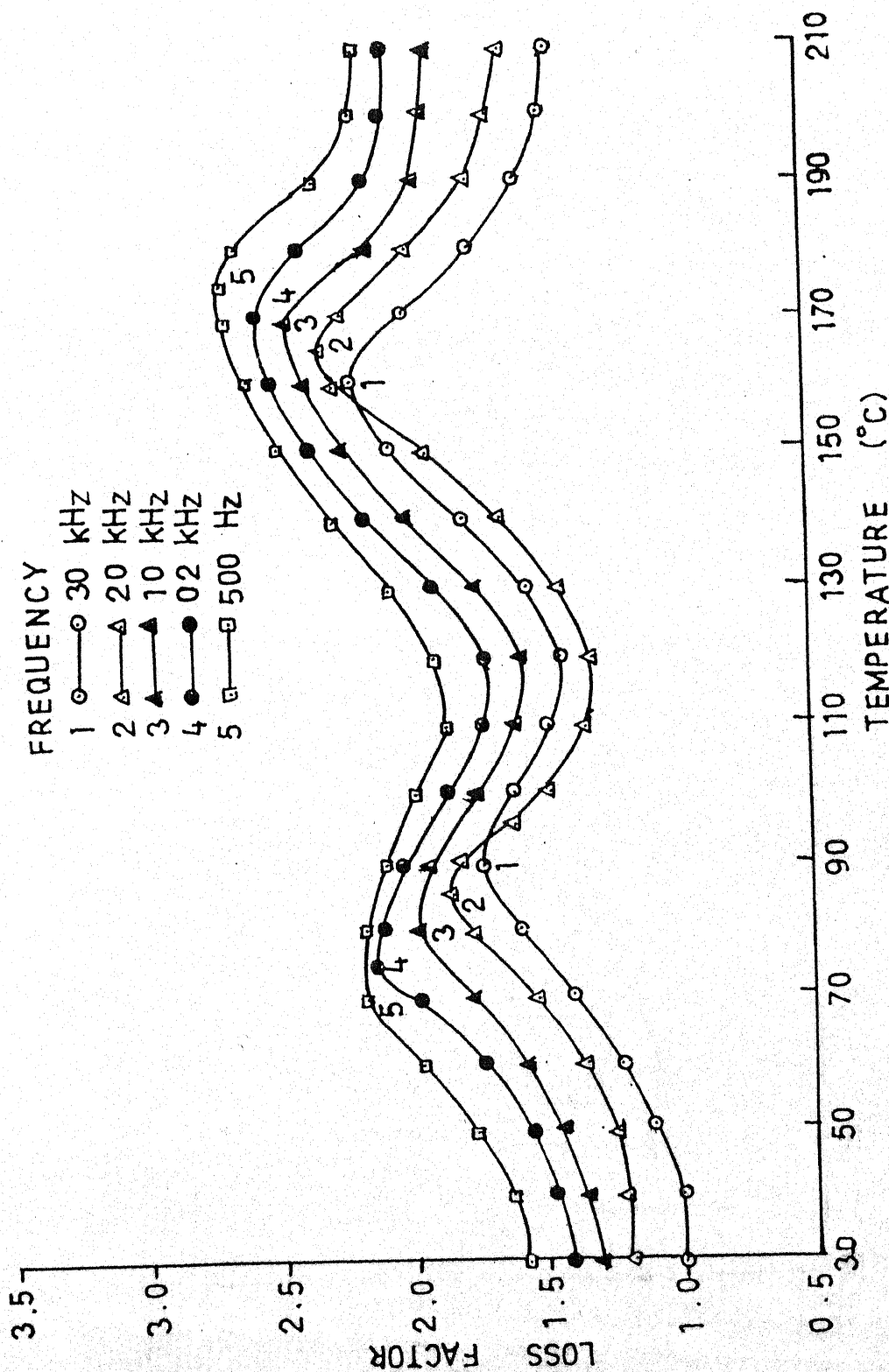


Fig.6.11 Variation of Loss factor with temperatures at different constant frequencies with Sn-Sn System.

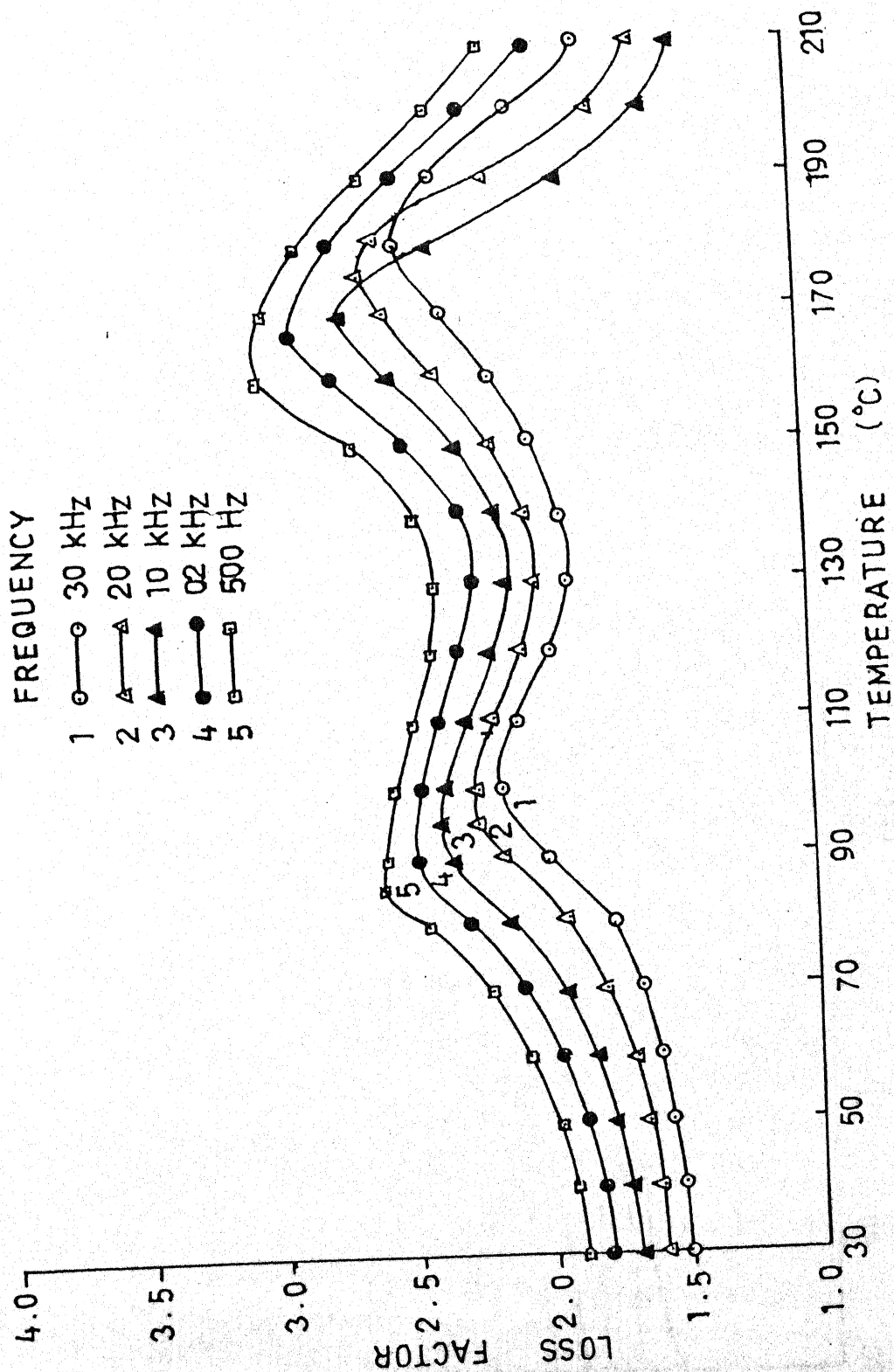


Fig.6.12 Variation of Loss factor with temperatures at different constant frequencies with Al-Ag System.

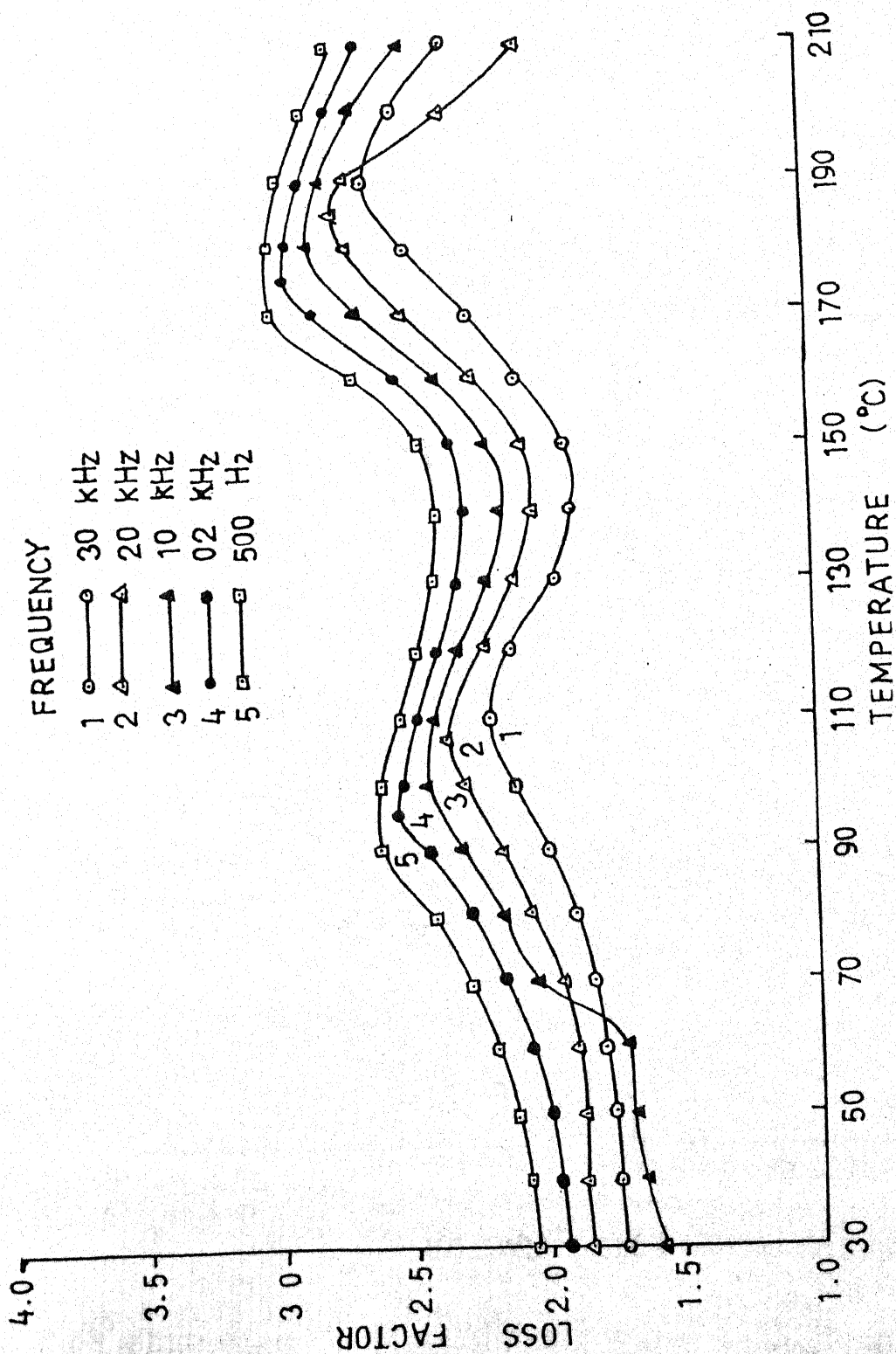


Fig.6.13 Variation of Loss factor with temperatures at different constant frequencies with Al-Cu System.

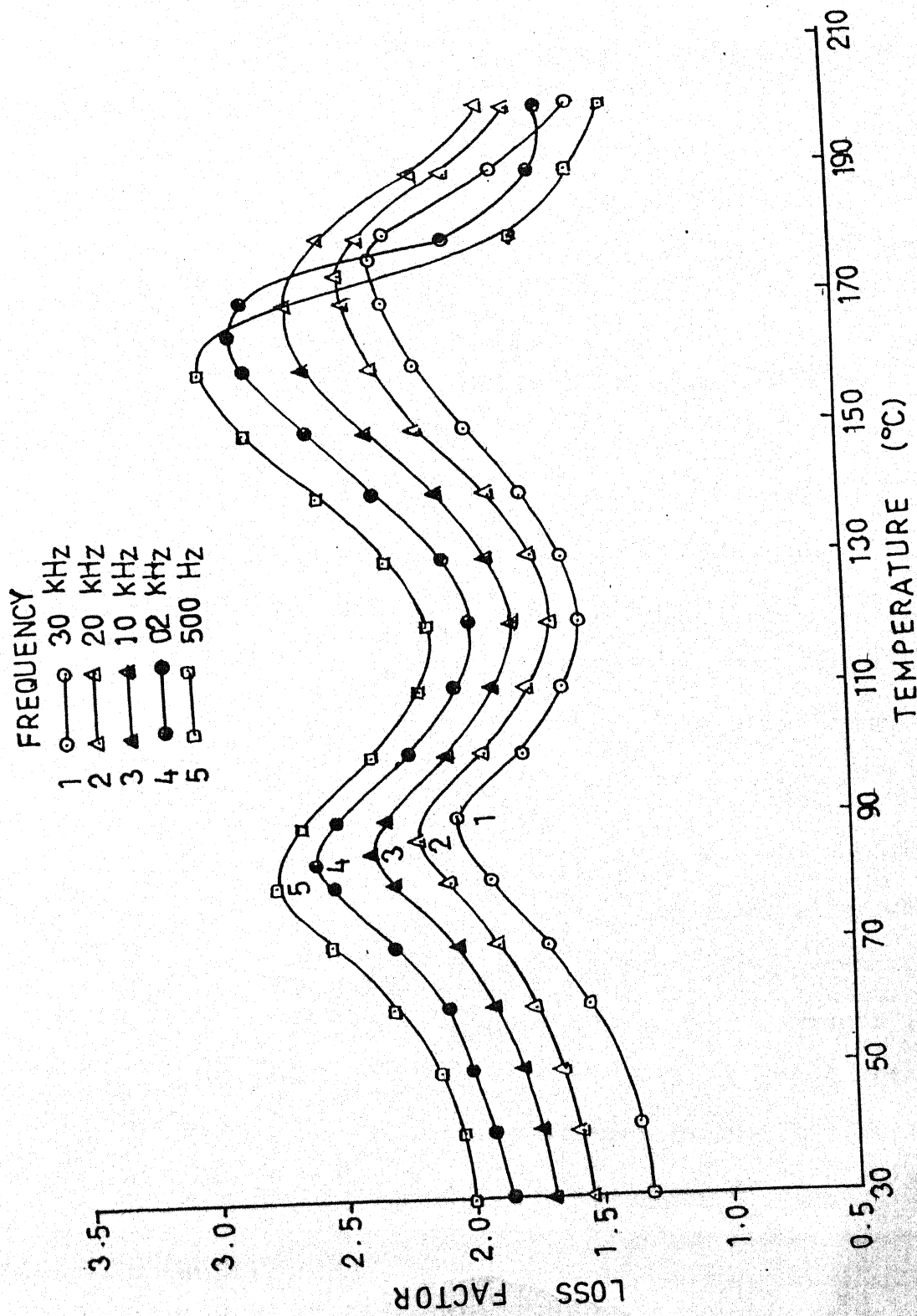


Fig.6.14 Variation of Loss factor with temperatures at different constant frequencies with Al-Sn System.

decrease in loss factor with temperature for the PVP foil is more pronounced. All thermograms, also show an increase in magnitude of both loss maxima, with the decrease in frequency. However, magnitude of ρ loss maxima is more than for α loss maxima.

Permittivity is the basic parameter of a dielectric describing its properties from the view point of the processes of its polarisation or propagation of electromagnetic waves in it, or more generally from the point of view of the processes of its interaction with an electric field. Permittivity is a microscopic parameter of a dielectric which reflects the properties of a given substance in a sufficiently large volume but not the properties of the separate atoms and molecules in the substance. There are three well known types of polarisations : electronic, ionic and dipole polarisation.

Electronic polarisation is the displacement of electrons with respect to the atomic nucleus, precisely - displacement under the action of an external field of the orbits in which negatively charged electrons move around a positively charged nucleus. This type of polarisation occurs in all atoms or ions and can be observed in all dielectrics irrespective of whether other types of polarisation are displaced in the dielectric. One specific feature of electronic polarisation is the fact that when an external field is superposed, this type of polarisation occurs during a very short interval of time (of the order of 10^{-15} s).

Ionic polarisation is the mutual displacement of ions forming a heteropolar (ionic) molecule. A shorter time is required for the process of ionic polarisation to set in, but it is longer than that for electronic polarisation, i.e., 10^{-12} s. On the whole, the process of electronic and ionic polarisation is much in common. Both phenomena may be regarded as the varieties of polarisation caused by deformation which is a displacement of charges with respect to each other, in the direction of the field. Apart from a very high velocity mentioned above, with which the state of polarisation sets in, it is important to bear in mind that the process of deformational polarisation is practically unaffected by the temperature of the dielectric. The electric energy required to polarise a molecule is completely returned to the energy sources after voltage is removed. For this reason, deformational polarisation does not entail any dielectric losses.

Polar dielectrics [30-32] exhibit a tendency towards dipole or orientational polarisation. The essence of this kind of polarisation can be reduced in a simplified manner, as has been first suggested by Debye, to the rotation of the molecules of a polar dielectric having a constant dipole moment in the direction of a field. If orientational polarisation is considered more strictly, it must be understood as the introduction by an electric field of a certain orderliness in the position of polar molecules being

in uninterrupted chaotic 'thermal' motion, and not as a direct rotation of polar molecules under the action of a field. For this reason, dipole polarisation is connected by its nature with the thermal motion of molecule, and temperature must exert an appreciable effect on the phenomenon of dipole polarisation.

After a dielectric is energised, the process establishing a dipole polarisation requires a relatively long time as compared with that of practically almost inertialess phenomena of deformational polarisation. As distinct from deformational polarisation, dipole polarisation and also other kinds of relaxation polarisation dissipate electric energy which transforms into heat in a dielectric, i.e. this energy causes dielectric losses.

In polymer, the dielectric loss behaviour may be attributed to the deformation of polymer chains [33-35]. The molecular flexibility of the chains are responsible for this characteristic property of the polymers. The other important mechanism for the dielectric losses in the polymers is considered to be the internal motions or the local movements of the molecular chains of the polymer. At high temperatures, especially at the glass transition temperature of the polymer such segmental motions are prominent. However, at low temperatures, these motions become less significant.

6.5-1 FREQUENCY DEPENDENCE OF CAPACITANCE

The capacitance and hence the dielectric constant of PVP foils decreases with the increase in frequency (Figs.6.1-6.7). This is so because the polarisation settles itself during a very short period of time. Dielectric constant of non-polar polymers remains invariable with frequency. In case of polar polymers like PVP, the dielectric constant begins to drop at a certain critical frequency and at very high frequencies it approaches the values typical of non-polar polymers. In amorphous polymers, structural polarisation is also possible. For this type of polarisation, the capacitance falls with the increase in frequency [36]. However, this behaviour can also be explained in the following manner.

Decrease of capacitance with frequency may be due to the failure of dipoles to settle themselves completely during the short time of one half period of applied voltage. This sort of polarisation like orientational component, atomic component, etc. further drops the value of capacitance. In our present investigation, we have observed a considerable change in capacitance value as expected in polar polymers. The dependence of capacitance on frequency is given by :

$$C = C_g + \frac{S\tau}{1 + \omega^2\tau^2}$$

where C_g is the geometrical capacitance.

It is obvious from the above equation that capacitance reaches its maximum width $W = 0$ (direct voltage) and is minimum when $W = \infty$.

6.5-2 TEMPERATURE DEPENDENCE OF CAPACITANCE

Whenever a dielectric is heated or energy is supplied in the form of heat, there is expansion of lattice. The ratio of the number of molecules to the effective length of dielectric diminishes when the temperature increases. As a result of this, the capacitance and hence dielectric constant should decrease but because of presence of dipoles in case of polar polymers like PVP, permittivity changes its behaviour. At the lower temperatures, the dipoles remains almost frozen in and are unable to orient themselves [38]. When the temperature is raised, the orientation of dipoles gets facilitated, which increases the permittivity. The increase in capacitance and dielectric constant with temperature may be partly due to ionic mechanism of polarisation.

6.5-3 ELECTRODE MATERIAL DEPENDENCE OF CAPACITANCE

Electrode material show marked dependence of permittivity (capacity). It is found that with Al-Ag/Cu/Sn combinations, permittivity is enhanced in lower temperature region at all frequencies, as compared to Al-Al/Cu-Cu/Ag-Ag/Sn-Sn system. This enhancement of permittivity is followed by a maximum at -100°C with Al-Ag/Cu/Sn combinations. Rise of

permittivity at a particular temperature may be due to maximum orientation of dipoles and then fall in permittivity value is because of loss of oriented dipoles as temperature further increases.

6.5-4 VARIATION IN LOSS FACTOR

In case of polar polymers like polyvinyl pyrrolidone, loss values depend strongly on temperature [39]. Two loss maxima are observed (Figs. 6.8-6.14). The first type of dielectric loss called dipole-segmental, is associated with orientation/rotation of the polar units of the macromolecule under conditions where segmental movement is possible, i.e., in the rubber-like state ($> T_g$) of the polymer. The second type - called dipole group is due to orientation of the polar groups themselves. Losses of this kind may also occur below the T_g , i.e., in the glassy state and above T_g , i.e., rubber like state. First loss maxima occur at $90 \pm 10^\circ\text{C}$ and the second loss maxima at $180 \pm 10^\circ\text{C}$. Incidentally, two current peaks have also been reported in Chapter IV of thermally stimulated discharge current studies with Al-Al electrode system, their location is also comparable.

Therefore, two loss maxima have been anticipated in the dielectric thermograms of PVP, since the dielectric properties are associated with the molecular relaxation modes of a system. Polymer is supposed to be a mixture of crystalline and amorphous phase. In crystalline region, the molecules

(dipoles) are bound with equilibrium position to the other. In the amorphous region the dipoles associated with one equilibrium position to another equilibrium position, can orient rather easily. The α relaxation process may be due to micro-Brownian motion in PVP which results in the orientation of dipoles due to the motion of main chain in PVP [40].

The polymer foils grown by solution technique, is a mixture of crystalline and amorphous regions. Due to amorphous nature, Vander Wall's force is weak and binding force is less. This facilitates the movements of segments. In the present investigation, ρ maxima occur at $180 \pm 10^\circ\text{C}$, which is slightly above T_g of PVP. Andrews and Kimmel [41,42] have discussed a high temperature transition in poly acrylonitrile which lies above its T_g . Therefore, ρ relaxation process in PVP foils may be attributed to the motion of the more mobil molecular chains in which the intermolecular forces between the crystalline regions are weakened due to thermally activated process. This weakening of forces causes the motion of the entire molecular chain and hence, the occurrence of ρ -relaxation.

REFERENCES

1. Cummins, S.E. and Cross, L.E., Appl. Phys. Lett. **10**, 14 (1967).
2. Cummins, S.E. and Cross, L.E., J. Appl. Phys. **30**, 2268 (1968).
3. Cross, L.E. and Pohanka, R.C., J. Appl. Phys. **39**, 3992 (1968).
4. Pulvari, C.F., Proc. Intern. Mtg. Ferroelectricity **1**, 347 (1966).
5. Kranjnik, N.N. et al., Fiz. Tverd. Tela **10**, 260 (1968).
6. Kawamura, Y., Nagai, S., Hirose, J. and Wada, Y., J. Polym. Sci. Pt. A-2 Polym. Phys. **7**, 1559 (1969).
7. Knizhnik, E.I., Mamchich, C.D. and Vyrokomolek, Soed. **11**, 1665 (1969).
8. Sasabe, H., Saito, S., Asahina, M. and Kakutani, H., J. Polym. Sci. Pt. A-2, Polym. Phys. **7**, 1405 (1969).
9. Kakutani, H. and Asahina, M., J. Polym. Sci. Pt. A-2 Polym. Phys. **7**, 1473 (1969).
10. Link, I.G.L., Dielectric Properties of Polymers, Volume 2, North Holland Publ. Co., Amsterdam (1972).
11. Aschcraft, C.R. and Boyd, R.H., J. Polym. Sci. Polym. Phys. Ed. **14**, 2153 (1976).
12. Pochan, J.M. and Hinman, D.F., J. Polym. Sci. Polym. Phys. Ed. **14**, 2285 (1976).
13. Philips, W.A., Proc. Res. Soc. **319**, 565 (1970).
14. Kulshrestha, Y.K. and Srivastava, A.P., Thin Solid Films **71**, (1980).
15. Srivastava, S.K. et al., Ind. J. Pure & Appl. Phys. **19**, 953 (1981).
16. Heston, W.M. and Symth, C.P., J. Am. Soc. **72**, 99 (1950).
17. Whiffen, D.H., Trans. Farad. Soc. **46**, 124 (1950).
18. Vonhippel, A.R., M.I.T. Vol. 1 (1944).
19. Sawaguchi, E. et al. J. Phys. Soc. Japan **17**, 1660 (1962).

20. Beans, W.R., Electronics of Solids, McGraw Hill Book Co., NY, 386 (1965).
21. Frohlich, H., 'Theory of Dielectrics', Clarendon Press, Oxford (1949).
22. Srivastava, S.K. et al., Indian J. Pure Appl. Phys. **19**, 935 (1981).
23. Chatterji, S.D. and Bhadra, T.C., Phys. Rev. **98**, 1728 (1955).
24. Bhargava, B., Ph.D. Thesis, University of Saugor, Saugor (1970).
25. Chatterji et al., Phys. Rev. **98**, 1728 (1955).
26. McMohan, W., J. Am. Chem. Soc. **14**, 3290 (1956).
27. Elgard, A.M., Fiz. Tverd. Tela **4**, 1320 (1962).
28. Lal, H.B., Indian J. Pure Appl. Phys. **7**, 370 (1969).
29. Kittle, C., 'Introduction to Solid State Phys', 2nd edn., John (1956).
30. Bucher, C.A., Polymers : Their structure and dielectric properties, 133rd meeting Electrochem. Soc., Boston, p.8 (1968).
31. Guicking, D. and Suss, K.J., Z. Angew. Phys. **28**, 238 (1970).
32. Kakutani, H., J. Polym. Sci. A-2, **8**, 1177 (1970).
33. Tanaka, A. and Ishida, Y., J. Polym. Sci. A-2, **8**, 1585 (1970).
34. Gibbs, D.F. and Jones, B.W., Brit. J. Appl. Phys. **3**, 157 (1970).
35. Cook, M. and Watts, D.C., Trans. Faraday Soc. **66**, 2503 (1970).
36. Knauss, C.J. and Smith, P.S., J. Polym. Sci. B-10, 737 (1972).
37. Schlosser, E. and Ranbach, H., Plaste and Kantsch (Germany) **24**, 182 (1977).
38. Ito, M. and Naktani, S. et al., J. Polym. Sci. Polym. Phys. Ed. **15**, 605 (1977).

9. Tareev, B., 'Physics of Dielectric Materials', Mir Pub., Moscow (1975).
10. Mahendru, P.C. and Jain, K. et al., J. Phys. D. Appl. Phys., 9 (1976).
11. Andrews, R.D. and Kimmel, R.M., J. Polym. Sc. Pl. B.3, 167 (1965).
12. Andrews, R.D., J. Polym. Sc. Pt. C14, 261 (1966).

CHAPTER VII

REVIEW AND CORRELATION OF THE RESULTS

7.1 REVIEW AND CORRELATION

Charge storage and polarization phenomena in dielectrics can be associated with two types of effects. A frozen-in polarization or trapped charges can either induce internal effects or create an external electric field. In the first case, the physical properties of the material can be modified leading, for instance, to piezoelectricity or to non linear effects. In the second case, an external electric field of large magnitude can be created.

As far as the internal effects are concerned, many attempts have been made to take advantage of the useful mechanical properties of the polymers, such as their low acoustical impedance, their flexibility, and the possibility to have them in large lateral or long linear dimensions. Piezoelectric polymers have found many applications, but still at a very reduced level. New developments are now being made in electro-optics and the potential here seems to be quite large.

As far as electrets which create an external field are concerned, large scale applications have already been developed; the main one being in the field of condensor microphones. Various types of sensors are also being studied out of the acoustical frequency range, for instance to produce or detect ultrasonic waves.

The interpretation of electrical charge storage and transport behaviour of polymers is not an easy task. There are at least two main difficulties :

- (i) Our knowledge about the energy band model of a real insulator is very small [1,2]. Polymers are characterized by very long chains formed of typical 10^3 - 10^5 strongly covalently bonded monomer molecules, each with their own electronic state. Consequently, it is difficult to approach the metal-polymer contact. To explain very large values of dielectric permittivity measured at low frequencies and/or high temperatures or the thermally stimulated depolarization current sign change, the contact is considered blocking [3]. Other results show that for many polymers the current voltage characteristic is independent of the electrode metal work function [4,5].
- (ii) On the other hand, dipolar charge and space charge coexist in the insulator and little experimental information can be obtained about the behaviour of each of the two charge types. The current in phase with the field called the conduction current leads as well to the space charge accumulation in the sample [6]. This charge, in turn, opposes the current flow and makes the interpretation of experimental results more difficult.

The specifications of the electrets required for in various applications are quite different. Therefore, a proper knowledge of charge storage and transport behaviour of materials is very important. A number of techniques have been employed to investigate the charge storage, transport and release from metal-polymer-metal structures. It has been found that a suitable combination of isothermal and non-isothermal techniques can be useful for consistent interpretation of charge storage behaviour in polymers. Various authors [7] have studied transient charging and discharging currents in combination with short circuit TSC measurements. Most polymers possess both surface as well as bulk traps. Unfortunately, both transient current and short circuit TSDC measurements do not, however, readily reveal the existence of surface traps and yield only limited information about the bulk traps. Further, distinction between excess charge decay by SCL drift and diffusion and by ohmic conduction cannot be made on the basis of short circuit TSDC measurements alone. More information can be obtained by employing the above two measurements in conjunction with the open circuit TSDC measurements of specimen. Much importance has been attached on the double layered films, in recent years, on the ground that there exists a possibility to adjust polarization distribution by adjusting the thickness of the films which is very meaningful for the applications [8].

thermally stimulated discharge current measurements, transient current measurements in charging and discharging modes, studies on steady state electrical conduction and dielectric properties have been, therefore, undertaken to provide information about polarisation and various relaxations occurring in polyvinyl pyrrolidone foil electrets.

With the view to present a unified picture of the various findings, we here review the various important results of the present investigation.

To determine the mechanisms responsible for polarisation in polyvinyl pyrrolidone foil electrets, an extensive study of sort circuit thermally stimulated depolarisation current measurements are made. It is observed that, in general, depolarisation current flows in the positive direction (as normally) corresponds to hetero charge for the samples polarised at lower temperatures with low fields. However, for higher polarising temperatures and higher fields, the observed currents becomes higher. Most of the thermograms are characterised by several peaks. Various peaks are considered to be located in three temperature intervals. In the temperature interval of 70-90°C, one peak is seen; a well resolved peak is observed around 160-170°C and a high temperature peak is found between 195-205°C. It is well established by Khare et al. [9-12] that three relaxation

been attributed to the molecular motion under the effect of external field. The ρ process is associated with the relaxations of permanent dipoles/orientation, of the main chain from polarised state to their equilibrium state, usually with large values of activation energy whereas the α process, having relatively small energy is due to the relaxations of side chain or smaller polar groups from polarised to the equilibrium state. At temperature lower than the glass transition temperatures, due to higher resistivity of the polymers, the mobility of molecular dipoles is so low that they are not able to get polarised under the influence of applied electric field and a small observed current peak (α) may be due to the depolarisation of sum loosely bound side groups. At temperatures higher than the glass transition temperature, the mobility of the molecules of the dipoles becomes sufficiently high and thus get polarised under the influence of the electric field. Therefore, two current maxima at about 170 and 200°C are observed in the TSDC thermograms of PVP foil electret.

The above experimental results suggest that in case of PVP trapping sites are centred around three well separated mean values of which the first gives a current peak below glass rubber transition temperature T_g and the second peak in the neighbourhood of T_g and the third peak well above it. Their activation energy, relaxation times are in ascending

order of magnitude. The observations suggest that the trapping sites in PVP is related to small groups segments, main chain/dipoles and crystalline amorphous region.

The values of activation energy associated with TSDC peaks of PVP increases with increase in poling temperature. The activation energy leads one to conclude that the trapping site itself is being destroyed due to increased molecular motion. Marked dependence of depolarising current on electrode materials, linear dependence of charge stored on applied field (not shown) and approximate linearity of steady state current voltage characteristics of PVP suggest carrier injection from electrodes. More emphasis is made to the importance of metal-polymer contact which is the origin of carriers responsible for conduction and surface charge.

Effect of electrode variation is being studied on TSD thermograms, current voltage measurement of PVP foil electret. In the depolarisation of an identically polarised specimen, current reversal is observed in high temperature region and is explained on the assumption that the contribution of hetero charge due to the included charges to the ρ' peak is relatively small as compared to that due to the injected charge carriers from the electrode to the surface of the polymer which finally form the space charge.

Electrical conduction study of PVP suggests a uniform distribution of traps. The flow of current is governed by the

trapping sites. The increase in conductivity with temperature is due to increase in mobility. At low temperature, Hopping like process invoked. The values of activation energy greater than 0.5 eV, the so called trap hopping mechanism is invoked. At higher temperature and field, space charge limited conduction is observed. The rise in conductivity in this region may be due to no free carriers and increase mobility of charge carriers. In our present investigation, the activation energy of conduction is about 1.07 eV which is in good agreement with that determined by TSDC method (1.05 eV).

Current-voltage (I-V) characteristics in pure PVP show different conduction mechanism one below glass transition temperature (T_g) and one above T_g . The mobility of charge carriers are low below T_g and conduction is described by Richardson-Schottky mechanism whereas at higher temperatures, due to increase in mobility of charge carriers the conduction is dominated by space charge.

The transient current in charging and discharging modes have been recorded in PVP foil electrets prepared under different conditions of electric stress and temperature and with different contact electrodes configurations. The currents have been found to follow the Curie von Schweilder law with two different slopes having index, n , values lying between 0.40 to 0.71 at short and from 1.26 to 1.98 at long times. The transient currents exhibited reversibility and a temperature

dependence; and have been characterised by an isochronal peak at 70°C. The associated activation energy values are, in general, found to increase at greater times in all the configurations and show a complex field dependence.

The observed results have been interpreted in terms of dipolar relaxations associated with the polar carbonyl group of polyvinyl pyrrolidone. Some indications of hopping of charge carriers amongst various localized states distributed in energy are also observed and cannot be completely ruled out. Strong evidence, however, in favour of injected and interfacial space charge formation are clearly perceptible. It has been observed that the magnitude of transient currents is higher in cases of dissimilar electrode combinations. This is considered to indicate towards more interfacial charge localization. The charging and discharging currents are found to mirror image of each other, in most of the cases of different configurations. The transient current in PVP decays according to t^{-n} law.

Frequency and temperature dependence of dielectric loss of PVP exhibited a maxima above/below the glass transition temperature of the polymer. Whereas TSDC thermograms of PVP exhibited three current maxima. These results suggest that α -relaxation process accompanied with small activation energy due to the rotational motion of side groups. This relaxation process could not be detected by the present study of dielectric properties in audio frequency range. The ρ

relaxation having large activation energy, is associated with a change of dipole orientation due to segmental rotation of the main chain. Besides these processes of polarisation, space charge polarisation due to injection of charge carriers from electrodes is also responsible for observed polarisation in PVP foils.

7.2 CONCLUDING REMARKS

The various results obtained in the present investigation have been discussed in detail in the light of the available literature, at appropriate sections. The results have indicated that dipolar relaxations, interfacial polarisations and space charge effects are jointly operative in the present case of polyvinyl pyrrolidone foil electrets. The space charges may be injected homo space charges and hetero space charges. Further, ohmic conduction also plays a prominent role. The charges are mainly injected into the bulk of the specimen.

On the basis of our results of various investigations brought about in electrical and dielectric phenomena in polyvinyl pyrrolidone foil electrets, following conclusions may be drawn.

- (i) Every polymer has a transitional temperature range. Near a transition temperature, appearance of peak in TSDC, dielectric loss maxima, change in

capacity, increase of current all are due to a certain region of temperature transition where the changes are mobile in a material.

- (ii) Activation energy (trap depth) calculated from different studies comes out to be nearly the same.

As poly vinyl pyrrolidone is most versatile polymer having numerous applications, as mentioned in Chapter Ist, it would be highly useful to extend these studies further. The study of the behaviour of the Corona, mono energetic electron beam and ion implanted polymer should appear to be a rewarding direction of further work. Thermally stimulated discharge current should be made by further observing doping effects, various heating effects and ageing effects. Recently, pulsed electro-acoustic (PEA) and laser induced pressure pulse (LIPP) techniques have been used [7,8] to measure the internal space charge and its actual distribution in the bulk of the polymer. The shape of the charge distribution obtained by these methods gives a clear indication about the polarity of charge carriers injected, actual location of accumulated charge with respect to the interface and transport of the injected charge into the bulk. Such techniques should be employed to get a better and more detailed information about charge accumulation.

However, the various results of the present investigations can be considered to be of considerable

technical importance to the synthetic chemist, solid state physicist, molecular spectroscopist and polymer material scientists. The work will capitalize on the potential of polyvinyl pyrrolidone as active electrical elements and has enabled us the better understandings of the basic phenomena, involved in charge storage capabilities of poly vinyl pyrrolidone foil electrets.

REFERENCES

1. Dissado, L.A. and Fother Gill, J.C., "Electrical degradaton and breakdown in polymers", U.K. (1992).
2. Lewis, T.J., J. Phys. D. Appl. Phys. 23, 469 (1990).
3. Braunlich, S.P., "Thermally stimulated relaxation in solids", Springer Verlag (1979).
4. DasGupta, D.K. and Joyner, K., J. Phys. D. Appl. Phys. 9, 829 (1976).
5. Kurtz, S.R. and Anderson, R.A., J. Phys. D. Appl. Phys. 60, 680 (1986).
6. Negu, R.E. et al., Proc. Ninth Int. Symp. on Electrets, Shunghai, 25 (1996).
7. Chen, G. et al., Proc. Ninth Int. Symp. on Electret Shunghai, 285 (1996).
8. Maeno, T. and Fukunago, K., Proc. Ninth Int. Symp. on Electret Shunghai, 207 (1996).
9. Khare, P.K. and Srivastava, A.P., Ind. J. Pure Appl. Phys. 30, 131 (1992).
10. Khare, P.K., Keller, J.M. and Datt, S., Ind. J. Pure Appl. Phys. 30, 768 (1992).
11. Khare, P.K., Bajpai Alka and Srivastava, A.P., Ind. J. Pure Appl. Phys. 31, 405 (1993).
12. Khare, P.K., Gaur, M.S. and Srivastava, A.P., Ind. J. Pure Appl. Phys. 31, 102 (1993).
